



# INŻYNIERIA MINERALNA

CZASOPISMO POLSKIEGO TOWARZYSTWA  
PRZERÓBKI KOPALIN

1(45)  
2020

TOM 2, NR 1 (45) 2020, STYCZEŃ – CZERWIEC

PL ISSN 1640 - 4920



JOURNAL OF THE POLISH  
MINERAL ENGINEERING SOCIETY

VOL. 2, NO. 1 (45) 2020, JANUARY – JUNE



**INŻYNIERIA  
MINERALNA**





# INŻYNIERIA MINERALNA

Inżynieria Mineralna  
CZASOPISMO POLSKIEGO TOWARZYSTWA PRZERÓBKI KOPALIN

Inżynieria Mineralna  
JOURNAL OF THE POLISH MINERAL ENGINEERING SOCIETY

1(45)/  
2020

VOL. 2

ROCZNIK XXII

# INŻYNIERIA MINERALNA

## Czasopismo Polskiego Towarzystwa Przeróbki Kopalnin

### JOURNAL OF THE POLISH MINERAL ENGINEERING SOCIETY

#### REDAKCJA – EDITORIAL BOARD

Redaktor Naczelny – Zastępca Redaktora Naczelnego, Redaktor Techniczny –	<b>Barbara TORA</b>	– Editor in Chief
	<b>Julia OKREGLICKA</b>	– Vice Editor, Technical Editor
Sekretarz Redakcji – Redaktor Statystyczny –	<b>Agnieszka SUROWIAK</b> <b>Tomasz NIEDOBA</b>	– Editorial Secretary – Statistical Editor

#### REDAKTORZY DZIAŁOWI BRANCH EDITORS

**Stanisław CIERPISZ**  
**Andrzej ŁUSZCZKIEWICZ**  
**Stanisława SANAK-RYDLEWSKA**  
**Tomasz SUPONIK**  
**Dariusz PROSTAŃSKI**  
**Alicja BAKALARZ**

#### MIEDZYNARODOWA RADA REDAKCYJNA INTERNATIONAL ADVISORY EDITORIAL BOARD

Rosja –	<b>Tatyana ALEXANDROVA</b>	– Russia
Grecja –	<b>Georgios ANASTASSAKIS</b>	– Greece
Polska –	<b>Wiesław BLASCHKE</b>	– Poland
Słowacja –	<b>Peter BLISTAN</b>	– Slovakia
Węgry –	<b>Ljudmilla BOKÁNYI</b>	– Hungary
Czechy –	<b>Vladimir ČABLÍK</b>	– Czech Republic
Czechy –	<b>Pavel ČERNOTA</b>	– Czech Republic
Rosja –	<b>Valentin A. CHANTURIYA</b>	– Russia
RPA –	<b>Johan DE KORTE</b>	– South Africa
Polska –	<b>Jan DRZYMAŁA</b>	– Poland
Słowacja –	<b>Juraj GAŠINEC</b>	– Slovakia
Węgry –	<b>Imre GOMBKÖTŐ</b>	– Hungary
Słowacja –	<b>Gabriel WEISS</b>	– Slovakia
Kanada –	<b>M.E. HOLUSZKO</b>	– Canada
Słowacja –	<b>Sławomir HREDZAK</b>	– Slovakia
W. Brytania –	<b>Douglas E. JENKINSON</b>	– United Kingdom
Polska –	<b>Przemysław KOWALCZUK</b>	– Poland
Rumunia –	<b>Sanda KRAUSZ</b>	– Romania
Polska –	<b>Janusz LASKOWSKI</b>	– Poland
Polska –	<b>Marcin LUTYŃSKI</b>	– Poland
Turcja –	<b>Gülhan ÖZBAYOĞLU</b>	– Turkey
USA –	<b>B. K. PAREKH</b>	– USA
RPA –	<b>David PEATFIELD</b>	– South Africa
Rosja –	<b>Yuliy B. RUBINSHTEIN</b>	– Russia
Polska –	<b>Jerzy SABLİK</b>	– Poland
Indie –	<b>Rai K. SACHDEV</b>	– India
Indie –	<b>Kalyan SEN</b>	– India
Chiny –	<b>Zhongjian SHAN</b>	– China
Słowacja –	<b>Jirí ŠKVARLA</b>	– Slovakia
Czechy –	<b>Hana STANKOVA</b>	– Czech Republic
Australia –	<b>Andrew SWANSON</b>	– Australia
Serbia –	<b>Rudolf A. TOMANEC</b>	– Serbia
Japonia –	<b>Masami TSUNEKAWA</b>	– Japan
Chiny –	<b>Xie WENBO</b>	– China
Ukraina –	<b>Olexandr YEGURNOV</b>	– Ukraine
Niemcy –	<b>Dieter ZIAJA</b>	– Germany

INŻYNIERIA MINERALNA JEST DOSTĘPNA (OPEN ACCESS) NA STRONIE WYDAWCY | WHOLE ISSUES OF INŻYNIERIA MINERALNA ARE AVAILABLE (OPEN ACCESS) ON PUBLISHER WEBSITE: POLSKA WWW.POTOPK.COM.PL/ARCHIWUM ENGLISH WWW.POTOPK.COM.PL/AN\_ARCHIWUM

INŻYNIERIA MINERALNA JEST INDEKSOWANA I ABSTRAKTOWANA | INŻYNIERIA MINERALNA IS INDEXED AND ABSTRACTED: SCOPUS (ELSEVIER), WEB OF SCIENCE, MASTER JOURNAL LIST – EMERGING SOURCES CITATION INDEX (CLARIVATE ANALITICS), POL-index, EBESCO, BAZTECH, Chemical Abstracts, Реферативный Журнал.  
Inżynieria Mineralna is a member of CROSSREF.

ADRES REDAKCJI | CORRESPONDANCE ADDRESS:  
POLSKIE TOWARZYSTWO PRZERÓBKI KOPALIN | POLISH MINERAL ENGINEERING SOCIETY  
MICKIEWICZA 30, 30-059 KRAKÓW  
MAIL: TORA@AGH.EDU.PL, C@NWH.PL

SKŁAD/ŁAMANIE/UKŁAD TYPOGRAFICZNY/OBSŁUGA: NOWY WSPANIAŁY HOLDING (NWH)  
KONTAKT: C@NWH.PL  
DRUK: DRUKARNIA TYPOGRAFIA – WWW.TYPOGRAFIA.COM.PL  
KONTAKT: TYPOGRAFIA@TYPOGRAFIA.COM.PL  
NAKŁAD: 200 egz.

© Inżynieria Mineralna, ISSN 1640-4920, Kraków 2020 by POLSKIE TOWARZYSTWO PRZERÓBKI KOPALIN  
Inżynieria Mineralna is licensed under CC-BY-SA 3.0 Creative Commons.  
© Articles by authors

Wydanie Inżynierii Mineralnej jest dofinansowane przez Ministerstwo Nauki i Szkolnictwa Wyższego w ramach działalności upowszechniającej naukę; numer umowy: 660/P-DUN/2018.







# Comparison of Mineral Processing Methods for Metal Recycling from Waste Printed Circuit Board

Gordan BEDEKOVIC<sup>1)</sup>, Vitomir PREMUR<sup>2)</sup>, Anđela IVIĆ<sup>3)</sup>

<sup>1)</sup> University of Zagreb, Faculty of Mining, Geology and Petroleum Engineering, Pierottijeva 6, 10000 Zagreb, Croatia;

email: gordan.bedekovic@rgn.hr

<sup>2)</sup> University of Zagreb, Faculty of Geotechnical Engineering, Hallerova aleja 7, 42000 Varaždin, Croatia; email: vitomir.premur@gfv.hr

<sup>3)</sup> University of Iceland, Faculty of Life and Environmental Sciences, Tækniagarður - Dunhagi 5, 107 Reykjavík, Iceland;

email: aivic1@hotmail.com

<http://doi.org/10.29227/IM-2020-01-29>

Submission date: 10-01-2020 | Review date: 02-04-2020

## Abstract

*Faster technology development, increasing of living standard and market availability are the main causes of faster obsolescence of electronic devices. Each electronic device contains printed circuit boards that are a valuable source of metal. The paper presents the results of preliminary research of the possibility for using various mineral processing methods in recycling of waste printed circuit boards. The gravity concentration (concentration table and Humphreys spiral concentrator), electrostatic separation and wet magnetic separation were used in this preliminary research and the obtained results were presented in the article.*

**Keywords:** waste printed circuit boards, recycling, metals, separation

## Introduction

Faster growth of the population and technology development, an increase in the standard of living and market availability have resulted in the waste electric and electronic equipment (WEEE) being one of the largest waste streams globally (Tanskanen, 2013) and more than 50 million tons generated yearly (Wang et al., 2013).

WEEE contains a large amount of metal, sometimes 30 to 40 times more than the primary raw material (minerals) from which certain metals are obtained (Robinson 2009), so it is an excellent secondary raw material for metals production. For example, copper content in ores today is approximately 0.4% (Freeport-Mcmoran 2013), while the content of copper in electronic components can be 18% (Veit, 2006), even more than 30% (Monal et al. 2011).

Today, almost every electrical or electronic device has a printed circuit board (PCB), and PCB constitutes about 3% of WEEE (Marques et al., 2013). The PCBs contain many valuable metals such as Cu, Al, Ag, Au, Pb, etc. (Bedeković, 2015).

PCB consists of a base (a thin insulating board that serves as a base for conductors and electronic components) and a conductive layer (usually copper in the form of thin lines tightly glued to the base).

The structure of the supporting insulating base is layered and is made by mixing the basic material with fillers. The base usually consists of cellulose fibres impregnated with phenol resin (pertenax) or glass fibres impregnated with epoxide resin (vitroplast). For higher frequencies, fluoropolymers and ceramics are used which are selected only in case when there is a price justification or when a different solution is not possible. Depending on the required thickness of the PCB, the desired number of layers of glass cloth is applied.

The conductive copper layer can be applied in several ways: depending on the desired quality of the finished PCBs, the quantity and the price vary between silk screen printing,

photo printing, printing methods such as lithotis and lithofecta printing, and mechanical methods of molding and shaping copper figures.

On average, the PCBs consist of over 70% nonmetals (plastic, epoxy resin and glass fiber), 16% copper, 4% solder, 3% iron, ferrites, 2% nickel, 0.05% silver, 0.03% of gold, 0.01% palladium and others (bismuth, antimony, tantalum etc.) with a share of less than 0.01% (Eswaraiyah, C., et al., 2008).

The most common classification of the PCBs is one-sided, two-sided and multiple although they can be classified according to different criteria. Single-sided have electronic components on one side (top side), and conductive connections on the other (bottom side). This type of PCBs is simple, the cost of production is low, which is advantageous, but with lower component density and poorer high-frequency properties.

Double-sided PCBs have conductive links on both sides of the PCB while the components are most commonly on one side. They have higher component density packing, better high-frequency properties, and easier component connectivity, but are more expensive than one-sided. They have weaker electrical properties and the possibility of realization very complex assemblies in relation to multilayer PCBs.

Multilayer PCBs are used in case when the density of conductive links is greater than is possible with double-sided PCBs or where precision data is required. It consists of several double-sided tiles between which is a thin layer of so-called pre-impregnated material and thus makes a multilayer PCB. This type of printed circuit board is characterized by very high component density, excellent high-frequency properties and the ability to control line impedance, but the production cost can be very high.

The previously described PCBs are solid PCBs (Fig.1 left), and except them there are flexible PCBs (Fig.1 right) which are also divided into single, double and multilayer. They



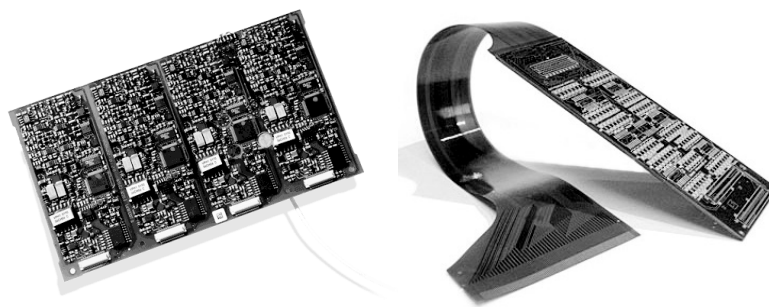


Fig. 1. Solid (left) and flexible (right) PCBs  
Rys. 1. Stałe (lewe) i elastyczne (prawe) płytki drukowane

are used as a replacement for multi-wire cables to achieve high-level complexity in small volumes, in mobile phones, video and photo cameras, calculators, etc. Their advantages are flexibility, 3D bending flexibility, low mass and dimensions, high density in small volumes, cheaper and more reliable connection of multiple PCBs. On the other hand, the design and manufacturing process is very complex and the production price is high. Solid PCBs have the advantage of flexible in most applications, and flexible ones are only selected when there is either a price justification or where it is not possible to implement a solution for a particular application.

#### Materials and methods

The aim of this study was to compare different methods for separating metals from solid waste PCBs.

A sample of 3.88 kg was delivered from Spectra Media d.o.o. which deals with the recycling of electronic waste. The electronic components have been previously removed from the PCBs, and the PCBs are cut to smaller dimensions for easier handling. The average size of the PCB in the sample was 5×5×0.2 cm.

The PCBs are made of glass fibers impregnated with epoxy resin (vitroplast). The metal (in this research valuable component) is attached to the PCB with the insulating base (non-valuable component). The precondition of separation is to interrupt the bonding of the metal with the base. Therefore, the first step in the research was comminution in order to achieve the liberation of metal from the insulating base. The metal mass content of the feed sample (PCB) was 33% and is determined by firing at a temperature of 400° to 600°C. PCBs were crushed in an impact crusher with an exit opening of 18 mm. However, crushing in the impact crusher did not satisfactory results due to small masses and small grits. Subsequently, the sample was crushed in a hammer crusher with a grid openings of 8 mm. After crushing, a granulometric analysis was carried out. Previous researching has found that by crushing the sample below the particle size of 2 mm almost completely liberate the metal from the base (Zhang and Forssberg, 1997). Therefore, the sieving was used to obtain samples of grain sizes 2/1 mm and 1/0.5 mm for further testing by gravity, magnetic and electrostatic concentration. Wilfley concentrating table and Humphreys spiral concentrator were used in gravity concentration. On the concentration table, two size classes (2/1 mm and 1/0.5 mm) were tested on three different slopes of the table (3°, 6° and 9°). The mass

of each sample was 30 grams. The wash water flow was 4 l/min. The same size class (2/1 mm and 1/0.5 mm) were also tested on the Humphreys spiral concentrator, with the heavy component exits completely closed on the first five bends and at the last one, sixth fully opened. The mass of the samples was 200 g. After the tests in these two devices, all the obtained products were dried and weighed. The electrostatic separator tests were conducted only in the size class 1/0.5 mm since the manufacturer prescribes an optimum particle size from 0.65 mm to 1.6 mm. In the first phase of the testing the drum speed was changed (40, 50, 60, 70 m/min), in the second ionization electrode voltage (17, 20 and 25 kV) and finally the influence of the ionization electrode distance from the drum (25 and 40 mm). The obtained products are weighed after the test. Tests in a wet low intensity magnetic separator were also performed in two classes (2/1 mm and 1/0.5 mm).

After each individual test, obtained products were dried and its composition were determined by hand sorting and weighing. Separation efficiency were estimated by two parameters: recovery (of metals) and grade of concentrate. The recovery represents the percentage of the total metal contained in the feed that is recovered into the concentrate. The recovery  $R$  can be expressed by follow equation:

$$R = 100 \cdot \frac{C \cdot c}{F \cdot f} \quad (\%)$$

where  $R$  is recovery in percentage,  $C$  is a mass of the concentrate in grams,  $c$  is a mass content of metal in concentrate in percentage,  $F$  is a mass of feed in grams and  $f$  is a mass content of metal in the feed material in percentage. Grade of concentrate represents the percentage of the metal contained in the concentrate as a final product and can be expressed by follow equation:

$$G_c = 100 \cdot \frac{m_m}{m_c} \quad (\%)$$

where  $G_c$  is grade of concentrate in percentage,  $m_m$  is mass of metal in concentrate in grams and  $m_c$  is mass of concentrate in grams.

#### Results and discussion

The results of the granulometric analysis of the crushed sample in hammer crusher were shown in Table 1. Since a grid with a 8 mm openings size was used during crushing, it is not surprising that almost half of the mass sample (49.23%) is larger

Tab. 1. Grain size distribution after crushing  
 Tab. 1. Rozkład wielkości ziarna po kruszeniu

Grain size (mm)	Screen retain		
	(g)	(%)	(cum. %)
8/2	21.66	49.23	49.23
2/1	5.58	12.68	61.91
1/0.5	5.56	12.64	74.55
0.5/0.1	8.28	18.82	93.36
- 0.1	2.92	6.64	100.00
Σ	44.00	100.00	-

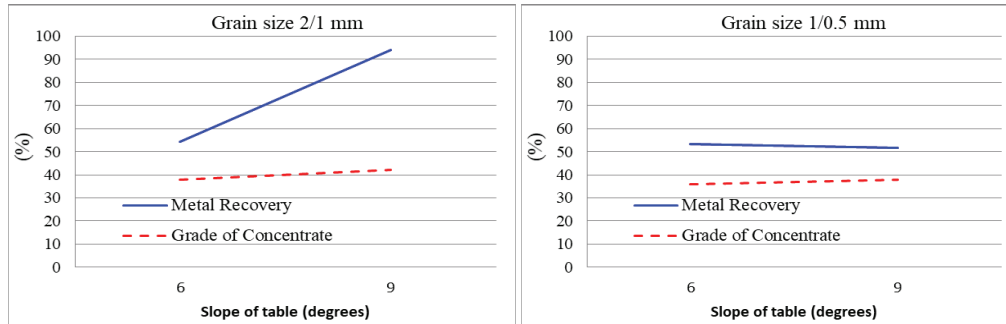


Fig. 2. Results of separation in Wilfley concentration table  
 Rys. 2. Wyniki rozdzielania w tabeli stężeń Wilfleya

than 2 mm. When the particles less than 2 mm are considered, the most common class is 0.5/0.1 mm (18.82%), and the lowest represented class is -0.1 mm (6.64%). The mass fraction of these two smaller classes together amounts to 25.46%, which is approximately half of the mass in the size class of -2 mm. The other half (25.32%) makes size classes 2/1 mm and 1/0.5 mm with approximately equal masses (12.68 and 12.82%), and separation tests were performed on those size classes.

Figure 2 shows the separation results of coarser size class 2/1 mm on the Wilfley concentration table. Although separation tests were carried out at three different slopes of the table (3°, 6°, 9°), only the results of tests performed at slopes of 6° and 9° were shown, as in the slope of 3° test results were far from satisfactory. From Figure 2 (left) it can be seen that with increasing slope there was also an increase in recovery and quality of concentrate (Grade) of grain size 2/1 mm. Thus, metal recovery grew by 40% (from 54.23 to 94.18%) and concentrate quality by 4% (from 38.08 to 42.12%).

The finer size class 1/0.5 mm did not show any significant changes with a change of table slope (Fig. 1 right). The recovery of the metal was somewhat over 50%, and the concentrate quality was slightly below 40%, which was worse than the results obtained by testing the size class 2/1 mm (Fig. 1 left).

In addition to the concentration table, the Humphreys spiral concentrator as well as at the concentration table for both size classes were used in gravity concentration. From the results (Fig. 3) it can be seen that in the spiral concentrator a better result is achieved with a coarser size class of 2/1 mm. In the coarser size class 2/1 mm test, the metal recovery was 56.95% with the concentrate quality of 78.12%. The finer size class 1/0.5 mm gave worse results in terms of metal recovery of 19.89% and concentrate quality of 50.98%.

When comparing the results of both devices used in the gravity concentration method, it can be seen that significantly higher metal recovery (up to 94.18%) can be achieved on the table than

the spiral concentrator (56.95%) but with a significantly lower concentrate quality of 42.12% (78.12% in a spiral concentrator). Based on these results, it would be recommended to use the concentration table in the first stage of separation when high recovery is desired, and then concentrate quality can be improved in the second stage by using a spiral concentrator to cleaning concentrate obtained in the first stage. In addition to the gravity concentration, the study was conducted using electrostatic concentration, and the results are shown in Figures 4 and 5. The electrostatic concentration tests was performed in three phases.

In the first phase of the testing the influence of drum speed on the separation (Figure 4 left) was researched. The first series of tests was performed by varying the drum speed from 40 to 70 m/min at the 25 kV electrode voltage and its distance from the drum of 25 mm. The figure shows recovery increasing up to 65.05% and concentrate quality up to 71.03% with drum speed up to 60 m/min. With a further increase in speed to 70 m/min, both parameters, recovery and quality of the concentrate decreased. The speed of 60 m/min was selected as the best, and a second phase of the tests was performed in which the influence of the electrode voltage was tested and the results are shown in Figure 4 (right).

In Figure 4 (right), it can be seen that by increasing the voltage from 15 to 20 kV practically hasn't influence on the separation parameters. With a further increase in the voltage of up to 25 kV, a slight increase in the quality of the concentrate and a significant increase in metal recovery are obtained. After testing the drum speed and the electrodes voltage, it was to be determined whether the electrode distance from the drum had a separation effect. For this purpose, tests with two different distances from drum (25 and 40 mm) at 25 kV and drum speed of 60 m/min were performed and the results are shown in Figure 5.

From Figure 5 it can be seen that with the increase of the electrode distance from the drum there is a significant reduc-

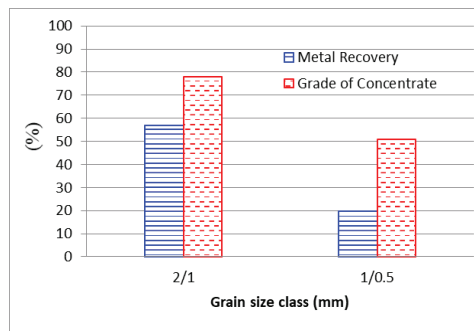


Fig. 3. Results of separation in Humphreys spiral concentrator (grain sizes 2/1 and 1/0.5 mm)  
 Rys. 3. Wyniki separacji w koncentratorze spiralnym Humphreysa (wielkość ziaren 2/1 i 1/0,5 mm)

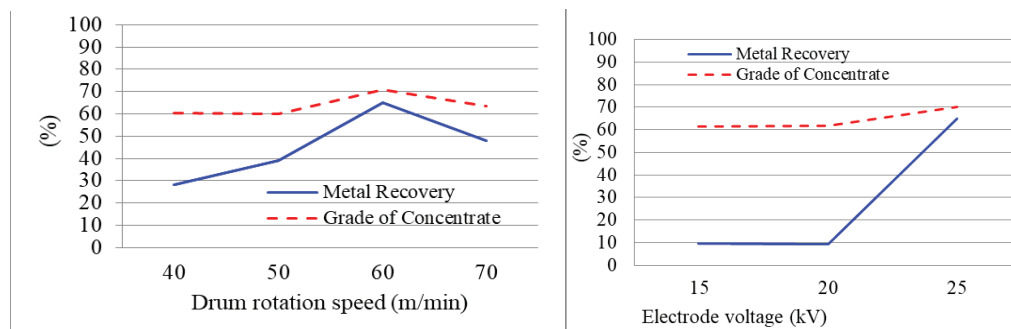


Fig. 4. Results of separation grain size 1/0.5 mm in Electrostatic separator at different drum speeds (left) and electrode voltage (right)  
 Rys. 4. Wyniki wielkości ziarna separacji 1/0,5 mm w separatorze elektrostatycznym przy różnych prędkościach bębna (po lewej) i napięciu elektrody (po prawej)

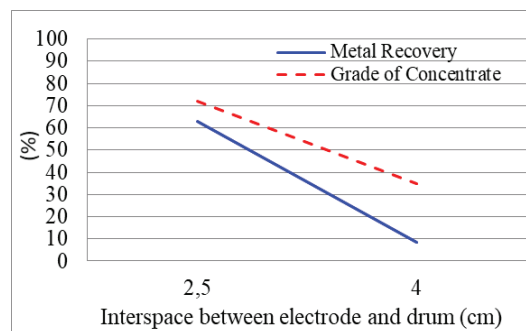


Fig. 5. Results of separation in Electrostatic separator at different distance between drum and electrode (grain size 1/0.5 mm)  
 Rys. 5. Wyniki separacji w separatorze elektrostatycznym w różnej odległości między bębniem a elektrodą (wielkość ziarna 1/0,5 mm)

tion of both observed parameters. Concentrate quality decreased from 72.11 to 35.03%, and metal recovery from 62.75 to 8.49%. Based on the results of the three-phase testing, it can be said that each of the tested independent variables can have a significant effect on the separation results. To determine the optimum separation conditions, a more detailed set of tests should be performed in the area of the value of the individual independent variables in which the greatest changes were observed (drum speed in the range from 55 to 65 m/min, electrode voltage from 25 to 30 kV and electrode distance of about 2.5 cm).

In a wet magnetic separator, the test was performed at a voltage of 57.5 V and a current of 10 A to generate a magnetic field. Two size classes were tested (2/1 mm and 1/0.5 mm), as well as gravity concentration. When testing the size class 2/1 mm, 10.5% of the mass of the sample was separated as a

magnetic component, while in the finer size class 1/0.5 mm it was significantly less (5.4%).

### Conclusion

This test compared several methods for separating metals from waste PCBs. Two crushers were used during comminution. It has been shown that due to the small weight and grit of the PCBs, hammer crusher is an incomparably better solution than the impact crusher. Gravitation concentrations on the Wilfley concentration table and Humphreys spiral concentrator were studied in two size classes (2/1 mm and 1/0.5 mm). On both devices, better results were obtained by separating the coarser grain size (2/1 mm). Comparison of the device showed that better results in terms of recovery were achieved at the concentration table and the concentrate quality with the spiral concentrator. Therefore, it may be recommended to use

a concentration table to achieve higher recovery in the first separation stage, and in the second use a Humphreys spiral concentrator for concentrate cleaning. The electrostatic separation tests were performed with the purpose of testing the influence of three independent variables (drum speed, electrode voltage and drum electrode distance). The results have shown that all three variables can have a significant effect on separation, depending on their values. Given the manufacturer's recommendations, a finer size class 1/0.5 mm was tested. It has been shown that recovery could be obtained somewhat over 60% (Humphreys spiral concentrator about 20%, Wilfley concentration table slightly more than 50%) and concentrate quality can be achieved, depending on separation conditions up to 70% (Humphreys spiral concentrator about 50%, con-

centration table Wilfley below 50%), which are better results than those in gravity concentration. With a wet magnetic concentration, about 5% of the magnetic component in the finer size class 1/0.5 mm and about 10% in the coarser size class 2/1 mm were obtained, which were worse than the first two methods. However, it should be kept in mind that the first two methods can practically separate all of metals, and a magnetic concentration just iron.

#### **Acknowledgements**

Dissemination process is supported by the Development Fund of the Faculty of Mining, Geology and Petroleum Engineering, University of Zagreb.

## Literatura – References

1. BEDEKOVIĆ, G. E-waste recycling by electrostatic separation. Handbook of research on advancements in environmental engineering. Hershey : IGI Global, 2015, p. 285-317, ISBN 978-1-4666-7336-6.
2. ESWARAIHAH, C., KAVITHA, T., VIDYASAGAR, S., NARAYANAN, S.S. Classification of metals and plastics from printed circuit boards (PCB) using air classifier. Chemical Engineering and Processing, 47(4), 2008, p. 565-576, ISSN 0255-2701.
3. FREEPORT-MCMORAN Copper & Gold Inc., Annual report pursuant to section 13 or 15(d) of the securities exchange act of 1934 [online]. Phoenix Arizona 2013 [cit. 2019-02-21]. URL: < <https://catalog.hathitrust.org/Record/101582359>>.
4. MARQUES, André Canal, CABRERA MARRERO, José-María, MALFATTI, Célia de Fraga. A review of the recycling of non-metallic fractions of printed circuit boards. Springer Plus a Springer Open Journal [online]. 2013, vol. 2, no. 521, April [cit. 2019-03-27]. Accessible from URL: < <https://www.ncbi.nlm.nih.gov/pmc/articles/PMC3930799/> >. ISSN 2193-1801.
5. MONAL, B., Shah, DEVAYANI, R., Tipre, SHAILLESH, R. Dave. Chemical and biological processes for multi-metal extraction from waste printed circuit boards of computers and mobile phones. Waste management & Research, 32(11), 2014, p. 1134-1141, ISSN 0734-242X.
6. ROBINSON, Brett H. E waste: An assessment of global production and environmental impacts. Science of the Total Environment, 408, 2009, p. 183-191, ISSN 0048-9697.
7. TANSKANEN, Pia. Management and recycling of electronic waste. Acta Materialia, 61(3), 2013, p. 1001-1011, ISSN 1359-6454.
8. VEIT, Hugo Marcelo, BERNARDES, Andréa Moura, FERREIRA, Jane Zoppas, SOARES TENORIO Jorge Alberto, MALFATTI, Célia de Fraga. Recovery of copper from printed circuit boards scraps by mechanical processing and electrometallurgy. Journal of Hazardous Materials, 137(3), 2006, p. 1704-1709, ISSN 0304-3894.
9. WANG, Feng, HUISMAN, Jaco, STEVELS, Ab, BALDE, Cornelis Peter. Enhancing e-waste estimates: Improving data quality by multivariate Input-Output Analysis. Waste management, 33(11), 2013, p. 2397-2407, ISSN 0956-053X.
10. ZHANG, Shunli, FORSSBERG, Eric. Mechanical separation-oriented characterization of electronic scrap. Resources, Conservation and Recycling, 21 (4), 1997, p. 247-269, ISSN 0921-3449.

### *Porównanie różnych metod odzysku metali z odpadowych płytek drukowanych*

*Szybki rozwój technologii, podwyższenie standardu życia i dostępność na rynku to główne przyczyny szybszego starzenia się urządzeń elektronicznych. Każde urządzenie elektroniczne zawiera płytki drukowane, które są cennym źródłem metalu. W pracy przedstawiono wyniki wstępnych badań możliwości zastosowania różnych metod przeróbki surowców w recyklingu zużytych obwodów drukowanych. W tych wstępnych badaniach wykorzystano wzbogacalnik grawitacyjny (stół wstrząsany i wzbogacalnik spiralny Humphreya), separację elektrostatyczną i separację magnetyczną na mokro, uzyskane wyniki przedstawiono w artykule.*

**Słowa kluczowe:** odpady obwodów drukowanych, recykling, metale, separacja



# Environmental Pollution Monitoring by Thin Metal Electrodes Prepared by Physical Vapor Deposition

Jaroslav BRIANČIN<sup>1)</sup>, Iraida KOLCUNOVÁ<sup>2)</sup>, Bystrík DOLNÍK<sup>2)</sup>,  
Juraj KURIMSKÝ<sup>2)</sup>, Jaroslav DŽMURA<sup>2)</sup>, Roman CIMBALA<sup>2)</sup>, Martin FABIÁN<sup>1)</sup>

<sup>1)</sup> Institute of Geotechnics, Slovak Academy of Sciences, Watsonova 45, 04001, Košice, Slovakia

briancin@saske.sk; fabianm@saske.sk

<sup>2)</sup> Faculty of Electrical Engineering and Informatics, Technical University of Košice, Letná 9, 04200, Košice, Slovakia; email: iraida.kolcunova@tuke.sk; bystrik.dolnik@tuke.sk; juraj.kurimsky@tuke.sk; jaroslav.dzmura@tuke.sk; roman.cimbala@tuke.sk

<http://doi.org/10.29227/IM-2020-01-30>

Submission date: 10-02-2020 | Review date: 02-04-2020

## Abstract

*This work is focused on environmental pollution monitoring utilizing thin metal electrodes on glassy/ceramic substrates prepared by physical vapour deposition. Besides others, it is well known that environmental pollution on electrical insulation is one of the problems faced by distribution utilities and electricity transmission system. Due to this reason there is a need to deal with monitoring of environmental pollution as it strongly influences their capability to withstand the high-voltage stress without the breakdown. It is the aim of present work to propose new system for environmental pollution monitoring based on application of extra-thin metal electrodes. The influence of morphology and chemical composition of pollutants on the surface resistance and conductivity of selected insulators is also discussed.*

**Keywords:** environmental pollution, metal electrodes, physical vapor deposition, electrical conductivity, insulators

## Introduction

Several activities forming modern society requires still higher consumption of electrical energy. Production and consumption of electrical energy are expressed in the regular calls of the European Commission's in the Framework Programme for Research and Innovation: Secure, clean and efficient energy [1–3]. In this context, European and national activities in this area are aimed at supporting the transition to reliable, sustainable and competitive energy systems. Contamination of high-voltage insulators is determined by the sources of pollution as well as meteorological factors in the locality and can vary during year [4]. Air pollution is recognized as environmental burden with negative great influence on environment as well as on different branches of industry. However, as electricity consumption increase, the electric energy consumption requires better quality of transmission networks. Pollution of the surface of the insulator increases its electrical conductivity and is therefore an unfavorable situation because it increases the risk of destruction of the insulator, mechanical damage to surrounding components as well as possible outages in the damaged part of the transmission or distribution network. It is known that during foggy weather, drizzle or dew form, contaminants are partially dissolved to form on the surface of the isolation the conductive regions, or the conductive layers and results in increase of electrical conductivity. Active monitoring of electric conductivity of contaminated parts of ceramic, glassy or polymer-based insulators allows early regulation (decrease of energy losses). In situ monitoring of conductivity of insulator surfaces can be used for control of environmental pollution caused by industrial activity. For these purposes, ultra-thin metal electrodes prepared by physical vapor deposition present alternative method to monitor electrical conductivity between them, and thus to follow insulating properties

of insulators. This paper deals with preparation and testing of thin metal electrodes introduced for environmental pollution monitoring.

## Materials and methods

### Preparation of silver electrodes on glazed ceramic surface

Colloid silver was used as a starting material for preparation of silver electrodes. A proper amount of colloid silver was mixed with solvent to form homogeneous paste. To obtain proper geometry of electrodes silver paste was applied on surface of glazed ceramic screen printing. Such prepared ceramic substrate was dried and annealed at 700°C for 30 min in air atmosphere. As-prepared electrodes with different geometries are shown in Figure 1.

### Electrical conductivity testing

Before all measurement the glazed ceramic sample was carefully cleaned in order to remove all traces of dirt and grease. The surface of the glazed ceramic sample is deemed to be sufficient clean and free from any grease if large continuous wet areas are observed. After cleaning, the insulating parts of the glazed ceramic sample were not touched by hand. Fairly uniform conducting electrolytic layer of a defined solid pollution, made from sodium chloride (NaCl) of commercial purity and tap water, was deposited on the dry sample surface representing the pollution layer in the service. The salinity of the prepared solution corresponds to four classes of pollution (I–IV) in accordance with [5, 6]. After drying of the deposited solution, uniformly distributed solid layer was formed.

The schematic diagram of the measuring circuit is shown in Figure 2. The applied voltage of sinusoidal shape connected to the electrodes was generated by wave signal generator Agilent 33220A. Amplitude of the testing voltage with sinusoi-

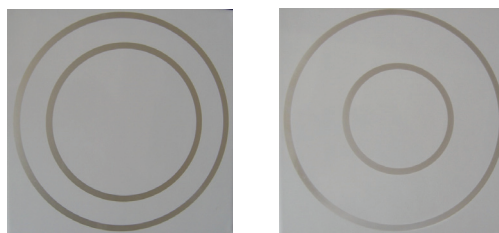


Fig. 1. Silver electrodes on glazed ceramic surface with 20 mm (left) and 40 mm (right) gap between them  
Rys. 1. Srebrne elektrody na szklawionej powierzchni ceramicznej z odstępem 20 mm (po lewej) i 40 mm (po prawej)

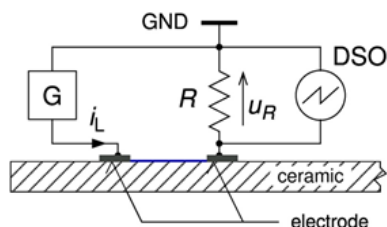


Fig. 2. Schematic diagram of the measuring circuit (G – wave signal generator, R – sensing resistor,  $i_L$  – leakage current,  $u_R$  – voltage, DSO – digital storage oscilloscope, GND – signal ground)

Rys. 2. Schemat obwodu pomiarowego (G – generator sygnału falowego, R – rezystor pomiarowy,  $i_L$  – prąd upływu,  $u_R$  – napięcie, DSO – cyfrowy oscyloskop magazynowy, GND – masa sygnału)

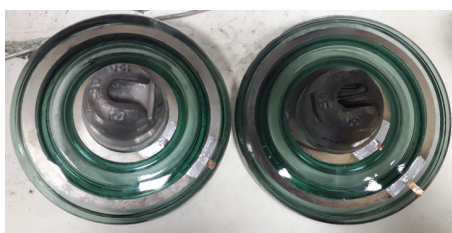


Fig. 3. Ultrathin aluminium-based metal electrodes deposited on high-voltage insulators  
Rys. 3. Ultracienkie elektrody metalowe na bazie aluminium osadzone na izolatorach wysokiego napięcia

dal shape was set from 1 V to 7 V and the frequencies ranges from 1 Hz to 10 kHz. The response of the electrode system to the applied voltage was measured with digital storage oscilloscope Agilent DSO 7104B. The amplitude of the leakage current on the surface of the sample was calculated according to the Ohm's law as the ratio of voltage and known resistance of resistor connected to one electrode. The resistance of sensing resistor is  $R = 3.3 \text{ M}\Omega$ .

At first, clean dry sample was measured. After measurement under dry conditions, the surface of the sample was wetted and the measurement was repeated. This procedure was then applied on sample with polluted layer (I class) under dry and wet conditions.

#### **Thin metal electrodes prepared by physical vapor deposition**

Thin metal electrodes were prepared on the surface of the high-voltage insulators by physical vapor deposition (PVD) of aluminium. Figure 3 shows examples of thin metal electrodes deposited.

#### **Results and discussion**

The values of leakage current flowing through the dry surface without contamination of the glazed ceramic surface between silver electrodes at different frequencies with sinusoidal shape is shown in Figure 4. As can be seen, the sensi-

tivity of measurement increases with increasing frequency of the testing voltage. Furthermore, it can be seen that with increasing testing voltage, the leakage current increases linearly.

Low frequencies (from 1 Hz to 100 Hz) does not result in satisfied sensitivity due to the presence of electromagnetic interference. Based on achieved results, for further experiments 1 kHz frequency was used.

The time course of the testing voltage and the surface leakage current on the uncontaminated sample in the time interval of 1 ms (one period at frequency 1 kHz) is depicted in Figure 5. Designation of individual lines is as follows: U represents the open circuit voltage applied to the silver electrodes,  $i_L$  dry is the leakage current flowing between silver electrodes on glazed ceramic surface without contamination and  $i_L$  wet is the leakage current flowing between silver electrodes on glazed ceramic surface with presence of humidity. It can be seen that leakage current has lower values for dry surface in comparison to surface after wetting. Thus it is shown that environment influences the conductivity between electrodes and measured voltage is higher in the case of humidity. It can be attributed to the better electric conductivity on the surface of glazed ceramic in the presence of humidity.

Based on achieved results it is clear that proposed methodology of environmental pollution monitoring is suitable and sensitive on in-situ study and monitoring of insulating

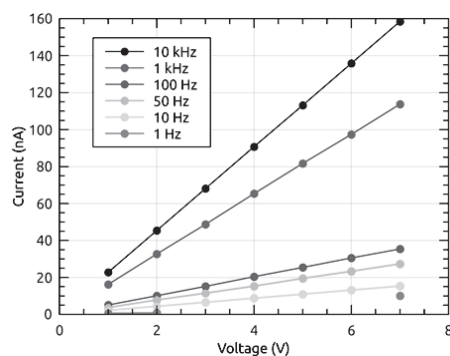


Fig. 4. Current vs. voltage at different frequencies recorded between silver electrodes on dry uncontaminated surface of glazed ceramic  
 Rys. 4. Zależność napięcia od prądu przy różnych częstotliwościach rejestrowane między elektrodami srebrnymi na suchej niezanieczyszczonej powierzchni szklawej ceramiki

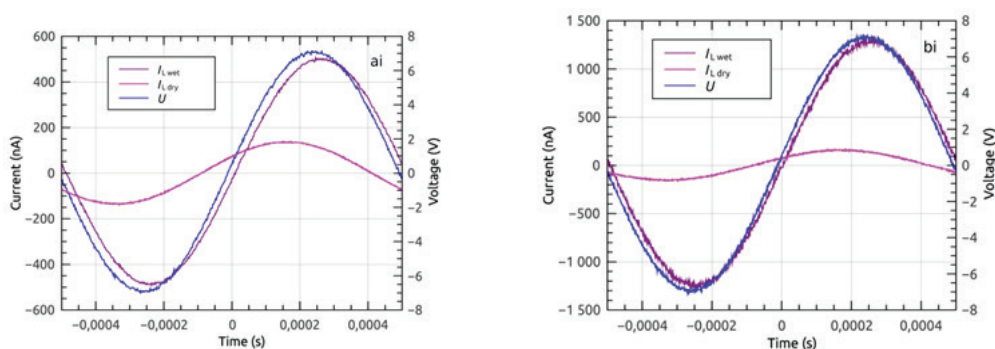


Fig. 5. Comparison of surface leakage current in measuring circuit supplied with sinusoidal voltage: left) dry and wet surface of glazed ceramic surface without contamination; right) dry and wet surface after contamination with solution class I  
 Rys. 5. Porównanie prądu upływu powierzchniowego w obwodzie pomiarowym zasilanym napięciem sinusoidalnym: po lewej – sucha i mokra powierzchnia oszklawej powierzchni ceramicznej bez zanieczyszczeń; po prawej – sucha i mokra powierzchnia po zanieczyszczeniu roztworem klasy I

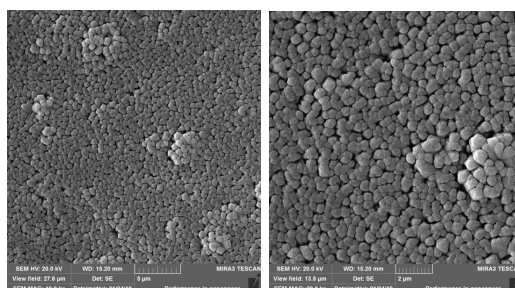


Fig. 6. SEM micrographs of surface of aluminium based metal electrodes with different magnifications  
 Rys. 6. Mikrografy SEM powierzchni elektrod metalowych na bazie aluminium o różnych powiększeniach

properties of high-voltage insulators and thus prediction of electrical losses.

For real applications, real metal electrodes replacing expensive silver should be proposed. In this manner we have prepared ultra-thin aluminium-based metal electrodes by PVD. Figure 6 shows SEM micrographs of their surface. Based on the electrical conductivity studies, performed on the silver electrodes, it is the plan of future work to test electrical conductivity of novel aluminium electrodes prepared by PVD on the surface of high-voltage insulators.

### Conclusions

Pollution layer on the insulation of electrical equipment has a visible effect on service life and reliable operation of installed electrical equipment. The aim of the experiment was to determine the effect of pollutants on the outer isolation.

From the measured data it is clear that environmental conditions have a great influence on the leakage current (surface resistivity) for pure and polluted insulation. The experimental results showed that the amplitude of the leakage current along the surface connected to testing voltage has increased on the polluted sample in wet conditions. The experimental results show that monitoring of leakage current along the surface of the external insulation is a useful indicator of the pollution of external insulation. PVD was used for preparation of aluminium-based electrodes. Improvement of their porosity and testing of their electrical properties is the aim of our future work.

### Acknowledgements

This work was supported by the Slovak Research and Development Agency under the contract No. APVV-15-0438.



#### Literatura – References

1. “Secure, Clean and Efficient Energy - Horizon 2020 - European Commission”, Horizon 2020. [Online]. Available at: <http://ec.europa.eu/programmes/horizon2020/en/h2020-section/secure-clean-and-efficient-energy>. [Cit: 21-okt-2015].
2. European Commission, Ed., Energy roadmap 2050. Luxembourg: Publications Office of the European Union, 2012.
3. European Commission, Ed., Energy infrastructure. Priorities for 2020 and beyond - A Blueprint for an integrated European energy network. Luxembourg: Publications Office of the European Union, 2011.
4. M. Amin, S. Amin, and M. Ali, “Monitoring of leakage current for composite insulators and electrical devices,” Review on Advanced Materials Science, vol. 21, no. 1, pp. 75–89, 2017.
5. IEC 60071-2: 1996, Insulation co-ordination – Part 2: Application guide. International standard.
6. IEC 507: 1991, Artificial pollution tests on high-voltage insulators to be used on a.c. systems. International standard.

#### *Monitorowanie zanieczyszczenia środowiska za pomocą cienkich elektrod metalowych przygotowanych przez fizyczne osadzanie z fazy gazowej*

*Artykuł dotyczy monitorowania zanieczyszczenia środowiska za pomocą cienkich elektrod metalowych na szklanych/ceramicznych podłożach przygotowanych przez fizyczne osadzanie z fazy gazowej. Widowym jest, że zanieczyszczenie środowiska odpadami izolacji elektrycznej jest jednym z problemów, przed którymi stoją firmy dystrybucyjne i system przesyłu energii elektrycznej. Z tego powodu istnieje potrzeba monitorowania zanieczyszczenia środowiska, ponieważ ma to duży wpływ niezawodność sieci wysokiego napięcia i jej awaryjność. Celem przedstawionych prac jest zaproponowanie nowego systemu monitorowania zanieczyszczenia środowiska w oparciu o zastosowanie bardzo cienkich elektrod metalowych. Omówiono także wpływ morfologii i składu chemicznego zanieczyszczeń na rezystancję powierzchniową i przewodnictwo wybranych izolatorów.*

**Słowa kluczowe:** zanieczyszczenie środowiska, elektrody metalowe, fizyczne osadzanie par, przewodnictwo elektryczne, izolatory



# The Need of Elastic Material Component between Rock Pressure Load and Metallic Structure Way of Receiving it in Order to Obtain a Uniform Load

Dănuț CHIRILĂ<sup>1)</sup>, Tamara Cristina DUMITRAȘCU<sup>1)</sup>, Aronel MATEI<sup>1)</sup>, Sorin MANGU<sup>1)</sup>

<sup>1)</sup> University of Petrosani, Romania

<http://doi.org/10.29227/IM-2020-01-31>

Submission date: 03-01-2020 | Review date: 09-03-2020

## Abstract

In galleries digged for different type of uses, but mostly for extracting coal, hydrotechnical adduction galleries but also for tunnels, after the dislocation of the rocks is done, the tensions in the rock changes massively. We take for example a metallic structure used as provisory structure until the rock pressure stabilize and used in Petroșani Romania, coal mines. The galleries are digged with explosives and the shockwave gives excessive cracks and disturb the rock pressure and its characteristics. The space between the metallic structure, rock walls and bolt is filled with wood, but this article suggests a rubber band material so the rock pressure to be distributed uniformly and not concentrated in the contact points between the wood and metal profile.

**Keywords:** galleries, dislocation, rocks, tension

## Introduction

In Romania the most common profiles used as temporary or definitive maintenance are TH and I profiles. The TH profile can be used in an elastic construction, but the I or doubled I profiles can only be used in rigid constructions. The elastic constructions have the advantage of interacting with the rock pressure. It allows the rock pressure to relax but not to change the geometrical profile. The characteristics of TH profiles and doubled I profiles are shown in table 1.

## Replacing the wood bars with rubber bands as filling materials between the rock walls, bolt and the metallic structure

The rubber band proposed to be used as filling material between metallic structure and the excavated profile can be made from recycled material in different shapes and mechanical characteristic as experimental material. We can also use broken rubber bands from the broken machines that need to be replaced or repaired. This space is usually filled with wood but this filling up material share out the tensions around the metallic structure concentrated in contact points and not uniform around the structure.

The metallic structure that is designed to receive the rock pressure is presented in figure 1.

## Comparative study between TH and I profiles considering the rock pressure and the rock proprieties

The distance between the profiles is given by their capacity of taking over the rock pressure of each profile. If we note with  $L$  the distance between the frameworks the calculation of it is given by the formula:

$$L = \frac{q}{P_M} [m]$$

where  $q$  is the capacity of taking over the rock pressure and  $P_M$  is the rock pressure.

For different values of the rock pressure the results are: for THN-21, in shale:

$$L_{THN21}^m = \frac{13,3}{18,4} = 0,73m$$

for double I-12 in shale:

$$L_{I12dublu}^m = \frac{9,73}{18,4} = 0,59m$$

for THN-21, in sandstone:

$$L_{THN21}^s = \frac{13,3}{11,6} = 1,14m$$

for double I-12, in sandstone:

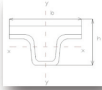
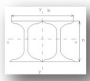
$$L_{I12dublu}^s = \frac{9,73}{11,6} = 0,83m$$

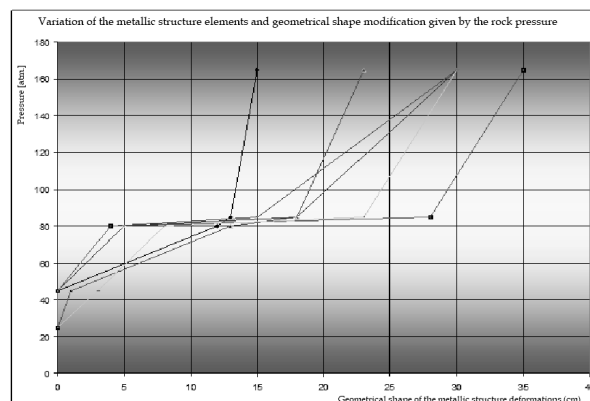
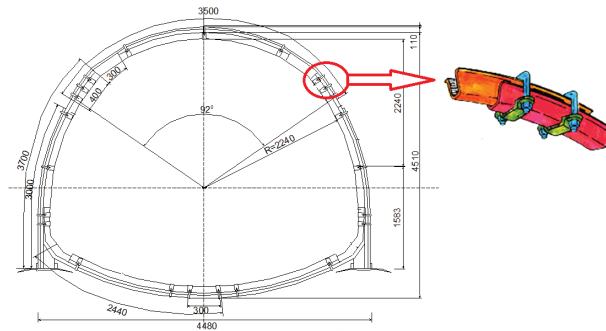
The results show that if the underground construction is made in rocks like shale, the distance between the frameworks is 0,73 meters and the I profiles needs 0,6 meters between the frameworks. For sandstone the TH profiles need one meter between the frameworks, and The I profiles need 0,8 meters. From this we can conclude that the TH profiles fits for rocks like shale but for rocks like sand stone the I profiles fits.

For evaluating the distance between the frameworks by considering the proprieties of the rocks and the dimension of the underground construction the formula is:

$$L = \frac{q \cdot f}{4 \cdot \gamma \cdot r^2 \cdot k_0} [m]$$

where  $f$  is the Protodiakonov clasification strenght coefficient,  $\gamma$  is the rock weight,  $r$  is the radius of the gallery and  $k_0$  is the rock uniformity coefficient. For values given to the formula the results are:

Name of the profile	Shape and dimension of the profile			Weight G kg/m	Transverse section F, cm <sup>2</sup>	Momentum				
	Shape	h, mm	b, mm			x-x W <sub>x</sub> cm <sup>3</sup>	y-y W <sub>y</sub> cm <sup>3</sup>	$\frac{W_x}{W_x}$ $\frac{cm^3}{cm^3}$	$\frac{W_x}{W_x}$ $\frac{1kg}{m}$	$\frac{W_y}{W_y}$ $\frac{1kg}{m}$
TH		85	98	12,9	16,4	32,0	30,6	0,96	2,5	2,4
		98	112	21,0	26,8	57,8	63,0	1,09	2,8	3,0
		119	149	29,0	37,0	99,6	107	1,11	3,4	3,7
		144	147	43,6	55,6	179,0	179	1,00	4,1	4,1
Double I		100	100	16,6	21,2	68,4	31,4	0,46	4,1	1,9



for shale:

$$L_{THN21}^m = \frac{13,3 \cdot 4}{4 \cdot 2,69 \cdot 2^2 \cdot 1,3} = 0,95m$$

for sandstone:

$$L_{THN21}^g = \frac{13,3 \cdot 6}{4 \cdot 2,73 \cdot 2^2 \cdot 1,3} = 1,4m$$

for shale:

$$L_{I12dublu}^m = \frac{9,73 \cdot 4}{4 \cdot 2,69 \cdot 2^2 \cdot 1,3} = 0,72m$$

for sandstone:

$$L_{I12dublu}^g = \frac{9,73 \cdot 6}{4 \cdot 2,73 \cdot 2^2 \cdot 1,3} = 1,08m$$

As the results shows, the TH profile as well as the I profile can be used, but the decision for choosing the right profile depends on financial reasons. A bigger distance between the

frameworks needs less frameworks so the price of the construction is smaller.

### Rock pressure limits for the metallic structure to receive by keeping the geometrical shape unmodified

The rock pressure values are variable and depends by the mechanical rock characteristics, the profile characteristics and geometrical shape of the gallery. The values obtained at University of Petroșani, Mine Faculty, Mining Constructions laboratory, are given in the graphic from figure 2.

### Conclusions

The dependence between the elastic behavior of the metallic structure and rock pressure was shown above. From the manifestation of the metallic structure it can be seen that an elastic material is needed to fill the place between the steel profile and rock wall so the pressure to be distributed uniform. In that case the graphic is expected to be more like a sine function.

#### Literatura – References

1. Chirilă D., Dura C., Herbei R., Morar M. - Comparative study of different types of metal profiles used in underground constructions in order to take over the rock pressure, 22nd Conference on Environment and Mineral Processing & Exhibition 2018, Technical University of Ostrava, Faculty of Mining and Geology, INSTITUTE OF ENVIRONMENTAL ENGINEERING, pag. 109-112, ISBN 978-80-248-4181-6;
2. F Faur, D MARCHIȘ, C Nistor - Evolution of the coal mining sector in Jiu Valley in terms of sustainable development and current socio-economic implications, Research Journal of Agricultural Science, 2017;
3. C Costa, D Pupazan, C Danciu, C Nistor - Implementing Modern Physical Training Methods for Mine Rescuers at Insemex Romania, SGEM2015 Conference Proceedings, ISBN 978-619-7105-33-9/ISSN 1314-2704;
4. N. Lețu, L. Radermacher – Metode de dimensionare a susținerilor metalice pentru lucrările miniere orizontale, Editura Institutul Național de Informare și Documentare, București 1, 85;
5. Cristian Radeanu, Larisa Chindris, Dan Paul Stefanescu, Ladislau Radermacher, Cristian Popa- MATHEMATICAL MODELS USED TO DETERMINE THE STRAIN OF EXPERIMENTAL WORKS JIU VALLEY MINING BASIN, International Multidisciplinary Scientific GeoConference: SGEM: Surveying Geology & mining Ecology Management, Surveying Geology & Mining Ecology Management (SGEM), 2017.

#### *Zastosowanie połączenia elastycznego pomiędzy wyrobiskiem a konstrukcją metalową w celu uzyskania jednolitego obciążenia*

*W wyrobiskach wybranych do różnego rodzaju zastosowań, głównie do wydobywania węgla, budowli hydrotechnicznych, tuneli, po zakończeniu wydobywania skał napięcie w skale zmienia się ogromnie. Jako przykład pokazano stabilizowanie się ciśnienia w wyrobiskach w kopalni węgla Petroșani w Rumunii. Eksploatacja jest prowadzona za pomocą materiałów wybuchowych, fala uderzeniowa powoduje nadmierne pęknięcia i zaburza ciśnienie w skałach. Przestrzeń między obudową a górotworem metalową jest wypełniona drewnem, ale w tym artykule przedstawiono zastosowanie gumy dla uzyskania równomiernego nacisku skały.*

**Słowa kluczowe:** wyrobiska, górotwór, przemieszczenia, naprężenie





# The Evaluation Potential as Micronized Calcite of White Marble Waste

Vedat DENİZ<sup>1)</sup>, Ercan POLAT<sup>2)</sup>

<sup>1)</sup> Department of Polymer Engineering, Hitit University, 19030, Corum, Turkey; email: vedatdeniz@hitit.edu.tr

<sup>2)</sup> Department of Mining Engineering, Mugla Sitki Kocman University, 48000, Mugla, Turkey; email: epolat@mugla.edu.tr

<http://doi.org/10.29227/IM-2020-01-32>

Submission date: 20-01-2020 | Review date: 28-03-2020

## Abstract

Natural calcium carbonates have a great importance in the world's economy due to their numerous applications areas such as calcium carbonate in the paper and paint industries. The final calcite products have rigorous quality specifications which are currently difficult to meet for local producers in Turkey. Therefore, large quantities of high white marble wastes have been transported long distances inside the country to supply the different industrial plants for using calcite. Marble wastes, located in Afyon and Kutahya regions, Turkey's mid-west, are used generally for concrete and highway purposes.

Evaluations of marble wastes are very important for the economic development of any country or region. This study aims at developing new perspective for evaluation of marble wastes as domestic calcite resources and serves as a guide for investment and decision making for the Turkey calcite industry.

This paper presents applied research work to determining the product quality for evaluation as micronized calcite of marble wastes and gives an overview of the market situation for the regional producers. The aim of the work is to characterize four different marble wastes and to determine the potential for production of the required quality for the Turkey calcite market;- to control the quality of the products by application tests, including the measurement some tests.

**Keywords:** calcite, marble wastes, micronized calcite, physical, chemical, physicochemical and mineralogical properties of micronized calcite

## Introduction

Limestone, which is composed mostly of calcite and aragonite minerals, i.e. different crystalline forms of calcium carbonate  $\text{CaCO}_3$ , abundant and widely distributed, comprises around 4% of the earth's crust [1]. Pure limestone ( $\text{CaCO}_3$ ) has 56.0% CaO and 44.0%  $\text{CO}_2$ . In practice, virtually all limestone contain impurities such as organic (bituminous) constituents, clay minerals, quartz, mica, iron-bearing minerals such as limonite or pyrite, feldspar, amphibole and pyroxene [2]. Limestone is also one of the cheapest commercially available inorganic materials [3], and therefore has innumerable industrial applications: it is used in paints, inks, coatings, paper products, plastics and films [4–5]. These carbonate minerals are precursors of marbles. Marble is a metamorphosed carbonate rock with re-crystallised minerals with size range from millimetre to several centimetres.

Storage of in certain areas or random disposal of marble wastes can cause both visual pollution and cause pollution of other natural resources as come together with other elements. This economic potential, which is accumulated hundreds of thousands or even millions of tons of waste in marble quarries and factories, is also important in terms of its contribution to the country's economy by making efforts to enable it to be an industrial product material. Nowadays, studies have been carried out by many researchers in recent years about the recycling of marble wastes. These can be considered as asphalt, concrete, aggregate and joint in the construction sector, in the agricultural sector as a soil conditioner and as animal feed. However, in these sectors, calcite can be recycled as low value added. On the other hand, white marble wastes can be recycled as micronized by having much more

added value. White marbles are called calcium carbonate or calcite [6].

Calcite, in other words calcium carbonate ( $\text{CaCO}_3$ ), glass shimmering, transparent, easily breakable, has Mosh hardness 3 and a specific gravity in range of 2.6–2.8, is a large crystal marble. It is micronized by grinding then classification processes is applied, and offered to the use as natural ground or ground and coated calcite according to sectors, usually as fillers, for the ceramic, glass, paint, paper and plastic sectors. In addition, micronized calcite is also used in certain rates for toothpaste, adhesive, chewing gum, sponge, rubber, carpet base and oil-cloth base. The use of calcite as a filler in papermaking permits the production of a brighter paper with a greater resistance to yellowing and ageing. In addition, when it is used as a part of the coating of the paper, it provides better opacity, printability, ink receptivity and smoothness, while its use as filler for plastics improves heat resistance and hardness [4].

There are basically three characteristics that define the quality of ground natural calcium carbonate (calcite) during use. These are the particle size, the chemical purity and the color parameters of calcite (whiteness, brightness and yellowness) in terms of optical property. Additionally, depending on the place of use; there are also sought features such as surface area, size distribution, electrochemical properties, oil absorption properties, dispersibility in solution etc. In the production of micronized calcite, the properties of marble wastes must be carefully examines to ensure that they meet the market conditions.

In this study, the potential of micronized calcite production of four different white marble wastes were investigated. For this purpose, initially, marble waste samples were

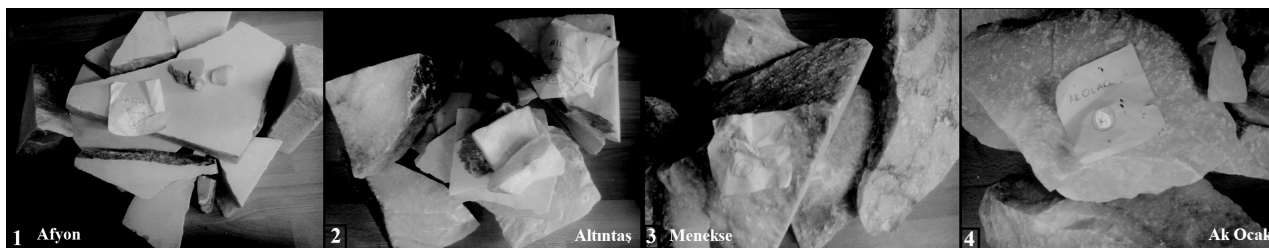


Fig. 1. General view of marble wastes used in experiments (Afyon [1], Altıntas [2], Menekse [3] and Ak Ocak [4])  
 Rys. 1. Widok ogólny odpadów marmurowych używanych w eksperymentach (Afyon [1], Altıntas [2], Menekse [3] i Ak Ocak [4])

Tab. 1. The results of chemical analysis by XRF of the marble wastes [\*LOI: Loss on ignition]

Tab. 1. Wyniki analizy chemicznej XRF odpadów marmurowych [\* LOI: Strata prażenia]

No	Sample Name	%								
		LOI*	CaO	MgO	SiO <sub>2</sub>	Fe <sub>2</sub> O <sub>3</sub>	Al <sub>2</sub> O <sub>3</sub>	SO <sub>3</sub>	K <sub>2</sub> O	Na <sub>2</sub> O
1	Afyon	44.01	51.30	2.75	1.34	0.21	0.15	0.19	0.06	0.00
2	Altıntas	43.21	54.90	0.26	1.19	0.13	0.14	0.13	0.04	0.00
3	Menekse	41.72	50.34	0.92	1.81	0.22	4.65	0.15	0.09	0.10
4	Ak Ocak	43.39	55.77	0.24	0.42	0.03	0.01	0.09	0.01	0.03

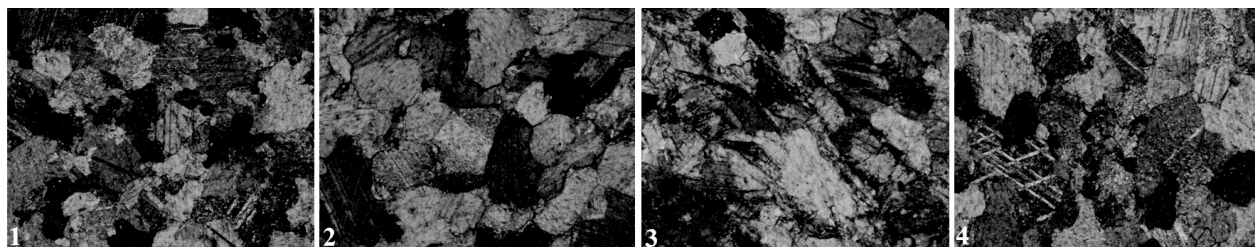


Fig. 3. Microstructure of fine crystalline marble used in experiment  
 Rys. 3. Mikrostruktura drobnego krystalicznego marmuru zastosowanego w eksperymencie

collected wastes from four different white marble quarries in Turkey. Then, the mineralogical, physical, chemical and physicochemical properties of the white marble wastes were investigated. According to the test results on the samples, micronized calcite obtained from four different marble wastes has been discussed whether it can be recycled according to the conditions demanded by the sector.

In this study, a comprehensive study was carried out on four different marble waste samples. These studies are listed as follows:

1. Chemical analysis (XRF),
2. Determination of rock structure (XRD),
3. Determination of mineralogical analysis (Polarized microscope),
4. Thermal Gravimetric Analysis (TGA),
5. Differential Thermal Analysis (DTA),
6. Morphological change status determinations of raw and ground samples (SEM),
7. Determination of rheological properties of samples in suspension (Viscometer),
8. Surface charge measurements of samples in suspension (Zeta meter),
9. Measurement of contact angle of samples (Contact angle meters),
10. The Bond grindability and work index determination ( $G_{bg}$  and  $W_i$ ),
11. Laboratory diameter grinding and size analysis to determine the studies,

12. Determination of optical properties of ground samples by grinding (RY, R457 and YI).

## Material and methods

### Material

The marble samples are located at mid-west Turkey. Many marble quarries are operated in this area and they produce in huge quantity of wastes. The marble wastes used in the experiments were taken from four different marble quarries in Afyon and Kutahya region (Turkey) by the whiteness, and the samples were called as Afyon (1), Altıntas (2), Menekse (3) and Ak Ocak (4). The samples consist of marble waste fragments from 50 to 400 mm. The best quality fragments were hand-picked from the marble wastes. Figure 1 shows the names and codes of the samples with the general image.

### Method

The mineralogical analyses of the marble samples were performed with a Zeiss polarized photomicroscope. Particle size distribution was conducted by Malvern laser particle size analysis equipment. The chemical analyses of the marble samples were made by XRF. The mineral composition of the marble sample was obtained by XRD. In respect to electrokinetic potential measurement of the marble samples, the surface charge (z.p.c.) was performed by Malvern zeta meter and surface tension was performed by contact angle meter. The determining of rheological properties in suspension of the marble samples was made by a Brookfield viscometer.

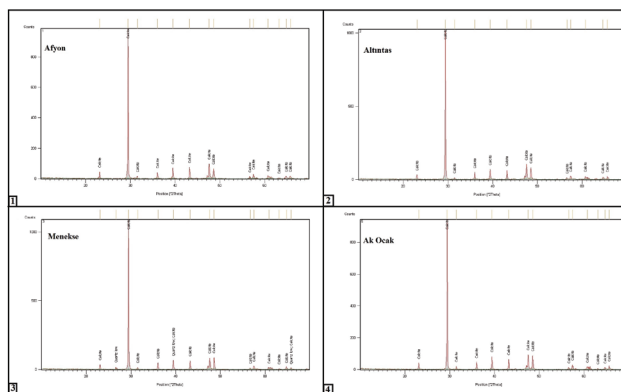


Fig. 2. The results of XRD pattern for four different marble wastes  
Rys. 2. Wyniki XRD dla czterech różnych odpadów marmurowych

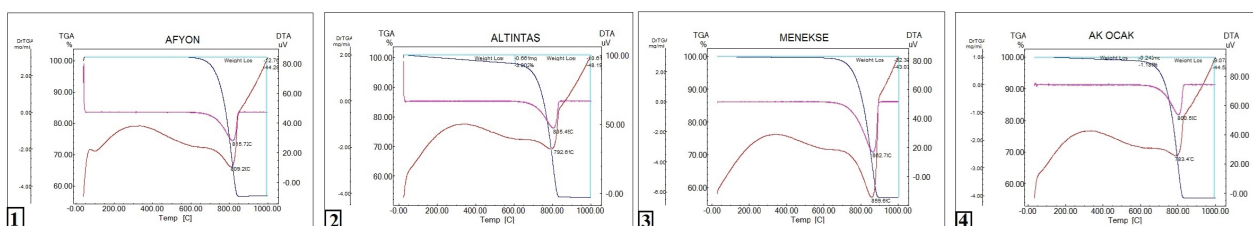


Fig. 4. TGA and DTA spectra of the marble wastes used in experiments  
Rys. 4. Widma TGA i DTA odpadów marmurowych użytych w doświadczeniach

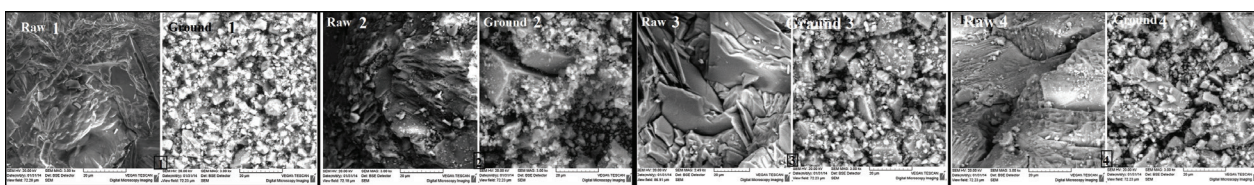


Fig. 5. SEM images of raw and ground marble wastes used in experiments  
Rys. 5. Obrazy SEM surowych i zmielonych odpadów marmurowych stosowanych w doświadczeniach

The changes in the weight loss of the marble samples were determined by differential thermal analysis (DTA) and thermogravimetric analysis (TGA). The resistance to grinding of the samples was obtained according to the Bond grindability. Optical properties (brightness, whiteness and yellowish) of the marble samples were determined by Datacolor Elrepho photoelectric spectrophotometer. SEM analyses have been made in terms of surface morphology characteristics of the raw and ground samples.

## Results and Discussion

### Chemical Analysis (XRF)

Each of the samples was analyzed by XRF device and the results are given in Table 1. As can be seen from the results, it is seen that all samples have high quality because of their high CaO content. In addition, low SiO<sub>2</sub> ratios are also important. From these data, it appears that 4 samples are suitable for the use of calcite. Specifically, sample no 2 and 4 were found to be more preferable because they had the highest CaCO<sub>3</sub> content.

### Rock Crystal Analysis Studies (XRD)

To understand the rock structure, rock analysis was performed by XRD. The results of XRD for each sample that

emerged in these studies are given in Figure 2. In the XRD studies, 4 samples were found to be calcite mineral. In Figure 2, a very small amount of quartz mineral was also detected in the Menekse (3) sample, but it has a little more quartz mineral than other samples. According to the results of chemical analysis (XRF), the fact that the highest SiO<sub>2</sub> value in the Menekse (3) sample is also support on the XRD results. From this point of view, each sample can be evaluated as calcite.

### Mineralogical Analysis Studies

For a better understanding of the properties of the samples, a detailed thin section microscopic study was carried out to determine the crystal structures, the mineralogical composition and particle sizes under the polarized microscope and to reveal the advantages or disadvantages in the grinding process. In investigation by microscope indicates that all sample types consist of more than 95% carbonate mineral.

The carbonate minerals identified in the marble waste samples are calcite. The most common silicate mineral in the samples is also quartz. It is necessary to limit the content of non-carbonate impurities in high-value carbonate products because of their adverse effect on the industrial processes where the carbonate product is used, mainly due to high abra-



Tab. 2. Viscosity values (cP) for different speed of the suspensions of marble wastes used in the experiments  
 Tab. 2. Wartości lepkości (cP) dla różnych prędkości zawiesin odpadów marmurowych użytych w doświadczeniach

Spindle Speed (rpm)	Calcite sample sold in the market cP	Afyon 1 cP	Altintas 2 cP	Menekse 3 cP	Ak Ocak 4 cP
10	680.0	621.18	952.96	971.39	974.39
20	312.5	289.41	464.51	510.81	511.38
50	102.0	86.66	164.07	201.57	204.62
100	46.0	18.46	60.85	86.66	112.46

Tab. 3. Surface tension results calculated from contact angle measurements at different pH of the marble wastes used in experiments  
 Tab. 3. Wyniki oznaczenia napięcia powierzchniowego obliczone na podstawie pomiarów kąta zwilżania przy różnym pH odpadów marmurowych użytych w doświadczeniach

Sample No	Surface tension (dyne/cm)			
	pH			
	4.16	7.12	9.30	11.29
Afyon (1)	38.51	45.51	38.83	39.98
Altintas (2)	43.75	47.75	43.25	47.63
Menekse (3)	53.13	52.75	56.13	54.13
Ak Ocak (4)	45.02	55.25	58.99	58.38

Tab. 4. The Bond grindability ( $G_{bg}$ ) and Bond work index ( $W_i$ ) values of marble wastes used in experiments  
 Tab. 4. Wartości podatności na mielenie Bonda ( $G_{bg}$ ) i wskaźnika pracy Bonda ( $W_i$ ) odpadów marmurowych użytych w doświadczeniach

Sample	$G_{bg}$ (g/rev)	$W_i$ (kWh/t)
1 (Afyon)	2.880	8.309
2 (Altintas)	3.748	6.870
3 (Menekse)	2.870	8.575
4 (Ak Ocak)	3.340	7.209

sion in machines. According to polarizing microscopy investigations on the marble wastes, it has been determined that each sample will not cause problems in grinding process due to excessive wear or not increase energy costs.

The typical carbonate and silicate minerals microstructures observed in thin sections are shown in Figure 3. Each marble wastes are finely crystallized, with particle sizes of less than 2 mm and mean particle sizes of 0.5 mm.

As samples 1 and 3 are examined, calcite crystals are generally locked with intricate boundaries. Intricate crystal boundaries can provide stronger clamping of crystals. The intricate crystal boundaries can be more difficult to micronize during grinding. However, as samples 2 and 4 are examined, the calcite crystal size is less than 1 mm, but the cleavage surfaces in the calcite crystals are well developed. The cleavage surfaces of growing calcite crystals by re-crystallisation processes become apparent. It can be thought that this feature will contribute positively to the process of grinding the calcite crystals. The polygonal crystal boundaries can be more easily micronized during grinding.

On the other hand, when sample 3 (Menekse) is examined; the impurities such as iron (hematite), silica (quartz), graphite and mica (muscovite) were detected. Addition, sample 4 (Ak Ocak) has the impurities such as iron and graphite. These very little impurities do not complicate the grinding process, but have a negative effect on the optical properties. This situation seems to may be a problem in terms of micronized calcite minerals for similar filler use like chemistry, paint and food.

#### Heat Weight Loss Study (TGA and DTA)

Tests were performed with TGA and DTA devices in order to determine the mass loss behaviors of the marble sam-

ples against temperature change. The results of DTA and TGA studies are presented in Figure 4.

As a result of these studies, it was found that there was a slight weight loss of mass due to very little organic matter in the samples 2 and 4. This is also determined by the presence of trace amounts of graphite in the mineralogical analyzes in the sample 4. This situation may cause negativity in the ceramic and glass industry demanding high temperatures. On the other hand, there will be no significant impact on the other usage areas.

#### Surface Morphology Studies (SEM)

SEM analyses were performed in terms of raw rock and the situation that might occur as a result of grinding in terms of surface morphology characteristics. The results of the SEM study are given in Figure 5.

Figure 5 analysed shows that the calcite crystal structure in rock form is similar for 4 samples, but some changes are observed as a result of grinding. As a result of the analysis, it was found that the sample 1 came to a more homogeneous thinness and brittle. It has been found that the sample 4 is ground as crusted and leafy crumb. The fact that the sample 3 is more heterogeneous compared to the other samples seems to be negative in terms of usage areas. The sample 2 was found to be more spherical of grinding. This makes micronized calcite more advantageous in terms of its (sample 2) use than the others.

#### Determination of Rheological Properties (Viscometer)

The viscosity values of the ground marble wastes in the suspension are important. Brookfield Rheometer was used

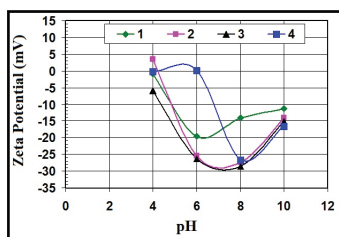


Fig. 6. Zeta potential-pH profile of the marble wastes used in the experiments  
Rys. 6. Potencjał Zeta vs pH odpadów marmurowych użytych w doświadczeniach

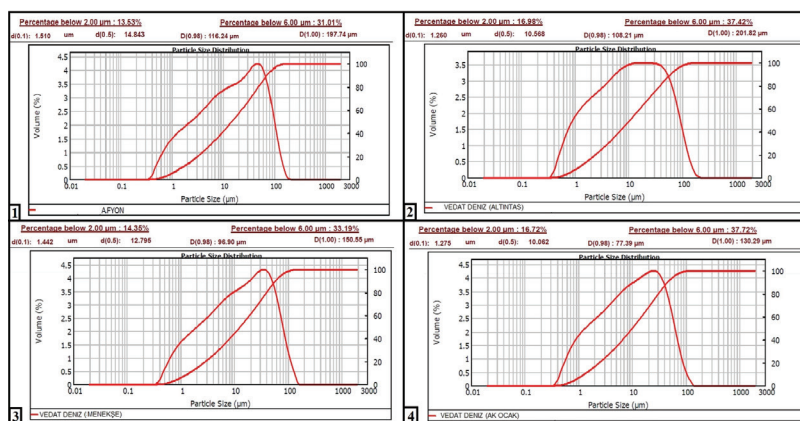


Fig. 7. Analysis of particle size distribution of the marble wastes used in experiments  
Rys. 7. Analiza rozkładu wielkości cząstek odpadów marmurowych użytych w doświadczeniach

for the rheological measurements. The viscosity measurement cell has equipment providing the water circulation. In this setup, dispersions remained at a constant temperature during the measurements ( $22 \pm 1^\circ\text{C}$ ). The viscosity measurements were carried out at using spindle # 1. The ground marble wastes were slurried to approximately 60% solids. The average size ( $d_{50}$ ) of the samples is about 10 microns. In this respect, the viscosity values (cP) of the samples were determined and the results are given in Table 2. Measurements were made 5 times each sample and the arithmetic mean was taken.

In terms of results, the viscosity values (cP) of a calcite sample sold in the market have almost same viscosity values of the sample 1 at different velocities of the viscometer. However, the viscosity values (cP) of the samples 2, 3 and 4 have slightly larger than calcite sample sold in the market, but do not have any effect on the dispersion in the suspension.

#### Contact Angle Measurement Studies

The contact angles are generally determined by techniques such as “sessile drop” or “captive bubble technique” in which a water drop or a bubble contact on a mineral surface is measured from the air or liquid phase.

In order to investigate the behavior of the marble samples at different pH levels in aqueous suspensions, surface tension was calculated by measuring the contact angles and the results are given in Table 3. As the data in Table 3, the hydrophobicity of the calcite sample increases due to the surface charge in the weak acidic suspension. The hydrophobic properties, especially at neutral pH, appear to increase in almost all samples, in this respect may cause problems in suspension.

In terms of contact angle, the sample 1 has the best hydrophilic property and it has an important advantage in the use of aqueous suspensions. The sample 1 will be dispersed more rapidly in the suspension and homogeneously suspended. In sample 2, it can be readily dispersed in the suspension, as in sample 1.

#### Surface Charge Measurement Studies (Zeta meter)

The indirect characterization of micronized marble suspensions by measuring zeta potential is feasible because the relationship between zeta potential and apparent viscosity is valid for a lot of solid/liquid system. The zeta potentials of micronized marbles were determined by Zetasizer Nano Z (Malvern Instruments) which uses micro- electrophoresis light scattering technology.

For each sample, 5 measurement results for different pH values were obtained as arithmetic mean.

The surface charge graph depending on pH values for each sample is given in Figure 6.

In the results of experiments, all samples have high surface charge at natural pH and all samples have hydrophilic. Thus, the facts that the samples can be wetted and dispersed easily with water when suspended are advantageous for all examples.

Zeta-potential measurements of calcite were made in a narrow pH range,  $\text{pH} = 6-10$ , because of the dissolution of calcite in acidic media. The potentials for calcite mineral are  $\text{Ca}^{2+}$ ,  $\text{CO}_2$ ,  $\text{OH}^-$ ,  $\text{H}^+$  and  $\text{HCO}_2^-$ . Therefore, the zeta potential of the calcite at a certain pH is zero. As shown in Figure 6, for marble waste samples, the point (z.p.c.) where the charge was zero for samples 1 and 3 could be determined, whereas

Tab. 5. Viscosity values (cP) for different speed of the suspensions of marble wastes used in the experiments  
Tab. 5. Wartości lepkości (cP) dla różnej prędkości zawiesin odpadów marmurowych użytych w eksperymencie

Sample	RY Whiteness	R457 Brightness	YI Yellowness
Afyon (1)	91.03	88.39	3.87
Altintas (2)	90.47	87.45	4.46
Menekse (3)	84.85	80.97	6.22
Ak Ocak (4)	88.53	85.39	4.67

the zero point charges (z.p.c.) for samples 2 and 4 were not determined.

### The Tests of the Bond Grindability and the Bond Work Index ( $G_{bg}$ and $W_i$ )

In the design of grinding circuits, the Bond grindability method is widely used for a particular material in dimensioning mills, power needs and the evaluation of performance. Its use as an industrial standard is very common provides satisfactory result in the all industrial applications. Despite having many advantages, this method has some drawbacks such as being tiring and requiring long test time also it needs a special mill [7].

The standard Bond grindability test is a closed-cycle dry grinding and screening process, which is carried out until steady state condition is obtained. This test was described as follow [8–12].

The material is packed to 700 cc volume using a vibrat-ing table. This is the volumetric weight of the material to be used for grinding tests. For the first grinding cycle, the mill is started with an arbitrarily chosen number of mill revolutions. At the end of each grinding cycle, the entire product is discharged from the mill and is screened on a test sieve ( $P_i$ ). Standard choice for  $P_i$  is 106 microns. The oversize fraction is returned to the mill for the second run together with fresh feed to make up the original weight corresponding to 700 cc. The weight of product per unit of mill revolution, called the ore grindability of the cycle, is then calculated and used to estimate the number of revolutions required for the second run to be equivalent to a circulating load of 250%. The process is continued until a constant value of the grindability is achieved, which is the equilibrium condition. This equilibrium condition may be reached in 6 to 12 grinding cycles. After reaching equilibrium, the grindabilities for the last three cycles are averaged. The average value is taken as the standard Bond grindability ( $G_{bg}$ ).

The products of the total final three cycles are combined to form the equilibrium rest product. Sieve analysis is carried out on the material and the results are plotted, to find the 80% passing size of the product ( $P_i$ ). The Bond work index values ( $W_i$ ) are calculated from equation below.

$$W_i = 1.1 * \frac{44.5}{P_i^{0.23} * G_{bg}^{0.82} * \left[ \left( \frac{10}{\sqrt{P_{80}}} \right) - \left( \frac{10}{\sqrt{F_{80}}} \right) \right]} \quad (1)$$

$W_i$ : work index, (kwh/t)

$P_i$ : screen size at which the test is performed (106  $\mu$ m)

$G_{bg}$ : Bond's standard ball mill grindability, net weight of ball mill product passing sieve size  $P_i$  produced per mill revolution, (g/rev)

$P_{80}$ : sieve opening which 80% of the product passes, ( $\mu$ m)

$F_{80}$ : sieve opening which 80% of the feed passes, ( $\mu$ m)

$G_{bg}$  and  $W_i$  values for each marble wastes are given in Table 4.

When Table 4 is examined, it is found that the easiest grindability is the sample 2 and the most difficult grindability is the sample 3. These results have also been demonstrated in mineralogical analysis.

### Micronized Grinding Tests in a Laboratory Scale Ball Mill

Micronized grinding tests of the marble wastes in a laboratory scale ball mill (0.20x0.20 m) at the same grinding conditions were performed. According to the results of the economic milling analysis, the obtained part size distribution graphs were determined by Malvern dimension analyzer and the results were given in Figure 7.

Figure 7 shows the differences in the particle size distribution of the samples milled under the same conditions. Samples 2 and 4 are the most advantageous in terms of energy cost in the grinding process because they are the largest in terms of quantities below 2 microns (16.98% and 16.72%, respectively). The sample 1 is the most disadvantageous in the grinding process because it is at least with 13.53% in terms of material content below 2 microns. The average particle size ( $d_{50}$ ) of the ground samples was found to be about 10 microns in the samples 2 and 4. Therefore, it is apparent that the samples 2 and 4 will be easier to grind compared to the other the samples 1 and 3.

### Determination of Optical Properties of Ground Samples by Grinding (RY, R457 and YI)

Calcite is capable of producing high quality concentrates with 98%  $\text{CaCO}_3$  grade or more, which conforms to most stringent market specifications for the chemical and oil industries. However, such highly pure calcite might not satisfy the product specifications especially for filler industries concerning the brightness, whiteness and yellowness indexes. Market price of calcite powder depends on its purity: market price of purest calcite powder may be as high as there to five times that paid for toothpaste, chewing gum, paint and paper sectors. Calcite powder for paint production can be separated by three elements according to the optical properties. These are whiteness (RY), brightness (R457) and yellowness indices (YI). On the market, for micronized calcite with  $d_{50}$  of 2 microns, RY and R457 values should be above 90 and 85, respectively, and YI values are desired to be below 4.

The optical properties of ground marble samples were determined by Elrepho Spectrophotometer. Colour analysis studies were carried out on average particle size  $d_{50}$ : 10–15 microns. Each test was repeated three times and the values given in Table 5 are the average of three measurements.

When  $d_{50} = 2$  microns, R457 and RY values will increase by 3–4 points and YI values will decrease by 2–3 points. From this point of view, it is seen that the samples 1 and 2 will easily

overcome the optical properties demanded by the market. It is determined that the sample 4 is within the acceptance limits of market and the sample 3 is difficult to carry the standards in terms of optical properties. However, when the white parts of the sample 3 were separated with the optic sorting devices, it was concluded that the desired values would be obtained.

### **Conclusions**

In terms of the general evaluation of many analysis performed on four different marble wastes; it is concluded that Afyon (1) and Altintas (2) samples can be used in many sec-

tors in terms of calcite. It was determined that it was not possible to evaluate the Menekse (3) sample as calcite. On the other hand, it can be seen that Ak Ocak (4) sample can be used in some applications by further studies.

Great colour heterogeneity (grey to white variations) was observed in the Menekse (3) sample so the optical sorting was must made as a separation process to obtain high whiteness grades.

As a result of this study, it has been revealed that the properties required by the market should be investigated first in order to evaluate any marble waste as calcite.

## Literatura – References

1. Liu, Q., Wang, Q., Xiang, L. 2008. Influence of poly acrylic acid on the dispersion of calcite nano-particles, Applied Surface Science, 254(21): 7104-7108.
2. Varela, J.J., Petter, C.O., Wotruba, H. 2006. Product quality improvement of Brazilian impure marble, Minerals Engineering, 19(4): 355-363.
3. Kumari, V., Dev, A., Gupta, A.P. 2014. Studies of poly(lactic acid) based calcium carbonate nanocomposites, Composites, Part B., 56: 184-188.
4. Garcia, F., Le Bolay, N., Frances, C. 2002. Changes of surface and volume properties of calcite during a batch wet grinding process, Chemical Engineering Journal, 85(2-3): 177-187.
5. Tsuzuki, T., Pethick, K., McCormick P.G. 2000. Synthesis of CaCO<sub>3</sub> nanoparticles by mechanochemical processing, Journal of Nanoparticle Research, 2(4): 375-380.
6. Deniz, V. 2018. Potential Evaluation of Marble Wastes as Micronized Calcite, Environmental Approaches in Marble Mining, (Eds: Guler ve Polat), ISBN:978-605-1839-14-8, Mugla Metropolitan Municipality Culture Publications: 6, 153-203, Mugla, Turkey (In Turkish).
7. Deniz, V., Ozdag, H. 2003. A new approach to Bond grindability and work index: dynamic elastic parameters, Minerals Engineering, 16: 211-217.
8. Bond, F.C., Maxson, W.L. 1943. Standard grindability tests and calculations, Transaction of Society Mining Engineering, AIME, 153: 362-372.
9. Austin, L.G., Brame, K. 1983. A comparison of the Bond method for sizing wet tumbling ball mills with a size-mass balance simulation model, Powder Technology, 34: 261-274.
10. Magdalinovic, N. 1989. A procedure for rapid determination of the Bond work index, International Journal of Mineral Processing, 27: 125-132.
11. Deniz, V. 2004. Relationships between Bond's grindability (G<sub>bg</sub>) and breakage parameters of grinding kinetic on limestone, Powder Technology, 109: 208-213.
12. Deniz, V., Akkurt, Y., Umucu, Y. 2005. A new model on breakage behaviour of a laboratory impact mill, Proceedings of the 19th International Mining Congress, 229-232, Izmir/Turkey.

## *Ocena potencjału pozyskania zmikronizowanego kalcytu z odpadów z białego marmuru*

*Naturalne węglany wapnia mają ogromne znaczenie w światowej gospodarce ze względu na ich liczne zastosowania, takie jak węgiel wapnia w przemyśle papierniczym i malarskim. Produkty handlowe kalcytu muszą spełniać rygorystyczne wymagania jakościowe, które obecnie są trudne do osiągnięcia przez lokalnych producentów w Turcji. Dlatego duże ilości odpadów z przeróbki białego marmuru zostały przetransportowane do zakładów przemysłowych które wykorzystują kalcyt. Odpady marmurowe, znajdujące się w regionach Afyon i Kutahya, w środkowo-zachodniej Turcji, są ogólnie wykorzystywane do betonu i budowy autostrad. Możliwość wykorzystania odpadów marmurowych jest bardzo ważna dla rozwoju gospodarczego każdego kraju lub regionu. W artykule przedstawiono nową metodę oceny odpadów marmurowych jako krajowych zasobów kalcytu. Metoda służy jako przewodnik dla inwestorów i do podejmowania decyzji w branży kalcytu w Turcji. W artykule przedstawiono prace badawcze prowadzone w celu określenia jakości produktu - zmikronizowanego kalcytu z odpadów marmurowych oraz przegląd sytuacji rynkowej producentów regionalnych. Celem artykułu jest scharakteryzowanie czterech różnych odpadów marmurowych i określenie potencjału produkcji kalcytu o wymaganej jakości w Turcji. Zaproponowano kontrolę jakości produktów poprzez testy aplikacyjne, w tym pomiary niektórych parametrów.*

**Słowa kluczowe:** kalcyt, odpady marmuru, kalcyt mikronizowany, właściwości fizyczne, chemiczne, fizykochemiczne i mineralogiczne mikronizowanego kalcytu



# Use of Solar Energy in Power Equipment

Ioan Lucian DIODIU<sup>1)</sup>, Daniel Alexandru DRAGOMIR<sup>1)</sup>, Aronel MATEI<sup>2)</sup>,  
Roxana Claudia HERBEI<sup>2)</sup>

<sup>1)</sup> SC ENERGOCONSULT SRL

<sup>2)</sup> University of Petrosani, "Dorin Pavel" Technical College, Alba Iulia, Romania

<http://doi.org/10.29227/IM-2020-01-33>

Submission date: 10-01-2020 | Review date: 15-03-2020

## Abstract

*A clean environment is essential for people's health and quality of life. Developing sectors that help to meet the needs and comfort, have a negative impact on the quality of the environment we live in.*

*The use of natural resources without care to meet the needs of humans leads to the destruction of the environment. Climate change, erosion, increasing the amount of carbon dioxide in the air we breathe, are the result of meeting other needs such as food, heat, transport, comfort in our own home, etc.*

**Keywords:** level CO<sub>2</sub>, solar energy, photovoltaic panels, distribution network

A clean environment is essential for people's health and quality of life. Developing sectors that help to meet the needs and comfort, have a negative impact on the quality of the environment we live in.

The use of natural resources without care to meet the needs of humans leads to the destruction of the environment. Climate change, erosion, increasing the amount of carbon dioxide in the air we breathe, are the result of meeting other needs such as food, heat, transport, comfort in our own home, etc.

Three major polluting directions can be identified, namely:

- power generation,
- transport and
- food.

Unfortunately, the electricity industry is the most polluting. The production and consumption of electricity has negative effects on the environment.

The old power energy production generates a large environmental pollution. In 2010 kWh of electricity for obtaining a (mix of wind, and hydro, coal, nuclear and gas) to generate 0.406 kg of CO<sub>2</sub> (Fig. 2. Connection point with internal services fed from a photovoltaic panel contains all other greenhouse gases – the remainder of the gases being converted to CO<sub>2</sub> equivalent for easier calculation). With the development of wind farms, the CO<sub>2</sub> level for producing a kWh decreased.

Thus, for the summer of 2018 the CO<sub>2</sub> level generated by the production of a kWh is 0.282 kg CO<sub>2</sub>/kWh, and for winter it is estimated to be 0.329 kg CO<sub>2</sub>/kWh.

The energy produced by solar panels is an energy we can enjoy without polluting the environment. They work on light and not on heat. Panels can also work in winter. Regarding the number of photovoltaic parks in Romania, there is no institution to centralize the information about these, but from the sources we can say that in the last 4–5 years there were built about 960 photovoltaic parks.

The tendencies of adapting photovoltaic panels, along with the development of new ones technologies for power

generation, brought major changes to distribution of electrical characteristics i.e. The energy produced by photovoltaic panels is a small part of the network injected in it, but their numbers increase and growth will have an effect on network distribution and use of electricity, and if their share will increase significantly and you will influence and transport networks.

The prospect of implementing widespread in electrical distribution networks as well as the users of distributed power sources based on photovoltaic panels, causes transformation network passive, networks active in the transfer of energy is two-way and level and which raise new safety issues to in service and quality and efficiency of energy.

Generating electricity using low-power distributed power sources enabling the delivery of electricity near users, and so a supplement for energy produced centrally benefits by reducing electricity losses during transportation and costs arising from the modernization of distribution networks.

As regards to you on users, low cost, high reliability, good quality of electrical energy and a certain autonomy reserves of energy are topics that interest when adopting the solution take the production of energy by the distributed energy sources, but this is possible only with additional investment.

By using distributed generation in the field of renewable energy technologies, such as are the solar ones ensure a beneficial effect on the environment.

The base unit of the photovoltaic plant is the photovoltaic cell. Typically, a photovoltaic cell has an electric power between 1 and 2 W.

To increase power, photovoltaic cells are electrically connected to return united to form larger, called modules (panels). Basically, a photovoltaic module consists of photovoltaic cells connected in series.

The modules (panels), in turn, may be connected in series and/or parallel to form united and higher, called strings (and rows).

Photovoltaic panel strings connected in series and/or parallel is an area of photovoltaic whose Definitions i.e. was adopted in ANSI/IEEE Std.928-1986.

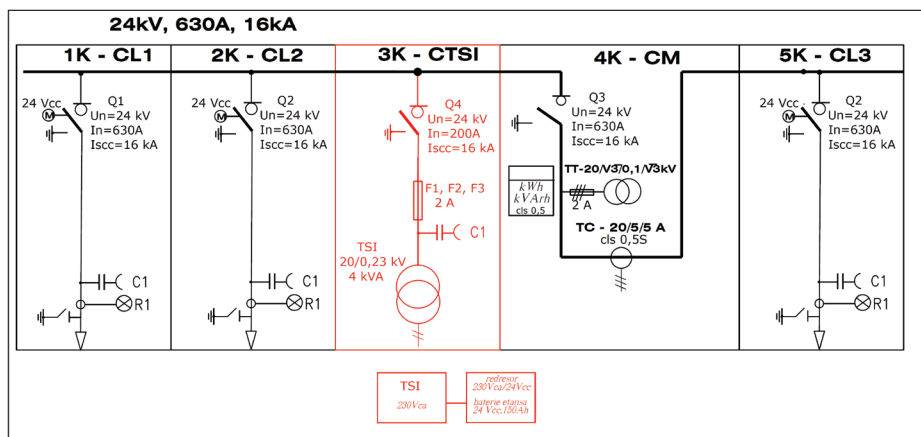


Fig. 1. The general scheme of a connection point  
Rys. 1. Ogólny schemat punktu przyłączenia

Photovoltaic technology has become a major player in the global electricity production and is now one of the most advanced technologies, the scale of essential residence applied up to the applied to industrial use.

Depending on the electronic power converter component, photovoltaic power plants may be:

- Simple photovoltaic power stage, which has a single converter of conversion DC-AC
- Many photovoltaic power stage, which has more converse converter and DC-DC-AC

Photovoltaic plant consists of:

- photovoltaic generator;
- electronic power converter;
- interface with electrical network supply distribution.

In literature, various converters and topologies condition of the environment was studied and determined. Operation of the points corresponding to maximum power at different levels of solar radiation and the temperature.

The relationship of current and voltage of the PV generator to vary during the day depending laid environmental condition. To find the maximum power points that the photovoltaic panel can generate, it is important to match the characteristic  $I = f(U)$  as close to the real values as it is very important to choose the characteristic  $I = f(U)$  of the photovoltaic panel in accordance with the characteristic  $I = f(U)$  a electric charge.

A general approach to reaction control t take power is to measure and maximize power across the load was applied and considers that maximum power of photovoltaic panel is equal to the maximum power load. This method, called s and direct connection method is applicable if direct connection of the load to the panel s and thus maximizes actually applied load and power and not the maximum power that the photovoltaic panel is charging.

Because power generated by the PV panel depends on the level of radiation and temperature it problem DEPA major need is to extract the maximum power available to change the condition DISCLOSURES environment in which it operates.

This effect is called and implemented a maximum power point tracker (MPPT) is a follow-up device and extracting the maximum power of the photovoltaic panel. This device is a

cc-cc converter inserted between the panel s and its electric charge. This converter is controlled by the types of algorithms, trying to find the most efficient solutions for extracting maximum power.

An application of these photovoltaic panels to support CO<sub>2</sub> reduction is to give up the internal service cell present at all connection points and replace it with a photovoltaic panel that generates energy for charging the battery of batteries needed for internal services as well as lighting the connection point tire.

A connection point has a general scheme shown in Figure 1.

Figure 1 shows that the internal services of the connection point are provided by a 3K-CTSI medium-voltage cell, connected to the medium voltage bars.

This cell has its component in medium voltage load separator, medium voltage fuses and an internal 20/0.23 kV internal power transformer of 4 kVA.

The internal service cell is mainly used to provide the 24 volt DC operating voltage required to power the drive motors of the load separators, command, protection and signaling voltage.

This voltage is permanently provided by a battery of 24V 150 Ah. Charging the battery is done by means of a buffer rectifier that ensures the current is up to 15A.

Considering that energy is consumed by charging storage battery is 500 W h/day, we can extrapolate a month at electricity consumed by 1,5 kWh per month.

Considering that there may be a large number of such cells on the territory of a city that provide operative voltage to power points or transformer stations, replacing them with renewable sources could reduce CO<sub>2</sub> levels.

For 100 transformer stations the electricity consumed would be 150 kWh/month.

The CO<sub>2</sub> emission for a mixed electricity product, equivalent to 150 kWh, calculated with a CO<sub>2</sub>=0,6170 factor, will be 0,9255 kg CO<sub>2</sub>.

Replacing the medium voltage of internal services with a photovoltaic panel capped to produce enough electrical energy to ensure operating voltage would reduce CO<sub>2</sub>.

The connection or transformation point, in addition to the advantages associated with the reliability of the so-called system, could under certain conditions also deliver voltage to the network.

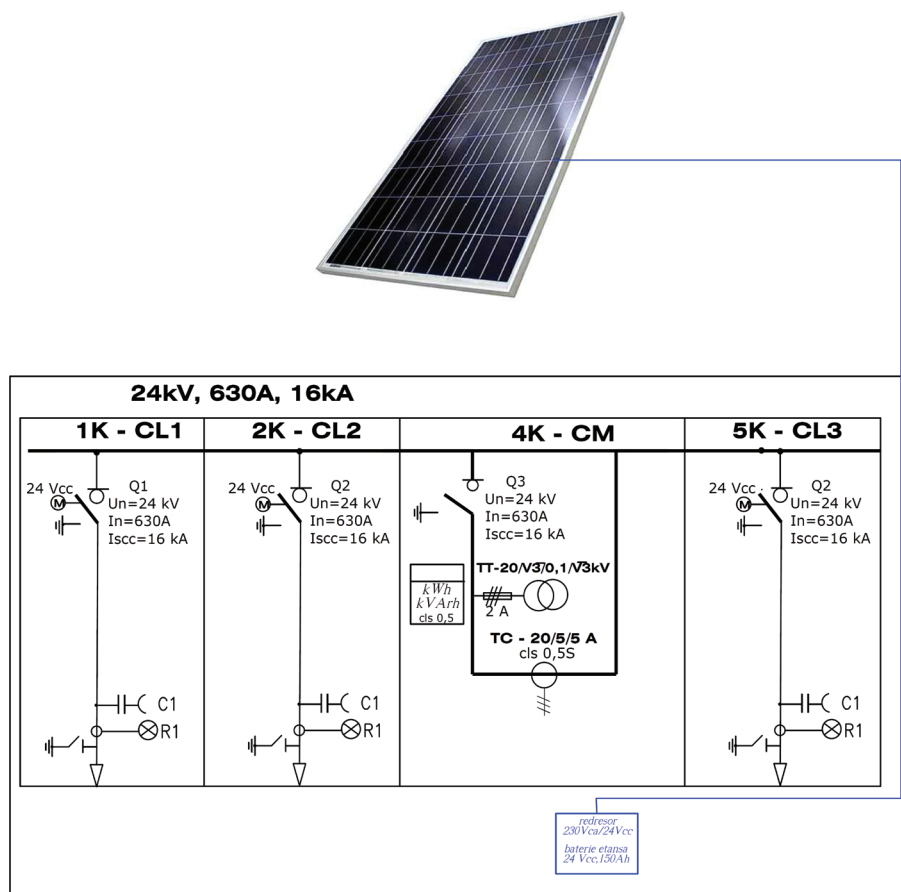


Fig. 2. Connection point with internal services fed from a photovoltaic panel  
 Rys. 2. Punkt połączenia z instalacją wewnętrzną zasilaną z panelu fotowoltaicznego

The features of a photovoltaic panel that could be used in such a configuration can be:

- Maximum power,  $P_{max} = 245$  [W];
- The voltage at  $P_{max}$ ,  $U_{mp} = 30,3$  [V];
- Current at  $P_{max}$ ,  $I = 8,09$  [A];
- Short-circuit current,  $I_{sc} = 8,34$  [A];
- Circuit voltage open,  $U_{oc} = 37,3$  [V];
- Temperature coefficient for  $I_{sc}$ ,  $a = 0.003/^\circ\text{C}$ ;
- Coefficient of temperature for  $U_{oc}$ ,  $\beta = -0,32/^\circ\text{C}$ .

Due to ability to generate “clean electricity” from the sun – without  $\text{CO}_2$  emission – photovoltaic systems are part of the solution to current energy and environmental problem.

Solar photovoltaic power can contribute to the gradual reduction of fossil fuel consumption, contributing signifi-

cantly to reducing greenhouse gas emissions in the electricity sector.

Photovoltaic modules contain materials that can be recovered and reused. Industrial recycling processes exist for both thin film modules and silicon modules. Materials such as glass, aluminum, and a variety of semiconductor materials are valuable when recovered.

Recycling brings benefits not only to the environment by reducing the amount of waste but also helps to reduce the amount of energy needed to supply raw materials and thereby reduce the cost and environmental impact of photovoltaic modules production.

Photovoltaic modules are designed to generate clean energy from renewable sources, a type of technology that has accumulated over 25 years of experience.



## Literatura – References

1. European Commission, Directive 2009/28 / EC of the European Parliament and of the Council of 23 April 2009 on the promotion of the use of energy from renewable sources, Official Journal of the European Union, 2009.
2. European Union law: <http://eur-lex.europa.eu>
3. European Photovoltaic Industry Association (EPIA), Global Market Perspective 2015 2011.
4. The European Photovoltaic Industry Association (EPIA), Greenpeace International, Solar Generation 6 - Solar photovoltaic power energizes the world, Feb 2011.
5. R. Alonso, E. Román (TECNALIA), T. Tsoutsos, Z. Gkouskos (ENV / TUC), O. Zabala, JR López (EVE), "The Potential and Benefits of BPIV", Intelligent Energy Europe (2009).
6. T. Tsoutsos, S. Turnaki, Z. Gkouskos, "PV Systems - Installation and Certification of Installers in Europe", Construction, Architecture and Technology, (June 2010).
7. T. Tsoutsos, S. Tournaki, Z. Gkouskos, E. Despotou, G. Masson, John Holden, "Training and Certification of Installers in Europe. Developing the PVTRIN Certification Scheme ", European Conference of European Photovoltaic Energy, 26th edition, Hamburg, Germany, 5-8 Sep., 2011.
8. Photovoltaic in DTI / PUB URN buildings 06/1972.
9. Concepts and common construction errors in commercial PV projects - 3E SERENE - Salerno 2nd July 2010.
10. Building integrated photovoltaics. A new design opportunity for architects. SUNRISE.
11. Building integrated photovoltaics. PREDAC.
12. Photovoltaic installations. Ed Garceta. 2010. Narciso Moreno, Lorena García Diaz.
13. GOOD PRACTICE GUIDE PROBE IN HOUSEHOLD PHOTOVOLTAIC LAND: Part I Project Management and Installation Problems (S / P2 / 00409 , URN 06/795).
14. GOOD PRACTICES GUIDE PROBE IN PHOTOVOLTAIC LAND.

## *Wykorzystanie energii słonecznej w urządzeniach energetycznych*

*Czyste środowisko jest niezbędne dla zdrowia ludzi i jakości życia. Rozwijające się sektory, które pomagają zaspokoić potrzeby i komfort, mają negatywny wpływ na jakość środowiska, w którym żyjemy. Wykorzystywanie zasobów naturalnych bez troski o potrzeby ludzi prowadzi do niszczenia środowiska. Zmiany klimatu, erozja, zwiększenie ilości dwutlenku węgla w powietrzu, którym oddychamy, są wynikiem zaspokojenia innych potrzeb, takich jak jedzenie, ciepło, transport, komfort w naszym domu.*

**Słowa kluczowe:** poziom CO<sub>2</sub>, energia słoneczna, panele fotowoltaiczne, sieć dystrybucyjna



# Sensory Network Monitoring the Air Condition, Installed in the Town of Litomerice

Josef DOUŠA<sup>1)</sup>

<sup>1)</sup> VSB-Technical University of Ostrava, Faculty of Mining and Geology, 17. listopadu Str. 15, 708 33 Ostrava - Poruba, Czech Republic; email: josef.dousa.st@vsb.cz

<http://doi.org/10.29227/IM-2020-01-34>

Submission date: 10-01-2020 | Review date: 05-03-2020

## Abstract

*There is a strong transit car traffic in Litomerice. A monitoring network was installed in the town of Litomerice (Czech Republic, Usti nad Labem Region) to explore the condition and impact on the environment. This monitoring uses a network of sensors and data is centralized.*

*In this work we will deal with the evaluation of the two-year operation of this network and function description.*

**Keywords:** sensors, monitoring network, protecting the city's environment

## Introduction

In most European cities, air quality is strongly affected by all kinds of human activities. Litomerice, as well as a number of other cities across Europe, face air pollution prevention problems. [1, 2] The low cost and availability of sensors and their involvement in measurement networks is becoming an effective option to monitor, evaluate and respond to air quality influences. In this work we will focus on the sensory network installed in the town of Litomerice and its almost two-year operation.

## Description

In Litomerice are historically operated two measuring stations. One owned by the Czech Hydrometeorological Institute (CHMI) – monitors PM<sub>10</sub>, SO<sub>2</sub>, CO and O<sub>3</sub> [3] and the other owned by the Institute of Health (ÚZ) – monitors SO<sub>2</sub>, PM<sub>10</sub>, O<sub>3</sub>, NO<sub>x</sub>, H<sub>2</sub>S and CS<sub>2</sub>.

In September 2017, a network of 12 measuring stations measuring PM<sub>1</sub>, PM<sub>2.5</sub> and PM<sub>10</sub>, 4 measuring stations VOC and one station measuring metrological values was installed for the city's needs. The location of the stations is shown in Figure 1. [4]

The installation was carried out with the assistance of The Faculty of Transportation Sciences, Czech Technical University in Prague.

The network is made up of AirTracker units that provide a comprehensive solution for on-line indicative environmental measurements (dust, noise, emissions). In addition to the sensors themselves, they are equipped with a wireless communication interface and a patented power supply system capable of uninterrupted operation from the public lighting network. The whole system is complemented by a web interface for visualization and analysis of current and historical data, see Figure 2. [4]

Measurements are thus PM<sub>1</sub> particulate concentrations (0.3 to 1.0 μm), PM<sub>2.5</sub> (1–2.5 μm), PM<sub>10</sub> (2.5–10 μm) in the range from 0 to 500 μg.m<sup>-3</sup> with an accuracy of 10%; maximum and average noise value (50–120 dB SPL), accuracy ± 1dB(A) SPL in full range; VOC concentrations with ionization potential <10.6 eV (range 1–1000 ppb, nonlinearity <3%). Optionally, the units can be supplemented with concentration measurements: CO, H<sub>2</sub>S, NO, NO<sub>2</sub>, O<sub>3</sub>, SO<sub>2</sub>. [5]

## Results and discussion

As can be seen from Table 1 [4], the amount of data as of January 12, 2019 collected by this sensory network is enough to allow us to evaluate this data. Prior to the actual evaluation, the data is adjusted by the float diameter with averaging window 500 and the finding and clearing of the outlier's data using the generalized extreme Student's test for outliers. This

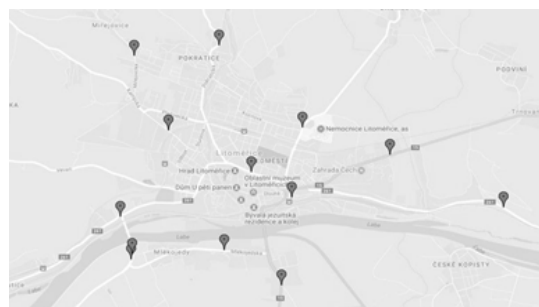


Fig. 1. Station locations [4]  
Rys. 1. Lokalizacje stacji [4]

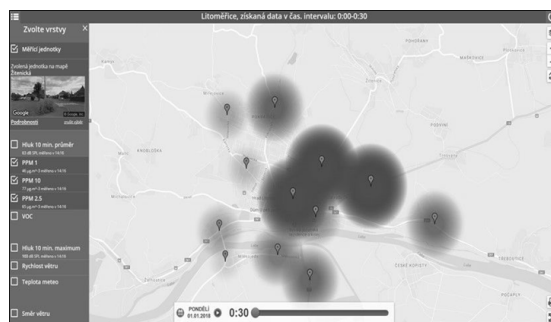


Fig. 2. Visualization interface [4]

Rys. 2. Interfejs wizualizacji [4]

Tab. 1. Number of measured data [4]

Tab. 1. Liczba zmierzonych danych [4]

ID of unit	number of data records
301 - Pokratická	148 312
302 - Miřejovická	176 779
303 - Kamýcká/ ČHMÚ	216 741
304 - Žitenická	134 529
305 - Na Valech / Tržnice	172 734
306 - Českolipská	191 115
307 - Ostrovní	207 990
308 - Žernosecká / Most G.Ch.	189 217
309 - Nádražní	188 841
311 - Mlékojedská	163 396
312 - Želetická	189 441
313 - AirTracker (metrological data)	88 101

Tab. 2. Measured data without outliers [4]

Tab. 2. Zmierzone dane bez wartości odstających [4]

ID of unit	number of data records	Outliers data
301 - Pokratická	148 312	340
302 - Miřejovická	176 329	403
303 - Kamýcká/ ČHMÚ	216 741	2 701
304 - Žitenická	134 529	9 874
305 - Na Valech / Tržnice	172 734	2 206
306 - Českolipská	191 115	1 995
307 - Ostrovní	207 990	885
308 - Žernosecká / Most G.Ch.	189 217	220
309 - Nádražní	188 841	3 801
310 - Mlékojedy most	218 754	14 876
311 - Mlékojedská	163 296	542
312 - Želetická	189 441	495
Celkem	2 197 299	38 338



Fig. 3. Installed humidifiers

Rys. 3. Zainstalowane nawilżacze

iterative method is useful when masking different outlier's data values, as shown in Table 2. [4]

### **Conclusion**

We will evaluate the cleaned data with the assistance of the Faculty of Transportation Sciences, Czech Technical University in Prague and the output should be the detection of causes of increased dustiness in Litomerice. Part of the monitoring of the air condition is the elaboration of a dispersion study in cooperation with CDV (Transport Research Center).

It is also possible to connect some sensors to humidifiers installed on public lighting poles, thus ensuring a controlled improvement of air at a critical time, see Figure 3.

In addition, sensors are connected to CO<sub>2</sub> sensors located in schools for efficient ventilation, excluding ventilation with poor air quality in the environment.

Despite the relative error of measurement or the amount of outliers data, sensory networks have a great potential for use in urban areas due to their relatively low purchase price and will certainly find their place in other fields and activities.

#### Literatura – References

1. U. A. Hvidtfeldt, M. Sørensen, C. Geels, M. Ketzel, J. Khan, A. Tjønneland, K. Overvad, J. Brandt and O. Raaschou-Nielsen, "Long-term residential exposure to PM2.5, PM10, black carbon, NO2, and ozone and mortality in a Danish cohort," *Environment International*, vol. 2019, no. 123, pp. 265-272, 2019.
2. "WHO | Air pollution," World Health Organization, 12. 05. 2016. [Online]. Available: <https://www.who.int/airpollution/en/>. [Accessed 14. 01. 2019].
3. ČHMÚ, "ČHMÚ," [Online]. Available: [http://portal.chmi.cz/files/portal/docs/uoco/web\\_generator/aqindex\\_slide4/mp\\_ULTTA\\_CZ.html](http://portal.chmi.cz/files/portal/docs/uoco/web_generator/aqindex_slide4/mp_ULTTA_CZ.html). [Accessed 15. 01. 2019].
4. "Litoměřice :: Mapa," [Online]. Available: <http://litomerice.fd.cvut.cz/index/publicmap/>. [Accessed 02. 03. 2019].
5. "Data sheet of AirTracker," FD CVUT, [Online]. Available: <https://security.fd.cvut.cz/wp-content/uploads/2017/09/Airtracker-CTU.pdf>. [Accessed 18 03 2019].

#### *Sieć sensoryczna monitorująca klimatyzację, zainstalowana w miejscowości Litomerice*

*W Litomericach panuje duży ruch tranzytowy. W mieście Litomerice (Czechy, Usti nad Labem) zainstalowano sieć monitorującą w celu zbadania stanu i wpływu na środowisko. Monitorowanie wykorzystuje sieć czujników, a dane są scentralizowane. W niniejszej pracy przedstawiono ocenę dwuletniego funkcjonowania tej sieci i opis funkcji.*

**Słowa kluczowe:** czujniki, sieć monitoringu, ochrona środowiska miasta



# EU Documents of Major Importance Relevant to Issues of Mineral Resource Utilisation

Jaroslav DVOŘÁČEK<sup>1)</sup>, Radmila SOUSEDÍKOVÁ<sup>2)</sup>, Ladislav MORAVEC<sup>3)</sup>

<sup>1)</sup> VŠB – Technical University of Ostrava, Faculty of Mining and Geology, 17. listopadu 2172/15, 708 00 Ostrava-Poruba, Czech Republic; email: jaroslav.dvoracek@vsb.cz

<sup>2)</sup> VŠB – Technical University of Ostrava, Faculty of Mining and Geology, 17. listopadu 2172/15, 708 00 Ostrava-Poruba, Czech Republic; email: radmila.sousedikova@vsb.cz

<sup>3)</sup> Havířovská teplárenská společnost, a.s., Konzumní 298/6a, 731 01 Havířov-Šumbark, Czech Republic; email: moravec@htsas.cz

<http://doi.org/10.29227/IM-2020-01-35>

Submission date: 22-01-2020 | Review date: 09-04-2020

## Abstract

*RAW MATERIALS INITIATIVE and REPORT ON CRITICAL RAW MATERIALS FOR THE EU are two documents of major importance as regards the issues of mineral resources of the European Union. The former document calls upon the EU Member States to maximize utilisation of domestic mineral resources, especially as regards those labelled as critical, the latter concerns occurrence of some such critical minerals in the Czech Republic. In actual fact, compliance with the implications of these documents means renewal of exploitation of residual mineral resources. Nonetheless, such activity anticipates positive economic results, and these are conditioned by investment means available for resumption of production. Both investment and operating expenses can be cut down if existing mining capacities are utilized. This paper investigates possibilities of mining resumption in the Czech Republic from the point of view of the methods employed for decommissioning and closure of mines. The so-called “wet” preservation of mines is recommended both for a future easy option of accessing decommissioned underground works and the possibilities of using pit water itself or employing its energy.*

**Keywords:** Raw Materials Initiative, Critical Raw Materials, resumption of mining, closure of mines

## Introduction

Mineral resource base is a prerequisite for development of any State. Relevant EU authorities became aware of the momentous significance of the matter, when they realized that major mineral resources are concentrated in only a few states, production is in the hands of a handful of big producers, and that some states dominate production or consumption of some minerals.

In 2008, the Commission of the European Communities issued the document, The raw materials initiative – meeting our critical needs for growth and jobs in Europe. It is the implication of the document that an integrated strategy for management of mineral resources should be adopted, where supply sustainability from EU sources proper plays a major role. At the same time, the Commission calls for a minute assessment of EU critical raw material availability. The exigency had been dealt with by compiling an initial list of 14 critical raw materials in 2011. An update of the list comprising 20 materials was issued in 2014, and a list of 27 items was published in 2017. The principal classifying criterion was constituted by economic importance of specific raw materials and their supply risks. It should be highlighted that some critical materials occur in the Czech Republic as exploitable resources, for example fluorite, natural graphite or tungsten. In the Czech Republic also other two raw materials feature European prominence, namely lithium and kaolin. Responding to demands of the mentioned document, Raw Material Initiative, actually means resumption of mining production.

## Is resuming of mining activities a real option?

The history of mining provides evidence of changing fortunes. We witnessed a major downturn of mining activities at

the beginning of the nineties of the past century. In the Czech Republic, a new prioritization initiative for national economy, termination of state subsidies, environmental issue emphasis, as well as political influence they all caused a complete termination of ore mining, an initial substantial reduction and later a complete closure of uranium mines. Production of lignite was almost halved in comparison to production maxima of the past mining operation. Nonetheless, reserves of formerly extracted or other minerals have been left at some mining localities.

Resuming of mining is not an issue of abstract theory. Also in the past, especially concerning ore deposits, closure or reopening of mines followed current supply and demand situation, solving of extraction technical and technological problems or simply the necessity of new mineral exploitation.

If the mine of Cínovec was closed after 600 hundred years of tin and tungsten production, it can be assumed that the production was hardly a continuous one. Apart from ore mining, also resumption of open-cast coal mining could be witnessed in the past.

Lignite mining: Very often, it has been the case that modern large-scale open pit lignite extraction comes across with remnants of former underground mining. The extraction meets with remainder of underground works, encounter unrelated materials or faces outburst of water from old mining works. Consequently, quality of the extracted lignite is impaired, people and machines are at risk of caving in, fires can start, upper bed cracks may occur, or hydrogeological equilibrium is disturbed (Zima, 2013). Nonetheless, problems are being solved and the open-cast mining continues, as only a

fraction of the lignite deposit was extracted by former underground mining.

Ore mining: Tin primary deposits in the territory of the Forest of Slavkov were exploited towards the end of the fourteenth century. From 17th to 19th century, tin mines were alternatively closed and mining resumed. Since the end of 19th century, apart from tin also tungsten has been extracted. The importance of mining for tungsten increased during the WWI and WWII.

Ore deposits of Jáchymov comprised not only silver but also uranium mineral pitchblende. The latter could find no demand and was waste heaped. At the beginning of 19th century, the pitchblende was used for colouring of glass and porcelain. Since the second half of 19th century, it has been the principal item of extraction. After WWII, uranium has become a strategic raw material.

Regarding options of resumed mining activities, on 11th October 2017, a breakthrough document, No. 713, was issued by the Government of the Czech Republic, namely „Zpráva o nutnosti zajištění ekonomických zájmů státu v oblasti využití kritických superstrategických surovin Evropské unie a některých dalších surovin (On Necessity of Safeguarding Economic Interests of the State in the Field of Utilizing Critical and Super-strategic Raw Materials of the European Union, and Some Other Raw Materials)“. The document implies increased governmental control of critical material utilization in the EU, and also tantalum, zirconium, titanium, gold, lithium, and uranium that are called strategic raw materials of the Czech Republic. The obvious burning issue is that of resuming mining activities at the locality of Cínovec.

Cínovec: The history of tin mining at the locality starts in 14th century. Over the centuries, the mining for tin and silver at the locality went through many vicissitudes. Since 1879, the importance of tungsten mining has been increasing. Old dump piles and fills were picked through to collect wolframite. Between 1931 and 1939, the pit was maintained without production. At the beginning of WWII, mining was resumed. Geological reserves of Cínovec I (old enterprise) were worked out in 1978. In 1980, mining activities at the deposit of Cínovec II (southern part of Cínovec) commenced to be finished in 1990.

In 1992, the whole mining area of Cínovec was decommissioned. The Pit I of Cínovec was flooded up to the level of the third floor, from which, through a system of gangways, water flows off at the German side of the Ore Mountains. The Pit II of Cínovec was flooded up to the top level. The third vertical opening – Winze, K 20225 – was backfilled (Kafka, 2003; RD Příbram, 2010).

The Czech mining company, Geomet Limited, was granted exploration permits for Sn, W, Li and other reserved minerals. This company is a subsidiary of the European Metal Holdings Limited (EMH). Recently, test boring has been realized by the company, EMH, and the results give evidence to the fact that the deposit of Cínovec is the largest lithium deposit in Europe and the fourth largest non-brine deposit of lithium in the world (European Metals, 2016). An investment presentation of the company, EMH, from November 2018 shows targeted production rates to be minimally p. a. 22 500 tons of lithium carbonate or p. a. 25 600 tons of lithium hydroxide, inclusive tin and tungsten by-products.

The presentation's investment costs are in excess of USD 390 million, and the isometric model of the underground mine implies usage of the existing underground works. As such, reopening of closed mines poses problem to be solved.

### Closure of mines and options for their reopening

Technical measures applied for decommissioning of ore mines included removing of machinery installations to avoid contamination of water by harmful substance, and disposal of entry and long workings. Pits and winzes were decommissioned by (Kafka, 2003):

- Complete fill-up and covering of the pit by a reinforced concrete slab installed at ground level.
- Installation of a reinforced concrete slab at a certain depth and filling the pit above the slab up to ground level.
- Closure of the pit entrance by a reinforced concrete slab, and progressive flooding of the mine.

The first method excludes possibility of resuming mining activities at the pit. If the fill-up had been hardened, putting down of a new shaft next to the filled-up working is necessary. This demands high financial investment and implementation time.

The second method would have been difficult to adopt because of safety precautions. The unhardened fill-up implies cavernous structure which, with lapse of time, may cause sinking of the backfill.

The third method is seemingly the simplest method to apply but it is not as easy as it seems to be.

Not only water from the pit itself but also water from all other underground rooms next to the pit must be removed. Cases might exist, when lowering of the water underground level would only be necessary, nevertheless, this option might also imply necessity of a long-term drainage of water and its purification before watercourse emptying.

### Discussion

So far, guiding principles for application of mine closure methods have consisted in execution cost and implementation rapidity. It is obvious that determining factors for mine closure implementation are constituted by efficient safety and precaution provisions. With regard to cyclical development of mining, mine closure planning should consider, whether the mineral deposit has been depleted or some reserve for future exploitation has been left.

If the depletion of currently exploited minerals or other accompanying minerals is the case, safety and financial costs determine adoption of the closure method.

If some mineral reserve exists at the locality, the mine closure method should be employed that would enable resuming of mining activities in future. Past experience and good practice suggest flooding of the pit, i.e. the “wet” method of preservation. Obviously, this is conditioned by stability of environment against contamination, which condition is usually satisfied as regards ore deposits.

If resuming of mining activities is considered an option, the decommissioning project and its implementation should be oriented by the simplest way of reopening the mine in future.

## **Conclusion**

From the point of view of safety, an ideal mine closure method is represented by placing of hardened backfill inside all underground workings. Domestic mining has practical experience with this method – ore mine of Křižanovice and coal pit, Jan Šverma, of Žacléř.

In perspective of renewing mining activities, it is the “wet” preservation, which is an obvious option. Even if the pit

is not reopened in future, it may serve the purpose of a water source or hydro energy reservoir.

## **Acknowledgements**

We thank organizers of the Project MERIDA, Research Fund for Coal and Steel, Grant Agreement, No, RF-CR-CT-2015-00004 that made investigation of this paper possible.



## Literatura – References

1. Commission of the European Communities (4. 11. 2008): The raw materials initiative – meeting our critical needs for growth and jobs in Europe. Communication from the Commission to the European Parliament and the Council. Brussel, COM (2008) 699 final.
2. European Commission (2018). Critical Raw Materials. Internal Market, Industry, Entrepreneurship and SMEs [online]. [vid. 2019-03-22]. Available from: [https://ec.europa.eu/growth/sectors/raw-materials/specific-interest/critical\\_en](https://ec.europa.eu/growth/sectors/raw-materials/specific-interest/critical_en)
3. European Metals. Cinovec lithium project: production of battery grade lithium carbonate from sodium sulphate roast. Company announcement 13 December 2016. [online]. [vid. 2019-03-18] Available from: <https://www.investi.com.au/api/announcements/emh/e238e68b-c4e.pdf>
4. European Metals. Cinovec a globally significant lithium & tin project in the heart of Europe. Investor presentation, November 2018. [online]. [vid. 2019-03-18]. Available from: <https://www.investi.com.au/api/announcements/emh/cabcb004-f95.pdf>
5. KAFKA, J. (Ed.) Rudné a uranové hornictví České republiky (Ore and Uranium Mining in the Czech Republic). Ostrava: ANAGRAM, 2003.
6. Rudné doly Příbram (2010). Důl Cínovec na Cínovci. [online]. [vid. 2018-11-20]. Available from: <http://www.zdarbuh.cz/reviry/rd-pribram/dul-cinovec/>
7. ZIMA, R. Optimalizace těžebních podmínek a toku těživa z oblasti zasaženou bývalou hlubinnou těžbou (Optimizing Mining Conditions and Material Flows Regarding Interference of Former Mining Activities). Ostrava, 2013. Disertační práce. VŠB – TUO Ostrava, HGF.

*Dokumenty UE o duším znaczeniu dla zagadnień wykorzystania zasobów mineralnych INICJATYWA W SPRAWIE SUROWCÓW i RAPORT NA TEMAT KRYTYCZNYCH SUROWCÓW DLA UE to dwa dokumenty o duším znaczeniu dla kwestii zasobów mineralnych Unii Europejskiej. Pierwszy dokument wzywa państwa członkowskie UE do maksymalnego wykorzystania krajowych zasobów mineralnych, zwłaszcza w odniesieniu do tych, które są oznaczone jako krytyczne, drugi dotyczy występowania niektórych takich krytycznych minerałów między innymi w Czechach. W rzeczywistości zgodność z implikacjami tych dokumentów oznacza odnowienie eksploatacji pozostałych zasobów mineralnych. Niemniej jednak taka działalność przewiduje pozytywne wyniki gospodarcze, które są uwarunkowane środkami inwestycyjnymi dostępnymi do wznowienia produkcji. Zarówno koszty inwestycyjne, jak i operacyjne można ograniczyć, jeżeli zostaną wykorzystane istniejące zdolności wydobywcze. W artykule przedstawiono możliwości wznowienia wydobywania w Czechach z punktu widzenia metod stosowanych do likwidacji i zamykania kopalń. Tak zwane „mokra” zamknięcie kopalni jest zalecana zarówno dla przyszłej łatwej opcji dostępu do wycofanych z eksploatacji robót podziemnych, jak i dla możliwości wykorzystania samej wody pitnej lub wykorzystania energii.*

**Słowa kluczowe:** inicjatywa na rzecz surowców, surowce krytyczne, wznowienie wydobywania, zamknięcie kopalń



# Reducing Environmental Degradation Caused by the Open-Cast Coal Mining Activities

*Tudor GOLDAN<sup>1)</sup>, Catalin Marian NISTOR<sup>1)</sup>, Aronel MATEI<sup>1)</sup>, Dimian MARU<sup>2)</sup>*

<sup>1)</sup> University of Petrosani, Romania

<sup>2)</sup> Hunedoara Energetical Complex

<http://doi.org/10.29227/IM-2020-01-36>

Submission date: 21-12-2019 | Review date: 02-02-2020

## Abstract

*Many types of changes are distinguished as a result of mining: degradation of land and vegetation, change in the natural topography which results in restrictions in the possibilities of using the land for other purposes, modification of surface and ground water balance and quality, changes in air quality and finally changes in the geotechnical conditions of the rock. The impact varies with local conditions of the specific site of mining.*

*Most surface mining methods are large scale, involving removal of massive volumes of material, including overburden, to extract the mineral deposit. Because the materials disposed in refuse dumps are physical-chemically heterogeneous and extremely diverse in terms of mineralogical composition (sand, gravel, clay, marl), over time there have been many occurrences of instability phenomena. Large amounts of waste can be produced in process. Surface mining also can cause noise and disturbance and may pollute air with dust.*

**Keywords:** *prevention, monitoring, environmental, impact, mining, activities, open pit*

## Introduction

Mining and its related activities have always resulted in changes in the environment. These changes differ from one area to another.

The process of removing, storing and subsequently replacing the soil during the mining activity lead to potential problems in relation to subsequent restoration. In this respect, a major distinction should be drawn between those sites where, for operational reasons, soil has to be stored for a period of years while the mining progresses, and those, usually larger, sites where a progressive system of restoration can be practiced.

The negative impacts of surface mining on environment can following:

- occupation of large farming areas needed for excavation and dumping operations;
- alteration of land morphology;
- disturbance of native fauna and flora;
- modification of surface and ground water balance;
- resettlement of residential areas, roads and railways;
- release of air, liquid and solid pollutants and noise pollution.

Soil destruction is one of the most crucial environmental impacts of open pit mining activities. Surface mining speeds up erosion and sedimentation and short duration, high intensity storms can be a violent force moving thousands of tons of soil. Physical characteristics of the overburden, degree and length of slope, climate, amount and rate of rainfall, type and percentage of vegetative ground cover affect the vulnerability of strip mined land erosion.

## Material and methods

The sources of data for this study comprised both primary and secondary sources. The primary sources of data were

observation and interview conducted at the various phases of the detailed study. Phase two involved data collection on existing land uses, thus detailed observation was made to identify the kinds of degradation that has occurred and also find out the use to which the heavily mined sites have been put.

Before starting the coal extraction there were performed the following workings: decommissioning of existing buildings, clearing the terrain, topsoil removal, preliminary excavations, achieving access routes, building production facilities and necessary annexes, building coal deposits, etc.

There were also conducted hydraulic water works like: diversion of watercourses; execution of dumps guard channels; flood embankment; shielding aquifer formations; arrangements for correcting torrents; water drainage and collection channels.

Simultaneously with the opening trenches execution there were built mounting platforms for technological equipment, slopes to access high capacity machines and for the location of belt conveyors.

Mining methods applied mainly have been those with transportation of the waste rock at dumps. They are used in all conditions and in any terrain configuration or lignite deposit settlement, whose inclination is in the range 5–8°.

Tailings disposed in landfills comes from the work of outcropping and sterile intercalations between the mined out lignite strata.

Observations on such dumps can be quantified as it follows below:

- the presence of uneven subsidence areas, which allows accumulation of rainfall and runoff in the body of dumps and results in the change of state of consistency, with negative effects on the stability;
- the occurrence of the thixotropic or liquefaction phenomenon during the rainfall season, which leads

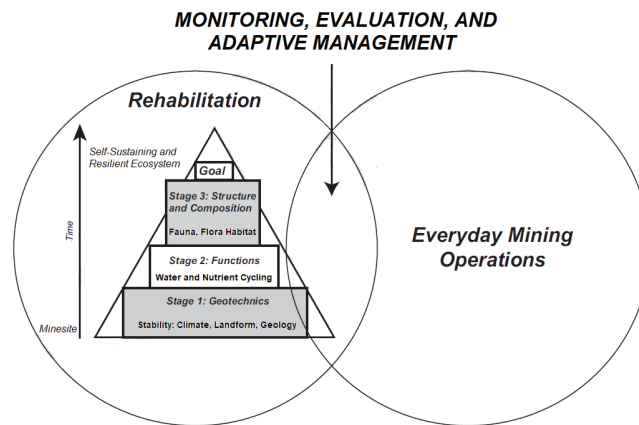


Fig. 1. Monitoring, Evaluation and Adaptive Management after mining operations  
 Rys. 1. Monitorowanie, ocena i zarządzanie adaptacyjne po zakończeniu operacji wydobywczych

to increased instability of dumped rock by reducing the shear strength;

- the increased humidity due to excess moisture leads to small size superficial slips of landfill slopes steps without affecting the overall stability of the;
- tilt slopes greater than 30° are crossed by ravines created by water flow.

Following the periods of excessive moisture, the presence of clays resulted in rocks swelling, leading ultimately to destabilize some of dumps.

Above realities combined with constructive deviations from the designed geometry of waste dumps favors the appearance of instability phenomena or reactivation of older, previously existing ones.

Moisture content in a dump is a fluctuating parameter which is influenced by the time of sampling, height of dump, stone content, amount of organic carbon, and the texture and thickness of litter layers on the dump surface. During the winter, the average moisture content of 5% was found to be sufficient for the plant growth. During high summer (May–June), moisture content in overburden dumps was reported to be as low as 2–3% moisture content of all the dumps was 5%.

Being loosened structures consisting of carbonaceous clay, sandy clay, dusty-marly sand and argillaceous sand, heaps are characterized by a great susceptibility to triggering geomorphological processes, of which the most common are runoff and gully, shallow landslides of steps and slopes, also their collapse, wind erosion, natural and anthropogenic compaction.

Rearrangement and rehabilitation works, which may be either to remove the visual effects of an existing mine site or to reduce the impact of a new mine site to a lowest degree, should be planned before starting operation and carried out in parallel with mining activities.

Rearrangement includes excavation and dumping according to the planning, stable design of dump sites and chamfers with proper slope and elevation, laying out of top humus layer and fertile soil right beneath it either directly or later, grading, drainage and water regime control, constructing surrounding drainage channels against floods, and constructing infrastructure and road network; whereas re-

habilitation comprises improvement of soil conditions and re-vegetation on topographically graded lands.

### Results and discussion

Unconsolidated surface mining operations usually require the removal of vegetative cover combined with the stripping of topsoil, overburden and spoil materials. These activities, along with construction of access roads, usually result in severe disturbance or complete destruction of soil structure, landscapes and vegetation. Without proper management and regulation, additional adverse impacts may include loss of topsoil and plant cover, changes in the quality and quantity of surface water and groundwater, and decline of wetland habitat.

After closure open pit mining activities it is necessary a monitoring management. Monitoring, evaluation and adaptive management is critical in mine rehabilitation (figure 1). Monitoring should also be used to determine the effectiveness of rehabilitation. Monitoring would become more complex over time, and together would demonstrate rehabilitation success.

Monitoring in an open pit should not only concentrate on surface movement, but systems should also be installed to monitor sub-surface movement. The timely collection and interpretation of the data, followed by distribution of the results, forms the complete slope monitoring system.

Measures commonly adopted to increase stability are draining surface water and groundwater, reducing the slope escarpment, covering them with plantations, building retaining walls.

In order to prevent instability of the surface land is used primarily the aquifer formations dewatering, process allowing that the water is drained and evacuated for operation under normal conditions. These works resulted in lowering the groundwater levels in areas with large extension.

Through the surface water drainage it is minimized the process of alteration of physical-mechanical properties of rocks. In this respect is necessary the surface land leveling and building drains for surface water leakage.

The underground drainage system lowers to groundwater levels, reducing pore water pressure and hydrostatic pressure in rocks's cracks.

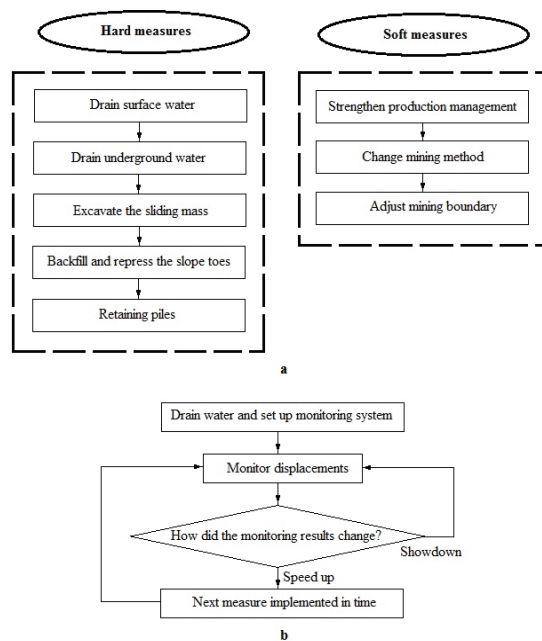


Fig. 2. Control measures and design procedures to landslides control: a – measures for landslides control; b – design procedures.  
 Rys. 2. Środki kontroli i procedury projektowania kontroli osuwisk: a – środki kontroli osuwisk; b – procedury projektowania

Leveling – which fall under mining units obligations – must create the conditions required to carry out the regeneration of soil fertility and plant cultivation or conditions for building and development purposes.

Creating plantations and afforestation are other measures with positive effect aimed to stabilize landslides, being applying after surface land leveling and provision of surface water drainage.

Another measure for landslide stabilization is to reduce slope gradients in order to achieve stable conditions.

Landscape and soil degradation involve a reduction in ecosystem functions and services. Thus, decisions about sustainable landscape management must consider the restoration of essential ecosystem services.

Restoration of coal mining landscapes has become an important area of focus with the pressure to reduce coal combustion, since coal combustion is a major contributors to the total anthropogenic emissions of 35 Gt CO<sub>2</sub>/yr. Restoration of these lands is critical to ecosystem functions and services.

## Conclusions

Effects of mining on the environment may not be evident immediately; many are usually noticed after some years. Surface mining requires large areas of land to be temporarily disturbed. The effects of open pit mining on the environment include a number of environmental challenges land degradation soil erosion, noise, dust, poisonous gases and pollution of water and so on. Open-pit mining changes the topography and vegetation, and include impacts on local biodiversity. From the noise and vibration point of view, drilling and blasting operations as well as application of heavy vehicles

are very important. Blasting, haulage and transportation are the main reasons for the dust generation.

Depending on the technology in use and the mining methods adopted, mining activities can cause considerable environmental degradation and industrial pollution. Mining dumps and tailings are frequently the principal source of solid waste as well as liquid waste pollution. Mining may also cause the contamination of ground and surface waters with toxic chemicals

Workings performed for extracting coal in open pits are large-scale developments and can lead to significant degradation of the surrounding terrain and waste dumps resulting from this activity.

Measures to ensure slope stability dumps can be qualified as "hard" or "soft". A first measure consist in respecting working technology, followed by dewatering, and drainage of surface water and groundwater, land leveling and creating plantations

All these measures requires continuous monitoring, which is a problem often neglected, most often due to limited financial resources or lack of communication between the involved parties.

Implementing pollution control measures, monitoring the effects of mining and rehabilitating mined areas, the mining industry minimises the impact of its activities on the neighbouring community, the immediate environment and on long term land capability.

It is necessary to understand the system requirements and specifications and to address human interface issues to improve component and system reliabilities, and minimize the occurrence of environmental damages.

## Literatura – References

1. BHATTACHARYA, A., ROUTH, J., JACKS, G., BHATTACHARYA, P., MORTH, M. Environmental Assessment of Abandoned Mine Tailings in Adak, Vasterbotten District (Northern Sweden). *Applied Geochemistry*, Volume 21, 2006, pp.1760-1780.
2. BELL, F.G., DONELLY, L.J. *Mining and Its Impact on the Environment*. Oxon, England: Taylor&Francis Group, 2006.
3. DRAKE, J., GREENE, R., MACDONALD, B.C.T., FIELD, J.B., PEARSON, G.L. A review of landscape rehabilitation frameworks ecosystem engineering for mine closure, *International Conference on Mine Closure 2010*, ed. Andy Fourie, Mark Tibbett, Jacques Wiertz, Australian Centre for Geomechanics, Perth, pp. 241-249.
4. HENDRYCHOVA, M. Reclamation Success in Post-Mining Landscapes in the Czech Republic: A Review of Pedological and Biological Studies. *Journal of Landscape Studies*, Volume 1, 2008, pp.63-78.
5. KAVOURIDES, C., PAVLOUDAKIS, F., FILIOS, P. Environmental protection and land reclamation works in West Macedonia Lignite Centre in North Greece current practice and future perspectives. In: Ciccu R. (ed.) *SWEMP 2002: Proceedings of the 7 th International Symposium on Environmental Issues and Waste Management in Energy and Mineral Production*, SWEMP 2002, 7-10 October 2002, Cagliari, Italy. University of Cagliari; 2002.
6. MAITI, S.K., GHOSE, M.K. Ecological restoration of acidic coal mine overburden dumps- an Indian case study. *Land Contamination and Reclamation*, 13(4), pp.361-369.
7. MIAO, Z., MARRS, R. Ecological Restoration and Land Reclamation in Open-Cast Mines in Shanxi Province, China. *Journal of Environmental Management*, Volume 59, 2000, pp. 205–215.
8. SENGUPTA, M. *Environmental Impacts of Mining: Monitoring, Restoration, and Control*. USA Lewis Publishers, 1993.
9. SHEORAN, V., SHEORAN, A.S., POONIA, P. Soil reclamation of abandoned mine land by revegetation: a review. *International Journal of Soil, Sediment and Water*, vol. 3(2), 2010.
10. SKLENICKA, P., KASPAROVA, I. Restoration of Visual Values in a Post-Mining Landscape. *Journal of Landscape Studies*, Volume 1, 2008, pp.1-10.
11. TONGWAY, D. Part 3: Interpretation of the data. In "The LFA Monitoring Procedure: A monitoring procedure to assess rehabilitation success". CSIRO Sustainable Ecosystems Presentation, 2005.

## *Ograniczanie degradacji środowiska spowodowanej działalnością wydobywczą węgla odkrywkowego*

*W wyniku wydobywania wyróżnia się wiele rodzajów zmian: degradacja gruntów i roślinności, zmiana naturalnej topografii, co powoduje ograniczenia możliwości wykorzystania gruntów do innych celów, modyfikację bilansu i jakości wód powierzchniowych i gruntowych, zmiany jakości powietrza i wreszcie zmiany warunków geotechnicznych.*

*Oddziaływanie różni się w zależności od lokalnych warunków miejsca wydobywania. Większość metod eksploatacji odkrywkowej odbywa się na dużą skalę, polega na usuwaniu ogromnych ilości materiału, w tym nadkładu, w celu wydobywania surowca mineralnego. Ponieważ materiały składowane na składowiskach odpadów są niejednorodne pod względem właściwości fizyczno-chemicznych i są niezwykle zróżnicowane pod względem składu mineralogicznego (piasek, żwir, glina, margiel), z czasem pojawiło się wiele niestabilności. Eksploatacja odkrywkowa może również powodować hałas i zakłócenia oraz może generować zanieczyszczenie powietrza pyłem.*

**Słowa kluczowe:** zapobieganie, monitorowanie, wpływ na środowisko, wydobywanie, działalność, kopalnia odkrywkowa



# Selected Characteristics of the Atmospheric Deposition in the Area of Košice

Jozef HANČULÁK<sup>1)</sup>, Tomislav ŠPALDON<sup>2)</sup>, Oľga ŠESTINOVA<sup>3)</sup>

<sup>1)</sup> Institute of Geotechnics of the Slovak Academy of Sciences, Watsonova 45, 040 01 Košice; email: hanculak@saske.sk

<sup>2)</sup> Institute of Geotechnics of the Slovak Academy of Sciences, Watsonova 45, 040 01 Košice; email: spaldon@saske.sk

<sup>3)</sup> Institute of Geotechnics of the Slovak Academy of Sciences, Watsonova 45, 040 01 Košice; email: sestinova@saske.sk

<http://doi.org/10.29227/IM-2020-01-37>

Submission date: 03-01-2020 | Review date: 12-03-2020

## Abstract

The contribution deals with the atmospheric deposition of solid particles and selected elements in the typical urban area with many sources of pollution. The main sources of pollution are represented by neighboring the iron and steel works and the thermal power station.

The samples were collected from the eleven sites, which are located from 3.6 to 16 km from the iron and steel works. Qualitative and quantitative characteristics of the total deposition of solid particles, the deposition fluxes of elements Fe, Al, Mn, Zn, Pb, Cu, Cr, Cd, As and their seasonal variations were studied. Results from the years of 2009–2018 are introduced.

The research has shown a significant influence of local sources of pollution on the studied parameters of atmospheric deposition. Compared to the values of deposition measured in the other areas, extremely high values of iron (28, 120), manganese (1,106) and chromium ( $34.1 \mu\text{g}\cdot\text{m}^{-2}\cdot\text{day}^{-1}$ ) deposition as well as high, above-average values of other monitored elements were measured in the proximity of the ironworks. The portion of emission sources of iron and steel works on the Fe fluxes at the individual sites in the city was calculated in the range from 24.7 to 54.1%. On the basis of the emission situation of the monitored area, it is possible to use selected compounds of the AD as an environment quality indicator and to quantify the contribution of emissions to area's environmental stress.

**Keywords:** atmospheric deposition, emissions, iron and steel works, metals

## Introduction

Atmospheric deposition (AD) is a significant source of many pollutants and their major input into the surface and other components of an environment. Specific anthropogenic emissions from the large sources of pollution have influence on the composition of AD. The study of qualitative composition AD and deposition fluxes of its components can be a suitable instrument for identifying sources of pollutants, their spatial distribution, variability, mass fluxes and provides important information for an assessment of air and environment quality. For this reason, many research studies deal with AD from point of view of various parameters and aspects in urban, suburban and rural areas (Azimi et al., 2005; Hančulák et al., 2011, 2015, 2016; Kara, M. et al., 2014; Mehrazin et al., 2017; Putaud et al., 2010, 2008; Wong et al., 2008).

The Košice area, in addition to typical urban pollution sources such as road traffic, municipal sphere, small industrial sources and construction, is long term environmentally loaded by the iron and steel works – the largest source of emissions of various pollutants including particulate matter and metals. Metals are regarded as very good markers of the specific natural and anthropogenic pollution sources, to a large extent they are used in studies dealing with determination and division of sources of solid particles (Nicolás et al., 2007). The contribution presents some results of the research of AD which was conducted by the bulk deposition methodology from 2009 to 2018 predominantly from viewpoint of deposition fluxes of selected elements (Fe, Al, Mn, Zn, Pb, Cu, Cr, Cd and As) and solid particles in relation to emissions from the iron and steel works.

## Characteristics of the area

The monitored area is located in the Košice Basin, in the valley of the river Hornád with north-south orientation in the eastern part of Slovakia. The prevailing winds in the area are northern (53.5%) and southern (31.6%), while the proportion of calm is 9.5%. Emissions of particulate matter (PM) have the greatest influence on its composition in terms of monitored components of AD. The decisive producer of particulate matter (PM) and gaseous emissions in the area of Košice, as well as the whole Slovakia is the iron and steel industry complex, the company U. S. Steel Košice, Ltd., located approx. 10 km south to southwest of the city center. Limekiln (Carmeuse Slovakia, Ltd.) and several other metallurgical companies are placed directly in the industrial estate of works. Directly, in the southern part of the city, a heating plant (TEKO) is located that produces heat and electricity based on coal and natural gas. Inventory emissions of PM and selected metals from crucial sources of pollution in the area are processed in Table 1 and Table 2. (NEIS).

## Materials and methods

Total atmospheric deposition i.e. both wet and dry ones, were collected monthly ( $35 \pm 5$  days) from eleven sites in the urban and suburban area in the vicinity of iron and steel works, from June 2009 to October 2018. The sampling sites were at a distance of 1–15 km from the main source of pollution. The localization of sampling sites is illustrated in Fig. 1.

In the urban area, the sites no. 1–6 were placed on the rooftops of blocks of flats and public buildings at 24–36 m height above the ground level, above the height of surround-

Tab. 1. The emissions of particulate matter (PM) from the largest sources in the Košice area [t.year<sup>-1</sup>]Tab. 1. Emisje pyłu zawieszzonego (PM) z największych źródeł na Koszycach [t.rok<sup>-1</sup>]

Source/Year	2009	2010	2011	2012	2013	2014	2015	2016	2017
City heating plant	56	92	90	96	76	85	37	2	2
Limekiln (Carmeuse)	518	333	169	137	12	12	15	31	22
U.S. Steel, Ltd.	2368	2746	2923	3130	3302	3335	2882	2703	2664

Tab. 2. The emissions selected metals from the iron and steel works U.S. Steel, Ltd [t.year<sup>-1</sup>]Tab. 2. Emisje wybranych metali z huty żelaza i stali U.S. Steel, Ltd [t.rok<sup>-1</sup>]

Year / Element	2009	2010	2011	2012	2013	2014	2015	2016	2017
As	0.158	0.147	0.119	0.026	0.025	0.031	0.039	0.243	0.258
Cd	0.107	0.134	0.149	0.062	0.058	0.072	0.073	0.125	0.124
Cr	0.707	0.785	0.876	0.191	0.042	0.045	0.045	0.028	0.048
Mn	2.418	2.386	2.263	2.807	3.09	3.959	7.69	0.728	0.910
Cu	0.613	0.794	0.932	0.001	0.001	0.001	0.002	0.002	0.011
Zn	7.141	8.553	8.043	5.132	2.988	2.802	3.189	6.395	7.037
Pb	13.44	16.315	17.785	17.834	17.244	21.329	20.871	60.74	61.219

ing buildings, 4–12 m in the case of suburban and rural sites no. 7–11. The four open polyethylene cylinders (inside diameter – 12.5 cm) filled with 200 ml of pure deionized water fitted on a stand were used for sampling. In laboratory the contents of cylinders were filtered by a vacuum filtration through 0.40 µm membrane filters to separate the “water soluble” and “insoluble” fractions (PM). The soluble fraction was analyzed after each sampling. The insoluble fraction designated for analysis was prepared by cumulation of six monthly samples into the one semi-annual sample – summer and winter period (mid-April – mid-October) and by mineralization using a microwave digestion. The elements were analyzed by the atomic absorption spectroscopy using the device VARIAN AA240 FS with GTA 120 and VGA-77. Since October 2012, the device ICP MS Agilent 7700 has been used for analysis. In the article, the results of 10 summer and 9 winter periods from 2009 to 2018 are processed.

## Results and discussion

Table 3 presents the average daily fluxes ( $\mu\text{g}\cdot\text{m}^{-2}\cdot\text{day}^{-1}$ ) of observed elements and solid particles – PM (“water insoluble” part of AD) from total bulk deposition and basic statistic parameters for all sampling sites and the whole monitored period (September 2009 – October 2018). Absolute values of deposition of observed elements and PM from sites north of ironworks are relatively balanced, without increased values at site No.5. The site is located in the city center with heavy traffic and high construction activities during monitored period, about 2 km northward of the thermal power station, which used coal apart from gas as fuel mainly in heating season. The maximum values of all studied metals and PM were recorded at sites localized southerly, near the ironworks. The average ratio between atmospheric deposition at site No. 9 and sites No. 1- 8 (ADSite 9/ADSites 1-8) for the observed elements were in the range 2.2 to 16.5 (Fe = 8.4, Al = 3.9, Mn = 16.5, Zn = 2.5, Pb = 5.2, Cu = 4.3, Cr = 6.3, Cd = 2.2 and As = 2.3).

In the table 4 is shown the average percentage representation of the deposition of trace elements bound to the “water-insoluble” (PM) part of AD and the ratio between summer and winter atmospheric deposition of the monitored elements and PM. To the insoluble phase, the monitored elements in order of Al, Fe, Mn Cr, Pb and As are bounded. Cd and Zn

are preferentially bounded to the soluble phase for sites north of ironworks. South of the ironworks representation of all observed metals in the solid insoluble phase is predominated and their representation is relatively high. Except monitored elements properties it is probably related with average size and thus with the surface of the particles. With increasing distance from the source of particulate emissions, proportion of smaller particles on their overall particle size distribution is rising.

Deposition of particulate matter and aluminum is significantly higher in summer period (ratio S/W - 0.55 and 0.60). There are better conditions for wind erosion and resuspension of particles from soil horizon, road traffic, agricultural and construction activities as well as the increased presence of organic detritus in the air in summer period. In winter, the deposition fluxes of solid particles are partially deprived of these effects. In winter seasons increased amount of components of AD, whose origin is in energy burning of fossil fuels on local and regional scale is assumed. In the area of Košice, slightly higher or balanced values of deposition fluxes in the order Pb, Cr, Fe, Mn, Cu and Cd ( $R_{w/s} = 1.21 - 1.00$ ) were found in winter. In the case of zinc ( $R_{w/s} = 0.79$ ) and arsenic ( $R_{w/s} = 0.63$ ) the higher values were recorded in the summer period. The smallest seasonal differences for all observed components were detected at sites near the ironworks (No. 9 and 10) and the station No. 5.

The relationship between the deposition of the observed elements and PM from all measured period and the distance from the iron and steel works was studied by regression analysis. The results are graphically presented in the figure 2. The significant dependence was found in descending order for the Mn, Fe, PM, Cr, Al and partly for Zn. In the case of elements Pb and Cu only small significant dependence was found. Deposition of Cd and As does not show dependence.

The statistical dependence between individual atmospheric deposition of observed metals and PM was evaluated by Pearson’s correlation analysis. The Pearson’s cross-correlation coefficients are summarized in the Table 5. The highest values of correlation coefficients ( $r = 0.82$  to  $0.94$ ) were calculated between elements where their dominant source are technologies of ironworks, namely Mn, Fe and Cr. The high values of the correlation coefficients were calculated for these

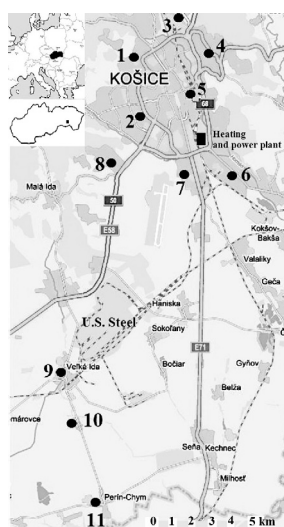


Fig. 1. Location of the sampling sites  
Rys. 1. Lokalizacja miejsc pobierania próbek

Tab. 3. The average daily fluxes of atmospheric deposition of particles (PM – insoluble fraction) and analyzed elements from 10 summer and 9 winter monitored periods (April 2009 – October 2018), [ $\mu\text{g}\cdot\text{m}^{-2}\cdot\text{day}^{-1}$ ] (\* – Finished April 2014, \*\* – Finished April 2017, # – Start sampling October 2011)  
Tab. 3. Średnie dzienne strumienie emisji cząstek do atmosfery (PM – frakcja nierozpuszczalna) i analizowane pierwiastki z 10 okresów letnich i 9 monitorowanych w okresie zimowym (kwiecień 2009 r. – październik 2018 r.), [ $\text{Mg}\cdot\text{m}^{-2}\cdot\text{dzień}^{-1}$ ] (\* – Zakończony kwietnia 2014 r., \*\* – Zakończony w kwietniu 2017 r., # – Początek pobierania próbek z października 2011 r.)

Site	PM	Fe	Al	Mn	Zn	Pb	Cu	Cr	Cd	As
1	37187	2970	1166	63	83	23.1	11.7	5.5	0.34	1.11
2	38290	3070	1315	62	69	24.8	10.1	5.9	0.26	1.24
3**	43916	2933	1039	60	87	19.9	8.7	5.4	0.40	0.87
4*	38840	3432	1007	64	83	9.8	9.3	4.8	0.27	1.14
5*	83909	5214	1751	96	112	14.4	17.3	8.6	0.34	1.26
6*	30919	2797	870	53	67	7.6	8.5	4.8	0.22	0.51
7	44318	5029	1288	92	102	39.2	11.2	6.2	0.32	1.37
8**	31201	3265	1031	75	116	23.9	9.0	5.2	0.28	0.74
9#	163694	28120	4310	1106	219	110.7	42.3	34.1	0.65	3.63
10#	129124	21206	3303	652	207	105.0	19.6	18.3	0.66	2.47
11#	49492	4438	1473	79	93	28.5	13.0	4.7	0.19	1.50
Average (n = 166)	60331	7131	1661	211	113	9.2	16.0	9.2	0.36	1.45
Min.	11019	1097	173	19	35	0.3	0.9	0.3	0.04	0.02
Max.	264981	34032	6922	1905	695	63.4	404.1	63.4	3.01	13.01
Median	43591	3528	1171	72	84	5.6	10.9	5.6	0.26	1.06

elements with Al ( $r = 0.70$  to  $0.82$ ), Pb ( $r = 0.39$  to  $0.68$ ) and Cu ( $r = 0.39$  to  $0.54$ ), relatively lower with Zn ( $r = 0.50$  to  $0.5$ ), Cd ( $r = 0.48$  to  $0.53$ ), and As ( $r = 0.35$  to  $0.55$ ). In the case of PM, the highest values of correlation coefficients were found for elements Fe, Al, Mn and Cr ( $r = 0.84$  to  $0.73$ ). Also, for other elements, the correlation values were relatively high ( $r = 0.57$  to  $0.44$ ).

The deposition fluxes of the elements from the area of Košice were compared with results from different urban and suburban areas (Prášková et al., 2008; Nicholson et al., 2008; Spiegel et al., 2008; Golomb et al., 1997; Mijić et al., 2011; Azimi et al., 2005; Wong et al., 2008). In this comparison, above average deposition of Fe, Mn and Cr, partially in the case of Zn was detected. The most significant differences were found for the deposition of iron and manganese. The average Fe deposition at stations in the city was 2–3, respectively 5–7 times higher compared with rural respectively urban areas. At the site No. 9, deposition of Fe and Mn was 15 or 38 times higher, deposition of Cr 2.5 or 6 times higher. The site is located approximately 1 km from the iron works area and their, almost 100% effect on Fe deposition can be assumed, which is fixed almost only to PM in AD. The calculated impact of

resources of ironworks on the deposition of Fe at other sites in the area was built on this fact. The average percentage of Fe deposition from PM at site No. 9 was taken as the basis 100% ( $B_{100\%}$ ) after deduction of regional background ( $AD_{\text{Fe Background}}$ ) of iron deposition:  $B_{100\%} = (AD_{\text{Fe Site No. 9}} - AD_{\text{Fe Background}}) / (AD_{\text{PM Site No. 9}} - AD_{\text{Fe Background}}) \cdot 100$ .

The corresponding values from the other sites were compared with the result of this calculation.

The average value of iron deposition from the area Kropachy (7 sites) obtained by using the same methodology was used as a background ( $AD_{\text{Fe Background}} = 600 \mu\text{g}\cdot\text{m}^{-2}\cdot\text{day}^{-1}$ ) [12]. Calculating contemplated with  $2 \times AD_{\text{Fe Background}} = 1200 \mu\text{g}\cdot\text{m}^{-2}\cdot\text{day}^{-1}$  for sites in the city (No. 1–8) due to the impact of other sources of emissions in urban environment. Iron in the  $\text{Fe}_2\text{O}_3$  form was taken in the calculation for correction of PM deposition. In the table 5 the calculated average percentage proportion of emission sources from iron and steel works on the AD of Fe fluxes at the individual sites is shown.

The portion of emission sources of iron and steel works on the Fe fluxes at the individual sites in the city was calculated in the range from 24.7 to 54.1%. The portion decreases proportionally with increasing distance as illustrated in Figure 3.



Tab. 4. The average element abundances in insoluble fraction (PM) [%] and the ratio between winter and summer atmospheric deposition of the observed elements and PM

Tab. 4. Średnia ilość pierwiastków we frakcji nierozpuszczalnej (PM) [%] oraz stosunek zimowej i letniej deponycji atmosferycznej obserwowanych pierwiastków do PM

Element	PM	Fe	Al	Mn	Zn	Pb	Cu	Cr	Cd	As
Element abundances [%]	-	96	97	58	23	58	42	71	24	65
Ratio between AD <sub>w</sub> /AD <sub>s</sub>	0.55	0.60	1.20	1.12	0.79	1.21	1.00	1.21	1.00	0.63

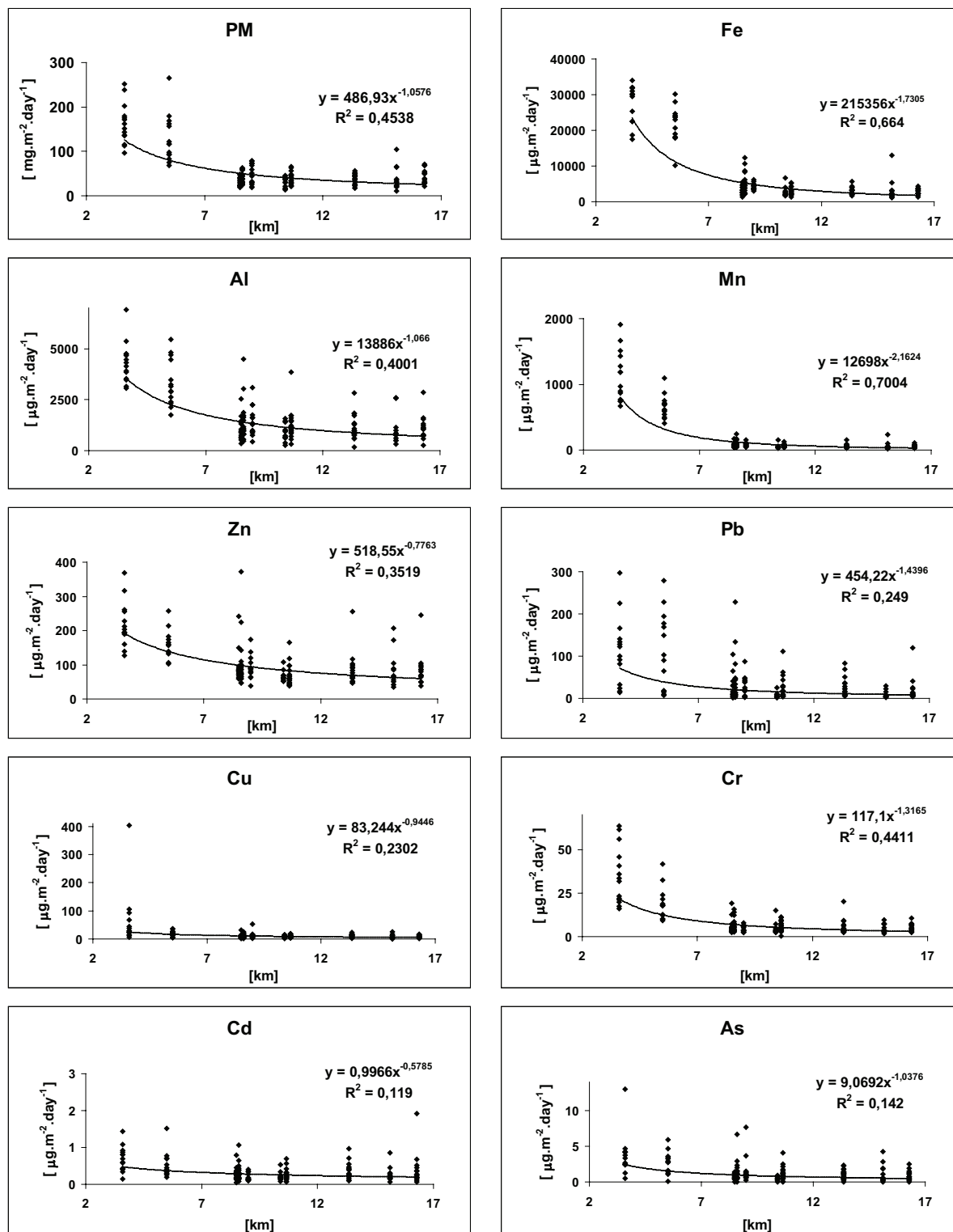


Fig. 2. The dependence between the deposition of the PM and observed elements and the distance from the iron and steel works U.S. Stel, Ltd.  
Rys. 2. Zależność między osadzeniem się PM a obserwowanymi pierwiastkami oraz odległością od huty żelaza i stali U.S. Stel, Ltd.

Tab. 5. The Pearson's cross-correlation coefficients between fluxes of trace elements (n = 166)  
 Tab. 5. Współczynniki korelacji krzyżowej Pearsona między strumieniami pierwiastków śladowych (n =166)

	Fe	Al	Mn	Zn	Pb	Cu	Cr	Cd	As
PM	0.84	0.84	0.82	0.57	0.44	0.51	0.73	0.44	0.51
Fe		0.82	0.94	0.52	0.68	0.44	0.82	0.45	0.55
Al	0.82		0.78	0.47	0.48	0.36	0.70	0.34	0.49
Mn	0.94	0.78		0.53	0.55	0.48	0.91	0.49	0.45
Zn	0.52	0.47	0.53		0.33	0.30	0.50	0.56	0.32
Pb	0.68	0.48	0.55	0.33		0.17	0.39	0.47	0.57
Cu	0.44	0.36	0.48	0.30	0.17		0.54	0.43	0.36
Cr	0.82	0.70	0.91	0.50	0.39	0.54		0.43	0.35
Cd	0.45	0.34	0.49	0.56	0.47	0.43	0.43		0.36
As	0.55	0.49	0.45	0.32	0.57	0.36	0.35	0.36	

Tab. 6. The average percentage portion of emission sources of iron and steel works on the Fe deposition fluxes at the individual sites  
 Tab. 6. Średnia procentowa wielkość emisji żelaza i stali w poszczególnych miejscach

Site	1	2	3	4	5	6	7	8	9	10	11
Distance from iron works (km)	13.4	10.7	16.3	15.1	12.3	10.4	8.6	8.5	3.6	5.5	9.0
The average percentage portion (%)	30.0	30.8	24.7	36.2	29.4	32.9	54.1	42.1	100.0	94.5	40.8

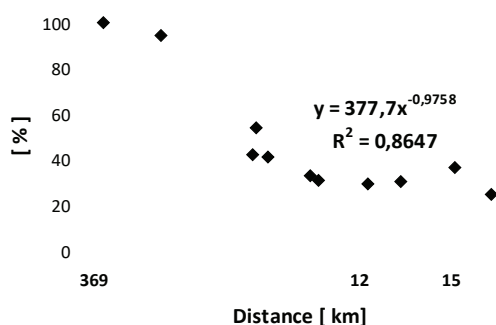


Fig. 3. The portion of emission sources of iron and steel works on the Fe deposition fluxes in depending on the distance sampling sites from sources of iron and steel works

Rys. 3. Emisja z hut żelaza i stali w zależności od odległości miejsc pobierania próbek od źródeł huty żelaza i stali

The lowest portion was found at the furthest station No. 3, the highest portions at the sites located closest to the ironworks. With respect to composition of emissions from ironworks, the iron is their major component and also of AD of PM. It can be assumed that this specified proportion of the ironworks sources on deposition is not valid only for Fe but also for PM and other components fixed mainly to particles produced from these sources.

### Conclusion

A detailed analysis of the atmospheric deposition of studied metals and solid particles proved a decisive influence of emissions from the ironworks on the composition of AD in the monitored area. Comparatively high seasonal and spatial variability of deposition of monitored elements and solid particles was detected on a relatively small area in urban and sub-

urban environment. The proportion of the ironworks sources of environmental burden on a monitored area was quantified based on the iron deposition. Compared to the values of deposition measured in the other areas, extremely high values of iron, manganese and chromium deposition as well as high, above-average values of other monitored elements were measured in the proximity of the ironworks. On the basis of the emission situation of the monitored area, it is possible to use selected compounds of the AD as an environment quality indicator and to quantify the contribution of emissions to area's environmental stress.

### Acknowledgment

The authors are grateful to the Slovak Grant Agency for Science (Grant No. 2/0165/19) for financial support of the work.

## Literatura – References

1. AZIMI, S.; ROCHER, V.; GARNAUD, S.; VARRAULT, G.; THEVENOT, D.R. Decrease of atmospheric deposition of heavy metals in an urban area from 1994 to 2002. *Chemosphere*. 2005, No. 6, p. 645-651. ISSN 0045-6535.
2. HANČULÁK, J., FEDOROVÁ, E., ŠESTINOVÁ, O., ŠPALDON, T., MATIK, M. Influence of iron ore works in Nižná Slaná on atmospheric deposition of heavy metals. In *Acta Montanistica Slovaca*, 16, 2011, p. 220-228. ISSN 1335-1788.
3. HANČULÁK, J. et al. Atmospheric Deposition of Solid Particles in the Area of Košice. *Solid State Phenomena*, 2016, vol. 244, p. 188-196.
4. HANČULÁK, J. et al. : Influence of Iron and Steel Industry on Selected Elements of Atmospheric Deposition in the Urban and Suburban Area of Košice (Slovakia). In *Inżynieria Mineralna – Journal of the Polish Mineral Engineering Society*, 2015, vol. 16, no. 2, p.95-102.
5. KARA, M. et. al. Seasonal and spatial variations of atmospheric trace elemental deposition in the Aliaga industrial region, Turkey. In: *Atmos. Res.*149 (2014) 204–216.
6. MIJIĆ, Z., STOJIC, A., PERIŠIĆ, M., RAJŠIĆ, S., TASIĆ, M., RADENKOVIĆ, M., JOKSIĆ, J. Seasonal variability and source apportionment of metals in the atmospheric deposition in Belgrade. *Atmospheric Environment*, 44,3, 2010, 3630-3637.
7. MEHRAZIN, O., RUBAN, V., RUBAN, G., LAMPREA, K. Assessment of atmospheric trace metal deposition in urban environments using direct and indirect measurement methodology and contributions from wet and dry depositions *Atmospheric Environment*, 168 (2017), 101-111.
8. NEIS (Národný emisný informačný systém) [online]. c2015 [cit. 2019-04-18]. Dostupné z WWW: <<http://www.air.sk> (National Emission Information System of Slovak Republic)
9. NICOLÁS, J.F. et. al., 2008. Quantification of Saharan and local dust impact in an arid Mediterranean area by the positive matrix factorization (PMF) technique. *Atmos. Environ.* 42, 8872-8882.
10. NICHOLSON, F.A. et al. An inventory of heavy metals inputs to agricultural soils in England and Wales. *Science of the Total Environment*. 2003, Vol. 311, p. 205-219. ISSN 0048-9697.
11. PRAŠKOVÁ, L.; KUBÍK, L.; MALÝ, S.: The control and extraneous matter monitoring in the farmlands and farm inputs. Annual report 2005. Central institute for supervising and testing in agriculture in Brno, 2006, p. 13.
12. PUTAUD, J.P. et al., 2010. A European aerosol phenomenology-3: physical and chemical characteristics of particulate matter from 60 rural, urban, and kerbside sites across Europe. *Atmos. Environ.* 44, 1308-1320.
13. QUEROL, X. et. al. 2007. Source origin of trace elements in PM from regional background, urban and industrial sites of Spain. *Atmos. Environ.* 41, 7219-7231
14. SPIEGEL H., BÖHM K.E., ROTH K. SAGER, M. Atmospheric deposition of trace metals onto arable land in Austria. *Proc. 7th Intern. Conf. On the Biogeochem. Of Trace Elements; Uppsala`03*, 2003, p. 90.
15. WONG, C.S.C.; LI, X.D.; ZHANG, S.H.Qi.; PENG, X.Z. Atmospheric deposition of heavy metals in the Pearl River Delta, China. *Atmospheric Environment*. 2003, Vol. 37, p. 767-776. ISSN 1352-2310.

### *Wybrane cechy charakterystyczne depozycji atmosferycznej na terenie Koszyc*

Artykuł dotyczy emisji do powietrza cząstek stałych i wybranych pierwiastków w typowym obszarze miejskim z wieloma źródłami zanieczyszczeń. Głównymi źródłami zanieczyszczeń są sąsiednie huty żelaza i stali oraz elektrownia ciepłna. Próbkę pobrano z jednego z miejsc, które znajdują się w odległości od 3,6 do 16 km od huty żelaza i stali. Badano cechy ilościowe i jakościowe całkowitej emisji cząstek stałych, strumienia osadzania pierwiastków Fe, Al, Mn, Zn, Pb, Cu, Cr, Cd, As oraz ich sezonowe zmiany. Przedstawiono wyniki z lat 2009–2018. Badania wykazały znaczący wpływ lokalnych źródeł zanieczyszczeń na badane parametry zanieczyszczeń w atmosferze. W porównaniu z wartościami depozycji zmierzonymi w innych obszarach, wyjątkowo wysokie wartości zawartości żelaza (28, 120), manganu (1106) i chromu ( $34,1 \mu\text{g}\cdot\text{m}^{-2}\cdot\text{dni}^{-1}$ ), a także wysokie, ponadprzeciętne wartości innych monitorowanych pierwiastków zmierzono w pobliżu huty. Część źródeł emisji hut żelaza i stali w poszczególnych lokalizacjach w mieście stwierdzono w przedziale od 24,7 do 54,1%. Na podstawie sytuacji emisyjnej monitorowanego obszaru można zastosować wybrane związki AD jako wskaźnik jakości środowiska i określić ilościowo udział emisji w obciążeniu środowiskowym obszaru.

**Słowa kluczowe:** emisja do atmosfery, emisja, huty żelaza i stali, metale



# Land Assessment Techniques

Roxana Claudia HERBEI<sup>1)</sup>, Aronel MATEI<sup>1)</sup>, Clementina MOLDOVAN<sup>1)</sup>,  
Danut CHIRILA<sup>1)</sup>

<sup>1)</sup> University of Petrosani, Romania

<http://doi.org/10.29227/IM-2020-01-38>

Submission date: 01-02-2020 | Review date: 02-03-2020

## Abstract

An assessment report may involve the assessment of unimproved land (the land that is developed for agricultural or development purposes), the land that constitutes a site (land set up and ready to be used for a specific purpose) or the land component of a built property. In each of these cases, the Valuer must describe and analyze the land in question. A description of a land or site is a detailed list that includes: legal description, other titles and information on the physical characteristics of the land. In the land or site analysis, this information is carefully studied in relation to the neighborhood characteristics that influence the usefulness and tenacity of the land or site are useful in determining the best use (considered as free) and in estimating the value of the land.

**Keywords:** assessment, report, land, method

## Introduction

The main methods used to describe real estate are: points and boundaries; a lot or part of a division, division or concession of division; a lot or part of a lot in an urban plan; reference plan; the number of a plot registered in the title plan over the land; and number of units in co-ownership or plan.

The point and boundary system describes the boundaries of a property in terms of reference points. The milestones comprise the starting point, which is also the point of return and all intermediate points that may be surveillance points, milestones, or monuments. Boundaries describe the course or angular direction in which a reference point moves to another. Distances are measured in the description of border and border points. The border and border system was first used to determine the boundaries of parcels of irregular shapes that could not be adequately described by rectangular tracking and some rights of servitude and crossing rights.

Reference Plans represent a description of the property design, which can also be highlighted through the system of margins and margins.

The Rectangular Section Surveillance System, Division and Concession Division has been established to facilitate the oversight and sale of public land.

The system of registered plans and lots simplifies the description of small plots through sections, divisions and the concession system. Subdivisions of the sections are divided into plans, which are then divided into lots and smaller plots.

The evaluator should consider development regulations, possible changes, building norms, physical limitations, and public land use programs, government policies to determine the best use of land or site. The value of taxing a property is rarely a solid indicator of market value. In order to describe the physical characteristics of the land plot or site, the assessor must consider the size and shape, corner influence, excess land, topography, utilities, site layout, location, physical and environmental factors. The evaluator should describe the width and depth of the site, the regularity and irregularity of

the shape, the façade and the depth-to-face ratio. The evaluator should study the interaction of topographic features with land use. The soil and subsoil characteristics are important in agriculture, while the slope, the natural drainage system and the foundation of the land are essential in building construction.

The evaluator collects and analyzes data on the land plot to be evaluated and comparable lots, identifies the related property rights, any legal restrictions, site physical characteristics, all utilities available, and site improvements that affect the site development potential. The value of a site or plot of land is based on its best use, considered free and fit for development in its best and most economical use. It is said that land has value while construction contributes to value. Buildings that do not contribute to the value of the property constitute a penalty for the value equal to the demolition cost. The best use of a site may be existing or different. Establishing the best use should be specific and justified by the market.

Land valuation techniques:

1. Direct comparison.
2. Proportion (allocation).
3. Extraction.
4. Parceling.
5. Residual value technique.
6. Capitalization of the basic rent.

The six procedures used in land valuation are derived from the three value approaches.

Direct comparison is the most commonly used and preferred method of land valuation when comparable data is available. In using this method are analyzed, compared, and corrected sales data of similar plots for differences in property valuation.

Compared items include:

- property rights;
- legal restrictions;
- financial conditions;

- sales and market conditions;
- location;
- physical characteristics;
- utilities available;
- zoning;
- best use.

The Proportion Procedure is based on the typical ratio between the value of the land and the value of the construction, for specific categories of real estate and specific locations. The report is more confident when the construction is more recent. The higher the age, the share of the value of the land in the total value decreases. Proportion is a less decisive method than others, but is useful if comparable transactions are not available.

Extraction is a similar procedure in which the construction contribution is deducted from the total property value. The value of the land derived from this procedure should be used to estimate the value of land in the properties built in rural areas and in cases where buildings contribute little to the total value of the property.

The plotting process is used for land valuation when plotting and development is the best use of the land to be assessed and sales data for such lots is available. The evaluator begins by determining the number and size of batch that can be created by land partitioning, physically, legally and economically. The lots are then analyzed to estimate the sales price most likely the development period and the rate of absorption of the proposed batches. From the anticipated gross sale price, the real state evaluator deducts all direct and indirect expenses and the entrepreneur's profit. Net sales revenue is brought to its present value at market capitalization rate for the period required for project development and market absorption. The resulting value indication should be compared with the prices paid for similar unprepared land parcels and having the best parcel use. There are some more sophisticated variants of this method.

The residual value technique is used when no sales data on similar free land parcels are available. In order to apply this procedure, it is necessary:

- the known or estimated value of the building;
- the known or estimated net operating income (SNE);
- capitalization rates for land and construction extracted from the market.

The evaluator determines which current or hypothetical construction is the best use of the site; then estimate the SNE annually stabilized, generated property. The SNE attributable to the building is deducted from the total VNE and what remains, the residual income of the land is capitalized at the market rate to obtain an estimate of the value of the land. In another variant of the residual land procedure, the evaluator simply evaluates the property as being built and reduces the construction cost and the entrepreneur's profits from the total value of the property.

Capitalization of the base rent is used in the land valuation when the basic rent corresponds to the value of the land owner's interest in the property. Derivative market capitalization rates are used to convert the base rent into an indication of the market value of the land. This procedure is useful when

comparable sales of leased land indicate a range of rents and capitalization rates.

### Evaluation of lands

The lands belonging to the commercial company with state capital at the date of their establishment, which are necessary for carrying out the activity according to their object of activity, are assessed in lei according to art. 6 of the Government Decision no.834/1991, by the Management Boards, on the basis of the following formula:

$$V_t = V_b ((1 + N) * k)$$

where in:

$V_t$  – the value of the land;

$V_b$  – the base value of the land determined as the minimum limit at a level of 495 lei/sq m; (this methodology now applies a multitude of updates  $k$  currency ratio – leu)

This value was determined on the basis of the price of 5 lei per square meter corrected by 99 years of the concession period; (it is mentioned that in some locations in Bucharest, the concession price per square meter is variable and higher, so the basic price may be considered higher in special cases).

$(1 + N)$  represents the correction coefficient of the base value of the land in which  $N$  reflects the sum of the scores granted on criteria and its level will be less than or equal to 9.

Criteria based on which the notes are required for train trains, in the assessment operation are as follows:

a) The category of the locality

- village 0, 1
- communal village 0,2
- city 0,4
- municipality 0,6
- the county seat of the city 1,0
- Bucharest 15 \*

b) Location of the land

- land outside the locality 0,0
- land in the peripheral area of the locality 0,5
- land in the middle part of the settlement 0,8
- land in the central area of the locality 1,0

c) Economic functions and social characteristics of the locality

- localities with predominant agricultural activity 0,5
- localities with complex economic functions in industry and services 0,8
- localities with complex economic functions (industrial, services, agriculture) 1,0

d) The position of the land in relation to access to transport networks

- road transport 0,2
- rail transport 0,3
- River transport 0,5
- maritime transport 0,5
- air transport 0,5

- e) The technical and municipal equipment of the area where the land is located
- water-channel networks 0,5
  - electricity networks 0,5
  - heating networks 0,5
  - Natural gas networks 0,5
  - telephone networks 0,5
  - urban transport networks 0,5
- f) Geotechnical characteristics of the land
- normal land 1,0
  - difficult foundation grounds that require improved compaction, cushions, earth or ballast, ballast ballasts, and so on. 0,2 – land requiring drainage and flood control measures 0,4
  - lands in unstable areas – slopes of slopes, landslides
  - shingles, shoreline breaks 0,7
- g) Restrictions on the use of land in accordance with the general and general urban plan
- related regulations
  - function incompatible with the urban plan -1,5
  - function compatible with the urban plan with restrictions -1,0
  - function compatible with the urban plan 0,5
- h) Polluted lands with waste
- gaseous -0,3
  - solids -0,5
  - liquids -0,7
  - \*) are the resorts and areas with spa, climatic and tourist potential.

There are, however, some additional points that can be taken into account by the experts, of course not in strict evaluation cases for a state unit.

This methodology was completed by MEF 71906/9.05.1992. "Rules of reevaluation Fixed assets "in accordance with GD no. 26 "1992, whereby the value of the land calculated according to HG. 834/1991, as supplemented by the HG. 500/1994, shall be updated on that date with the coefficient  $K_i = 8,873$ .

The formula becomes  $V_t = V_b ((1 + N) (8,873) k)$ , where  $k$  will of course be taken into account by the currency exchange only on 30.05.1992 ( $\$ = \dots$ )

#### Evaluation of extra-urban (rural)

In order to be better understood some methods of free-valuation of agricultural land in urban and out-of-town areas, methods to be completed with the details of the land (locations, fertility, access, production, etc.)

It should be noted that there is no official or general binding methodology for evaluations.

At the free market price and because of the bureaucratic restrictions included in Law 18/1991, there are practically no transactions in this area, and when selling in this field, the land purchaser believes he will transfer it as intravilan land (as in big wholesale on access roads), and the price is traded no longer through direct transactions without complying with a specific methodology.

In this respect it is worth noting the obviously increased value of all land, likely to become neighborhoods of exclusive villas, wholesale, central warehouses. Comparable values are given in the comparative tables on the localities, a series of prices on the free market.

The lands inside the villages and communes each have a number of individualized micro indications, as shown below, which are indicative, and they can be filled in to best adapt to the reality and the specific situation of each land.

The following macros are to be considered in this spirit:

a) In the countryside, the optimal land for a normal individual household is 1000 square meters.

If this area is below 400 sqm, a decrease of 3–5% is applied. For plots of more than 100 square meters, which can be used for the vegetable, orchard or vineyard, an increase of 5–8% can be granted.

b) The land is located in a commune with access to a paved road or there is a railway station or a dump. Otherwise, a decrease of 3–8% will be applied.

c) Whether or not one has regular bus lines or is linked to a larger number of lands, a 3–5% increase can be granted.

d) The land is – inside the commune – close to the administrative center (town hall, school, shops, police, church) and with good road and road links with the road or railway station, this location gives the right to a 2–5% increase.

e) If the land has the possibility of separate access, in whole or in part, giving the opportunity to lease the vegetable garden or orchard, a 10% increase can be applied.

f) If the land, through its location, makes it possible to transform the building built on it and facing the street – in a commercial space, it is a great advantage and leads to a 10–15% increase.

g) The land is located on a paved street or even on the national road that passes through the town; this is a small extra advantage that can lead to an increase of 2–3%.

#### Land valuation based on agricultural production

Elements to be considered when establishing the strict production potential of the assessed land are:

a) the nature of the land from a pedological point of view: chernozems, reddish brown, brancig, podzol, saltings, intermediate soils;

b) the area's pebble and area-specific crop, which will be the basis for setting production, including the multi-annual rainfall average;

c) groundwater level.

These (a, b and c) are defined elements of the production taken into account in the assessment of agricultural land.

It is noted that for irrigated land, either from a local or even local system, the production taken into account will be multiplied by a coefficient of 1.3–1.5 compared to a land in the same micro-zone but not irrigated.

The determining factors for determining the costs of exploitation (agricultural works, transport, recovery).

The calculation of the annual net income is made up of the total value of the basic production + secondary production (straw, cocoons, etc.) and then the production costs are deducted.

Production costs are generally considered to be 40% of the gross production value for the vast majority of crops, a level

accepted under conditions of mechanization of agricultural works. This 40% level of production expenditure is calculated for land which in principle meets the following conditions:

- plan land with a tilt of up to 5%;
- land located within a maximum of 2 km from the edge of the locality where the land is located;
- the land next to a practicable road in all seasons;
- land so placed that the largest side has at least 300 m linear;
- ground a groundwater is at a depth greater than 2 m.

If the land surveyed does not meet these conditions, production costs ("CPs") will be corrected with "K" correction coefficients, which will be added to the CP, thus decreasing the annual net income.

The proposed K correction coefficients are:

K1 = 5% for land with a slope of 6-12%;

K2 = 10% for land with a slope above 12%;

K3 = 1% for each additional km above the 2 Km limit from the boundary of the building site, presented in point b;

K4 = 5% for land not adjacent to a modernized road, practicable in all seasons;

K5 = 5% for sloping land of over 6% and not having the minimum side 300 m linear.

#### Land valuation in urban areas – categories of land use

The land use category is determined by its economic destination, determined either naturally or artificially by the owner of the land. In general, there are two major groups of land use:

- A. Group of agricultural use;
- B. Non-agricultural use group.

Each of the two groups has five categories of use:

- A. arable land;
  - pastures;
  - meadows;
  - are you coming;
  - orchards.
- B. forests and other land with forest vegetation;
  - land with water and sulfur;
  - non-productive land;
  - roads and railways;
  - land with construction and other uses.

Each of the ten categories of land use is subdivided into subcategories. The names of the categories and subcategories of use are accompanied by symbols that are noted in cadastral plans and registers.

The definition of agricultural land use categories is presented below.

Arable land – means land that grows every year or several years and is cultivated with annual or melon plants. Within the arable land are different:

- arable itself;
- arranged for irrigation from which the rice crops, arable with broken trees.

When integrating into arable land, the following criteria are considered:

- a) Land for perennial forage crops, which are up to six years old at a time, is arable land;
- b) Arable land plundered as well as those under development;
- c) Arable land left unhealthy due to floods or other causes, is recorded in arable land;
- d) Arable lands landscaped or improved by desertification, irrigation; only direct productive areas and the areas occupied by the canals are delimited and included in the arable category. They are measured and plotted as linear details and are not included in the production area;
- e) Greenhouse, solarium and planting lands – are delineated on the perimeter of the construction and fall into categories of arable use, making that mention.

Pastures are either grassland or land naturally or artificially grounded by re-seed at 15–20 years. The following subcategories of use are distinguished:

- a) Pastures clean or covered only with grass vegetation;
- b) Wooded pastures are those pastures that apart from grassy vegetation and vegetation vegetation; only those with forest vegetation coverage of 10 ÷ 60% are considered forested pastures. When the forest vegetation is more than 60%, the wooded pasture is considered forest with legal regime in administration;
- c) Grassland pastures are rarely planted pastures with fruit trees to prevent landslides or those from orchards;
- d) Grazing and bush pastures are those pastures where bush and bush have an anti-erosive role and cannot be deflected.

Hayfields are those naturally or artificially grounded or under growed fields through reseeded. The following subcategories appear:

- a) Clean pots are covered with grassy vegetation only;
- b) The wooded meadows are partially covered with forest vegetation or invasion with bush, the coverage being less than 40%;
- c) Hedges with fruit trees come from degraded orchards or pastures where breeding perimeters have been formed and grazing is forbidden;
- d) Hedges with bush and bush are those in which bush and bush have anti-erosional value and cannot be gutted.

The vines comprise all the fields planted with vines. They have the following subcategories:

- a) living grafted and indigenous. Vine grafts are those that are based on a rootstock. Indigenous people are unpatched, developed on their own principles;
- b) live hybrids are those that are also called direct products. This category is endangered because the legislation in force forbids its planting, and the existing ones are isolated, hinders the mechanization process;
- c) vineyard nurseries are land intended for the production of vineyard material;
- d) hop plantations whose fruits are used in brewing.

With the identification and elevation of the area occupied by the vineyards, some details (such as troughs, canals, alleys) are measured and recorded on the topographic plane.

Live crops include all land planted with fruit trees or fruit plantations. These are the following subcategories:

Categories of use	Coefficient of arable transformation of the category of use
1. Arable	1 ha / 1 ha
2. Pastures	1 ha of pasture / 1 hectare of arable land, when the pasture can be turned into arable soil and relief quality. Where pasture differs from arable land around the land, relief and other factors that diminish the production potential, the arable equivalent will be set between 1 ÷ 0.4 ha arable for 1 ha of pastureland.
3. Hay	1 ha = 1 ha arable equivalent in arable land will be between 1 ÷ 0.5 ha arable for 1 ha of pasture.
4. The hybrid lives	1 ha live hybrid = 1 hectare of arable land
5. Noble living	1 hectare of noble can be equivalent to 1 ÷ 4 arable land, depending on soil quality, relief, planting age.
6. Classic cattle	1 ha of classical orchard may be equivalent to 1 ÷ 2 hectares of arable land, depending on soil quality, relief, planting age, well-established fruit basins, and plant production potential.
7. Intensive and superintensive livestock	1 hectare intensive and super intensive orchard may be equivalent to 1 ÷ 3,5 hectares of arable land, depending on the quality of the soil, the arrangement system, etc.

- a) intensive orchard - is the plantation that has a high density of trees at the surface unit, and trees are cared for by a specific technology. Also here are the super - intensive orchards with a density of over 2000 trees / ha;
- b) planting of fruit trees;
- c) fruit nurseries for the production of fruit propagating material;
- d) lobster plantations.

The criteria for equalizing agricultural land by category of use in arable equivalent are presented in the table.

#### Conclusions

The evaluator should consider development regulations, possible changes, building norms, physical limita-

tions, and public land use programs, government policies to determine the best use of land or site. The value of taxing a property is rarely a solid indicator of market value. In order to describe the physical characteristics of the land plot or site, the assessor must consider the size and shape, corner influence, excess land, topography, utilities, site layout, location, physical and environmental factors. The evaluator should describe the width and depth of the site, the regularity and irregularity of the shape, the façade and the depth-to-face ratio. The evaluator should study the interaction of topographic features with land use. The soil and subsoil characteristics are important in agriculture, while the slope, the natural drainage system and the foundation of the land are essential in building construction.



### Literatura – References

1. EGER, Albert F. Canadian Real Estate Finance : A Typical Transaction, 1st edition. Montreal: Ad Valorem Press Inc., 1990
2. GIMMY, Arthur E., and Martin E. BENSON. Golf Courses and Century Clubs: A Guide to Appraisal, Market Analysis and Financing. Chicago: Appraisal Institute, 1992
3. SAHLING Leonard. Real Estate Economics Special Report. "Rent or Buy: A Market Analyzes". New York: Merrill Lynch, June, 1990
4. HERBEI O. ULAR R. - Valuation of Real Estate, UNIVERSITAS Publishing House, Petrosani, 2006.
5. MATRIXROM CATALOAGES - RAPID ASSESSMENT OF BUILDINGS - HOUSES, HOUSES, HOTELS, 1995.
6. PADURE I, PALAMARIU M. - Evaluation of Real Estate, Global Media Image Publishing House, Deva, 2001.
7. HERBEI Roxana Claudia - Evaluation of Real Estate, Universitas Publishing House, Petrosani, 2013

### *Techniki oceny terenu*

*Raport oceniający grunt może obejmować ocenę nieulepszonych gruntów (gruntów zagospodarowanych pod cele rolnicze lub rozwojowe), gruntów stanowiących teren (gruntów utworzonych i gotowych do wykorzystania w określonym celu) lub części gruntu zabudowanego własność. W każdym z tych przypadków Valuer musi opisać i przeanalizować dany grunt. Opis gruntu lub terenu to szczegółowa lista, która obejmuje: opis prawny, inne tytuły i informacje o fizycznych cechach gruntu. W analizie terenu lub terenu informacje te są dokładnie badane w odniesieniu do cech sąsiedztwa, które wpływają na użyteczność i trwałość gruntu lub terenu, są przydatne w określaniu najlepszego wykorzystania (uznanego za bezpłatne) i szacowaniu wartości terenu.*

**Słowa kluczowe:** ocena, raport, grunt, metoda



# Carbon Quantum Dots (CQDs) Prepared from Waste Biomass as a New Class of Biomaterials with Luminescent Properties

*Lukasz JANUS, Marek PIĄTKOWSKI, Julia RADWAN-PRAGŁOWSKA<sup>1)</sup>, Aleksandra SIERAKOWSKA*

<sup>1)</sup> Cracow University of Technology, Faculty of Chemical Engineering and Technology, Warszawska 24 Street, 31-155 Cracow, Poland; email: jrpragłowska@chemia.pk.edu.pl

<http://doi.org/10.29227/IM-2020-01-39>

Submission date: 11-01-2020 | Review date: 05-04-2020

## Abstract

*Carbon Quantum Dots (CQDs) are objects with a size less than 10 nm that have the ability to emit radiation in the visible range from blue to red depending on the excitation radiation used. Quantum dots are used in in vitro bioimaging of cell structures or creation of biosensors. In contrast to classic nanodots, which are obtained from simple sulphides, selenides or metal tellurides, carbon quantum dots are constructed from a non-toxic, biocompatible carbon core, thanks to which it is possible to apply quantum carbon dots in bio-imaging in-vitro or in-vivo biological structures with minimal cytotoxic effect on cells.*

*The aim of the research was to obtain carbon nanodots capable of emitting fluorescence using lignin from waste biomass. The CQDs were functionalized with amino-acids. The result of the work was to obtain a series of CQDs with advanced luminescence properties using hydrothermal and microwave assisted methods. Ready products were investigated over their cytotoxicity.*

**Keywords:** carbon quantum dots, nanomaterials, waste biomass, biomaterials, luminescence

## Introduction

In the past few years, the scientists have focused on the nanomaterials development since the objects of the size below 100 nm tend to exhibit extraordinary optical, electrical and biological properties. Among nanorods, nanofibers or nanowires a new type of nanoparticles have been discovered – quantum dots. The nanomaterials can be described as objects of the size below 10 nm. Their most unique property is the ability to emit radiation in the visible region from blue to red. The emission depends on the excitation radiation which is applied. Therefore, such nanomaterials have a great potential in the industry and may successfully replace traditional fluorescence dyes [WANG, Youfu et al. 2014, LIANG, Zicheng et al. 2016, ZUO, Jun et al. 2015]. A special attention is paid to the so-called carbon quantum dots (CQDs) which are superior to other types of quantum dots with metallic or semi-metallic cores due to their lack of cytotoxicity [CAYUELA, Angelina et al 2016]. CQDs can be prepared from both synthetic and natural raw materials. The most interesting carbon quantum dots preparation strategy involves the application of biomass. As a feedstock, any organic component may be used. Carbon quantum dots can be obtained by various methods, including laser ablation, microwave radiation, conventional heating or ultrasounds. Carbon nanomaterials have a great potential in medicine and pharmacy, since they are water-soluble [ZUO, Jun et al. 2015, WANG, Ru et al. 2017]. Moreover, CQDs can undergo surface modification due to the presence of certain functional groups, which may differ depending on the raw material applied.

The surface functionalization may result in the enhancement of water-solubility [ZHANG, Miaomiao et al. 2016]. Also, it can positively affect luminescence properties such as

fluorescence quantum yield or photostability as well as resistance to photobleaching and photoblinking. The functionalization can be carried out using natural substances containing sulphur or nitrogen atoms [ROY, Prathik et al 2015, PIRES, Natalia et al 2015]. Currently, it is believed, that carbon quantum dots can replace traditional dyes, drug carriers and labelling agents in medicine and pharmacy due to their nanosize and ability to permeate cell membranes. CQDs can be applied in cells labelling and diagnostics since they may help to visualise various cell components. Carbon quantum dots can be modified by various biomolecules including proteins which help them to detect cancer cells [DAS, Rahul et al. 2017]. Functionalization of the nanomaterials with compounds containing phenol rings may give them antioxidant properties.

The functionalization process can be performed simultaneously with the nanodots formation during carbonization process, or after. The right choice of the modifying agent results in the preparation of the nanomaterials with desired characteristics [GAO, Xiaohui et al, 2016, PANDA, Snigdharani et al. 2018].

Lignin which is one of the most abundant polymers in the environment rich in carbon atoms [CHEN, Jao et al, 2016]. Thus, it is a cheap and easily accessible raw material for the quantum dots synthesis.

In this article, a strategy for the novel type of nanodots synthesis is proposed. The obtained nanomaterials were investigated over their physicochemical, especially spectroscopic and luminescence properties. Also, their cytotoxicity was investigated to verify their potential in medicine and pharmacy.

## Materials and methods

### Materials

Tab. 1. CQDs synthesis parameters

Tab. 1. Parametry syntezy CQD

Sample	Lignin, g	HCl, ml	water, ml	Modifying agent, g	Modifying agent	Time, h	Temperature, °C
1	0.50	0.50	5.00	0.10	L-lysine	12	180
2					L-glutamic acid		
3					L-aspartic acid		
4					L-cystein		

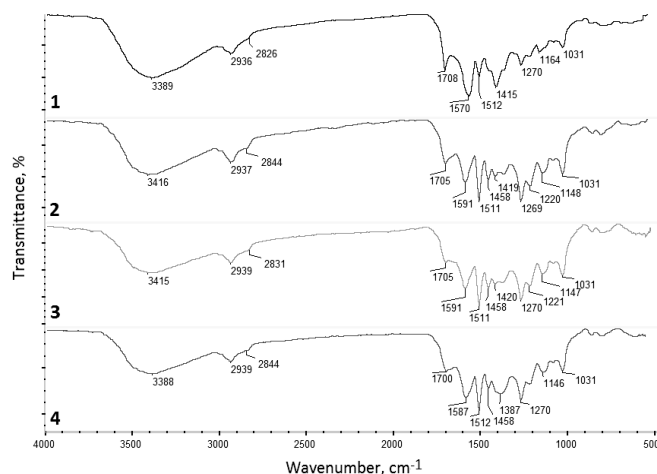


Fig. 1. Presents FTIR spectra of the obtained samples

Rys. 1. Przedstawia widma FTIR uzyskanych próbek

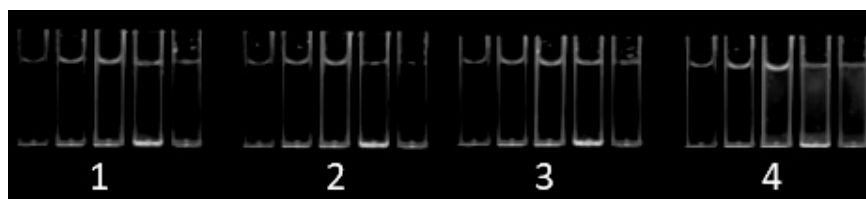


Fig. 2. Luminescence properties of the prepared samples

Rys. 2. Właściwości luminescencyjne przygotowanych próbek

Fibroblast growth medium (FGM) and human dermal fibroblasts (HDF), aminoacids (L-lysine, L-glutamic acid, L-aspartic acid, L-cystein), XTT assay were purchased from Sigma Aldrich, Poland. Ethanol, methanol, NaOH were purchased from Avantor, Poland. Lignin was obtained from the wood during extraction process.

### Methods

#### Carbon quantum dots synthesis

Carbon quantum dots were obtained by hydrothermal method using lignin as a raw material.

As modifying agents aminoacids were used (L-lysine, L-glutamic acid, L-aspartic acid, L-cystein).

The nanomaterials synthesis was carried out in autoclave (parameters given in Table 1). After reaction, the products were neutralized with NaOH solution and purified on membranes for 96h and dialysed on 500–1000 MWCO to remove contaminants.

#### Antioxidant properties study

To perform antioxidant properties study a solution of DPPH in methanol was prepared with absorbance = 1. The measurements were performed using Aligent 8453 spectrophotometer at 517 nm.

To determine the capability of free radicals removal, 0.10 g of each sample was placed in 5 ml of DPPH solution and left in darkness for 1 hour. Then, the absorbance of each solution was measured at 517 nm. The percentage of the free radicals removed was calculated using following Equation:

$$\%S = \frac{A_s - A_c}{A_c}$$

where:

%S – the % of the free radicals which were neutralized

$A_c$  – the absorbance of the DPPH solution without the sample

$A_s$  – the absorbance of the DPPH solution containing sample

#### Luminescence properties analysis

The quantum yield of the obtained products was determined according to following Equation:

$$Q_s = Q_r \left( \frac{A_r}{A_s} \right) \left( \frac{E_s}{E_r} \right) \left( \frac{\eta_s}{\eta_r} \right)^2$$

Q = Fluorescence quantum yield

$\eta$  = Refractive index of the solvent

A = Absorbance of the solution

E = Integrated fluorescence intensity of emitted light

Tab. 2. CQDs fluorescence quantum yield  
 Tab. 2. Wydajność kwantowa fluorescencji CQD

Sample	Fluorescence Quantum Yield, %	Fluorescence Quantum Yield after 30 days, %
1	9	9
2	6	5
3	7	7
4	11	11

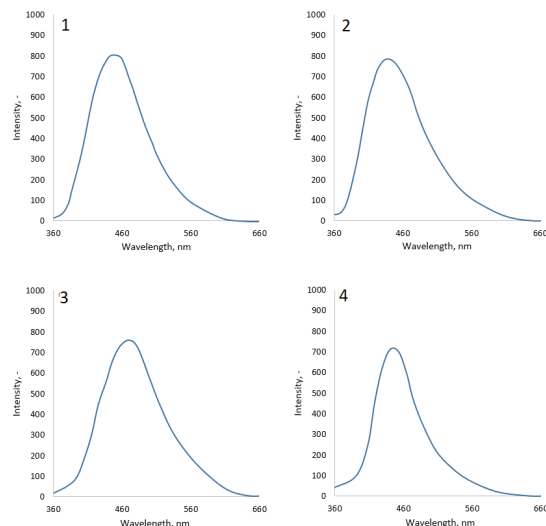


Fig. 3. Fluorescence spectra of the prepared samples  
 Rys. 3. Widma fluorescencji przygotowanych próbek

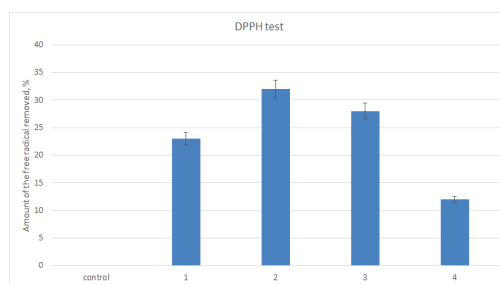


Fig. 4. Antioxidant properties of the prepared CQDs  
 Rys. 4. Właściwości przeciwutleniające przygotowanych CQD

Subscripts 'r' and 's' refer to the reference and unknown fluorophore respectively

The fluorescence quantum yield was determined by comparison to quinine sulphate standard solutions, which exhibited a fluorescence quantum yield of 0.54 at 365 nm.

#### Cytotoxicity study

Cytotoxicity of the CQDs was investigated using HDF (primary cells). The culture was performed for 48h at 37°C (95% CO<sub>2</sub>). As a culture medium complete FGM was applied. The cells were monitored under Delta Optics inverted microscope. The cytotoxicity was measured by XTT assay.

### Results and discussion

#### FTIR analysis

It can be noticed that all samples spectra show bands typical for lignin such as 3416–3388 cm<sup>-1</sup> that confirm the presence of hydroxyl functional groups coming from phenolic and

alcoholic groups. Wide and broad bands in the range between 3600–2600 cm<sup>-1</sup> 1708–1700 cm<sup>-1</sup> indicate presence of carboxylic functional groups in the structure of polymeric nanomaterials. Moreover aromatic groups vibrations can be observed at 1512–1511 cm<sup>-1</sup> and 1458–1415 cm<sup>-1</sup>. What is important some additional bands can be noticed coming from the incorporated modifying agents (amino acids). Amino groups presence can be confirmed by bands located at 1591–1570 cm<sup>-1</sup>.

#### Luminescence properties analysis

It can be noticed that all samples had luminescence properties under UV radiation and it depends on their concentration. One may also observe, that the best properties exhibit sample 1 and 4. The obtained spectra are typical for carbon quantum dot with luminescent properties.

#### Fluorescence quantum yield

Table 2 presents results of fluorescence quantum yield of the prepared nanomaterials. All of the CQDs have fluores-

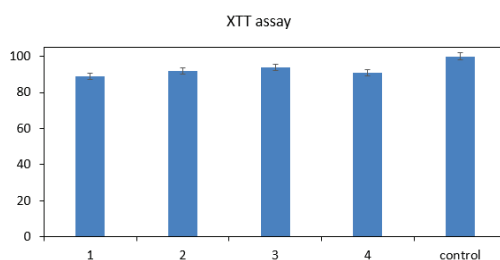


Fig. 5. Cytotoxicity of the prepared biomaterials  
Rys. 5. Cytotoksyczność przygotowanych biomateriałów

cence properties. It can be noticed that this property depends on the modifying agent was applied. The highest FQY can be observed in the case of nanodots obtained from lignin and doped with cysteine. Also, very good results were obtained for the sample functionalized with lysine. Moreover, all samples had very good photostability since no decrease of luminescence properties had been noticed after 30 days.

#### **Antioxidant properties study**

Figure 4 presents results of the antioxidant properties study performed by DPPH method. It can be observed that all of the obtained samples exhibited an ability to remove free radical. The highest antioxidant activity was observed for sample 2 and 3 which can be assigned to the presence of free amino groups coming from aspartic and glutamic acids incorporated into carbon dot. The lowest ability of free radicals scavenging was noticed for sample 4 prepared using cysteine as functionalizing agent.

#### **Cytotoxicity study**

Figure 5 presents results of cytotoxicity study carried out on human dermal fibroblasts. It can be noticed, that prepared nanomaterials are non-toxic to the prepared carbon dots since no any significant decrease in the amount of living cells

when comparing to the control culture can be noticed. Lack of cytotoxicity is correlated with the application of natural raw materials as well as carefully proceeded purification.

#### **Conclusion**

The aim of the following research was to obtain biocompatible carbon-based nanomaterials using waste biomass (lignin) as a raw material. Performed studies showed that proposed carbon quantum dot preparation strategy enabled obtainment of the advanced nanomaterials functionalized with aminoacids which enhance their biological activity. The modification of the carbon core was confirmed by FT-IR method. Luminescence properties study showed that CQDs had good fluorescence quantum yield and were photostable for 30 days. Moreover, it was shown that the samples had antioxidant activity. Finally, it was confirmed that prepared nanomaterials are not cytotoxic so they can be safely used in medicine and pharmacy, especially for bioimaging and cells labelling applications.

#### **Acknowledgements**

The research was supported financially by the Preludium project National Science Centre, Poland, Grant no. UMO-2017/25/N/ST8/02952.

## Literatura – References

1. CAYUELA, Angelina et al. Semiconductor and carbon-based fluorescent nanodots: The need for consistency. *Chemical Communications*, 52, 2016, 1311-1326, ISSN 1359-7345.
2. CHEN, Jao et al. Enhancing the quality of bio-oil from catalytic pyrolysis of kraft black liquor lignin. *RSC Advances*, 109, 2016, p. 107970-107976, ISSN 2046-2069.
3. DAS, Rahul et al. Highly luminescent, heteroatom-doped carbon quantum dots for ultrasensitive sensing of glucosamine and targeted imaging of liver cancer cells. *Journal of Materials Chemistry B*, 5, 2017, p. 2190-2197, ISSN 2050-750X.
4. GAO, Xiaohui et al. Carbon quantum dot-based nanoprobe for metal ion detection. *Journal of Materials Chemistry C*, 4, 2016, p. 6927-6945, ISSN 2050-7526.
5. LIANG, Zicheng et al. Probing Energy and Electron Transfer Mechanisms in Fluorescence Quenching of Biomass Carbon Quantum Dots. *ACS Applied Materials & Interfaces*, 8, 2016, p. 17478–17488, ISSN 1944-8244.
6. PANDA, Snigdharani et al. A novel carbon quantum dot-based fluorescent nanosensor for selective detection of flumioxazin in real samples. *New Journal of Chemistry*, 42, 2018, p. 2074-2080, ISSN 1144-0546
7. PIRES, Natalia et al. Novel and Fast Microwave-Assisted Synthesis of Carbon Quantum Dots from Raw Cashew Gum. *Journal of the Brazilian Chemical Society*, 26 (6), 2015, p. 1274-1282, ISSN 0103-5053.
8. ROY, Prathik et al. Photoluminescent carbon nanodots: synthesis, physicochemical properties and analytical applications. *Materials Today*, 18 (8), 2015, p. 1369-7021, ISSN 1369-7021.
9. WANG, Ru et al. Recent progress in carbon quantum dots: synthesis, properties and applications in photocatalysis. *Journal of Materials Chemistry A*, 5, 2017, p. 3717–3734 ISSN 2050-7488.
10. WANG, Youfu et al. Carbon quantum dots: synthesis, properties and applications. *Journal of Materials Chemistry C*, 2014, 2, 6921–6939. ISSN 2050-7526.
11. ZHANG, Miaomiao et al. Hyaluronic acid functionalized Nitrogen-doped carbon quantum dots for targeted specific bioimaging. *RSC Advances*, 2016,6, p. 104979-104984, ISSN 2046-2069.
12. ZUO, Jun et al. Preparation and Application of Fluorescent Carbon Dots. *Journal of Nanomaterials* 2015, 2015, p. 1-13, ISSN 1687-4110.

### *Kropki kwantowe węgla (CQD) przygotowane z biomasy odpadowej jako nowa klasa biomateriałów o właściwościach luminescencyjnych*

*Kropki kwantowe węgla (Carbon Quantum Dots – CQD) to obiekty o rozmiarze mniejszym niż 10 nm, które mają zdolność emitowania promieniowania w zakresie widzialnym od niebieskiego do czerwonego w zależności od zastosowanego promieniowania wzbudzenia. Kropki kwantowe stosuje się w bioobrazowaniu in vitro struktur komórkowych lub tworzeniu bioczuJNIKÓW. W przeciwieństwie do klasycznych nanodotów, które są otrzymywane z prostych siarczków, selenków lub tellurków metali, kropki kwantowe węgla są zbudowane z nietoksycznego, biokompatybilnego rdzenia węglowego, dzięki czemu możliwe jest zastosowanie kwantowych kropek węgla w bioobrazowaniu struktur biologicznych in vitro lub in vivo przy minimalnym działaniu cytotoksycznym na komórki. Celem badań było uzyskanie nanodotów węglowych zdolnych do emitowania fluorescencji przy użyciu ligniny z biomasy odpadowej. CQD sfunkcjonalizowano aminokwasami. Rezultatem prac było uzyskanie serii CQD o zaawansowanych właściwościach luminescencyjnych z zastosowaniem metod hydrotermalnych i mikrofalowych. Gotowe produkty badano pod kątem ich cytotoksyczności.*

**Słowa kluczowe:** kropki kwantowe węgla, Carbon Quantum Dots, nanomateriały, biomasa odpadowa, biomateriały, luminescencja





# Removal of Contaminants from Water by Bacterial Activity

Jana JENČÁROVÁ<sup>1)</sup>, Alena LUPTÁKOVÁ<sup>2)</sup>, Daniel KUPKA<sup>2)</sup>

<sup>1)</sup> Institute of Geotechnics, Slovak Academy of Sciences, Watsonova 45, 040 01 Košice, Slovakia; email: jencarova@saske.sk

<sup>2)</sup> Institute of Geotechnics, Slovak Academy of Sciences, Watsonova 45, 040 01 Košice, Slovakia

<http://doi.org/10.29227/IM-2020-01-40>

Submission date: 22-12-2019 | Review date: 01-02-2020

## Abstract

High concentration of sulphates and metals in waters is often as a consequence of anthropogenic activity and industry. The principles of the biological-chemical methods for pollution removal include various processes. The most widely metabolic pathway of sulphate-reducing bacteria - overall dissimilatory reduction - is the complete reduction of sulphate to hydrogen sulphide. Two major metabolic groups are known, depending on whether or not they can oxidize acetate. One group utilizes lactate, fumarate, propionate, butyrate, pyruvate, and aromatic compounds, which they typically oxidize to acetate, while the other group oxidizes acetate to CO<sub>2</sub> and H<sub>2</sub>O. Sulphate is reduced to H<sub>2</sub>S through a series of intermediate reactions. The end product of this reaction, hydrogen sulphide, can react with metal ions to form insoluble metal sulphides or reduce soluble toxic metals, often to less toxic or less soluble forms. This way, sulphate-reducing bacteria are utilizable in bio-elimination of sulphate and metal from water.

**Keywords:** pollution, sulphates, bacteria, reduction

## Introduction

Wastewaters coming from various industries are often characterized by numerous pollutants. High levels of metals, sulphates and other salt constituents and low pH are common characteristics of wastewater produced in mining and metal processing (Lens and Pol, 2000). The concentration of sulphates often exceeds legislative limits. 250 mg/L is a value allowed to be discharged according to SR Government Regulation 269/2010. Therefore, there is a need to treat these waters before being released to the environment.

Many techniques exist to remove sulphates from water, but in many cases they are generally expensive and produce high sludge volumes. There is an increasing interest in the potential biotechnological applications of bacterial sulphate reduction as an alternative method for sulphate removal from environmental contamination.

Sulphate-reducing bacteria (SRB) are those prokaryotic microorganisms that can use sulphate as the terminal electron acceptor in their energy metabolism, i.e. that are capable of dissimilatory sulphate reduction. Most of the SRB belong to one of the four following phylogenetic lineages (with some examples of genera): (i) the mesophilic  $\delta$ -proteobacteria with the genera *Desulfovibrio*, *Desulfobacterium*, *Desulfobacter*; (ii) the thermophilic Gram-negative bacteria with the genus *Thermodesulfovibrio*; (iii) the Gram-positive bacteria with the genus *Desulfotomaculum*; and (iv) the Euryarchaeota with the genus *Archaeoglobus* (Castro et al., 2000). They are considered to be chemoorganotrophic and strictly anaerobic bacteria with the ability to perform dissimilatory sulphate reduction with the simultaneous oxidation of the organic substrates (Postgate, 1984). Two major metabolic groups are known, depending on whether or not they can oxidize acetate (Widdel et al., 1993). Group of complete oxidizers (acetate oxidizers) has the ability to oxidize the organic compound to carbon dioxide, incomplete oxidizers (non-acetate oxidizers) carry out

the incomplete oxidation of the organic compound to acetate. Some species of the genera *Desulfobacter*, *Desulfococcus*, *Desulfosarcina*, *Desulfoarculus*, *Desulfomonile*, as well as *Desulfotomaculum acetoxidans* and *Desulfovibrio baarsii* belong to the group of complete oxidizers (Rabus et al., 2006). The incomplete oxidizers include *Desulfovibrio*, *Desulfomicrobium*, *Desulfobotulus*, *Desulfotomaculum*, *Desulfobacula*, *Archaeoglobus*, *Desulfobulbus* and *Thermodesulfovibrio* (Colleran et al., 1995). The growth kinetics for incomplete oxidizers is generally faster than the complete oxidizers. While the group of “complete oxidizers” oxidizes acetate to CO<sub>2</sub>, the incomplete oxidizers utilize lactate, fumarate, propionate, butyrate, pyruvate, and aromatic compounds, which they typically oxidize to acetate (Cao et al., 2012; Teclu et al., 2009; Liamleam and Annachatre, 2007). Sulphate is reduced to H<sub>2</sub>S through a series of intermediate reactions that include trithionate, thiosulphate and some organic sulphur compounds (Oluwaseun et al., 2009; Peck, 1993). The energy produced serves for growth and maintenance.

The aim of this work is to study the removal of sulphates from waters as a consequence of metabolic activity of bacteria and follow the associated processes and by-products.

In some cases, treatment by biological sulphate reduction is not pleasant because of odorous sulphide production. Nevertheless, it has been recognized as an efficient method for removing sulphate from wastewater and as a mean for treating a variety of sulphate-containing industrial effluents (Moosa et al., 2002). The main advantages of using SRB are minimal sludge production and removal of metals (Van den Brand et al., 2015). Biogenically produced hydrogen sulphide can react with dissolved metals to form metal sulphide precipitates since the solubility of most toxic metal sulphides is generally very low (Jong and Parry, 2006). Moreover, valuable metals from biologically precipitated metal sulphide can be recovered and recycled.



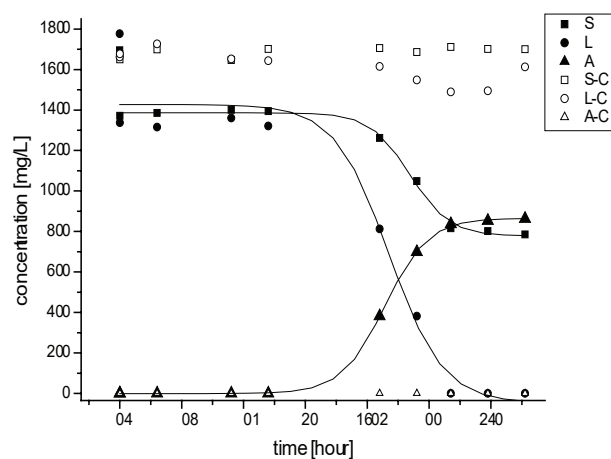


Fig. 1. Changes in nutrient medium Postgate's C influenced by bacterial sulphate reduction (S - sulphates, L - sodium lactate, A - acetate, S-C - sulphates in control sample, L-C - sodium lactate in control sample, A-C - acetate in control sample)

Rys. 1. Zmiany w pożywce C pod wpływem bakteryjnej redukcji siarczany (S - siarczany, L - mleczan sodu, A - octan, S-C - siarczany w próbce kontrolnej, L-C - mleczan sodu w próbce kontrolnej, A-C - octan w próbce kontrolnej)

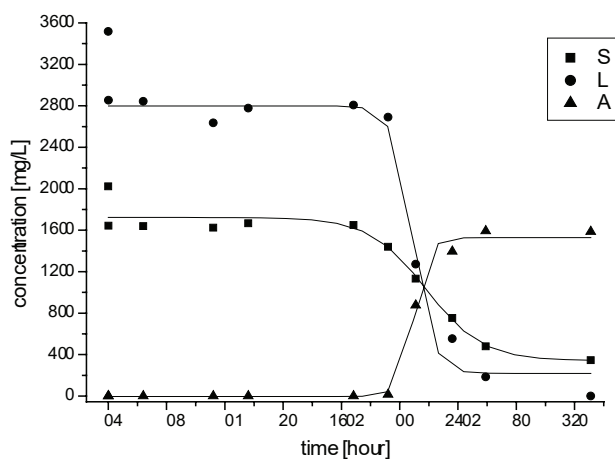


Fig. 2. Changes in modified nutrient medium Postgate's C influenced by bacterial sulphate reduction (S - sulphates, L - sodium lactate, A - acetate)

Rys. 2. Zmiany w zmodyfikowanej pożywce C pod wpływem bakteryjnej redukcji siarczany (S - siarczany, L - mleczan sodu, A - octan)

## Materials and methods

### Nutrient medium

Selective nutrient medium for bacteria enrichment – Postgate's C has the following composition (per liter of distilled water): 0.5 g  $\text{KH}_2\text{PO}_4$ , 1 g  $\text{NH}_4\text{Cl}$ , 4.5 g  $\text{Na}_2\text{SO}_4$ , 0.2 g sodium acetate, 2 g  $\text{MgSO}_4 \cdot 7\text{H}_2\text{O}$ , 0.1 g  $\text{CaCl}_2 \cdot \text{H}_2\text{O}$ , 1 g yeast extract, 0.1 g sodium thioglycollate, 0.1 g ascorbic acid, 0.5–1 g  $\text{FeSO}_4 \cdot 7\text{H}_2\text{O}$  and resazurin (Postgate, 1984).

### Growth and source of bacteria

The growth studies were performed in duplicate using a 20% inoculum. All cultures were stored in thermostat at temperature 30°C for 2–4 weeks.

Mixed culture of sulphate-reducing bacteria was obtained from mineral spring Gajdovka (Košice, Slovakia). This water is classified as potable, natural, mineralized water with pH 7–8 and strong  $\text{H}_2\text{S}$  odour.

### Source of organic substrate and sulphates

Sodium lactate (60 % w/w) was used as a carbon source in an assay to determine the sulphidogenic metabolic potential. Experimental cultures were grown with different concentrations of sodium lactate (2 and 4 g/L).

Stock solution with sulphate concentration 2 g/L was prepared by dissolving  $\text{K}_2\text{SO}_4$  (p.a. grade) in distilled water.

### Experiments of sulphates removal

Elimination of sulphates from water was studied in 2 different experiments. First of them was carried out in 1L glass bottles using medium Postgate's C, with concentration of sodium lactate 2 and 4 g/L,  $\text{FeSO}_4 \cdot 7\text{H}_2\text{O}$  dose 0.5 and 1 g/L and SRB inoculum 20%. The second study involved the usage of model solution instead of "classic" nutrient medium. 1L glass bottles were filled with 850 mL of model solution and 15% of SRB inoculum. Sodium lactate dose was 4 g/L. Trace elements according to Postgate's medium, sodium thioglycollate, ascorbic acid were added too. As a control for both experiments, same media were used, with lactate as carbon sources but without bacteria. The pH of solutions before experiments was adjusted at  $7.5 \pm 0.1$  with 0.01 M NaOH and 0.01 M HCl.

The experiments took 14 days, they were realized at room temperature and sampling was carried out in selected time intervals in order to determine sulphates decrease and lactate utilization.

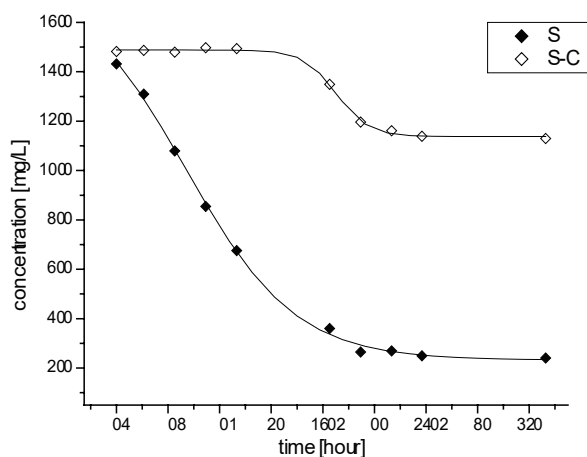


Fig. 3. Bacterial sulphate reduction in model solution (S – sulphates, S-C – sulphates in control sample)  
Rys. 3. Bakteryjna redukcja siarczanu w roztworze modelowym (S – siarczany, S-C – siarczany w próbce kontrolnej)

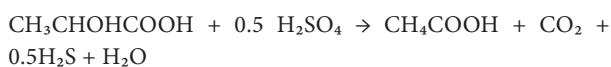
### Methods

Growth of the SRB was monitored microscopically using an optical microscope Nikon Eclipse 400. Measurement of sulphate, lactate and acetate concentrations were made by the Dionex ICS-5000 Ion Chromatograph.

### Results and discussion

The requirements for SRB development: a near-neutral pH, appropriate temperature, a reducing environment, a source of organic carbon, a source of sulphate and nutrients were fulfilled at the beginning of all experiments. In experimental cultures SRB occurrence was confirmed by light microscope, with predominance of genus *Desulfovibrio*. An attendant phenomenon was the formation of black precipitates at the bottom and the walls of the glass flasks during the first week after inoculation, which confirms expecting sulphate reduction and “FeS” formation. In addition, the smell of hydrogen sulphide was obvious.

*Desulfovibrio* belongs to the incomplete oxidizers and can use lactate as an electron donor and carbon source. Sulphate reduction using lactate can be described as follows:



Two moles of lactate are oxidized per mole of sulphate reduced by *D. desulfuricans*, and this stoichiometric ratio is not temperature dependent (Liamleam and Annachhatre, 2007).

Study of sulphates elimination caused by bacterial activity in nutrient medium without modification ( $\text{FeSO}_4 \cdot 7\text{H}_2\text{O}$  dose 0.5 g/L) illustrates Figure 1. We can see that bacteria reduce sulphates in medium until the complete lactate consumption. After this time (about 10 days of experiment duration) the process was stopped. The amount of acetate production corresponds to the quantity of oxidized lactate. The reduction of sulphates was about 50%. Changes of sulphates, lactate and acetate concentration in abiotic controls are negligible. Samples without bacterial cultures were “inactive”.

On Figure 2 are experimental results from modified nutrient medium, i.e. sodium lactate dose was doubled in order to achieve more effective sulphate elimination.  $\text{FeSO}_4 \cdot 7\text{H}_2\text{O}$  dose in this case was 1 g/L. Initial concentration of total sulphates in solution 2000 mg/L was lowered to 400 mg/L (80% reduction) when 4 g/L of sodium lactate was oxidized completely. This process took 14 days. For total sulphate reduction is necessary to use even higher lactate dosage and prolong the experiment duration, respectively.

The influence of SRB on the sulphate removal process in experiment with model solution was studied in the next step. The results verified by measuring of sulphate concentration decrease are shown on Figure 3. The initial concentration 1450 mg/L declined to the 240 mg/L within 14 days. This value meets the water quality requirements for the discharging into the recipient. Initial sodium lactate amount was 4 g/L. The concentration of sulphates in control sample without bacteria was reduced a little, probably because of some chemical reaction in solution. The measurements of sodium lactate and acetate concentration during experiment with model solution were not performed, they will be studied in the next stage.

### Conclusion

The purpose of this work was to investigate sulphate-reducing bacteria utilization for the removal of high levels of sulphates from water. These results refer to the need of sufficient organic substrate amount for the growth of sulphate-reducing bacteria with respect to initial sulphate concentration. SRB eliminated about 84% of sulphates from model solution within 14 days and final concentration achieved a value allowed to be discharged – below 250 mg/L. Presented theoretical knowledge as well as our experimental results from sulphate elimination using SRB allows to note that their natural metabolic activity can be used in environmental technology for treatment of industrial waste water with excessive content of sulphates.

### Acknowledgements

This work was supported by the Scientific Grant Agency under the contract 2/0142/19.

## Literatura – References

1. CAO, J. et al. Influence of electron donors on the growth and activity of sulfate-reducing bacteria. *International Journal of Mineral Processing*, 106–109, 2012, p. 58-64.
2. CASTRO, H.F. et al. Phylogeny of sulphate-reducing bacteria. *FEMS Microbiology Ecology*, 31(1), 2000, p. 1-9.
3. COLLERAN, E. et al. Anaerobic treatment of sulphate-containing waste streams. *Antonie van Leeuwenhoek Journal of Microbiology*, 67 (1), 1995, p. 29-46.
4. JONG, T., PARRY, D.L. Microbial sulfate reduction under sequentially acidic conditions in an upflow anaerobic packed bed bioreactor. *Water Research*, 40, 2006, p. 2561-2571.
5. LENS, P., POL, L.H. *Environmental Technologies to Treat Sulphur Pollution – Principles and Engineering*. IWA Publishing, London, 2000, 550 p. e-ISBN 9781780403038.
6. LIAMLEAM, W., ANNACHHATRE, A.P. Electron donors for biological sulfate reduction. *Biotechnology Advances*, 25 (5), 2007, p. 452-463.
7. MOOSA, S. et al. A kinetic study on anaerobic reduction of sulphate, Part I: Effect of sulphate concentration. *Chemical Engineering Science*, 57, 2002, p. 2773-2780.
8. OLUWASEUN, O.O. et al. Study of anaerobic lactate metabolism under biosulfidogenic conditions. *Water Research*, 43, 2009, p. 3345-3354.
9. PECK, H.D. Bioenergetic Strategies of the Sulfate-Reducing Bacteria. In: Odom, J.M., Rivers Singleton, J.R., editors. *The Sulfate-Reducing Bacteria: Contemporary Perspectives*. Springer-Verlag, New York, 1993, p. 41-76.
10. POSTGATE, J.R. *The sulphate-reducing bacteria*. 2nd edition. Cambridge University Press, Cambridge, 1984, 208 p. ISBN 0521257913.
11. RABUS, R. et al. Dissimilatory sulfate- and sulfur-reducing prokaryotes. In: Dworkin, M., Falkow, S., Rosenberg, E., Schleifer, K.H., Stackebrandt, E., editors. *The Prokaryotes*. Springer, New York, 2006, p. 659-768.
12. Regulation of the Slovak Government 269/2010 defining the requirements for achieving good status of waters (in Slovak) [online]. [ cit. 2019-04-17]. <<https://www.noveaspi.sk/products/lawText/1/71240/1/2>>.
13. TECLU, D. et al. Determination of the elemental composition of molasses and its suitability as carbon source for growth of sulphate-reducing bacteria. *Journal of Hazardous Materials*, 161, 2009, p. 1157-1165.
14. VAN DEN BRAND, T.P.H. et al. Potential for beneficial application of sulfate reducing bacteria in sulfate containing domestic wastewater treatment. *World Journal of Microbiology and Biotechnology*, 31, 2015, p. 1675-1681.
15. WIDDEL, F. et al. Ferrous iron oxidation by anoxygenic phototrophic bacteria. *Nature*, 362, 1993, p. 834-836.

### *Usuwanie zanieczyszczeń z wody za pomocą bakterii*

Wysokie stężenie siarczanów i metali w wodach jest często konsekwencją działalności antropogenicznej i przemysłu. Zasady biologiczno-chemicznych metod usuwania zanieczyszczeń obejmują różne procesy. Najszerszym szlakiem metabolicznym bakterii redukujących siarczany – ogólna redukcja dyssymilacyjna – jest całkowita redukcja siarczanu do siarkowodoru. Znane są dwie główne grupy metaboliczne, w zależności od tego, czy mogą utleniać octan. Jedna grupa wykorzystuje mleczan, fumaran, propionian, bmaslan, pirogronian i związki aromatyczne, które zwykle utleniają do octanu, podczas gdy druga grupa utlenia octan do CO<sub>2</sub> i H<sub>2</sub>O. Siarczan jest redukowany do H<sub>2</sub>S poprzez szereg reakcji pośrednich. Produkt końcowy tej reakcji – siarkowódor – może reagować z jonami metali, tworząc nierozpuszczalne siarczki i metale lub redukować rozpuszczalne metale toksyczne, często do postaci mniej toksycznych lub mniej rozpuszczalnych. W ten sposób bakterie redukujące siarczany są wykorzystywane do bio-eliminacji siarczanu i metali z wody.

**Słowa kluczowe:** zanieczyszczenie, siarczany, bakterie, redukcja



# Effect of Wastewater Sample Pre-Treatment on Determination of Selected Heavy Metals Using ICP-MS Method

Iva KOTALOVÁ<sup>1)</sup>, Katrin CALÁBKOVÁ<sup>2)</sup>, Martina NOVÁČKOVÁ<sup>3)</sup>,  
Silvie DRABINOVÁ<sup>4)</sup>, Silvie HEVIÁNKOVÁ<sup>5)</sup>

<sup>1)</sup> VSB – Technical University of Ostrava, Faculty of Mining and Geology, 17. listopadu 15, 708 33 Ostrava-Poruba, Czech Republic; email: iva.kotalova@vsb.cz,

<sup>2)</sup> VSB – Technical University of Ostrava, Faculty of Mining and Geology, 17. listopadu 15, 708 33 Ostrava-Poruba, Czech Republic; email: katrin.calabkova@vsb.cz

<sup>3)</sup> VSB – Technical University of Ostrava, Faculty of Mining and Geology, 17. listopadu 15, 708 33 Ostrava-Poruba, Czech Republic; email: martina.novackova@vsb.cz

<sup>4)</sup> VSB – Technical University of Ostrava, Faculty of Mining and Geology, 17. listopadu 15, 708 33 Ostrava-Poruba, Czech Republic; email: silvie.drabinova@vsb.cz

<sup>5)</sup> VSB – Technical University of Ostrava, Faculty of Mining and Geology, 17. listopadu 15, 708 33 Ostrava-Poruba, Czech Republic; email: silvie.heviankova@vsb.cz

<http://doi.org/10.29227/IM-2020-01-41>

Submission date: 04-01-2020 | Review date: 24-02-2020

## Abstract

*Polychlorinated substances, polyaromatic hydrocarbons, heavy metals and pesticides are among the priority even at low concentrations. The problem, however, is that such low concentrations are impossible to measure using most available methods. This research focused on the determination of selected priority substances – heavy metals, namely lead and cadmium, in which the determination of Pb and Cd in wastewater by Inductively Coupled Plasma Mass Spectrometry (ICP-MS) was preceded by water sample pre-treatment. The paper deals with the influence of the pre-treatment on the resulting measured values. Two processes were selected as pre-treatment processes. The first pre-treatment procedure was a simple filtration using a filter paper for moderate filtration. As the second procedure, we applied decomposition of the sample by nitric acid in the open system. The pre-treated wastewater samples were subsequently examined using ICP-MS. Based on the obtained results, we can conclude that decomposition of the sample by nitric acid in the open system is a more suitable pre-treatment method for water samples.*

**Keywords:** heavy metals, lead, cadmium, wastewater, pre-treatment filtration

## Introduction

Priority substances are defined by the Water Framework Directive as a significant risk to the aquatic environment. Priority substances are persistent, toxic and have a high accumulation capacity. They also include heavy metals - lead and cadmium, which this research is focused on. [1,2]

Lead is obtained from lead ore – Galenite (PbS). Especially in the past, there were significant anthropogenic sources, when lead made parts of gasoline, resulting in lead accumulation in the vegetation along the roads. Lead contamination also occurred when water was in contact with corrosive parts of water piping. At present, lead is contained in wastewaters from ore processing and battery production. [3,4,5]

Cadmium is potentially carcinogenic and teratogenic, so its use is minimal. It gets into the aquatic environment from the industry (electroplating and battery production) and fertilizers. It is mainly accumulated in water sediments. In humans, cadmium accumulates mainly in kidneys and liver. Cadmium causes decalcification of bones and affects blood pressure. [3,4,6]

In the Czech Republic, heavy metal concentrations in wastewater are regulated by Regulation 401/2015 Coll., which also contains environmental quality standards (EQS). The standards specify the EQS-AA limits: an environmental qual-

ity standard expressed as an annual average value and EQS-MAC: an environmental quality standard expressed as the maximum allowable concentration that must not be exceeded. For the purposes of this paper, the EQS-MAC limits have been used to assess and compare the measured values. The permissible values of Cd and Pb concentration according to NEK-MAC are given in Table 1. According to the measured values of Cd concentration, wastewater is divided into five classes.

Priority substances have a negative impact on the aquatic environment even at very low concentrations. Such low concentrations are generally difficult to determine. For this reason, ICP-MS method was chosen for this research. This method is able to detect concentrations in ppb units.

Sample pre-processing is very important for ICP-MS. The aim of the pre-treatment is to ensure the removal of interfering compounds and to concentrate the measured analyte in the sample. Basic processes of pre-treatment include, for example, filtration, centrifugation, extraction or microwave decomposition of the sample. [8]

## Materials and Methods

Two sewage samples were selected for this experiment. The first was wastewater taken from the municipal Waste-

Tab. 1. Allowable concentrations of cadmium and lead for each class according to EQS-MAC [7]

Tab. 1. Dopuszczalne stężenia kadmu i ołowiu dla każdej klasy zgodnie z EQS-MAC [7]

Heavy metal	Class	EQS-MAC [ppb]
Cd	1	≤ 0.45
	2	0.45
	3	0.6
	4	0.9
	5	1.5
Pb		14

Tab. 2. Results obtained by ICP-MS analysis for Sample 1

Tab. 2. Wyniki uzyskane za pomocą analizy ICP-MS dla próbki 1

	Filtration		Decomposition	
	Cd [ppb]	Pb [ppb]	Cd [ppb]	Pb [ppb]
1	0.0593	0.1089	0.0834	0.9691
2	0.0553	0.1311	0.0851	1.0449
3	0.0566	0.1188	0.0723	1.0270
<b>avg.</b>	<b>0.0571</b>	<b>0.1196</b>	<b>0.0803</b>	<b>1.0137</b>

Tab. 3. Results obtained by ICP-MS analysis for Sample 2

Tab. 3. Wyniki uzyskane za pomocą analizy ICP-MS dla próbki 2

	Filtration		Decomposition	
	Cd [ppb]	Pb [ppb]	Cd [ppb]	Pb [ppb]
1	0.5220	0.3679	1.2504	2.7350
2	0.5652	0.3163	1.3236	2.7495
3	0.5378	0.3395	1.2504	2.6925
<b>avg.</b>	<b>0.5417</b>	<b>0.3412</b>	<b>1.2748</b>	<b>2.7257</b>

water Treatment Plant (Sample 1). The second sample can be referred to as industrial wastewater, because it comes from a wastewater treatment plant of the company that deals with the production of nickel-cadmium batteries (Sample 2).

Selected samples were analyzed by ICP-MS. This method is one of the modern analytical methods using which the trace amount of individual elements contained in the analyzed samples can be determined. One of the advantages of this method is the possibility of fast and multi-element analysis. The basis of ICP-MS is the ion source, which serves to ionize the elements in the sample. The resulting ions are further fed to a mass analyzer. In the analyzer, the individual ions are divided by their mass and charge ( $m/z$ ). This is followed by their detection, where the ions separated by the analyzer pass into the detector, whose main task is to convert the ion current into an electron current. This is followed by a PC evaluation. [9, 10, 11]

Before using the ICP-MS analytical method, it is important to pre-treat all the analyzed samples.

In this research, both samples were pre-treated using two procedures. The first procedure was simple filtration. Filtration paper was used for medium filtration rate. 50 ml of each sample were filtered. After filtration, 0.5 ml of nitric acid was added to each sample for stabilization. All chemicals used in this analysis must be of p.p purity.

As the second procedure we chose the decomposition of the sample by nitric nitrate in the open system. 50 ml of each sample was boiled. The boil was terminated when the volume of boiled samples dropped to half – 25 ml sample. After boiling, the samples were cooled and also filtered through medium filtering paper. The filtrates obtained were filled up to 50 ml with distilled water.

All the pre-treated samples were further analyzed by ICP-MS the next day. Analysis of each sample was performed 3 times, to avoid measurement errors. Analyses were performed on the instrument Analytik Jena PlasmaQuant MS Elite.

## Result and Discussion

The results obtained by ICP-MS analysis are summarized in Tables 2 and 3. The values of each individual measurement were averaged and further compared with the EQS-MAC.

The results show that the concentration of cadmium in Sample 1 after both pre-treatment methods is very low and the results are of the order of magnitude, with all the measured values of the sample

pre-treated with nitric acid decomposition are higher. By comparison with EQS-MAC this sample belongs to class 1 in indicator Cd.

After analysis of sample 2, which was pre-treated by filtration, concentration of cadmium of 0.5417 ppb was measured. In this case, sample belongs to class 2 according to EQS-MAC. After nitric acid decomposition, the sample had a Cd concentration of 1.2748 ppb, which corresponds to class 4 according to EQS-MAC. The Cd concentration values obtained differ. After both pre-treatment methods, Pb concentrations measured for Sample 2 were lower than the EQS-MAC value. These values also differ from one another. Again, the values found for samples that were pre-treated with simple filtration are lower.

The heavy metals concentration values measured in the municipal waste water (Sample 1) were lower than the concentrations found in industrial wastewater (Sample 2).

## **Conclusion**

The results show that the pre-treatment of the sample affects the subsequent determination of selected heavy metals in wastewater samples. The concentration of both metals was shown to be lower for samples that were only filtered prior to ICP-MS analysis. Thus, according to EQS-MAC these samples belong to a lower quality class and appear to be of superior quality. However, for ICP-MS analysis, it is preferable to pre-treat the analyzed samples by decomposing the sample with nitric acid in an open system. By this pre-treatment process,

sufficient removal of interfering compounds in the sample was achieved over simple filtration.

## **Acknowledgements**

This article was written within the Project SP2019/87 – "Study of the occurrence of selected priority substances in wastewater from wastewater treatment plants and their removal". The project is supported by Student Grant Competition and the Ministry of Education, Youth and Sports of the Czech Republic.

## Literatura – References

1. Babel, T.A. Kurniawan, Low-cost adsorbents for heavy metals uptake from contaminated water: a review, *J. Hazard. Mater.* 97 (2003) 219–243.
2. W.W.S. Nagh, M.A.K.M. Hanafiah, Removal of heavy metal ions from waste water by chemically modified plant wastes as adsorbents: a review, *Bioresour. Technol.* 99 (2008) 3935–3948.
3. Těžké kovy. Arnika [online]. Praha, 2014 [cit. 2019-05-02]. Available at: <https://arnika.org/tezke-kovy-2>
4. PITTER, Pavel. *Hydrochemie*. 4. aktualiz. vyd. Praha: Vydavatelství VŠCHT, 2009. ISBN 978-80-7080-701-9.
5. BAYSAL, Asli, Nil OZBEK a Suleyman AKM. Determination of Trace Metals in Waste Water and Their Removal Processes. GARCA EINSCHLAG, Fernando Sebastin, ed. *Waste Water - Treatment Technologies and Recent Analytical Developments* [online]. InTech, 2013, 2013-01-16 [cit. 2019-05-02]. DOI: 10.5772/52025. ISBN 978-953-51-0882-5.
6. VELÍŠEK, Jan. *Chemie potravin I*. Tábor: Osis, 1999. 352 s. ISBN 80-902391-3-7.
7. Vyhláška č. 401/2015 Sb., o ukazatelích a hodnotách přípustného znečištění povrchových vod a odpadních vod, náležitostech povolení k vypouštění odpadních vod do vod povrchových a do kanalizací a o citlivých oblastech, ze dne 30. 12. 2015, ve znění pozdějších předpisů.
8. MADER, P., ČURDOVÁ E.: Metody rozkladu biologických materiálů pro stanovení stopových prvků, *Eurochem*. online: [http://archiv.eurochem.cz/polavolt/anorg/priprava\\_vzorku/mader\\_curdova.htm](http://archiv.eurochem.cz/polavolt/anorg/priprava_vzorku/mader_curdova.htm)
9. MIHALJEVIČ, M., STRNAD, L., ŠEBEK, O.: Využití hmotnostní spektroskopie s indukčně vázaným plazmatem v geochemii, *Chemické listy, Chem. Listy* 98, 123 – 130 2004.
10. HILL, S.J.: *Inductively coupled plasma spectrometry and its applications*, Blackwell publishing, Oxford, 2007.
11. MESTEK, O., *Hmotnostní spektrometrie s indukčně vázaným plazmatem – pracovní text*, Vysoká škola chemicko – technologická v Praze, Ústav analytické chemie, Praha.

## *Wpływ wstępnej obróbki próbek ścieków na oznaczanie wybranych metali ciężkich metodą ICP-MS*

*Zawartość substancje polichlorowanych, węglowodorów poliaromatycznych, metali ciężkich i pestycydów ma ogromne znaczenie nawet przy niskich stężeniach. Problem polega na tym, że niskich stężeń nie można zmierzyć przy użyciu większości dostępnych metod. Badania koncentrowały się na oznaczeniu wybranych substancji priorytetowych – metali ciężkich, a mianowicie ołowiu i kadmu, w których oznaczanie Pb i Cd w ściekach metodą indukcyjnie sprzężonej plazmowej spektrometrii masowej (ICP-MS) poprzedziło wstępne uzdatnianie próbki wody. Artykuł dotyczy wpływu obróbki wstępnej na uzyskane wartości pomiarowe. Dwa procesy wybrano jako procesy obróbki wstępnej. Pierwszą procedurą wstępnej obróbki była prosta filtracja z użyciem bibuły filtracyjnej do umiarkowanej filtracji. W drugiej procedurze zastosowano rozkład próbki kwasem azotowym w układzie otwartym. Wstępnie oczyszczone próbki ścieków zostały następnie zbadane przy użyciu ICP-MS. Na podstawie uzyskanych wyników stwierdzono, że rozkład próbki kwasem azotowym w układzie otwartym jest bardziej odpowiednią metodą wstępnej obróbki próbek wody.*

**Słowa kluczowe:** metale ciężkie, ołów, kadm, ścieki, filtracja wstępna



# Removal of Fluoride Ions from the Mine Water

*Eugenia KRASAVTSEVA<sup>1)</sup>, Anton SVETLOV<sup>2)</sup>, Andrey GORYACHEV<sup>3)</sup>,  
Dmitry MAKAROV<sup>4)</sup>, Vladimir MASLOBOEV<sup>5)</sup>*

<sup>1)</sup> Institute of Industrial North Ecology Problems of the Kola Science Centre of RAS, Fersman St., 14a, Apatity, Murmansk Region, 184209, Russia; email: vandeleur2012@yandex.ru

<sup>2)</sup> Institute of Industrial North Ecology Problems of the Kola Science Centre of RAS, Fersman St., 14a, Apatity, Murmansk Region, 184209, Russia; email: antonsvetlov@mail.ru

<sup>3)</sup> Institute of Industrial North Ecology Problems of the Kola Science Centre of RAS, Fersman St., 14a, Apatity, Murmansk Region, 184209, Russia; email: andrej.goria4ev@yandex.ru

<sup>4)</sup> Institute of Industrial North Ecology Problems of the Kola Science Centre of RAS, Fersman St., 14a, Apatity, Murmansk Region, 184209, Russia; email: mdv\_2008@mail.ru,

<sup>5)</sup> Institute of Industrial North Ecology Problems of the Kola Science Centre of RAS, Fersman St., 14a, Apatity, Murmansk Region, 184209, Russia; email: masloboev@mail.ru

<http://doi.org/10.29227/IM-2020-01-42>

Submission date: 12-12-2019 | Review date: 07-02-2020

## Abstract

*Murmansk Region is home to some major mining and mineral sites. One of the most challenging environmental problems in the mining industry is mine water treatment. For example, the rocks of the deposit operated by Lovozero Mining and Mineral Processing Company contain villiomite (NaF). It is highly soluble in water, and the mine waters at the site have a high content of fluoride ions – significantly above the maximum permissible values.*

*Lab-scale experiments were conducted to test various reagents and different initial concentrations of fluoride ions in the treatment of model solutions and mine water. Depending on the initial concentrations, magnesium and calcium-containing sorbents are proposed for the defluorization of water. Using scanning electron microscopy and microprobe analysis, it was found that fluorine can be bound in poorly soluble compounds, such as, for example, fluorite.*

*Pilot trials are planned.*

**Keywords:** usuwanie fluoru, ścieki, sorbenty zawierające magnez i wapń

## Introduction

The mining industry is highly active in Russia's Murmansk Region. Mining operations lead to the formation of wastewater with a high content of fluorine, often discharged into potable and fisheries water bodies without prior treatment or after inadequate treatment.

The urgency of developing simpler technologies for wastewater treatment using local materials or production waste is explained by large volume of wastewater requiring treatment, as well as the remoteness of the mining and mineral processing facilities from reagent and building materials manufacturers. In most cases, the implementation process of any proposed water treatment technology aimed at removing fluorine stops at the stage of a full-scale trial and requires further development of the technology.

Lovozero MMPC is located in the center of the Kola Peninsula and is the primary employer in the town of Revda. Karnasurt Concentrator has two fresh water intakes and six wastewater outlets used to discharge household, process, and drainage wastewater. At present, untreated mine water is discharged into the Sergevan River, a first order tributary of Lake Lovozero, classified in the highest category of fisheries water bodies. In addition, in 2011, due to an increase in the site's output, there was an increase in the amount of polluted wastewater discharged without treatment to 12.042 million m<sup>3</sup>.

It should be noted that the ore mined by Lovozero MMPC at the Karnasurt Mine contains villiomite (NaF), character-

ized by high water-solubility, therefore, the mine water in the mine has an elevated level of fluoride ions, significantly exceeding the existing maximum permissible values.

In this paper, we examine the possibility of using the reagents recovered from the waste and by-products of Murmansk Region's mining and minerals industry to remove fluoride ions from the wastewater.

## Materials and methods

The following sorbent samples were used to defluorize the solutions: thermally activated (500°C, 2 hours) brucite, calcined (900°C, 2 hours) carbonatite, a 1:1 (by weight) mixture of thermally activated brucite and calcined carbonatite, AlCl<sub>3</sub>·3H<sub>2</sub>O.

The proposed reagents were tested on model solutions with a concentration of 10 and 100 mg/l, as well as on actual mine water, collected in one of the Karnasurt mine's discharge outlets and containing 51 mg/l of fluorine.

The dependence of the fluoride ion sorption on the initial concentration was studied using the following method: 200 ml of the initial solution of a known concentration (10, 100 mg/l) was placed in a 250 ml conical flask, the sample was added, the mixture was shaken periodically and the residual fluorine concentration in the filtrate was measured. The residence time ranged from 0.5 to 24 hours, reagent flow rate from 0.25 g/l to 5 g/l. The pH value of the solutions was adjusted by adding H<sub>2</sub>SO<sub>4</sub> and NaOH solutions.



Tab. 1. Removal of fluoride ions from the model solution, 10 mg/l  
 Tab. 1. Usuwanie jonów fluorkowych z roztworu modelowego, 10 mg/l

Time, h	Termoactivated brucite			Calcined carbonatite			Brucite:Carbonatite 1:1			AlCl <sub>3</sub> ·3H <sub>2</sub> O		
	0.5	1	5	0.5	1	5	0.5	1	5	0.25	0.5	0.75
Consumption, g/l	0.5	1	5	0.5	1	5	0.5	1	5	0.25	0.5	0.75
0.5	5.3	13.7	43.2	9.1	12.6	19.9	8.3	19.9	20.9	85.8	90.5	96.4
1	14.6	28.3	51.3	18	20.2	28.7	15.6	28.1	32.1	86	90.8	96.6
24	63.6	71.9	97.2	30.2	31.4	40.1	42.3	46.3	56.4	86.1	91	96.7

Tab. 2. Removal of fluoride ions from the model solution, 100 mg/l  
 Tab. 2. Usuwanie jonów fluorkowych z roztworu modelowego, 100 mg/l

Time, h	Termoactivated brucite			Calcined carbonatite			Brucite:Carbonatite 1:1			AlCl <sub>3</sub> ·3H <sub>2</sub> O		
	0.5	1	5	0.5	1	5	0.5	1	5	0.25	0.5	0.75
Consumption, g/l	0.5	1	5	0.5	1	5	0.5	1	5	0.25	0.5	0.75
0.5	19.3	37.8	91.42	77.9	80.31	84.40	64.2	77.2	88.4	64.6	87.35	89.05
1	34.7	52.46	92.36	81.4	86.68	91.88	72.6	79.4	92.65	64.9	87.7	89.2
24	68.4	73.65	94.68	89.62	92.5	95.95	81.1	89.3	95.82	65.1	87.8	89.2

Tab. 3. Removal of fluoride ions from the real waste water, 51 mg/l  
 Tab. 3. Usuwanie jonów fluorkowych z rzeczywistych ścieków, 51 mg/l

Time, h	Termoactivated brucite, 1 g/l	Calcined carbonatite, 1 g/l	Brucite:Carbonatite 1:1, 1 g/l
0.5	22.94	24.31	20.20
add 0.5 g/l AlCl <sub>3</sub> ·3H <sub>2</sub> O			
0.5	98.23	97.02	97.51

Fluoride ion concentration in water was measured by the potentiometric method using an electrode system composed of a fluoride ion-selective electrode and an additional chlorine-silver electrode. The filter precipitates were examined by scanning electron microscopy and X-ray microprobe analysis using the measurement instrument SEM LEO 1450. The residual concentration of chlorine anions, where the water was treated with aluminum chloride, was measured by liquid chromatography.

## Results

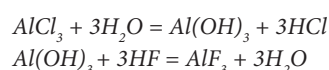
The results of the experiments on the model solutions are presented in the tables 1, 2.

The mechanism of sorption by brucite and carbonatite, as well as by a mixture of the two, is explained by isomorphous substitution of hydroxyl/carbonate ions by fluorine with the formation of poorly soluble calcium and magnesium fluorides without changes in the crystal lattice; the solubility of MgF<sub>2</sub> is 0.13 g/l, of CaF<sub>2</sub> 0.018 g/l at 25°C (Solubility Handbook, 1961). To regenerate the sorbent, a 2% caustic soda solution can be used.

In the dried precipitate of the reaction of thermally activated brucite and calcined carbonatite with the model solutions, calcium fluorides (fluorite) and magnesium fluorides were found both on the surfaces and in the newly formed phases.

In the process of water treatment using aluminum chloride, hydrolysis occurs with the formation of flocculent compounds with a general formula of the form [Al<sub>n</sub>(H<sub>2</sub>O)<sub>3n</sub>(OH)<sub>3n-x</sub>]<sup>x+</sup> + xOH<sup>-</sup>, where x OH<sup>-</sup> ions are found in

the outer layer, and 3n-x OH<sup>-</sup> ions are locked in the flakes. In the hydroxyl ions of the outer layer, the charge is only partially compensated by the hydration shell and sorbed anions; in general, the particle acquires a positive charge. With a decrease in pH as a result of the partial neutralization of the charge of the OH<sup>-</sup> ions by the hydrogen ions, the flake particles become more positively charged; hydroxyl ions, as a result of the weakening of the bond with the main matrix, improve their ability to exchange with anions in the external environment (Rozhdov and Silaeva, 2008).



The optimum pH value for the formation of stable Al(OH)<sub>3</sub> flakes and maximum absorption of F lies in the pH range of 5.5–7 (Mamyachenkov et al., 2016; Belikov and Lokshin, 2018). NaOH solution was added to the solution containing aluminum chloride until the pH was 6–7. Already during the first half hour at a minimum reagent flow rate, it was possible to reduce the concentration of fluoride ions to 1.42 mg/l and 35.4% in the model solutions containing 10 and 100 mg/l of fluorine. Secondary contamination with chloride ions does not exceed the maximum permissible.

The examined calcium and magnesium-containing reagents reduce the concentration of fluoride ions to the maximum permissible concentration at a high flow rate of 5 g/l, which is hardly viable in a production environment. These sorbents can be applied in smaller quantities for the pre-treatment of wastewater.

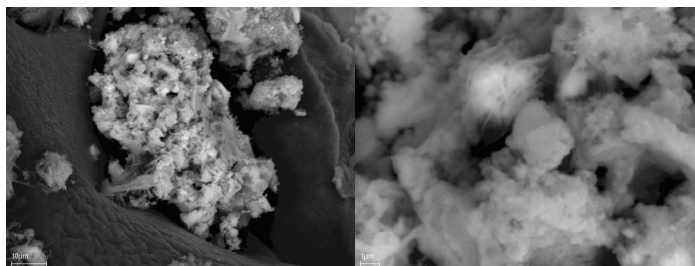


Fig. 1. Micrographs of precipitated fluorides on a thermally activated brucite surface  
Rys. 1. Mikrografy strąconych fluorków na termicznie aktywowanej powierzchni brucytowej

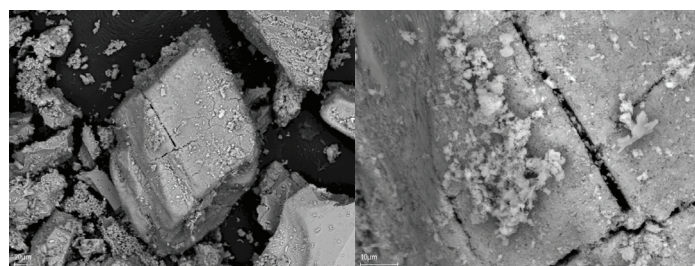


Fig. 2. Micrographs of precipitated fluorides on a calcined carbonatite surface  
Rys. 2. Mikrografy wytrąconych fluorków na kalcynowanej powierzchni węglanu

In further treatment, reagents, e.g. aluminum chloride, can be used.

Using the actual mine water with an initial fluoride concentration of 51 mg/l, a two-stage treatment process.

Magnesium and calcium-containing reagents raised the pH to almost 10 and the addition of aluminum salt reduced it to 6.1–6.3; no additional adjustment of the pH was necessary.

### Conclusion

Lab-scale experiments were carried out under static conditions on model solutions and the actual mine water from the Karnasurt Mine. The following reagents were tested: thermally activated (500°C, 2 hours) brucite, calcined (900°C, 2 hours) carbonatite, a 1:1 (by weight) mixture of thermally activated brucite and calcined carbonatite,  $\text{AlCl}_3 \cdot 3\text{H}_2\text{O}$ . The experiments showed that a high degree of fluorine removal is achieved when using a reagent based on brucite and carbonatite.

It was found that the most promising processes for the removal of fluorine from the wastewater of the mining industry

are processes combining chemical precipitation, coagulation, and sorption, making it possible to irreversibly and efficiently remove fluorine in a wide range of concentrations.

For initial fluorine concentrations of the order of 100 mg/l, chemical precipitation processes capable of removing up to 95% of fluorine are considered efficient. Either lime or magnesite, or both, will be effective in the pre-treatment stage. To further reduce the concentration of fluoride ions, it is possible to use aluminum chloride; at a low flow rate, secondary contamination with chlorine ions is unlikely.

A process is described for the separation of the mine wastewater from the Karnasurt Mine to reduce the volume of the polluted mine water and increase the concentration of the pollutant, which will improve the efficiency of fluoride ion removal using both conventional and novel methods.

### Acknowledgments

The study has been performed with financial support of the RFFR (project No 18-05-60142 Arctic).

#### Literatura – References

1. BELIKOV, Maxim, LOKSHIN, Efroim. Wastewater treatment from fluorine compounds of iron and aluminum. Non-ferrous metals, 2018; No 1, pp. 39–43. ISSN: 0372-2929.
2. MAMYACHENKOV, Sergey et al., Overview of promising methods for the removal of fluoride and chloride ions from solutions for the preparation of zinc electrolyte to the stage of electroextraction. Bulletin of ISTU, 2016; No 4 (111), pp. 155–169. ISSN: 1814-3520.
3. ROZHDOV, Joseph, SILAEVA, Elena. The study of ion-exchange properties of aluminum hydroxide, obtained by treatment with aluminum oxychloride. News of universities. North Caucasus region. Technical science, 2008; No 2, pp. 65–67. ISSN: 0321-3005.
4. SOLUBILITY HANDBOOK, ed. V.V. Kafarova. B. 1, Binary systems. L.: Publishing House of the Academy of Sciences USSR, 1961, 961 p.

#### *Usuwanie jonów fluorkowych z wody kopalnianej*

*Region Murmański jest regionem silnie uprzemysłowionym, jest lokalizacją wielu kopalń. Jednym z najtrudniejszych problemów środowiskowych w górnictwie jest uzdatnianie wód kopalnianych. Przedstawiono przykład kopalni Lovozero Mining and Mineral Processing. Złoże zawiera villiaumit (NaF). Jest to minerał dobrze rozpuszczalny w wodzie. Wody kopalniane w tym miejscu mają wysoką zawartość jonów fluorkowych - znacznie powyżej maksymalnych dopuszczalnych wartości. Przeprowadzono eksperymenty na skalę laboratoryjną w celu przetestowania różnych odczynników i różnych początkowych stężeń jonów fluorkowych w obróbce roztworów modelowych i wody kopalnianej. W zależności od początkowych stężeń do odfluoryzacji wody proponuje się sorbenty zawierające magnez i wapń. Za pomocą skaningowej mikroskopii elektronowej i analizy mikropróbek stwierdzono, że fluor może wiązać się w słabo rozpuszczalnych związkach, takich jak na przykład fluoryt. Planowane są próby pilotażowe.*

**Słowa kluczowe:** usuwanie fluoru, ścieki, sorbenty zawierające magnez i wapń



# Technical Infrastructure Increasing Resistance in the Natural Environment

Šárka KROČOVÁ<sup>1)</sup>

<sup>1)</sup> VSB-Technical University of Ostrava, Faculty of Safety Engineering, 700 13 Ostrava-Výškovice, Lumírova Str. 13, Czech Republic; email: sarka.krocova@vsb.cz

<http://doi.org/10.29227/IM-2020-01-43>

Submission date: 12-01-2020 | Review date: 17-04-2020

## Abstract

*The natural environment has its specific patterns that a human must take into account during realisation of any technical infrastructure of the world countries. Underestimating the dangers that can arise from natural phenomena has often serious consequences. For some constructions of technical infrastructure, especially their line constructions, there will be a high number of operational accidents with extremely negative impact on the supplied regions with energy or drinking water. Other types of technical infrastructure for example in nuclear power have a potential to create a natural emergency threaten the environment not only in the country of their dislocation but also in the long term to change living conditions in entire regions.*

*The following article deals with this issue in a sufficient basic range suggests chat ways and means to recognize the threat of danger and then based on risk analysis to eliminate the consequences to an acceptable level.*

**Keywords:** technical infrastructure, system resistance, risk, risk analysis, consequences elimination

## Introduction

When constructing any technical work, the designer must take into account local natural conditions. According to different regions and climatic zones, the building in question may have different functional characteristic and safety parameters and conditions. These differences are manifested not only on the object above the ground but especially on the line constructions.

The object or line structure must meet the specified parameters of resistance to the effect of normal natural influence and at the same time according to the specific conditions of its dislocation in the area, other conditions that have the potential to arise only periodically at different intervals. In Europe these include in particular floods, landslides, soil load-bearing instability, like undermining, and water conditions. Also in some regions seismic influences of varying intensity and probability of their occurrence are present as well.

When assessing them it is necessary to start with historical records as well as geophysical, climatic and hydrological knowledge of the environment. Failure or underestimation of this information very often reduces the resistance of buildings and their assemblies, increases operating costs and also shortens the buildings life.

### 1. Potential of nature emergencies and their negative consequences

In order to build an object or line structure in any country, such as Europe, the building's investor must respect local legislative (building law, water law,..) for the location of the building as well as the common EU legislation. Their adherence increases the resistance of buildings to the effect of extraordinary events and in particular protects the original natural environment.

However some objects and line structures of technical and transport infrastructure (water works, bridge structures, security elements) must be also built in areas with an increased risk risk of emergencies of a natural character:

- floodplains of recipients,
- territory with seismic activity,
- significantly sloping areas in mountain locations.

In practice, the above-mentioned natural hazards are often simultaneously amplified by concurrent anthropogenic safety influences in industrial areas or territories through which certain types of pipelines (oil pipelines, transport of chemicals, wastewater treatment by the industry) pass. The highest probability of occurrence of an extraordinary event and extent of extensive consequential damages are buildings which must be for technical reasons (gravity water inflow) located in the flood areas of the recipients such as wastewater treatment plants, see Fig. 1. and other water works, eventually transport infrastructure construction.

As a rule in the case of transport infrastructure constructions there is no permanent or long-term reduction in utility values or subsequent secondary damage. They are designed and built for high resistance to the effect of natural influences caused by floods. A similar statement applies to a large part of the water works (dams, rainwater and wastewater outlets).

Specific water works with relatively complex technologies such as sewage treatment plants, wastewater pumping stations, monitoring systems, have a low degree of natural flood resistance. Since they are of irreplaceable importance in the area and it the natural environment protection, it is always necessary to count on the risk of buildings flooding and their technologies and to prepare for an extraordinary event, for example in the manner specified in chapter 3 in this article.

The potential for other emergencies caused by natural phenomena is different depending on the type of facility and its location in the area. To a fundamental extent, natural events on the technical infrastructure cause the following conditions:

- breaks and cracks in pipe systems during landslides,



Fig. 1. Destruction of gas tank due to floods in Ostrava in 1997 [1]

Rys. 1. Zniszczenie zbiornika gazu z powodu powodzi w Ostrawie w 1997 r. [1]

<i>Accident probability</i>	Extremely high-almost certainly				
	High-can occur relatively often				
	Small-can happen only by rare coincidence				
	Very small-almost impossible to occur				
		Slight	Small scale	Extensively	Catastrophic
<i>Accident consequences</i>					

Fig. 2. Model of MU risk rate matrix and its consequences in technical infrastructure [3]

Rys. 2. Model macierzy stopy ryzyka MU i jego konsekwencje dla infrastruktury technicznej [3]

- foundation structural joints disruption of building structures,
- spot and area corrosion of metallic materials deposited in the ground,
- in extreme cases the destruction of object structures.

Taken together the above events can seriously undermine the general infrastructure of whole regions for a number of days or even weeks. However the self-preparation prevention for addressing the different kinds of natural influences on technical infrastructure must result from risk analysis using appropriate methods and optimizing ways of recognising the treats in question.

## 2. Means and methods of emergencies recognition

Current knowledge and possibilities of technology can be detected in time by a number of potentials hazards [2] In their practical application, technical tools for project management and management need to be put in the place. One way to proceed with risk analysis is to use an appropriate analysis method. The following is the technical infrastructure for which the region is largely dependent on operability and reliability.

Already in the first engineering risk analysis phase to develop risk checklist in accordance with the overall concept included in the mind map, see Table 1 and 2 which indicate weaknesses and strengths of the system.

Subsequently from the primary information from the checklist the risk analysis need to be continued using for example the FMEA method through a sequential step involving a risk matrix. The matrix can take various forms. One of the alternative form and structure options for the matrix is shown in the following Figure 2.

From the matrix output the individual relationships must always be sufficiently clear from the point of view of the extraordi-

nary risk events, its probability and consequences for the operating systems of assessed operating set. Of course, the other ways of engineering risk analysis can also be used in practice. However each used method must have the outputs sufficiently understandable to the user, for example the state administration, the municipal authorities and also the infrastructure managers [4].

## 3. Possibilities of technical residence increasing in the area

The resilience of each technical infrastructure is always based on the knowledge of the environment in which is located and preventive preparedness to deal with emergencies. This knowledge will result from the risk analysis performed before any construction on the technical infrastructure. From a pragmatic point of view it is advisable to increase the resilience of the subject infrastructure in two steps.

### *Increasing the infrastructure buildings resilience*

Underground or overground buildings have almost always a major impact on the reliability of energy supplies or drinking water for the region in question. Their purpose is to increase or decrease the hydraulic and technical parameters of the system or to accumulate the transported medium. These objects can be relatively well protected from the effects of anthropogenic influences. Substantially more complicated, before the occurrence of natural phenomena, depending on the different types displacement of object structures.

To increase the infrastructure buildings operational resistance can be done for example:

- always know in detail the stability of the soil environment under the building and its weaknesses when changing climatic conditions,
- knowledge of the risk object flooding and potential levels of flooding at different levels of risk,

Tab. 1. Selection of vulnerability checklist – gas supply to the region  
 Tab. 1. Wybór listy kontrolnej podatności na zagrożenia – dostawa gazu do regionu

MUTUAL DEPENDENCES				
<b>1.1</b>	<b>Underground gas storage facility</b>	Yes	No	Note
1.1.1	Does the natural gas storage facility have the sufficient capacity to overcome MU,extrenal supply lockouts for a region of more than 65 days?	yes		The tray capacity is realized for max 97 days of average consumption.
1.1.2	Can the gas supply from this reservoir be a serve for the neighboring region in the event of a crisis on the primary multinational distribution system?		no	There is insufficient capacitive interconnection through the piping of both regions, including additional technical system equipment.

Tab. 2. Selection of vulnerability checklist – drinking water sources for consumer  
 Tab. 2. Wybór listy kontrolnej podatności na zagrożenia – źródła wody pitnej dla konsumenta

MUTUAL DEPENDENCES				
<b>2.1</b>	<b>Raw surface water source for drinking water treatment</b>	Yes	No	Note
2.1.1	Does the drinking water source for the water supply system have sufficient passive and active elements when entering the contaminant into the water tank?	yes		Operational and safety measures allow water to be taken from the water treatment plant for several different horizons of accumulated raw water.
2.1.2	Does the drinking water treatment plant have sufficient technological equipment to treat water of quality significantly exceeding the raw water parametres in A3 category?		no	UV technology is equipped with a technology for water treatment of category A2.

- proposes based od previous points, to suggest building foundation in a way that avoids the reduction of its static stability in crisis situations,
- at the alternative hazard mentioned to allow the emergency threat,easy and rapid evacuation of threatened technology elements,
- to incorporate operational and handling rules into strategic object buildings and in general also into crisis management plats of relevant region.

#### **Increasing the line construction building infrastructure**

Line structures of technical infrastructure are almost always extremely threatened by natural influences. The intensity and probability of their occurrence arises from the type of territory, its geological character and climate zone in which the infrastructure is located. For example to increase the resistance of liner structures to the natural environment effects:

- physicochemical properties knowledge of the soil in which the corrosion environment inducing the steel piping system of the technical infrastructure are found,
- in a hazardous environment to increase the passive and active means of protecting the equipment in question to the highest attainable level,
- in the extremely sloping areas, implemet horizontal stress relief emelemts on the pipe system (compensators),
- in to floodplains, before its beggining and ens, place shut off valves on the pipeline, allowing for quick shut-down of the area in question, in case of an akcident caused by natural influences,
- in critical areas with unstable subsoil, redistribute the distribution system with a back-up pipeline, allowing the transport of the specified emergency quantity medium,

- to have a kontrol and monitoring system in place to enable remote monitoring and subsequent operational management of crisis processes.

The above-mentioned basic and other measures have the potentials to substantially increase the resilience of buildings and line structures of technical infrastructure. In the upcoming new climatic conditions in Europe, periodically reccuring intense incidents can be almost assured which will affect the technical infrastructure operating systems reliability [5]. Most countries in the world have already sufficient sfientific information on the risk and with appropriate international cooperation also the means by which the hazard can be appropriately and economically eliminated to the extent feasible.

#### **4. International cooperation and prevent coordination of emergencies in technical infrastructure**

The substantial part especially the energy infrastructure of the wold is not built for its own specific state but has an international character. In many cases it converts the medium in question to several states to the point of consumption. In the years to come this form of international cooperation can be expected to deepen. Due to the lenght of pipe systems converting media or power lines, the occurrence likelihood of especially natural emergencies increases with the pipe systems lenght. For example to reduce the occurrence likelihood:

- carry out the following measures on the distribution systém from new discovered energy sources to transport the relevant commodity to the consumption destination
  - in the risk sections of the product route endangering its own operation or secondarily the natural environment to build specific monitoring systems enabling rapid recognition of the emergency occurrence,

- carry out the transmission of information by the current most efficient transmission technology and monitoring equipment,
- the purchase of this technice by international agrément, regardless of the real international political situation and orientation of the state in which the deposits of necessary energy are located,

- to implement new elements of passive and active protection, equipment against existing natural influences on operating systems on existing production and especially distribution systems,

- to use strictly the latest climate knowledge in the new 21st century global climate conditions, based on the OSN conclusions to reduce the various types of hazards to operational infrastructure systems.

The increased number of hazards threatening the transnational technical production and distribution equipment can no longer be solved only segmentally. International cooperaton and coordination of activities will not only increase the potential and probability of a successful solution but will also save

economic costs resulting from the implementation of security measures [6].

### Conclusion

From the article it is clear that new threats to technical infrastructure and increasing their resilience to the effects of natural phenomena or anthropogenic events can no longer be addressed by local means. Such solutions would not be only costly for the state concerned, but would also lack a higher level of dimension. In most cases such cooperation already exists between states. However new climatic threats and resulting consequences are clearly solvable only by means of the examples given in several cases in this article. The aim of the article is to initiate, among other things, a discussion of the issue and thus other new solutions to existing and deepening problems in infrastructure operating systems.

### Acknowledgments

This work was supported by the research project VI20152019049 „RESILIENCE 2015: Dynamic Resilience Evaluation of Interrelated Critical Infrastructure Subsystems“, supported by the Ministry of the Interior of the Czech Republic in the years 2015–2019.

### Literatura – References

1. Ondeo Suez[online], [cit:12.11.2007], dostępne z: <http://www.ondeo.cz/>
2. KAVAN, S., MUDROCHOVA, S. SpecialTrainingofBrigadeMembers on a Software Training Simulator. In 5th International Multidisciplinary Scientific Conference on Social Sciences & Arts, Conference Proceedings. SGEM International, MultidisciplinaryScientificConference on Social Science and Arts. Volume 5, Issue 3.5 Education and EducationalResearch. Bulgaria, 2018. ISBN 978-619-7408-57-7. ISSN 2367-5659. DOI: 10.5593/sgemsocial2018/3.5
3. upraveno dle ČSN EN 31010 Management rizik – Techniky posuzování rizik
4. BERNATIK, A., SENOVSKY, P., SENOVSKY, M., a D. REHAK. (2013). Territorial risk analysis and mapping. Chemical Engineering Transactions, 31, 79-84.
5. KROCOVA, S. 2017 Industrial Lanscape in the Period Drought.InženieraMineralna 2017 vol. 39. No. 1 p 39-32 ISSN 1803-569-8X.
6. KAVAN, Š., BREHOVSKÁ, L. CooperationofSouth Bohemia and Cross-BorderRegionswith a Focus on Civil Protection. In Klímová, V., Žítek, V. (eds.) 19th International Colloquium on RegionalSciences. ConferenceProceedings. Brno : Masarykova univerzita, 2016. pp. 907-914. ISBN 978-80-210-8273-1. DOI: 10.5817/CZ.MUNI.P210-8273-2016-117.

### *Infrastruktura techniczna zwiększająca oporność w środowisku naturalnym*

*Środowisko naturalne ma swoje specyficzne wzorce, które człowiek musi wziąć pod uwagę przy realizacji dowolnej infrastruktury technicznej krajów świata. Niedocenianie zagrożeń, które mogą wynikać ze zjawisk naturalnych, ma często poważne konsekwencje. W przypadku niektórych konstrukcji infrastruktury technicznej, zwłaszcza ich konstrukcji liniowych, występuje duża liczba wypadków operacyjnych, które mają wyjątkowo negatywny wpływ na regiony zaopatrywane w energię lub wodę pitną. Inne rodzaje infrastruktury technicznej, na przykład w energetyce jądrowej, mogą potencjalnie stworzyć naturalny stan zagrożenia, zagrażając środowisku nie tylko w kraju, ale także w perspektywie długoterminowej i może wywołać zmiany warunków życia w całych regionach. Poniższy artykuł zajmuje się tym problemem w zakresie podstawowym, proponuje sposoby rozpoznawania zagrożenia, a następnie rozwiązania oparte na analizie ryzyka w celu zredukowania konsekwencji do akceptowalnego poziomu.*

**Słowa kluczowe:** infrastruktura techniczna, oporność systemu, ryzyko, analiza ryzyka, eliminacja skutków



# Steelmaking Dust: Speciation of Zinc by Sequential Leaching

Christof LANZERSTORFER<sup>1)</sup>, Wilfried PREITSCHOPF<sup>2)</sup>

<sup>1)</sup> University of Applied Sciences Upper Austria, School of Engineering, Stelzhamerstraße 23, 4600Wels, Austria; email: c.lanzerstorfer@fh-wels.at

<sup>2)</sup> University of Applied Sciences Upper Austria, School of Engineering, Stelzhamerstraße 23, 4600Wels, Austria; email: wilfried.preitschopf@fh-wels.at

<http://doi.org/10.29227/IM-2020-01-44>

Submission date: 28-12-2019 | Review date: 02-02-2020

## Abstract

*In electric arc furnace (EAF) steelmaking significant amounts of dust are generated. The main component in the dust is usually iron. Additionally, increased concentrations of metals which are volatile in the steelmaking process like zinc are found in the dusts. During cooling of the off-gas in the off-gas system the volatile metals are deposited on the dust particles. In electric arc furnace dust the zinc can be present in different compounds, for example as zinc oxide and zinc ferrite. Although recycling of EAF dust and utilization for zinc recovery are practiced in several countries approximately 50% of the EAF dust produced worldwide is still goes to landfill. In this study the EAF dust from a mini mill was investigated by chemical fractionation. The experiment was carried out in a sequence of five leaching steps, where the residue from a leaching step was treated in the next step. The total zinc content of the EAF dust was approximately 6.4%. In the water-soluble fraction no zinc was found, while the carbonated fraction and the oxide fraction each contained approximately 25% of the zinc. The reduced fraction contained approximately 8% of the zinc and the majority of the zinc was in the residual fraction.*

**Keywords:** steelmaking dust, sequential leaching, zinc

## Introduction

In electric arc furnace (EAF) steelmaking in mini mills significant amounts of dust in the range of 10-30 kg per ton of liquid steel (kg/t LS) are produced (Remus et al., 2013). Fe is usually the main component in EAF dust. For metals which are volatile under steelmaking conditions like Zn increased concentrations are often found in EAF dusts. These metals enter the furnace with the scrap and are subsequently volatilized because of the high temperature in the furnace and the reducing conditions. These metals leave the furnace with the off-gas and are deposited on the dust particles during off-gas cooling. Reported Zn concentrations of EAF dust are in the range of 2–43% (Remus et al., 2013). According to the literature, Zn is mainly present as Zn oxide (ZnO, zincite) and Zn ferrite (ZnFe<sub>2</sub>O<sub>4</sub>, franklinite) (Machado et al., 2006; Grillo et al., 2014). Although recycling of EAF dust and utilization for Zn recovery are practiced in several countries (Doronin and Svyazhin, 2011; Lin et al., 2017) approximately 50% of the EAF dust produced worldwide (4.5 million tons per year) is still landfilled (Antrekowitsch et al., 2015).

In this study the EAF dust from a mini mill was investigated for the distribution of Zn in various compounds.

## Materials and methods

Two dust samples were collected at the dust discharge of the off-gas dedusting filter of an industrial EAF plant. In the laboratory the samples were dried and subsequently the sample volume was reduced to a volume suitable for the various laboratory tests using sample dividers (Haver&Boecker HAVER RT and Quantachrome Micro Riffler). If required, the sample dividers were applied repeatedly.

The particle size distribution of the dusts was measured using a laser diffraction instrument with dry sample dispersion from Sympatec, type HELOS/RODOS.

The leaching experiment was carried out in a sequence of five leaching steps, where the residue from a leaching step was used for the treatment in the next leaching step. Thereby, the amount of Zn can be separately determined in different fractions: the exchangeable, easily water-soluble fraction (L1), the carbonated fraction (L2), the oxides (L3), the reduced fraction (L4) and the residual fraction (L5).

Zn would be present in these fractions, for example, mostly as ZnCl<sub>2</sub> or ZnSO<sub>4</sub> (L1), as ZnCO<sub>3</sub> (L2), as ZnO (L3), as ZnS (L4) or as ZnFe<sub>2</sub>O<sub>4</sub> (L5).

The leaching procedure, which was adapted from published leaching procedures (Sammur et al., 2008), is described in detail in Table 1.

During the leaching procedure the vessel was stirred at 250 rpm with a magnetic stirrer. After the leaching the undissolved residue was separated from the liquid by vacuum filtration. The filtrate was saved for chemical analysis, while the filter cake was transferred to the next leaching step.

The concentrations of Zn in the solutions were measured by Inductive Coupled Plasma Optical Emission Spectroscopy (iCAP 7000 Plus Series).

## Results and discussion

The average particle size distribution is shown in Figure 1. Generally, the particle size of the dusts was very small. The average values of the d<sub>10</sub>, d<sub>50</sub> and d<sub>90</sub> were 0.38 μm, 1.27 μm and 24 μm respectively. This is within the range of reported data for EAF dust (da Silva et al. 2008; Lanzerstorfer, 2018).



Tab. 1. Leaching procedure (a special preparation procedure was applied)  
 Tab. 1. Procedura wymywania (zastosowano specjalną procedurę przygotowawczą)

Step	Leachate	Temperature	Time
L1	H <sub>2</sub> O <sub>demi</sub> (60 mL)	60°C	3h
L2	CH <sub>3</sub> COONa (1 M, 54 mL) and CH <sub>3</sub> COOH (1 M, 6 mL)	Room temperature	3h
L3	Na <sub>2</sub> S <sub>2</sub> O <sub>4</sub> (0.3 M, 20 mL), Na-citrate (1.175 M, 20 mL) and H-citrate (0.025 M, 20 mL)	Room temperature	4h
L4	H <sub>2</sub> O <sub>2</sub> (30%, 24 mL) in HNO <sub>3</sub> <sup>a</sup> (60 mL)	refluxed at 95°C	3h
L5	Aqua Regia (HCl/HNO <sub>3</sub> , 3:1, 60 mL)	refluxed at 90°C	3h

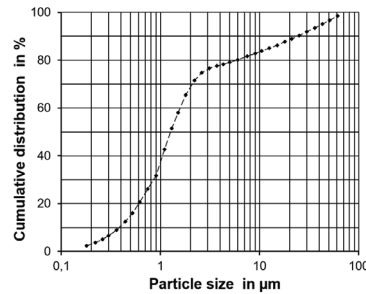


Fig. 1. Average size distribution of the EAF dusts  
 Rys. 1. Średni rozkład wielkości pyłów EAF

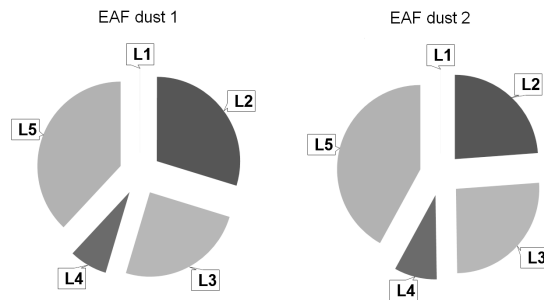


Fig. 2. Fraction of Zn in the various leaching fractions  
 Rys. 2. Frakcja Zn w różnych frakcjach ługujących

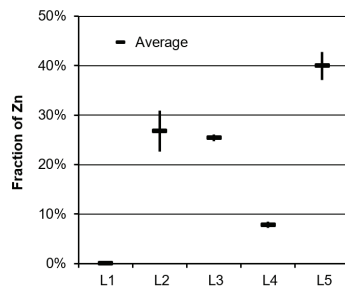


Fig. 3. Fraction of Zn in the various leaching fractions  
 Rys. 3. Frakcja Zn w różnych frakcjach ługujących

The total Zn content was  $6.5 \pm 0.4\%$  for the first EAF dust sample and  $6.4 \pm 0.3\%$  for the second sample. The distribution of the Zn in the various leaching fractions L1 to L5 is shown in Figure 2. The differences between the two samples were quite small.

Figure 3 shows the variation of the Zn fraction (average fraction  $\pm$  standard deviation) found in the leachates. In the water-soluble fraction (L1) no Zn was found. In the carbonated fraction (L2) as well as in the oxide fraction (L3) approximately 25% of the Zn was found. However, the variation

was larger for the carbonated fraction. The reduced fraction (L4) contained approximately 8% of the Zn. The majority of the Zn, approximately 40%, was found in the residual fraction (L5).

The presence of Zn in the form of Zn oxide and Zn ferrite is in accordance with published data. (Machado et al., 2006; Grillo et al., 2014). However, the presence of approximately one third of the Zn in the carbonated and reduced fraction is somewhat surprising. Further investigations are required to confirm these findings.

## Conclusion

The investigated EAF dust samples were within the typical values with respect to particle size and total Zn content.

The speciation of Zn by sequential leaching revealed that approximately two thirds of the total Zn can be found as Zn oxide and Zn ferrite. However, the remaining third of the total Zn content was found in the carbonated and reduced fractions. To confirm these findings further investigations are required.

## Acknowledgements

Laboratory work by K.F. Dale is gratefully acknowledged. The study was financially supported by K1-MET. K1-MET is a member of COMET – Competence Centers for Excellent Technologies and is financially supported by the BMVIT (Federal Ministry for Transport, Innovation and Technology), BMWFJ (Federal Ministry of Economy, Family and Youth), the federal states of Upper Austria, Styria and Tyrol, SFG and Tiroler Zukunftsstiftung. COMET is managed by FFG (Austrian research promotion agency).

## Literatura – References

1. ANTREKOWITSCH, Jürgen; RÖSLER, Gernot; STEINACKER, Stephan. State of the Art in Steel Mill Dust Recycling. In *Chemie Ingenieur Technik*, 87 (11), 2015, p. 1498-1503, ISSN 1522-2640.
2. DA SILVA, M.C.; BERNARDES, A.M.; BERGMANN, C.P.; TENORIO, J.A.S.; ESPINOSA, D.C.R. Characterization of electric arc furnace dust generated during plain carbon steel production. *Ironmaking and Steelmaking*, 35 (4), 2008, p. 315-320, ISSN 0301-9233.
3. DORONIN, I. E.; SVYAZHIN, A. G. Commercial methods of recycling dust from steelmaking. *Metallurgist*, 54 (9-10), 2011, p. 673-681, ISSN 0026-0894.
4. GRILLO, F.F., COLETTI, J.L., ESPINOSA, D.C.R., OLIVEIRA, J.R., TENORIO, J.A.S. Zn and Fe Recovery from Electric Arc Furnace Dusts. In *Materials Transactions*, 55 (2), 2014, p. 351-356, ISSN 1347-5320.
5. LANZERSTORFER, Christof. Properties of steelmaking dusts from dry dust separators. Ostrava : Tanger Ltd., 2018. p. 41-48. ISBN 978-80-87294-84-0.
6. LIN, Xiaolong; PENG, Zhiwei; YAN, Jiaying; LI, Zhizhong; HWANG, Jiann-Yang; ZHANG, Yuanbo; LI, Guanghui; JIANG, Tao. Pyrometallurgical recycling of electric arc furnace dust. In *Journal of Cleaner Production*, 149, 2017, p. 1079-1100, ISSN 0959-6526.
7. MACHADO, Janaina G.M.S.; BREHM, Feliciane Andrade; MORAES, Carlos Alberto Mendes; DOS SANTOS, Carlos Alberto; VILELA, Antônio Cezar Faria; DA CUNHA, João Batista Marimon. Chemical, physical, structural, and morphological characterization of electric arc furnace dust. In *Journal of Hazardous Materials*, B136 (3), 2006, p. 953-960, ISSN 0304-3894.
8. REMUS, Rainer; AGUADO MONSONET, Miguel A.; ROUDIER, Serge; DELGADO SANCHO, Luis. Best Available Techniques (BAT) Reference Document for Iron and Steel Production, Industrial Emissions Directive 2010/75/EU, Integrated Pollution Prevention and Control. Publications Office of the European Union, Luxembourg, 2013.
9. SAMMUT, M.L.; ROSE, J.; MASON, A.; FIANI, E.; DEPOUX, M.; ZIEBEL, A.; HAZEMANN, J.L.; PROUX, O.; BORSCHNECK, D.; NOACK, Y. Determination of zinc speciation in basic oxygen furnace flying dust by chemical extractions and X-ray spectroscopy. In *Chemosphere*, 70 (11), 2008, p. 1945-1951, ISSN 0045-6535.

### *Pył stalowniczy: specjacja cynku metodą sekwencyjnego ługowania*

*W elektrycznym piecu łukowym (EAF) wytwarzającym stal wytwarzane są znaczne ilości pyłu. Głównym składnikiem pyłu jest zwykłe żelazo. Ponadto w pyłach znajdują się podwyższone stężenia metali lotnych w procesie hutnictwa, takich jak cynk. Podczas chłodzenia gazu odlotowego w układzie gazu odlotowego lotne metale osadzają się na cząstkach pyłu. W pyłach z elektrycznych pieców łukowych cynk może występować w różnych związkach, na przykład jako tlenek cynku i ferryt cynku. Chociaż recykling pyłu z EAF i wykorzystanie do odzysku cynku są praktykowane w kilku krajach, około 50% pyłu z EAF wytwarzanego na całym świecie nadal trafia na składowisko odpadów. W przedstawionych badaniach pył EAF z mini-młyna zbadano przez frakcjonowanie chemiczne. Eksperyment przeprowadzono w sekwencji pięciu etapów ługowania, przy czym pozostałość z etapu ługowania poddawano obróbce w następnym etapie. Całkowita zawartość cynku w pyłach EAF wyniosła około 6,4%. We frakcji rozpuszczalnej w wodzie nie znaleziono cynku, podczas gdy frakcja węglanowa i frakcja tlenkowa zawierały około 25% cynku. Zredukowana frakcja zawierała około 8% cynku, a większość cynku znajdowała się we frakcji resztkowej.*

**Słowa kluczowe:** pył stalowy, ługowanie sekwencyjne, cynk



# Combination of Chemical and Biological-Chemical Methods for Elimination of Metals from Acid Mine Drainage

Alena LUPTÁKOVÁ<sup>1)</sup>, Eva MAČINGOVÁ<sup>1)</sup>, Stefano UBALDINI<sup>2)</sup>,  
Miloslav LUPTÁK<sup>3)</sup>

<sup>1)</sup> Slovak Academy of Sciences, Institute of Geotechnics, Watsonova 45, 040 01 Košice, Slovak Republic; email: luptakal@saske.sk

<sup>2)</sup> Institute of Environmental Geology and Geoengineering, CNR, Area della Ricerca di Roma RM 1 – Montelibretti, Via Salaria Km 29 300, Roma, Italy

<sup>3)</sup> Technical University of Košice, Faculty of Materials, Metallurgy and Recycling, Letná 9, 042 00 Košice, Slovak Republic

<http://doi.org/10.29227/IM-2020-01-45>

Submission date: 29-12-2019 | Review date: 16-02-2020

## Abstract

Each acid mine drainage has a specific composition, but always contains sulphuric acid, dissolved heavy metals, sulphates, iron precipitates and their pH can be very low. The elimination of metals from the acid mine drainage is a severe environmental problem and has been a long-standing major concern to scientists, engineers, industry and governments. Various methods are used for the metals removal from waters, but any of them have been applied under commercial-scale conditions. Mostly studied are chemical and biological-chemical methods. Main aim of the paper was to interpret the combination of chemical and biological-chemical methods for the heavy metals elimination from the synthetic solution of acid mine drainage, coming from the zinc mine located in Tünel Kingsmill outlet of the Rio Yauli (district of Yauli – Perú). The metals selective precipitation as hydroxides (chemical method) and sulphides (biological-chemical method) at the various values of pH acid mine drainage is the fundamental of the examined process. For the hydrogen sulphide production the sulphate-reducing bacteria of genus *Desulfovibrio* was used. The selective sequential precipitation process reaches the selective precipitation of chosen metals with 97–99% efficiency – Fe, As, Al and Mn in the form of metal hydroxides, Cu and Zn as metal sulphides.

**Keywords:** acid mine drainage, sulphate-reducing bacteria, metal sulphides, selective sequential precipitation

## Introduction

Acid mine drainage (AMD) is considered as one of the most dangerous forms of water pollution in areas of the world that have active or historic mining operations. The source of acid mine drainage is the residues of mining activity mainly after the mining of deposits with the content of sulfide minerals. AMD always contains sulfuric acid, dissolved heavy metals, sulfates and iron precipitates. Its value of pH is very low, about 1.5–2.0 (Johnson and Hallberg, 2003). AMD cause the decomposition of other minerals, the devastation of the surrounding environment, the contamination of underground water and water streams by a wide range of elements, including the toxic ones, the penetration of metals into the food chain, etc.

Generally are used two strategies for treating AMD: active and passive technologies (Skousen et al., 1998). Conventionally, hydroxide precipitation is the most commonly applied method for the treatment of metal containing waters (Kalin et al., 2006). The production of the high quantities of the unstable metal hydroxides mixture, which also lead to a greater disposal expense, is the main disadvantage of the method. The high operating costs and the production of a bulky sludge, which must be disposed, are the disadvantages of the traditional chemical treatment.

In the treatment of AMD the application of bacterially produced hydrogen sulfide by sulfate-reducing bacteria (SRB) is becoming an alternative to conventional chemical treatment (Kaksonen and Puhakka, 2007). The basic metabolic process

of SRB is the anaerobic reduction of sulphates in which organic substrate (lactate, malate, etc.) or gaseous hydrogen is the electron donor and sulphate is the electron acceptor (Odom and Singleton, 1993). The research and development of the appropriate combinations of the chemical and biological-chemical methods for the metals selective recovery from AMD, suggested the interesting solving problems concerning the AMD treatment. These methods constitute the possibility of the recovery metals in a suitable form for commercial or industrial utilization (Costa et al., 2008).

The combination of the metal precipitation using the sodium hydroxide (chemical methods) with the metal precipitation using the bacterially produced hydrogen sulfide (biological-chemical method) presents the base of the selective sequential precipitation (SSP) (Tabak et al., 2003). It is the environmentally friendly way for elimination metals and metalloids from AMD.

In this study the synthetic solutions of AMD from a lead and zinc mine located in Tünel Kingsmill outlet of the Rio Yauli (district of Yauli – Perú) was used. The Kingsmill Tunnel was built between 1929 and 1934 by the Cerro de Pasco Copper Corporation. The tunnel drains mines Morococha mining district in Yauli River, which then flows into the Mantaro, affecting about 900000 inhabitants of the Mantaro Valley, Junín Region. Currently, an acidic water pouring Kingsmill Tunnel is approximately 1,250 liters per second, with a pH of 3.5–5.0. The river is contaminated by water of the tunnel when they are discharged into their flow, as these are oxidized prior to

Tab. 1. Metals concentration and pH of AMD sample from Tünel Kingsmill (district of Yauli – Perù)

Tab. 1. Stężenie metali i pH próbki AMD z Tünel Kingsmill (dystrykt Yauli – Perù)

	pH	Concentration (mg/L)					
		Fe	As	Al	Cu	Zn	Mn
Value	3.0	129	2	8	12	70	50

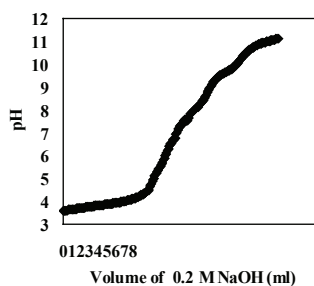


Fig. 1. Integral titration curve

Rys. 1. Całkowa krzywa miareczkowania

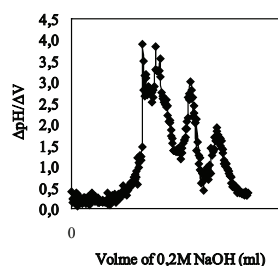


Fig. 2. The first derivation of the integral titration curve

Rys. 2. Pierwsze wyprowadzenie całkowitej krzywej miareczkowania

making contact with the minerals and metals. Peruvian mining companies are finalizing the feasibility studies using conventional remediation technologies involving the addition of lime.

The main objective of the paper was to interpret SSP as a way to separate chosen metals (Fe, As, Cu, Al, Zn and Mn) from the model solution of Peruvian AMD.

## Materials and methods

### Synthetic Solution of Acid Mine Drainage

The experiments were carried out at the laboratory scale using a synthetic solution of an AMD coming from the zinc mine located in Tünel Kingsmill outlet of the Rio Yauli (district of Yauli – Perù).

A synthetic solution with similar properties to the real sample of AMD was prepared. Reagents with a high analytical degree of purity were used (RPE Carlo Erba). Based on the concentration of metals in the real AMD sample, the corresponding salts were weighed and dissolved in deionized water. The solution with a pH of 3.0 was achieved after adjusting the pH value using 5M NaOH. The annual average metals concentration and pH values of peruvian AMD describes Table 1.

### Metals precipitation by NaOH

The precipitation by 0.2M NaOH solutions was used for the informative removal of metals as hydroxides. 100ml of the AMD synthetic solution was titrated at a pH ranging from 3.0 to 10 using a 0.2M NaOH solution. During titration the

solution was continuously stirred. Changes of pH using a pH-meter PHM210 MetLab were monitored. Accrued precipitates were not removal form liquid phase. The metals concentration (Fe, As, Cu, Al, Zn and Mn) in solution by atomic absorption spectrometry (AAS) was determined.

The detailed determination of the metals precipitation pH values from studied model solution was performed by the acid-base titration – alkalimetry using automatic titrator TitrLab 850 in connection with PC program TitrMaster 85. Titration agent was 0,2M NaOH solution. After precipitation of individual metals, accrued precipitates were removed by filtration. The concentration of metals in liquid phase by the AAS was determined.

### Metals precipitation by bacterially produced H<sub>2</sub>S

The informative precipitation of heavy metals at pH 3.0 (initial pH the AMD synthetic solution), in the form of sulfides was performed in two interconnected tanks with a capacity 500 ml (the first tank - the bacterial production of hydrogen sulfide) and 250 ml (the second tank - the heavy metals precipitation by the bacterially produced H<sub>2</sub>S) (Luptakova et al., 2002). For the hydrogen sulfide production the cultures of SRB (genus *Desulfovibrio*) were used. Bacteria were isolated from the potable mineral water (Gajdovka spring, Kosice-north, Slovakia). The genus *Desulfovibrio* was enriched from the mixed cultures SRB using the nutrient Postgate's medium C (Postgate, 1984; Luptakova et al., 2011). The SRB cultivation for the bacterial production of hydrogen sulfide was carried

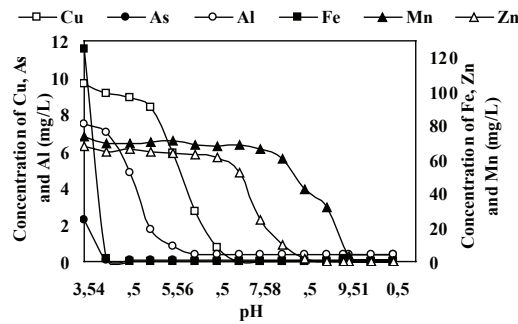


Fig. 3. Chemical analysis of the AMD synthetic solution during titration by 0.2 M NaOH  
Rys. 3. Analiza chemiczna syntetycznego roztworu AMD podczas miareczkowania 0,2 M NaOH

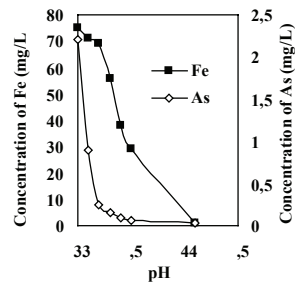


Fig. 4. The co-precipitation of Fe and As in the form of hydroxides  
Rys. 4. Współstrącanie Fe i As w postaci wodorotlenków

Tab. 2. Precipitation of Cu and As by bacterially produced  $H_2S$  at initial pH of model solution – 3.0)  
Tab. 2. Wytrącanie Cu i As przez bakteryjnie wytwarzany  $H_2S$  przy początkowym pH roztworu modelowego – 3,0)

Time (min)	Concentration of metals (mg/L)					
	Fe	As	Al	Cu	Zn	Mn
0	129	<b>2.00</b>	8.00	<b>12.00</b>	70.00	50.00
5	128	<b>1.89</b>	7.98	<b>0.57</b>	69.80	49.98
10	129	<b>1.08</b>	8.00	<b>0.02</b>	70.00	49.96
15	127	<b>0.93</b>	8.00	<b>0.02</b>	70.00	49.98
30	127	<b>0.56</b>	7.97	<b>0.02</b>	70.00	50.00
60	128	<b>0.53</b>	7.98	<b>0.02</b>	70.00	49.97

Tab. 3. Metals precipitation by NaOH and bacterially produced  $H_2S$  (initial pH of AMD synthetic solution 3.5)  
Tab. 3. Wytrącanie metali przez NaOH i bakteryjnie wytwarzany  $H_2S$  (początkowe pH syntetycznego roztworu AMD 3,5)

Step	pH	Precipitating agent	Removed metals
1.	3.5 → 4.5	NaOH	Fe, As
2.	4.5 → 3.9	$H_2S$	Cu
3.	4.0 → 5.8	NaOH	Al
4.	5.8 → 6.5	$H_2S$	Zn
5.	6.8 → 10.5	NaOH	Mn

out using the same nutrient medium. The heavy metals concentration in the liquid samples taken from the second tank by the AAS was determined.

### Selective Sequential Precipitation

The selective sequential precipitation was realized to using the combined application of sodium hydroxide solution and hydrogen sulfide produced by sulfate-reducing bacteria. The bases of SSP were next principal steps: 1 – addition of 0,2M NaOH solution by the automatic titrator TitraLab 850; 2 – filtration of precipitates; 3 – addition of bacterially produced hydrogen sulfide by the equipment consist of two interconnected tanks. After each addition of the precipitating agent and metals precipitation, accrued precipitates were removal by filtration. The concentration of metals in the fil-

trates during SSP by the AAS was determined. For the hydrogen sulfide production in the framework of 2.step the same cultures of SRB (genus *Desulfovibrio*) were used, as in case of aforementioned experiments concerning of the metals precipitation by bacterially produced  $H_2S$ . A little amount of  $H_2O_2$  has been added to the synthetic solution with the aim to provide the presence of Fe, As and Mn in the form of  $Fe^{3+}$ ,  $As^{5+}$  and  $Mn^{2+}$ . The suitable pH values for selective precipitation of metals using automatic titrator TitraLab 850 in connection with PC program TitraMaster 85 were performed. Titration agent was 0,2M NaOH solution.

### Results and discussion

Each metal in aqueous solution precipitates by addition of sodium hydroxide solution or hydrogen sulfide at specific pH

levels (Tabak et al., 2003). The acid-base titration – alkalimetry is simple and convenient method for the suitable pH values determination of the metals selective precipitation from aqueous solution (Totsche et al., 2003). It helps to explain the AMD forming procedure and helps to find the treat method. The issue of alkalimetry is the titration curve. Its shaped like a staircase. Vertical part shows the process OH<sup>-</sup> ions neutralizing H<sup>+</sup> ions, which increases the pH of water. Horizontal part indicates OH<sup>-</sup> ions precipitate metal ions into metal hydroxides, which will act as a buffer, using hydroxide from the titrant, keeping the pH constant for a brief time until a specific metal has completely precipitated. When pH reaches certain level the metal ions will precipitate and be eliminated from the water. This forms the stair steps of the titration curve.

For all that the first part of experiments was oriented on the metals precipitation pH values determination using the acid-base titration with 0.2 M NaOH. The initial pH of AMD solution was 3.5. Figure 1 describes the shapes of the AMD synthetic solution integral titration curve and Figure 2 its the first derivation. The chemical analysis of the AMD synthetic solution during titration (Figures 3 and 4) documented the co-precipitation of Fe and As at pH <3.5–4.0>. Next the successive precipitation of Al (pH 5.8), Cu (pH 6.5), Zn (pH 8.5) and Mn (10.2) were observed. The co-precipitation of Fe and As is in accordance with results of many authors (Kaksonen and Puhakka, 2007), because the arsenic compounds have the high affinity for adsorption on the iron hydroxide.

During the metals precipitation by bacterially produced hydrogen sulfide at the initial pH of the AMD synthetic solution, the co-precipitation of Cu and As were observed. Table 2 presents that at pH 3.0 Cu was effectively recovered using biologically produced H<sub>2</sub>S. After 10 minutes the concentration of Cu was 0.02 mg/L. The selective precipitation of Cu

was not achieved because was evidenced the decreasing of As concentration too (Table 2.).

After determination of the suitable pH values for metals selective precipitation were realized experiments concerning of the SSP. The metals selective precipitation as hydroxides or sulphides at the various values of pH AMD is the fundamental of the examined process. The working conditions, occurrence of metal precipitates and obtained results of the selective sequential precipitation of heavy metals from AMD synthetic solution illustrates Table 3. Bacterially produced hydrogen sulphide reacts with the available metal ions in AMD to form insoluble metal sulphides at the appropriate values of pH. When pH of the studied solution is adjusted by sodium hydroxide come to consequent precipitation of metals in the form of hydroxides.

### Conclusion

SSP process demonstrates the removal of heavy metals from aforementioned AMD synthetic solution by the combined application of sodium hydroxide solution and bacterially produced hydrogen sulfide. SSP is able to sequentially precipitate of Fe<sup>3+</sup>, As<sup>5+</sup>, Al<sup>3+</sup> and Mn<sup>2+</sup> in the form of hydroxides; Cu<sup>2+</sup> and Zn<sup>2+</sup> in the form of sulfides. For the removal of Cu and Zn in the form of sulfides were received excellent results. For the removal of Al and Mn in the form of hydroxides were received good results (the minor co-precipitation was observed). Was not come to good results point of view of the Fe and As the selective precipitation, because was determined the co-precipitation of Fe and As.

### Acknowledgements

This work has been supported by Grant Agency of Slovak Republic (project No. 2/0142/19 and No. 1/0326/18).

## Literatura – References

1. COSTA, Maria Clara et al. Treatment of Acid Mine Drainage by Sulphate-reducing Bacteria Using Low Cost Matrices. *Water Air Soil Pollution*, 189, 1, 2008, pp. 149, ISSN: 0049-6979.
2. JOHNSON, Barrie, and Hallberg, Kevin. The microbiology of acidic mine waters. *Research in Microbiology* 154, 7, 2003, p. 466-473, ISSN: 0923-2508.
3. KAKSONEN, Anna and PUHAKKA, Jaakko. Sulfate reduction based bioprocesses for the treatment of acid mine drainage and the recovery of metals. *Engineering in Life Sciences*, 7, 2007, pp. 541–564, ISSN: 1618-2863.
4. KALIN, Margarete et al. The chemistry of conventional and alternative treatment systems for the neutralization of acid mine drainage. *Science of the Total Environment*, 366, 2 – 3, 2006, pp. 395–408, ISSN
5. LUPTAKOVA, Alena et al. Application of Physical-chemical and Biological-chemical Methods for Heavy Metals Removal from Acid Mine Drainage. *Process Biochemistry*, 47, 11, 2011, p. 1633-1639, ISSN 1359-5113.
6. LUPTAKOVA, Alena et al. Mineral biotechnology II. – Sulfuretum in nature and industry. Ostrava : Publishing services department VŠB-TU Ostrava, 2002, p. 152, ISBN 80-248-0114-0. (in Slovak).
7. ODOM, J.M., SINGLETON, R. The Sulfate-reducing Bacteria: Contemporary Perspectives. Springer-Verlag, New York, 1993, p. 249. ISBN 387978658.
8. POSTGATE, John Raymond. The sulphate-reducing bacteria. 2nd edition. Cambridge : Cambridge University Press , 1984, p. 208, ISBN 0521257913.
9. SKOUSEN, Jeffrey et al. A Handbook of Technologies for Avoidance and Remediation of Acid Mine Drainage. West Virginia: The National Mine Land Reclamation Center at West Virginia University in Morgantown, 1998, p. 130.
10. TABAK, H.H. et al. Advances in biotreatment of acid mine drainage and biorecovery of metals: 1. Metal precipitation for recovery and recycle. *Biodegradation*, 14, 6, 2003, p. 423-436, ISSN: 0923-9820.
11. TOTSCHE, Oliver et al. Titration Curves, A Useful Instrument for Assessing the Buffer Systems of Acidic Mining Waters. *Environmental Science and Pollution Research*, 13, 4, 2006, p. 215 – 224, ISSN: 0944-1344.

## *Połączenie chemicznych i biologiczno-chemicznych metod eliminacji metali z kwaśnego drenażu kopalnianego*

*Każdy kwaśny drenaż kopalniany ma określony skład, ale zawsze zawiera kwas siarkowy, rozpuszczone metale ciężkie, siarczany, osady żelaza, a jego pH może być bardzo niskie. Eliminacja metali z kwaśnego drenażu kopalnianego jest poważnym problemem środowiskowym i od dawna stanowi poważny problem dla naukowców, inżynierów, przemysłu i rządów. Różne metody są stosowane do usuwania metali z wód, ale żadna z nich została zastosowana w warunkach komercyjnych. Przeważnie badane są metody chemiczne i biologiczno-chemiczne. Głównym celem pracy była interpretacja połączenia chemicznych i biologiczno-chemicznych metod eliminacji metali ciężkich z syntetycznego roztworu kwaśnego drenażu kopalnianego pochodzącego z kopalni cynku zlokalizowanej w wylocie Túnel Kingsmill w Rio Yauli (dzielnica Yauli – Peru). Podstawą badanego procesu jest selektywne wytrącanie metali w postaci wodorotlenków (metoda chemiczna) i siarczków (metoda biologiczno-chemiczna) przy różnych wartościach pH kwaśnego drenażu kopalnianego. Do produkcji siarkowodoru wykorzystano bakterie redukujące siarczany z rodzaju *Desulfovibrio*. Proces selektywnego sekwencyjnego wytrącania osiąga selektywne wytrącanie wybranych metali z wydajnością 97–99% – Fe, As, Al i Mn w postaci wodorotlenków metali, Cu i Zn jako siarczków metali.*

**Słowa kluczowe:** kwaśny drenaż kopalniany, bakterie redukujące siarczany, siarczki metali, selektywne sekwencyjne wytrącanie







# Development of Filling Material with Fly Ash and Slag as Lubricant in Pipe Jacking Under Acid Sulfate Soils

Kazuki MAEHARA<sup>1)</sup>, Hideki SHIMADA<sup>2)</sup>, Takashi SASAOKA<sup>3)</sup>,  
Akihiro HAMANAKA<sup>4)</sup>

<sup>1)</sup> Kyushu University, Department of Earth Resources Engineering, 744, Motoooka, Nishi-ku, Fukuoka, Japan; email: maehara17r@mine.kyushu-u.ac.jp

<sup>2)</sup> Kyushu University, Department of Earth Resources Engineering, 744, Motoooka, Nishi-ku, Fukuoka, Japan; email: shimada@mine.kyushu-u.ac.jp

<sup>3)</sup> Kyushu University, Department of Earth Resources Engineering, 744, Motoooka, Nishi-ku, Fukuoka, Japan; email: sasaoka@mine.kyushu-u.ac.jp

<sup>4)</sup> Kyushu University, Department of Earth Resources Engineering, 744, Motoooka, Nishi-ku, Fukuoka, Japan; email: hamanaka@mine.kyushu-u.ac.jp

<http://doi.org/10.29227/IM-2020-01-46>

Submission date: 03-01-2020 | Review date: 13-03-20120

## Abstract

*The pipe jacking method is relatively reasonable among trenchless construction methods.*

*For the application of this method, the acid sulfate soils have negative impacts on filling materials (one of the cement materials) injected into the tail-void which are over-cutting areas formed to reduce the friction between the pipes and the surrounding soils. In this study, the application of fly ash and slag is discussed to minimize the effect of sulfur acid to filling materials. As the results of the experiments, the addition of fly ash and slag can control the gelling time and prevent the reduction of uniaxial strength of filling materials under the acid sulfate soils. In addition, the filling materials added slag lowered frictional resistance compared to that of fly ash. Filling materials with the lower frictional resistance are preferred to apply for the smooth pipe jacking constructions. Therefore, filling materials added slag would show better performance than that of fly ash under the acid sulfate soils due to its lower frictional resistance.*

**Keywords:** pipe jacking method, acid sulfate soils, slag, fly ash

## Introduction

In the large cities in Southeast Asian countries, the demand for infrastructure constructions has increased with the growth of the economy and the population (Arc Center of Excellence in Population Ageing Research, 2013). The social infrastructure, however, has to be established under the underground since most of the area is occupied by structures. In Japan, there are social infrastructures including subways, water and sewage systems, and gas pipelines. Two methods are mainly used in Japan to construct the infrastructures under the ground: the open-cut methods and the trenchless construction methods. Although the open-cut method is generally used because of low cost and simplicity, this method causes some social problems such as traffic jams and regulation of traffic in the large cities. On the other hand, trenchless construction methods, such as the shield method and pipe jacking method, allow us to construct the infrastructures under the ground without the problems since they are directly constructed underground. Therefore, trenchless construction methods, especially pipe jacking method, have been widely utilized for the underground construction in Japan (Japan Tunneling Association, 1997).

Pipe jacking is a technique for installing pipelines, ducts, and culverts under the ground. The thrust and the reception pits are constructed, as the pre-construction work. After the construction, the pipelines are installed by transmitting the jacking force with some jacks. The thrust wall is to balance

against the jacking force which is changed depending on the pipe size, the strength of the pipeline, the installed length, and the friction resistance (Attandana and Vacharotavan, 1986). Additionally, the tail-void is formed between pipes and surrounding soils in order to smoothly construct underground pipelines by using pipe jacking.

The filling materials are injected into the tail-void as skid during the constructions so as to decrease the friction resistance and to sustain against the overburden pressure as shown in Figure 1. The performance of the filling materials for pipe jacking construction can be summarized as follows:

1. Reducing the frictions between pipes and surrounding soils efficiently
2. Filling through the tail-voids completely
3. Securing the spaces of the tail-voids
4. Sustaining against the overburden pressure

Recently, the pipe jacking method is expected to be used in Southeast Asian countries in order to construct infrastructures underground without the negative effects on the structures on the ground. However, acid sulfate soils which are often observed in the countries may have the negative impacts on cement which are often used in concrete and the filling material (Yamaji et al., 2007). The pH of acid sulfate soils is below 4 (Attandana and Vacharotavan, 1986). The needle-shaped crystals “Ettringite ( $6\text{CaO} \cdot \text{Al}_2\text{O}_3 \cdot 3\text{SO}_4 \cdot 32\text{H}_2\text{O}$ )” are created by the reaction of sulfur acid in acid sulfate soils and hy-

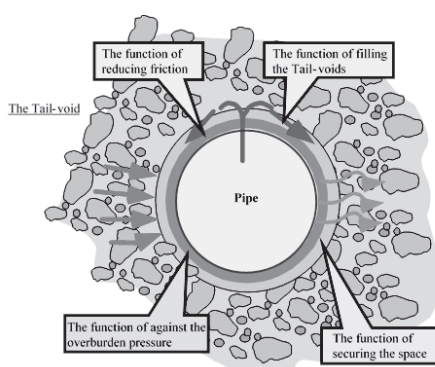


Fig. 1. The functions of filling materials in the tail-void  
Rys. 1. Funkcje wypełniania materiałów w pustce końcowej

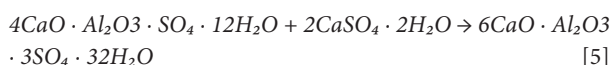
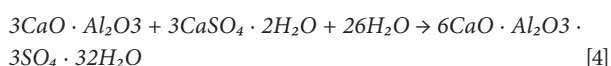
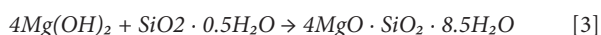
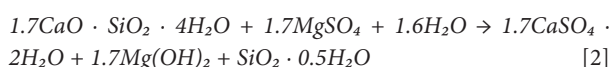
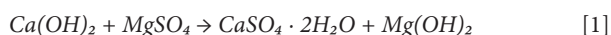
Tab. 1. Contents of the new filling material  
Tab. 1. Skład nowego materiału wypełniającego

Cement	Fly ash	Gypsum	Bentonite	Additive	Fly ash	Slag	Water	Sodium silicate
(g)	(g)	(g)	(g)	(g)	(g)	(g)	(mL)	(mL)
100	140	20	40	8.5	0~20	0~70	830	35



Fig. 2. Rotational friction meter  
Rys. 2. Miernik tarcia obrotowego

drate, which is formed by the reaction of clinker (CaO) (main elements of cement) and water, as follows:



Ettringite causes the swelling inside of the filling materials, resulting in the formation of vacant spaces and the decrease of the densities of the materials. This causes the deterioration of the performance of the filling materials. To reduce the effects on the durability of concrete, fly ash and slag are used in some cases. However, fly ash and slag have never been used for the sake of reducing the effect of acid sulfate soils on

the filling materials in the construction of underground pipe by pipe jacking methods. From these backgrounds, the application of fly ash and slag is discussed to minimize the effect of sulfur acid to filling materials in this study.

## Material and methods

### Gelling time measurement

Setting appropriate gelling time is significantly important for pipe jacking construction. Excess of gelling time causes an outflow of the filling material on the ground. On the other hand, the shortage of gelling time blocks the injection of pipes. Therefore, gelling time of new filling materials added fly ash and slag, shown in Table 1, were measured. Fly ash was taken in the coal-fired power plant in Japan. Here, the concentrations of sulfur acid for the water of the new filling material is arranged to 0 ppm and 100 ppm in order to discuss the effects of sulfur acid on its gelling time.

### Uniaxial compressive strength (UCS) test

The filling materials injected into the tail-void have to support overburden with enough mechanical strength to keep the space of the tail-void. In order to discuss the impact of sulfur acid on the strength of filling materials, the samples of

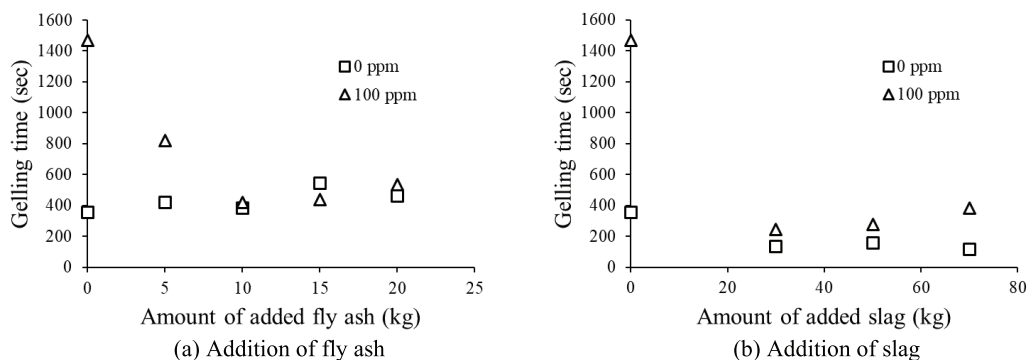


Fig. 3. Results of gelling time measurements with and without sulfur acid  
Rys. 3. Wyniki pomiarów czasu żelowania z i bez kwasu siarkowego

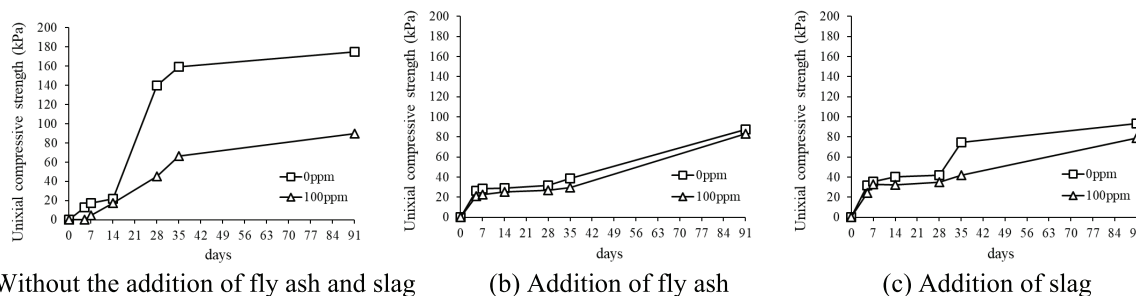


Fig. 4. Results of UCS test  
Rys. 4. Wyniki testu LUW

the filling materials are immersed in sulfur acid during their curing terms. Curing times were 5, 7, 14, 28, 35, and 91 days. The concentrations of sulfur acid were set 0 ppm and 100 ppm. On a basis of the results of gelling time measurements, one filling material which shows the smallest gap between the gelling times of the filling materials with and without sulfur acid was selected from the filling materials added fly ash and slag, respectively. UCS test was performed to the two filling materials.

#### Coefficient of friction measurement

The smaller the coefficient of friction of the filling materials is, the less driving force is necessary, leading to reasonable constructions. It is significantly important to understand the coefficient of friction of the filling materials in a sulfuric acid environment. Hence, coefficients of friction of filling materials were measured with the rotational friction meter as shown in Figure 2. In the bottom part of this meter, 2 types of soil were set, respectively: the one was the soil, whose water content was around 10% with water (neutral soil) and another one was the soil, whose water content was around 10% with sulfur acid (acid soil). The pH of acid soil was around 4. At first, the coefficients of friction of neutral and acid soil were measured. After these measurements, the filling materials with fly ash and slag were set on each soil type, respectively in order to understand the performance for the reduction of friction. These measurements were continued for 20 minutes for soils, and 25 minutes for the filling materials.

### Results and discussion

#### Gelling time measurement

The filling materials did not contain fly ash or slag were strongly influenced by sulfur acid (see Figures 3 and 4). Generally, the clinker (CaO) in the filling materials react with water to generate calcium hydroxide (Ca(OH)<sub>2</sub>) which causes solidification of the filling material (Glasser, 1997). In a sulfuric acid environment, however, the clinker more likely to react with sulfur acid than water to form calcium sulfate (CaSO<sub>4</sub> · H<sub>2</sub>O). This reaction resulted in the formulation of calcium hydroxide, leading to prevent the solidification. Therefore, conventional filling material showed long gelling time in a sulfuric acid environment. On the other hand, the changes of gelling time in a sulfuric acid environment can be minimized by added fly ash and slag. This is because fly ash and slag has alkalinity (Dermatas and Meng, 2003, Manso et al., 2006), meaning that the neutralization occurred before the hydrate reaction. Because of the neutralization, the amount of sulfur acid reduced and the formation of calcium sulfate was prevented, leading to shortening the gelling time. On the basis of these results, the filling materials added 10 g of fly ash and 30 g of slag was selected, respectively, as the sample for UCS test and coefficient of friction measurement.

#### UCS test

At first, the effect of acid on the strength of the filling material without the addition of fly ash and slag is discussed (Figure 4 (a)). The strength of the filling material does not show potential strength in a sulfuric acid environment. The final strength of the sample cured in 100 ppm sulfur acid is approximately half, compared to the final strength of the samples cured in water. In a sulfuric acid environment, the ettringite reaction is likely to occur, resulting in expansion of

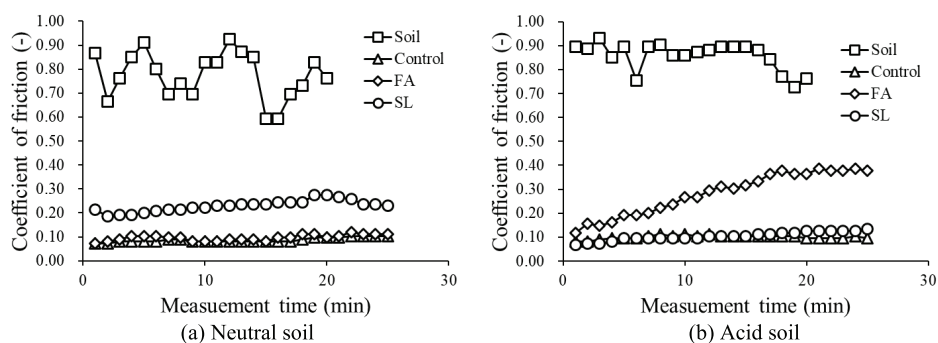


Fig. 5. Results of coefficient of friction measurements  
Rys. 5. Wyniki współczynnika tarcia

the sample. Moreover, the expansion induces generation of new cracks inside the sample and sulfur acid easily ingress into the samples, resulting in deterioration of the strength of filling materials (Grubesa et al., 2016). However, fly ash and slag can control the deterioration of strength because there is less gap between the strength of samples cured in water and sulfur acid (see Figures 4 (b) and (c)). In the case of adding fly ash, silicate oxide ( $\text{SiO}_2$ ) and aluminum oxide ( $\text{Al}_2\text{O}_3$ ) in fly ash react with cement in the filling material (pozzolanic reaction). Because of this reaction, durability and water-tightness of the filling material increase, which control the deterioration of the strength (Yamamoto and Kanezu, 2007). On the other hand, slag can increase the density of filling materials, which makes the sample harder (Ueki, 2014). In addition, because of the increase of the density, the pores inside the filling material decrease, leading to block the penetration of sulfur acid into the filling materials and control the deterioration of the strength. Based on these results, it is suggested that fly ash and slag can control deteriorations of strength from sulfur acid.

#### Coefficient of friction measurement

The coefficient of friction of the filling materials is lower than the soil in both neutral and acid soil (see Figures 5 (a) and (b)). For the filling material without fly ash and slag (Control), the coefficient of friction is decreased dramatically in both neutral and acid soil. In a sulfuric acid environment, however, the coefficient of friction of the filling material with fly ash (FA) gradually increases with time elapsed. Fly ash is generally dominated by small particles and initial strength of fly ash is relatively weak. That is, the filling materials added fly ash does not have enough strength to support the upper part

of the rotational friction meter. Because of this, the upper part of the rotational friction meter is likely to contact the soils, resulting in an increase of the coefficient of friction. On the other hand, the coefficient of friction of the filling material with slag (SL) in acid soil is smaller than that of SL in the neutral soil. Slag has a function as the aggregate and maintaining the volume and/or density of the filling materials, leading to support the upper part of the rotational friction meter (Manso et al., 2006). Hence, the upper part of the rotational friction meter hardly contacts with the soils, resulting in controlling of the coefficient of friction. Above all discussions, although both of the new filling materials with the addition of fly ash and slag can be applied to the constructions of pipe jacking in Southeast Asian countries, the addition of slag would show better performance than that of fly ash in terms of coefficient of friction.

#### Conclusion

From all discussions, the following conclusions can be obtained.

- (1) Sulfur acid causes increasing the gelling time and deterioration of strength of the filling materials.
- (2) The new filling material added fly ash and slag can control increasing the gelling times caused by sulfur acid. Moreover, the addition of fly ash and slag can also control deterioration from sulfur acid, leading to maintain the strength of the filling materials.
- (3) The coefficient of friction of the filling materials added fly ash increases with time elapsed. This result indicates that the filling materials added slag would show better performance than the filling materials added fly ash in Southeast Asian countries

## Literatura – References

1. Arc Center of Excellence in Population Ageing Research, Asia in the aging century, [online]. c2013 [cit. 2019-04-25]. Dostępny z WWW: <<https://www.neura.edu.au/project/arc-centre-of-excellence-in-population-ageing-research/>>.
2. Japan Tunneling Association. Trend of using deep underground and activity report, [online]. C1997 [cit. 2019-04-25]. Dostępny z WWW: <<http://www.japan-tunnel.org/>>. (Japanese).
3. ATTANANDANA, Tasnee., VACHAROTAYAN, Sorasith. Acid sulfate soils: Their characteristics, Genesis, Amelioration and utilization. Southeast Asian Studies, Vol. 24, No. 2, 1986, p. 155-180, ISSN 0563-8682.
4. YAMAJI, Toru et al. Study on a simple factor on the deterioration of concrete submerged in seawater for long term. Technical note of the port and airport research institute, No. 1150, 2007, ISSN 1346-7840.
5. GLASSER, F P. Fundamental aspects of cement solidification and stabilization. Journal of Hazardous Materials, vol. 52, 1997, p. 151-170, ISSN 0304-3894.
6. DERMATAS, Dimitris and MENG, Xiaoguang. Utilization of fly ash stabilization / solidification of heavy metal contaminated soils. Engineering Geology, Vol. 70, 2003, p. 377-394, ISSN 0013-7952.
7. MANSO, Juan M et al. Durability of concrete made with EAF slag as aggregate. Cement & Concrete Composites, Vol. 28, 2006, p. 528-534, ISSN 0958-9465.
8. GRUBESA, Ivanka Netinger et al. Characteristics and uses of steel slag in building construction. Woodhead Publishing Series in Civil and Structural Engineering, 2016, p. 15-30, ISBN 978-0-08-100368-8.
9. YAMAMOTO, Takeshi and KANAZU, Tsutomu. Experimental explanation of compacting effect on hydration phases and strength development mechanism from pozzolanic reaction of fly ash. Journal of JSCE, Vol. 63, No. 1, 2007, p. 52-65, ISSN 1880-6066.
10. UEKI, Yasutomo. History and utilization of portland blast furnace slag cement. Nippon Steel & Sumitomo Metal Technical Reports, No. 399, 2014, p. 110-114, ISSN 0916-7609.

### *Materiał wypełniający z popiołem lotnym i żużlem jako środkiem smarnym w przeciskaniu rur pod kwaśnymi gruntami siarczanowymi*

*Metoda przeciskania rur jest zaliczana do metod budowy bezwykopowej. W przypadku zastosowania tej metody kwaśne gleby siarczanowe mają negatywny wpływ na materiały wypełniające (jeden z materiałów cementowych) wstrzykiwane w pustkę końcową, które są obszarami utworzonymi w celu zmniejszenia tarcia między rurami a otaczającymi glebami. W artykule omówiono zastosowanie popiołu lotnego i żużla w celu zminimalizowania wpływu kwasu siarkowego na materiały wypełniające. W wyniku eksperymentów stwierdzono, że dodanie popiołu lotnego i żużla pozwala na kontrolowanie czasu żelowania i zapobiega zmniejszeniu jednoosiowej wytrzymałości materiałów wypełniających. Ponadto dodany materiał wypełniający obniżył opór tarcia w porównaniu z popiołem lotnym. W przypadku gładkich konstrukcji rurowych zaleca się stosowanie materiałów wypełniających o niższym oporze tarcia. Dlatego dodany żużel z materiałów wypełniających wykazywałby lepszą wydajność niż popioły lotne ze względu na niższy opór tarcia.*

**Słowa kluczowe:** metoda przeciskania rur, kwaśne gleby siarczanowe, żużel, popioły lotne





# Hidden Microcosmos in Slovak Gold Mine Rozalia – Microbial Gold Miners?

*Lenka MALINIČOVÁ*<sup>1)</sup>, *Lea NOSÁLOVÁ*<sup>2)</sup>, *Ivana TIMKOVÁ*<sup>3)</sup>, *Peter PRISTAŠ*<sup>4)</sup>,  
*Jana SEDLÁKOVÁ-KADUKOVÁ*<sup>5)</sup>

<sup>1)</sup> Department of Microbiology, Institute of Biology and Ecology, Faculty of Science, Pavol Jozef Šafárik University in Košice, Šrobárova 2, 04154 Košice, Slovakia; email: lenka.malinicova@upjs.sk

<sup>2)</sup> Department of Microbiology, Institute of Biology and Ecology, Faculty of Science, Pavol Jozef Šafárik University in Košice, Šrobárova 2, 04154 Košice, Slovakia; email: nosalova.lea11@gmail.com

<sup>3)</sup> Department of Microbiology, Institute of Biology and Ecology, Faculty of Science, Pavol Jozef Šafárik University in Košice, Šrobárova 2, 04154 Košice, Slovakia; email: ivana.timkova@student.upjs.sk

<sup>4)</sup> Department of Microbiology, Institute of Biology and Ecology, Faculty of Science, Pavol Jozef Šafárik University in Košice, Šrobárova 2, 04154 Košice, Slovakia; email: jana.sedlakova@upjs.sk

<sup>5)</sup> Department of Microbiology, Institute of Biology and Ecology, Faculty of Science, Pavol Jozef Šafárik University in Košice, Šrobárova 2, 04154 Košice, Slovakia; email: peter.pristas@upjs.sk

<http://doi.org/10.29227/IM-2020-01-47>

Submission date: 02-01-2020 | Review date: 01-04-2020

## Abstract

*Biogeochemical cycling of gold involves dispersion and reconcentration of gold (Au) due to physical, chemical and biological processes in Earth surface environments. These processes are evoked by a metabolic activity of different microbial taxa but many of them (and also their biogeochemical potential) are still unexplored. Understanding the gold cycling is necessary for developing innovative, environmentally friendly gold processing techniques. Our experiments were aimed on isolation and identification of heterotrophic bacteria from ore and ore storage dump samples collected in Rozalia gold mine in Hodruša-Hámre. Using culture-based approach followed by combination of MALDI-TOF MS protein profiling and 16S rDNA sequencing, 18 different bacterial genera were identified in studied microbiota. The participation of several representatives of these genera in individual gold cycling steps has already been reported. The real involvement of bacterial isolates in gold transformation reactions and their biogeochemical potential will be studied in subsequent experiments.*

**Keywords:** gold mine, biogeochemical cycle, bacterial diversity

## Introduction

Geomicrobiology is the scientific field studying the role that microorganisms have played in the geologic past from the time of their first appearance on our planet to the present, the role they are playing today and will probably play in the future in some of the geologically important processes (Ehrlich and Newmann, 2009). Microorganisms participate in many processes including biotransformation of metals and minerals, as well as related substances, and they are intimately involved in metal biogeochemistry with a variety of mechanisms determining mobility and bioavailability (Gadd, 2010).

Gold (Au) is one of the rarest metals on earth. Based on its increased global demand in industry and nanotechnology, the need to supply Au will continue well into the future, despite the increasingly reduced availability of conventional economically and environmentally-viable sources. Therefore, searching for new gold deposits in the nature has become very important. On the other hand, waste products from several industrial processes contain residual gold, that could be recovered and reused. There is an essential need to develop alternative cost-effective and environmentally friendly methods for recovering gold from waste products (Lengke et al., 2006). Research in gold geomicrobiology has developed extensively over the last decade, more and more mechanisms are being discovered by which microbes interact with gold

in its biogeochemical cycle. In weathering environments, Au is mobile, taking the form of oxidized, soluble complexes or reduced, elemental Au nanoparticles. There is still growing evidence that microbes can directly influence solubilization, Au-nanoparticle formation, nanoparticle aggregation, and Au (re)distribution within the natural environment (Shuster and Reith, 2018). These microbial abilities make them suitable tool for biomining - inexpensive and ecological way to extract gold (and other precious metals) from metal-containing ores, waste products and concentrates using microbiological technology.

Ore mining and capacities of ore deposits in Slovakia, formerly very important, are in quite difficult situation nowadays. During last years the gold mining in Slovakia has been complicated due to objective economic conditions resulting from changes at the world metal exchange. Especially, it was the extensive variation of the price and sudden decline of the demands to produce gold that caused the difficulties with the gold mining in Hodruša-Hámre (Bauer et al., 2002).

The Rozalia mine (48°27'N, 18°51'E) at Banská Hodruša, located in the Middle Miocene Štiavnica stratovolcano on the inner side of the Carpathian arc in Slovakia, is the last operating ore mine in Slovakia. Since 1992 the base- and precious metal mineralization has been mined by the company Slovenská banská, Ltd., with variable annual production from 70 to 500 kg of gold. The eastern part of the deposit currently



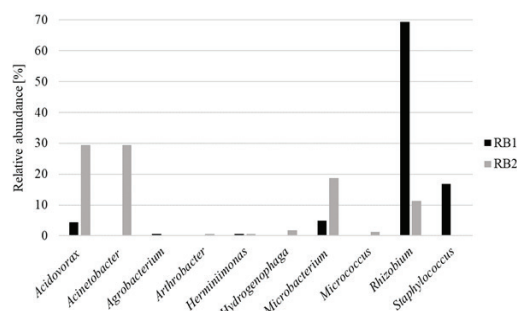


Fig. 1. Genus-level distribution of bacterial isolates obtained from two underground vein exposures RB1 and RB2  
Rys. 1. Rozkład rodzaju izolatów bakteryjnych uzyskanych z dwóch podziemnych żył RB1 i RB2

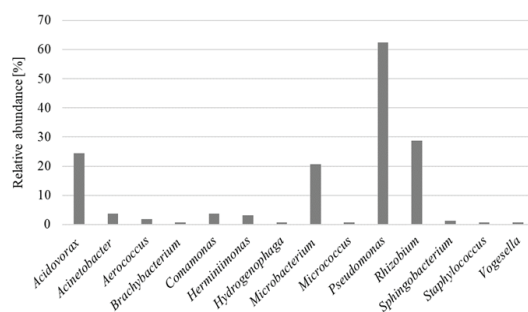


Fig. 2. Genus-level distribution of bacterial isolates obtained from ore storage dump sample H1  
Rys. 2. Rozkład rodzaju izolatów bakteryjnych uzyskanych z próbki H1 składowiska rudy

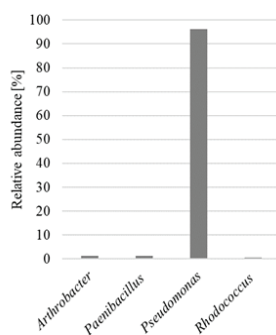


Fig. 3. Genus-level distribution of bacterial isolates obtained from soil sample P1  
Rys. 3. Rozkład rodzaju izolatów bakteryjnych uzyskanych z próbki gleby P1

has an annual production of approximately 30–45 kt of ore containing 450–500 kg of Au (Kubač et al., 2018). The residual material from the ore treatment stored in the ore storage dump at Hodruša-Hámre still contains some residual gold, which is not efficient to recover by conventional processes. The aim of this work was to isolate and identify autochthonous heterotrophic bacteria from both subsurface mine environment and above-ground sites associated with the mine.

### Materials and methods

Samples of ore material from two underground vein exposures in the XIV level of the Rozália mine (sample RB1 – two days after exposure and RB2 – one month after exposure), one sample (H1) from ore storage dump and one sample of soil (P1) from the site immediately near mine entrance were collected under sterile conditions.

1.0 g of each sample was mixed separately with 10 mL of sterile phosphate buffered saline, decimal dilution of samples was prepared and 100  $\mu$ L aliquots of all dilutions were spread

in parallels on four types of culture media (TSA – Trypticase Soy Agar, NA2 – Nutrient Agar no. 2, 10 $\times$ NA2 – 10  $\times$  diluted Nutrient Agar no. 2, and R2A – Reasoner's 2A agar). Cultivation was performed overnight at room temperature under aerobic conditions. From each of studied sample collection sites and each type of culture media, 40 randomly selected bacterial colonies were isolated and subcultured (640 colonies in total).

All bacterial isolates were subjected to identification using MALDI-TOF mass spectrometry protein profiling according to the manufacturer's manual (Microflex LT, Bruker Daltonics, Germany). Total bacterial DNA from isolates unidentified by MALDI-TOF MS was subsequently extracted using GenElute<sup>TM</sup> Bacterial Genomic DNA kit (SIGMA-ALDRICH, Germany). Obtained DNA samples were used as templates for PCR amplification of 16S rRNA gene. PCR amplification was performed on C1000<sup>TM</sup> Thermal Cycler (BIO-RAD Laboratories, USA) and for preparation of reaction mixtures Taq Core kit/high yield (JENA Bioscience,

Tab. 1. Bacterial genera with proven participation in the biogeochemical cycle of gold  
 Tab 1. Rodzaje bakterii o udowodnionym udziale w biogeochemicznym cyklu złota

Bacterial genus	Potential effect on Au-cycling process		Reference
<i>Arthrobacter</i> <i>Microbacterium</i> <i>Micrococcus</i> <i>Staphylococcus</i>	Mediation of initial colonization of the Au-grains surface		Rea et al., 2016
<i>Acinetobacter</i> <i>Pseudomonas</i>	Biofilm growth and recruitment	Stabilisation of the biofilm through the production of extracellular polymeric substances	Pal and Paul, 2008
<i>Rhizobium</i> <i>Acidovorax</i> <i>Pseudomonas</i>		Nitrogen fixation N <sub>2</sub> cycling and continuous supply of usable nitrogen to other biofilm organisms	Rea et al., 2016
<i>Acinetobacter</i> <i>Arthrobacter</i> <i>Pseudomonas</i>		Metabolic turnover of complex organics, xenobiotic and toxins	
<i>Pseudomonas</i>	Au solubilization Precipitation of gold colloids		Reith et al., 2006

Germany) was used. Each PCR reaction mixture (50 µL) contained 1 µM of fD1 primer, 1µM of rP2 primer (Weisburg et al., 1991) and 50 ng of DNA template. The PCR included an initial denaturation at 94°C for 5 minutes followed by 35 cycles of denaturation at 94°C for 1 minute, annealing at 53°C for 1 minute, and extension at 72°C for 1 minute 30 seconds and final extension at 72°C for 10 minutes. Amplified fragments were purified using Wizard SV Gel and PCR Clean-Up System (Promega, USA). Sequencing of PCR amplicons was performed using both primers at Eurofins Genomics, Germany. The obtained sequences were assembled and the entire 16S rRNA gene sequences were subjected to BLAST search against GenBank database.

## Results and discussion

From the biological point of view mines represent an extreme environment with low content of nutrients and often high concentration of metals. Our results showed surprisingly presence of many different bacterial genera inhabiting both subsurface and above-ground sites associated with the mine.

We expected that the variability of microorganisms would be higher in the above-ground environments (H1 and P1), which are influenced by external factors (weather conditions, contact with macro-organisms, etc.). In line with our expectations the highest genus-level distribution (14 genera) was observed in the ore storage dump sample H1 (Fig. 2), 6 and 8 bacterial genera were identified in the subsurface samples RB1 and RB2 respectively (Fig. 1). However, the lowest variability (4 genera) was unexpectedly observed in the soil P1 sample (Fig. 3). We need to take into consideration the fact that until today it is not entirely clear how accurately cultivable microorganisms represent the overall microbial diversity in the environment. The culture-based approach is limited as most of these microorganisms cannot be cultivated under laboratory conditions (Štursa et al., 2009). The overall abundance of cultivable microorganisms in the studied samples was also interesting, with hundreds of thousands of CFU (colony forming units) in 1 gram of sample (from  $2,18 \times 10^5$  CFU per 1.0 gram of the RB1 sample to  $4,51 \times 10^5$  per 1.0 gram of the P1 sample).

The presence of several bacterial genera identified in the samples from Rozália mine and mine-associated sites

was also observed in other studies dealing with the microbial diversity of the gold mine environment or the biogeochemical cycle of gold. For example, the genus *Paenibacillus* which was found in the sample collected from the deep subsurface (1.5 km depth) of the Homestake gold mine in Lead, South Dakota, USA (Rastogi et al., 2009), other genera such as *Arthrobacter*, *Microbacterium*, *Micrococcus*, *Pseudomonas* and *Sphingomonas* represented a significant proportion of the identified taxa in the samples from the gold mine in Złoty Stok, Poland (Drewniak et al., 2008). Our results also show an overlap with other work in identifying the presence of the genera *Acidovorax*, *Acinetobacter*, *Hydrogenophaga*, *Micrococcus*, *Pseudomonas*, *Rhizobium*, *Sphingomonas* and *Staphylococcus* in biofilms on Au grains and nuggets from Australia, New Zealand and South America (Rea et al., 2016).

The mechanisms of participating in the biogeochemical cycle of gold have already been described in several bacterial genera which have also been identified in our samples (Tab. 1).

## Conclusion

The exploration of gold mine-associated autochthonous microbiota and its biogeochemical potential provides new findings and possibilities in the field of precious metals microbial biomining. Our work deals with study of bacteria inhabiting deep subsurface environment of Rozália gold mine in Hodruša-Hámre and above-ground sites associated with mine. Although these locations represent a certain type of extreme environments our results demonstrate the presence of a relatively diverse bacterial population. Using combination of culture-based and molecular methods, 18 different bacterial genera were identified in the examined samples. The role of several of these genera in the biogeochemical cycle of gold has already been reported. The real participation of our bacterial isolates in the individual steps of gold cycle and their potential in biomining will be the subject of subsequent experiments.

## Acknowledgements

The work was financially supported by the Slovak Grant Agency for Science VEGA grant no. 1/0229/17 and by the The Slovak Research and Development Agency grant no. APVV SK-PL-18-0012.

## Literatura – References

1. BAUER, V. et al. Present state of ore mining in Slovak republic. In *Acta Metallurgica Slovaca*, 1, 2002, p. 59–68, ISSN 1338–1156.
2. DREWNIAK, L. et al. Bacteria, hypertolerant to arsenic in the rocks of an ancient gold mine, and their potential role in dissemination arsenic pollution. In *Environmental pollution*. 156(3), 2008, p. 1069–1074. ISSN 0269–7491.
3. EHRLICH, H., NEWMANN, D. *Geomicrobiology*. 5th edition. Boca Raton : CRC Press, 2009. p. 628. ISBN 978-0-8493-7906-2.
4. GADD, G. M. Microbial Role in Global Biogeochemical Cycling of Metals and Metalloids at the Interfaces in the Earth's Critical Zone. In: XU J., HUANG P. M. (eds) *Molecular Environmental Soil Science at the Interfaces in the Earth's Critical Zone*. Berlin, Heidelberg : Springer, 2010, p. 5–7. ISBN 978-3-642-05296-5.
5. KUBAČ, A. et al. Mineralogy of the epithermal precious and base metal deposit Banská Hodruša at the Rozália Mine (Slovakia). In *Mineralogy and Petrology*. 112(5), 2018, p. 705–731. ISSN 1438–1168.
6. LENGKE, M. et al. Mechanisms of gold bioaccumulation by filamentous cyanobacteria from gold(III)-chloride complex. In *Environmental Science & Technology*. 40(20), 2006, p. 6304–6309. ISSN 1520–5851.
7. PAL, A., PAUL A. Microbial extracellular polymeric substances: central elements in heavy metal bioremediation. In *Indian journal of microbiology*. 48(1), 2008, p. 49–64. ISSN 0973–7715.
8. RASTOGI, G. et al. Isolation and characterization of cellulose-degrading bacteria from deep subsurface of the Homestake gold mine, Lead, South Dakota, USA. In *Journal of industrial microbiology and biotechnology*. 36(4), 2009, p. 585–598. ISSN 1476–5535.
9. REA, M. et al. 2016. Bacterial biofilms on gold grains – implication for geomicrobial transformations of gold. In *FEMS Microbiology Ecology*. 92(6), 2016, fiw082, ISSN 0168–6496.
10. REITH, F. et al. 2006. Biomineralization of gold: Biofilms on bacterioform gold. In *Science*, 303(5784), 2006, p. 233–235. ISSN 1095–9203.
11. SHUSTER, J., REITH, F. Reflecting on Gold Geomicrobiology Research: Thoughts and Considerations for Future Endeavors. In *Minerals*, 8(9), 2018, p. 401. ISSN 2075–163X.
12. ŠTURSA, P. et al. Approaches for diversity analysis of cultivable and non-cultivable bacteria in real soil. In *Plant Soil and Environment*, 55(9), 2009, p. 389–396, ISSN 1214–1178.
13. WEISBURG, W. G. et al. 16S ribosomal DNA amplification for phylogenetic study. In *Journal of bacteriology*, 173(2), 1991, p. 697–703, ISSN 1098–5530.

### *Ukryty mikrokosmos w słowackiej kopalni złota Rozalia – drobnoustroje górnkami złota?*

*Cykl biogeochemiczny złota obejmuje dyspersję i ponowne zateżnienie złota (Au) w wyniku procesów fizycznych, chemicznych i biologicznych w środowiskach powierzchni Ziemi. Procesy te są wywoływane przez aktywność metaboliczną różnych taksonów drobnoustrojowych, ale wiele z nich (a także ich potencjał biogeochemiczny) jest wciąż niezbadanych. Zrozumienie obiegu złota jest niezbędne do opracowania innowacyjnych, przyjaznych dla środowiska technik przetwarzania złota. Nasze eksperymenty miały na celu izolację i identyfikację bakterii heterotroficznych z próbek rudy i składowiska rudy zebranych w kopalni złota Rozália w Hodruša-Hámre. Stosując podejście oparte na hodowli, a następnie połączenie profilowania białka MALDI-TOF MS i sekwencjonowania 16S rDNA, zidentyfikowano 18 różnych rodzajów bakterii w badanej mikroflorze. Stwierdzono udział kilku przedstawicieli tych rodzajów w poszczególnych etapach złotego cyklu. Rzeczywiste zaangażowanie izolatów bakteryjnych w reakcje transformacji złota i ich potencjał biogeochemiczny zostaną zbadane w kolejnych eksperymentach.*

**Słowa kluczowe:** kopalnia złota, cykl biogeochemiczny, różnorodność bakterii



# Concepts of Necessary Costs to Be Used in the Minimum Enterprise Decisions

Sorin-Iuliu MANGU<sup>1)</sup>, Diana-Cornelia CSIMINGA<sup>1)</sup>, Mirela ILOIU<sup>1)</sup>,  
Roxana Claudia HERBEI<sup>1)</sup>

<sup>1)</sup> University of Petrosani, Romania

<http://doi.org/10.29227/IM-2020-01-48>

Submission date: 04-01-2020 | Review date: 07-04-2020

## Abstract

*For the correct substantiation of many managerial decisions, the costs provided by the calculations are not sufficient. Because of its complexity, managerial decision may require consideration of costs other than accounting. Under these circumstances, the management of the mining enterprise is subject to the requirement of an economic (net different from the accounting, based on the result of calculations) approach of the decisional situation, which implies the ability to identify and quantify the costs of opportunity, implicit costs, relevant costs, influenced, the costs "sunk".*

**Keywords:** *decision, cost, management*

## Introduction

The decision-making component holds a privileged position in the architecture, functionality and performance of the management system of any enterprise. No other organizational element has such a pronounced managerial specificity and so much impact on all their business plans and business results.

As a result, most management authors view the decision as the essential element of the management process and the specific tool for expressing managers. In essence, the qualitative level of the way an enterprise is run is best expressed through the results achieved by the decisions made and implemented. The decision is the "resistance piece" of management, its most dynamic expression, through which it expresses its functions in full.

Perhaps no other economic category has such high connotations and influences on the decision-making process as the costs. In their various forms of expression, structured in relation to some or other of the criteria, costs are most often the essential element underlying management decisions.

The explanation of this importance, we consider, is as simple as possible: the cost reflects the best, quantitatively, but especially qualitative, the processes that take place within the enterprise. In order to achieve its economic objectives (maximizing profit, maximizing value) and fulfilling its social responsibilities (assuring consumers of goods and/or services), the enterprise consumes resources, the costs being one of the fundamental elements expressing the efficiency of their consumption.

## The cost of opportunity

In its most general definition, the cost of opportunity is "the value of the opportunity or opportunity lost or sacrificed due to the action taken or the option made" [5]. According to this vision, the entrepreneur who uses his own capital to finance certain businesses, in fact, eludes him from other uses, thus incurring the cost of the opportunity (chance) lost to using that capital to fund other projects. Faced with this perspective, the cost of opportunity is the most significant

economic criterion against which the economic efficiency of different capital investment alternatives must be assessed.

Relating the importance of opportunity cost to decision-making can be achieved by considering a simple example. A mining construction company has a stock of 50 tons of steel purchased at the price of 100 m/ton. The current market price for such steel is 120 m/ton. The company's decision on the price at which it accepts a paper in which it consumes the entire steel stock cannot disregard the current steel price, 120 um/ton, because the sale of steel (to the detriment of its use in carrying out a work) an alternative, an option that cannot be neglected in any decisional analysis. If the business does not achieve at least a price equal to the current market price for the steel, it means that it has made the wrong choice because accepting the project means sacrificing the opportunity to sell steel. This example makes it possible to note the weak link between the historical cost and the final decision to be taken. Basically, this cost is neglected in decision-making.

The cost of opportunity is the cost behind price formation on the free market. For example, the price of steel used to manufacture a mechanized abatement complex is determined by its value in other alternative uses. A mining company will therefore have to pay for the steel it consumes a price equal to the one paid by the companies using steel for other uses (car, ship, agricultural machinery, etc.). If the mining company does not do so, if it does not pay the price for the withdrawal of steel from alternative uses, it will practically not produce mining equipment, the steel being used exclusively for the construction of cars, ships, agricultural machinery, and so on

Economic resources are of value to the extent they can be used to produce goods and/or services for consumption. When an enterprise purchases a resource for a particular use, it has to pay a sufficient price for it to withdraw it from other alternative uses (the applicant for the project has to pay for steel from the stock of the construction company a sufficiently high price to withdraw it from the sale on the market). Basically, the price of a resource is determined by its value in the best alternative use.

The sizing of state grants should be based on the cost of opportunity. For the mining industry in Romania, such assessments were not used in such decisions.

### Implicit costs

Normally, the cost of using resources for productive purposes implies one or more payments, called explicit costs, and other non-payment costs, called default costs. Payments of materials, wages, utilities, interest, dividends are all examples of explicit costs. However, the implicit costs associated with a decision-making situation are more difficult to identify and estimate. These costs do not involve cash payments, and as a result, they are often neglected in decisional analyzes. Examples of default costs are numerous, the most common ones being:

- which a cash holder would charge if he made a bank deposit with money, and would not keep them "sock";
- the rent that the owner of an uninhabited building would pay if he hired it;
- the income that the owner of a farmed land will receive if he rents it.

To clarify the difference between the two types of costs, explicit and implicit, can be considered as the following example. Two entrepreneurs, A and B, are analyzing the business of buying a small mining enterprise that exploits an ornamental rock deposit in its quarry. To take over the business it would require 800. The entrepreneur A has the capital needed to buy the career, unlike the entrepreneur B, who has only 500 u of his own capital but can contract from a bank in the form of a loan with a rate annual nominal interest rate of 30%, difference of 300 um Assuming that the results and operation of the small mining enterprise will be the same, regardless of the entrepreneur who will take over the business, the question is: entrepreneur B, who pays an annual interest of 90 um, does it have higher career costs than entrepreneur A? From the point of view of explicit costs, the answer to the question is affirmative, because entrepreneur B has annual payments higher by 90 um than entrepreneur A. For decision-making purposes, management, the answer to the question is negative. The two entrepreneurs cannot have different annual total costs, even if they have different explicit costs. Entrepreneur B has more explicit costs because of the borrowing interest he pays. The total (implicit and explicit) costs of the two entrepreneurs are the same. Entrepreneur A carries a default cost of capital opportunity equal to the amount that he could have earned in an alternative use of the capital invested for taking over the career. At the limit, if in another business it would have obtained a 30% return on the invested capital, it means that it carries an implicit annual cost of opportunity equal to 240 um In turn, entrepreneur B also bears a default cost of opportunity due to capital own investment, in an annual amount of 150 um, which amounts to the 90-um paid annual interest, leads to the same annual cost, 240 um, equal to that of the entrepreneur A.

In the first alternative was taken into account the implicit cost of the capital opportunity, but the implicit management costs were not taken into account. In order to introduce them into the analysis, we will assume that entrepreneurs will also ensure the management of the small mining enterprise. Entrepreneur A is an engineer and could earn as an employee 90 m/y, while entrepreneur B is a clerk and could earn as an

employee 40 m/y. Under these circumstances, the total annual operating costs of the quarry are no longer equal for the two entrepreneurs. Entrepreneur A will incur a default cost of 50µm/year (90–40) than entrepreneur B.

From the entire example presented, one can see how the decisional situation is affected by the implicit costs.

At this point of the paper we should emphasize a particular qualitative aspect of the calculations, taken from the work "Calculation and cost management". When addressing the issue of cost-based costing, a distinct type of cost is so-called "computer interest", expressed in particular by "entrepreneur's salary" and "interest on equity". The two kinds of costs are, in essence, implicit costs, of the opportunity, by taking them into account, the cost calculation increasing in difficulty, but closer to the requirements imposed by rigorous and complete substantiation of managerial decisions.

### Relevant costs

"Not all costs are the basis for decision-making, but only relevant ones" [3]. Almost every decisional situation involves identifying and determining the amount of certain costs. The costs that the manager should consider when analyzing decisional alternatives are called the relevant costs.

Even though the definition of the relevant costs is relatively simple (the costs to be decided), their identification is not so easy. Every decisional situation has its own specificity, the relevant costs in a given situation becoming irrelevant in another. For example, in determining the cost of completing income tax determination, accountants are required to use the actual amounts spent on materials, labor, utilities and services provided by third parties. Also, the legal framework determines the methods for calculating fixed assets' depreciation and provisioning. In conclusion, for the purposes of taxing profit, the relevant costs are past expense. These costs are also relevant for other official, legal purposes. For managerial decisions, however, these past costs, already incurred, may not be relevant, as they are not appropriate, as management costs are generally more relevant to the current costs or future projected costs.

A suggestive example comes in support of the previous statement. A mining enterprise has in its heritage a scrap combination that has been used to exploit coal reserves in several slaughter fields, being completely depreciated from the accounting point of view. However, a technical analysis of the state of the combine shows that it could still be used to extract the coal from another slaughter field. If, however, the combine would be scrapped, different components could be recovered in a total value of 80 um

In these circumstances, can the zero cost of using the combine to extract the coal from the new abatement field be considered as zero? The answer to this question is affirmative only if we analyze the situation from a strictly accounting point of view (combining being fully amortized, the cost of using it further is zero). From an economic point of view, the future use cost of the combine is not equal to zero, but represents 80 um, the value of the components that could be recovered today but which will no longer have any value when the reserve in the new field is exhausted Peaks. It means that for the decision to use the combination to continue or to dismantle it, the past accounting cost has no relevance, the cost of future use of the combine being equal to 80 um

Another example is to outline the concept of relevant cost more clearly, but at the same time proposes to move to another category of costs of particular importance for managerial decisions in the mining sector. A mining enterprise, in the idea of starting a new project, purchased a forwarding combine, paying for it the sum of 1,000. The project was not started, and the combine of advancing remained unused for four years. Attempts to sell it have failed, and the analysis of the mining machinery market shows that there are no prospects for finding a buyer in the future either. However, the opening of coal reserves to a new horizon is a possibility to use the combine. In this situation, the following question arises: what is the relevant cost of using the combine? Perhaps an accountant will calculate the amortization for the duration of the combine and will assume that it is the cost of using it. An experienced manager will, however, consider that the use of the combine harvester generates a relevant zero cost because if the opportunity does not appear, it will still be unused. Combine is an integral part of the mining enterprise's patrimony.

It has been bought in the past but has economic value only to the extent that it will be used in the future. The amount paid when buying the combine is a past cost, definitely borne, irrelevant to the decision to use or not to combine without other alternatives.

With all their simplicity, the two previous examples can serve as a basis for assessing the importance of cost-related aspects of decision-making. The issue of cost relevance becomes complex when coupled with cost calculations in order to substantiate complex decisions such as continuing or stopping the exploitation of reserves in certain mining perimeters, ie the transition to another phase development of the operating unit.

### Influenced costs

The relevant cost concept leads to another cost-critical concept for decision-making. It's the cost that's influenced. Impaired costs are costs that vary with a particular decision. Hence, the conclusion that, in any decision, the relevant costs are also influenced costs (costs affected by the decision).

Influenced costs should not be confused with marginal costs. The marginal cost is just a particular case of influenced cost, with the multitude of influenced costs not being reduced to marginal costs. The marginal cost is a cost influenced by the change in activity level, while the generally influenced cost is a cost influenced by any change, including the level of activity. For example, we can talk about the cost influenced by the introduction of a new product in the manufacturing, the cost influenced by the adopted transport system, the cost influenced by the abatement technology applied, the cost influenced by the decision to close a zone and the extraction of the reserve another geological block, etc.

With all the simplicity of the concept, in many decisional analyzes, influenced costs are not properly quantified or even neglected. The following example confirms this observation. An enterprise refuses a special order representing the production of a particular mark (for which there is excess capacity) and selling it at the 2-um price because an accounting calculation indicates a full unit cost of 2.2 um (obtained by adding to the cost marginally of 1.6 um of a common cost share of 0.6 um). Referring to the influenced cost concept,

two fundamental questions can be answered: "What costs are incurred if the order is accepted?" Respectively "What costs are incurred if the order is declined?" Accepting the order involves only marginal costing of 1.6 um (decision-relevant cost, decision-priced cost) because the shared cost share (0.6 um) is anyway supported, whether or not the order is accepted. Accepting the order means earning a unit contribution margin of 0.4 um (2-1.6), while rejecting the order means losing this contribution to cover fixed costs and generating the result of the period. In conclusion, an addition of uninfluenced costs (allocated on the basis of certain rules or allocation coefficients) to the costs influenced by the decision may entail erroneous decisions resulting in the rejection of certain profitable opportunities, as the undertaking concerned did.

Situations such as those presented in the example are common in companies experiencing a temporary reduction in demand, a reduction that generates excess capacity. These undertakings often accept contracts at a sufficient price only to cover direct costs, but not fully cover the corresponding share of common costs. In this way, the enterprise cannot function "infinitely". As a result, such alternatives, concretized in accepting pricing orders above the estimated cost level but below the full cost, should only be considered as short-term solutions, and in the long run it is necessary to identify and exploit opportunities that provide at least normal profits, because only in this way can the enterprise aspire to development and strengthen the competitive position.

For a developing business, a decision can generate new costs, suppress some old costs and keep them unchanged (obviously an old cost that remains unchanged after the decision, intervenes as a constant, without affecting the outcome of the decision). Similar influences may also be known for profits, which in turn should be treated as costs of opportunity. In such a decision, the final effect is a result of all the influences mentioned, being determined by the relationship

$$[\text{result of the decision}] = [\text{new generated costs}] - [\text{old cost suppressed}] + [\text{old profits lost}] - [\text{new profits earned}]$$

A positive value of the result obtained on the basis of the previous relationship indicates a wrong decision, while a negative value indicates a correct decision.

### Costs "SUNK"

Consideration and acceptance of the influenced cost concept inherently implies the principle that any cost that is not affected by the decision is irrelevant for the purpose of that decision. Irrelevant costs in relation to decisional alternatives are called "sunk" costs because they "play no role in determining the optimal course of action" [5]. These costs have been generated by past decisions and cannot be influenced at present, regardless of the adopted decision alternatives. As a result, they "are not relevant to future events, and can be ignored in making the decision" [3].

At least until 1990, according to our knowledge, the Romanian economy did not have the problem of identifying and analyzing such costs, so that the lack of a consecrated equivalent language term reflecting the concept is justified. Subsequently, at least two reference works in the field of costs pre-

sented and illustrated the concept, under the name of "hidden cost" [3], ie "cost indifferent or submerged"[8].

The importance of these costs in decision-making is significant, but even in the US economy, where the concept originates; there is a relatively high frequency of their incorrect treatment.

The mining branch, through its specific activities, offers many examples of "sunk" costs. In the patrimony of the mining enterprises, the special share is represented by the special constructions, represented mainly by the mining works and the various fittings and installations related thereto. From a decision-making point of view, all of these assets are past, definitively borne costs, "sunk" costs, irrelevant to many current and future decisions regarding the future exploitation of reserves.

This economic feature of capital participation in mining is essential to properly assessing the assets of mining companies in investment start-ups, start-ups or curtailments, as well as in reinvestment to maintain their business or to invest further to develop capacity production.

### Conclusions

Cost-oriented control and decision-making has become one of the core components of the company's profitable management mechanism. It has even come to the design of a system of rules (cost-based) that allows the company to compete on the market in performance conditions, a system designated by the concept of "controlling". The cost calculation, as a process by which identification, assessment, grouping, division and aggregation of expenditure items and structures is achieved in order to obtain the cost of the resource used, the place of activity, the activity or the process as a whole, respectively of the product or period, the clear distinction between two notions which, very often, are attributed the same meaning: costs and costs. The full definition of "expenditure" can only be achieved in an integrating process, with four main coordinates: the generator element, the place of production, the carrier, and the reference period. Instead, the main features that ensure the individualization of the notion of "cost" are: resource consumption, link to achievements, monetary expression. The distinction between costs and costs, reported on the basis of the ratio between financial accounting and management accounting, can be quantified in four different ways: in terms of belonging to one of the two branches of accounting, in terms of differences in nature, in terms of evaluation in monetary terms, from the point of view of the reference period. All these nuances allow for a hierarchy of

the relationship between costs and costs, materialized in the areas of costing: by cost types, by cost carriers, by cost places.

In the particular case of the mining company, several questions can be asked about the elements of the definition of the concept of cost, namely:

- what resources do you work with?
- how resources buy from the market?
- how do they get these resources?
- all expenses generate the purchase of resources?
- can consume to get goods?
- the costs are "born" with the consumption of resources?
- is the term "resource consumption" appropriate to define the costs of the mining company?

Answers to such questions are likely to illustrate a number of peculiarities of mining activities that cannot be ignored in the calculation process.

Once the cost is defined, the result can also be defined in relation to it. Cost-to-detail cost analyzes look at places of activity (costs) and cost carriers. Places of work, also referred to as management centers, are essentially cost-generating places and results, which in the organizational structure are identified with a department that is entrusted with responsibilities related to a function, activity, work, project, goal, etc., and for which the associated expenditure-income relationship can be determined. The planning and control tool of management centers is the revenue and expenditure budget. Particularities of cost locations in mining enterprises are related to their diversity and different destinations of achievements. Thus, a place of costs may be: an opening work (corporeal immobilization), a preparation work ("stock" intended for internal consumption in future exercises), a montage or repair work (for the current exercise or for several future exercises), a cut-off (the actual extraction site of the useful mineral), a process (transport, water evacuation, aeration). Cost carriers are the final products (limited to the object of activity, in limited numbers, coal types, ore concentrates, and useful rocks), ie work and services destined for internal consumption.

Due to the complexity of the need to ensure a correct substantiation, the management decision may require consideration of costs other than accounting (calculation products). A new approach has been developed in which the concepts of opportunity cost, implicit cost, relevant cost, influenced cost, cost "sunk" prevail.

## Literatura – References

1. Abrudan, I. - Premises and landmarks of Romanian managerial culture, Dacia Publishing House, Cluj-Napoca, 1999.
2. Angelescu, C. (coordinator) - Economics, 5th Edition, Economic Publishing House, Bucharest, 2000.
3. Cristea, H. - Accounting and calculations in the company management, Mirton Publishing House, Timișoara, 1997.
4. Gherasim, T. - Microeconomics, vol. I, II, Economic Publishing House, Bucharest, 1993.
5. Heyne, P. - Economic Thought, Didactic and Pedagogical Publishing House, Bucharest, 1991.
6. Hodor, P.; Dobrițoiu, N.; Simionescu, A. - Fundamental Management Decisions in Mine Design, Universitas Publishing House, Petrosani, 2000.
7. Nicolescu, O.; Verboncu, I. - Management, Economic Publishing House, Bucharest, 1995.
8. Ristea, M.; Possler, L.; Ebbeken, K. - Calculation and Cost Management, Teora Publishing House, Bucharest, 2000.
9. Simionescu, A. (coordinator) - General Management, Economic Engineering Manual, Dacia Publishing House, Cluj-Napoca, 2002.
10. Simionescu, A.; Bud, N.; Biber, E. - Evaluation of Projects, Economic Publishing House, Bucharest, 2005.
11. Simionescu, A.; Mangu SI - Microeconomics, Focus Publishing House, Petrosani, 2004.

### *Koncepcje niezbędnych kosztów, które należy zastosować w minimalnych decyzjach przedsiębiorstwa*

*Dla prawidłowego uzasadnienia wielu decyzji zarządczych koszty przedstawione w obliczeniach nie są wystarczające. Ze względu na złożoność decyzje kierownictwa mogą wymagać uwzględnienia kosztów innych niż koszty księgowe. W tych okolicznościach kierownictwo przedsiębiorstwa górniczego podlega wymogom ekonomicznym (innego niż rachunkowość netto, opartego na wynikach obliczeń), podejścia decyzyjnego do sytuacji, co oznacza możliwość zidentyfikowania i oszacowania kosztów alternatywnych, kosztów ukrytych, kosztów utraconych możliwości, kosztów ukrytych.*

**Słowa kluczowe:** decyzja, koszt, zarządzanie







# Possibilities of Tetrahedrite Separation from Polymetallic Ore

Michal MARCIN<sup>1)</sup>, Martin SISOL, Peter VARGA, Ivan BREZÁNI,  
Michal MAŤAŠOVSKÝ, Andrea ORAVCOVA

<sup>1)</sup> Technical University of Košice, Faculty of Mining, Ecology, Process Control and Geotechnologies, Institute of earth resources, Department of mineral processing, Park Komenského 19, 042 00, Košice, Slovak Republic; email: michal.marcin@tuke.sk

<http://doi.org/10.29227/IM-2020-01-49>

Submission date: 26-01-2020 | Review date: 22-04-2020

## Abstract

Using the separation methods, the tetrahedrite concentrate, which contains multiple elements, was obtained from the tetrahedrite ore. We focused mainly on copper, but also on iron and antimony. Ore also contains undesirable elements such as arsenic or mercury. The aim of this paper is an efficient separation of the utility components. Gravity separation and flotation was used. The first processing step was gravity separation on shaking table the second step was froth flotation in flotation column.

**Keywords:** flotation, shaking table, recovery, tetrahedrite

## Introduction

Flotation is based on different physical-chemical properties of each mineral surface. Flotation is a process of separation mineral particles by their selective attachment on fluid-liquid interface. Particles can be hydrophobic (water repulsive) or hydrophilic (water attracted) [1]. Flotation is used mostly on separation valuable minerals from rocks and fine coal from clay, sludge, slate and more coal bearing materials. Preparation process is generally crushing a grinding. After flotation can follow other metallurgical processes [1].

The three main forces acting on a particle moving through a fluid include the external force (gravitational or centrifugal force), the buoyant force (acting parallel to the external force but in the opposite direction) and the drag force (as a result of relative motion between the particle and fluid). Gravity separation involves the separation of minerals of different specific gravity by their relative movement in response to the three forces acting on the mineral particles in a viscous medium such as heavy media, water or, less commonly, air [2][3]. A marked difference in density must exist between the mineral of interest and the gangue to ensure an effective separation. An idea of separation potential can be gained from the concentration criterion [2][3], calculated using the expression [3].

The shaking table is a typical conventional gravity concentrator that has been used extensively over the years. During its operation, separation is principally effected according to the specific gravity, particle size, and particle shape of the minerals in the feed [4][5]. Detailed description of the operation of the shaking table has been presented in the literature [3][4][5]. The table has riffles where vertical stratification of mineral particles due to the shaking action takes place. The heaviest particles report to the bottom, whilst the coarsest and lightest particles migrate to the top. The lightest gangue mineral particles eventually ride over the riffles and are discharged at the lower end of the table along with the flowing film of wash water. The concentrates are then recovered at the unriffled upper section of the deck.

The crystal structure of tetrahedrite and related phases was solved and re-solved many times. The structure is commonly viewed as a complicated derivative of the sphalerite structure, and less commonly as a maximally collapsed sodalite-type framework [6]. The crystal chemical formula of this mineral group is  $\text{Cu}_3\text{6}(\text{Cu}, \dots)\text{4}_6(\text{Sb,As})\text{3}_4\text{S}_4\text{12S}_6$ , with many substitutions possible. Compositions with  $\text{Cu}^{2+}$  are less stable than the composition without this species.  $\text{Cu}^{2+}$  is thus avoided by substitution of Zn, Fe, Hg, Cd, Mn, Co, Ni, or Pb into the tetrahedral sites; note that not all these metals are found in appreciable quantities in natural members of the tetrahedrite-tennantite series [7][8]. In terms of terminology, the compositions with prevailing Sb are tetrahedrite (i.e., not only the Sb end-member) and the As-dominated compositions are tennantite.

## Materials and methods

Material for separation was obtained from local Slovakian deposit Roznava. Sample was mostly tetrahedrite. Main components were Cu and Fe, but also contain Si and Sb. Our focus was mainly to obtain Cu and Fe.

Sample was from mine so size reduction was necessary. Two steps of crushing and one step of milling was performed. After crushing material was screened and then proceeded to shaking table or to another step of size reduction by laboratory mill. After last step of reduction flotation tests were performed in laboratory flotation column. Sample for flotation tests was weighted and 8 kg of material was used in every flotation in total 8 tests were performed. Reagent regime was 4 g.l<sup>-1</sup> MIBC used as frother and 10 g.l<sup>-1</sup> SIPX used as collector. Flowsheet of comminution is on figure 1.

All products after gravity separation and froth flotation were weighted and set for chemical analysis.

## Results

Flotation test showed that copper from tetrahedrite was successfully recovered in froth product. Copper in feed was 1523, 2 g and in concentrate 1034 g so calculated recovery

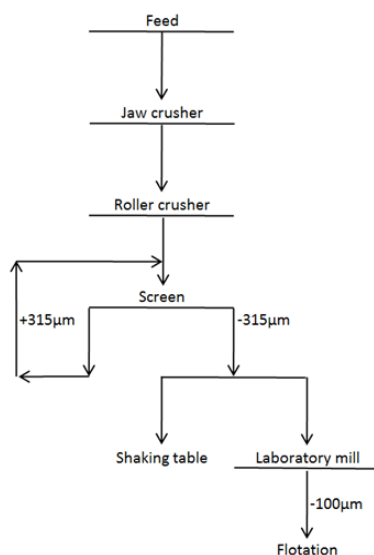


Fig. 1. Flowsheet of comminution  
Rys. 1. Schemat rozdrabniania

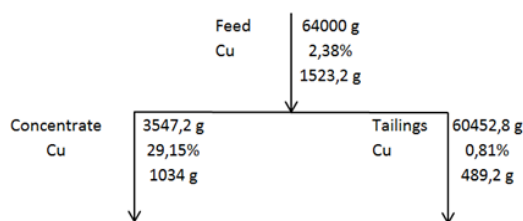


Fig. 2. Scheme of flotation tests  
Rys. 2. Schemat flotacji

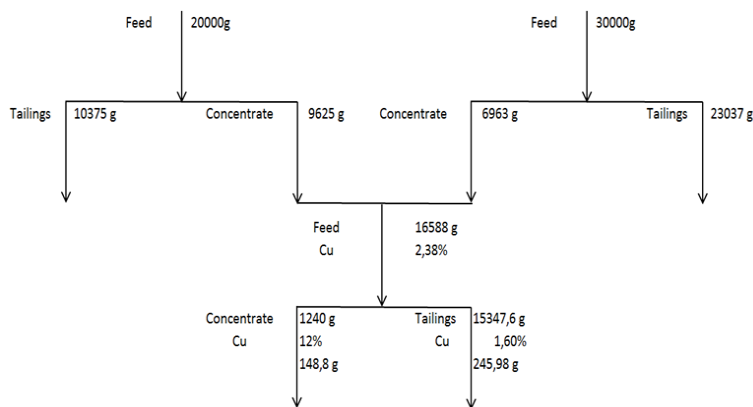


Fig. 3. Scheme of gravity separation test  
Rys. 3. Schemat separacji grawitacyjnej

was 67,88%. There were no cleansing steps after first flotation, but in next experiment we decided to perform this step to increase recovery of copper. Also it is in consideration to little bit change reagent regime and increase the dosage of collector used in flotation.

Another type of tetrahedrite processing was gravity concentration on shaking table. Three tests were performed. Concentrate from this first two tests were then mixed to create new feed on shaking table and cleansing operation was followed.

On figures 2 and 3 are shown schemes and results of flotation and gravity separation tests. Recovery of copper after two steps of gravity separation was calculated 37,69%. This product can be used in further flotation test but conducted in flotation cell, because the amount of material left is not enough to fill the flotation column.

### Conclusion

Froth flotation, using frother such as MIBC and collector SIPX as the only two reagents was found to be a good method

for achieving a high recovery of copper to froth product at natural pH. Such an approach could be advised for roughing or scavenging operations of the tetrahedrite ore processing using the froth flotation method.

After conducting all tests recovery of copper from flotation column is much better than from gravity separation on shaking table. Shaking table should be advised to create higher grade feed for succeeding froth flotation.

Main aim of this work was to find the most suitable method for laboratory tetrahedrite processing. After all conducted experiment, the results are very obvious. The best method for copper recovery from tetrahedrite is froth flotation.

#### **Acknowledgments**

This work was supported by the research grant project VEGA, no. 1/0472/18.

#### Literatura – References

1. A.V. Nguyen, Froth Flotation, In Reference Module in Chemistry, Molecular Sciences and Chemical Engineering, Elsevier, 2013, ISBN 9780124095472,
2. F.F. Aplan, Gravity Concentration M.C. Fuerstenau, K.N. Han (Eds.), Principles of Mineral Processing, SME, Colorado (2003), pp. 185-241
3. B.A. Wills, T.J. Napier-Munn Wills' Mineral Processing Technology: An Introduction to the Practical Aspects of Ore Treatment and Mineral Recovery (7th ed.), Elsevier Science & Technology Books (2006)
4. J. Abols, P. Grady Maximizing Gravity Recovery through the Application of Multiple Gravity Devices Gekko Systems, Vancouver (2006)
5. A. Falconer Gravity separation: old technique/new methods Phys. Sep. Sci. Eng., 12 (2003), pp. 31-48
6. E. Makovicky, Crystal structures of sulfides and other chalcogenides, Rev. Mineral. Geochem., 61 (2006), pp. 7-125
7. S. Karup-Møller, E. Makovicky, Exploratory studies of the solubility of minor elements in tetrahedrite VI. Zinc and the combined zinc-mercury and iron-mercury substitutions, N. Jb. Miner. Mh., 2004 (2004), pp. 508-524
8. M. Klünder-Hansen, S. Karup-Møller, E. Makovicky, Exploratory studies on substitutions in tetrahedrite-tennantite solid solution. Part III. The solubility of bismuth in tetrahedrite-tennantite containing iron and zinc, N. Jb. Miner. Mh., 2003 (2003), pp. 153-175

#### *Możliwość separacji tetraedrytu z rud polimetalicznych*

*Stosując metody separacji otrzymano z tetraedrytu koncentrat który zawiera wiele pierwiastków, Autorzy skupili się głównie na miedzi, żelazie i antymonie. Ruda zawiera również niepożądane pierwiastki, takie jak arsen lub rtęć. Celem przedstawionej pracy jest efektywne oddzielenie składników użytecznych. Zastosowano separację grawitacyjną i flotację. Pierwszym etapem przetwarzania było oddzielenie grawitacyjne na stole wytrząsającym, drugim etapem była flotacja pianowa w kolumnie flotacyjnej.*

**Słowa kluczowe:** flotacja, stół koncentracyjny, odzysk, tetraedryt



# Study of Chemical Pollutants and the Methods of Economic Reconstruction of the Rovinar Basin

Raluca MATEI<sup>1)</sup>, Emilia-Cornelia DUNCA<sup>2)</sup>, Aronel MATEI<sup>2)</sup>

<sup>1)</sup> Company of Mine Closing Jiu Valley

<sup>2)</sup> University of Petrosani, Romania

<http://doi.org/10.29227/IM-2020-01-50>

Submission date: 21-01-2020 | Review date: 11-04-2020

## Abstract

Soil being considered as a resource at anyone's disposal in quantities at its discretion, so there is currently no interest from economic agents to recover and use it efficiently. At the global level, both law and NGOs increasingly require ongoing land use monitoring for the purpose of soil conservation, requiring studies, field and laboratory investigations, prevention, prevention and control projects, methods and techniques. The paper will focus on the analysis of chemical parameters and pollutants (pH, humus, SB, T, total content of N, P, K, Ca, Mg, total Fe, Mn, Cu, Co, Ni, Pb, sulphites, nitrites, pesticides, complex hydrocarbons), the concentration of heavy metals (Cd, Hg, Zn, Pb) of the objectives in the Rovinari basin.

**Keywords:** flotation, shaking table, recovery, tetrahedrite

## Introduction

The purpose of this paper is to provide answers on the importance of the concept of ecological reconstruction, but also to highlight the long-term advantages of its implementation in the context of the management of chemical polluted soils and the concentration of heavy metals in the soil-plant-fruit circuit in the mining objectives in the Rovinari basin. [3, 4, 5]

The paper wishes to provide answers as to how prepared we are, as consumers, to understand this necessary change of approach to how to consume products from these mining areas. To contribute actively through methods of quality and innovation in the field of the environment, to accept and adapt in this direction, and last but not least, how willing we are to participate from a cross-responsible perspective in order to quantify the implementation and gradual development of the new vision in Romania regarding the ecological reconstruction of soils polluted chemically in mining areas. [12]

The importance and necessity of addressing this issue is the continuing decrease in the amount of non-renewable resources worldwide, along with the continuing increase in global population, putting pressure on new approaches to the use and restoration of chemically polluted lands. In this context, a gradual step from a linear economy to a circular economy would have a good environmental, economic and social impact. Under these circumstances, the United Nations has underlined the importance of sustainable development, as defined in principle number 3 of the Rio Declaration, as the right of a country to develop only by taking into account "equitable satisfaction of both developmental and the environment of present and future generations." In order to promote such sustainable development, a new business model is a necessity, one that can take into account the principles of sustainable development. [8, 9, 11]

Transposing the provisions of Directive 2013/34/EU, on Transparency Rules for Mining in the Mining Law on Transparency in the Exploitation of Natural Resources, which in-

cludes a set of clear and concrete principles of integrity and accountability that guarantee the management of natural resources to the benefit of the state and with real economic and social benefits. [13]

In order to provide citizens with assurance as to how the state manages, concessions to exploitation, exploits mineral resources, and fails to violate fundamental rights to safety, property and ecological balance, clear and concrete measures of transparency need to be adopted, integrity and responsibility in the exploitation of natural resources.

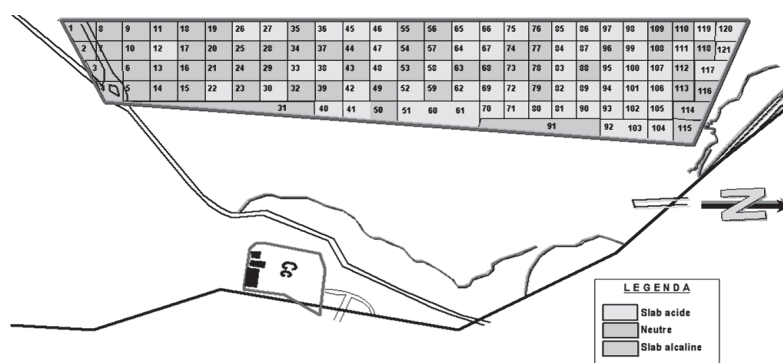
## Research methodology

Studies will primarily focus on soils polluted chemically in the Rovinari mining basin. The study will consist of two parts, namely:

1) Soil sampling in the Tismana waste area. This step is designed to determine the composition and characteristics of chemically polluted soils, the results of a concrete index in the subsequent way of map development with the distribution of chemical pollutants needed in the planning of the ecological reconstruction step, eco-system functionality. [10]

2) Research by experimental methods based on soil chemical characteristics to identify new models of ecological reconstruction of chemically polluted soils. The results of this research will be a starting point in achieving the last of the objectives by establishing a link between the theoretical and practical aspects of finding suitable business models for managing these chemically polluted soils. [2, 3, 9]

3) Organic rehabilitation of chemically polluted soils for their reuse in agriculture, as fruit crops with apple and hazelnut varieties, raspberry and blackcurrant crops; all these activities will be done with a view to gathering accurate, accurate and accurate information so that it is possible to resort to the final stage of proposing a model of ecological reconstruction of chemically polluted soils in order to increase the degree of use and rational reuse of polluted land.



CARTOGRAMA pH

Fig. 1. Cartographic pH

Rys. 1. Rozkład pH

The agrochemical study compiled the following phases of work: A. Preparatory Phase, B. Field Phase, C. Laboratory phase, D. Phase of office, E. the final phase. [3, 11]

#### A. Preparatory Phase

This phase included the following actions: the link with the beneficiary unit (EM Rovinari); preparing the topographic base for the study of agro chemistry; preparation of field materials for harvesting agrochemical soil samples.

#### B. Field Phase

It consisted of the following actions: presentation to the beneficiary unit, drafting of the work plan, recognition of the territory; the actual harvesting of agrochemical soil samples; guidance and field control.

The following are written on the working plan: the perimeter surface; the number of harvested samples.

From the 30-hectare area of the Tismana II internal heap, 121 samples of agrochemical average soil were harvested.

The area of the harvest plot was  $0,25 \div 0,30$  ha at the plan scale of 1: 2000, and the harvesting depth was  $0 \div 20$  cm.

#### C. Laboratory phase

This phase took place at the laboratory of the Gorj Office for Pedological and Agrochemical Studies and covered all laboratory operations from the moment the samples arrived at the laboratory and until handing over the cartography analysis bulletins.

Samples were recorded by laboratory numbers according to the numbering system adopted by OSPA Gorj laboratory.

Large series and small series analysis were performed in this phase.

#### Large series analyzes

The indicators for the full range of agrochemical samples were represented by:

- pH in aqueous suspension pH H<sub>2</sub>O – determined at soil ratio: water 1: 2.5, potentiometer with a couple of glass-calomel electrodes;
- mobile phosphorus content – determined by the Egner-Riehm-Domingo method, in acetate-ammonium lactate extract at pH 3,7 (P-AL);
- the content of mobile potassium – determined in the same extractive solutions as mobile phosphorus and K-AL respectively.

#### Small series analyzes

Additional indicators for small series of agrochemical samples are as follows: In 10% of the soil samples chosen to represent the main soil types in the mapped area, determine the humus content by the modified Donkey's Walkley-Black Oxidometric Method. The data obtained are used for the calculation of the nitrogen index which serves to assess the nitrogen level of the soil.

#### D. Office Phase

It includes the activities carried out by the cartography sector and the study sector – the agro-chemistry department – from the moment of receipt of the analysis bulletins to the finalization of the agro-chemistry file, including the endorsement of the paper.

The office phase consists in finalizing the topographic base, drawing up cartograms, supplementary analytical bulletins, diagrams and synthetic situations on soil reaction and the level of phosphorus and potassium supply.

In the phase of the office, recommendations are also made for chemical fertilizer doses, amendments, depending on the crops expected to be obtained and the supply of soil in nutrients.

As regards the soil reaction state, synthetic situation and laboratory analyzes the following results:

- 15.37 ha, representing 51% of the total area of 30 ha, have a weak acid reaction
- 12.15 ha, representing 41% of the total area, have a neutral reaction
- 2.48 ha, representing 8% of the total area, have a weak alkaline reaction.

It follows from the above that soil reaction (pH) is within optimal limits for the growth of fruit and bushes under normal conditions. (Figure 1)

#### Results

The ecological rehabilitation of land released by technological tasks is a slow and long process.

The greatest weight is to restore vitality and fertility to edaphic environments.

Through ecological rehabilitation (stage I), the land is attracted to the land for agricultural technologies, and by recultivation (stage II) the new edaphic environment is created to create the potential to produce economically.

## SYNTHETIC SITUATION

of the soil reaction state depending on the pH in aqueous suspension

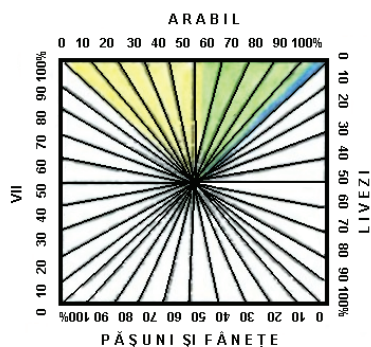
Tismana I waste material

EM Rovinari

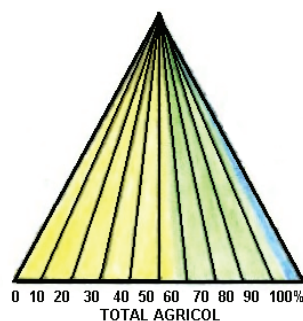
County Gorj

### A. The synoptic situation of the reaction state

a. by category of use



b. on total agricultural



### B. Reaction state structure by category of use

Category of use	Samples or hectares		The reaction											
			Strongly acidic		Moderately acidic		Slightly acidic		neutral		Slightly alkaline		Moderate / Strong alkaline	
			No.	%	No.	%	No.	%	No.	%	No.	%	No.	%
Arable	samples	121	-	-	-	-	62	51	49	41	10	8	-	-
	ha	30	-	-	-	-	15.37	51	12.15	41	2.48	8	-	-
pastures	samples	-	-	-	-	-	-	-	-	-	-	-	-	-
	ha	-	-	-	-	-	-	-	-	-	-	-	-	-
Rough	samples	-	-	-	-	-	-	-	-	-	-	-	-	-
	ha	-	-	-	-	-	-	-	-	-	-	-	-	-
Are you coming	samples	-	-	-	-	-	-	-	-	-	-	-	-	-
	ha	-	-	-	-	-	-	-	-	-	-	-	-	-
orchards	samples	-	-	-	-	-	-	-	-	-	-	-	-	-
	ha	-	-	-	-	-	-	-	-	-	-	-	-	-
Agricultural	samples	121	-	-	-	-	62	51	49	41	10	8	-	-
	ha	30	-	-	-	-	15.37	51	12.15	41	2.48	8	-	-
The color legend														

At the analyzed objective, the Tismana II indoor waste dumps, with a surface of 30 ha following the reconstruction of the lands, resulted in flat, slightly inclined surfaces, the land being suitable for productive agricultural and forestry activities.

The new environment created by the arrangement has good physical and chemical properties for the root system to develop under normal conditions in most of the anthropic ecosystems practiced in the area.

Under these conditions, a structured recultivation program is recommended for the designer for at least 2 years as follows:

- in the first year to practice cultures that could be used as green fertilizer, if possible two crops per year,
- in the second year, to plant fruit trees and fruit bushes practiced by the agricultural producers in the area (apple, hazelnut etc.).

The structure of crops in the 2 years is the following: jar-rye green-lucerne-goat mass. The four cultures can be grouped into at least two variants:

#### Variant 1

- year I - jar-rye green meal
- 2nd year - apple - hazelnuts

#### Variant 2

- 1st year - lucerne - naked
- 2nd year - fruit shrubs

It also incorporates all remaining plant remains after harvesting of bark, clover and alfalfa.

The need for mineral fertilizers is ensured according to the fertilization plan for each crop individually and every year.

If by applying a complete technology the production results for each crop are economic, after 3 years of re-cultivation land can be handed over to the beneficiaries.

Otherwise, the process of re-cultivation continues, focusing on works aimed at increasing the production capacity.

In case of planting of forest plantations, two variants are recommended:

- variant 1 - fertilizer spread over the entire surface and saplings planting
- variant 2 - setting up orchards, planting seedlings with fertilizers at the planting pit (without touching the roots) on land with a slope of more than 10%.

#### Need to apply organic-mineral fertilizers

In order to complement the stock of nutrients in the soil in order to obtain large and economically efficient crops for all crops and all uses, it is necessary to apply organic-mineral fertilizers.



Types of recommended organic-mineral fertilizers can be applied to the range of crops proposed within the Biological Recultivate Project at the tailings dumbbell Tismana II are:

- L-200 (20% N + 20% AH) = 40% active substance
- L-300 (30% N + 12% AH) = 42% active substance.

in which: AH – humic acids.

By the method and the application period, it is intended that the nutrients applied as fertilizers should be as far as possible in the active absorption zone and the utilization rate should be as high as possible.

Annual grass rotation for annual plants is carried out with the deep soil work at the time when it is recommended to perform it (usually in autumn), but also with other soil works that are done before sowing.

In the case of organic-mineral fertilizers it is recommended to apply nitrogen and humic acids.

In the case of nitrogen, phosphorus and potassium fertilizers, it is recommended that nitrogen be applied physically (both under base and during vegetation) and phosphorus and potassium entirely under the basic soil in the preparation of the sowing field at the time of application, depending on the culture to be set up.

For setting up forest plantations (hardwoods), the chemical fertilization periods are as follows:

- nitrogen – 1 / 2 of the nitrogen dose is applied early spring with phosphorus and potassium; 1A is given in one or two halves in the first part of the vegetation;
- phosphorus – is given early spring;
- Potassium – is given early spring (preferably potassium sulphate).

Taking into account the fact that in the long run the objective in its entirety must be ensured stability, it is recommended that the areas with slopes higher than 2-5% be arranged and used for forest productive activities.

In the fertilization plan the fertilizer and forestry (hardwood) needs were calculated.

## Conclusions

The investigations carried out in the mining Rovinari between 2018–2019, several conclusions can be drawn:

Pollution caused by the up-to-date exploitation of lignite in the Rovinari mining perimeter of the soil and subsoil is a long-term local and area and relates to:

1. The degradation of the natural geological environment:
  - the impossibility of recovering the soil layer from deforested forest lands, and as a result it is destroyed;
  - roads are dislodged, excavated, transported and stored on sites down to the depths of tens and even hundreds of meters;

- the resulting, sterile and useful mining masses acquire geotechnical features other than basic rock;
- deposited tailings create new compaction and stability effects on new sites;
- the physico-chemical imbalance in the basement produced by excavations and landfills is extended also in the areas pertaining to the mining perimeter.

2. Disturbance of the physico-chemical equilibrium of the geological environment caused by geological, hydrogeological and geotechnical prospecting through drillings with insignificant, inevitable and irreversible effects on groundwater and groundwater systems, on small surfaces and volumes and in limited time;

3. Soil and subsoil damage through the construction of buildings, roads, infrastructure and mining mass transport, etc ;

4. Soil degradation and decrease of fertility class on large areas, by changing the initial destination of agricultural or forest lands and organizing activities related to exploitation.

The quality of the soil environmental factor in the mining and exploitation mining perimeter is entirely negatively affected by the direct and related exploitation activities of the lignite. The same is true of the basement, where the exploitation activity effectively destroys the natural geological environment. Soil and subsoil pollution is also linked to the risk of accidents or catastrophes, which relate to:

- the risk of environmental accidents that cause lignite self-ignition in the bed or surface deposits;
- accidents or catastrophes leading to major disruptions of the geological environment, mixtures of aquifers, penetration of surface pollutants;
- the adoption of organizational measures and exploitation technologies, which do not limit the actual "in situ" action to the strict necessity and are not adapted to the specific geological structure, can amplify and diversify the complexity of the exploitation/coal on the ground and subsoil;
- local accentuation of geological strain instability and favoring landslides and sediments.

The tailings dumps, besides the permanent occupation of the land on which they are stored, also constitute a permanent source of pollution, by the entrainment of the material and the dissolution of the metal ions.

Analyzes on soil quality indicate a decrease in nitrogen, phosphorus and potassium in agricultural land, the emergence of new types of soils on tailings dumps of the non-evolved type with surface rock on the surface.

## Literatura – References

1. Botnariuc, N, 1999, Evolution of supra-individual biological systems, Bucharest University Publishing House.
2. Cioacă A., Dinu M., 1998 - Restructuring of lignite mining in Romania and its environmental effects with special reference to landforms, Romanian Revue of Geographie, Tome 42, Academia Publishing House, Bucharest.
3. Constandache, C., 2000, Reclamation, Improvement and / or Substitution of Inappropriate Stands on Degraded Land, ICAS Bucharest.
4. Dumitrescu I., 2002, Environmental pollution, FOCUS Publishing House, Petrosani;
5. Dumitru M., Popescu I., Blaga Gh., Dumitru Elisabeta, 1999, Recultivation of land degraded by the Oltenia coal basin, "Transilvania Press" Publishing House, Cluj-Napoca.
6. Fodor, D., Baican, G., 2001, Impact of the mining industry on the environment. INFOMIN Publishing House, Deva.
7. Geanbașu, N., 1995, Some theoretical aspects regarding the ecological reconstruction of damaged forest ecosystems - Forest Journal, No. 2.
8. Lazar M, Dumitrescu I., 2006, Ecological Rehabilitation, Universitas Publishing House, Petroșani.
9. Olteanu A., 1991, Agricultural landscaping. Practical workshop. Lithographed, N. Agronomic Institute Bălcescu ", Bucharest.
10. Răgălie S., Rusu C., 2008, - Assessment of the current state and prospects of the mining industry in Romania. Romanian Academy. National Institute of Economic Research. Center of Industry and Services Economy
11. Rojanschi, V., Bran, F., Diaconu, Gh., 1998, Protection and Environmental Engineering. Economic Publishing House.
12. Rojanschi, V., Bran, F., Diaconu, Gh., 2002, Protection and Environmental Engineering. Second Edition, Economic Publishing House.
13. Traci, C., 1990, Reconstruction of forest ecosystems on degraded land, volume Ecological bases for forestry and prairie culture, Bucharest.

### *Badanie zanieczyszczeń chemicznych i metod rekonstrukcji gospodarczej basenu Rovinar*

*Gleba jest uważana za zasób do dyspozycji każdego w ilościach według własnego uznania, więc podmioty gospodarcze nie są obecnie zainteresowane odzyskaniem i efektywnym wykorzystaniem. Na poziomie globalnym zarówno prawo, jak i organizacje pozarządowe coraz częściej wymagają ciągłego monitorowania użytkowania gruntów w celu ochrony gleby, wymagając badań, badań terenowych i laboratoryjnych, projektów, metod i technik zapobiegania, zapobiegania i kontroli. Artykuł koncentruje się na analizie parametrów chemicznych i zanieczyszczeń (pH, próchnicy, SB, T, całkowitej zawartości N, P, K, Ca, Mg, całkowitej Fe, Mn, Cu, Co, Ni, Pb, siarczynów, azotynów, pestycydy, złożone węglowodory), stężenie metali ciężkich (Cd, Hg, Zn, Pb) terenów w dorzeczu Rovinari.*

**Słowa kluczowe:** flotacja, stół wytrząsający, odzyskiwanie, tetraedryt





# Investigation of Groundwater Flow Using $\Delta^{18}\text{O}$ and $\Delta\text{D}$ in a Sulfur Mine in Japan

Shinji MATSUMOTO<sup>1)</sup>, Isao MACHIDA<sup>2)</sup>

<sup>1)</sup> National Institute of Advanced Industrial Science and Technology, Geological Survey of Japan, Geo-Resources and Environment, Groundwater Research Group Central 7, 1-1-1, Higashi, Tsukuba, Ibaraki, Japan; email: shin.matsumoto@aist.go.jp

<sup>2)</sup> National Institute of Advanced Industrial Science and Technology, Geological Survey of Japan, Geo-Resources and Environment, Groundwater Research Group Central 7, 1-1-1, Higashi, Tsukuba, Ibaraki, Japan; email: i-machida@aist.go.jp

<http://doi.org/10.29227/IM-2020-01-51>

Submission date: 02-01-2020 | Review date: 21-02-2020

## Abstract

The A sulfur mine is located in the Iwate Prefecture of Japan. This mine has both surface and underground parts and was operated from the late 1800s to the late 1900s. Since the early 1900s, acid mine drainage (AMD) has been reported in this mine, and the waste water has been neutralized in a treatment plant since the mine was closed. Recently, reducing the AMD volume by decreasing water inflow to the underground mine has been considered as a way to reduce the AMD treatment cost. The first step in such an approach is to understand in detail the groundwater flow around the mine. However, part of the study area is covered by lava and comprises crystalline rocks with complicated structures, making it difficult to understand the groundwater flow. Therefore, the present study investigated the groundwater flow around this mine by focusing on water quality, such as pH and electrical conductivity (EC), stable isotopes (i.e.  $\delta^{18}\text{O}$  and  $\delta\text{D}$ ) and  $^3\text{H}$  in the surface and ground water. The spatial distributions of pH, Stiff diagrams, and  $\delta^{18}\text{O}$  and  $\delta\text{D}$  values in the surface and ground water indicated that the groundwater flow system was divided into three basins in the study area, as predicted from geomorphological information. Moreover, the spatial distribution of  $\delta^{18}\text{O}$  and  $\delta\text{D}$  in the surface and ground water suggested that the groundwater recharged at the highest altitudes in the B mountain in the northwest of the mine might flow in the underground mine. Furthermore, the  $^3\text{H}$  values in the waste water discharged from the underground part of mine implied that the groundwater age was no more than approximately 60 years old.

**Keywords:** mine closure, acid mine drainage (AMD), waste water, stable isotopes, groundwater flow

## Introduction

The A sulfur mine is located in the Iwate Prefecture of Japan. This mine has both surface and underground parts. This mine began operation in the late 1800s but was closed in the late 1900s because of falling demand for sulfur. Since the early 1900s, the serious water-pollution problem of acid mine drainage (AMD) has been reported in this mine, and the waste water discharged from the underground mine has been neutralized in a treatment plant since the mine closed. However, treating this AMD is very expensive and voluminous (e.g., approximately 9.1 million cubic meters of AMD with a pH of 2.3 were treated in 2006). Reducing the AMD volume by decreasing water inflow to the underground mine has been considered as a way to reduce the AMD treatment cost. The first step in such an approach is to understand the groundwater flow around the mine. A reliable method for understanding groundwater flow is to use information about the stable isotopes of water, such as  $\delta^{18}\text{O}$  and  $\delta\text{D}$ . The isotope tracer technique began in the 1950s in the field of hydrology, and by the late 1960s isotopes were being used widely in hydrology research worldwide (Huang and Wang, 2017). In recent years, the composition of stable water isotopes has been used effectively to investigate groundwater flow around mine sites. Gammons et al. (2010) used  $\delta^{18}\text{O}$  and  $\delta\text{D}$  to understand the recharge area of inflow into abandoned coal mines, and Toughzaoui et al. (2015) used  $\delta^{18}\text{O}$  and  $\delta\text{D}$  isotope analysis to investigate hydrological processes around an abandoned mine watershed. Huang and Wang (2017) showed several examples

of using  $\delta^{18}\text{O}$  and  $\delta\text{D}$  as mine groundwater tracers, and they used the isotopic data of water samples taken from the study area to simulate numerically the groundwater recharge area. Furthermore, the impact of AMD can be discussed based on the  $\delta^{18}\text{O}$  and  $\delta\text{D}$  values of surface water around a mine area (Sun et al., 2014). However, part of the area in the present study is covered by lava and comprises crystalline rocks with complicated structures, making it difficult to understand the groundwater flow. In addition,  $\delta^{18}\text{O}$  and  $\delta\text{D}$  have not been used previously to investigate water inflow to the underground part of this mine. Therefore, the present study investigates the groundwater flow around the A sulfur mine by using geochemical methods, water quality, such as pH and electrical conductivity (EC), stable isotopes (i.e.  $\delta^{18}\text{O}$  and  $\delta\text{D}$  which are used widely as tracers), and  $^3\text{H}$  in surface and ground water.

## Materials and methods

Figure 1 shows a topographic map of the study area with the locations of (i) the sampling sites (A1–A6, B1–B17, and C1–C8), (ii) the B mountain, and (iii) the underground mine area. Figure 2 provides geological information about the study area (Kawano and Uemura, 1962). The underground mine area is located at approximately 1,000 m above sea level. In Fig. 1, based on the geomorphological information, the groundwater flow system is divided into basins A, B, and C. In Fig. 2, the alteration zones, which are affected by silicification and argillation, include sulfur deposits (L1 and L2) and are covered with unaltered lava (L3–L5) (Kawano and Uemura,

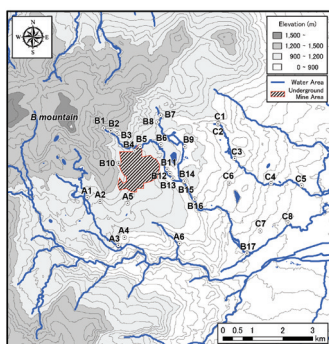


Fig. 1. Topographic map of study area with locations of sampling sites, B mountain, and underground mine area  
 Rys. 1. Mapa topograficzna obszaru badań z lokalizacjami miejsc pobierania próbek, góry B i obszaru kopalni podziemnej

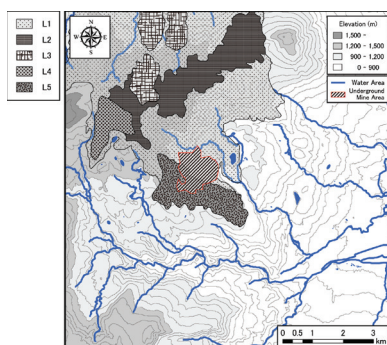


Fig. 2. Geological map of study area: L1 is andesitic tuff with augite-hypersthene andesite lava; L2 is quartz-bearing olivine-augite-hypersthene andesite and augite-hypersthene andesite; L3 is augite-hypersthene-olivine basalt; L4 is augite-olivine-hypersthene andesite; L5 is olivine-augite-hypersthene andesite (Kawano and Uemura, 1962)

Rys. 2. Mapa geologiczna badanego obszaru: L1 jest tufem andezytycznym z lawą andezytową hiperstenem; L2 to zawierający kwarc oliwinowy augit-augit-hipersten andezyt i augit-hipersten-oliwin bazaltem; L3 to andezyt-augit-oliwin-hiperten; L5 jest andezytem oliwinu-augitu-hiperstenu (Kawano i Uemura, 1962)

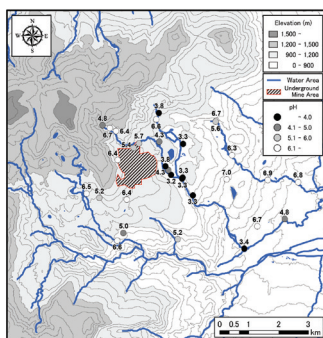


Fig. 3. Spatial distribution of pH of water samples  
 Rys. 3. Przestrzenny rozkład pH próbek wody

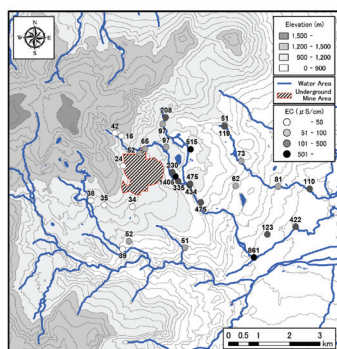


Fig. 4. Spatial distribution of EC of water samples  
 Rys. 4. Przestrzenny rozkład EC próbek wody

Tab. 1. Chemical characteristics of surface and ground water in study area  
 Tab. 1. Charakterystyka chemiczna wód powierzchniowych i gruntowych na badanym obszarze

Samples	Temp (°C)	pH (-)	EC ( $\mu\text{S}/\text{cm}$ )	Fe <sup>total</sup> (mg/L)	Na <sup>+</sup> (mg/L)	K <sup>+</sup> (mg/L)	Ca <sup>2+</sup> (mg/L)	Mg <sup>2+</sup> (mg/L)	Cl <sup>-</sup> (mg/L)	HCO <sub>3</sub> <sup>-</sup> (mg/L)	SO <sub>4</sub> <sup>2-</sup> (mg/L)	$\delta^{18}\text{O}$ (‰)	$\delta\text{D}$ (‰)	<sup>3</sup> H (T.U.)
A1	5.1	6.5	40	0.1	2.6	0.5	3.1	1.0	3.2	6.5	2.6	-10.4	-66	3.9
A2	5.4	5.2	40	0.0	2.3	0.5	2.0	0.9	3.9	7.7	5.4	-10.2	-63	-
A3	5.3	6.6	40	0.0	2.5	0.5	3.2	1.0	3.4	11.8	2.2	-10.7	-65	-
A4	5.4	5.0	50	0.0	2.9	0.7	3.3	1.3	3.8	2.4	13.3	-10.4	-64	-
A5	5.1	6.4	30	0.0	2.3	0.4	2.9	0.8	2.1	11.8	2.7	-11.8	-74	-
A6	5.0	5.2	50	0.0	2.5	0.6	3.4	1.3	2.7	6.9	13.8	-11.0	-69	3.9
B1	-	4.8	-	0.1	2.3	0.5	3.6	1.4	2.4	0.0	20.3	-11.4	-70	3.8
B2	3.6	6.7	40	0.0	3.0	0.7	3.3	1.2	2.6	4.5	7.4	-11.6	-73	3.5
B3	3.0	6.4	20	0.0	1.5	0.3	1.1	0.5	2.6	6.1	2.3	-10.6	-66	-
B4	5.4	5.4	50	0.1	2.3	0.5	4.4	1.5	2.8	6.9	16.3	-10.8	-67	-
B5	3.4	5.7	70	0.1	2.3	0.5	4.7	1.6	2.5	0.0	21.0	-11.4	-71	-
B6	5.2	4.3	100	0.1	2.3	0.7	5.2	1.4	3.0	0.0	30.5	-10.3	-63	-
B7	5.4	3.8	210	0.1	2.8	0.8	7.1	2.2	2.2	0.0	68.0	-11.2	-69	4.6
B8	5.7	6.6	100	0.0	4.8	0.6	8.9	2.4	2.7	8.5	33.9	-11.8	-74	3.8
B9	7.4	3.3	520	0.3	5.5	2.4	30.0	3.8	3.9	0.0	152.1	-11.1	-69	-
B10	5.4	6.4	20	0.0	1.8	0.3	1.9	0.7	2.0	8.1	5.5	-11.7	-73	-
B11	4.4	3.8	230	0.1	3.1	0.8	9.9	2.8	2.8	0.0	81.2	-11.0	-68	-
B12	13.0	4.3	1410	0.0	8.4	3.2	254.4	8.7	2.6	0.0	877.2	-11.8	-74	-
B13	7.3	3.2	340	0.3	3.2	0.8	6.5	2.1	2.2	0.0	86.3	-11.5	-73	3.8
B14	8.0	3.3	480	0.2	5.5	3.2	30.1	3.8	4.6	0.0	150.3	-11.0	-68	-
B15	7.4	3.3	430	0.4	3.7	1.2	17.3	3.3	3.1	0.0	157.0	-10.4	-63	-
B16	7.5	3.3	480	0.5	4.2	1.7	22.1	3.3	3.4	0.0	160.4	-10.5	-63	-
B17	9.5	3.4	860	0.2	6.7	2.5	109.6	6.3	3.0	0.0	446.8	-11.2	-70	-
C1	7.1	6.7	50	0.0	3.1	1.2	4.3	1.5	2.6	30.5	4.2	-11.8	-75	3.5
C2	8.7	5.6	120	0.0	5.4	1.7	8.1	2.9	4.2	6.5	37.4	-11.3	-71	0.6
C3	5.8	6.3	70	0.1	3.7	1.1	5.6	2.0	3.3	9.4	21.8	-11.4	-72	-
C4	5.2	6.9	80	0.0	3.8	1.1	5.8	2.1	3.2	9.4	22.6	-11.4	-73	-
C5	8.1	6.8	110	0.0	4.6	1.2	10.6	3.1	3.3	15.5	31.9	-11.4	-73	-
C6	7.8	7.0	60	0.0	3.1	0.4	4.8	2.3	4.9	29.7	32.0	-11.5	-74	2.9
C7	7.5	6.7	120	0.0	4.5	1.7	12.0	3.2	4.1	10.6	43.3	-10.6	-68	-
C8	9.7	4.8	420	0.0	10.4	2.9	44.3	9.2	6.4	0.0	205.0	-10.5	-68	3.3
Average	6.4	5.3	220	0.1	3.8	1.1	20.4	2.6	3.2	6.2	87.9	-11.1	-69	3.4

1962). The waste water from the underground mine is neutralized in the treatment plant at B12 in Fig. 1 before being discharged into the river (the pH of the final effluent water is maintained at above 4.0 based on the limits regarding the waste water quality in this mine). There is also a water drain hole at B10 to decrease the volume of recharging water into the underground mine.

Samples of surface and ground water for chemical and isotopic analyses were taken between October 30, 2018 and November 1, 2018 at the 31 sampling sites shown in Fig. 1. During the sampling, the chemical characteristics of the water [i.e., temperature, pH, and EC] were measured in the field using a colorimetric pH measuring device (ATC series; Advantec, Japan), a pH meter (D52S; Horiba, Japan), and an EC meter (YSI-Pro30; YSI, USA). Collected in 100 mL polyethylene bottles, the water samples were analyzed for alkalinity, inorganic ions (Fe<sup>total</sup>, Na<sup>+</sup>, K<sup>+</sup>, Ca<sup>2+</sup>, Mg<sup>2+</sup>, Cl<sup>-</sup>, SO<sub>4</sub><sup>2-</sup>), and stable isotope of water ( $\delta^{18}\text{O}$  and  $\delta\text{D}$ ) after filtration using disposable 0.45  $\mu\text{m}$  in-line filters. The alkalinity (pH 4.8) was measured using 0.02N H<sub>2</sub>SO<sub>4</sub> titration method, and the result was converted to a concentration of HCO<sub>3</sub><sup>-</sup>. The concentrations of Fe<sup>total</sup> and Mg<sup>2+</sup> were measured using ICP-MS (NexION 300; PerkinElmer, USA) after adding HNO<sub>3</sub> to lower the pH to below 2, and those of Na<sup>+</sup>, K<sup>+</sup>, Ca<sup>2+</sup>, Cl<sup>-</sup>, and SO<sub>4</sub><sup>2-</sup> were measured using ion chromatography (ICS-5000; Dionex, USA). The  $\delta^{18}\text{O}$  and  $\delta\text{D}$  values were determined using a liquid water isotope analyzer (L2140-i; Picarro, USA) employing a cavity ring-down spectrometer with analytical errors within  $\pm 0.1\text{‰}$  for  $\delta^{18}\text{O}$  and  $\pm 1\text{‰}$  for  $\delta\text{D}$ . The  $\delta^{18}\text{O}$  and  $\delta\text{D}$  values were expressed relative to Vienna Standard Mean Ocean Water. Additionally, water samples in 1,000 mL polyethylene bot-

tles were taken at 11 sampling sites for <sup>3</sup>H analysis. They were distilled under reduced pressure using an automated evaporator (NVC2200 and N-2100; Eyela, Japan) prior to electrolytic accumulation of <sup>3</sup>H by an electrolysis instrument (Tori Pure; Permec, Japan). The <sup>3</sup>H concentrations of the samples were determined using a liquid scintillation counter (AccuFLEX LSC-LB7; Hitachi Aloka, Japan) with an analytical error within  $\pm 0.28$  tritium unit (T.U.). The analytical data were plotted using ArcGIS 10.5 (ESRI, USA).

## Results and discussion

The quality of the water samples is summarized in Table 1, and Figs. 3 and 4 show the spatial distributions of pH and EC in the study area. The B12 water sample had the highest temperature, EC, and SO<sub>4</sub><sup>2-</sup>. Because the treatment plant for the waste water from the underground mine is at B12, the pH there exceeded 4.0 and was within the regulations for waste water quality in this mine. Although the surface water at A1–A4 showed pH values greater than 5.0 (the average pH was 5.8) and that at C1–C5 showed pH values greater than 5.6 (the average pH was 6.5), a low pH was observed in the surface water around the underground mine area in Fig. 3; the pH values at B9 and B13–B16 were less than 3.3. Given that the pH of the treated water at B12 was 4.3, the low pH around the underground mine area is not due to the waste water from the underground mine. In Fig. 2, the alteration zones (L1) including the sulfur deposit cover the B7, B9, B11, B13, and B14 sampling sites, where the pH of the surface water was less than 4.0. Furthermore, the SO<sub>4</sub><sup>2-</sup> concentration exceeded 68.0 mg/L (the average value was 107.6 mg/L) and that of Fe<sup>total</sup> exceeded 0.1 mg/L (the average value was 0.2 mg/L), show-

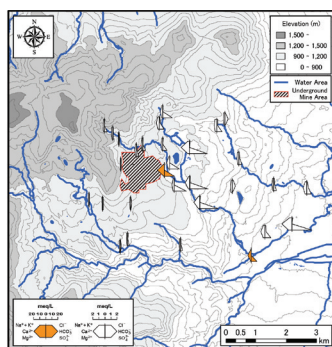


Fig. 5. Stiff diagrams of water samples  
Rys. 5. Diagramy Stiffa próbek wody

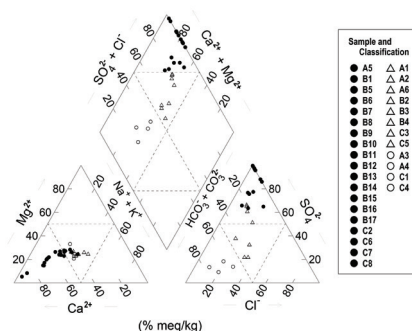


Fig. 6. Piper diagram of water samples  
Rys. 6. Chemizm próbek wody

ing higher values than the overall average values of  $\text{SO}_4^{2-}$  and  $\text{Fe}^{\text{total}}$  in the study area. This indicates that the acidic water ( $\text{pH} < 4.0$ ) may be due to the exposure of sulfide minerals in the L1 layer in Fig. 2, leading to the pH being less than 3.4 at B9 and B13–B16.

In Table 1, the  $^3\text{H}$  values are between 2.9 and 4.6 at all sampling sites except C2. The C2 water sample was collected in wetland with stagnant water areas, causing an  $^3\text{H}$  value of 0.6 T.U. According to Kazemi et al. (2006), the concentration of  $^3\text{H}$  in rainfall was observed as early as 1953 because of thermonuclear tests around the world; it peaked in 1963 and 1964 and has decreased since then. This suggests that the groundwater ages around the underground mine are less than approximately 60 years old.

Figure 5 shows the spatial distribution of Stiff diagrams, and Fig. 6 shows the Piper diagram based on the water quality in Table 1. The Stiff diagrams with high concentration of  $\text{SO}_4^{2-}$  and  $\text{Ca}^{2+}$  were plotted at the middle stream and downstream of the river located east of the underground mine, although the Stiff diagrams were smaller upstream of the river. The Stiff diagrams at A1–A6 were the smallest, followed by those at C1–C7. These results show that the groundwater flow system can be divided into three basins in the study area (A, B, and C), as predicted based on geomorphological information. In Fig. 6, most of the analytical results at B1–B17 as shown in Table 1 were plotted in the Piper diagram with  $\text{SO}_4^{2-} + \text{Cl}^- > 60\%$  and  $\text{Ca}^{2+} + \text{Mg}^{2+} > 60\%$ . By contrast, surface water with  $\text{SO}_4^{2-} + \text{Cl}^- < 50\%$  and  $\text{Ca}^{2+} + \text{Mg}^{2+} > 60\%$  was sampled at A3, A4, C1, and C4. Thus, the quality of the surface water and groundwater in the study area is characterized by  $\text{SO}_4^{2-}$ , which is attributed to the generation of AMD.

The spatial distributions of stable isotopes of the water samples ( $\delta^{18}\text{O}$  and  $\delta\text{D}$ ) are summarized in Fig. 7 based on the analytical data in Table 1, and the relationship between  $\delta^{18}\text{O}$  and  $\delta\text{D}$  is described in Fig. 8. The respective values of  $\delta^{18}\text{O}$  and  $\delta\text{D}$  were  $-11.7\text{‰}$  and  $-73\text{‰}$  at B10 and  $-11.8\text{‰}$  and  $-74\text{‰}$  at A5 and B12, indicating lower  $\delta^{18}\text{O}$  and  $\delta\text{D}$  values than the overall average ones. The values of  $\delta^{18}\text{O}$  and  $\delta\text{D}$  are generally lower in water from higher altitude (known as the altitude effect) (Florea et al., 2017; Clark and Fritz, 1997). Regarding the spatial distributions of  $\delta^{18}\text{O}$  and  $\delta\text{D}$ , the rain water recharged at the B mountain with the highest altitude of approximately 1,600 m in the study area may flow in B10, A5, and B12 through the underground mine area. The values of  $\delta^{18}\text{O}$  and  $\delta\text{D}$  at A1–A4 were  $\delta^{18}\text{O} \geq -10.7\text{‰}$  and  $\delta\text{D} \geq -66\text{‰}$ , suggesting that the surface water at the sampling sites comes from an area lower than B mountain. By contrast, the average values of  $\delta^{18}\text{O}$  and  $\delta\text{D}$  at C1–C5 were  $-11.5\text{‰}$  and  $-73\text{‰}$ , respectively, showing lower values than the overall average ones. Therefore, the surface water at C1–C5 may come from the high-altitude area in the northeast of the study area. Because lava is generally porous and cannot hold water (Leopold et al., 2016), rain water may be supplied to the underground mine area from B mountain through lava described as L3, L4, and L5 in Fig. 2 on the basis of the spatial distributions of  $\delta^{18}\text{O}$  and  $\delta\text{D}$ . In addition, Fig. 8 shows good correlation between  $\delta^{18}\text{O}$  and  $\delta\text{D}$ . The values were plotted between the meteoric water line with “d-excess” values of 10 and 25, and the same trend was observed in a previous study (Suzuki and Tase, 2014).

Consequently, the quality of the surface and groundwater in the present study was characterized by  $\text{SO}_4^{2-}$  from sulfide minerals in the sulfur deposit. The acidic water at the middle

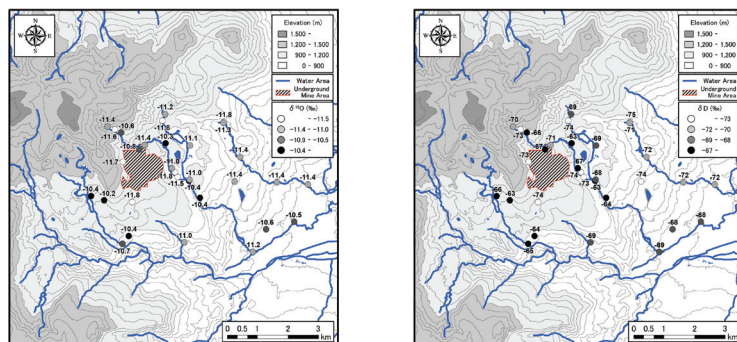


Fig. 7. Spatial distributions of  $\delta^{18}\text{O}$  (left) and  $\delta\text{D}$  (right) in water samples  
 Rys. 7. Rozkłady przestrzenne  $\delta^{18}\text{O}$  (po lewej) i  $\delta\text{D}$  (po prawej) w próbkach wody

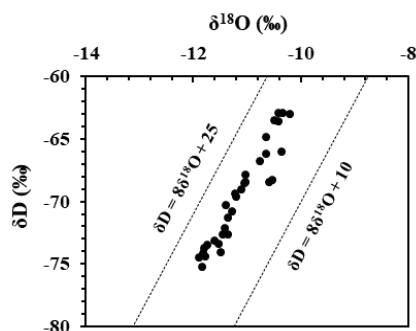


Fig. 8. Relationship between  $\delta^{18}\text{O}$  and  $\delta\text{D}$  in water samples  
 Rys. 8. Zależność między  $\delta^{18}\text{O}$  i  $\delta\text{D}$  w próbkach wody

and downstream of the river located east of the underground mine is not attributed to waste water from the underground mine. The surface and ground water at A5 and B10 might come from water recharged in the B mountain area based on the spatial distributions of  $\delta^{18}\text{O}$  and  $\delta\text{D}$ , and it flows into B12 through the underground mine area. Although more data are required to determine the area recharging the underground mine area, doing so would help to reduce the AMD volume by decreasing water inflow to the underground mine. Thus, the hydrogeochemical and isotopic data of surface and ground water can provide information that is important for understanding hydrological processes around the mine site and assessing how the mine waste water impacts the surrounding environment.

### Conclusions

This research investigates groundwater flow around the A sulfur mine by using geochemical methods, water quality, such as pH and EC, stable isotopes (i.e.  $\delta^{18}\text{O}$  and  $\delta\text{D}$ ) and  $^3\text{H}$  in surface and ground water. The distributions of pH, Stiff

diagrams, and  $\delta^{18}\text{O}$  and  $\delta\text{D}$  in surface and ground water indicated that the groundwater flow system was divided into three basins in the study area, corresponding to the flow system predicted based on geomorphological information. The results also suggested that the quality of the surface and ground water in the study area was characterized by  $\text{SO}_4^{2-}$  from sulfide minerals in the sulfur deposit. Furthermore, the groundwater recharged at the highest altitudes in the B mountain in the northwest of the underground mine might flow in the underground mine based on the distribution of  $\delta^{18}\text{O}$  and  $\delta\text{D}$  in the surface and ground water. Furthermore, the value of  $^3\text{H}$  in the waste water from the underground part of mine implied that the groundwater age was less than approximately 60 years old.

### Acknowledgments

The authors are grateful to Suimon LLC Co., Ltd. for measuring the water quality on site and providing water samples. The authors would like to thank Enago ([www.enago.jp](http://www.enago.jp)) for the English language review.



## Literatura – References

1. CLARK, D. Ian and FRITZ, Peter. Environmental isotopes in hydrogeology. Lewis Publishers: New York, 1997, p. 352.
2. FLOREA, Lee et al. Stable isotopes of river water and groundwater along altitudinal gradients in the high Himalayas and the Eastern Nyainqentanghla mountains. In Journal of Hydrology: Regional Studies, 14, 2017, p.37-48.
3. GAMMONS, H. Christopher et al. Geochemistry and stable isotope investigation of acid mine drainage associated with abandoned coal mines in central Montana, USA. In Chemical Geology, 269(1-2), 2010, p. 100-112.
4. HUANG, Pinghua and WANG, Xinyi. Applying environmental isotope theory to groundwater recharge in the Jiaozuo mining area, China. In Geofluids, 2017(1), 2017, p. 1-11.
5. KAWANO, Yoshinori and UEMURA, Fujio. Explanatory text of the geological map of Japan, Scale 1:50000, Hachimantai. Geological Survey of Japan, 1962.
6. KAZEMI, A. Gholam et al. Groundwater Age. John Wiley & Sons: Hoboken, 2006, p. 346.
7. LEOPOLD, Matthias et al. Subsurface architecture of two tropical alpine desert cinder cones that hold water. In Journal of Geophysical Research: Earth Surface, 121(6), 2016, p. 1148-1160.
8. SUN, Jing et al. Hydrogen and oxygen isotopic composition of karst waters with and without acid mine drainage: impacts at a SW China coalfield. In Science of the Total Environment, 487(15), 2014, p. 123-129.
9. SUZUKI, Hidekazu and TASE, Norio. Origin and geochemistry of a flowing confined groundwater at the northern foot of Mt. Iwate, Northeast Japan. In Komazawa Journal of Geography, 50, 2014, p. 101-111, In Japanese.
10. TOUGHZAOU, Sana et al. Hydrogeochemical and isotopic studies of the Kettara mine watershed, Morocco. In Mine Water and the Environment, 34(3), 2015, p. 308-319.

### *Badanie przepływu wód podziemnych za pomocą $\Delta^{18}\text{O}$ i $\Delta\text{D}$ w kopalni siarki w Japonii*

*Kopalnia siarki znajduje się w prefekturze Iwate w Japonii. Kopalnia ma zarówno części naziemne, jak i podziemne i działała od końca 1800 roku do końca XX wieku. Od początku XX wieku odnotowano w tej kopalni kwaśny drenaż kopalniany (AMD), a ścieki były zneutralizowane w oczyszczalni do czasu zamknięcia kopalni. Ostatnio uznano, że zmniejszenie objętości AMD przez zmniejszenie dopływu wody do podziemnej kopalni jest dobrym sposobem na zmniejszenie kosztów neutralizacji AMD. Pierwszym krokiem w takim podejściu jest szczegółowa analiza przepływu wód gruntowych wokół kopalni. Jednak część obszaru objętego badaniem jest pokryta lawą i obejmuje skały krystaliczne o skomplikowanych strukturach, co utrudnia zrozumienie przepływu wód gruntowych. Dlatego w niniejszych badaniach określono przepływ wód podziemnych wokół tej kopalni, koncentrując się na jakości wody, określono parametry takie jak pH i przewodność elektryczna (EC), stabilne izotopy (tj.  $\Delta^{18}\text{O}$  i  $\delta\text{D}$ ) oraz 3H w wodzie powierzchniowej i gruntowej. Przestrzenne rozkłady odczynu pH, wartości  $\delta^{18}\text{O}$  i  $\delta\text{D}$  w wodzie powierzchniowej i gruntowej wskazały, że system przepływu wód podziemnych został podzielony na trzy baseny na badanym obszarze, zgodnie z przewidywaniami z informacji geomorfologicznej. Ponadto rozkład przestrzenny  $\delta^{18}\text{O}$  i  $\delta\text{D}$  w wodach powierzchniowych i gruntowych sugerował, że wody gruntowe dopływające na najwyższych wysokościach w północno-zachodniej części kopalni mogą płynąć do części podziemnej kopalni. Co więcej, wartości 3H w ściekach odprowadzanych z podziemnej części kopalni sugerowały, że wiek wód podziemnych wyniósł nie więcej niż około 60 lat.*

*Słowa kluczowe: zamknięcie kopalni, kwaśny drenaż kopalniany (AMD), ścieki, stabilne izotopy, przepływ wód gruntowych*



# Assessment of IM-50 and TOFA Adsorbed Layer on Cassiterite in Flotation of Tin Sulfide Wastes

Tamara MATVEEVA<sup>1)</sup>, Nadezhda GROMOVA<sup>1)</sup>

<sup>1)</sup> Institute of Comprehensive Exploitation of Mineral Resources, Russian Academy of Sciences, (ICERM RAS), Moscow, Russia

<http://doi.org/10.29227/IM-2020-01-52>

Submission date: 14-01-2020 | Review date: 01-04-2020

## Abstract

The paper presents the results of experimental study of the adsorption characteristic of the IM-50 and tall oil fatty acids (TOFA) collector reagents on cassiterite. UV-spectrophotometric method, scanning electron and laser microscopy were applied to analyze the adsorption of the reagents. SHIMADZU UV 1800 was used to obtain the UV spectra of aqueous solutions of IM-50 reagents and saponified TOFA at varied concentrations. IM-50 has not got characteristic adsorption maxima in ultraviolet and visible spectrum. TOFA has a weakly pronounced maximum absorption in the range of 233-244 nm. Microscopic photographs of cassiterite sections were obtained with LEO 1420VP INCA equipped OXFORD ENERGY 350 analyzer. Reagent IM-50 and TOFA collector reagent, Newly formed organic matter phases of IM-50 and TOFA were detected. X-ray spectra characterized the increased carbon content indicating adsorption on the surface of cassiterite IM-50 and TOFA.

By measuring the surface relief parameters of polished cassiterite, using KEYENCE VK-9700 scanning laser microscopy and VK-Analyzer software, a qualitative and quantitative assessment of the IM-50 and TOFA reagent layer on the cassiterite surface was performed. Measurements were performed in the several fields of view and showed the degree of IM-50 coating varied from 40.5 to 42.6% of the surface area, and TOFA average coating was 38.5%. Subsequent washing with water does not remove the reagents from the surface of the mineral and indicates a strong fixation of IM-50 and TOFA on cassiterite, which can have a positive effect on flotation extraction of sludge tin fractions.

Qualitative and quantitative results of the reagent adsorption helped to make a forecast of their floatability by the studied collectors. This study is supported by the Russian Science Foundation (project No. 17-17-01292).

**Keywords:** sulfide tin ores, cassiterite, tailings, flotation, IM-50, TOFA, adsorption

## Introduction

Cassiterite is the main tin mineral. Cassiterite is found in association with quartz, muscovite, lepidolite, topaz, scheelite, fluorite, albite, tourmalines, ferro-columbite, manganocolbit, beryl, spodumene, wolframite, pyrite, arsenopyrite, pyrrhotite, sphalerite, chrysoberyl, etc., and pyrite, pyrite, arsenopyrite, pyrrhotite, sphalerite, chrysoberyl, and certrum; Cassiterite is formed in the vein and skarn deposits of W-Mo-Sn ores (hydrothermal origin); in greisens (pneumatolite-hydrothermal); forms uneven clusters in rare-metal granite pegmatites (pegmatite); as an accessory mineral in acidic rocks (igneous). Cassiterite of exogenous origin is found in zones of oxidation of deposits with tin sulfides.

The main deposits of tin sulfide type in Russia are located in the Khabarovsk Territory. At present, the recycled tails of the Solnechny Mining and Processing Plant with a tin content of 0.22–0.4% are involved in processing [1–3].

A distinctive feature of the Russian tin deposits of sulfide, less commonly silicate industrial types of the Far East is their complex mineral composition - in addition to tin, ores contain in industrial quantities copper, lead, zinc, tungsten, silver, rare and trace elements (indium, scandium, etc.). For example, in the fields of the Komsomolsk tin ore district, the ores and tailings of which are planned to be recycled in the near future, contain tin in the form of cassiterite, stannine and sulfostannate, sulphides of non-ferrous metals – copper, zinc, lead, silver, rare and trace elements (indium, scandium, etc.). At the same time, a significant proportion of sulfides is represented by pyrite, pyrrhotite and arsenopyrite, the presence

of which in concentrates of non-ferrous metals worsens their quality (for example, arsenic in copper concentrate) and complicates further metallurgical redistribution [1].

Flotation is the most effective method for sulfide-tin ores treatment. Hydroxamic acids and tall oil fat acids (TOFA) are used for flotation of cassiterite [4–6]. Application of selective collectors and modifiers may provide effective recovery of valuable metals into flotation concentrates.

Due to the fact, that the choice of the optimal conditions for the formation of the hydrophobic layer of the collector on the surface of valuable minerals is a determining factor in improving the recovery of non-ferrous metals from refractory ores, a detailed study of the nature of its adsorption on the mineral surface has been performed.

The aim of the study is to analyze the adsorbed species and percentage covering of collecting agents on cassiterite surface in flotation conditions and forecast the dosage of flotation reagents under processing of refractory tin sulfide ores

In this paper, collecting agents IM-50 and TOFA have been tested in adsorption and flotation of cassiterite from one of the sulfide-tin deposits of Russia.

## Materials and Methods

Mineral fraction of cassiterite was selected from one of the sulfide-tin deposits of Russia. Microphoto and X-ray spectrum of cassiterite sample (LEO 1420VP + INCA Oxford 350) is shown Figure 1.

Newly formed species of collector IM-50 and TOFA on polished sections of cassiterite (10×10×2 mm in size) were

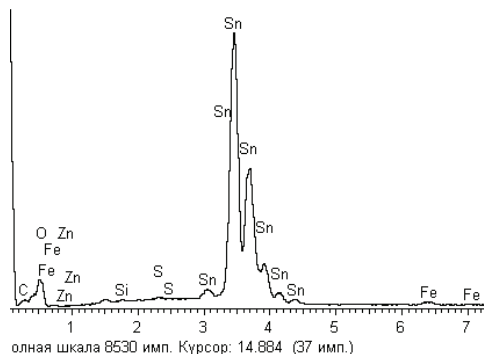
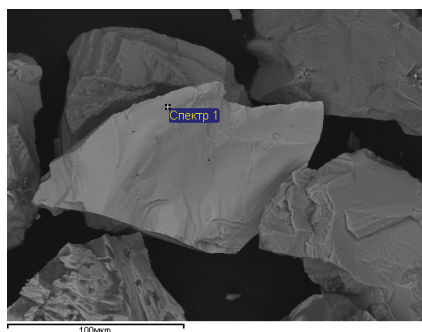
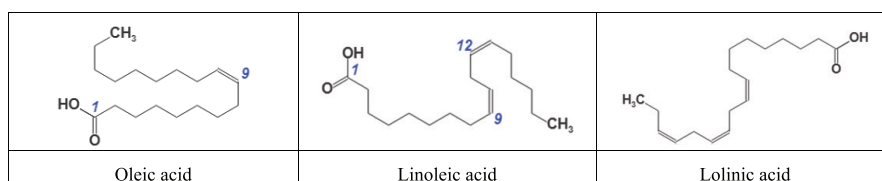
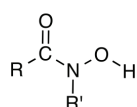


Fig. 1. Microphoto and X-ray spectrum of cassiterite sample (LEO 1420VP + INCA Oxford 350)  
Rys. 1. Widmo mikrofotograficzne i rentgenowskie próbki kasyterytu (LEO 1420VP + INCA Oxford 350)



studied by analytical scanning electron (LEO 1420VP + INCA Oxford 350), and a laser microscope (KEYENCE VK-9700 with 1 nm resolution). Research methods are optical, confocal laser, analytical electronic, scanning probe microscopy, UV-spectrophotometry of reagent solutions, flotation of minerals. The KEYENCE scanning laser microscope with the surface analysis module VK-9700 enables making a non-contact measurement of the roughness of the surface of minerals and thus determining the height and size of the new formations obtained as a result of interaction with the reagents. The electronic microscope with energy-dispersive micro analyzer LEO-1420 VP INCA-350 allows determining the elemental composition of micro- and nanophases of reagents on the surface of minerals. UV-spectrophotometry was used to analyze the IM-50 and TOFA concentration in aqua phase of mineral suspension before and after contact with ground fractions (-0.1 + 0.063 mm) of cassiterite. The liquid phase was decanted after centrifugation and the residual concentration of the components of IM-50 and TOFA was analyzed by spectrophotometer SHIMADZU-1700.

Hydroxamic acids are selective collectors for ores containing rare metals: tantalum, niobium, rare earth, etc., as well as tin. The general formula of hydroxamic acids:



Reagent IM-50 is a mixture of alkyl hydroxamic acids (C7-C9 fraction). IM-50 is a brownish-red liquid with a strongly alkaline reaction, with an ammonia smell. The technology for producing this reagent was developed at the Mekhanobr Institute, Russia. The reagent contains 75–78% hydroxamic acids, 10–12% carboxylic acids, 10–12% moisture, and up to 4.5% inorganic impurities. Hydroxamic acids are weaker than fatty acids, the pKa values for capron (C6) -, enanth (C7) - and capryl hydroxamic (C8) acids are 9.65; 9.67 and 9.69. As a result, they form much stronger complexes than fatty acids.

Tall oil fat acids (TOFA) are the oily liquid of light yellow color, consisting of a mixture of high-molecular unsaturated

organic acids (C18–C20) obtained by rectification of crude tall oil. The mixture includes oleic, linoleic, lolinic acids and their isomers. Resin acids (up to 2%), unsinkable substances (up to 2%), and also saturated fatty acids: palmitic, stearic, their isomers, etc. are present as undesirable impurities.

The spectrophotometer SHIMADZU UV 1800 was used to obtain the UV spectra of aqueous solutions of IM-50 reagents and saponified TOFA (various concentrations). On the spectra of IM-50 the characteristic maxima of absorption were not determined. The spectra of TOFA have a weakly pronounced maximum absorption in the range of 233–244 nm.

## Results and Discussion

The images of polished sections of cassiterite that were observed by analytical scanning electron (LEO 1420VP + INCA Oxford 350) and laser microscope (KEYENCE VK-9700 with 1 nm resolution) have shown the characteristic molecular shape of adsorbed phase of collector after its contact with the IM-50 (Figure 1a) and TOFA (Figure 1b) solutions. Microscopic photographs of polished sections of cassiterite shows with IM-50 and TOFA reagent reveal characteristic dark round or oval spots with a diameter of 0.1 to 15 microns. X-ray spectra of the spots are characterized by an increased content of carbon C, which indicates adsorption of carbon-containing organic reagent on the surface of cassiterite.

Newly formed carbon-containing organic species of the reactant firmly anchored on the surface and did not dissolve in water at a subsequent washing.

Laser microscopy (KEYENCEVK-9700) data indicated the appearance of adsorbed IM-50 neoplasms on the surface of cassiterite in the form of films and rounded islands, the size of which is 9–29  $\mu\text{m}$  in diameter, 1–1.5  $\mu\text{m}$  in height, reaching a maximum height of 2  $\mu\text{m}$  (Fig. 3a). After washing, the dimensions of the newly formed phases did not actually change. TOFA is fixed in the form of films and rounded droplets with a diameter of 10  $\mu\text{m}$  on average and 1–2  $\mu\text{m}$  in height (Fig. 3b).

Thus, as a result of the selective interaction of cassiterite with IM-50 and TOFA reagents, the surface of the mineral is modified by stable Sn-reagent complexes, namely (RR<sub>1</sub>C-

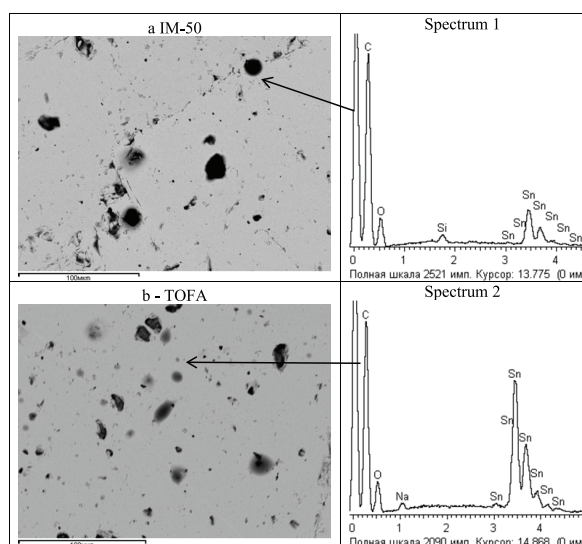


Fig. 2. Image of polished cassiterite after IM-50 (a) and TOFA (b) treatment ( $C = 100 \text{ mg/l}$ ) (LEO 1420VP + INCA Oxford 350) (b) and X-ray spectra of adsorbed phase of collector (Label 100 microns)

Rys. 2. Obraz kasyterytu po obróbce IM-50 (a) i TOFA (b) ( $C = 100 \text{ mg/l}$ ) (LEO 1420VP + INCA Oxford 350) (b) i widma rentgenowskie zaadsorbowanej fazy kolektora (Etykieta 100 mikronów)

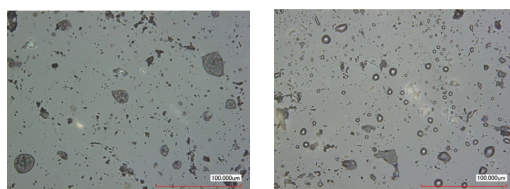


Fig. 3. Image of polished cassiterite after IM-50 (a) and TOFA (b) treatment ( $C = 100 \text{ mg/l}$ ) (KEYENCE VK-9700) (Label 100 microns) Magnification of 50X

Rys. 3. Obraz kasyterytu po obróbce IM-50 (a) i TOFA (b) ( $C = 100 \text{ mg/l}$ ) (KEYENCE VK-9700) (Etykieta 100 mikronów) Powiększenie 50X

Reagent	Magnification	Mineral surface area, $\mu\text{m}^2$	Surface area covered by a reagent, $\mu\text{m}^2$	Percentage of coverage by a reagent, %
IM-50	10X	2907542	1208357	41,5
TOFA	10X	3683390	1418055	38,5

$\text{NOO}_2\text{Sn}$ ,  $(\text{C}_{17}\text{H}_{31}\text{COO})_n\text{Sn}$ , which contributes to the efficient extraction of tin from sulfide-tin ores.

In ICERM RAS an original technique was developed to quantify the adsorption of the reagent on the surface of sulfide minerals in flotation conditions. The originality and novelty of the approach to the study of thin reagent films on the surface of mineral surfaces is to compare the numerical measurements of the unevenness of the relief of a mineral before and after its contact with the reagent solutions [7–8].

The measurement of the surface area of the polished mineral coated with the newly formed reagent phase was made on the color image by filling the area of the object with a selected gradient. A layer of adsorbed reagent was highlighted and the corresponding area was measured. Thus, the area ( $\mu\text{m}^2$ ) of the total mineral surface and the surface covered with the reagent were estimated. The percentage degree of coating the surface of the mineral with a reagent (%) was calculated.

The area of the newly formed reagent phases on cassiterite polished sections treated with IM-50 and TOFA was determined at various magnifications of the image (10X, 20X, 50X). Measurements were made in several areas of the field of view. The results are presented in the Table.

Measurements of the adsorption layer of reagents on the surface of cassiterite in several areas of the field of view showed that the degree of coverage with the IM-50 reagent on the surface of cassiterite with an increase of 10X and 20X is 40.5–42.6%, washing with water practically does not desorb the reagent, the degree of coverage is 41.5%, i.e. IM-50 is firmly entrenched on the surface of the mineral. The degree of coating with the reagent TOFA of the surface of cassiterite is 38.5% (with an increase of 10X).

## Conclusions

Microscopic photographs of the cassiterite sections obtained using a LEO 1420VP scanning electron microscope with the INCA OXFORD ENERGY 350 energy dispersive analyzer, after being treated with IM-50 and TOFA collectors, reveal dark, round sections, whose X-ray spectra are characterized by an increased carbon content, which indicates adsorption on the surface of cassiterite carbon-containing organic reagent.

According to the method developed in ICERM RAS, which consists in comparing numerical measurements of the irregularities of the relief of a mineral before and after con-

tact with a reagent solution obtained by KEYENCE VK-9700 scanning laser microscopy using VK-Analyzer software, an IM-50 adsorption layer of reagents was measured and GCTM on the surface of cassiterite.

Measurements of the adsorption layer of reagents on the surface of cassiterite in several areas of the field of view showed that the degree of coverage with the IM-50 reagent on the surface of cassiterite with an increase of 10X and 20X is 40.5–42.6%, washing with water practically does not desorb the reagent, the degree of coverage is 41, 5%, i.e. IM-50 is

firmly entrenched on the surface of the mineral. The degree of coating with the reagent GCTM of the surface of cassiterite is 38.5% (with an increase of 10X). Qualitative and quantitative assessment of the adsorption of reagent on minerals could help to make a forecast of their floatability by the studied collectors.

#### Acknowledgments

This study is supported by the Russian Science Foundation (project No. 17-17-01292).

#### Literatura – References

1. Khanchuk, A.I., Kemkina, R.A., Kemkin, I.V., Zvereva, V.P. KRAUNZ. Earth Sciences. - 2012. - № 1 (19).
2. Yusupov, TS, Kondratyev, S.A., Baksheeva, I.I., Structural-chemical and technological properties of minerals of cassiterite-sulfide technogenic raw materials, Obogashchenie rud. - 2016. - № 5. - P. 26 - 31.
3. Gazaleeva G.I., Nazarenko L.N., Shikhov N.V., Shigaeva V.N., Boykov I.S. Development of the enrichment technology for tin-containing tails of the Solar Mining Plant // Scientific principles and practice of processing ores and technogenic raw materials: materials XIII International scientific and technical conf. - Ekaterinburg: Fort Dialog-Iset, 2018. - p. 11 - 16.
4. Leistner T., Embrechts M., Leißner T., Chehren Chelgani S., Osbahr I., Mockel R., Peuker U. A., and Rudolph M. A study of the reprocessing of fine and ultrafine cassiterite from gravity tailing residues by using various flotation techniques, Minerals Engineering. - 2016. Vol. 96 - 97. — P. 94 - 98.
5. Angadi S.I., Sreenivas T., Ho-Seok Jeon, Sang-Ho Baek, and Mishra B. K. A review of cassiterite beneficiation fundamentals and plant practices, Minerals Engineering, 2015, Vol. 70. — P. 178 - 200.
6. López F. A., García-Díaz I., Rodríguez Largo O., Polonio F. G., and Llorens T. Recovery and purification of tin from tailings from the Penouta Sn-Ta-Nb Deposit, Minerals, 2018, Vol. 8, № 1. — P. 20.
7. Matveeva, T.N., Chanturiya, V.A., Gromova, N., K., Lantsova, L., B. Study of the effect of chemical and phase composition on adsorption and flotation properties of sulfide-tin ore tails using dibutyliditiocarbamate, J Mining Science. - 2018.
8. Matveeva, T., N., Gromova, N., K., Minaev, V.A. Quantitative assessment of adsorbed layer of combined diethylditiocarbamate on chalcopyrite and arsenopyrite by measuring relief parameters, Tsventnye metally. - 2018. - № 7. - P.27-32.

#### *Adsorpcja kolektorów IM-50 i TOFA na kasyteryście w procesie flotacji odpadów siarczków cyny*

*W pracy przedstawiono wyniki badań eksperymentalnych charakterystyki adsorpcji odczynników kolektorowych IM-50 i kwasów tłuszczowych oleju talowego (TOFA) na kasyteryście. Do analizy adsorpcji odczynników zastosowano metodę spektrofotometryczną UV, skaningową mikroskopię elektronową i laserową. SHIMADZU UV 1800 zastosowano do uzyskania widm UV wodnych roztworów odczynników IM-50 i zmydlonego TOFA w różnych stężeniach. IM-50 nie ma charakterystycznych maksimów adsorpcji w widmie ultrafioletowym i widzialnym. TOFA ma słabo wyraźną maksymalną absorpcję w zakresie 233–244 nm. Zdjęcia mikroskopowe przekrojów kasyterytów uzyskano za pomocą analizatora OXFORD ENERGY 350 wyposażonego w LEO 1420VP INCA. Wykryto nowo powstałe fazy materii organicznej IM-50 i TOFA. Widma rentgenowskie charakteryzowały zwiększoną zawartość węgla wskazującą na adsorpcję na powierzchni kasyterytów IM-50 i TOFA. Mierząc parametry wypukłości powierzchni polerowanego kasyterytu, stosując skaningową mikroskopię laserową KEYENCE VK-9700 i oprogramowanie VK-Analyzer, przeprowadzono jakościową i ilościową ocenę warstwy odczynnika IM-50 i TOFA na powierzchni kasyterytu. Pomiar przeprowadzono w kilku polach widzenia i stwierdzono no stopień pokrycia IM-50 wahający się od 40,5 do 42,6% pola powierzchni, a średnie pokrycie TOFA wynosiło 38,5%. Późniejsze przemycie wodą nie usuwa odczynników z powierzchni minerału i wskazuje na silne utrwalenie IM-50 i TOFA na kasyteryście, co może mieć pozytywny wpływ na ekstrakcję flotacyjną frakcji szlamu i cyny. Jakościowe i ilościowe wyniki adsorpcji odczynników pomogły w opracowaniu prognozy ich flotowalności za pomocą badanych kolektorów. Badanie jest wspierane przez Russian Science Foundation (projekt nr 17-17-01292).*

*Słowa kluczowe: rudy siarczkowe cyny, kasyteryt, odpady poflotacyjne, flotacja, IM-50, TOFA, adsorpcja*



# The Influence of Coal Tars over the Environment

Clementina MOLDOVAN<sup>1)</sup>, Aronel MATEI<sup>1)</sup>, Roxana Claudia HERBEI<sup>1)</sup>,  
Raluca MATEI<sup>2)</sup>

<sup>1)</sup> University of Petrosani, Romania

<sup>2)</sup> Company of Mine Closing Jiu Valley

<http://doi.org/10.29227/IM-2020-01-53>

Submission date: 03-01-2020 | Review date: 27-02-2020

## Abstract

Coal is a macromolecular compound. At high temperatures, by coal pyrogenesis, coke and volatile products will result. The volatile products from coal form the coke gas and coke tar from which a very large number of aromatic compounds can be extracted. The aromatic compounds extracted from domestic and foreign coal tar were compared in this paper, together with their effects over the human and animal health.

**Keywords:** compounds, macromolecular, coke gas

## Introduction

The standard methods which are used during coal processing are very important in defining the subsequent potential of coal chemical treatment because the processes employed in the destructive processing of coal have provided the raw material base for the chemical synthesis and the fundamental principles for laying the base of upcoming technologies.

Coal pyrogenation at low temperatures (400–600°C), in the absence of air, leads to the simultaneous formation of some products with smaller molecular weight and of some products with a molecular weight higher than the primary coal. The products with a smaller molecular weight form the volatile matters, released as tar vapors, water and gases and the products with a higher molecular weight that gives the solid residue of carbonization (semi-coke and coke).

## Coal chemical treatment

Basically, coal pyrogenation at low temperatures (semi-coking) takes place as follows:

- Up to 100–150°C hygroscopic water and adsorbed gases are being emitted;
- Between 200°C and 250°C occurs a thermal decomposition revealed by the coming of the pyrogenetic water and of some gases, such as: CO<sub>2</sub>, CO and H<sub>2</sub>S;
- At around 300°C starts the emission of tar vapors;
- Between 350°C and 400°C takes place an intense decomposition and the amount of the emitted gases increases abruptly; the gases become combustible because there increases highly the content of hydrocarbons (methane and homologues), as well they start to have increasing amounts of hydrogen;

At high temperatures (coking), the following processes take place:

- Between 50°C and 150°C coal dries out and gases are being emitted;

- Between 150°C and 300°C the marginal functional groups, carboxyl, hydroxyl, tionil break up and CO<sub>2</sub>, H<sub>2</sub>O and H<sub>2</sub>S are being emitted;
- Between 400°C and 550°C, full aliphatic chains and heterocycles with oxygen and nitrogen break up and aliphatic, hydro aromatic hydrocarbons and superior phenols are being formed;
- The maximum temperature for tar emission is between 400°C and 550°C and tar formation ends at 500°C and 550°C;
- Above 600°C there are emitted gaseous products (CH<sub>4</sub> and especially H<sub>2</sub>) that are being formed by breaking the bonds C–H and the breaking off the groups CH<sub>3</sub>. The emission of condensable products (tars) ends at around 550–600°C. There also occur conversions that lead to the formation of pyridinic and kinoleic alkali, to the occurrence of phenol, of ammonia and even of the elementary nitrogen.

As a result, both the structure and the percentage weighting of the co-products acquired from the coal pyrogenation shall depend on the quality of the raw material that is being used and on the parameters of the processing method: temperature, pressure and the operating period of temperature over the coaly mass, also called the standstill period.

Figures 1a, 1b and 1c show the variation in the structure of gaseous phase, liquid phase and solid phase in relation to the carbonization temperature.

Table 1 shows, by comparison, the products acquired through hard coal pyrogenation, during semi-coking at 500°C and during cooking at 1000°C.

The analysis of charts and of data submitted shows that a process of secondary carbonization occurs simultaneously with the temperature rise together with the diminution of the tar efficiency and increasing the efficiency for formation of gaseous components. Pyrogenation at higher temperatures increases the weight of aromatic hydrocarbons from the tar and of hydrogen from the gaseous phase.

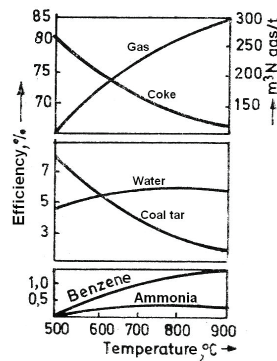


Fig. 1a. Variation in the efficiency of hard coal pyrogenation depending on temperature  
Rys. 1a. Zróżnicowanie wydajności pirogenizacji węgla kamiennego w zależności od temperatury

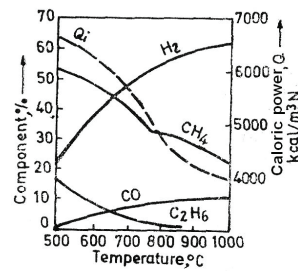


Fig. 1b. Variation in the gas structure depending on temperature  
Rys. 1b. Zmienność struktury gazu w zależności od temperatury

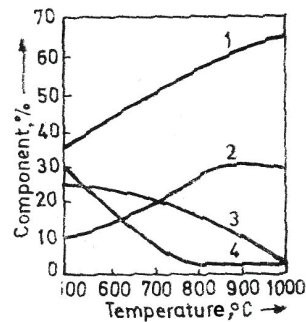


Fig. 1c. Variation in the tar composition in relation to temperature: 1. pitch; 2. aromatic oils; 3. acids and phenols; 4. saturated hydrocarbons  
Rys. 1c. Zróżnicowanie składu smoły w zależności od temperatury: 1. pitch; 2. oleje aromatyczne; 3. kwasy i fenole; 4. nasycone węglowodory

### Chemical structure of tar resulted after hard coal coking and semi-coking

High and low temperature tar comprises a large array of fractions that can be separated in accordance with the needs and opportunities related to their trading.

Table 2 shows the main products separated from the high temperature tar (coking tar) that are being used by the chemical synthesis technology.

The table shows that the coking tar is a complex mixture of aromatic hydrocarbons, phenols, derivatives with nitrogen, oxygen, sulphur, etc.

The capitalization of the coking tars can be made through direct processing, meaning the separation of relatively homogeneous fractions and getting some components of different purity degrees and through chemical treatment, hydrogenation, cracking, processes that lead to the acquiring of new fractions that comprise intermediate products for the petrochemical industry.

The methods that are being used for a direct capitalization of tars implement traditional physical operations, such as

decanting, filtering, distillation, rectification, crystallization, sublimation and selective extractions, refining with acids, alkali, chemical operations, etc. As a result, there are being used substances of different purity degrees necessary for the chemical industry: benzene, toluene, xylene, naphthalene, anthracene, pyridinic alkali, components with nitrogen, components with sulphur, etc.

Tars derived from semi-coking display specific structures and features that differentiate them from the tar acquired through the coking process. These tars include mainly alkenes and aromatic hydrocarbons in very small quantities. Nevertheless, there can be noticed high concentrations of oxygenated compounds from the category of phenols and especially, through the contents of phenols.

The processing of semi-coking tar shall give products similar to the ones that result through oil processing: gasoline, diesel oil, mineral oils, phenols and a solid distillation residue, asphalt.

Tab. 1. Products acquired during hard coal semi-coking and coking

Tab. 1. Produkty uzyskane podczas półkoksowania i koksowania węgla kamiennego

Products and specific features	U.M.	Semi – coking (500°C)	Coking (1000°C)
<b>Solid product</b>	-	Semi – coke	Coke
- efficiency	%	70 - 81	65 – 70
- volatile matters	%	10 - 18	0.5 – 1.5
<b>Tar</b>	-	Alkaline	Aromatic
- efficiency	%	7 – 12	2 – 4
- content of phenols	%	20	2
- content of phenol	%	-	1 – 1.7
- content of tar	%	40	60
- density	Kg/m <sup>3</sup>	0.9 – 1.0 × 10 <sup>3</sup>	1.1 – 1.2 × 10 <sup>3</sup>
<b>Gas</b>	-	of semi – coke	of coke
- efficiency	Nm <sup>3</sup> /t	60 - 80	330 – 350
- superior calorific power	Kcal/Nm <sup>3</sup>	6000 - 8000	3800 – 4500
- density	Kg/m <sup>3</sup>	0.85- 0.95	0.4 – 0.4
<b>Light oils in gas</b>	-	gasoline from gas	raw benzene
- efficiency	%	0.3 – 0.5	1.0 – 1.2
- content of benzene (C <sub>6</sub> H <sub>6</sub> )	%	traces	50 – 75
Ammonia	-	From semi – coke gas	From coke gas
- efficiency	%	Traces	0.20 – 0.35

Tab. 2. Separable products from coal tar

Tab. 2. Produkty, które można oddzielić od smoły węglowej

No.	Name	Boiling temperature °C	Melting temperature °C	% (g)
0	1	2	3	4
1	Components above 1%			
	naphthalene	217,95	80,29	10,0
	fenantrene	338,4	100	5,0
	fluoroantrene	383,5	111	5,3
	pyrene	393,5	150	2,1
	acenaftylene	270	93	2,0
	fluorene	297,9	115	2,0
	chrysene	441	256	2,0
	anthracene	340	218	1,9
	carbazole	354,76	244,4	1,5
	2 – methylnaphthalene	241,05	34,58	1,5
	diphenylenoxide	285,1	85	1,0
	indene	182,44	-1,5	1,0
2	Components below 1%			
	acridine	343,9	111	0,6
	1 - methylnaphthalene	244,68	-30,8	0,5
	phenol	181,83	40,9	0,4
	m - cresol	202,23	12,22	0,4
	benzene	80,1	5,53	0,4
	diphenyl	255,0	69,2	0,4
	acenaphthene	227,0	95	0,3
	2 - phenylnaphthalene	359,8	101	0,3
	toluene	110,62	-94,99	0,3
	quinoline	237,1	-14,2	0,3
	diphenyl sulphide	331,4	97	0,3
	tionaphtene	219,0	31,32	0,3
	m – xylene	139,10	-47,87	0,2
	o - cresol	191,00	30,99	0,2
	p - cresol	201,94	34,69	0,2
	isoquinoline	243,25	26,48	0,2
	quinidine	247,6	-1	0,2
	fenantridine	349,5	107	0,2
	7, 8 - benzoquinoline	340,2	52	0,2
	2, 3 – benzo diphenyl oxide	394,5	208	0,2
	indole	254,7	52,5	0,2
	3, 5 - dimetylphenol	221,69	63,27	0,1
	2, 4 - dimetylphenol	210,93	24,54	0,1
	2 – methylpyridine (α – picoline)	129,40	-66,7	0,02
	3 – methylpyridine (β – picoline)	144,14	-18,25	0,01
	4 – methylpyridine (γ – picoline)	145,35	3,65	0,01
	2, 6 – dimetylpyridine (2,6 - lutidine)	144,04	-6,1	0,01
	2, 4 – dimetylpyridine (2,4 - lutidine)	158,40	-63,96	0,01
	pyridine	115,25	-41,8	0,02

Tab. 3. Classification of toxicity

Tab. 3. Klasyfikacja toksyczności

LD (mg / kg)	Classification
< 25	Very toxic substances
Between 25 and 200	Toxic substances
Between 200 and 2000	Hazardous substances
2000 >	Substances which are not toxic



Tab. 4. LD and LD<sub>50</sub> for the compounds come from the hard coal tarTab. 4. LD i LD<sub>50</sub> dla związków pochodzących ze smoły węglowej

Name of the aromatic compound	LD (oral ingestion, at rats) (mg / kg)	LD <sub>50</sub> (oral ingestion, at rats) (mg / kg)
Aniline		440
Antracene	> 16000	
Benzene		3800
Ethylbenzene		3500
O - cresol		121
Naphthalene	> 16000	
Fenantrene	> 16000	
Phenol		414
Pyrene	> 16000	
Styrene		5000
Toluene		5000
o - xylene		5000
m - xylene		5000
p - xylene		5000

Tab. 5. OELV and AOELV for the compounds come from the hard coal tar

Tab. 5. OELV i AOELV dla związków pochodzących ze smoły węglowej

Name of the compound	AOELV (mg / m <sup>3</sup> )	OELV (mg / m <sup>3</sup> )
Aniline	10	
Benzene	16	
Cresols	22	
Indene	45	
Naphthalene	50	
Diphenyl oxide	7	
Phenol	19	
Pyridine	15	30
Styrene	215	
Toluene	375	550
Xylenes	435	650

### Toxic effect of aromatic compounds extracted from hard coal tars

It is very important to know the compounds that result after the processing of tar coal tar because these chemical compounds are very poisonous both for the man's health and for animals health.

### Toxicity of certain aromatic compounds extracted from hard coal tars

#### Toxicological information

##### Ingestion

The effects of toxicity due to ingestion are being tested on animal (usually on rats) and the measurement unit is the lethal dose (LD); it is expressed in mg of substance ingested per kilogram of animal body weight. (LD) represents a dose at which a given percentage of animals will die (see table 3).

LD<sub>50</sub> indicator allows an assessment of chronic toxicity; it is dose at which 50% of subjects will die within a determined period of time.

##### Respiratory tract

The French Ministry of Labor has settled the permissible occupational exposure values with the view to preventing the occurrence of occupational diseases triggered by the polluting substances in the atmosphere of the workplace. There are two values that evaluate the maximum permissible concentrations in the atmosphere of the workplace.

- the occupational exposure limit value (OELV) that measured all trough a maximum exposure period of 15 minutes; the observance of this value shall lead to

a short - time avoidance of adverse effects due to the toxic substances;

- the average occupational exposure limit value (AOELV) measured or estimated over an 8 - hour period (see table no. 5).

This table comprises several products which are also very toxic when reaching the skin. These products are aniline, cresols and phenol.

##### Water

Phenol, cresols, xylenes and naphthalene are being classified as "marine pollutants". For cresols, for a 96 hour - period the lethal concentrations (LC<sub>50</sub>) vary between 5 and 20 mg/l, depending on the species concerned.

For naphtalene, for a 96 hour - period the lethal concentrations (LC<sub>50</sub>) vary between 0.1 and 150 mg/l, depending on the species concerned. These products are biodegradable at low concentrations.

### Carcinogenetic risks

Benzene and tar vapors are well - known as carcinogenic agents for man so they are subject to strict regulations in relation to the labeling of packages that contain these products.

Starting with the month of august 1997, several substances that can be found in the hard coal tar vapors have been classified as carcinogenic for man. Here are included certain compounds that have 4, 5 or 6 aromatic nuclei, the most well - known being perylene. Their boiling temperature is > 400°C and this is why they are dangerous only in certain conditions of use. Cresols are also part of this classification.

## Conclusions

1. Coal pyrogenation gives the following main products:

- semi-coke and coke;
- gases that contain products which can be chemically treated, such as: ethane, ethene, propene, acetylene, methane, hydrogen, water vapors, etc.;
- semi-coking and coking tar is a mixture of around 10,000 chemical substances, among which 350 were separated with the help of chemical treatment;
- ammoniacal waters.

2. The chemical composition of coking tar differs from the chemical composition of semi-coking tar;

- The coking tar is a complex mixture of aromatic hydrocarbons, phenols, derivatives with nitrogen, oxygen, sulphur, etc.;
- The semi-coking tar includes alkenes and aromatic hydrocarbons at very low concentrations and oxygenated compounds from the category of phenols and especially of superior phenols, at high concentrations;
- The compounds resulted from the processing of hard coal tar are very bad for the human health and for the health of the animals.

#### Literatura – References

1. Victor Părăușanu, Tehnologii Chimice, Editura Științifică și Enciclopedică, București, 1982
2. Constantin Gosselin, Ingénieur de l'École nationale supérieure de chimie de Lille Chef d'établissement de la société HGD (Huiles, Goudrons et Dérivés)
3. Victor Părăușanu, Mihai Corobea, Gavril Musca, Economia Hidrocarburilor, Editura Științifică și Enciclopedică, București, 1980

#### *Wpływ smoły węglowej na środowisko*

*Węgiel jest związkiem makrocząsteczkowym. W wysokich temperaturach, w wyniku pirolizacji węgla, powstaje koks i produkty lotne. Lotne produkty z węgla tworzą gaz koksowniczy i smołę koksową, z której można uzyskać bardzo dużą liczbę związków aromatycznych.*

*W pracy porównano związki aromatyczne uzyskane ze smoły węglowej pochodzenia krajowego i zagranicznego, wraz z ich wpływem na zdrowie ludzi i zwierząt*

**Słowa kluczowe:** związki, makrocząsteczki, gaz koksowniczy



# Utilization Range of By-Products from Coal Combustion in Earth Structures of Transport Infrastructure

Václav MRÁZ<sup>1)</sup>, Jan SUDA<sup>2)</sup>, Vít LOJDA<sup>3)</sup>, Adam CULKA<sup>4)</sup>, Jakub TRUBAČ<sup>5)</sup>

<sup>1)</sup> Czech Technical University in Prague, Faculty of Civil Engineering, Thákurova 7, 166 29 Praha, Czech Republic; email: vaclav.mraz@fsv.cvut.cz

<sup>2)</sup> Czech Technical University in Prague, Faculty of Civil Engineering, Thákurova 7, 166 29 Praha, Czech Republic; email: jan.suda@fsv.cvut.cz

<sup>3)</sup> Czech Technical University in Prague, Faculty of Civil Engineering, Thákurova 7, 166 29 Praha, Czech Republic; email: vit.lojda@fsv.cvut.cz

<sup>4)</sup> Charles University, Faculty of Science, Institute of Geochemistry, Albertov 6, 128 43 Praha, Czech Republic; email: culka@natur.cuni.cz

<sup>5)</sup> Charles University, Faculty of Science, Institute of Geochemistry, Albertov 6, 128 43 Praha, Czech Republic; email: trubac@natur.cuni.cz

<http://doi.org/10.29227/IM-2020-01-54>

Submission date: 14-12-2019 | Review date: 07-02-2020

## Abstract

*In transportation engineering, earthwork is the main structural material which geotechnical properties can be positively modified with admixtures. This article focuses on the application of energy by-products in earthwork of transportation line structures and summarizes their advantages and define the scope of their utilization. Earthwork construction demands the considerable volume of quality material and therefore, the effort to optimize traditional material substitution is made. One possibility is to apply solid by-products emerging when combusting coal, which is referred to as secondary energy products. These include various types of fly-ash, slag, bottom ash or gypsum. Requisite for their further widespread utilization is the application in the construction and modernization of transport infrastructure, including road and rail construction, or in the case of flood control dams within the framework of water management measures against flooding. They can be utilized also as municipal waste dumps covering. However, the application of fly ashes in earthwork constructions delivers certain limits. When contacting with rain ingress or groundwater, the leaching containing heavy and toxic metals depending on energy by-product type may occur. Alternatively, the limitation of their application can be relatively low mechanical resistance to cyclic saturation and frost effect and consequent volume changes. This article deals with long-term observation results of the energy by-products saturation and additivity influence on volume changes. For the investigation purpose of failure causes, the phase composition using X-ray crystallography and Raman spectroscopy was determined.*

**Keywords:** coal combustion, fly ash, earth structures, transport infrastructure, volume changes, ettringite

## Introduction

The cementing or modification of solid coal products is an effective method for using materials otherwise difficult to apply, often classified as waste. The secondary energy products (CCPs) coming from the combustion and desulphurisation technologies used in power stations and heating plants includes, among others, different kinds of fly ash, slag, ash or mineral gypsum (calcium sulphate). Every year around 15 million tons of secondary energy products are produced in the Czech Republic. Only 20-30% of this production is used in the construction industry. Most products are deposited or used to load excavated areas after mining (Fečko, 2005). Within the scope of applicability in the ground constructions of road structures, CCPs, often mixed with a binder (lime or cement) and water, are often used. These modified CCPs are referred to as fly ash based stabilizers (Lidmila, 2015). The fly ash based stabilizer can also be produced by wetting the mixture of fluid fly ash or bed ash (Kresta, 2012).

There are not so much experience with using of fly ash for constructing railway embankment.

The more detailed study for utilization of fly ash as a structural fill material for railway embankment for rail metro was done in Japan (Sunaga, 1992), another study for the rail-

way substructure was done in Serbia (Vukićević, 2016). The real application of fly ash in railway structures in the form of fly ash based stabilizer was applied in the railway line at Smřice station in 2005. The earthwork, which contains a layer of dangerously freezing and swellable clay limestone, was protected from the effect of frost and penetration of water by a layer of fly ash based stabilizer. After more than 13 years from the implementation of the fly ash based stabilizer layer in the track bed construction, all requirements of SŽDC S4 regulation (Lojda, 2017) are still met.

The use of ash stabilizers for building earthworks brings major problems associated with volume changes (Yoon, 2007). When long term contacting the fluid fly ashes with water new secondary minerals are created, especially ettringite  $\text{Ca}_6\text{Al}_2(\text{SO}_4)_3(\text{OH})_{12}\cdot 26(\text{H}_2\text{O})$  and calcium carbonates, which can cause volume changes causing defects of road construction layers. In terms of the risk of loss of mechanical strength and ultimately of overall stability, the most dangerous is the formation and growth of ettringite minerals (Dermatas, 1995). Another risk factor for the use of fly ash based stabilizers in ground constructions is their relatively low resistance to repeated contact with water and frost (Chen 2009, Sear 2011) and the risk of partially unsatisfactory hygienic and ecological parameters (Vaniček, 2003).

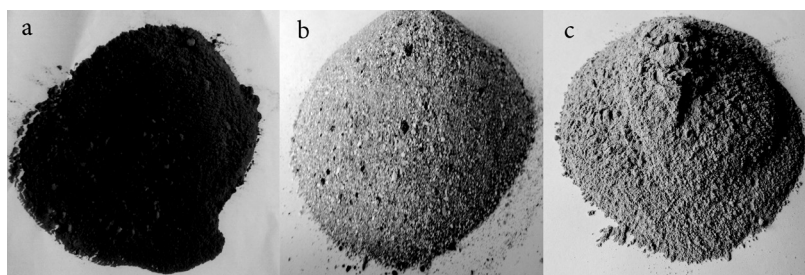


Fig. 1. a) Fly ash from Mělník power station, b) fluid bed ash from Ledvice power station, c) fluid filter ash from Tisová power station  
 Rys. 1. a) Popiół lotny z elektrowni Mělník, b) popiół ze złoża fluidalnego z elektrowni Ledvice, c) popiół z filtru płynnego z elektrowni Tisová

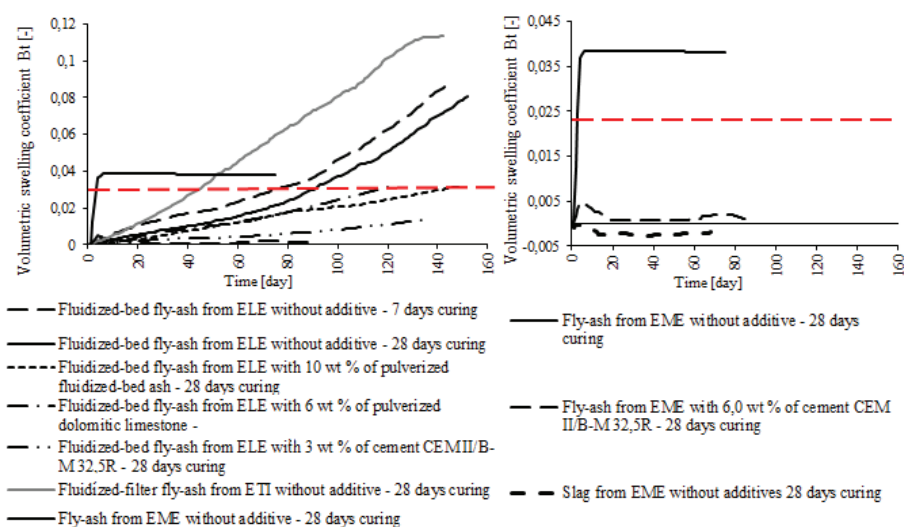


Fig. 2. Time course of volumetric changes of tested fly ash based stabilizers

Rys. 2. Przebieg zmian objętościowych w czasie badanych stabilizatorów na bazie popiołu lotnego

In relation to the risk of undesirable volumetric changes, this article focuses on the issue of CCP swelling. The long-term influence of saturation and influence of used additives in the investigated mixtures on volumetric changes of CCPs were studied within experimental research.

## Materials

For the purpose of experimental research of coal combustion by-products, samples (see Figure 1) were taken from three power stations in the Czech Republic, namely fly ash from the Mělník power station, fluid bed ash from the Ledvice power station, and filter fly ash from the Tisová power station. In addition, a fly ash-based stabilizer sample was taken from the trial section trackbed at the Smiřice railway station within the Pardubice–Liberec railway line, where stabilizer from the Chvaletice power plant (ECHVA) was used.

The above-mentioned power stations represent two basic types of desulphurisation and each produces by-products with other technical parameters. In Mělník, desulphurization is done by wet limestone solution. From Ledvice and Tisová have been used fluid combustion products. All three power stations burn brown coal.

High-temperature fly ash (Mělník) from wet limestone solution consists mainly of aluminosilicates (mullite, quartz). Fluid bed ash from Ledvice is mostly formed of  $\text{CaSO}_4$ ,  $\text{CaCO}_3$ ,  $\text{CaO}$  and aluminosilicates (mullite, quartz) (Mráz, 2015).

As additives the following materials were used:

- Calcitic-dolomitic crystalline limestone from Krtyně mine, which was subjected to mechanical activation in a two-rotor repulsion high-speed mill;
- Mechanically-chemically activated fluid ash from the Pilsen heating plant;
- Cement CEM II/B-M 32,5 R in accordance with ČSN EN 197-1.

The fly ash stabilizer from the Chvaletice Power Station was used as part of the test section verifying the use of fly ash stabilizer in the railway substructure construction, as described for example in (Lidmila, 2015). The fly ash stabilizer from Chvaletice Power Station consisted (weight composition) of fly ash (52%), gypsum, (25%), calcium oxide mined in Kotouč Štrambersk (3%) and water (20%). Furthermore, crystals of  $\text{CaSO}_4$  (gypsum) and fragments of minerals of quartz, K feldspar, plagioclase, biotite, calcite, zirconium,  $\text{BaSO}_4$  and KCl were present in fly ash stabilizer. Gypsum and mineral debris form accumulation sites.

## Methodology

Laboratory compatibility determination of fly ash mixtures by Proctor standard tests according to ČSN EN 13286-2 were carried out at Czech Technical University in Prague, the Faculty of Civil Engineering. In order to verify the resistance to the effects of transport loads, the stress tests according to

Tab. 1. XRF elemental analysis of fluid filter fly ash and slag from wet limestone scrubbing  
 Tab. 1. Analiza elementarna XRF popiołu lotnego i żużła z filtra z przemywania wapienia

Element	Fluid filter fly ash from Tisová	Slag from wet limestone solution from Mělník	Fluid filter fly ash without additives from Tisová	Slag from wet limestone solution without additives from Mělník
			After volume changes monitoring is complete	
(wt. %)				
Al	14,4	15,4	14,3	11,4
Si	16,0	17,7	16,8	13,5
Ti	6,5	2,0	4,1	2,5
Fe	4,5	6,4	4,6	4,4
Mg	0,5	0,3	0,7	0,5
Sx	3,8	4,3	6,4	5,9

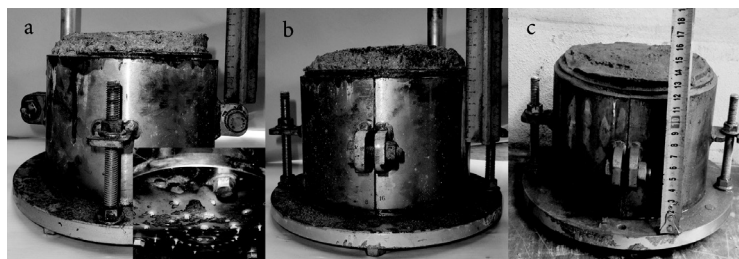


Fig. 3. Testing bodies of fly ash based stabilizers after the volume changes monitoring, a) fluid fly ash without additives from Tisová after 28 days of curing - (ETI\_mineral), b) fluid bed ash without additives from Ledvice after 28 days of curing, c) fly ash without additives from Mělník after 28 days of curing

Rys. 3. Badanie stabilizatorów na bazie popiołu lotnego po monitorowaniu zmian objętości, a) płynny popiół lotny bez dodatków Tisová po 28 dniach utwardzania - (ETI\_mineral), b) popiół fluidalny bez dodatków Ledvice po 28 dniach utwardzania, c) popioły lotne bez dodatków z Mielnika po 28 dniach utwardzania

ČSN EN 13286-41 were performed. To determine the resistance to the effects of climatic conditions, suitability for water effect and reduction under freezing according to ČSN EN 14227-14 was assessed. The greatest attention was paid to the long-term influence of saturation and the influence of additives in examined mixtures on volume changes.

Mixtures of both combustion and desulphurisation technologies and with different binder ratios were tested separately. In the case of CCPs, commonly used binders were replaced by inorganic bulk binders obtained by mechanical-chemical activation of fluid fly ash or by mechanical activation of dolomitic limestones.

One of the purposes of applying mechanically-chemically activated materials to CCPs was to eliminate the formation of ettringite.

#### Methodology of analysis of elemental and phase composition

To describe the causes of volume changes was in the laboratory of University of Chemistry and Technology analysed the elemental composition by X-ray fluorescence spectroscopy (XRF) and determining the phase composition using X-ray diffraction analysis (XRD). XRD analysis was performed on 5 samples of fly ash mixtures. It was a fly bed ash from Ledvice without additives, a fluid bed ash from Ledvice with 10 wt. % of mechanically-chemically activated fluid fly ash, fluid bed ash with 6 wt. % mechanically-chemically activated dolomite limestone, slag from Mělník without admixtures, non-admixed fly ash from Tisová. XRD data were obtained at room ambient temperature using  $\theta$ - $\theta$  powder diffractometer Bruker AXS D8 'Pert PRO in Bragg-Brentano para focusing geometry with wave length CoK $\alpha$  radiation ( $\lambda = 1.7903 \text{ \AA}$ ,  $U = 34 \text{ kV}$ ,  $I = 20$  or  $30 \text{ mA}$ ). Data were scanned using hi-speed detector LynxEye in angle range of  $30$ – $80^\circ$  ( $2\theta$ ) with

measurement step of  $0.0196^\circ$  ( $2\theta$ ) and adding time of 19.2 per step. Data processing and evaluation was done in HighScore Plus 3.0e software.

XRF analysis was performed using the ARL 9400 XP sequenced wave-dispersive X-ray spectrometer. This spectrometer is equipped with an X-ray tube with Rh anode type 4GN with an end Be window of  $50 \mu\text{m}$  thickness. All intensity of the spectral lines of the elements were measured in vacuum by WinXRF. The combination of generator-collimator-crystal-detector settings has been optimized for 82 measured elements with a time of 6 seconds per element. The obtained intensities were processed by Uniquant 4 without the need to measure standards. The analysed powder samples were extruded into tablets of 5 mm thickness and 40 mm in diameter without the use of a binder (or using Dentacryl as a binder) and with or without a  $4 \mu\text{m}$  thick polypropylene film (PP). The time of measuring of one sample was approximately 15 minutes.

Analysis by Raman microspectroscopy method were conducted at several randomly selected locations individual coarsely powdered samples using a Renishaw instrument InVia Reflex Raman spectrometer Renishaw linked with a Leica microscope using a  $50\times$  objective lens. As an excitation, an argon laser ( $\lambda = 514 \text{ nm}$ ) and a diode laser ( $\lambda = 785 \text{ nm}$ ) were used. Laser energy was limited to 10% to eliminate thermal changes in samples. The spectra were taken in the range of  $100$ – $2000 \text{ cm}^{-1}$  with the following settings: 20 seconds of one accumulation time and 10–20 of these accumulations were recorded for the resulting spectrum with an optimized signal to noise ratio. The instrument was calibrated on a Raman diamond strip of  $1332 \text{ cm}^{-1}$ . Spectrum manipulation (baseline correction) was performed in GRAMS/AI 9.1.

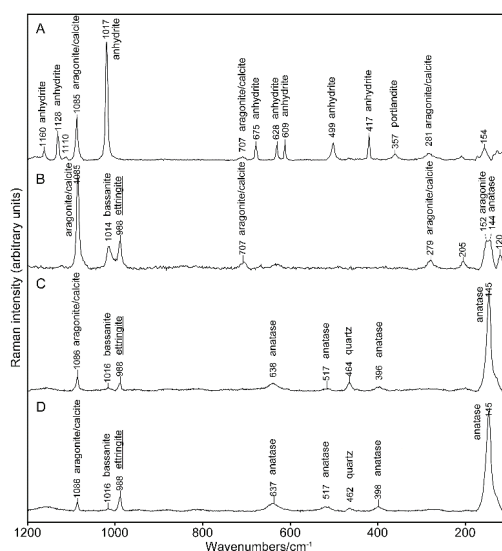


Fig. 4. Raman's spectrum of fluid bed ash from Ledvice power station  
 Sys. 4. Widmo Ramana popiołu ze złoża fluidalnego z elektrowni Ledvice

### Verification of volumetric stability of ash stabilizer

The purpose of the measuring the volume changes of ash stabilizer was the determination of the volume swelling coefficient. For this test, the CBR mortar and other equipment used for the preparation and execution of the CBR test according to ČSN EN 13286-47 was used. The mixture moisturized to optimal moisture was compacted in the CBR by the energy Proctor Standard. The ash stabilizers were aged for 7 or 28 days in a mold at 20°C in a sealed package and then saturated with water until the deformation subsides. In time intervals, the change in the height of the surface of the compacted, saturated sample loaded with load was measured.

The volume swelling coefficient  $B_t$  was determined according to following relationship (1) (see appendix 3 of TP 93):

$$B_t = \Delta V_t / V_1 \quad (1)$$

where:  $V_1$  ( $m^3$ ) is the original volume of the sample and  $\Delta V_t$  ( $m^3$ ) is the change of volume of the sample in the time  $t$ .

In the experiment, fluid bed ash samples, non-additive fluid filter fly ash, and various admixtures (10 wt. % of mechanically chemically activated fluid fly ash, 3 wt. % of cement CEM II/B 32.5 R, 6 wt. % of micronized dolomite limestone) were subjected to the laboratory testing. Additionally, samples of high temperature fly ash and slag without additives and with 6 wt. % of cement CEM II/B 32.5 R were tested.

### Results

The results of volumetric changes in fly ash based stabilizers are shown in the Figure 2. The evolution of volumetric changes in fly ash mixture made of wet limestone solution without additives technology and their values indicate that most volume changes occurred during the first week. At mixtures of high-temperature fly ash without additives, it has occurred to volumetric changes after watering. Volume changes of high temperature fly ash without additives in saturation of compacted samples can be attributed to the release of negative pore pressures. This value was up to 4%. Since it is not a

swelling, i.e. a change in volume due to chemical reactions, it is not necessary to modify by binders the fly ash tested for applications in transport structures. Sample fly ash samples with 6 wt. % of cement can be considered as volume-stable. In the case of slag from wet limestone solution, it has been shown that the test procedure does not change its volume.

The largest increase in volume (more than 10%) show fly ash based stabilizers from fluid bed ash from Ledvice and fluid fly ash without additives from Tisová. Even after 160 days, there are no signs of stabilization. In the case of the additive mixtures, the volume increase occurs more slowly with approximately linear growth. It can be assumed that for all other tested fly ash based stabilizers the maximum permissible volume changes for use in earth structures (<3% swelling in the CBR cylinder according to TP 93) will be achieved after longer observation.

An important finding of swelling measurements during solidification and hardening of the ash stabilizer prepared from fluid combustion technology products is that the addition of mechanically-chemically activated additives into the fly ash mixture results in a decrease in swelling. For example, the effect of mechanically-chemically activated fluid fly ash and mechanically activated dolomite limestone applied to the mixture with fluid bed ash indicates a decrease of swelling to about half.

The XRF and XRD analysis was then performed on the tested fly ash mixtures. XRF analysis showed that the fly ash mixture is significantly represented by Al, Si, (Ti, Fe). The elemental composition of fly ash mixtures remains virtually unchanged during curing. XRD and XRF analyses show a heterogeneous distribution of iron FeO concentrations. In the case of slag from wet limestone solution, the iron concentration is reduced during the sample curing, probably due to precipitation reactions. Examples of XRF analyses for fluid fly ash and slag from wet limestone solution are given in Table 1.

From made XRD analyses, the crystalline phases are in fly ash mixtures represented mainly by anhydrite ( $CaSO_4$ ), quartz ( $SiO_2$ ), anortit ( $CaAl_2Si_2O_8$ ), mullite ( $Al_6Si_2O_{13}$ ) and calcium ( $CaCO_3$ ). The results of XRD analysis showed that

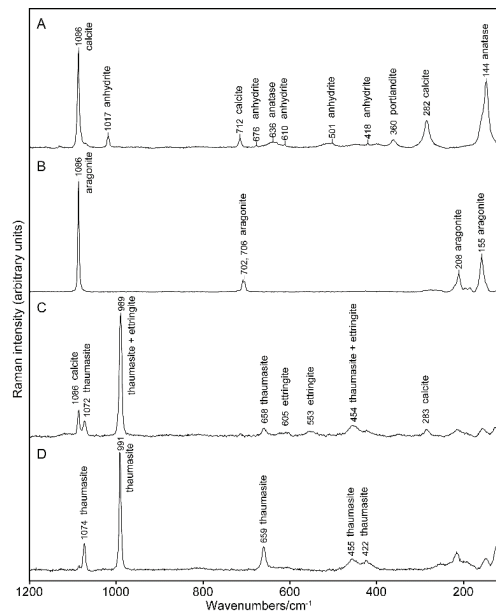


Fig. 5. Raman's spectrum of fluid fly ash from Tisová power station  
Rys. 5. Widmo plynnego popiołu lotnego Ramana z elektrowni Tisová

due to swelling, the phase composition of the studied samples changed. Expansive behaviour of fly ash based stabilizers can be therefore attributed to the formation of ettringite  $\text{Ca}_6\text{Al}_2(\text{SO}_4)_3(\text{OH})_{12}\cdot 26(\text{H}_2\text{O})$  and thaumasite  $\text{Ca}_6[\text{Si}(\text{OH})_6]_2(\text{CO}_3)_2(\text{SO}_4)_2\cdot 24\text{H}_2\text{O}$ .

XRD analysis of fly ash-based stabilizer extracted from structural layer of trackbed from the trial section showed that most of the fly ash material is represented by  $\text{Al}_2\text{O}_3$ - $\text{SiO}_2$  particles, with variable Ca, Fe, Mg +/- Ti and K contents. The particles are mostly porous with many "bubbles", or smaller spherical particles are present. Heavy particles are Fe oxides and silicates, or they are rich in Ti. Other particles consist of amorphous glass, some of them contain automorphic, sometimes skeletal growths of Fe (magnetite) oxides. To a small extent, Fe sulphide (corresponding to pyrrhotine) is present in these particles.

### Raman's spectroscopy

All of the analysed samples were in the form of a coarse powder material consisting of a complex mixture of minerals and amorphous phases. This fact is reflected in the obtained spectra which, even when a microscope and a micrometric laser track is used, often contain Raman strips of several different minerals. Using a 785 nm wavelength laser often has a large amount of luminescence/fluorescence, which corresponds to previous experience in analysing similar samples containing anhydrite or silicate minerals. This luminescence can be caused by the presence of trace amounts of elements from the REE group and sometimes completely overlaps the Raman's mineral signal. The presented spectra (Figures 4 and 5) are therefore cases where negative fluorescence occurred only to a limited extent. In the spectra obtained from the sample from Ledvice power station (Figure 4A) before swelling, the following minerals were identified in the white base mass: anhydrite, aragonite/calcite, portlandite. Quartz has also been identified. Dark minerals have been identified as anatase and hematite. In addition to the Raman strips corresponding to

the aragonite/calcite, basanite, quartz, and anatase minerals, the strip  $988\text{ cm}^{-1}$  was identified in the samples obtained from Ledvice power station (Figure 4B, C) after swelling and from Ledvice power station with addition of milled fluid fly ash (Figure 4D), which corresponds to the ettringite mineral. This strip is related to symmetrical valence vibration in  $\text{SO}_4$  tetrahedra and corresponds to a reference value of  $988\text{ cm}^{-1}$  (Deb et al., 2003). Other Raman strips of ettringite have much less intensity and were not detected in the samples.

Samples from Tisová power station were also analysed. In the sample of fluid fly ash from Tisová power station before swelling (Figure 5A), the calcite, anatase, anhydrite and portlandite minerals were clearly identified. The aragonite was dominated by spectra obtained from the sample taken after swelling from the outside of the base of the test form (Figure 5B). Significant changes, however, were recorded in the spectra obtained from the sample from Tisová power station after swelling. As can be seen from Figure 5C, D spectra are dominated by a strong Raman strip at the  $900\text{ cm}^{-1}$  position. This strip shows the presence of thaumasite and ettringite minerals. Additional bands corresponding to the thaumasite mineral were identified at  $1072$ ,  $658$  and  $454\text{ cm}^{-1}$ , and for the ettringite mineral at  $605$ ,  $553$  and  $454\text{ cm}^{-1}$ . Figure 5D shows a spectrum of almost exclusively thaumasite, and the positions of the Raman strips are in very good agreement with the reference values (Brough and Atkinson, 2001). The strip at  $1074\text{ cm}^{-1}$  ( $1072$  reference value) is assigned to a symmetrical valence vibration of the  $\text{CO}_3$  group, the  $991\text{ cm}^{-1}$  ( $990$ ) strip corresponds to the symmetrical valence vibration of the  $\text{SO}_4$  group, and the  $659\text{ cm}^{-1}$  ( $658$ ) to the vibration of the  $\text{Si}(\text{OH})_6$  group. Strips at  $455$  and  $422\text{ cm}^{-1}$  are probably to exhibit a deformation vibration of the  $\text{SO}_4$  group.

### Conclusions

The strip at  $1074\text{ cm}^{-1}$  ( $1072$  reference value) is assigned to a symmetrical valence vibration of the  $\text{CO}_3$  group, the  $991\text{ cm}^{-1}$  ( $990$ ) strip corresponds to the symmetrical valence vi-



bration of the  $\text{SO}_4$  group, and the  $659\text{ cm}^{-1}$  ( $658$ ) strip to the vibration of the  $\text{Si}(\text{OH})_6$  group. Strips at  $455$  and  $422\text{ cm}^{-1}$  are probably to exhibit a deformation vibration of the  $\text{SO}_4$  group.

From the results obtained from the XRD method and the Raman spectroscopy analysis, it is clear that the samples after swelling from Ledvice power station contain the newly formed ettringite mineral, and the samples after swelling from Tisová power station contain a larger amount of newly formed thaumasite mineral and a smaller amount of ettringite mineral. As for the realization of the fly ash stabilizer layer in the sleeper structure, all requirements of the SŽDC S4 regulation are still fulfilled after more than 10 years of implementation. The ash stabilizer layer performs its protective and insulating function in the structure and does not show a vertical alignment by measuring the track geometry parameters, which means that the stabilizer does not swell.

One of the ways to avoid the creation of ettringite and consequently the degradation of road construction layers is to use

suitable additives. By performing the above-mentioned experiments, it has been shown that by adding additives, especially micronized fly ash or micronized dolomitic limestone, volume changes can be significantly reduced. When installing CCPs into the ground, other factors, especially the geological, hydrogeological and mechanical properties of the underlying earth, must be considered. An additional saturation of the earth structure with built-in CCPs with water can cause a further increase of the newly formed sulphate and carbonate crystals, which can cause a degradation of the road construction layers.

#### **Acknowledgement**

Financial support for the research presented in this paper was granted from Competence Centres programme of Technology Agency of the Czech Republic (TAČR) within the Centre for Effective and Sustainable Transport Infrastructure (CESTI), project number TE01020168. This support is hereby gratefully acknowledged.

## Literatura – References

1. BROUGH, Adrian, ATKINSON, Alan. Micro-Raman spectroscopy of thaumasite. In Cement Concrete Research 31, 2001, p. 421-424, ISSN: 0008-8846.
2. CHEN, Zhiguo, WANG, Zheren, WANG, Xiwei, and ZHAO, Yufeng. Study on the Frost Resistance Test Method of Lime-Fly Ash Stabilized Material Base Course, Proceeding of the ICCTP 2009, Harbin, China, Aug 5-9, 2009.
3. DEB, Stephan et al. Raman scattering and x-ray diffraction study of the thermal decomposition of an ettringite-group crystal. In Phys Chem Minerals 30, 2003, p. 31-38, ISSN: 1432-2021.
4. DERMATAS, Dimitris. Ettringite-Induced Swelling in Soils: State-of-the-art. In Applied Mechanics Review, Vol.48, No. 10, 1995, pp. 659-673, ISSN:2379-0407.
5. FEČKO, Peter et al. Fly ash. Monograph, Ostrava: Publishing services department VŠB-TU Ostrava, 2005, p. 191, ISBN 80-248-0836-6.
6. KRESTA František. Secondary materials in highway engineering, Publishing services department VŠB-TU Ostrava, 2012, p. 144, ISBN 978-80-248-2890-0.
7. LIDMILA, Martin, et al.: Fly ash-based stabilizer in railway trackbed, Monograph, University of technology in Brno, p. 125, 2015, ISBN 978-80-214-5250-3.
8. LOJDA, Vít et al. Microstructural Analysis of Fly Ash-Based Stabilizer for Track Bed. In Key Engineering Materials 731, 2017, p. 66–73. ISSN 1662-9795.
9. MRÁZ, Václav et al. Experimental Assessment of Fly-Ash Stabilized and Recycled Mixes, In Journal of Testing and Evaluation, ASTM, Philadelphia, 2015, p. 264 – 278, ISSN:0090-3973.
10. SEAR, Linton. Properties and Use of Coal Fly Ash. London: Thomas Telford Ltd, 2001. ISBN: 9780727738479 072773847X.
11. SUNAGA, Makoto, Sekine, Etsuo. Utilization of Fly Ash as Materials for Railway Embankment, In Japanese Railway Engineering 121, 1992, p. 13, ISSN 0448-8938.
12. VANÍČEK, Martin. Contaminant transport in the host rock, numerical modelling and laboratory work, Ph.D. thesis, CTU in Prague Publishing house, p. 128.
13. VUKIČEVIĆ, Mirjana et al. Fly Ash and Slag Utilization for the Serbian Railway Substructure, In Vilnius Gediminas Technical University (VGTU) Press, 2016, ISSN 1648-4142.
14. YOON, Sungmin, BALUNAINI, Umashankar and PREZZI, Monica. Forensic Examination of the Severe Heaving of an Embankment Constructed with Fluidized-Bed-Combustion (FBC) Ash, In Journal of the Transportation Research Board (TRB), National Research Council, 2007, ISSN: 2169-4052.

### *Zakres wykorzystania ubocznych produktów spalania węgla w infrastrukturze transportowej*

*W inżynierii transportu masy ziemne są głównym materiałem konstrukcyjnym, którego właściwości geotechniczne można pozytywnie modyfikować za pomocą domieszek. Artykuł koncentruje się na zastosowaniu produktów ubocznych spalania w pracach ziemnych w konstrukcji linii transportowych ocenia ich zalety oraz określa zakres ich wykorzystania. Konstrukcja robót ziemnych wymaga znacznej ilości wysokiej jakości materiału, dlatego podejmowane są wysiłki w celu optymalizacji zastępowania materiałów. Jedną z możliwości jest zastosowanie stałych ubocznych produktów spalania węgla, które są określane jako wtórne produkty energetyczne. Należą do nich różne rodzaje popiołów lotnych, żużli, popiołów dennych lub gipsu. Kierunkiem ich wykorzystania jest zastosowanie w budowie i modernizacji infrastruktury transportowej, w tym w budownictwie drogowym, kolejowym, budowie zapór przeciwpodziowych. Zastosowanie popiołów lotnych w konstrukcjach ziemnych ma jednak pewne ograniczenia. Podczas kontaktu z wnikającymi deszczami lub wodami gruntowymi może wystąpić ługowanie metali ciężkich i toksycznych w zależności od składu ubocznego produktu spalania. Ograniczeniem ich zastosowania może być względnie niska odporność mechaniczna i mrozoodporność. Artykuł dotyczy wyników długoterminowych obserwacji dodatku ubocznych produktów spalania na zmiany objętości. Skład fazowy określono za pomocą krystalografii rentgenowskiej i spektroskopii Ramana.*

**Słowa kluczowe:** spalanie węgla, popioły lotne, struktura gruntu, infrastruktura transportowa, zmiany objętości, ettringit





# Biosorption of Lead and Cadmium Ions on the Green Parts of *Daucus Carota*

Martin MUCHA<sup>1)</sup>

<sup>1)</sup> University of Ostrava, Faculty of Science, Department of chemistry, 30. dubna 22, 701 03 Ostrava, Czech Republic;  
email: martin.mucha@osu.cz

<http://doi.org/10.29227/IM-2020-01-55>

Submission date: 12-01-2020 | Review date: 04-03-2020

## Abstract

*This study deals with utilization of milled stems and leaves of carrot (*Daucus carota*) for the adsorptive removal of Pb(II) and Cd(II) from the aqueous solution. Carrot was bought in the local grocery, it was dried at the laboratory temperature and milled. Prepared material was analysed by the infrared spectrometry which confirms good structural homogeneity of the sample. Kinetic measurements were performed for estimation of adsorption equilibrium time. Equilibrium of Pb(II) adsorption was established after 6 hours of contact time, equilibrium of Cd(II) adsorption was established after 24 hours of contact time. The isotherms' measurements were realized with the contact time 24 hours for the estimation of adsorption capacities of the studied sorbent. Adsorption capacities were around 47 mg/g for Cd(II) and 154 mg/g for Pb(II). Changes of pH values of the sorption solutions were negligible but some amount of Ca(II), Mg(II), K(I) and Na(I) ions was released to the solution during adsorption process. *Daucus carota* stems and leaves exhibit good sorption capacities and they could be utilized for adsorptive removal of Pb(II) and Cd(II) ions from the aqueous solutions.*

**Keywords:** biosorption, carrot, lead, cadmium

## Introduction

Heavy metals represent potentially dangerous species for the plants, animals and human health. They negatively affect many biochemical processes (Chen et al., 2017). Heavy metals ions can be released to the environment through some types of pesticides, by the combustion of fossil fuels or they can get to the environment from the industrial wastes (Kafka and Punčochářová, 2002). Processing of industrial wastes containing heavy metals is currently widely studied (Al-Enezi et al., 2004; Sreesai and Sthiannopkao, 2009). Industrial wastewater containing heavy metals can be decontaminated by various techniques such as precipitation (Wu, 2019), electrodeposition (Vivas et al., 2019), or adsorption (Mohan et al., 2007). Adsorption represents the most utilized technique for heavy metals removal. Clays (mainly bentonites) (Yang et al., 2010) and activated carbons (Mohan et al., 2007) belong to the most common adsorbents used in the praxis. Sorption capacities of these materials vary for various metals ions. They can be up to tens of mg/g of sorbent (Mohan et al. 2007; Yang et al., 2010). Unfortunately, clays belong to the exhaustible resources and production of activated carbons is relatively energy-intensive. Research in the field of heavy metals adsorption is currently targeted to the utilization of various waste materials (Bláhová et al., 2018; Wang et al., 2015). Slags as a by-product from the metallurgical industry exhibit promising sorption properties. Sorption capacity of blast furnace slag for Pb(II) can be around 20 mg/g but sorption capacity of steelmaking slag for Pb(II) can reach 70 mg/g of material (Bláhová et al., 2018). Unfortunately slags interact with water, they cause increase of the solution's pH value as well as they release some ions to the solution. Therefore they are potentially dangerous, which limit their utilization for the wastewater treatment (Mucha, 2018). Biosorption represents other approach to the research of the new sorption materials. Plants or their parts (Dubey

and Mishra, 2017, Mucha and Mucha, 2015) or fungi (Zhao et al., 2016) can be utilized as sorption materials. These materials are of natural origin and compounds which can be released from these materials would not be dangerous for environment in the comparison to waste materials. Biosorbents can reach or even exceed the sorption capacities of above mentioned materials (Mucha and Mucha, 2015).

Presented work deals with utilization of carrot (*Daucus carota*) dried and milled stems and leaves for adsorption of Pb(II) and Cd(II) ions from the aqueous environment. Material was characterized by infrared spectroscopy and kinetics and adsorption isotherms were measured.

## Materials and methods

Carrot (*Daucus carota*) was purchased in the local grocery. Green parts (stems and leaves) were separated from the root and they were dried at laboratory temperature. Green parts were milled after the drying and they were characterized by infrared spectrometry (FTIR) on the Nicolet 6700 FTIR spectrometer (Thermo scientific, USA). Spectra were measured by ATR technique with single bounce diamond crystal at 256 scans and with resolution 4 cm<sup>-1</sup>. The bulk density, loss by drying at 105°C (using the Memmert UNB 300 dryer, Memmert GmbH, Germany) and loss of ignition (amount of ash) at 1100°C (using the muffle furnace, LAC Ltd. Czech Republic) were determined. Material was decomposed by 1:1 HNO<sub>3</sub> (p.a., Mach chemicals Ltd., Czech Republic) and contents of Ca(II), Mg(II), K(I), Na(I), Pb(II) and Cd(II) were determined by atomic absorption spectrometry (AAS) at Varian AA240FS spectrometer (Varian, USA). Standards of particular cations were supplied by Sigma-Aldrich GmbH (Germany), wavelengths 422,7 nm (Ca), 202,6 nm (Mg), 404,4 nm (K), 330,3 nm (Na), 205,3 nm (Pb) and 326,1 nm (Cd) were utilized for analysis. Adsorption experiments were carried out by batch

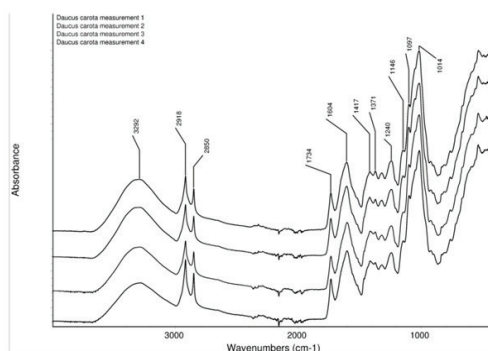


Fig. 1. Infrared spectra of various portions of the studied material  
Rys. 1. Widma w podczerwieni różnych części badanego materiału

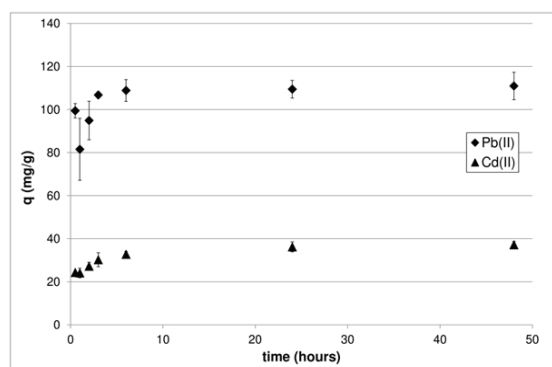


Fig. 2. Kinetics of Cd(II) and Pb(II) adsorption on the carrot biomass  
Rys. 2. Kinetyka adsorpcji Cd (II) i Pb (II) na biomacie z marchwi

method. Kinetic experiments were realized at times 0.5, 1, 2, 3, 6, 24 and 48 hours. Concentrations of studied cations in the sorption solutions were 5 mmol/L. Sorption solutions were prepared from  $\text{Pb}(\text{NO}_3)_2$  (p.a., LachNer Ltd., Czech Republic) and  $\text{Cd}(\text{NO}_3)_2 \cdot 4\text{H}_2\text{O}$  (p.a., Sigma-Aldrich GmbH, Germany). The mass 0.25 g of carrot biomass was weighted to the centrifugation tube and 50 mL of sorption solution was added. Samples were occasionally stirred and filtered after given time period. The pH values of the solutions were measured by WTW InoLab 735 equipped by WTW SenTix 41 electrode (WTW GmbH, Germany). Concentrations of Pb(II), Cd(II), Ca(II), Mg(II), K(I) and Na(I) were determined by above mentioned AAS methods. Equilibrium measurements of isotherms were carried out in the centrifugation tubes with 0.25 g of carrot biomass and 50 mL of sorption solution. Concentrations of the Pb(II) and Cd(II) cations in the sorption solutions were 0.1, 0.5, 1, 2.5, 5, 10 and 20 mmol/L. Contact time was 24 hours and it was selected according to kinetic measurements. Samples were filtered after 24 hours and contents of Pb(II), Cd(II), Ca(II), Mg(II), K(I) and Na(I) were determined by AAS method. All sorption experiments were carried out in 3 parallel assessments at temperature  $22 \pm 1^\circ\text{C}$ .

## Results and discussion

Dried and milled sorption material (carrot biomass) was characterized at first. It was found out that material contains  $9.4 \pm 1.7\%$  of free water (moisture) and  $6.9 \pm 0.8\%$  of ash. Bulk density of the used carrot biomass was  $172.4 \pm 6.8 \text{ kg/m}^3$ . Contents of selected ions in the used material were  $17.98$

$\pm 3.25 \text{ mg/g}$  (Ca),  $5.45 \pm 0.26 \text{ mg/g}$  (Mg),  $33.59 \pm 4.38 \text{ mg/g}$  (K),  $14.21 \pm 0.87$  (Na),  $< 3.14 \pm 0.07 \text{ mg/g}$  (Pb) and  $< 5.84 \pm 0.14 \text{ mg/g}$  (Cd). It can be stated that contents of Pb(II) and Cd(II) in the studied material were negligible for purposes of this study.

Infrared spectra were measured for the verification of homogeneity of the sample as well as for the description of material's chemical composition. Measured spectra are depicted on the Fig. 1. It can be seen that spectra of various portions of biomass are almost identical, only negligible changes occur in the region of  $-\text{CH}_2-$  and  $-\text{CH}_3$  groups deformation vibrations ( $1417$  and  $1371 \text{ cm}^{-1}$ ). It can be stated that material is homogeneous enough for the utilization in sorption experiments in this study. Chemical composition of the carrot biomass is mainly organic. The broad band at  $3292 \text{ cm}^{-1}$  can be assigned to the stretch vibration of O–H or N–H bonds. Bands at  $2918$  and  $2850 \text{ cm}^{-1}$  belong to the stretch vibrations of C–H bond in the saturated hydrocarbons. Presence of carbonyl group (C=O, aldehydes, ketones or carboxylic acids) is confirmed by the band at  $1734 \text{ cm}^{-1}$ . Broad band around  $1604 \text{ cm}^{-1}$  can be assigned to the stretch vibration of C=C in aromates and it can contain the band of C=O stretch vibration in carboxylates as well. Bands of deformation vibrations of  $-\text{CH}_2-$  and  $-\text{CH}_3$  groups occur at  $1417$  and  $1371 \text{ cm}^{-1}$ . Content of C–O or C–N bonds in various functional groups can be assumed from the presence of bands at  $1240$ ,  $1146$ ,  $1097$  and  $1014 \text{ cm}^{-1}$ . Studied material contains aliphatic as well as aromatic hydrocarbon parts and mainly hydroxyl, amine and carboxyl functional groups (Socrates, 2007). Heavy metals cations could bond

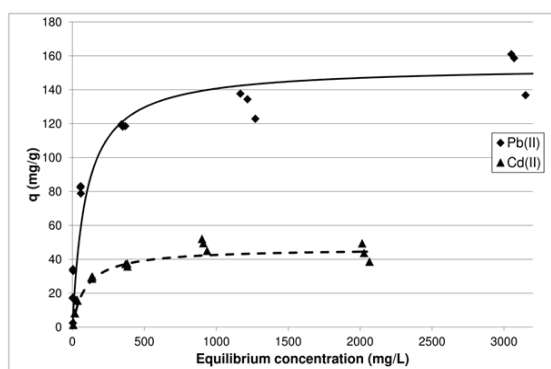


Fig. 3. Adsorption isotherms of Cd(II) and Pb(II) on the carrot biomass  
Rys. 3. Izotermy adsorpcji Cd (II) i Pb (II) na biomacie z marchwi

Tab. 1. Parameters of Langmuir isotherm for studied cations ( $q_{\max}$  – maximal adsorbed amount)  
Tab. 1. Parametry izotermy Langmuira dla badanych kationów ( $q_{\max}$  - maksymalna zaadsorbowana ilość)

Metal cation	$q_{\max}$ [mg/g]	$b$ [L/mg]
Pb(II)	$154,50 \pm 13,70$	$0,011 \pm 0,005$
Cd(II)	$47,26 \pm 6,97$	$0,011 \pm 0,004$

on the surface of carrot biomass probably on the carboxylic groups via chemisorption or on the hydroxyl or amine functional groups or on the  $\pi$ -electron systems by the electrostatic interactions.

The results of kinetic measurements are shown on the Fig. 2. It can be stated that equilibrium of the sorption on carrot biomass is established after 6 hours of contact time in the case of Pb(II) ions and after 24 hours of contact time in the case of Cd(II) ions. The adsorbed amount of Cd(II) increases continuously with increasing contact time. The adsorbed amount of Pb(II) ions increases significantly in the first 0.5 hour, then small decrease in the adsorbed amount occurs after 1 hour and then further increase of adsorbed amount occurs. The decrease can be probably caused by changes in the composition of the Pb(II) complex particles on the biomass surface or by reorganization of adsorbed Pb(II) cations on the surface due to chemical reactions with surface functional groups (chemisorption), which can lead to the release of small amount of Pb(II) ions back to the solution. The changes of the pH values during sorption were negligible (maximal 0.5 pH units after 48 hours). These changes can be caused by changes of the solution composition during sorption as Pb(II) or Cd(II) were removed from the solution and other cations were released from the material. Each cation forms various aqua- and hydroxo- complexes in the aqueous environment and therefore changes in the cationic composition of solution can cause small changes of the pH values. Carrot biomass contains higher amounts of Ca(II), Mg(II), K(I) and Na(I) which are released to the solution during sorption. The amount of released K(I) was up to  $33.14 \pm 1.22$  mg/g, released amount of Na(I) was  $14.87 \pm 1.34$  mg/g, released amount of Mg(II) reach  $3.52 \pm 0.21$  mg/g and released amount of Ca(II) was up to  $15.12 \pm 0.83$  mg/g. It can be stated that almost all of cations present in the material were released to the solution during the sorption. Chemisorption can be other factor that influences the solution pH value. If the chemisorption on the carboxylic functional groups occurs during contact of biomass with solution, small amount of H(I) ions or other cations can be released to the solution due to formation of carboxylates

containing Pb(II) or Cd(II) ions. Release of H(I) ions as well as the formation of hydroxocomplexes of cations present in the solution can cause the pH values decrease. Adsorption of Cd(II) and Pb(II) on the carrot biomass take probably place by combination of physisorption and chemisorption, which can be concluded from the fast first stage of adsorption but the longer time to reach equilibrium as well as from the release of cations from the material.

Adsorption isotherms were measured for contact time 24 hours and they are depicted on the Fig. 3. The model of Langmuir isotherm is more suitable in the case of both studied cations. Model isotherms were calculated using linear forms of isotherms' equations. The coefficients of determination of the linear forms of isotherms were 0.98 (Pb(II) isotherm) and 0.97 (Cd(II) isotherm) in the case of Langmuir model in the comparison to 0.68 (Pb(II) isotherm) and 0.79 (Cd(II) isotherm) in the case of Freundlich model. Parameters of Langmuir isotherms calculated from measured data are shown in the Table 1. The maximal adsorption capacities ( $q_{\max}$ ) of the carrot biomass were  $154.5 \pm 13.7$  mg/g for Pb(II) and  $47.3 \pm 7.0$  mg/g for Cd(II) ions. The sorption capacities recalculated to molar expression were 0.75 mmol/g for Pb(II) and 0.42 mmol/g for Cd(II), so it can be stated that carrot biomass has higher affinity to Pb(II) ions in the comparison to Cd(II) ions. Changes of the pH values during sorption were negligible as in the case of kinetic measurements. Cations (Ca(II), Mg(II), K(I) and Na(I)) were released to the solution as well. The amount of released cations is practically independent at the initial concentration of Pb(II) or Cd(II) in the case of Mg(II) and Na(I) and it increases with increasing initial concentration of Pb(II) or Cd(II) in the case of Ca(II) and K(I). Studied heavy metals cations probably interact with various parts of biomass surface because Ca(II) release is more affected compared to K(I) release in the case of Pb(II) sorption but release of cations exhibits opposite trend (more affected K(I) release than Ca(II) release) in the case of Cd(II) sorption. Estimated adsorption capacities are comparable or higher than adsorption capacities of other materials studied for the removal of heavy metals cations from the aqueous solutions. Other stud-

ies state sorption capacities for bentonite 47.9 mg/g of Pb(II) (Yang et al. 2010) or 117.6 mg/g of Pb(II) (Mucha and Mucha, 2015). The sorption capacities for activated carbons around 30.1 mg/g of Pb(II) and 8.0 mg/g of Cd(II) were published (Mohan et al. 2007). Slags were studied as sorption material as well with sorption capacities of Pb(II) around 22.8 mg/g for blast furnace slag and 78.7 mg/g for steelmaking slag (Bláhová et al. 2018). It can be stated that carrot biomass could be promising material for sorption purposes.

### Conclusion

Carrot (*Daucus Carota*) biomass obtained by drying and milling of green parts (stems and leaves) of carrot was utilized for removal of Pb(II) and Cd(II) cations from the aqueous solutions. Sorption material was characterized to determine basic parameters (moisture content, ash content, bulk density) and information about chemical composition. It was found out using infrared spectroscopy that material is homo-

geneous enough for utilization as sorbent. Kinetic measurements reveal that sorption equilibrium was reached after 24 hours in the case of Cd(II) ions and it was reached after 6 hours in the case of Pb(II) ions. Only negligible changes of the pH values occur during contact of carrot biomass with solutions containing Pb(II) or Cd(II) ions and various cations (Ca(II), Mg(II), Na(I) and K(I)) were released to the sorption solution during contact with sorbent. Equilibrium measurements show that adsorption of Pb(II) and Cd(II) ions on the carrot biomass takes place according to Langmuir isotherm model and the adsorption capacities of the studied sorbent were  $154.5 \pm 13.7$  mg/g for Pb(II) and  $47.3 \pm 7.0$  mg/g for Cd(II) ions. These sorption capacities are comparable or higher than capacities of other sorption materials (bentonite, activated carbon, slags) published in the literature. Carrot biomass could be utilized as alternative sorbent for the Pb(II) and Cd(II) ions removal from the aqueous solutions.

## Literatura – References

1. AL-ENEZI, G. et al. Ion Exchange Extraction of Heavy Metals from Wastewater Sludges. *Journal of Environmental Science and Health, Part A.*, r. 39, 2004, p. 455-464, ISSN 1093-4529.
2. BLÁHOVÁ, Lenka et al. Influence of the slags treatment on the heavy metals binding. *International Journal of Environmental Science and Technology*, p. 15, 2018, p. 697-706, ISSN 1735-1472.
3. CHEN, Yongchun et al. The accumulation characteristics and potential health risks of heavy metals in vegetables from reclaimed area of China. *Human and Ecological Risk Assessment: An International Journal*, r. 24, 2017, p. 949-960, ISSN 1080-7039.
4. DUBEY, Abha; MISHRA Anuradha. A Novel Plant-Based Biosorbent for Removal of Copper (II) from Aqueous Solutions: Biosorption of Copper (II) by Dried Plant Biomass. *Journal of Renewable Materials*, r. 5, 2017, p. 54-61. ISSN 2164-6325.
5. KAFKA, Zdeněk; PUNČOCHÁŘOVÁ Jana. Těžké kovy v přírodě a jejich toxicita. *Chemické listy*, r. 96, 2002, p. 611-617, ISSN 1213-7103.
6. MOHAN, Dinesh et al. Sorption of arsenic, cadmium, and lead by chars produced from fast pyrolysis of wood and bark during bio-oil production. *Journal of Colloid and Interface Science*, r. 310, 2007, p. 57-73, ISSN 0021-9797.
7. MUCHA Marek; MUCHA Martin. Utilization of Knotweed for the Sorption of Lead Ions. *Spektrum*, r. 15(2), 2015, p. 10-13, ISSN 1804-1639.
8. MUCHA Martin. Stability of blast furnace slag in the demineralized water. *Waste forum*, (4), 2018, p. 484-493, ISSN 1804-0195.
9. SOCRATES, George. *Infrared and raman characteristic group frequencies: tables and charts* 3rd ed. West Sussex: John Wiley, 2007. ISBN 978-047-0093-078.
10. SREESAI, Siranee; STHIANNOPKAO Suthipong. Utilization of zeolite industrial wastewater for removal of copper and zinc from copper-brass pipe industrial. *Canadian Journal of Civil Engineering*, r. 36, 2009, p. 709-719, ISSN 0315-1468.
11. VIVAS, Eleazer L. et al. Comparative evaluation of alkali precipitation and electrodeposition for copper removal in artisanal gold smelting wastewater in the Philippines. *Desalination and water treatment*, r. 150, 2019, p. 396-405, ISSN 1944-3986.
12. WANG, Jianlong et al. Adsorption characteristics of construction waste for heavy metals from urban stormwater runoff. *Chinese Journal of Chemical Engineering*, r. 23, 2015, p. 1542-1550, ISSN 1004-9541.
13. WU, Ruiping. Removal of Heavy Metal Ions from Industrial Wastewater Based on Chemical Precipitation Method. *Ekoloji*, r. 28, 2019, p. 2443-2452, ISSN 1300-1361.
14. YANG, Shitong et al. Impact of environmental conditions on the sorption behavior of Pb(II) in Na-bentonite suspensions. *Journal of Hazardous Materials*, r. 183, 2010, p. 632-640. ISSN 0304-3894.
15. ZHAO, Changsong et al. Characteristics of uranium biosorption from aqueous solutions on fungus *Pleurotus ostreatus*. *Environmental Science and Pollution Research*, r. 23, 2016, p. 24846-24856, ISSN 0944-1344.

### *Biosorpcja jonów ołowiu I kadmu na zielonych częściach marchwi Daucus Carota*

Artykuł dotyczy wykorzystania zmielonych łodyg i liści marchwi (*Daucus carota*) do adsorpcyjnego usuwania Pb (II) i Cd (II) z roztworu wodnego. Marchewkę kupiono w lokalnym sklepie spożywczym, wysuszono w laboratorium i zmielono. Przygotowany materiał analizowano za pomocą spektrometrii w podczerwieni, co potwierdziło dobrą jednorodność strukturalną próbki. Pomiary kinetyczne przeprowadzono w celu oszacowania czasu osiągnięcia równowagi adsorpcji.

Równowagę adsorpcji Pb (II) ustalono po 6 godzinach czasu kontaktu, równowagę adsorpcji Cd (II) ustalono po 24 godzinach czasu kontaktu. Pomiary izoterm wykonano z czasem kontaktu 24 godziny w celu oszacowania zdolności adsorpcji badanego sorbentu. Zdolności adsorpcyjne wynosiły około 47 mg / g dla Cd (II) i 154 mg / g dla Pb (II). Zmiany wartości pH roztworów sorpcyjnych były znikome, ale pewna ilość jonów Ca (II), Mg (II), K (I) i Na (I) została uwolniona do roztworu podczas procesu adsorpcji. Łodygi i liście *Daucus carota* wykazują dobre zdolności sorpcyjne i można je wykorzystać do adsorpcyjnego usuwania jonów Pb (II) i Cd (II) z roztworów wodnych.

**Słowa kluczowe:** biosorpcja, marchew, ołów, kadm







# Online X-Ray Fluorescence Monitoring of Coarse Ore for Silver at the Process Conveyors at Kazakhmys Corporation LLC

Aydar NIGMATULIN<sup>1)</sup>, Zauze ABDRAKHMANOVA<sup>1)</sup>, Andrey KAN<sup>1)</sup>,  
Sergey EFIMENKO<sup>2)</sup>, Dmitry MAKAROV<sup>3)</sup>

<sup>1)</sup> Kazakhmys Corporation LLC Metallurgov pl. 1, Zhezkazgan, 101300, Kazakhstan

<sup>2)</sup> Kazakhmys Corporation LLC Metallurgov pl. 1, Zhezkazgan, 101300, Kazakhstan; email: serg\_yef@mail.ru

<sup>3)</sup> Institute of Industrial North Ecology Problems of the Kola Science Centre of RAS, Akademgorodok, 14a, 184209, Apatity, Russia; email: mdv\_2008@mail.ru

<http://doi.org/10.29227/IM-2020-01-56>

Submission date: 14-02-2020 | Review date: 07-04-20120

## Abstract

*This paper examines the process and methodological aspects of implementing online X-ray fluorescence monitoring of ore in terms of its silver, cadmium, zinc, lead, molybdenum, and iron grade at the process conveyors at Balkhash and Karagaily Concentrators and the main conveyor of the Nurkazgan underground mine operated by Kazakhmys Corporation LLC. The research was complicated by the need to: a) ensure reliable measurement of silver and cadmium in the range of 1+ ppm, molybdenum in the range of 10+ ppm, as well as copper, zinc, lead, and iron in the ore size class -300 mm; b) implement monitoring of the grade of these elements (except molybdenum) at Balkhash Concentrator in the waste slag of Balkhash Copper Smelter, characterized by a very complex elemental matrix. A modification of the ore monitoring station RLP-21T (by Aspap Geo LLC, Alma-Ata) was developed, implemented, and thoroughly tested for online monitoring of low-grade silver ore flows. Energy dispersive X-ray fluorescence method was adopted for ore assays. Instrument spectra were measured every second. Silver, cadmium, and molybdenum grade was calculated based on 40 measurements, copper, zinc, lead, and iron grade – based on 20 measurements.*

**Keywords:** X-ray fluorescence method, RLP-21T ore monitoring station, copper, silver, cadmium, molybdenum, online monitoring of ore grade, process conveyors

## Introduction

The existing literature on the implementation of effective online monitoring of silver, cadmium, copper, lead, zinc, and iron in the run-of-the-mine ore from the copper sandstone deposits Zhezkazgan and Zhaman-Aibat fed to the Zhezkazgan Concentrators 1 (ZC-1) and 2 (ZC-2), using energy dispersive X-ray fluorescence (EDRFXF) ore monitoring stations (OMS) at on belt process conveyors, was reviewed in detail in [1–3]. As a result of the studies conducted at ZC-1 and ZC-2 from October 2016 to January 2017, for the first time in Kazakhstan the most pressing production problem was solved: highly effective online monitoring was implemented of primary (Cu, Pb, Zn) and secondary (Ag, Cd) commercial elements in ores of the size class -300 mm with a low (5+ ppm) silver grade, transported by heavy-duty belt conveyors at concentrator plants.

Zhezkazgan industrial site and the Zhomart mine now have access to: a) real-time information on the grade of the ore fed to the concentrator plants during the shift, day, and since the beginning of the month and can quickly make the necessary adjustments to the mining and concentration process; b) reliable evidence for the purposes of substantiating their proposals concerning ore grade when the concentrator's output is allocated at the end of the calendar month.

The research goal was to develop a single high-performance system for online monitoring of the chemical composition of the salable copper polymetallic ores at the mining operations of Kazakhmys Corporation LLC, focused not only on the core element (copper), but also secondary elements

(silver, cadmium, molybdenum). The goal was achieved at some of the operations at the Zhezkazgan industrial site.

But Kazakhmys Corporation LLC also controls the deposits developed by the mining operations at the Karaganda and Balkhash industrial sites: the gold and copper porphyry deposit Nurkazgan (Cu, Au, Ag, Mo, Se, S), the pyrite-copper-lead-zinc deposits Kusmuryan (Cu, Zn, Pb, Au, Ag, Cd, Se, Te, S) and Akbastau (Cu, Zn, Pb, Au, Ag, Cd, Se, S, Te), the gold-pyrite-copper-lead-zinc deposit Abyz (Pb, Zn, Cu, Au, Ag, S, Se, Te, Cd, In, Hg), the Sayak group of copper skarn deposits (Cu, Mo, Fe, Au, Ag, Co, Bi, Te, Se, Re), the porphyry copper deposits Shatyrykol (Cu, Mo, Au, Ag, Te, Se, U) and Konyrat (Cu, Mo, S, Au, Ag, Re, Se, Te), as well as the concentrators (Balkhash (BC), Karagaily (KC), Nurkazgan (NC)) processing the ores.

The research goal was to deploy a single high-performance system for online monitoring of the chemical composition of salable copper polymetallic ores at the mining and processing operations of the Karagandy and Balkhash industrial sites controlled by Kazakhmys Corporation LLC.

The ores of the deposits listed above are characterized by a broad grade range of the primary and associated elements, a very low (1+ ppm) silver grade, and a large number of process ore grades, i.e. are more challenging in terms of implementing an X-ray fluorescence online monitoring of the ore grade at the process belt conveyors compared to the ore coming from the homogeneous (copper sandstone) deposits Zhezkazgan and Zhaman-Aibat.

Balkhash Concentrator is fed ore from the mines Konyrat, Sayak (Sayak-1 and Tastau), Shatyrykol, Nurkazgan, Akzhal



Fig. 1. RLP-21T at the conveyors 2 and 2A, Balkhash Concentrator. Conveyor gallery with the OMS installed (a) and ore monitoring station RLP-21T (b)  
 Rys. 1. RLP – 21T na przenośnikach 2 i 2A, koncentratorka Balkhash. Galeria przenośników z zainstalowanym OMS (a) i stacją monitorowania rudy RLP – 21T (b)

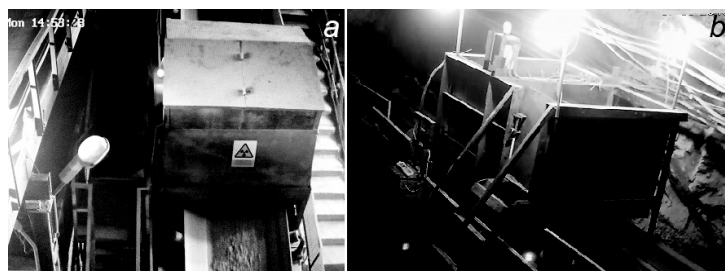


Fig. 2. RLP-21T at the conveyors of Karagaily Concentrator and Nurkazgan mine. Conveyor 4 at Karagaily Concentrator (a) and conveyor at the Nurkazgan mine (b)

Rys. 2. RLP – 21T na przenośnikach w zakładzie wzbogacania Karagaily i kopalni Nurkazgan. Przenośnik 4 w zakładzie Karagaily (a) i przenośnik w kopalni Nurkazgan (b)

and waste slags of Balkhash Copper Smelter. Karagaily Concentrator is fed ore from the mines Akbastau, Kusmuryr, and Abyz. The ore produced by the Nurkazgan underground mine (NM) is processed at NC.

The research task was the most difficult at BC, simultaneously receiving ore from heterogeneous sources, such as deposits, and a virtually homogeneous source, i.e. the slag waste dump at Balkhash Copper Smelter. The copper ores being processed have high (Shatyrkol), medium (Sayak-1, Tastau, Nurkazgan), low (Konyrat), and poor (Akzhal) grades. The waste slags from Balkhash Copper Smelter have a complex elemental composition: Cu — up to 1.15%, Zn — up to 6.0%, Pb — up to 0.70%, Fe — up to 47.0%. Ore grain size: -300 mm. OMS was planned to be installed at the heavy-duty belt conveyors 2 and 2A. Monitored elements: Cu, Pb, Zn, Ag, Cd, Fe.

At KC, one OMS unit was to be installed at the conveyor 4. Ore grain size: -50 mm. Monitored elements: Cu, Pb, Zn, Ag, Cd, Fe. Due to the more favorable ore size distribution, this research task was considered the least difficult.

At NM, one OMS was planned to be installed at the mine's main conveyor. Ore grain size: -300 mm. Monitored elements: Cu, Pb, Zn, Ag, Mo, Fe. Ore properties: a) very low silver grade (the deposit averages 2.9 ppm); b) molybdenum in the ore (110 ppm on average).

Due to the fact that the global non-ferrous metals industry offers no examples of effective online monitoring of the primary and associated ore component grades at an ore size of -300 mm and silver and cadmium grade higher than 1+ ppm using EDXRF OMS, the research problem is of high theoretical and practical relevance.

#### Study area/Materials and methods

A detailed review of the OMS market is available in [1-3]. Due to the fact that effective online monitoring of the primary

and associated ore component grades at ZC-1 and ZC-2 was successfully implemented with the help of EDXRF OMS RLP-21T, for BC, KC, and NM we chose: OMS RLP-21T, X-ray fluorescence ore assay; an X-ray tube with side end radiation emission coupled with combined targets as the excitation source; silicon drift detector (SDD) with an internal collimator as the radiation detector, which, together with a digital signal processor, provides a high energy resolution (130 eV along the 5.9 keV line).

Ensuring the stable operation of the OMS in ores with an extremely low silver, cadmium, and molybdenum grade for X-ray fluorescence is an extremely challenging task in terms of instruments and methods. To achieve the set goals, RLP-21T OMS was configured with more powerful X-ray tubes (a significantly higher pulse loading of the spectrometric tract and, consequently, a higher sensitivity of X-ray fluorescence measurements of silver, cadmium, and molybdenum was achieved); large-area silicon drift detectors (FAST SDD® 25 mm<sup>2</sup> (500 μm/0.5 mil Be/ML) (the detectors are capable of operating at loads up to 1 Gb/s, which is extremely important, because only at such loads RLP-21T OMS can handle ores low in silver, cadmium, and molybdenum); the most advanced (high-speed) electronics; individual collimators of the X-ray tube primary radiation beam tube (clean conveyor belt sections containing zinc should not get into the exposed area of the ore surface).

To reduce the conveyor stopping time for the OMS operability checks, an artificial control sample was added to RLP-21T OMS, which is mounted onto the openings of the X-ray tube and SDD on the side end of the RLP-21T OMS body and held by magnets. Elemental composition of the control sample: Cu – 1.38%, Ag – 12.0 ppm, Zn – 0.05%, Pb – 0.20%, Cd – 1.8 ppm, Fe – 4.65%.

Tab. 1. RLP-21T performance at BC in 2018

Tab. 1. Wydajność RLP – 21T w BC w 2018

Month of 2018	Copper, %				Silver, ppm			
	Underflow	OMS	$\Delta$	$\sigma$ , %	Underflow	OMS	$\Delta$	$\sigma$ , %
5	0.85	0.85	0	0				
6	0.93	0.93	0	0				
7	0.93	0.95	-0.02	2.15				
8	0.92	0.95	-0.03	3.26	5.33	4.51	0.82	15.38
9	0.94	0.95	-0.01	1.06	5.35	4.49	0.86	16.07
10	1.04	1.05	-0.01	0.96	5.53	4.60	0.93	16.82
11	0.98	0.95	0.03	3.06	4.50	4.34	0.16	3.56
12	1.11	1.10	0.01	0.90	5.81	6.01	-0.20	3.44
Year total	0.963	0.966	-0.004	0.39	5.304	4.790	0.514	9.69

Tab. 2. RLP-21T performance at BC in November 2018

Tab. 2. Wyniki RLP – 21T w BC w listopadzie 2018

Mine	Copper, %				Silver, ppm			
	Underflow	OMS	$\Delta$	$\sigma$ , %	Underflow	OMS	$\Delta$	$\sigma$ , %
Shatyrkol	2.34	2.27	0.07	2.99	3.85	3.70	0.15	3.90
Sayak	1.04	1.00	0.04	3.85	5.59	5.37	0.22	3.94
Nurkazgan	1.05	1.02	0.03	2.86	3.25	3.12	0.13	4.00
Konyrat	0.28	0.37	0.01	2.63	2.88	2.77	0.11	3.82
Slag	0.73	0.72	0.02	2.70	7.88	7.57	0.31	3.93
Total	0.98	0.95	0.03	3.06	4.52	4.34	0.18	3.98

Dedicated research was carried out for the purposes of the more complex analytical tasks, as a result of which major upgrades were made to the OMS RLP-21T software. In the software, in particular, the components were upgraded responsible for the following: compensation for the variable profile of ore loading onto the belt conveyor (variable sensor-ore gap); compensation for the matrix effect; automatic selection of conversion equations for each ore supplier to BC, etc. In addition, Aspap Geo LLC had to deviate from its basic principle: since the online monitoring objects are different, ore types are different, ore processing products are different, they had to switch to custom scales. The scale was selected automatically depending on the content of a group of elements (primarily copper and iron).

Prior to installation on the conveyors, all OMS RLP-21T units underwent mandatory bench tests. The research objects were specially prepared ore sample sets from each of the deposits with a known content of the six elements. Each set included three types of samples: powdered samples, size fraction after the roller crusher (-3 mm), size fraction after the jaw crusher (-10 mm). After each OMS was suspended directly at the conveyors, the entire test cycle repeated, but taking into account the limitations on the stopping time of the conveyors for the tests.

At the OMS intended for the BC, KC, and NM conveyors, the ore assay process tested at ZC-1 and ZC-2 [2, 3] was kept with a single measurement exposure of 1 sec. The only difference was that at BC, copper, lead, zinc, and iron grades are averaged based on 20 single measurements, silver and cadmium grades are averaged based on 40 single measurements; at KC and NM, all grades were averaged over five-minute intervals.

## Results and discussion

The main research findings are discussed below.

1. At BC, OMS RLP-21T were installed at the heavy-duty belt conveyors 2 and 2A and put into operation on May 4, 2018 (Figure 1).

The performance of RLP-21T at BC is shown in Table 1 (for silver, the differences in August–October 2018 were due to technical reasons; these were later eliminated, as indicated by the data from November and December). The interpretation of the performance data of RLP-21T in November 2018 is given in Table 2.

In July 2018, the QC testing station at the KKD 1500/180 crusher was shut down. As the data is collected, the grade calculation algorithms for some ore suppliers are being refined.

Attention should be paid to the fact that, over the 11 months of operation, the maximum silver grade in a single train recorded by the OMS was 11.5 ppm (Tastau) and 12.3 ppm (waste slag), and the minimum grade was 1.9 ppm (Kounrad). This is much lower than the silver grade of the ores fed to ZC-1 and ZC-2. Moreover, for the first time in the world practice, an EDXRF OMS was able to detect that low silver grades in ores sized -300 mm.

2. At KC, OMS RLP-21T was put into operation at conveyor 4 on July 27, 2018 (Figure 2a). The silver grades recorded by OMS over one five-minute interval were: 19.6 ppm (maximum) and 6.5 ppm (minimum). This is another evidence of the uniqueness of the methodological approach and numerical models underlying RLP-21T.

3. RLP-21T at the Nurkazgan underground mine. RLP-21T on the main belt conveyor was put into operation on June 14, 2018 (Figure 2b). The grades recorded by OMS over one five-minute interval were: 7.4 ppm (maximum) and 1.1 ppm (minimum) for silver, 0.1105% (maximum) and 0.0008% (minimum) for molybdenum.

## Conclusion

1. A system for online monitoring of the primary (Cu, Pb, Zn) and associated (Ag, Cd, Mo) elements in the copper polymetallic ores processed at Balkhash Concentrator, Karagaily

Concentrator, and the Nurkazgan underground mine was developed, thoroughly tested, and commercialized. The system is based on the EDXRF ore monitoring station RLP-21T.

2. Four ore monitoring stations RLP-21T were put into operation: two at BC (heavy-duty belt conveyors 2 and 2A, monitored elements: Cu, Pb, Zn, Ag, Cd, Fe), one at KC (belt conveyor 4, monitored elements: Cu, Pb, Zn, Ag, Cd, Fe), one at NM (main belt conveyor, monitored elements: Cu, Pb, Zn, Ag, Mo, Fe).

3. For the first time at a large-scale mining project in Kazakhstan (Kazakhmys Corporation LLC), a practical solution was implemented for online monitoring of primary (Cu, Pb,

Zn) and, most importantly, associated (Ag, Cd, Mo) elements at low (1+ ppm) silver and cadmium and (10+ ppm) molybdenum grades and an ore size of -300 mm at process belt conveyors. Thus, the groundwork has been laid for ore grade management according to the content of the primary and associated elements (most importantly, silver).

#### Acknowledgments

The authors express their deep gratitude to Alexander Lezin and Nursultan Takenov at Aspap Geo LLC for their invaluable assistance in the conduct of this study.

#### Literatura – References

1. YEFIMENKO, Sergey et al. Multicomponent online analysis of coarse ore on conveyors of Kazakhmys LLC processing plants. 21th Conference on Environment and Mineral Processing. Ostrava : VŠB-TU Ostrava, 2017, p. 245-249. ISBN 978-80-248-4049-9
2. YEFIMENKO, Sergey et al. Technologies of «on-line» quality control of ores and their processing products at Kazakhmys corporation LLP. Innovative development of resource-saving technologies for mining. Multi-Author ed monograph. Sofia : Publishing House «St. Ivan Rilski», 2018, p. 245-268.
3. NIGMATULIN, Aydar et al. Nuclear-geophysical technologies of «on-line» control of the chemical composition of copper-containing polymetallic ores. Resource and resource-saving technologies in minerals mining and processing. Multi-authored monograph. Petrosani, Romania: UNIVERSITAS Publishing, 2018, p. 162-179.

#### *Monitorowanie online za pomocą fluorescencji rentgenowskiej gruboziarnistej rudy srebra na przenośnikach w zakładzie przeróbki w Kazakhmys Corporation LLC*

*W artykule przeanalizowano proces i aspekty metodologiczne wdrażania zdalnego monitorowania zawartości srebra, kadmu, cynku, ołowiu, molibdenu i żelaza w zakładach wzbogacania Balkhash i Karagaily oraz na głównym przenośniku w kopalni podziemnej Nurkazgan obsługiwanej przez Kazakhmys Corporation LLC. Badania były skomplikowane ze względu na konieczność: a) zapewnienia niezawodnego pomiaru srebra i kadmu w zakresie 1+ ppm, molibdenu w zakresie 10+ ppm, a także miedzi, cynku, ołowiu i żelaza w klasie -300 mm; b) wdrożyć monitorowanie tych pierwiastków (z wyjątkiem molibdenu) w koncentracjach Balkhash, w żużlu odpadowym Huty Miedzi Balkhash, charakteryzującym się bardzo złożoną matrycą elementarną. Opracowano, wdrożono i dokładnie przetestowano modyfikację stacji monitorowania rudy RLP-21T (firmy Aspap Geo LLC, Alma-Ata) do monitorowania online przepływów rudy srebra o niskiej jakości. Do fluorescencji rentgenowskiej zastosowano dyspersyjną metodę rentgenowską. Widma mierzono co sekundę. Zawartość srebra, kadmu i molibdenu obliczono na podstawie 40 pomiarów, a miedzi, cynku, ołowiu i żelaza – na podstawie 20 pomiarów.*

**Słowa kluczowe:** rentgenowska metoda fluorescencji, stacja monitorowania rudy RLP-21T, miedź, srebro, kadm, molibden, monitoring online rudy, przenośniki taśmowe



# Oil Production by Polish Companies in Poland and Abroad

Tadeusz OLKUSKI<sup>1)</sup>, Janusz ZYŚK<sup>1)</sup>, Barbara TORA<sup>2)</sup>,  
Wacław ANDRUSIKIEWICZ<sup>2)</sup>, Adam SZURLEJ<sup>3)</sup>, Kaja JEDLIŃSKA<sup>4)</sup>

<sup>1)</sup> AGH University of Science and Technology, Faculty of Energy and Fuels, Krakow, Poland; email: olkuski@agh.edu.pl

<sup>2)</sup> AGH University of Science and Technology, Faculty of Mining and Geoengineering, Krakow, Poland

<sup>3)</sup> AGH University of Science and Technology, Faculty of Drilling, Oil and Gas, Krakow, Poland

<sup>4)</sup> Graduate of the AGH University of Science and Technology, Faculty of Energy and Fuels, Krakow, Poland

<http://doi.org/10.29227/IM-2020-01-57>

Submission date: 02-02-2020 | Review date: 08-04-2020

## Abstract

The article discusses a very important problem of oil production. Oil, recognized as a major source of economic development, is the main energy source of the modern world. Unfortunately, Poland has limited oil reserves. However, the production, which meets only about 4% of the demand, is carried out. Oil deposits in Poland are found in the Carpathians, in the Carpathian Foredeep, in the Polish Lowlands, and in the Polish Exclusive Economic Zone of the Baltic Sea. Initially, deposits in the Carpathians were of the greatest economic importance, but these are already depleted to a great extent. Currently, oil deposits in the Polish Lowlands are of the greatest economic importance. The largest deposit is BMB (Barnówko-Mostno-Buszewo) near Gorzów Wielkopolski. In total, in Poland oil resources amount to 23 598.46 thousand tons, of which 61.37% accounts for industrial resources (14 482.15 thousand tons). The article presents crude oil resources in Poland by regions, i.e. Polish Lowlands, the Carpathians, the Carpathian Foredeep, and the Polish Exclusive Economic Zone. The resources were divided into anticipated economic, industrial, undeveloped resources and abandoned deposits. In addition, the three Polish companies involved in the extraction of oil, namely PGNiG S.A., the LOTOS Group S.A. and ORLEN Upstream sp. z o.o., were presented. The locations where exploitation is carried out and the volume of oil production in the last few years were discussed.

**Keywords:** crude oil, resources, production

## Introduction

Crude oil, as the basic energy source, has become the subject of interest among global economic powers and the source of income for oil states over the last decades. The exploration, extraction, and processing industries are still growing dynamically despite the fact that numerous commercial banks have decided to cut their investments in fossil fuels. However, the abundance of resources is not always beneficial. The economically and militarily stronger countries put pressure on countries dependent on raw materials, forcing them to sell oil at the lowest possible prices. This often causes conflicts and leads to wars, while the raw material, instead of lifting the country out of crisis, becomes its curse. There are many examples, such as continuous armed conflicts in the Persian Gulf, Africa, or Central America. For this reason, it is extremely important to have own energy resources to avoid dependence on imports, which is always associated with supply interruption and price increase risks.

It is worth adding that at the beginning of the 20th century the province of Galicia in the eastern part of the Austro-Hungarian Empire (now Poland) was the center of the European petroleum industry.

On July 31, 1853, the first kerosene lamp designed by Ignacy Łukasiewicz was used in a hospital in Lviv; a year later, the oil mine in Bóbrka near Krosno was opened. By 1909, approximately 1.9 million tons of crude oil were produced in Borysław and the Galicia was an important region in the world in terms of oil production (Boiko O., Szurlej A. 2018). In 1909, the production in the Galicia amounted to 2.75

million tons. Currently, Poland has limited oil reserves, the reserves-to-production ratio (RPR or R/P) is 23 (BP 2018), which is why most of the crude oil (around 96%) must be imported from abroad. This is not a comfortable situation. Therefore, if large imports cannot be avoided, they must be diversified so as not to rely on raw material from only one supplier. Until recently, Poland imported crude oil only from the east; for example in 2014 the share of crude oil from Russia in supplies to domestic refineries amounted to 91%. In recent years, Poland started to reduce the dependence on supplies from Russia and imported oil from Iraq, Azerbaijan, Kazakhstan, Venezuela, Angola, the United States, the United Arab Emirates, and Nigeria. In 2018, the share of Russian oil decreased to 76% and should further decrease in 2019 in favor of, inter alia, supplies from Saudi Arabia (POPiHN (Polish Organization of Oil Industry and Trade) 2019)). Oil production is also carried out by Polish companies outside the country, mainly in Norway, but also in Lithuania and Canada.

## Oil reserves in Poland

According to the data contained in the balance of mineral resources deposits in Poland as of December 31, 2017 (Bilans 2018), 86 oil fields were documented in Poland, including 29 deposits in the Carpathians, 12 in the Carpathian Foredeep, 43 in the Polish Lowlands, and 2 deposits in the Polish Exclusive Economic Zone. The oil deposits in the Carpathians, the oldest deposits in Poland, are now becoming depleted. The Carpathian crude oil deposits are mainly oil-gas deposits. The

Tab. 1. Oil resources in Poland by region, thousand tons. Source: Own work based on the balance of mineral resources deposits in Poland as of 31.12.2017

Tab. 1. Zasoby ropy naftowej w Polsce z podziałem na regiony, tys. ton

Region	Anticipated economic resources	Industrial resources
Polish Lowlands	15 360.17	8 130.53
The Carpathians	679.05	143.93
The Carpathian Foredeep	355.84	60.83
The Polish Exclusive Economic Zone	6 765.55	6 728.33
TOTAL	23 160.61	14 365.27

Tab. 2. Undeveloped resources, thousand tons. Source: Own work based on the balance of mineral resources deposits in Poland as of 31.12.2017

Tab. 2. Zasoby złóż niezagospodarowanych, tys. ton

Region	Anticipated economic resources	Industrial resources
Polish Lowlands	266.10	116.50
The Carpathian Foredeep	115.93	-
TOTAL	382.03	116.50

Tab. 3. Abandoned oil fields, thousand tons. Source: Own work based on the balance of mineral resources deposits in Poland as of 31.12.2017

Tab. 3. Zasoby złóż ropy naftowej, w których zaniechano eksploatacji, tys. ton

Region	Anticipated economic resources	Industrial resources
Polish Lowlands	49.74	0.38
The Carpathians	1.50	-
The Carpathian Foredeep	4.58	-
TOTAL	55.82	0.38

Tab. 4. Oil and natural gas mines in the PGNiG branches in Sanok and Zielona Góra. Source: Own work based on of the PGNiG report for the year 2017; 2018

Tab. 4. Kopalnie ropy naftowej i gazu ziemnego w oddziałach PGNiG w Sanoku i Zielonej Górze

The number of mines	Sanok	Zielona Góra
Oil mines	5	1
Oil and gas mines	13	7
Natural gas mines	18	10
TOTAL	36	18

Tab. 5. Oil production in Poland by the PGNiG (fractions, thousand tons). Source: Own work based on of the PGNiG report for the year 2017; 2018

Tab. 5. Wydobycie ropy naftowej w Polsce wraz z frakcjami przez PGNiG, tys. ton

Production site	Years				
	2013	2014	2015	2016	2017
The branch in Zielona Góra	766	742	719	719	747
The branch in Sanok	49	47	46	44	40
Total number in Poland	815	789	765	763	787
In Norway	283	418	664	555	470
TOTAL	1098	1207	1429	1318	1257

crude oil density ranges from 0.750 to 0.943 g/cm<sup>3</sup> while the paraffin content is in the range from 3.5 to 7.0%. These are sulfur-free deposits. The Carpathian oil deposits are limited, depending on the size and nature of the structures in which they occur. As a result of many years of exploitation, a significant depletion of resources in this area can be observed. The oils found in the Carpathian Foredeep are classified as light and medium oils (with a density in the range of 0.811–0.846 g/cm<sup>3</sup>). The paraffin and sulfur contents range from 2.32 to 9.37% and from 0.45 to 0.85%, respectively.

Currently, oil fields in the Polish Lowlands are of the greatest economic importance. The paraffin and sulfur contents of these oils are between 4.3–7.4% and slightly above 1%, respectively. Their density is in the range 0.857–0.870 g/cm<sup>3</sup>. These deposits occur in the Permian, Carboniferous, and Cambrian formations. The largest deposit is BMB (Barnówko-Mostono-Buszewo) near Gorzów Wielkopolski. The resources of

this deposit were more than twice that of Poland. In total, in Poland oil resources amount to 23 598.46 thousand tons, of which 61.37% accounts for industrial resources (14 482.15 thousand tons). Table 1 presents oil resources in Poland in currently exploited deposits broken down into regions; tables 2 and 3 present the resources of undeveloped and abandoned deposits, respectively. Industrial resources that can be subject to economically viable and technically possible exploitation have been separated from anticipated economic resources. Crude oil resources also include oil condensate, whose share in total resources is 5.76%.

### Crude oil production

In Poland, the production of hydrocarbons is carried out by the three companies. They include: PGNiG S. A., The LOTOS Group S. A., and Orlen Upstream sp. z o.o. However, it must be clearly emphasized that domestic extraction is not

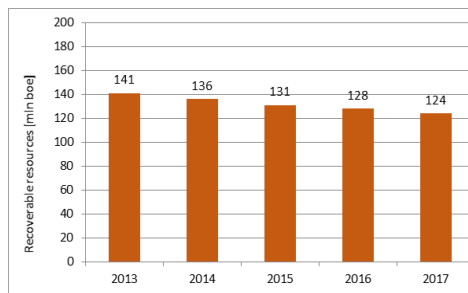


Fig. 1. The total exploitable resources (PGNiG data). Source: Own work based on the PGNiG report for the year 2017; 2018

Rys. 1. Zasoby wydobywalne ropy naftowej udokumentowane przez PGNiG

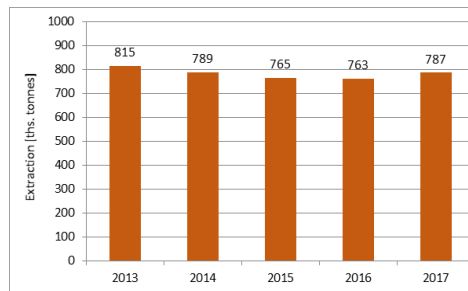


Fig. 2. The production of oil, condensate, and NLG by the PGNiG Group in Poland. Source: Own work based on the PGNiG report for the years 2017; 2018

Rys. 2. Wydobycie ropy naftowej, kondensatu i NLG w Grupie PGNiG w Polsce

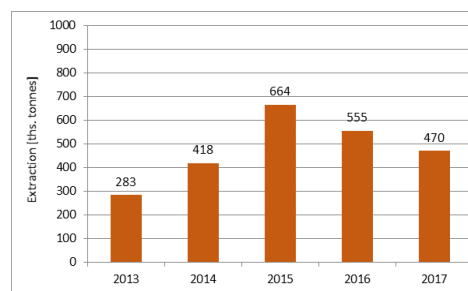


Fig. 3. The production of oil, condensate, and NLG by the PGNiG Group in Norway. Source: Own work based on the PGNiG report for the year 2017; 2018

Rys. 3. Wydobycie ropy naftowej, kondensatu i NLG w Grupie PGNiG w Norwegii

able to meet domestic needs and the vast majority of crude oil must be imported from abroad.

#### PGNiG S. A.

PGNiG is one of the largest companies specializing in oil production in the country, in 2017 its production amounted to almost 800 thousand tons, which gives about 80% share in the domestic extraction. The company has even larger share, about 90%, in the production of natural gas. At the end of December 2017, PGNiG held 58 licenses for exploration and production of crude oil and natural gas (The PGNiG report for the year 2017; 2018). Table 4 shows the number of oil and gas mines owned by the PGNiG, while Table 5 shows the extraction of crude oil (including fractions) in Poland by this company.

PGNiG UN holds exploration and production licenses on the Norwegian Continental Shelf located in the Norwegian, North, and Barents Seas. The cooperation with partners in Norway involves the extraction of hydrocarbons from the Skarv, Morvin, Vilje, Vale, and Gina Krog fields, and the development of Ærfugl (formerly Snadd) and Skogul (former Storklakken) fields. The remaining licenses are exploration li-

censes. The most important is the Skarv field. In 2017, PGNiG UN extracted 470 thousand tons of crude oil (all fractions, per ton of oil equivalent) and 548 million m<sup>3</sup> of natural gas from the Skarv, Morvin, Vilje, Vale, and Gina Krog deposits. In 2017, an increase from 78 million boe to 83 million boe in the documented resources in Norway has been reported by the PGNiG UN (The PGNiG report for the year 2017; 2018).

Crude oil extracted in Norway is sold directly from deposits to Shell International Trading and Shipping Company Ltd (from Skarv, Vilje, Vale, and Gina Krog fields) and TOTSA Total Oil Trading SA (from the Morvin field). In the case of all fields, with the exception of Vilje, natural gas is also extracted along with oil; it is sent via gas pipeline to Germany, where it received by the PST. The main sales markets are Norway, Germany, and the United Kingdom.

PGNiG also conducts exploratory activities in Pakistan under a license for the exploration and exploitation of hydrocarbons in the Kirthar area, awarded on 18 May 2005 by the Pakistani government. Exploration activities in the Kirthar block are carried out jointly with Pakistan Petroleum Ltd. (PPL), according to the division of shares and costs (PGNiG (operator) – 70%, PPL – 30%). Two natural gas deposits, Reh-





Fig. 4. The areas covered by exploration and production licenses in the sea and land areas of Poland. Source: <http://www.lotosp.pl/repository/49397/pl/>  
Rys. 4. Obszary objęte koncesjami poszukiwawczymi i wydobywczymi na obszarach morskich RP oraz na lądzie

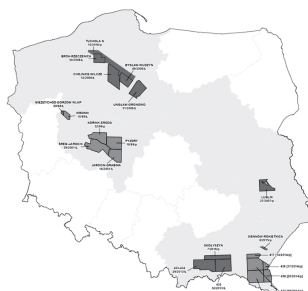


Fig. 5. The area of prospecting and exploration activities in Poland. Source: Projekt 2019  
Rys. 5. Obszar działalności poszukiwawczo-wydobywczej w Polsce

man and Rizq, have been discovered in the course of previous exploration activities within the concession.

In addition, the PGNiG also conducted exploratory activities in Libya and Iran, but, due to the unstable political situation in these countries, these works were limited.

The PGNiG S.A. conducts intensive research work on the documentation of hydrocarbon resources. In the case of crude oil, the volume of documented exploitable resources (reserves) is gradually decreasing each year. And so, in 2013 they amounted to 141 million boe, and in 2017 only 124 million boe (Fig. 1).

When it comes to oil production, it is highly variable over the last five years. While the production in Poland is relatively stable, ranging from 763 thousand tons in 2016 to 815 thousand tons in 2013 (Fig. 2), the production of Norwegian deposits is highly variable. In 2013, it amounted to PLN 282 thousand tons and in just two years has increased to 664 thousand tons. In the next two years, however, it decreased to 555 thousand tons in 2016 and 470 thousand tons in 2017 (Fig. 3). Nevertheless, the Norwegian oil fields constitute an important element in the production of oil by PGNiG.

Taking into account the above data, it should be stated that the PGNiG S.A. is the most important Polish company involved in the exploration and extraction of both crude oil and natural gas.

#### **The LOTOS Group S. A.**

The LOTOS S.A. Group is another Polish entity involved in hydrocarbon extraction. The LOTOS Group consists of 17 companies and capital groups operating not only in Poland, but also in Norway and Lithuania. The group is focused on the exploration, extraction, production, trade, and services. It is the owner or co-owner of 33 sea licenses and 10 land concessions. It extracts oil in the Polish Exclusive Economic Zone,

on the Norwegian Continental Shelf, in Poland, and Lithuania. In 2017, the total potential of the LOTOS 2P reserves amounted to 88.4 million barrels, while the output reached the level of 8.1 million barrels (Jednostkowy... 2018). To clarify, it is worth mentioning that, according to the international classification of resources (H-C) PRMS, 2P are probable reserves, i.e. determined on the basis of indirect, e.g. geophysical, analysis. They determine the size of the hydrocarbon trap but do not indicate the amount of resources.

In 2017, the LOTOS Upstream was established, which in December 2017 acquired its foreign assets from LOTOS Petrobaltic, i.e. LOTOS Norge and Geonafra. The aim of LOTOS Upstream was to manage international exploration and production activities. LOTOS Petrobaltic S.A. holds licenses for extracting crude oil and accompanying natural gas from the B3 field as well as a concession for oil extraction and co-occurring natural gas from the B8 field (B8 Sp. z o.o. BALTIC SKA). The company also holds 3 licenses for prospecting and exploration of crude oil and natural gas deposits and gas production from fields in the sea areas of Poland with a total area of 3177 km<sup>2</sup> (LOTOS Petrobaltic Koncesje 2018).

Fig. 4. presents the areas covered by exploration and production licenses.

The newest land license is the prospecting and exploration license for oil and gas deposits in the Młynary area in the Warmian-Masurian Voivodeship. This was the first land license acquired by LOTOS Petrobaltic in September 2016.

LOTOS Exploration & Production Norge (LOTOS Norge 2018) is involved in hydrocarbon exploration and production on the Norwegian Continental Shelf. It belongs to the LOTOS Upstream Capital Group, in which it is responsible for implementing the strategy of the LOTOS extraction segment in the North Sea and the Norwegian Sea. At the end of 2017, LOTOS Norge held 26 licenses for prospecting, exploration

Tab. 6. Oil production by the LOTOS S.A. Group in Norway, Poland, and Lithuania, million boe. Source: Own work based on LOTOS S. A. 2019

Tab. 6. Wydobycie ropy naftowej przez Grupę LOTOS S.A. w Norwegii, w Polsce i na Litwie, mln boe

Production site	Year	
	2017	2018
Norway	6.2	5.5
Poland	1.8	1.6
Lithuania	0.4	0.3



Fig. 6. The main areas of activity of ORLEN Upstream in Canada. Source: Projekty 2019

Rys. 6. Główne obszary działalności ORLEN Upstrim w Kanadzie

and production of hydrocarbon deposits on the Norwegian Continental Shelf. Later on, the Norwegian authorities offered two new licenses, so their total number increased to 28. The output of LOTOS from Norwegian deposits in 2017 was at an average level of 17.0 thousand boe/day, which is 74% of the total volume of the segment. As at the end of 2017, the 2P reserves of Baltic deposits amounted to 39.3 million boe (including: 2.9 million tons of oil and 2.7 billion m<sup>3</sup> of natural gas), which accounts for 45% of the total reserves (LOTOS Norge 2018). Key assets under the concessions held include: The Heimdal area, purchased in December 2013, including Atla (LEPN share: 20%), Skirne (30% share), Vale (share 25.8%), Heimdal (5% share) and the remaining fields in north from Heimdal: FriggGammaDelta, Langfjellet, Rind, Fulla, and Froy with an average share of the LOTOS Group at 10%. In 2017, in cooperation with the operator (AkerBP), LOTOS conducted an analysis of the optimal variant of development of deposits under the so-called Greater Heimdal project. The resource potential of the abovementioned deposits is about 34 million boe (LOTOS share).

The second is the Sleipner area purchased in December 2015 including the Sleipner Vest and Sleipner East fields, with the Gungne and Loke satellite fields. The exploitable resources of the Sleipner fields in the 2P category amount to 15,5 million boe as of 31.12.2017. The second deposit is the Utgard field, which is in the development phase, operated by Statoil. The exploitable resources of the Utgard deposit are 8.1 million boe (LOTOS share). The commercial production in the field is planned for the beginning of 2020. In the first five years of operation, an annual production volume of 4.000 boe/day is expected (the LOTOS share). In addition, LOTOS holds a 20% interest in the Yme field, which is being prepared for re-use and launch of oil production. The exploitable resources of the Yme field are 12.9 million bbl of crude oil (the LOTOS share). The commercial production in the field is scheduled for the first half of 2020 (LOTOS Norge 2018).

In addition, the LOTOS Group S.A. extracts oil in Lithuania. The AB LOTOS Geonafta, a company in the LOTOS Group and a daughter company to LOTOS Upstream, has carried out activities in Lithuania since 2000. As of today, crude oil is produced in land-based deposits, the potential of which has been greatly reduced over the years. It is necessary to conduct extraction at sea, which at the same time will increase Lithuania's energy security. Table 6 presents oil production by the LOTOS Group S.A. in Norway, Poland, and Lithuania in the last two years.

LOTOS strives to increase its activity in this country. The attention is focused on the possibility of exploration and extraction of oil from deposits located in Lithuanian territorial waters.

#### **Orlen Upstream sp. z o.o.**

The Orlen Upstream sp. z o.o. operates both in Poland and Canada. In total, in Poland and Canada, it has 153 million boe of reserves (Raport Zintegrowany2017). In Poland, the ORLEN Group is focused on exploration and production activities in the Greater Poland, Pomeranian, Podkarpackie, and Lesser Poland voivodships, the Lublin region, and Mazovia. At the end of 2017, the company's 2P reserves in Poland amounted to 11 million boe, while the production in the second quarter of 2018 reached 900 boe per day. The upstream segment holds 13 licenses for prospecting, exploration and production of hydrocarbon deposits in Poland; the next 13 licenses are held jointly with business partners. Formally, 8 concessions were granted by the Ministry of the Environment to ORLEN Upstream, while the next 5 were granted to FX Energy Poland, acquired by the ORLEN Group and integrated into the company's structures in 2015 (Projekty 2019).

The Orlen Upstream sp. z o.o. also cooperates with PGNiG S.A. on the Sieraków, Płotki, Bieszczady, and Warszawa Południe projects. The areas of activity of the Orlen Group in Poland are shown in Fig. 5.

In North America, the Orlen Group has been operating since 2013. At the end of 2017, 2P reserves in Canada amounted to 141 million boe, while the average production in the second quarter of 2018 remained at 17 100 boe /d. The key Canadian assets of the group are located within the province of Alberta, in the following regions: Kakwa (Montney formation), Ferrier Strachan (Cardium formation), Lochend (Cardium formation), Pouce Coupe (Montney formation), and Kaybob (Dunvegan formation). The most important assets of Orlen Upstream in Canada (Projekty 2019) are described below:

Ferrier Strachan – one of the two main areas of activity of ORLEN Upstream Canada, very perspective for the development of coastal sandstones of the Cretaceous Cardium formation.

An interesting fact is a high variability of the extracted mineral – ranging from gas with a small amount of oil to crude oil with a relatively small amount of gas.

Kakwa – is one of the most promising regions in the Alberta region. The activities are carried out in the Lower Triassic Montney Formation. The main storage medium in the Kakwa region is gas with a high content of condensate.

Kaybob – the main reason for drillings in this region are the sandy delta deposits that were deposited during the Cretaceous period, forming part of the Dunvegan formation. They are distinguished by very good reservoir parameters and a high share of oil in the volume of extraction.

Lochend – An area just a few kilometers from the suburbs of Calgary is the foundation on which the ORLEN Upstream Canada project portfolio was built. In the area of several dozen square kilometers, the Upper Cretaceous Cardium Formation is perspective in at least two reservoir levels, from which light oil and gas are extracted.

Pouce Coupe – is one of the first three areas of activity of the ORLEN Upstream Canada. The extraction is carried

out from mudstones of the Montney Triassic Formation. The main storage medium in the Pouce Coupe region is gas with a low liquid hydrocarbon content.

Stoney Creek – Stoney Creek in New Brunswick is one of the oldest discovered oil fields in this part of Canada. It was documented in 1909 within the assemblage of sandstones of the Dawson Settlement Member of the Carboniferous Albert Formation.

Goldboro LNG – ORLEN Upstream Canada has a 7.4% percent stake in the Pieridae Energy, which is responsible for the construction of the LNG terminal on the east coast of Canada. Preparatory works are underway on the basis of which an investment decision on the further direction of the project will be made.

Fig. 6 shows the main areas of ORLEN Upstream activity in Canada.

### Conclusions

According to the Energy Policy of Poland until 2040 (PEP2040) (Projekt 2018), the demand for fuels in Poland will increase in the coming years, although this will be moderate due to the change in the structure of energy demand in the economy. When determining the future demand for oil in the transport sector, the use of alternative fuels, electricity, and biocomponents in transport must be taken into account. The draft states that the refining companies should focus on the production and trade of fuels, while the state is to take full control over the key assets of the energy security in the fields of pipeline transport and storage of oil and fuels. To maintain their position in the international market, the two largest entities in the fuel sector, i.e. ORLEN S.A. and LOTOS S.A. will be merged. Oil and gas exploratory projects will also be carried out, but the production will not be increased.

## Literatura – References

1. Boiko O., Szurlej A., 2018 – Porównanie bezpieczeństwa energetycznego Polski i Ukrainy (Comparison of the energy security of Poland and Ukraine) (in Polish). Bulletin of the Mineral and Energy Economy Research Institute of the Polish Academy of Sciences, Kraków, No. 104, pp. 19–30.
2. BP 2018: BP Statistical Review of World Energy. [Online] [www.bp.com](http://www.bp.com) [Accessed on: 02.08.2018].
3. <http://www.lotost.pl/repository/49397/pl/>; accessed on: 25.03.2019
4. Jednostkowy 2018 – Jednostkowy raport roczny Grupy LOTOS S.A. (Non-consolidated Annual Report), p.257
5. LOTOS Norge 2018 – ([http://www.lotost.pl/164/grupa\\_kapitalowa/nasze\\_spolki/lotost\\_exploration\\_\\_production\\_norge](http://www.lotost.pl/164/grupa_kapitalowa/nasze_spolki/lotost_exploration__production_norge)); accessed on: 25.03.2019
6. LOTOS Petrobaltic Koncesje 2018 - ([http://www.lotost.pl/350/grupa\\_kapitalowa/nasze\\_spolki/lotost\\_petrobaltic/koncesje](http://www.lotost.pl/350/grupa_kapitalowa/nasze_spolki/lotost_petrobaltic/koncesje)); accessed on: 25.03.2019
7. LOTOS S.A. – ([www.lotost.pl](http://www.lotost.pl)); accessed on 17.04.2019
8. POPiHN (Polish Organization of Oil Industry and Trade) 2019 – <http://www.popihn.pl/>; accessed on 20.04.2019
9. Projekt 2018 – Polityka energetyczna Polski do 2040 roku – Projekt (The Energy Policy of Poland until 2040 – a draft version). The Ministry Of Energy. Warsaw 2018.
10. Projekty 2019 – (<http://www.ornenupstream.pl/PL/Projekty/dzialalnoscwpolsce/Strony/default.aspx>); accessed on: 17.04.2019
11. Raport Zintegrowany 2017 – Raport Zintegrowany Grupy Orlen 2017 (<https://raportzintegrowany2017.ornen.pl/pl-ornen-2017-2017>) accessed on: 17.04.2019
12. The balance of mineral resources deposits in Poland as of 31.12.2017. The Polish Geological Institute – National Research Institute Warsaw 2018.
13. The PGNiG report for the years 2017–2018 – (<http://pgnig2017.pl/dzialalnosc-w-2017-roku/poszuki-i-wydobycie/dzialalnosc-w-2017-r/>); accessed on: 5.04.2019.

## *Pozyskiwanie ropy naftowej przez polskie firmy wydobywcze na terenie kraju i poza jego granicami*

*W artykule poruszono bardzo ważny problem jakim jest pozyskiwanie ropy naftowej. Ropa jest podstawowym surowcem energetycznym w świecie i źródłem tak spektakularnego rozwoju gospodarczego jaki obserwujemy od czasu jest odkrycia. Polska jest niestety krajem ubogim w zasoby tego surowca, niemniej jednak prowadzone jest wydobywanie, które zaspokaja zaledwie około 4% potrzeb. Zasoby ropy naftowej w Polsce znajdują się w Karpatach, w zapadlisku przedkarpackim, na Niżu Polskim oraz w polskiej strefie ekonomicznej Bałtyku. Początkowo największe znaczenie gospodarcze miały złoża w Karpatach, ale uległy one już w znacznym stopniu wyczerpaniu. Obecnie największe znaczenie mają złoża ropy występujące na Niżu Polskim. Największym złożem jest BMB (skrót od nazw miejscowości Barnówko-Mostno-Buszewo) koło Gorzowa Wielkopolskiego. Ogółem w Polsce zasoby ropy naftowej wynoszą 23 598,46 tys. ton, w tym zasoby przemysłowe 14 482,15 tys. ton, co stanowi 61,37% zasobów ogółem. W artykule przedstawiono zasoby ropy naftowej w Polsce z podziałem na regiony, tzn. Niż Polski, Karpaty, Zapadlisko przedkarpackie, oraz polską strefę ekonomiczną Bałtyku.*

*Zasoby podzielono na zasoby bilansowe, przemysłowe, niezagospodarowane oraz złoża, w których zaniechano eksploatacji. Przedstawiono również trzy polskie firmy, które zajmują się wydobywaniem tego surowca, czyli PGNiG S.A., Grupę LOTOS S.A. oraz ORLEN Upstream sp. z o.o. Pokazano miejsca, w których prowadzona jest eksploatacja oraz jej wielkość w kilku ostatnich latach.*

**Słowa kluczowe:** ropa naftowa, zasoby, wydobywanie





# An Investigation on the Turbidity Removal from Natural Stone Processing Plant Wastewater by Flocculation

Savas OZUN<sup>1)</sup>, Dilan AGIRTMIS ULUS<sup>2)</sup>

<sup>1)</sup> Suleyman Demirel University, Faculty of Engineering, Department of Mining Engineering, E7 Building, West Campus, Isparta, Turkey; email: savasozun@sdu.edu.tr

<sup>2)</sup> Suleyman Demirel University, Faculty of Engineering, Department of Mining Engineering, E7 Building, West Campus, Isparta, Turkey; email: dilanagrtrms@hotmail.com

<http://doi.org/10.29227/IM-2020-01-58>

Submission date: 14-01-2020 | Review date: 09-04-2020

## Abstract

*This study aimed to determine the effects of three different high molecular weight (HMW) flocculants (anionic, cationic and non-ionic flocculants) on the fine particles removal from natural stone (foid-bearing rock) processing plant wastewater at alkaline pH conditions. The test results were investigated in terms of turbidity values depending on pH of the medium, flocculant concentration and time (0–60 min). According to the results obtained, the turbidity values of the wastewater in the absence of the flocculants were pH dependent and decreased as the pH increased, resulted in the minimum turbidity values at pH 12. In the presence of the flocculants, the pH depended turbidity removal efficiencies varied with flocculant type, flocculant concentration and time. The best results were obtained at highly alkaline pH values (pH 12) with the turbidity removal efficiency of  $\leq 99\%$  in the presence of non-ionic flocculant. In the case of anionic and cationic flocculants, the minimum turbidity values were also obtained at pH 12 with turbidity removal efficiencies over 90%.*

**Keywords:** natural stone processing plant wastewater, turbidity removal, flocculant addition, flocculant concentration, pH, time

## Introduction

Water has vital importance in almost every step of the mining industry, starting from the pre-mining operations to an obtaining salable concentrate after the ore preparation/mineral processing operations.

In general, it is used for machine cooling (cutting parts), removing the ore bodies from the surface of the excavation/cutting processes in open pit mining, underground mining and natural stone processing (sizing of natural stones such as marble and granite) and applied as water sprays for suppressing dust (Ediz vd. 2001; Mavis, 2003; Ağırtaş, 2017). The wastewater can have 2–10% solid content (by Wt) which approximately contain 25–40% (by Wt) of the products formed during mining operations (Wright et al., 1976; Ashton et al., 2001; Thomashausen et al., 2018). Thus, the water used in the mining/processing plants for different purposes contains solid (mostly mineral particles) having with a wide size distribution, from millimeter to microns, depending on the method applied.

In the case of the wastewater is recirculated to the system without solid/liquid separation, it will negatively affect the life and cutting performance of the cutting units as well as causing clogging of water transfer pumps and pipes etc. (Acar, 2001; Celik et al., 2008). As there is a high density difference between mineral particles and water in the wastewater of the natural stone processing plants, the solid/liquid separation processes are usually applied by sedimentation method (İpekoglu, 1997; Svarovsky, 2000). In the sedimentation process, the settling rate of the mineral particles is mostly affected by the density and size of the particles. The bigger the size and the higher the density of the mineral particles the faster the settling velocity (Bradby, 1993; Table 1). The solid particles

in the size range of 1 nm–0.1 nm, which are called colloids, cannot be removed by classical physical treatment methods because they cannot settle easily by themselves (Öztürk et al. 2005). The other factors affecting the settling velocity are the shape, the charge of the particles and pH of the medium etc. (Leschonski, 1993; Ersoy, 2005; Tripathy et al., 2006; Tasdemir et al., 2012; Watanabe, 2017) and can be increased by the use of natural/synthetic flocculants. In addition, the hardness of the process and recycle water, the presence of high-valence cations like  $\text{Ca}^{2+}$  and  $\text{Mg}^{2+}$ , may aid coagulation by reducing the magnitude of potential and/or neutralizing the surface charge of the mineral particles. Therefore, their presence may promote flocculation efficiency with the use of lower flocculant concentrations (Hosten et al., 2013; Wang et al., 2009).

The most of the researches on the removal of fines in natural stone processing plant wastewaters have been done on the effluents of processing plants which only contain marble or travertine fines (Ersoy, 2005; Tasdemir et al., 2012; Bayraktar et al., 1996; Sabah et al., 2012; Arslan et al., 2005). In this regard, this study aimed to determine the effect of the presence and the concentration of three different flocculants with different charging mechanisms (anionic, cationic and non-ionic flocculants) depending on pH and time on flocculation behavior of foid-bearing rock fines; containing silicates, clays and iron-bearing minerals etc., in processing plant wastewater.

## Materials and methods

The wastewater sample was obtained and collected in sealed pet bottles from a wastewater pond of a foid-bearing rock processing plant (FRPP) located near Isparta, Turkey. The schematic presentation of the processing plant and the particle size distribution of the sample are given in Fig. 1.

Tab. 1. Classification of particle sizes (Bratby, 1993) [\*mineral particles having specific gravity of 2.65]

Tab. 1. Klasyfikacja wielkości cząstek (Bratby, 1993) [\* cząstki mineralne o ciężarze właściwym 2,65]

Particle size (mm)	Classification	Examples	Time required to settle 100 mm*
10	Coarse dispersion (visible to naked eye)	Gravel, coarse sand, mineral substances, precipitated and flocculated particles, silt, macroplankton	0.1 s
1			1 s
10 <sup>-1</sup>			13 s
10 <sup>-2</sup>	Fine particulate dispersion (visible under microscope)	Mineral substances, precipitated and flocculated particles, silt, bacteria, plankton and other organisms	11 min
10 <sup>-3</sup>			20 hours
10 <sup>-4</sup>			80 days
10 <sup>-5</sup>	Colloidal dispersion (submicroscopic)	Mineral substances, hydrolysis and precipitated products, macromolecules, biopolymers,	1 years
10 <sup>-6</sup>			20 years

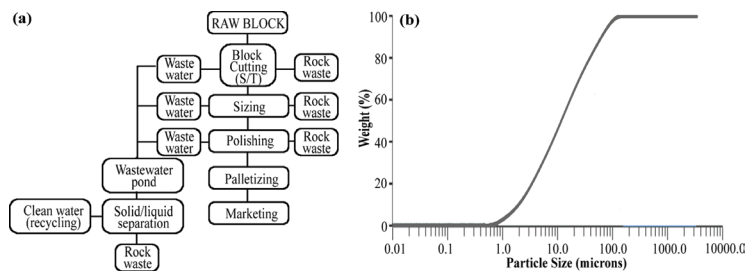


Fig. 1. (a) Schematic presentation of the FRPP and (b) particle size distribution of the sample  
Rys. 1. (a) Schematyczne przedstawienie FRPP i (b) rozkład wielkości cząstek w próbce

Tab. 2. XRF analysis of particles in wastewater

Tab. 2. Analiza XRF cząstek w ściekach

Content	%	Content	%
SiO <sub>2</sub>	58.14	Fe <sub>2</sub> O <sub>3</sub>	4.54
Al <sub>2</sub> O <sub>3</sub>	18.38	CaO	3.99
Na <sub>2</sub> O	6.32	MgO	0.78
K <sub>2</sub> O	6.02	SO <sub>3</sub>	0.19

According to the results given in Figure 1(b), the wastewater contains mineral particles having sizes -3 mm (d<sub>80</sub>: -0.040 mm) with a pulp density of 1.25 ± 0.15% (by Wt).

According to the results of the mineralogical analysis, the sample contains approximately 45% nepheline, 25% orthoclase, 15% oligoclase, 8% amphibole, 2% pyroxene, 5% opaque minerals mostly composed of magnetite and ilmenite. The rock also has illite and kaolin clay formations, which are formed by the alteration of nepheline and orthoclase. The chemical analysis of the minerals in wastewater is given in Table 2.

The HMW-flocculants having high bridging ability; anionic (Cyfloc A-150) and non-ionic (N-100) flocculants were obtained from Cytec Inc., and cationic flocculant (425Ca) was obtained from ECS Chemicals. The stock solutions (0.1 g/100 ml) of each flocculant were diluted to desired flocculant concentrations with appropriate amounts of distilled water before the experimental analysis. After the dilute flocculant addition, the pulp (wastewater) was conditioned in previously determined optimum parameters: 5 min at a stirring speed of 500 rpm. Then the sample was transferred in the 500-ml graduated cylinder, shaken 10 times gently to prevent breaking of the flocs, and then left to stand still. The turbidity measurements of the wastewater were carried out by Hanna HI 93703 por-

table turbidity meter with a sensitivity of ±0.5 FTU between 0.00 and 1000 NTU (Nephelometric Turbidity Unit).

## Results and discussion

### Turbidity of fooid-bearing rock processing plant wastewater

In this research study it was aimed to determine the effect of different flocculants on turbidity removal from FRPP wastewater at three different alkaline pH conditions. Even so, the turbidity values of wastewater were also determined depending on pH (pH 8–12) and time (0–120 min) in order to make the results more comparable and the results are given in Figure 2.

In Figure 2, the results show that the initial turbidity value of as-received wastewater at natural pH value (pH 8.5 ± 0.5) was about 760 NTU after the mixing process. However, as the high settling velocity of the coarse particles in the wastewater a turbulent flow conditions created leading higher turbidity value of 1000 NTU a min after mixing process. The turbidity values remained constant at 1000 NTU between 1 and 20 min due to slow settling rate of very fine particles and then gradually decreased to 445 NTU after 60 min and 120 NTU with a turbidity removal efficiency of 88% after 120 min. The turbidity values at pH 8 displayed similarities with the results of the as-received wastewater sample at the original pH condition.

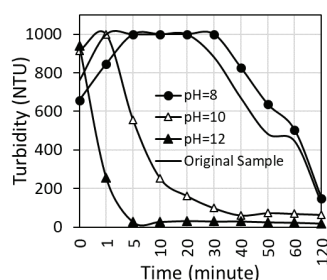


Fig. 2. Turbidity vs time profiles of FRPP wastewater  
Rys. 2. Profile zmętnienia w funkcji czasu FRPP

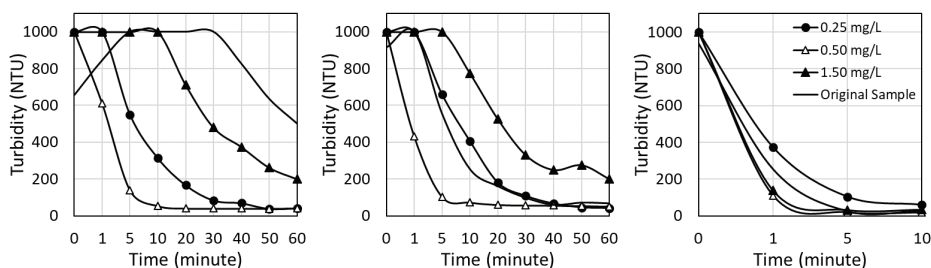


Fig. 3. Turbidity vs time profiles of wastewater with anionic flocculant at; (a) pH 8, (b) pH 10 and (c) pH 12  
Rys. 3. Profile zmętnienia w funkcji czasu, dodatek flokulantu anionowego; (a) pH = 8, (b) pH = 10 i (c) pH = 12

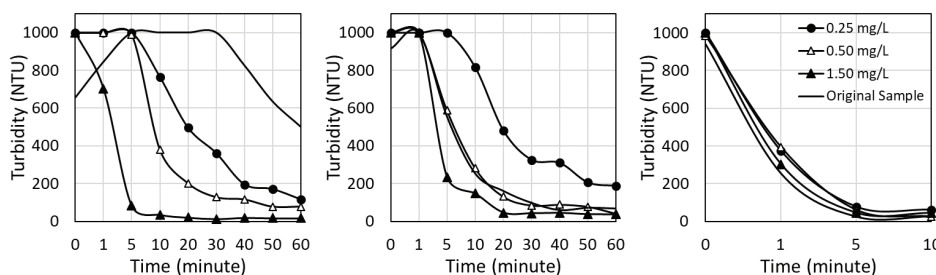


Fig. 4. Turbidity vs time profiles of wastewater with cationic flocculant at; (a) pH 8, (b) pH 10 and (c) pH 12  
Rys. 4. Profile zmętnienia w funkcji czasu, dodatek flokulantu kationowego; (a) pH = 8, (b) pH = 10 i (c) pH = 12

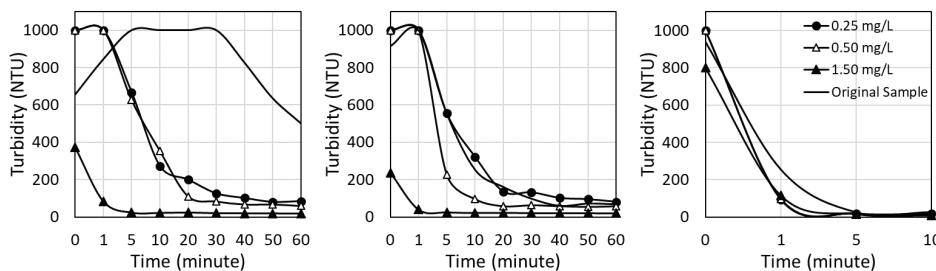


Fig. 5. Turbidity vs time profiles of wastewater with non-ionic flocculant at; (a) pH 8, (b) pH 10 and (c) pH 12  
Rys. 5. Profile zmętnienia w funkcji czasu, dodatek flokulantu niejonowego; (a) pH = 8, (b) pH = 10 i (c) pH = 12

As the pH increased to higher alkaline pH conditions, at pH 10, the turbidity values decreased rapidly from initial turbidity of over 900 NTU to below 250 NTU after 10 min and decreased gradually to about 60 NTU at the end of 40 min. When the zeta potential values of the minerals in wastewater are taken into account, as they have been reported to have highly negative values at alkaline pH conditions (Kolarik and Priestly, 1995; Nduwa-Mushidi et al., 2017; Ozun et al., 2019a), it is expected that the mineral particles will repel each other, leading to higher turbidity values. However, the mineral

particles aggregated and settled rapidly over pH 9 due to the increasing effectiveness of the polyvalent ions ( $\text{Ca}^{2+}$  and  $\text{Mg}^{2+}$ ) in wastewater on turbidity removal (Clark et al., 1968; Ozkan et al., 2009).

#### **Turbidity of foiled-bearing rock processing plant wastewater with flocculants**

In Figure 3-5, the effects of HMW flocculants (anionic, cationic, non-ionic) on turbidity removal from the FRPP wastewater were given as graphical presentation depending



on the flocculant concentration (0.25–1.50 mg/L) and time (0–60 min) at three alkaline pH values (pH 8–12). According to the results obtained in the presence of each flocculant, the turbidity values varied depending on concentration, pH value and time.

In Figure 3, the results show that the effectiveness of anionic flocculant on turbidity removal from wastewater increased with increasing flocculant concentration up to 0.50 mg/L. In the presence of 0.25 mg/L flocculant concentration, compared to those without flocculant, the turbidity values at pH 8 decreased rapidly from initial turbidity value of 1000 NTU to about 550 NTU with a turbidity removal efficiency of 45% after 5 min, and decreased to 50 NTU after 60 min. With increasing flocculant concentration (0.50 mg/L), the turbidity of the supernatant decreased more resulting in lower turbidity values of <150 NTU with a turbidity removal efficiency of >85% after 5 min and about 50 NTU after 10 min.

The similar trend with pH 8 was obtained at pH 10 with each flocculant concentration. The test results with 1.50 mg/L flocculant concentration exhibited much higher turbidity values than those with lower flocculant concentrations (0.25–0.50 mg/L). In the case of turbidity removal at pH 12, as the mineral particles in wastewater displayed a stable behavior in the pulp because of they had highly negative (–) zeta potential values at alkaline pH values, a strong electrostatic repulsion between the anionic flocculant and the mineral particles was expected. However, a rapid settlement of the mineral particles was observed resulting in the minimum turbidity values <100 NTU after 5 min of flocculation. The reason might be interaction of the oppositely charged high-valence ions ( $\text{Ca}^{2+}$  and  $\text{Mg}^{2+}$ ) with mineral particles in the plant wastewater causing charge neutralization on their surfaces (Ozun et al., 2019a).

In the presence of cationic flocculant (Figure 4), considering that all mineral particles had negative zeta potential values for the given pH value, the turbidity values at pH 8 decreased because of an electrostatic attraction occurred between mineral particles and oppositely charged flocculant species.

The results also show that the turbidity values in the presence of 0.25 mg/L and 0.50 exhibited higher turbidity values compared to those in the presence of 1.50 mg/L flocculant concentration having 92% turbidity removal efficiency after 5 min. However, with increasing pH, the turbidity removal efficiencies at pH 10 and pH 12 were much lower contrary to expectations even though mineral particles and flocculant had oppositely charged. Because of the charge neutralization effect of mono and polyvalent ions present in the wastewater, the mineral particles exhibited unstable behavior leading insufficient interaction with the oppositely charged flocculant species.

In the case of turbidity removal with non-ionic flocculant, the results given in Figure 5 show that the effect of

non-ionic flocculant on turbidity removal from wastewater especially at pH 8, which is the closest pH value to the natural pH of the wastewater, was superior compared to those with ionic flocculants. The results also showed that at any pH values tested, the turbidity values obtained with 0.25 mg/L and 0.50 mg/L of non-ionic flocculant concentrations displayed similarities with each other. The turbidity values for the given flocculant concentrations decreased from the initial turbidity of 1000 NTU to >180 NTU after 20 min of flocculation. However, the best turbidity removal efficiencies were obtained with 1.50 mg/L non-ionic flocculant concentration at any pH conditions tested. After 1 min of flocculation, the initial turbidity value of <400 NTU decreased down to <100 NTU at pH 8 and decreased down to 40 NTU at pH 10. The turbidity values then decreased less than to 25 NTU after 5 min of flocculation for both pH conditions. In the case of flocculation at pH 12, the turbidity values obtained with each flocculant concentration were lower than the turbidity values of the original sample.

The turbidity values started to decrease from the initial turbidity value of about 1000 NTU to  $\leq 100$  NTU after 1 min, decreased to <5 NTU with a turbidity removal efficiency of  $\leq 99\%$  after 60 min.

## Conclusion

According to the results obtained with experimental analyses, the settling velocities of mineral particles in FRPP wastewater varied depending on pH conditions, flocculant type, flocculant concentration and time. The settling velocities increased with increasing flocculant concentration, resulting in the minimum turbidity values at certain circumstances.

The turbidity values obtained with non-ionic flocculant at any pH values tested were found to be superior compared to those with anionic and cationic flocculants. The best results with each flocculant were obtained at highly alkaline pH conditions (pH 12) due to the effect of the polyvalent  $\text{Ca}^{2+}$  and  $\text{Mg}^{2+}$  ions present in wastewater and the high concentration of sodium hydroxide used to adjust pH conditions. Their presence might be one of the reasons which promoted the flocculation behaviour of mineral particles at certain pH values (>pH 9) by reducing the magnitude of potential and/or neutralizing the surface charge of the mineral particles, resulted in  $\leq 99\%$  turbidity removal efficiency at pH 12.

## Acknowledgements

This study was financially supported by Süleyman Demirel University, BAP #4897-L1-17. The authors would like to thank Dr. Kadioglu and Dr. Karacabey for their valuable contribution to improving the quality of the study.

## Literatura – References

1. ACAR, H. Attention Must be Paid to Matters During the Establishment and the Running of a Wastewater Clarity Unit for a Marble Processing Plant, The Third Marble Symposium, Afyon, Turkey, 2001, s. 289–296.
2. AGIRTMIS, Dilan. Purification of Wastewater of Phonolite Processing Plant by Coagulation and Flocculation Methods. Isparta: Süleyman Demirel University, Graduate School of Natural and Applied Sciences, MSc. Thesis, 2017.
3. ARSLAN, Emine Işıl et al. Physico-chemical treatment of marble processing wastewater and recycling of its sludge. *Waste Management & Research*, 23, 2005, p. 550–559, ISSN 0734242X.
4. ASHTON, Peter et al. An overview of the impact of mining and mineral processing operations on water resources and water quality in the Zambezi, Limpopo and Olifants Catchments in Southern Africa. Contract Report to the Mining, Minerals and Sustainable Development (Southern Africa) Project, by CSIR-Environmentek, Pretoria and Geology Department, University of Zimbabwe Harare. Report No. ENV-PC, 2001, vol. 42.
5. BAYRAKTAR, Irfan et al. Wastewater treatment in the marble industry. In: M. Kemal, V. Arslan, A. Akar, M. Canbazoglu (Eds.), *Changing Scopes in Mineral Processing*, Balkema, Rotterdam, NL 1996, s. 673–677. ISBN 9789054108290.
6. BRATBY, John. *Coagulation and Flocculation with an Emphasis on Water and Wastewater Treatment* (2nd ed.). Croydon, England: Uplands Press Ltd, 2006, ISBN 1843391066.
7. CELIK, Mustafa Yavuz et al. Geological and technical characterization of Iscehisar (Afyon Turkey) marble deposits and the impact of marble waste on environmental pollution. *Journal of Environmental Management*, 87 (1), 2008, 106–116, ISSN 0301-4797.
8. CLARK, S.W. et al. Adsorption of calcium, magnesium and sodium ion by quartz. *Trans. AIME* 241, 1968, s. 334–341.
9. EDIZ, I. Goktay, et al. Madencilikte Toz Kaynakları ve Kontrolü. *Journal of Science and Technology of Dumlupınar University*, 2, 2001, p. 121-132, e-ISSN 2651-2769.
10. ERSOY, Bahri. Effect of pH and polymer charge density on settling rate and turbidity of natural stone suspensions. *International Journal of Mineral Processing*, 75, 2005, p. 207–216, ISSN 0301-7516.
11. HOŞTEN, Çetin et al. Flocculation behavior of clayey dolomites in borax solutions. *Powder Technology*, 235, 2013, p. 263–270, ISSN 0032-5910.
12. İPEKOĞLU, Uner. *Susuzlandırma ve Yöntemleri*. Dokuz Eylül University, Engineering Faculty Press, Izmir, 1997.
13. KOLARIK, Luise Otokar et al. *Modern Techniques in Water and Wastewater Treatment*. Victoria, Australia: CSIRO Publishing, 1995, ISBN 9780643105089.
14. LESCHONSKI, Kurt. The characterisation of particles using the settling rate dependent movement in two phase flows. *Particle & Particle Systems Characterization*, 10 (4), 1993, p. 159–166, ISSN 1521-4117.
15. MAVIS, Jim. *Water Use in Industries of the Future: Mining Industry*. Center for Waste Reduction Technologies for U.S. Department of Energy, Office of Energy Efficiency and Renewable Energy, Industrial Technologies Program, Washington, D.C., 2003, 47-53.
16. NDUWA-MUSHIDI, Josie et al. Surface chemistry and flotation behaviors of monazite, apatite, ilmenite, quartz, rutile, zircon with octanohydroxamic acid collector. *Journal of Sustainable Metallurgy*, 3 (1), 2017, p. 62–72, ISSN 2199-3823.
17. OZKAN, Alper et al. Comparison of stages in oil agglomeration process of quartz with sodium oleate in the presence of Ca(II) and Mg(II) ions. *Journal of Colloid and Interface Science*, 329 (1), 2009, p. 81–88, ISSN 0021-9797.
18. OZTURK, İzzet et al. *Aritımın Esasları*. Republic of Turkey, Ministry of Environment and Forestry Press, Ankara.
19. OZUN, Savas et al. Study of adsorption characteristics of long chain alkyl amine and petroleum sulfonate on silicates by electrokinetic potential microflotation FTIR and AFM analyses. *Particulate Science and Technology*, 37(4), 2019, p. 488-499, ISSN 0272-6351.
20. OZUN, Savas et al. Coagulation and flocculation behavior of fines in foid-bearing rock processing plant (FRPP) wastewater at alkaline environment. *Powder Technology*, 344, 2019, p. 335-342, ISSN 0032-5910.
21. SABAH, Eyup. Flocculation performance of fine particles in travertine slime suspension. *Physicochemical Problems of Mineral Processing* 48 (2), 2012, p. 555–566, ISSN 1643-1049.
22. SVAROVSKY, Ladislav. *Solid-Liquid Separation*, Butterworth-Heinemann, Oxford, 2000, eBook ISBN: 9780080541440.
23. TASDEMİR, Tugba et al. Fine particle removal from natural stone processing effluent by flocculation. *Environmental Progress & Sustainable Energy*, 32 (2), 2012, p. 317–324, ISSN 1944-7450.
24. THOMASHAUSEN, Sophie et al. A comparative overview of legal frameworks governing water use and waste water discharge in the mining sector. *Resources Policy*, 55, 2018, p. 143–151, ISSN 0301-4207.

25. TRIPATHY, Tridip et al. Flocculation: a new way to treat the waste water. *Journal of Physical Sciences*, 10, 2006, p. 93–127, ISSN 1675-3402.
26. WANG, Yan et al. The effect of total hardness on the coagulation performance of aluminum salts with different Al species. *Separation and Purification Technology*, 66 (3), 2009, p. 457–462, ISSN 1383-5866.
27. WATANABE, Yoshimasa. Flocculation and me. *Water Research*, 114, 2017, p. 88–103, ISSN 0043-1354.
28. WRIGHT, H.J.L., et al. The problem of dewatering clay Slurries: factors controlling filtrability. *Journal of Colloid and Interface Science*, 56, 1976, p. 57–65, ISSN 0021-9797.

### *Badanie usuwania zmętnienia ze ścieków z zakładu przeróbki kamienia naturalnego w procesie flokulacji*

*Badania miały na celu określenie wpływu trzech różnych flokulantów o wysokiej masie cząsteczkowej (HMW) (flokulanty anionowe, kationowe i niejonowe) na usuwanie drobnych cząstek (pyłu kamiennego) ze ścieków z zakładów przeróbki kamienia naturalnego w alkalicznym pH.*

*Zbadano zmętnienie w zależności od pH, stężenia flokulantu i czasu (0–6 min). Zgodnie z uzyskanymi wynikami, wartości zmętnienia ścieków przy braku flokulantów zależy od pH i zmniejszały się wraz ze wzrostem pH, co skutkowało minimalnymi wartościami zmętnienia przy pH 12. W obecności flokulantów wydajność klarowania zależy od rodzaju flokulantu, stężenia flokulantu i czasu. Najlepsze wyniki uzyskano przy wysokich alkalicznych wartościach pH (pH 12) ze skutecznością usuwania zmętnienia  $\leq 99\%$  w obecności flokulanta niejonowego. W przypadku anionów i flokulantów kationowych minimalne wartości zmętnienia uzyskano również przy pH 12 przy skuteczności usuwania zmętnienia powyżej 90%.*

**Słowa kluczowe:** ścieki z zakładów przeróbki kamienia naturalnego, usuwanie zmętnienia, dodawanie flokulantu, stężenie flokulantu, pH, czas



# Advanced Biomaterials with Semiconductive Properties Based on Fungal Chitosan

Marek PIĄTKOWSKI<sup>1)</sup>, Aleksandra SIERAKOWSKA<sup>2)</sup>, Łukasz JANUS<sup>2)</sup>,  
Julia RADWAN-PRAGŁOWSKA<sup>2)</sup>

<sup>1)</sup> Cracow University of Technology, Faculty of Chemical Engineering and Technology, Warszawska 24 Street, 31-155 Cracow, Poland; email: mpiatkowski@chemia.pk.edu.pl

<sup>2)</sup> Cracow University of Technology, Faculty of Chemical Engineering and Technology, Warszawska 24 Street, 31-155 Cracow, Poland

<http://doi.org/10.29227/IM-2020-01-59>

Submission date: 10-01-2020 | Review date: 11-03-2020

## Abstract

Tissue engineering is a branch of science that focuses on methods and techniques for the creation of new tissues and organs for the therapeutic reconstruction of the damaged organ by providing support structures, cells, molecular and mechanical signals for regeneration to the desired region. Conventional implants made of inert materials can eliminate only physical and mechanical defects of damaged tissues. The goal of tissue engineering is to restore biological functions, that is regeneration of tissues, and not only to replace it with a substitute made of synthetic material. The most important challenges of tissue engineering include the development of new biomaterials that will be used as three-dimensional scaffolds for cell cultures. Such scaffolding must be characterized by biocompatibility and biodegradability.

The aim of the research was to obtain biomaterials based on acylated chitosan. The result of the work was to obtain three-dimensional scaffolding with bioactive properties based on raw materials of natural origin. The biomaterials were modified with ferrimagnetic nanoparticles which are capable of electromagnetic stimulation of proliferation.

**Keywords:** waste biomass, chitosan, semi-conductive materials, Green Chemistry, scaffolds

## Introduction

Regenerative medicine is an alternative to traditional transplantation. It enables obtainment of tissues under in vitro conditions using primary cells derived from the patients. Cells are cultured on three-dimensional scaffolds which mimic their natural environment. The substrates can be prepared from synthetic polymers and biopolymers. Natural polymers are known of their excellent biocompatibility and biodegradability. However, their mechanical durability is quite low. Thus biomaterials prepared from them are modified with various substances both organic and inorganic. An interesting approach constitutes the application of nanoparticles to enhance raw polymer properties [PIĄTKOWSKI, Marek et al., 2019].

Nanotechnology is currently the most dynamically developing field of science. Rapid development is caused by great interest, financing of many studies and the possibility of using nanomaterials in almost all fields of science and everyday life. The goal of nanotechnology is to obtain new nanomaterials with the desired properties. Iron oxide nanoparticles, thanks to their size similar to the size of cells and due to their superparamagnetic properties, have been used in diagnostics (enhancing contrast in magnetic resonance imaging), therapies (hyperthermia, drug delivery) and industry (bioseparation) [FATIMA, Hira et al. 2018, LAURENT, Sophie et al. 2008, SIMONSEN, Galina et al. 2018]. There are two possibilities for obtaining nanoparticles. The first of these is the "top-down" method consisting in reducing the particle size of classical matter by, for example, grinding in a mill. This process is long-term, time-consuming and energy-intensive. The second and more common approach is the "bottom-up" method, which consists in the production of liquid-phase nanoparticles. The most commonly used syntheses of this type include: coprecipitation, sol-gel, colloidal and solvothermal methods. Coprecipita-

tion is a simple process. It consists of adding a basic alkaline reagent to aqueous salt solutions. The pH then rises and new seeds are formed, then they grow and age until the saturation level is reached. In the sol-gel method, the sol should first be obtained, a suspension in which the solid particles are not sedimented. Precursors including inorganic metal salts, metal alkoxides, acetates together with the solvent form a sol that then turns into a gel. The solvothermal methods consist in carrying out chemical reactions at a temperature exceeding the boiling point of the solvent and at elevated pressure. They are most often used to change the amorphous material into a crystalline one [CHEN, Zhou et al. 2018, R.V. MEHTA, 2017].

In order to give certain properties, reduce the tendency to agglomerate, protect against environmental factors and increase biocompatibility, magnetic nanoparticles are functionalised by surface coating using suitable polymeric stabilizers or surfactants, e.g. polyvinyl alcohol (PVA), polyethylene glycol (PEG), or by depositing several atomic metal layers (e.g. gold) or non-metals (e.g. graphite); the production of polymeric coatings that prevent the growth of clusters after nucleation and keep the domains of particles away from the attraction forces; by creating lipid coatings around the magnetic core [REDDY, Harivardhan et al. 2012].

Chitosan is a natural polymer known of its cytocompatibility and biodegradability. The biopolymer is built from two type of mers – aminoglucose and N-acetylaminoglucose. It may undergo numerous chemical and physical modifications due to presence of free hydroxy and amino functional groups. Until now, the scientists were focused on the application of chitosan obtained from shrips, crabs and lobsters. However, the potential of fungal chitosan is still not fully discovered. Fibroblasts are the most common cells of the connective tissue. They are a building part of skin (dermis). They are responsible for extracellular ma-

Tab. 1. Chitosan scaffolds synthesis parameters  
 Tab. 1. Parametry syntezy rusztowań chitozanowych

Sample	Chitosan, g	Aspartic acid, g	Propylene glycol, ml	Fe <sub>3</sub> O <sub>4</sub> NPs, %	Time, min	Temperature, °C
1	0.50	0.74	7		45	120
2				0.5		125
3						130
4						135

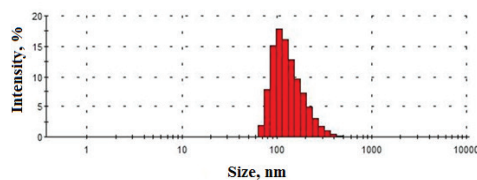


Fig. 1. The particle size distribution of obtained sample using ultrasounds without the addition of polymer  
 Rys. 1. Rozkład wielkości cząstek uzyskanej próbki za pomocą ultradźwięków bez dodatku polimeru

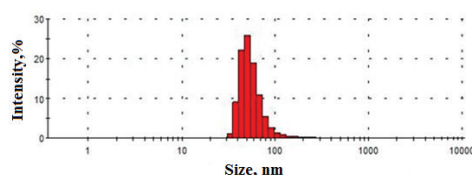


Fig. 2. The particle size distribution of obtained systems using ultrasounds stabilized by 0.1 mL PVA 14000  
 Rys. 2. Rozkład wielkości ziaren otrzymanych z wykorzystaniem ultradźwięków stabilizowane 0,1 ml PVA 14000

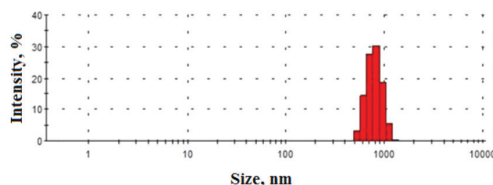


Fig. 3. The particle size distribution of obtained systems using ultrasounds stabilized by 0.2 mL PVA 14000  
 Rys. 3. Rozkład wielkości cząstek otrzymanych z wykorzystaniem ultradźwięków stabilizowanych 0,2 ml PVA 14000

trix components secretion [BALAKRISHNAN, Biji et al. 2011, PIĄTKOWSKI, Marek et al., 2019, SHAHID, Mohammad et al.2013, SHAMSHINA, Julia et al. 2019, VLIERBERGHE, Van et al. 2011]. In this article, a novel strategy of bioactive scaffolds synthesis strategy is presented using fungal chitosan as a raw material and ferrimagnetic.

## Materials and methods

### Materials

Chitosan was purchased from Polaura, Poland. The iron (III) chloride, ammonium and iron (VI) sulfate, ammonia, sodium citrate, poly(vinyl alcohol), poly(ethylene glycol), poly(vinylpyrrolidone) were received from Avantor Performance Materials Poland. All compounds were characterized by analytical purity. L-Aspartic acid, fibroblast growth medium (FGM) and human dermal fibroblasts (HDF) were purchased from Sigma Aldrich, Poland. Ethanol was purchased from Avantor, Poland.

### Methods

#### Biomaterials preparation pathway

The solutions were prepared by dissolving 0.584 g FeCl<sub>3</sub> and 0.423 g Mohr salt in 100 mL of distilled water. 10% stabi-

lizer solutions were prepared by dissolving 5 g of polymer in 45 g distilled water. Three methods of energy supply were used in the experiment: a heating plate, a microwave reactor and an ultrasonic cleaner with a heating function. Various volumes of stabilizers were added to the precursor solutions. The whole was heated to 60°C, and then 15 mL of a 5% ammonia solution was added dropwise. The produced precipitate was rinsed twice with distilled water to get rid of the salts which had not reacted. Then, aspartic acid was dissolved in the distilled water containing Fe<sub>3</sub>O<sub>4</sub> NPs. Next, chitosan and propylene glycol were added and reaction was carried out under microwave radiation using Prolabo Synthwave reactor. Finally, the products were lyophilised.

#### DLS analysis

DLS analysis was performed using zeta sizer analyser.

#### FT-IR analysis

FT-IR analysis was performed using IR Thermo Nicolet Nexus X 470 spectrometer (diamond crystal ATR), USA. The range was between 400 and 4000 cm<sup>-1</sup> with 32 scans and 4 cm<sup>-1</sup> resolution.

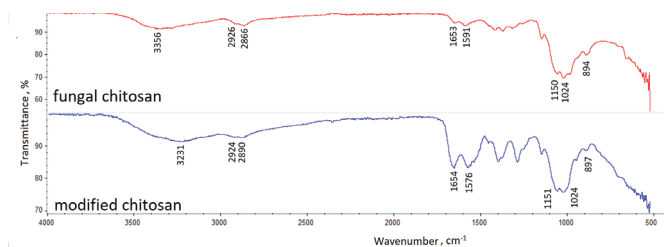


Fig. 4. FT-IR spectra of the prepared biomaterials  
Rys. 4. Widma FT-IR przygotowanych biomateriałów

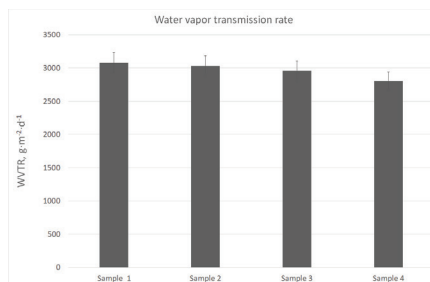


Fig. 5. Water vapor transmission rate of the prepared biomaterials  
Rys. 5. Szybkość przenikania pary wodnej przygotowanych biomateriałów

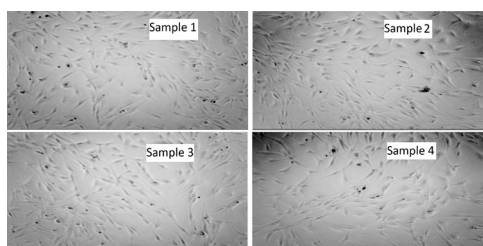


Fig. 6. Human dermal fibroblasts after cell culture in the presence of the prepared biomaterials  
Rys. 6. Ludzkie fibroblasty skórne po hodowli komórkowej w obecności przygotowanych biomateriałów

#### Water vapor transmission rate (WVTR)

Water vapor transmission rate was performed by placing weighed samples on the vessels containing 10 mL of distilled water. The biomaterials were fixed with glue to cover the container. The vessels were left for 24h at 37°C. Next, the amount of the evaporated water was determined. To calculate WVTR the following equation was used:

$$WVTR = (W_t - W_0) / (tA) \quad (g \cdot m^{-2} \cdot d^{-1})$$

where:  $W_t$  – the weight after time  $t$ ,  $W_0$  – the initial weight,  $t$  – the measuring time,  $A$  – the area of the opening of polystyrene well

#### Cytotoxicity study

To verify cytotoxicity of the prepared biomaterials cell culture of the primary cells – human dermal fibroblasts was carried out. The culture was performed for 48h at 37°C and 95% CO<sub>2</sub> concentration. As a culture medium fibroblast growth medium was used. The cells were investigated under inverted microscope.

## Results and discussion

### DLS analysis

Figures 1–3 presents results of particles size determination by DLS method. For particles obtained in synthesis 1 had size of 100 nm, synthesis 2–50 nm, while in synthesis 3–900 nm.

Differences in the size of the obtained particles indicate the importance of choosing the right stabilizer concentration during the synthesis. In synthesis 2, the addition of 0.1 mL of PVA solution favored the formation of nanometric size particles. The increase in the stabilizer concentration decreased the scatter of results, increased the homogeneity of the obtained samples. This was due to the stabilizer properties, which adsorbed on the particles prevented their agglomeration.

### FT-IR analysis

Figure 4 shows the chemical structure of the raw and modified chitosan. Pure polymer prepared from fungi shows all bands typical for chitosan coming from free hydroxyl and amino groups, alkyl groups, glucopyranose rings and glycosidic bonds. FT-IR spectrum of the modified chitosan proves acylation reaction occurrence since it can be noticed that new amide bonds were formed between polymer amino groups and carboxylic groups of amino acid. At the same time, it can be noticed that the rest of the bands are similar which means that no degradation of chitosan took place. Thanks to the presence of the hydrophilic groups including amino, carboxyl and hydroxyl the ob-

tained material had a hydrogel nature and was capable of water sorption.

#### ***Water vapor transmission rate***

Biomaterials dedicated to applications in skin tissue regeneration must meet various conditions, such as good water vapor permeability. Appropriate humidity and gas exchange are crucial for damage skin recovery. Results shown in Figure 4 indicate, that all prepared samples are permeable for water vapor in the similar manner. Such permeability can be caused by the very porous structure of the biomaterials which was achieved by the lyophilization of the swollen samples. After freezing, water molecules increased their volume creating spread pores in the polymeric matrix as a result of sublimation.

#### ***Cytotoxicity study***

The proposed biomaterials are dedicated to tissue engineering applications and should provide appropriate environment for skin cells adhesion and multiplication. The raw chitosan is known of its biocompatibility. However, its chemical modification can deteriorate this feature. Also, the addition of nanoparticles may sometime induce undesired cellular responses, including apoptosis. Figure 6 presents results of cytotoxicity study carried

out on human dermal fibroblasts. It can be observed that cells are of standard morphology and have spindle-like shape. Additionally, their nuclei are flat and oval and no grains in cytoplasm can be noticed. Therefore, it can be stated that the prepared biomaterials are non-cytotoxic. Additionally, comparing to the cells cultured without biomaterials it can be noticed that the proliferation activity is higher.

#### **Conclusion**

The aim of this research was to obtain novel type of material using chitosan prepared from fungi as a main component. Also,  $\text{Fe}_3\text{O}_4$  nanoparticles were prepared under synthesis conditions. The polymer was successfully modified by acylation using L-aspartic acid and obtained ferrimagnetic NPs. Ready products were examined over their physicochemical properties. Finally, their biocompatibility and bioactivity were confirmed on human dermal fibroblasts. Overall, the proposed biomaterials have a great potential in tissue engineering, especially of skin tissue.

#### **Acknowledgements**

The research was supported financially by the Sonata project National Science Centre, Poland, Grant no. 2017/26/D/ST8/00979.

## Literatura – References

1. BALAKRISHNAN, Biji et al. Biopolymer-based hydrogels for cartilage tissue engineering. *Chemical Reviews*, 111 (8), 2011, p. 84453-4474, ISSN 0009-2665.
2. FATIMA, Hira et al. Iron-based magnetic nanoparticles for magnetic resonance imaging. *Advanced Powder Technology*, 29, 2018, p. 2678–2685, ISSN 0921-8831.
3. CHEN, Zhou et al. Synthesis, functionalization, and nanomedical applications of functional magnetic nanoparticles. *Chinese Chemical Letters*, 29, 2018, p. 1601–1608 ISSN 1001-8417.
4. LAURENT, Sophie et al. Magnetic iron oxide nanoparticles: synthesis, stabilization, vectorization, physicochemical characterizations, and biological applications. *Chemical Reviews*, 108, 2008, p. 2064–2110, ISSN 0009-2665.
5. PIĄTKOWSKI, Marek et al. Microwave-assisted synthesis and characterization of chitosan aerogels doped with Au-NPs for skin regeneration. *Polymer Testing*, 73, 2019, p. 366-376, ISSN 0142-9418.
6. R.V. MEHTA, Synthesis of magnetic nanoparticles and their dispersions with special reference to applications in biomedicine and biotechnology. *Materials Science and Engineering C*, 79, 2017, p. 901–916, ISSN 0928-4931.
7. REDDY, Harivardhan et al. Magnetic nanoparticles: design and characterization, toxicity and biocompatibility, pharmaceutical and biomedical applications. *Chemical Reviews*, 112, 2012, p. 5818–5878, ISSN 0009-2665.
8. SHAHID, Mohammad et al. Green Chemistry Approaches to Develop Antimicrobial Textiles Based on Sustainable Biopolymers—A Review. *Industrial & Engineering Chemistry Research*, 52 (15), 2013, p. 5245-5260, ISSN 0888-5885.
9. SHAMSHINA, Julia et al. Advances in functional chitin materials: a review. *ACS Sustainable Chemistry & Engineering*, 7, 2019, p. 6444-6457, ISSN 2168-0485.
10. SIMONSEN, Galina et al. Potential applications of magnetic nanoparticles within separation in the petroleum industry. *Journal of Petroleum Science and Engineering*, 165, 2018, p. 488–495, ISSN 0920-4105.
11. VLIERBERGHE, Van et al. Biopolymer-based hydrogels as scaffolds for tissue engineering applications: a review. *Bio-macromolecules*, 12 (5), 2011, p. 1387-1408, ISSN 1525-7797.

## *Zaawansowane biomateriały o właściwościach półprzewodnikowych oparte chitozanie pochodzącym z grzybów*

*Inżynieria tkankowa jest dziedziną nauki, która koncentruje się na metodach i technikach tworzenia nowych tkanek i narządów do terapeutycznej rekonstrukcji uszkodzonego narządu poprzez dostarczenie struktur wspierających, komórek, sygnałów molekularnych i mechanicznych do regeneracji w pożądanym kierunku. Konwencjonalne implanty wykonane z materiałów obojętnych mogą wyeliminować fizyczne i mechaniczne wady uszkodzonych tkanek. Celem inżynierii tkankowej jest przywrócenie funkcji biologicznych, czyli regeneracja tkanek, a nie tylko zastąpienie jej substytutem wykonanym z materiału syntetycznego. Najważniejsze wyzwania inżynierii tkankowej obejmują rozwój nowych biomateriałów, które będą wykorzystywane jako trójwymiarowe rusztowania do hodowli komórkowych. Takie rusztowanie musi charakteryzować się biokompatybilnością i biodegradowalnością. Celem badań było uzyskanie biomateriałów na bazie acylowanego chitozanu. Rezultatem prac było uzyskanie trójwymiarowego rusztowania o właściwościach bioaktywnych na bazie surowców pochodzenia naturalnego. Biomateriały zmodyfikowano nanocząstkami ferrimagnetycznymi, które są zdolne do elektromagnetycznej stymulacji proliferacji.*

**Słowa kluczowe:** *odpadowa biomasa, chitozan, materiały półprzewodnikowe, Zielona Chemia, rusztowania chitozanowe*







# Bioactive Scaffolds for Skin Tissue Engineering Doped with Gold Nanoparticles Prepared from Waste Biomass

Julia RADWAN-PRAGŁOWSKA<sup>1)</sup>, Łukasz JANUS<sup>2)</sup>, Marek PIĄTKOWSKI<sup>2)</sup>, Aleksandra SIERAKOWSKA<sup>2)</sup>, Dariusz BOGDAŁ<sup>2)</sup>

<sup>1)</sup> Cracow University of Technology, Faculty of Chemical Engineering and Technology, Warszawska 24 Street, 31-155 Cracow, Poland; email: jrpragłowska@chemia.pk.edu.pl

<sup>2)</sup> Cracow University of Technology, Faculty of Chemical Engineering and Technology, Warszawska 24 Street, 31-155 Cracow, Poland

<http://doi.org/10.29227/IM-2020-01-61>

Submission date: 04-01-2020 | Review date: 02-03-2020

## Abstract

Skin is the first barrier against pathogens and harmful external factors. Each damage of this tissue may cause microbial infection and danger to internal organs. Burns which may be a result of the exposure to radiation, chemicals or high temperature leads to the significant disruption of skin functions. The most promising method for this tissue recovery is regenerative medicine which requires application of three-dimensional biocompatible scaffolds. The biomaterials enable skin cells proliferation and new tissue formation under *in vitro* conditions. They can be prepared from synthetic and natural polymers and their combination. The application of additional components such as nanoparticles may enhance their mechanical properties and have a positive impact on fibroblasts divisions and extra cellular formation. One of the most promising raw materials for scaffolds is chitosan - a chitin derivative. It may be obtained from waste biomass such as crabs, shrimps and lobsters exoskeletons. Chitosan is non-toxic, biodegradable and have antibacterial properties. The aim of the following study was to obtain novel chitosan derivatives doped with the gold nanoparticles using only natural components such as orange peels and fatty acid derivative. Proposed modification strategy resulted in the preparation of the novel, biodegradable and biocompatible material with interesting properties. The products were analysed by UV-Vis and FT-IR methods. The scaffolds were investigated over their susceptibility to enzymatic degradation. Finally, the biomaterials were verified over their cyto-compatibility with human dermal fibroblasts. The results showed that the proposed synthesis pathway resulted in the obtained of the chitosan biomaterials with high potential in medicine.

**Keywords:** waste biomass, gold nanoparticles, chitosan, biomaterials, Green Chemistry

## Introduction

Annually, 20,000 patients await skin grafts as a result of burns. Currently, the only solution for these people are autogenous, allogenic and xenogeneic grafts. These types of treatments are associated with a limited amount of available tissue. Alternative to transplantation is regenerative medicine and tissue engineering. They enable the cultivation of skin cells on special substrates that can be transplanted to the patient [AMBEKAR, Rushikesh et al. 2019, BARGUES, L et al. 2011].

Cell cultures are carried out on three-dimensional scaffolds, which must be non-toxic and biocompatible, as well as allow the flow of nutrients. In order to ensure proper tissue regeneration, scaffolds should be characterized by controlled biodegradability under the influence of enzymes naturally occurring in the human body. They should also promote cells proliferation [AHMED, Shakeel et al. 2018, RADWAN-PRAGŁOWSKA, Julia et al. 2019].

Chitosan is a biodegradable polymer obtained as a result of deacetylation of chitin, which is a biopolymer present in exoskeletons of crustaceans constituting a large-scale food industry waste, especially shells of shrimps, crabs and lobsters [KNIDRI, Hakima et al.2018, VLIERBERGHE, Van et al. 2011].

Chitosan due to its favorable features such as biocompatibility and biodegradability is widely applied in medicine and

pharmacy as a component of wound dressings or controlled drug delivery and release systems [MITTAL, Hemant et al.2018, SHARIATINIA, Zahra et al. 2019]. Gold nanoparticles which are particles below 100 nm are known of their positive impact of extracellular matrix components secretion, especially collagen [PIĄTKOWSKI, Marek et al. 2019, THAKOR, A. S. et al. 2011].

The aim of the research was to obtain new chitosan derivatives with controlled biodegradability, which can be used in regeneration of full skin thickness. The biomaterials were modified with gold nanoparticles which have positive impact on new extracellular matrix formation.

## Materials and methods

### Materials

Chloroauric acid, triethylamine, acetone, oleoyl chloride, fibroblast growth medium (FGM) and human dermal fibroblasts (HDF), simulated body fluid (SBF) and lysozyme were purchased from Sigma Aldrich, Poland. Acetone, ethanol and methanol were purchased from POCH, Poland.

### Methods

#### Biomaterials preparation pathway

Gold nanoparticles were obtained in a reduction reaction of chloroauric acid. As a reducing agent orange peel extract was used which was prepared under microwave-as-

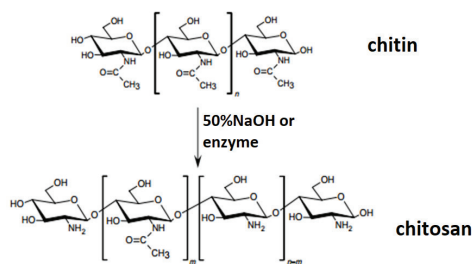


Fig. 1. Chitosan preparation  
Rys. 1. Przygotowanie chitozanu

Tab. 1. Chitosan biomaterials synthesis parameters  
Tab. 1. Parametry syntezy biomateriałów chitozanu

Sample	Chitosan, g	Acetone, ml	TEA, ml	Oleic acid chloride, ml	Deacetylation degree	Time, min	Temperature, °C
1	0.50	20	4.2	3	80	45	140
2					85		
3					90		
4					95		

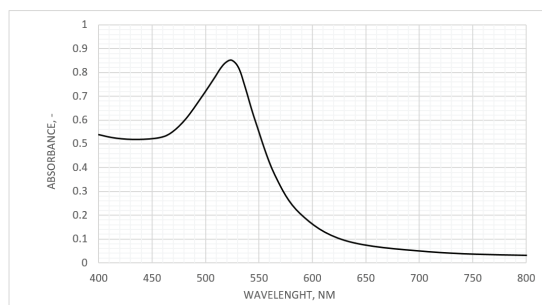


Fig. 2. UV-Vis spectrum of the prepared Au nanoparticles  
Rys. 2. Widmo UV-Vis przygotowanych nanocząstek Au

sisted conditions. In brief, chopped orange peel fragments were placed in the Prolabo Synthwave microwave reactor for 5 min (80°C).

The extract was further purified on membrane filters. Chitosan acylation reaction was performed using as a raw material polymer of various deacetylation degree (80%, 85%, 90% and 95%) obtained from shrimps' exoskeletons. The acylation reaction was carried out using microwave irradiation. In the first step chitosan was activated using triethylamine dissolved in acetone. Then, acylation reaction was performed according to data presented in Table 1. To obtain 3D scaffolds, modified chitosan previously washed out with methanol and dried was swollen with 20 ml of the solution containing Au nanoparticles. Then, biomaterials were freeze-dried.

#### UV Vis spectroscopy analysis

UV-Vis spectrum was performed using Aligent 8453 spectrophotometer.

#### FT-IR analysis

FT-IR analysis was performed using IR Thermo Nicolet Nexus X 470 spectrometer (diamond crystal ATR), USA.

#### Biodegradation study

For the degradation study weighed samples were placed in the sterile SBF solution and their weight loss was determined after fixed time intervals according to the Equation 1. To verify their biodegradability, the samples were placed in the sterile SBF solution containing lysozyme – human enzyme which is present in various body fluids such as tears. The weight loss was determined using Equation 1:

$$(B)D = \frac{W_0 - W_t}{W_0} \cdot 100\% \quad (1)$$

where:

(B)D – (bio)degradation degree, %,  $W_0$  – Initial weight of the analyzed sample, g,  $W_t$  – Sample weight after time = t, min

#### Cytotoxicity study

To verify cytotoxicity of the prepared biomaterials cell culture of the primary cells – human dermal fibroblasts was carried out. The culture was performed for 48h at 37°C and 95% CO<sub>2</sub> concentration. As a culture medium fibroblast growth medium was used. The cells were investigated under inverted microscope.

## Results and discussion

### UV-Vis analysis

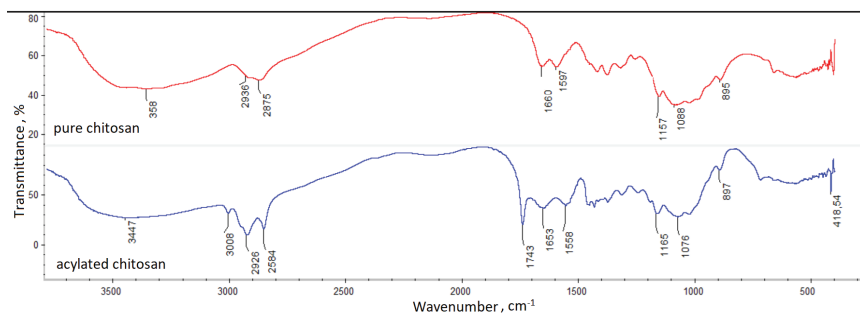


Fig. 3. FT-IR spectra of the prepared biomaterials  
Rys. 3. Widma FT-IR przygotowanych biomateriałów

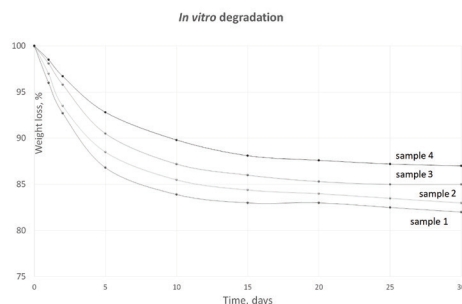


Fig. 4. Degradation study of the prepared biomaterials  
Rys. 4. Badanie degradacji przygotowanych biomateriałów

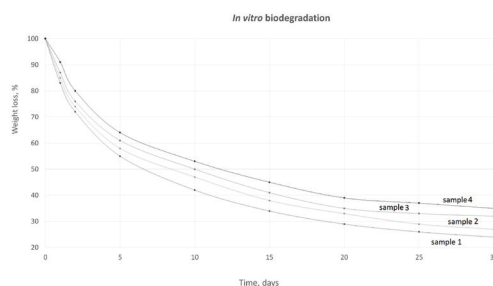


Fig. 5. Biodegradation study of the prepared biomaterials  
Rys. 5. Badanie biodegradacji przygotowanych biomateriałów

Figure 2 presents UV-Vis spectrum of the prepared particles. It can be noticed, that the maximum absorption peak wavelength is typical for the Au NPs diameter of 20 nm. Therefore, it can be concluded that the nanoparticles were successfully obtained and their size is above 10 nm which will prevent their bioaccumulation and cytotoxicity.

#### FT-IR analysis

Figure 3 presents spectra of the pure chitosan and obtained samples. It can be noticed that unmodified chitosan spectrum shows some typical band coming from free hydroxyl groups as well as acyl groups. Moreover, at the band corresponding to amide bonds present in acylated chitosan unit is visible as well as bands which are typical for free amino groups in deacetylated units. Additionally, band characteristic for glycosidic bonds as well as glucopyranose rings are noticeable. The other spectra show chitosan after acylation. It can be noticed that in the case of all samples some changes are visi-

ble. One may observe, that the intensity of amide bonds has significantly increased, whereas the intensity of free amino groups decreased. Moreover, bands coming from  $-CH-$  and  $-CH_2-$  are of much higher intensity which proves acyl chain incorporation. At the same time, bands coming from free hydroxyl groups as well as glycosidic bonds and pyranose rings are still presents which proves that no significant chitosan degradation has occurred.

#### Biodegradation study

Figure 4 presents results of in vitro degradation and biodegradation study carried out under human-like conditions. It can be noticed that all samples exhibited very good stability in the simulated body fluids since their weight loss in 30 days is up to 20%. On the other hand, one may observe that the biomaterials undergo biodegradation process in the presence of lysozyme which naturally occurs in human body and hydrolyses glycosidic bonds. Chitosan is a biodegradable poly-

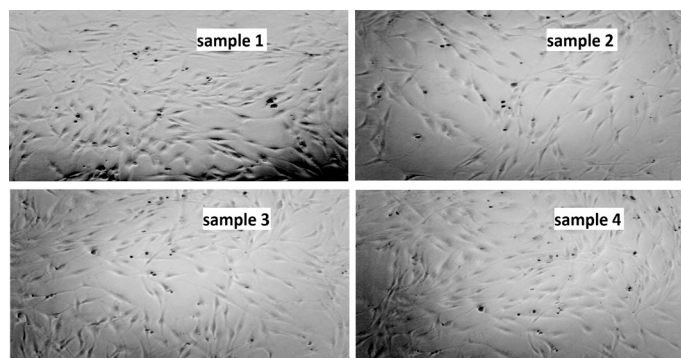


Fig. 6. Cytotoxicity of the prepared biomaterials  
Rys. 6. Cytotoksyczność przygotowanych biomateriałów

mer, however chemical modification may hamper this property. The proposed strategy of bioactive scaffolds preparation enables obtainment of the biomaterials susceptible to natural degradation. It can be noticed (Figure 5) that all samples degraded in more than 60%. Thus, they can be considered as biodegradable and may be used under both in vitro and in vivo conditions since new tissue formation will be parallel with the materials degradation. The scaffolds will be naturally removed from the body and no reoperation will be needed which is very important for the patient.

#### **Cytotoxicity study**

The prepared biomaterials are dedicated to skin tissue engineering. The application of waste biomass may negatively affect the scaffolds cytocompatibility. The Figure 6 presents microphotographs (40x) of the human dermal fibroblasts after 48 hours of the study. It can be observed that the fibroblasts cultured in the presence of the biomaterials were flattened and of normal morphology without visible grains. Therefore,

it can be stated that obtained scaffolds are biocompatible and provide appropriate environment for skin cells.

#### **Conclusion**

In this article a novel approach to chitosan was proposed. The scaffolds dedicated to full-thickness skin transplantation were prepared by acylation reaction using fatty acid derivative as modifying agent. The biomaterials were further modified with gold nanoparticles to enhance their bioactivity. The products were biodegradable under human-like conditions and had a positive impact on skin cells proliferation. Taken all together, the results confirmed preparation of novel biomaterials which can be successfully applied for damaged skin regeneration under in vitro conditions.

#### **Acknowledgements**

The research was supported financially by National Science Centre, Poland, grant number: 2016/23/N/ST8/01273.

## Literatura – References

1. AHMED, Shakeel et al. A review on chitosan centred scaffolds and their applications in tissue engineering. *International Journal of Biological Macromolecules*, 116, 2018, p. 849-862, ISSN 0141-8130
2. AMBEKAR, Rushikesh et al. Progress in the advancement of porous biopolymer scaffold: tissue engineering application. *Industrial & Engineering Chemistry Research*, 58 (16), 2019, p. 6163-6194, ISSN 0888-5885
3. BARGUES, L et al. Present and future of cell therapy in burns. *Pathologie Biologie*, 59, 2011, p. 49–56 ISSN 0369-8114
4. KNIDRI, Hakima et al. Extraction, Chemical modification and characterization of chitin and chitosan. *International Journal of Biological Macromolecules*, 120 (A), 2018, p. 1181-1189, ISSN 0141-8130
5. MITTAL, Hemant et al. Recent progress in the structural modification of chitosan for applications in diversified bio-medical fields. *European Polymer Journal*, 109, 2018, p. 402-434, ISSN 0014-3057
6. PIĄTKOWSKI, Marek et al. Microwave-assisted synthesis and characterization of chitosan aerogels doped with Au-NPs for skin regeneration. *Polymer Testing*, 73, 2019, p. 366-376, ISSN 0142-9418
7. RADWAN-PRAGŁOWSKA, Julia et al. 3D scaffolds prepared from acylated chitosan applicable in skin regeneration – synthesis and characterization. *International Journal of Polymer Analysis and Characterization*, 24, 2019, p. 75-86, ISSN 1563-5341
8. SHARIATINIA, Zahra et al. Pharmaceutical applications of chitosan. *Advances in Colloid and Interface Science*, 263, 2019, p. 131-194, ISSN 0001-8686
9. THAKOR, A. S. et al. Gold nanoparticles: a revival in precious metal administration to patients. *Nano Letters*, 2011, 11 (10), p. 4029-4036, ISSN 1530-6984
10. VLIERBERGHE, Van et al. Biopolymer-based hydrogels as scaffolds for tissue engineering applications: a review. *Bio-macromolecules*, 12 (5), 2011, p. 1387-1408, ISSN 1525-7797

### *Bioaktywne rusztowania do inżynierii tkanek skóry domieszkowane złotymi nanocząstkami przygotowanymi z biomasy odpadowej*

Skóra jest pierwszą barierą przed patogenami i szkodliwymi czynnikami zewnętrznymi. Każde uszkodzenie tej tkanki może powodować zakażenie drobnoustrojami i zagrożenie dla narządów wewnętrznych. Oparzenia, które mogą być wynikiem narażenia na promieniowanie, chemikalia lub wysoką temperaturę, prowadzą do znacznego zakłócenia funkcji skóry. Najbardziej obiecującą metodą tego odzyskiwania tkanki jest medycyna regeneracyjna, która wymaga zastosowania trójwymiarowych biokompatybilnych rusztowań. Biomateriały umożliwiają namnażanie komórek skóry i tworzenie nowych tkanek w warunkach *in vitro*. Można je wytwarzać z polimerów syntetycznych i naturalnych oraz ich kombinacji. Zastosowanie dodatkowych składników, takich jak nanocząstki, może poprawić ich właściwości mechaniczne i mieć pozytywny wpływ na podziały fibroblastów i tworzenie się komórek. Jednym z najbardziej obiecujących surowców na rusztowania jest chitozan - pochodna chityny. Można go uzyskać z biomasy odpadowej, takiej jak egzoszkielety krabów, krewetek i homarów. Chitozan jest nietoksyczny, biodegradowalny i ma właściwości antybakteryjne.

Celem przedstawionych badań było uzyskanie nowych pochodnych chitozanu domieszkowanych nanocząstkami złota przy użyciu wyłącznie naturalnych składników, takich jak skórki pomarańczy i pochodna kwasu tłuszczowego. Proponowana strategia modyfikacji zaowocowała przygotowaniem nowego, biodegradowalnego i biokompatybilnego materiału o interesujących właściwościach. Produkty analizowano metodami UV-Vis i FT-IR. Rusztowania badano pod kątem ich podatności na degradację enzymatyczną. Na koniec biomateriały zweryfikowano pod kątem ich zgodności cytologicznej z ludzkimi fibroblastami skórnymi. Wyniki wykazały, że proponowany szlak syntezy zaowocował uzyskaniem biomateriałów chitozanu o wysokim potencjale w medycynie.

**Słowa kluczowe:** odpady biomasy, nanocząstki złota, chitozan, biomateriały, Zielona Chemia





# Reduction of Pollution During Composite Machining

Jan RAŠKA<sup>1)</sup>, Libor HLAVÁČ<sup>1)</sup>, Adam ŠTEFEK<sup>1)</sup>, Martin TYČ<sup>1)</sup>

<sup>1)</sup> PWR Composite s.r.o., Sadová 1892/41, 702 00 Moravská Ostrava a Přívoz, Czech Republic

<http://doi.org/10.29227/IM-2020-01-62>

Submission date: 07-01-2020 | Review date: 22-02-2020

## Abstract

Machining of composite materials through classical way, i.e. using conventional tools for turning, drilling, milling, grinding and polishing, produces a lot of very small particles - dust. These particles enter the air, because machining should be performed with a minimum of sprinkling to protect composite material properties and to avoid delamination or swelling. Sometimes, even some burning of epoxide used as binder takes place during machining. Dust produced during machining of the composite material might have negative impact on health and may cause explosion. Skin inflammation or inhalation of the toxic epoxide resin, are some of the examples. Common solution of this problem is suction of particles and fume using machines creating negative pressure. Subsequent removing of these harmful substances from air is quite demanding and expensive. Moreover, using of common suction systems is many times less efficient than declared by producers. This contribution presents a new way of fighting with pollution caused by composite machining. The alternative machining tool for composite machining is abrasive water jet (AWJ). This tool is efficient in all basic machining processes and produces in air only about 1% of dangerous pollution comparing to classical tools. Progress of the AWJ machining system based on robot as a movement device is presented and the first results are commented. The main attention is aimed at machining quality possibilities. However, a part of the contemporary research focused on pollution suppression is also presented in the contribution.

**Keywords:** composite, abrasive water jet, cutting, turning, pollution

## Introduction

Abrasive water jet (AWJ) machining is a technique known since eighties of the twenties century when firstly introduced, described and presented by Hashish (1984). It is used namely for cutting, but applications of abrasive water jets for milling (Rabani et al., 2016), turning (Zohourkari et al., 2014), grinding (Liang et al., 2015) or polishing (Che et al., 2008) are tested more and more often, because they bring some benefits regarding classical machining processes. Utilization of abrasive water jet as a machining tool for composite materials is tested more and more often (Ming et al. 2018, Wong et al. 2018, Ruiz-Garcia et al., 2019). One of the most important benefits of AWJ utilization is substantial reduction of dust pollution in air. Dust pollution, often carcinogenic or silicosis causing, arising from classical machining of composites, though reduced by exhausters, is a quite serious problem. The dust removal from the air and its subsequent storage and/or neutralization, disposal of clogged filters and other measures to reduce the risk of operator injury could be substantially reduced applying AWJ. Therefore, some of the most dangerous materials, like glass fabric with epoxy, have been tested to check precision of their machining by AWJ with a view to changing from conventional machining to unconventional one.

## Theoretical background

The theoretical base of the new procedures applied during solving the problems with AWJ machining of composites has been published by Hlavac et al. (2012) and Hlavac et al. (2015). They are focused on the two main problems of AWJ machining accuracy – the trailback and taper. The typical simplistic description of jet penetration through material is replacement of the real trajectory by simple curves, namely

parabolic shape. The respective equations describing the trailback and the taper are presented in the shapes published in Hlaváč et al. (2012) and Hlaváč et al. (2015) respectively:

$$\sigma = \frac{2}{5} H \operatorname{tg} \left[ \theta_{\lim} \left( \frac{v_p}{v_{p\lim}} \right)^{\frac{2}{5}} \right] \quad (1)$$

$\sigma$  – the trailback,  $H$  – material thickness,  $\theta_{\lim}$  – the limit declination angle,  $v_p$  – the actual traverse speed,  $v_{p\lim}$  – the limit traverse speed for material thickness  $H$ ;

$$\varphi = \varphi_{\lim} \left( \frac{h}{h_{\lim}} \right)^{\frac{2}{5}} + q \quad (2)$$

$\varphi$  – the inclination angle,  $\varphi_{\lim}$  – the limit inclination angle,  $h$  – actual depth of AWJ penetration into material,  $h_{\lim}$  – the limit depth of penetration of AWJ into material for selected traverse speed (namely material thickness  $H$ ),  $q$  – a constant characterizing ductility and brittleness of material.

The resulting theoretical equation combining influence of trailback and taper has been presented in Hlaváč et al. (2018) enables calculation of the bottom diameter in the curved parts of trajectories:

$$D_{bc} = 2 \left[ \sqrt{\left( \frac{2}{5} H \tan \theta \right)^2 + R^2} + \frac{2}{5} H \tan \varphi \right] + d_a \quad (3)$$

$D_{bc}$  – the bottom diameter of the circular part of cutting trajectory, variables  $H$ ,  $\theta$  and  $\varphi$  are identical with to those used in Eq. (1) and (2),  $R$  – set radius of cutting trajectory,  $d_a$  – the diameter of an abrasive focussing tube.

## Experimental results

Experiments were performed with two abrasive water jets having different origin pressure and flow rate. The deforma-



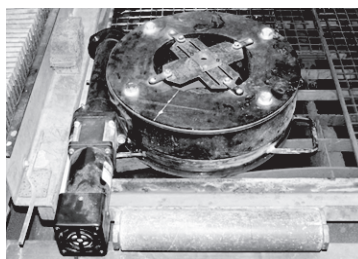


Fig. 1. Device for rotating with sample under the AWJ cutting head  
Rys. 1. Urządzenie do obróbki z głowicą tnącą AWJ



Fig. 2. Column cut without AWJ head tilting (left) and with tilting (right)  
Rys. 2. Cięcie kolumny bez przechylania głowicy AWJ (po lewej) i przechyleniu (po prawej)

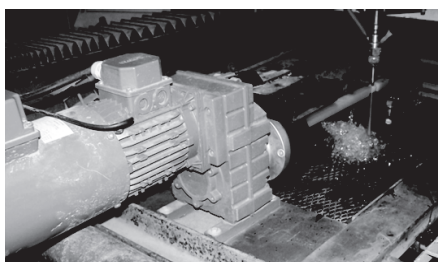


Fig. 3. Device with horizontal axis for sample turning  
Rys. 3. Urządzenie z osią poziomą do obracania próbki

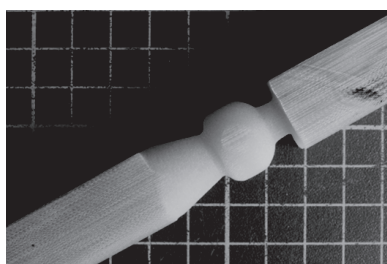


Fig. 4. Sample documenting possibility of composite with glass fibre turning by AWJ  
Rys. 4. Przykładowa dokumentacja możliwości toczenia kompozytu z włóknem szklanym przez AWJ

tion of column samples and reduction of difference between top and bottom diameter has been tested using low pressure but high flow rate pump. A special device for sample rotation under the tilted cutting head has been used for this test (Fig. 1). The experimental conditions are summarized in Table 1. Results of column cutting with cutting head without and with tilting are presented in Fig. 2.

Figure 2 shows the typical striations on the samples' walls. It is evident that non-tilted jet makes more noticeable striations and the sample is rather truncated cone shaped then "column" shaped. By contrast to it the tilted jet produces rather barrel shaped samples with striations better visible even in the bottom part. It can be also mentioned that diam-

eter of the top base of the sample produced by a non-tilted jet is smaller than that of the tilted jet and some slight increase of the diameter of the bottom base can be also noticeable.

Several columns were cut: one half of them with jet axis perpendicular to the surface of the plan-parallel sheet of composite plate, the second half with tilting of the cutting head compensating deformation caused by trailback. Both sets of samples were measured on the top and bottom to compare their diameters with each other. The respective average top and bottom diameters for a non tilted jet are 16.46 mm and 18.58 mm. Values for tilted jet are 18.26 mm and 19.28 mm. The setup diameter was 20 mm for all experimental tests. The increase of top and bottom diameters for tilted regarding the non-tilted

Tab. 1. Parameters used in experiments  
 Tab. 1. Parametry stosowane w eksperymentach

Factor	Constant cutting parameters on two testing workplaces	
	Low pressure workplace	High pressure workplace
Pressure in pump	23 MPa	380 MPa
Water jet diameter	1.2 mm	0.254 mm
Focusing tube diameter	3 mm	1.02 mm
Focusing tube length	152 mm	76 mm
Abrasive mass flow rate	300 g/min	250 g/min
Mean abrasive grain size <sup>a</sup>	0.375 mm (50 mesh) <sup>b</sup>	0.25 mm (80 mesh) <sup>b</sup>
Abrasive type	Australian garnet (almandine)	Australian garnet (almandine)
Traverse speed	100 mm/min	50 mm/min
Rotational axis	vertical	Horizontal
Revolutions	1.6 min <sup>-1</sup>	600 min <sup>-1</sup>
Stand-off distance	2 mm	2 – 5 mm

<sup>a</sup> Mean grain size is determined on the commercial particles size analyzer.

<sup>b</sup> The “mesh” specification is commercial indication provided by suppliers.

jets correlated with findings presented by Hlaváč et al. (2018).

The second experiment was performed with high-pressure and low flow rate pump and device used for turning of material (see Fig. 3). The experimental conditions are also summarized in Table 1. Sample result of material turning is presented in Fig. 4. The testing shape has been prepared so that it includes all basic possible movements applied during material turning. Movement of the tool towards rotational axis, along it, combined movement towards and/or from the axis necessary for turning spherical or conical shapes. The testing shape has been prepared from prism to test also deformation caused by deflection of the jet on the edges. The testing trajectory has been set so, that the spherical part exceeds the dimensions of prism to study the influence of the partial material removing on the resulting quality of surface.

All results have proved that the quality is very good and difference in shape dimensions is negligible.

## Discussion

Preliminary results aimed at column sample distortion proved that tilting of the cutting head is a proper way for reduction of trailback and the taper. The difference between diameters of column bases on the inlet and the outlet surface has been reduced by 208% eliminating the trailback. Elimination of the taper causes additional 50% of reduction. The resulting average diameters after tilting in both directions (compensation of trailback and taper) are 18.46 mm on the top and 18.56 mm on the bottom, i.e. the diameter difference is only 0.1 which means 0.54% of real top diameter (0.50% for set-up diameter). Difference between set-up and real diameter is caused by leaving out the jet radius being about 1.5 mm. For real object diameter 20 mm the set-up diameter should be approximately 21.5 mm. The experiments have also proved that even low pressure AWJ can efficiently cut composite materials. Therefore, cutting costs can be reduced, because pump pressure can be lowered and it means much lower capital costs and also operational costs (pump maintenance). The benefit of the AWJ composite cutting is negligible production of air pollution, namely composite material dust and fumes.

Very good results were obtained also with turning. The shape distortion is below 0.5% for non-optimized set of parameters. The surface roughness Ra is below 3.2 μm and it can be further improved by tuning respective parameters. The most important and closely connected parameters are the traverse speed (i.e. the velocity of jet movement along the rotational axis simultaneously with movement to this axis and from it) and the angular velocity (given by revolutions). Optimization of these two parameters is the main task to be solved on the way to commercial application of AWJ for turning. Nevertheless, the most important benefit of AWJ machining tool is elimination of the dangerous dust, namely glass particles, and toxic fumes from burning epoxy binder produced by conventional tools. Thus the application of AWJ machining can substantially reduce capital and operational costs necessary for exhausters and filters.

Provided that robot is used for manipulation with cutting head the possibilities of 3D machining will be increased substantially. Unfortunately, programming of cutting of the 3D objects by abrasive water jet is quite difficult, because it is necessary to take into account that residual energy of the AWJ is still efficient in material damage. Therefore, the programming process needs to calculate with anticipated directions of residual jet deflection. The merit of 3D AWJ machining is namely reduction of pollution, but some operations, when well prepared, can be less time consuming and more precise. However, the proper programming is not possible without deep and exact knowledge of deflected jet behaviour.

To obtain all necessary information the further research of AWJ, both theoretical and experimental, is inevitable.

## Conclusions

The preliminary experiments aimed at AWJ machining of composite materials proved that such machining is possible with a relatively high precision and inconsiderable amount of dust pollution in air. The accuracy of the machining is limited by precision of used machines and respective operation software. Nevertheless, the first tests show that product distortion and/or difference from entered contour can be substantially lower than 1 %. All these results indicate that correct optimization process can

improve production of final products by AWJ to be competitive with classical machining tools producing, simultaneously, much lower amount of health hazardous and risky by-products like dust and fumes. Therefore, further research and development aimed at improvement of AWJ machining for composite materials is strongly recommended.

#### Acknowledgements

Research presented in this contribution was supported by project CZ.01.1.02/0.0/0.0/15\_018/0004857 of the Ministry of Industry and Trade of the Czech Republic.

#### Literatura – References

1. CHE, C.L., HUANG, C.Z., WANG, J., ZHU, H.T., LI, Q.L. Theoretical model of surface roughness for polishing super hard materials with Abrasive Waterjet. *Advances in Machining and Manufacturing Technology IX, Key Engineering Materials*, 375-376, 2008, p. 465-469, ISSN 1662-9795.
2. HASHISH, M. A Modelling Study of Metal Cutting with Abrasive-Waterjets. *Journal of Engineering Materials and Technology – Transactions of the ASME*, 106(1), 1984, p. 88-100, ISSN 0094-4289.
3. HLAVÁČ, L.M., HLAVÁČOVÁ, I.M., GERYK, V., PLANČÁR, Š. Investigation of the taper of kerfs cut in steels by AWJ. *International Journal of Advanced Manufacturing Technology*, 77(9-12), 2015, p. 1811-1818, ISSN 0268-3768.
4. HLAVÁČ, L.M., HLAVÁČOVÁ, I.M., PLANČÁR, Š., KRENICKÝ, T., GERYK, V. Deformation of products cut on AWJ x-y tables and its suppression. *IOP Conference Series: Materials Science and Engineering*, 307 (1), 2018, Article number 0120152017, ISSN 1757-8981.
5. HLAVÁČ, L.M., STRNADEL, B., KALIČINSKÝ, J., GEMBALOVÁ, L. The model of product distortion in AWJ cutting. *International Journal of Advanced Manufacturing Technology*, 62(1-4), 2012, p. 157-166, ISSN 0268-3768.
6. LIANG, Z., XIE, B., LIAO, S., ZHOU, J. Concentration degree prediction of AWJ grinding effectiveness based on turbulence characteristics and the improved ANFIS. *International Journal of Advanced Manufacturing Technology*, 80(5-8), 2015, p. 887-905, ISSN 0268-3768.
7. MING, I.W.M., AZMI, A.L., CHUAN, L.C., MANSOR, A.F. Experimental study and empirical analyses of abrasive waterjet machining for hybrid carbon/glass fiber – reinforced composites for improved surface quality. *International Journal of Advanced Manufacturing Technology*, 95, 2018, p. 3809-3822, ISSN 0268-3768.
8. RABANI, A., MADARIAGA, J., BOUVIER, C., AXINTE, D. An approach for using iterative learning for controlling the jet penetration depth in abrasive waterjet milling. *Journal of Manufacturing Processes*, 22, 2016, p. 99-107, ISSN 1526-6125.
9. RUIZ-GARCIA, R., ARES, P.F.M., VAZQUEZ-MARTINEZ, J.M., GOMEZ, J.S. Influence of Abrasive Waterjet Parameters on the Cutting and Drilling of CFRP/UNS A97075 and UNS A97075/CFRP Stacks. *Materials*, 12, 2019, p. 1-18, ISSN 1996-1944.
10. WONG, M.M.I., AZMI, A.L., LEE, C.C., MANSOR, A.F. Kerf taper and delamination damage minimization of FRP hybrid composites under abrasive water-jet machining. *International Journal of Advanced Manufacturing Technology*, 94, 2018, p. 1727-1744, ISSN 0268-3768.
11. ZOHOURKARI, I., ZOHOOR, M., ANNONI, M. Investigation of the Effects of Machining Parameters on Material Removal Rate in Abrasive Waterjet Turning. *Advances in Mechanical Engineering*, 2014, Article Number 624203, ISSN 1687-8140.

#### *Redukcja zanieczyszczenia podczas obróbki kompozytów*

*Obróbka materiałów kompozytowych klasycznym sposobem, tj. przy użyciu konwencjonalnych narzędzi do toczenia, wiercenia, frezowania, szlifowania i polerowania, powoduje powstawanie bardzo małych cząstek – pyłu. Cząsteczki te dostają się do powietrza, ponieważ obróbkę należy wykonywać przy minimalnym zraszaniu, aby chronić właściwości materiału kompozytowego i uniknąć rozwarstwienia lub pęcznienia. Stosowana jest również obróbka epoksydu stosowanego jako spoiwo. Pył powstający podczas obróbki materiału kompozytowego może mieć negatywny wpływ na zdrowie i spowodować wybuch. Zapalenie skóry lub wdychanie toksycznej żywicy epoksydowej to tylko niektóre z przykładów. Powszechnym rozwiązaniem tego problemu jest odsysanie cząstek i oparów za pomocą maszyn wytwarzających podciśnienie. Usunięcie tych szkodliwych substancji z powietrza jest dość wymagające i kosztowne. Co więcej, stosowanie popularnych systemów ssących jest wielokrotnie mniej wydajne niż deklarowane przez producentów. W artykule przedstawiono nowy sposób walki z zanieczyszczeniami powodowanymi przez obróbkę kompozytów. Alternatywnym sposobem do obróbki kompozytów jest ścieranie strumieniem wody (AWJ). Ten sposób jest wydajny we wszystkich podstawowych procesach obróbki i powoduje powstawanie w powietrzu tylko około 1% niebezpiecznych zanieczyszczeń w porównaniu do klasycznych narzędzi. Przedstawiono postępy systemu obróbki AWJ opartego na robocie jako urządzeniu ruchowym i komentowano pierwsze wyniki. Główna uwaga skupiona jest na możliwościach obróbki strumieniem wody. Przedstawiono również inne współczesne badania koncentrujące się na zmniejszeniu tłumieniu zanieczyszczeń z procesu obróbki kompozytów.*

**Słowa kluczowe:** kompozyt, cięcie strumieniem wody, cięcie, toczenie, zanieczyszczenie



# Influence of High-Power Electromagnetic Pulses on the Structural-Chemical and Physicochemical Properties of Rare-Earth Minerals

Valentine A. CHANTURIYA, Igor Zh. BUNIN, Maria V. RYAZANTSEVA<sup>1)</sup>

<sup>1)</sup> Institute of Comprehensive Exploitation of Mineral Resources Russian academy of Sciences named after academician N. V. Mel'nikov, 4. Krukovsky tupic, 111020 Moscow, Russia; email: ryzanceva@mail.ru

<http://doi.org/10.29227/IM-2020-01-63>

Submission date: 14-02-2020 | Review date: 22-04-2020

## Abstract

*The investigation of the structural-chemical state and sorption properties modification of columbite and eudialite surface under the impact of high-power nanosecond pulses (HPEMP) was performed using XPS and FTIR. It was defined that preliminarily treatment of rare-metal minerals with high-power nanosecond pulses is promising tool for the directional changes in their physicochemical and structural-chemical properties as it was confirmed by the increasing of mineral's sorption activity.*

**Keywords:** columbite, eudialite, high – power electromagnetic pulses, XPS, FTIR

## Introduction

The flotation of rare earth minerals is important for the economic recovery of rare earth minerals from their ores. Flotation is a key step in the industrial production of RE materials, understanding the process of RE flotation will facilitate improvement in the flotation recovery and more efficient production of RE s for their numerous application. Systematic studies on RE flotation are urgently required, the research presented in this study id directed toward the better understanding the RE minerals flotation regularities.

## Materials and methods

The mineral samples of columbite and eudialite used in this study (size fractions - 100 + 63  $\mu\text{m}$ ) contained about 98% of the studied mineral according to XRD results.

The treatment of minerals 'samples by high-power nanosecond video pulses [1] was carried out in air atmosphere under standard conditions and the following electro physical parameters of the impulse treatment:  $\tau \sim 1 - 5 \text{ ns}$  – pulse front,  $\tau \sim 50 \text{ ns}$  – pulse duration,  $U \sim 25 \text{ kV}$  – pulse amplitude,  $E \sim 107 \text{ V/m}$ , pulse repetition rate is 100 Hz, pulse energy  $\sim 0.1 \text{ J}$ , processing time (t) of mineral samples were varied from 10 s to 150 s. Before electromagnetic pulse treatment, the concentrate samples were wetted with distilled water with ration of solid to liquid respect to S: L = 5: 1 according to recommendations [2].

X-ray photoelectron spectra were obtained on a Versa Probe II spectrometer (ULVAC-PHI; Material Science and Metallurgy Collective Center) at NITU MISiS using monochromatic Al K $\alpha$  radiation with an energy of 1486.6 eV; power X - ray source  $\sim 50 \text{ watts}$ . The XPS spectra were recorded in the constant transmit energy mode of the analyzer, which was 160 eV for the recording of survey spectra, and 29.35 eV for recording the spectrum of Si 2 p. The survey spectrum was recorded with a step of 1.0 eV, the high resolution spectrum of the 2 p line of silicon – with a step of 0.1 eV.

To prevent the effect of charging minerals, powder samples were pressed into an indium plate, then the samples were

placed in the spectrometer chamber and examined at room temperature under vacuum with a residual pressure of less than  $6.7 \times 10^{-8} \text{ Pa}$ , the diameter of the analysis area was 200  $\mu\text{m}$ .

To eliminate the effect of charging the samples the registration of spectra was performed using double neutralization. The obtained spectra were calibrated by the binding energy of the low-energy component in the spectrum of 1 s electrons of carbon atoms (C 1s line) of hydrocarbons adsorbed on the sample surface; The binding energy of this component was assumed to be 285.0 eV. To obtain qualitative and quantitative information on the composition of the surface of minerals, the spectra of individual lines of elements were fitted according to standard procedures using the Casa XPS program.

The technique of the adsorption experiment was as follows: a 0.5 g mineral was placed in the cell of a laboratory flotation machine and agitated in distilled water for 3 minutes (S: L = 1: 20), then the pH was adjusted to the required value (NaOl - pH 9.0 (NaOH); Flotisor sm 15 – pH 3.5 (H<sub>2</sub>SO<sub>4</sub>); CH<sub>3</sub> (CH<sub>2</sub>)<sub>6</sub> C (O) N (H) OH – 6.0 (HCl) and the reagent was added (300 mg / l), the contact time with the collector – 3 minutes, after that the solid phase was separated by filtration, washed with a tenfold volume of distilled water and dried in air.

IR spectra were obtained in the wavelength range from 4000  $\text{cm}^{-1}$  to 400  $\text{cm}^{-1}$  (spectral resolution 4  $\text{cm}^{-1}$ ) using an Fourier transform spectrometer (IR – Affinity, Shimadzu) and the diffuse reflectance attachment (Diffuse IR, Pike Technologies). For each sample, at least five spectra were obtained; the number of scans was 50 for each spectra.

## Results and discussion

### XPS

Table 1 presents the experimental results of the columbite (manganocolumbite) surface chemical composition 'changes as a result of pulsed energy impact; the chemical composition was determined by the survey XPS spectra. The compo-

Tab. 1. Influence of high-power electromagnetic pulses on the chemical composition of the columbite surface according to XPS results, at. %  
 Tab. 1. Wpływ impulsów elektromagnetycznych dużej mocy na skład chemiczny powierzchni kolumbitu zgodnie z wynikami XPS, przy. %

N pulses, 10 <sup>3</sup>	Nb	Ta	O	Fe	Si	Al	F	Zn	Pb	Th	C
0	1.7	0.2	54.2	5.5	6.9	3.4	1.3	0.7	1.2	0.3	24.6
1	1.2	0.2	53.4	5.2	7.3	3.3	1.3	0.5	1.0	0.2	26.6
5	1.7	0.3	52.4	4.3	6.6	3.5	1.1	0.7	1.0	0.3	28.3
10	2.0	0.1	51.9	4.9	5.4	3.1	1.5	0.5	1.1	0.2	29.4
15	2.2	0.1	48.8	8.3	5.5	2.6	2.4	0.7	1.4	0.2	25.7
30	2.4	0.7	53.0	6.1	5.5	2.8	1.9	0.6	1.2	0.4	23.8

Tab. 2. Influence of the treatment by high-power electromagnetic pulses on the columbite surface state according to XPS, at. %  
 Tab. 2. Wpływ obróbki impulsami elektromagnetycznymi o dużej mocy na stan powierzchni kolumbitu określone XPS, przy. %

N pulses, 10 <sup>3</sup>	O 1s	
	$E_{CB} = 530.0 \text{ eV}$ Nb <sub>2</sub> O <sub>5</sub> , Fe <sub>2</sub> O <sub>3</sub>	$E_{CB} = 532.0 \text{ eV}$ SiO <sub>2</sub> , Al <sub>2</sub> O <sub>3</sub> , OH, H <sub>2</sub> O <sub>adsorbed</sub> , O-C <sub>opr</sub>
0	15	85
1	15	85
5	20	80
10	20	80
15	23	77
30	24	76

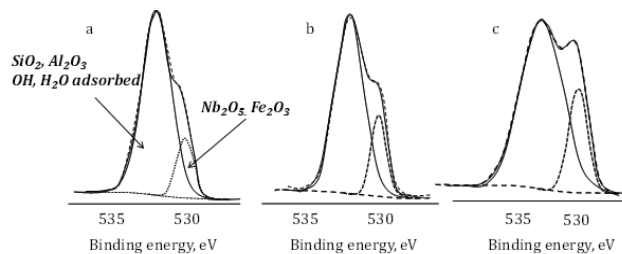


Fig. 1. O 1s line of columbite samples before (a) and after (b), (c) the treatment by high – power electromagnetic pulses during 150 s (b) and 300 s (c)  
 Rys. 1. Linia O 1s próbek kolumbitu przed (a) i po (b), (c) obróbki impulsami elektromagnetycznymi o dużej mocy przez 150 s (b) i 300 s (c)

sition of the mineral surface before and after the treatment was characterized by the presence of Nb, O and Fe atoms in an amount sufficient to analyze their chemical and valent state by XPS.

Registration and subsequent analysis of the Nb 3d, Fe 2p lines showed that the spectral characteristics did not change as result of the treatment, namely, the Nb 3d 5/2 doublet (BE = 206.9–207.0 eV) corresponded to the state of niobium pentoxide Nb<sub>2</sub>O<sub>5</sub> [3]; The position of the Fe 2p3/2 peak (BE = 711.4–711.8 eV) indicated that the chemical state of the iron atoms in the surface layer of the particles of the studied mineral was close to maghemite ( $\gamma$  – Fe<sub>2</sub>O<sub>3</sub>) or lepidocrocite ( $\gamma$  – FeO (OH)) [4].

The O 1s line (figure 1) was fitted with two components: the first with a binding energy BE ~ 530.0 eV corresponded to structural oxygen in the structure of Nb<sub>2</sub>O<sub>5</sub> and  $\gamma$  – Fe<sub>2</sub>O<sub>3</sub> ( $\gamma$  – FeOOH); the second contribution with BE ~ 532.0 eV was attributed to silicon and aluminum oxides and, presumably, hydroxogroups adsorbed on the surface of the mineral, oxygen in organic pollutants, and chemisorbed water molecules [5].

The a result of the columbite samples electromagnetic treatment for 10–150 s (range from 103 to 1.5 × 10<sup>4</sup> pulses) is a consistent increase in the O 1s spectra component with a binding energy of BE ~ 530.0 eV, corresponding to structural oxygen atoms in niobium and iron oxides (Table 2, Fig. 1), and a decrease by 5–9 at.% of the the high-energy com-

ponent with BE ~ 532.0 eV, which characterizes the presence on the mineral surface of SiO<sub>2</sub>, Al<sub>2</sub>O<sub>3</sub>, adsorbed water and functional hydrosogroups (Table 2). Since the surface concentration of Si and Al (at.%) remained constant during the treatment (Table 1), it can be assumed that at long treatment times (1.5–3.0) × 10<sup>4</sup>, 2.5–5.0 min) were accompanied by thermal removal of hydroxo groups and chemisorbed water molecules from the surface of columbite (dihydroxylation – dehydration) due to local temperature increase [6].

#### DRIFT

IR spectra of columbite samples after contact with the collector in the initial state, as well as after treatment by high-power nanosecond electromagnetic pulses are given in the figure 2. IR spectra of the columbite sample in the initial state (Figure 2 a) demonstrate the presence of the bands indicating the adsorption of the collector. The presence of a peak at 1530 cm<sup>-1</sup> and 1600 cm<sup>-1</sup> indicates the formation of Fe (III), tantalum and niobium on the surface [7, 8], and a weak shoulder at 1670 cm<sup>-1</sup> indicates the presence of a physically adsorbed hydroxamic acid [9]. Based on this, capryl-hydroxamic acid is adsorbed chemically on the surface of columbite predominantly, with the formation of complex compounds with metal atoms; the amount of physically adsorbed hydroxamic acid is small. A comparative analysis of the IR spectra showed a profile change: the shoulder at 1670 cm<sup>-1</sup> identified for the initial sample and corresponding to

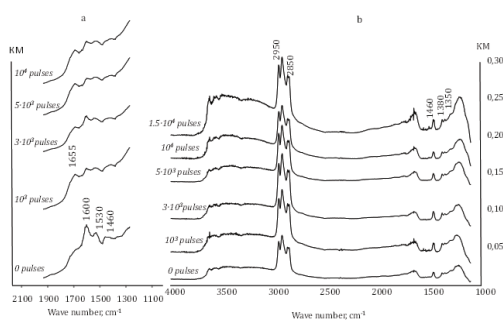


Fig. 2. DRIFT spectra of columbite (a) and eudialite (b) samples after the interaction with Flotisor sm 15 for untreated samples (0 pulses) and samples after the treatment by high-power electromagnetic pulses

Rys. 2. Widma DRIFT próbek kolumbitu (a) i eudialitu (b) po interakcji z Flotisor sm 15 dla próbek nietraktowanych (0 impulsów) i próbek po obróbce impulsami elektromagnetycznymi o dużej mocy

the physical sorption of hydroxamic acid transform into the clear band (Figure 2a) for the samples after the treatment by high-power electromagnetic pulses that indicates an increase in the quantity of physically adsorbed collector.

IR spectra of treated and untreated eudialite samples after the contact with Flotisor sm 15 are shown in Figure 2 b. The presence of the bands indicating the adsorption of the reagent were identified:  $1350\text{ cm}^{-1}$ ;  $1380\text{ cm}^{-1}$ ;  $1460\text{ cm}^{-1}$ ;  $2850\text{ cm}^{-1}$ ;  $2950\text{ cm}^{-1}$ . At the same time, the position of the spectral peaks for the adsorbed Flotisor sm 15 coincides with the spectrum of the pure substance indicating the physical adsorption of the collector.

The calculation of the spectra ' peak areas demonstrates that the preliminary high-power electromagnetic treatment of eudialyte results in the increasing of the Flotisor sm 15 adsorption. The area of the band at  $1380\text{ cm}^{-1}$  increases 4.3–7 times (from 0.03 (untreated sample) to 0.124 relative units ( $10^3$  pulses) and further to 0.22 ( $5 \cdot 10^3$  pulses), the area of the peak at  $1460\text{ cm}^{-1}$  increases by 3.5–7 times (from 0.05 (0 pulses) to 0.18 ( $10^3$  pulses) and further to 0.35 ( $5 \cdot 10^3$  pulses).

As a result of studies, it was identified that the use of pulsed energy (high-power electromagnetic pulses) gives a possibility of the minerals technological properties regulation. It was found that usage of high-power electromagnetic treatment of eudialite before the acid leaching allows to increase the zirconium recovery of 1.7 times and  $\Sigma\text{ REE}$  – 1.4 times [10]. It is shown that the usage of high – power electromagnetic treatment ( $N\text{ pulses} = 5 \times 10^3 \div 10^4$ ) allows to improve the columbite floatability by 4–9% [11].

## Conclusion

The structural and chemical transformations of the manganocolumbite surface as a result of non-thermal treatment by high-power nanosecond electromagnetic pulses were studied. According to XPS data, at the initial stages at low treatment durations (from  $10^3$  pulses to  $5 \times 10^3$  pulses), the surface state of mineral was characterized by the presence of hydroxyl groups and adsorbed water molecules. With the increasing of the treatment duration up to  $5 \times 10^3 - 1.5 \times 10^4$ , chemisorbed water and hydroxogroups were removed from the surface of columbite.

With usage of DRIF was defined that treatment by high-power electromagnetic pulses allows to control the physicochemical properties of columbite and eudialyte. The growth of the sorption activity for eudialyte towards Flotisor sm 15 was defined. It was identified that the areas of the bands describing the adsorption of the reagent into mineral surface increased on average 4 to 7 times for the samples after the high-power electromagnetic treatment. It is shown that treatment by high-power electromagnetic pulses results to the increasing of the of manganocolumbite sorption activity towards octanohydroxamic acid. The shoulder at  $1670\text{ cm}^{-1}$ , identified for the untreated sample and corresponding to the physically adsorbed reagent transform in the clear absorption band in the case of the sample that was treated by high-power electromagnetic pulses.

## Acknowledgements

This work was supported by the Russian Science Foundation (project № 16 – 17 – 10061).

## Literatura – References

1. Bunin I. Zh. et. al. Experimental study of non-thermal effects of high - power electromagnetic pulses on refractory gold - bearing raw materials. *Izv. RAS. Ser. Physical*, 65, 2001, p. 1788 – 1792.
2. Chanturiya V.A. et. al. Synergistic effect of powerful electromagnetic pulses and pore moisture on the opening of gold-bearing raw materials. *Academy of Sciences Reports*, 379, 2001, p. 372 – 376.
3. Ozer N. et. al. Preparation and properties of spin-coated Nb2O5 film by the sol-gel process for electrochromic application. *Thin Solid Films*, 277, 1996, p. 162 – 168.
4. Grosvenor A. P. et. al. Investigation of multiplets splitting of Fe 2p XPS spectra and bonding in iron compounds. *Surface and interface analysis*, 36, 2004, p. 1564 – 1574.
5. Wagner C. D., Naumkin A. V., Kraut-Vass A. et al. NIST X-ray photoelectron spectroscopy database, standard reference database 20, Vers. 3.4, Web version, 2000 – 2008, <http://srdata.nist.gov/xps>
6. Chanturiya V.A. et. al. Energy concentration in electrical discharges between particles of semiconductor sulfide minerals during the interaction with high – power nanosecond pulses. *Izv. RAS. Ser. Physical*, 8, 2008, p. 1118 – 1121.
7. Brown D. A. et. al. The infrared spectra of monohydroxamic acid complexes of copper, iron and nickel. *Inorganica Chimica Acta*, 35, 1979, p. 57 – 60.
8. Cui Jianlan et. al. Spectroscopic investigation of the interaction of hydroxamate with bastnaesite (cerium) and rare earth oxides. *Minerals Engineering*, 36 – 38, 2012, p. 91–99.
9. Raghavan S. and Furstenau D.W. The adsorption of aqueous octylhydroxamate on ferric oxide. *Journal of colloid and interface science*, 50, 1975, p. 319 – 330.
10. Chanturiya V.A. et. al. Intensification of eudialyte concentrate leaching process with usage of high – power electromagnetic pulses. *Physical and technical problems of mining*, 4, 2015, p. 134 – 144.
11. Chanturiya V.A. et. al. Modification of the structural-chemical and technological properties of rare metals minerals with usage of high – power electromagnetic pulses. *Physical and technical problems of mining*, 4, 2017, p. 117 – 134.

## *Wpływ impulsów elektromagnetycznych dużej mocy na właściwości strukturalne, chemiczne i fizykochemiczne minerałów ziem rzadkich*

*Badanie modyfikacji stanu strukturalno-chemicznego i właściwości sorpcyjnych powierzchni kolumbitu i eudialitu pod wpływem impulsów nanosekundowych o dużej mocy (HPEMP) przeprowadzono za pomocą XPS i FTIR. Ustalono, że wstępna obróbka minerałów metali rzadkich impulsami nanosekundowymi o dużej mocy jest obiecującym narzędziem do kierunkowych zmian ich właściwości fizykochemicznych i strukturalno-chemicznych, co zostało potwierdzone przez zwiększenie aktywności sorpcyjnej minerału.*

**Słowa kluczowe:** kolumbit, eudialyte, impulsy elektromagnetyczne dużej mocy, XPS, FTIR



# Study on Addition of Surfactants Agents to Improve the Behavior of High Water Content Sediment for Rare Earth Mining in Deep Sea

Takashi SASAOKA<sup>1)</sup>, Akihiro HAMANAKA<sup>1)</sup>, Takahiro FUNATSU<sup>1)</sup>,  
Hideki SHIMADA<sup>1)</sup>, Keisuke TAKAHASHI<sup>2)</sup>

<sup>1)</sup> Kyushu University, Department of Earth Resources Engineering, 744, Motoooka, Nishi-ku, Fukuoka, Japan;  
email: hamanaka@mine.kyushu-u.ac.jp, funatsu@mine.kyushu-u.ac.jp, sasaoka@mine.kyushu-u.ac.jp, shimada@mine.kyushu-u.ac.jp,  
keisuke@mine.kyushu-u.ac.jp

<sup>2)</sup> Construction Materials Research Center, Ube industries, Ltd., 1-6, Okinoyama, Kogushi, Ube, Yamaguchi, Japan;  
email: takahashi@ube-ind.co.jp

<http://doi.org/10.29227/IM-2020-01-64>

Submission date: 04-02-2020 | Review date: 12-03-2020

## Abstract

Importance of rare mineral metal resources is increasing currently. Therefore, the rare earth elements rich mud which exist on the deep-sea floor has the potential to be developed to fulfill their demand. As one of the effective mining method, a suction mining method is expected to apply to seabed mining. The seabed sediment containing rare earth element shows the very high water content, more than 100%. And the sediment movement during the suction is greatly affected by the water content ( $W_c$ ) and liquid limit ( $W_L$ ) of the material. Therefore, it is important to modify the liquid limit by adding a chemical agent to control the behavior of sediment. We selected eight different surfactants which can be divided into three types. They are dispersant type, water retention type, and thickener type. We carried out a liquid limit test and viscosity measurement of the sediment mixed with the agents. It is found that the water-absorbing polymer and the hydroxyethyl cellulose increase the liquid limit and viscosity. Whereas, the alkyl ammonium salt surfactant and the alkyl ammonium salt, alkyl aryl sulfonate blend decrease the liquid limit and viscosity. It is possible to control sediment behavior by adding suitable surfactants.

**Keywords:** deep sea mining, high water content sediment, rare earth, surfactants agent

## Introduction

In recent years, the demand for rare mineral resources has grown and a lot of investigations have been conducted to discover new ore deposits all over the world. As a result, it was discovered that abundant rare-earth elements-rich mud exists on the deep sea floor (Kato et al., 2011, Hirai, 2014, Agency for Natural Resources and Energy, 2016). In recent years, some seabed mining method by using road header, drum cutter, or suction pump were developed all over the world (JOGMEC, 2010). Especially, suction pump mining is considered as one of effective methods for rare-earth elements-rich mud mining because it needs smaller-scale machine and less cost than other mining methods. However, it is required to evaluate the deformation behavior of rare-earth elements-rich mud in seabed mining because it will cause suspension and topographic variation (Ministry of the Environment, 2011) though there are some researches to minimize the environmental disturbance by adopting cement-based sealants (Sakamoto et al., 2016, Takahashi et al., 2017). For this reason, it is important to control the deformation behavior of rare-earth elements-rich mud in order to evaluate environmental impact in seabed mining. In the previous study, Tagami et al. (Tagami et al., 2017) reported that the deformation behavior of the mined seabed sediments is classified based on the ratio of water content and liquid limit as shown in Figures 1 (a)~(c). Therefore, if the liquid limit of the sediment can be varied by adding materials such as surfactants agents, the deformation behavior of the sediment can be controlled in order to obtain

more suitable behavior for mining. This paper discussed the deformation behavior of seabed sediment by adding several different types of surfactants agents and measure the liquid limit and viscosity to evaluate the effectiveness.

## Material and methods

### Preparation of simulated sediment sample

Rare-earth elements-rich mud is classified as clay on soil classification. However, liquid limit and water content of rare-earth elements-rich mud are different depending on the place and it is expected that these difference change the deformation behavior of rare-earth elements-rich mud on suction mining. The geotechnical properties of rare earth rich mud are shown in Table 1. The simulated sediment samples which had the liquid limit and water content were prepared and used in the laboratory test. Those soil samples were prepared by blending two types of bentonite clay in different mixing ratio. Liquid limit and water content of the sample are 120% and 130% respectively.

The flowability of the particles suspended in the liquid generally depends on the dispersion and aggregation of the suspended particles. When a strong attractive force is generated between the particles and strongly aggregated primary aggregates or secondary aggregates due to the weak attraction are formed, the water restrained between the particles increases and the free water involved in the fluidity decreases and the fluidity decreases. On the other hand, when a strong repulsive force acts on the particles, the particles are dis-



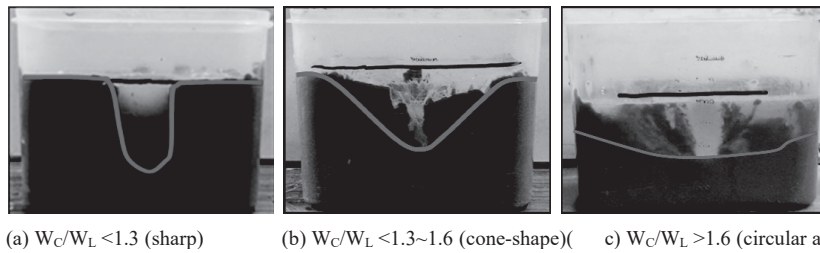


Fig. 1. Classification of deformation behavior of simulated soil based on the water content ( $W_c$ ) and the liquid limit ( $W_L$ )  
 Rys. 1. Klasyfikacja deformacji dla symulowanej charakterystyki gleby na podstawie zawartości wody ( $W_c$ ) oraz limitu ciecizy ( $W_L$ )

Tab. 1. Properties of sample of rare-earth elements-rich mud (Agency for Natural Resources and Energy, 2016)  
 Tab.1. Właściwości próbki podłoża z pierwiastkami ziem rzadkich (Agency for Natural Resources and Energy, 2016)

	A-1	A-2	A-3	A-4	B	C
Density ( $\text{g}/\text{cm}^3$ )	2.850	2.831	2.792	2.792	2.833	2.821
Liquid limit (%)	116.3	111.1	98.7	105.4	117.1	109.8
Water content (%)	124.1	138.9	156.3	140.3	128.8	146.1

Tab. 2. Surfactants used in this study

Tab. 2. Odczynniki powierzchniowe zastosowane w badaniu

Group	Surfactant	Addition ratio (%)		
		0.2	0.5	1.0
Dispersant	Low molecular weight polycarboxylic acid ethers	0.2	0.5	1.0
	High molecular weight polycarboxylic acid ethers	0.2	0.5	1.0
Water retention agent	Alkyl ammonium salt	0.2	0.5	1.0
	Hydroxypropylmethylcellulose	0.2	0.5	1.0
	Water-absorbing polymer	0.2	0.5	1.0
Thickener	Hydroxyethyl cellulose	0.2	0.5	1.0
	Alkyl ammonium salt, Alkyl aryl sulfonate blend	0.2	0.5	1.0
	Polyacrylamide	0.2	0.5	1.0

persed, restrained water is reduced, and fluidity is improved. Considering those mechanisms above, the surfactants agents which are classified as three groups as shown in Table 2 were added with 0.2~1.0% by the weight of the simulated sediment samples in order to control the dispersion and aggregation of the suspended particles.

Liquid limit and viscosity were measured to evaluate the properties of the sediment samples. Liquid limit tests were conducted according to the test method for liquid limit and plastic limit of soils (JIS A 1205:2009). Soil sample is put in a brass dish with a thickness of 1 cm and cut a groove in the sample in the cup. Turn the handle of the device at a ratio of 2 drops per second. Count the number of blows until the two halves of the soil sample come in contact along a distance of 1.5 cm. Adding or evaporating water to collect the data. The viscosity of the sample was measured by B type viscometer. One cycle of changing the rotational speed in the order of 0.3, 0.6, 1.5, 3.0, 6.0, 12, 30, 60, 30, 12, 6.0, 3.0, 1.5, 0.6, 0.3 rpm. The cycle is repeated for a total of 4 times. The interval of each speed is 30 seconds. The average viscosity of the 60 rpm from the 2nd to 4th cycle was calculated as the viscosity during suction pumping.

#### Suction pump test

In order to evaluate the deformation behavior of simulated soil samples, suction quantity and influence range were measured by a suction pump test. Conceptual diagram of a suction pump test is shown in Figure 2. The suction force of the pump was adjusted in 4.0 kPa (maximum suction force of the pump is 21.4 kPa). The caliber of a suction pump was 10 mm and the suction time was 8 seconds. The suction area was

50 mm depth from the simulated soil surface. After the suction pump test, deformation behavior of simulated soil was observed and the maximum vertical length ( $V$ ) and horizontal length ( $H$ ) of the deformation area were measured. Influence range was defined as  $H/V$ . Furthermore, the ratio of water content and liquid limit ( $W_c/W_L$ ) was defined in order to evaluate the fluidity of simulated soil samples quantitatively.

## Results and discussion

### Properties of sediment sample by addition of surfactant agents

Figures 3 (a)~(c) show the relationship between the liquid limit and addition ratio. When water retention agents were added, liquid limit increased, whereas, dispersant type agents tend to reduce the liquid limit. For the thickener type agents, a specific trend was not observed. Further, when the hydroxyethyl cellulose and the water absorbing surfactant were added, a larger effect of increasing the liquid limit was obtained as compared with other surfactants. On the other hand, the alkyl ammonium salt and the alkyl ammonium salt, alkyl sulfonate blend was used, the liquid limit decreased significantly. Figures 4 (a)~(c) show the relationship between the ratio of water content to liquid limit ( $W_c/W_L$ ) and the addition ratio of each surfactant when the water content of sediment sample is 130%. As the water content is constant, the trend of the variation of the ratio is similar to the trend of liquid limit variation.

The viscosity test was conducted on each sample under the same conditions of  $W_c/W_L$  indicated in Figure 4. Figures 5 (a)~(c) show the relationship between the viscosity and the addition ratio of each surfactant. As shown in the figure,

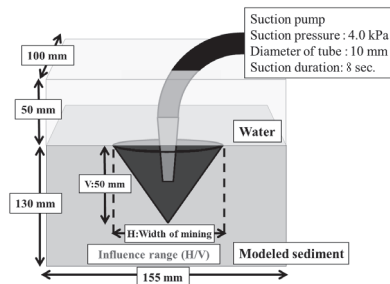


Fig. 2. Conceptual diagram of suction pump test  
Rys. 2. Diagram koncepcyjny testu pompy ssącej

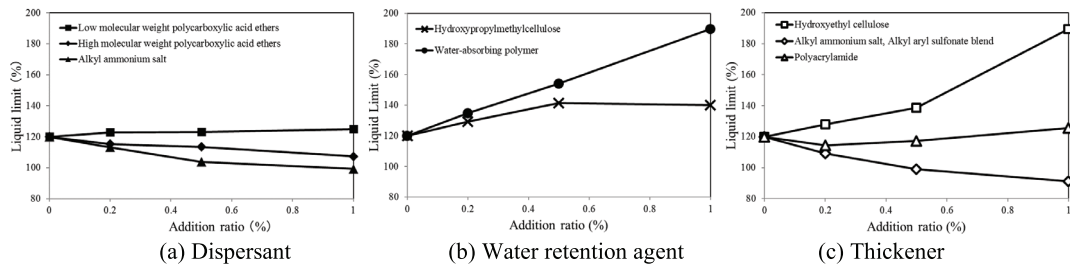


Fig. 3. Relationship between liquid limit and addition ratio of each surfactant

Rys. 3. Zależność pomiędzy limitem cieczy a stopniem dodania każdego odczynnika powierzchniowego

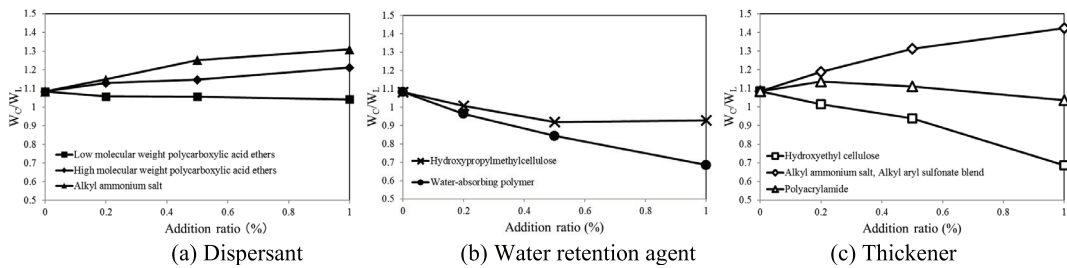


Fig. 4. Relationship between the ratio of water content to liquid limit ( $W_c/W_L$ ) and addition ratio of each surfactant

Rys. 4. Zależność pomiędzy zawartością wody a limitem cieczy ( $W_c/W_L$ ) oraz stopniem dodania każdego odczynnika powierzchniowego

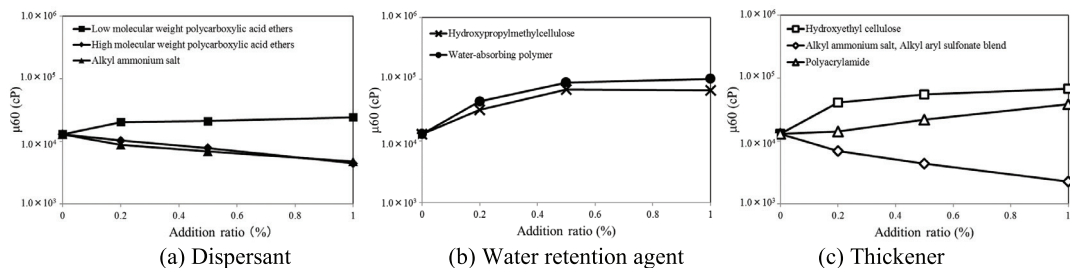


Fig. 5. Relationship between viscosity and addition ratio of each surfactant

Rys. 5. Zależność pomiędzy lepkością a stopniem dodania każdego odczynnika powierzchniowego

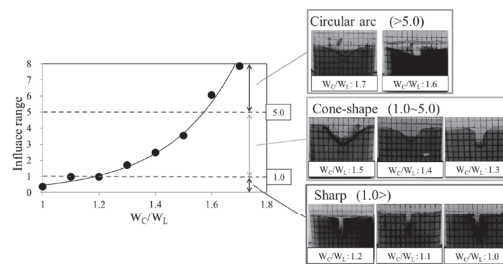


Fig. 6. Definition of influence range for 3 types based on  $W_c/W_L$ : circular arc, cone-shape, and sharp

Rys. 6. Definicja stopnia wpływu dla trzech typów na podstawie  $W_c/W_L$ : łuk kolisty, kształt stożkowy oraz łuk ostry

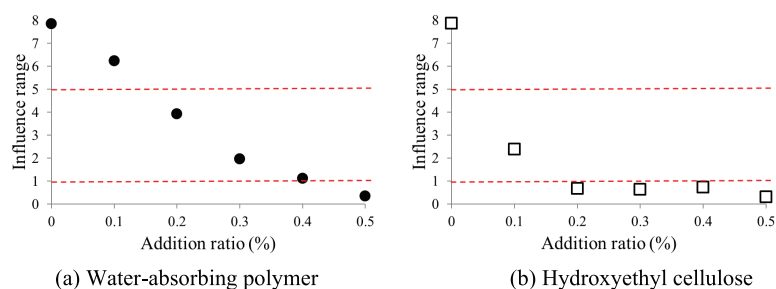


Fig. 7. Modification effect by suction test: circular to cone-shape

Rys. 7. Wpływ modyfikacji typu łuku kołowego na kształt stożkowy w teście ssania

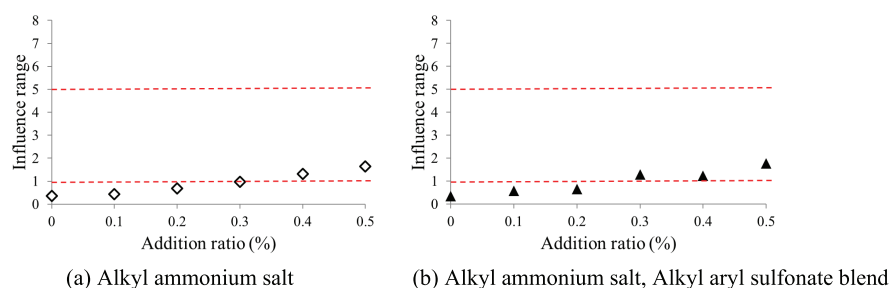


Fig. 8. Modification effect by suction test: sharp to cone-shape

Rys. 8. Wpływ modyfikacji kształtu ostrego na kształt stożkowy w teście ssania

when the water absorbent polymer, hydroxypropyl methylcellulose, and hydroxyethyl cellulose were added, the viscosity increased more than the other surfactants. In addition, when the alkyl ammonium salt, high molecular weight polycarboxylic acid ethers, and the alkyl ammonium salt, alkyl sulfonate blend surfactants were added, the viscosity decreased. These results agree with those of the relationship between the liquid limit.

Considering the modification of liquid limit and viscosity, the surfactants of water-absorbing polymer and hydroxyethyl cellulose seem to be effective to change the deformation behavior from circular arc to cone-shape while alkyl ammonium salt and alkyl ammonium salt, alkyl aryl sulfonate blend seem to be effective for the changing the behavior from sharp to cone-shape. Therefore, the actual deformation behavior owing to the suction mining is discussed in the next section.

#### Deformation behavior of sediment sample in suction pump test

In order to confirm the effectiveness to control the deformation behavior by adding surfactants, the suction pump test was carried out. The deformation behavior was evaluated by using the influence range defined as 3 types: circular arc, cone-shape, and sharp. Figure 6 shows a definition of influence range in this study for 3 types based on  $W_c/W_L$ .

Figures 7 (a) and (b) show the results of deformation behavior when water-absorbing polymer and hydroxyethyl cellulose are added. From these results, both surfactants are effective to change the deformation behavior from circular arc to cone-shape because the influence range is reduced with the increase of addition ratio. Additionally, the hydroxyethyl cellulose is more effective to control the deformation behavior of sediments because the less adding of the surfactant is enough to change the deformation behavior. This result is inconsistent with the fundamental properties of the sediment sample; the  $WC/WL$  is higher and the viscosity is smaller in the sediment

sample added hydroxyethyl cellulose compared to that of water-absorbing polymer. Therefore, a more detailed study will be needed to conduct the quantitative evaluation of the effects to change deformation behavior such as viscoelasticity properties and the viscosity under the different rotational speed.

Figures 8 (a) and (b) show the results of deformation behavior when alkyl ammonium salt and alkyl ammonium salt, alkyl aryl sulfonate blend are added. These results indicate the effectiveness of the addition of both surfactants to change the deformation behavior from sharp to cone-shape. Additionally, both surfactants have an almost similar effect to change the deformation. However, the addition of alkyl ammonium salt and alkyl ammonium salt, alkyl aryl sulfonate blend is less effective to control the deformation behavior than that of water-absorbing polymer and hydroxyethyl cellulose. This can be explained by the fundamental properties of the sediment samples; the changing of liquid limit, viscosity, and  $WC/WL$  are less compared to the surfactants of water-absorbing polymer and hydroxyethyl cellulose.

From the above results, in the modification of the suction behavior of the simulated sediment, it is possible to select the suitable surfactants agents. For example, if the behavior have to be modified from a circular arc structure to a cone-shape one, it is considered that the water-absorbing polymer and hydroxyethyl cellulose are applicable. When the behavior have to be modified from a sharp structure to a cone-shape one, it is preferable to use an alkyl ammonium salt surfactant and an alkyl ammonium salt, alkyl aryl sulfonate blend.

#### Conclusion

In order to investigate the modification method of rare earth sediment fluidity, a series of laboratory experiments were conducted. We selected 8 different surfactants which can be divided into 3 types. They are dispersant type, water reten-

tion type, and thickener type. The fundamental properties of the sediment mixed with the surfactants were measured by the liquid limit test and viscosity measurement. Additionally, the suction pump test was carried out to confirm the effectiveness to control the deformation behavior during suction mining. As a result, proper selection of surfactants can modify the liquid limit and viscosity and lead to control the deformation behavior of the sediments. In order to conduct the quantita-

tive evaluation of the effects to change deformation behavior, a more detailed study has to be needed such as viscoelasticity properties and the viscosity under the different rotational speed.

#### **Acknowledgements**

This work was supported by JSPS KAKENHI Grant Number JP 19K05351.

## Literatura – References

1. KATO, Yasuhiro et al. Deep-sea mud in the Pacific Ocean as a potential resource for rare-earth elements. *Nature Geoscience*, 4, 2011, p. 13-24, 2011, ISSN 1752-0894.
2. HIRAKI, Koji. Trends in Metal Resource Development and Strategies for Resource Security, *Surface Science for Resource*, 35(2), 2014, p. 114-115, ISSN 1881-4743.
3. Agency for Natural Resources and Energy, Report of Resource Potential Assessment for Rare Earth Sediments, [online]. c2016 [cit. 2019-04-02]. Dostępny z WWW: < <https://www.meti.go.jp/press/2016/07/20160706004/20160706004-2.pdf>>. (Japanese).
4. JOGMEC, Study of Mining System of Seafloor Hydrothermal Deposits [online]. c2010 [cit. 2019-04-02]. Dostępny z WWW: < [http://mric.jogmec.go.jp/kouenkai\\_index/2010/briefing\\_100527\\_5.pdf](http://mric.jogmec.go.jp/kouenkai_index/2010/briefing_100527_5.pdf)>. (Japanese).
5. Ministry of the Environment, Report of Technology Assessment of Environmental Impact, [online]. c2011 [cit. 2019-04-02]. Dostępny z WWW: < [http://warp.da.ndl.go.jp/info:ndljp/pid/11057318/www.neti.env.go.jp/policy/assess/4-1-report/file/h23\\_08i.pdf](http://warp.da.ndl.go.jp/info:ndljp/pid/11057318/www.neti.env.go.jp/policy/assess/4-1-report/file/h23_08i.pdf)>. (Japanese).
6. SAKAMOTO, Seiichi et al. Fundamental Study on Deformation Behavior of Seafloor Covered with Sealing Materials in Seabed Mining, *Proc. International Symposium on Earth Science and Technology 2016*, 2016, 74-78. ISBN 978-4-9902356-5-9.
7. TAKAHASHI, Keisuke et al. Application of Cement-based Sealants for Prevention and Remediation of Environmental Impact of Submarine Resource Mining, *Proc. of 26th International Symposium on Mine Planning & Equipment Selection*, 2017, 363-367. ISBN 978-91-7583-935-6.
8. TAGAMI, Taiko et al. Study on Deformation Behavior of Rare-Earth Elements-Rich Mud and Applicability of Sealing Materials in Seabed Mining, *Proc. International Symposium on Earth Science and Technology 2017*, 2017, 161-164. ISBN 978-4-9902356-6-6.

## *Badanie wpływu odczynników powierzchniowych na poprawę właściwości osadu pod kątem głębinowego górnictwa pierwiastków rzadkich*

Złoża metali rzadkich są bardzo ważne a ich istotność wzrasta w ostatnich latach. Zatem, dno morskie, które zawiera duże ilości tego typu pierwiastków posiada potencjał do zaspokojenia potrzeb w tym zakresie. Jako jedną z efektywnych metod górniczych w tym aspekcie należy traktować ssanie. Osad denny z dna morskiego, który zawiera pierwiastki ziem rzadkich wykazuje bardzo dużą zawartość wody. Ruch osadu podczas ssania jest uzależniony w dużym stopniu od zawartości wody ( $W_c$ ) oraz krytycznego limitu cieczy ( $W_c$ ) materiału. Zatem, ważnym jest aby zmodyfikować limit cieczy poprzez dodatek odczynnika chemicznego w celu kontrolowania zachowania się osadu. Wybrano osiem różnych odczynników powierzchniowych, które mogą być podzielona na trzy typy. Są to odczynniki typu dyspergującego, typu retencji wody oraz typu zagęszczającego. Przeprowadzono test limitu cieczy i pomiaru lepkości osadu wymieszanego z odczynnikami. Stwierdzono, że polimer absorbujący wodę oraz hydroksyetyloceluloza zwiększają limit cieczy oraz lepkość. Z kolei, sól amoniowo-alkilowa oraz blenda alkiloarylosulfonianowa zmniejszają te wielkości. Możliwa jest kontrola zachowania się osadu poprzez dodatek odpowiednich odczynników powierzchniowych.

**Słowa kluczowe:** górnictwo głębinowe, osad o dużej zawartości wody, pierwiastki ziem rzadkich, odczynniki powierzchniowe



# Sulphate Removal from Mining-Process Water by Capacitive Deionization

Maria SINCHE-GONZALEZ<sup>1)</sup>, Raul MOLLEHUARA CANALES<sup>2)</sup>

<sup>1)</sup> University of Oulu, Oulu Mining School, P.O.Box 3000, FI-90014, Finland; email: maria.sinchegonzalez@oulu.fi

<sup>2)</sup> University of Oulu, Oulu Mining School, P.O.Box 3000, FI-90014, Finland; email: raul.mollehuaracanales@oulu.fi

<http://doi.org/10.29227/IM-2020-01-65>

Submission date: 29-12-2019 | Review date: 15-01-2020

## Abstract

The removal of dissolved sulphate ions in water is one of the main challenges in the industry. Dissolved sulphate ions are ubiquitous in mining influenced waters because of its physical and chemical stability in aqueous solutions, including in process-water used by mineral beneficiation processes. It is a major problem for the mining industry because it can have negative impacts on the mineral beneficiation process and bring other issues for equipment and piping infrastructure. Not to mention the quality requirements for environmental water release. For instance, when water is recycled to the concentrator plant, dissolved sulphates can build up to increased concentration levels that can have negative effects in the processing of minerals.

This work proposes a new approach for the removal of sulphate ions from mining influenced waters, including process water, which is the capacitive deionization technique (CADI).

The technique can provide good quality water with low sulphate content suitable for recycling to the beneficiation process and meet adequate quality for recycling and safe release to the environment.

Synthetic process-water with sulphate concentrations similar to those in mining and mineral process water was prepared and treated by CADI at fixed conditions of electric current and residence time. The original sulphate concentration in water was 1000, 2000, 3000 mg/L; and reduction rates achieved of sulphate concentrations of 275 mg/L, 712 mg/L and 1015 mg/L, respectively. The results show effective removal of sulphate ions.

**Keywords:** water, sulphate, capacitive deionization

## Introduction

This project aims to develop a new approach to remove sulphate ions from mining process-water by the CADI technique. The target is a low-sulphate water quality for utilisation and recycling in mineral processing, and for disposal into the environment.

Many industrial wastewaters, particularly those associated with mining operations and mineral processes contain high concentrations of sulphate ions exceeding quality standards for drinking water or ecological and biodiversity requirements. The water discharge in mining environments does not follow a uniform criterion because this is restricted to concentration limits based on ecological risk assessments and the sensitivity of the ecosystem receptors.

Table 1 shows permitted maximum sulphate concentrations for release in mining influenced waters in different jurisdictions. Countries with traditional mining activities can have sulphate concentration limits up to 1000 mg/L; but this is only a guideline. Environmental policies for water discharge depends on ecological risk assessments and water quality criteria for final uses.

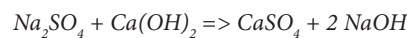
Sulphur-containing ions, particularly sulphate and thio-sulphate ions (Barskii et al., 1985) are present in the water of mining and mineral processing environments.

In mining and process recycled water, sulphate ions originate from the ore and reagents (Broman 1980) that accumulate in the liquid phase in appreciable concentration (>1500 mg/L). When the water is recycled, the concentration of sulphate can build up to high levels that may have an important harmful bearing on the mineral bene-

ficiation (Sinche et al., 2013), equipment, piping and to the environment.

Different ions react differently with sulphate, forming soluble and insoluble complexes (Silva et al. 2010) and may cause various kinds of problems in mineral treatment depending on concentration and associated species (Morris, Levy 1983) such as adsorption, depression, activation, others.

The most common method for removing high concentrations of sulphate from water is through the addition of hydrated lime ( $\text{Ca}(\text{OH})_2$ ), which precipitates calcium sulphate:



Calcium sulphate hydrates to form the common mineral gypsum, which solubility is approximately 1467 mg/L as sulphate at 25°C. Sulphate reduction below 2000 mg/L has been possible in the past only through expensive technologies such as reverse osmosis (RO) or ion exchange (IX). RO and IX generate large volumes of liquid waste, which typically create additional treatment and disposal costs.

## Capacitive Deionization – CADI

Capacitive deionization called desalination or electrochemical desalination is a relatively new method. It applies to water softening in seawater desalination and it is presented as a low-cost/low-energy, high yield method better than reverse osmosis (RO) and electrodialysis (ED) and with the advantage of removing all ionic contaminants (Weinstein, Dash 2013).

The technology is based on ion electrosorption at the surface of a pair of electrically charged electrodes, common-

Tab. 1. Recommended maximum sulphate levels (Ramachandran, 2012)  
 Tab. 1. Rekomendowane poziomy maksymalne siarczanów (Ramachandran, 2012)

Authority	Sulphate Concentration (mg/L)
USA	500
Canada	1000
European Union	1000
South Africa	600
Australia	1000
World Health Organization (drinking water)	250

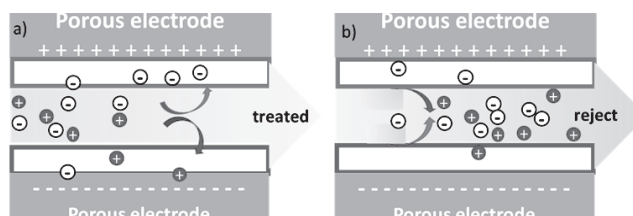


Fig. 1. Purification (a), Regeneration (b) stages in the capacitive deionization treatment  
 Rys. 1. Fazy oczyszczania (a) i regeneracji (b) w procesie dejonizacji objętościowej

ly composed of highly porous carbon materials. It showed a wide range of capacities and it features real-time remote monitoring of pressure, flow, conductivity and desalination characteristics.

The water treatment has two stages purification and regeneration (Figure 1). In the stage of purification, the water passes between oppositely charged electrodes, which electrostatically remove dissolved ions, leaving pure water (treated) flowing out of the cell. The deionization cycle continues until the electrodes are saturated with ions. In the regeneration, the feed water flushed through the cell at a lower flow rate, while electrode polarity is reversed. Ions are ejected from the electrode surface, concentrated in the flow channel and slushed from the cell, producing a concentrate solution (reject) and electrodes are regenerated.

## Materials and methods

### Synthetic water

Mining influenced waters can contain large amounts of dissolved sulphate ions >1500 mg/l, and waters with less than 1000 mg/l are difficult for sulphate removal. Synthetic water containing 1000, 2000 and 3000 mg/L (Table 2) with and without interfering metal ions was prepared and used with the CADI treatment.

Ultrapure water and milliQ water, and reagents of analytical grade (i.e.  $\text{CuSO}_4$ ,  $\text{NiSO}_4$ ,  $\text{ZnSO}_4$ ,  $\text{Na}_2\text{SO}_4$ ,  $\text{NaNO}_3$ ,  $\text{NH}_4\text{Cl}$ ,  $\text{NaCl}$ ) were used to prepare synthetic water of various qualities for the research.

### Capacitive Deionization – CADI tests

The tests were conducted in the Center of Technological Investigation of Water in the Desert-Ceitsaza, Chile.

The experimental work used a Capacitive Deionization equipment (Kit Model C-3-20FclFRG Voltea) with a 1.0  $\mu\text{m}$  filter for pre-filtration (Figure 2). The Voltea program monitored and recorded in real time the experiments and experimental conditions as the equipment is logged for the entire duration of the experiments. The data was collected during

the experiments included a wide range of data on electric capacity, electric conductivity, electrical potential, cycle times, pressure, and flow. For every cycle, the average conductivity and voltage values were calculated.

Triplicate tests with synthetic water at various sulphate concentrations were conducted for reproducibility.

The capacitive deionization treatment relied upon the constant electricity operation. First, the water conductivity was measured and the sulphate removal percentage was set up by adjusting the residence time and outflows for the final streams (treated- and reject water). Treated water is the product water with low-sulphate concentration and the reject water is the residual brackish solution with high-sulphate concentration (Figure 3). The electric current in the cell is set up to a maximum of 60 Amperes (A) and the recovery of treated water is calculated in percentage as shown the Table 3.

### Analysis of sulphate in water samples

Sampling and analysis were conducted on the feed, treated and reject waters. Sulphate determination was conducted by the gravimetric method with the ignition of residues. The method used hydrochloric acid (HCl) and barium chloride solution ( $\text{BaCl}_2$ ) as reagents.

## Results and discussion

### Capacitive Deionization – CADI

The experimental work conducted several runs with varying conditions (i.e. removal rate, volume flow, retention time). Settings for the resultant treated – and reject waters were fixed as shown in Table 4 after measurement of the conductivity. The conductivity was 3.2, 3.22, 5.5 and 8.68 mS/cm for 1000, 2000 and 3000 mg/L of sulphate in synthetic water respectively.

The removal rate for water with a sulphate concentration of 1000 mg/L was 75%. A lower removal rate of 65% and longer retention time was required for water with a sulphate concentration of 2000 mg/L.

A 64% removal rate was achieved for a higher sulphate concentration of 3000 mg/L, but with a reduction in the re-

Tab. 2. Synthetic water at initial concentrations of 1000, 2000 and 3000 mg/L of sulphate, with interfering ions  
 Tab. 2. Woda syntetyczna w początkowych stężeniach 1000, 2000 i 3000 mg/L siarczanu, z jonami przeszkadzającymi

Ions	Low without metal ions	Concentration, mg/l		
		Low	Medium	High
SO <sub>4</sub> <sup>2-</sup>	1000	1000	2000	3000
NO <sub>3</sub> <sup>-</sup>	20	20	40	60
Cl <sup>-*</sup>	100	100	200	300
Cu <sup>2+</sup>		2	5	8
Ni <sup>2+</sup>		2	5	8
Zn <sup>2+</sup>		5	10	15
NH <sub>4</sub> <sup>+</sup>		10	20	30

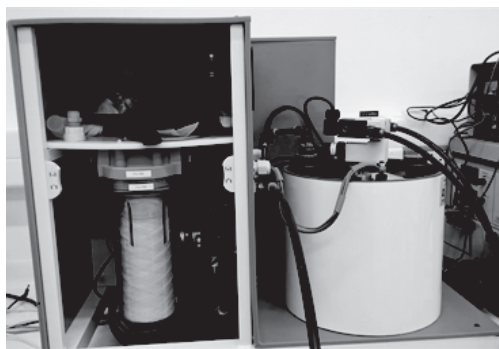


Fig. 2. Capacitive Deionization equipment (Ceitsaza, Chile)  
 Rys. 2. Sprzęt do dejonizacji objętościowej (Ceitsaza, Chile)

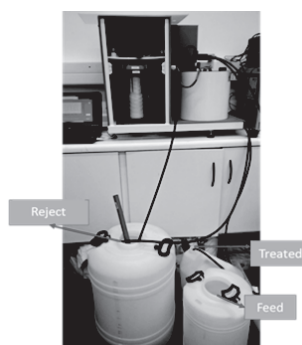


Fig. 3. Feed, treated and reject solutions from the CADI treatment  
 Rys. 3. Nadawa, produkty i odpady z procesu CADI

tention time and the volume flows (treated water from 1 to 0.65 L/min; reject water from ~0.4 to 0.2 L/min). The experiment attempted higher electric current values but this was not possible as the values exceeded the capacity of the equipment.

A higher sulphate removal rate was obtained in the absence of interfering ions such as Cu, Ni, Zn in the water. The test was carried out for a low-sulphate concentration only (1000 mg/L), with a removal rate of 80%.

The result using the CADI method should be interpreted not only in terms of sulphate removal rates but also in terms of the final products that is the amount of water treated in a continuous flow (treated water and reject water).

Table 5 presents the results for effective removals and volume recoveries. The reconciled volume flow in the feed water (1.47 L/min) was maintained constant. Maximum volume recovery was achieved from low-sulphate concentration water (1000mg/L) in absence of interfering ions, resulting in 77% water recovery (1.13 out of 1.47 L/min), and 80% sulphate

removal rate (1000 to 200 mg/L). In the presence of interfering ions, the water recovery is similar (1.16 L/m), but the sulphate removal decreases to 75% (250 mg/L). For synthetic water with a sulphate concentration of 2000 mg/L, the water recovery is 68% (1 L/min) but the removal rate decreases to 65% (2000 to 700 mg/L). For higher concentration of sulphate (3000 mg/L), the recovery rate is 70% (1.03 L/min), with only 64% of sulphate removal (3000 to 1080 mg/L).

The results show that the CADI method can achieve water volume recoveries in the range of 68–79% in a wide range of sulphate concentrations (1000–3000 mg/L) in water. However, the resulting brackish solution or reject water requires further investigation for treatment. In Chile, the alternative is the natural solar evaporation as in the treatment of brines with potential sulphur recovery.

In the case of water with 3000 mg/L of sulphate, the reduction is to 1080 mg/L. A secondary treatment stage could further reduce the concentration levels and increase the recovery rate to at least 75% (as for the case of synthetic water



Tab. 3. Setting up the variables for calculation of current and recovery of the treated water. Feed water 2000 mg/L, conductivity 5.50 mS/cm  
 Tab. 3. Ustawienie zmiennych dla obliczenia napięcia i odzysku wody procesowej. Woda w nadawie 2000 mg/L, przewodność 5,50 mS/cm

Constant Current Operation					
Settings Calculator					
Adjustable Settings			Calculated Settings		
Conductivity	5.5	mS/cm	Treated Current	59.5	A
Removal	65	%	Reject Current	60	A
PreTreated Flow	1	l/min			
Treated Flow	1	l/min	Recovery	68	%
Reject Flow	0.4	l/min			
PreTreated Time	5	sec			
Treated Time	115	sec			
Reject Time	125	sec			

Tab. 4. Setting the conditions to treated water with different concentrations  
 Tab. 4. Ustalenie warunków dla wody procesowej o różnych koncentracjach

Ions	Units	Water with Sulphate			
		Low	Medium	High	Low (not metals)
SO <sub>4</sub> <sup>2-</sup>	mg/L	1000	2000	3000	1000
Conductivity	mS/cm	3.22	5.5	8.68	3.2
Removal	%	<b>75</b>	<b>65</b>	<b>64</b>	<b>80</b>
PreTreated flow	L/min	1.0	1.0	0.65	0.9
Treated flow	L/min	1.0	1.0	0.65	0.9
Reject flow	L/min	0.3	0.4	0.2	0.3
PreTreated time	sec	5.0	5.0	5.0	5.0
Treated time	sec	110	115	64	110
Reject time	sec	82	125	70	82
Treated current	A	40.3	59.5	60.1	38.7
Reject current	A	59.4	60.0	59.5	57.0
<b>Recovery</b>	<b>%</b>	<b>79</b>	<b>68</b>	<b>70</b>	<b>77</b>

Tab. 5. Calculated water recovery and sulphate removal  
 Tab. 5. Obliczony uzysk wody i stopień usunięcia siarczanów

Ions	Units	Water with Sulphate			
		Low	Medium	High	Low not metals
SO <sub>4</sub> <sup>2-</sup>	mg/L	1000	2000	3000	1000
Reconciled feed to maximum flow treated	L/min	1.47	1.47	1.47	1.47
Recovery	%	79	68	70	77
Treated flow	L/min	1.16	1.00	1.03	1.13
Removal	%	75	65	64	80
Final sulphate in treated, calculated	mg/L	250	700	1080	200
Concentrate flow, calculated	L/min	0.31	0.47	0.44	0.34

Tab. 6. Summary of various sulphate concentration in synthetic water treated (calculated and analysed)  
 Tab. 6. Podsumowanie różnych koncentracji siarczanów w sztucznej wodzie procesowej (obliczone i empiryczne)

Calculated SO <sub>4</sub> (mg/L)	Analysed SO <sub>4</sub> (mg/L)			pH			Conductivity mS/cm
	Feed	Treated	Reject	Feed	Treated	Reject	
1000	1073	275	3041	8.18	9.73	8.12	3.22
2000	1925	712	3706	6.98	7.37	6.58	5.5
3000	3008	1015	5354	6.18	6.63	6.24	8.68

with 1000 mg/L). This requires additional investigations to evaluate the technical and economic pros and cons.

Results of sulphate concentration in the feed, treated and reject waters are shown in Table 6, which is comparable with the calculated values from Table 5. In addition, the chemical analysis of the sample shows a good correlation with the calculated amounts of reagents required to prepare the synthetic waters (~1.3% difference). It is also observed

that the removal of sulphate resulted in an increase of the pH (~ 1 unit) which is also an indication of reduction of the acidity.

Figure 4 shows the concentration in the feed and in the products (treated and reject) after treatment. Results show a linear trend for the three solutions indicating that removal rates are proportional to concentrations of sulphate in the feed.

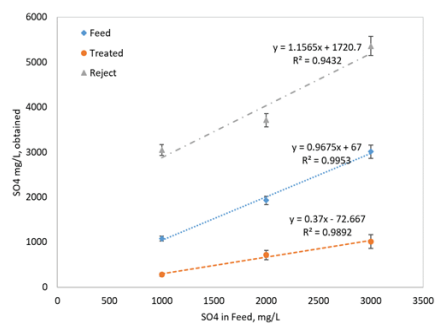


Fig. 4. Chemical analysis of sulphate concentration in synthetic water before and after treatment  
 Rys. 4. Analiza chemiczna stężenia siarczanów w sztucznej wodzie procesowej przed i po procesie

## Conclusions

Capacitive deionization is an alternative treatment option for sulphate containing waters.

The advantage of the technique is its capacity for a continuous flow treatment process.

Capacitive deionization shows to decrease sulphate ions from a wide range of concentration solutions.

Capacitive deionization proved to yield higher recovery rates compared to RO that has a recovery rate of 50% or less. The technique is of low power consumption and uses only 0.5 KWhr/m<sup>3</sup> of treated water.

Synthetic water with similar concentration to those found in process and mining water were tested. The use of real pro-

cess-water is the next step to evaluate the technique. The challenge, in this case, is the presence of solids in suspension and fines particles.

The testing technique in this work generated a residue called here as reject water, which requires further investigation to handle it.

## Acknowledgements

The authors thanks the funds provided by K. H. Renlund Foundation. Also with grateful acknowledgement to the staff at Ceitsaza-Chile and the travel grant of UOA.

#### Literatura – References

1. BARSKII, L.A., RYBAS, V, FAT'YANOVA, M. a and PONOMAREV, G.P, 1985. Influence of sulfur-containing ions on selective flotation of copper-nickel ores. Soviet Mining. 1985. Vol. 22, no. 4, p. 310–316.
2. GREENWOOD, N and FARNSHAW, A, 1997. Chemistry of the Elements. Pergamont Press.
3. MORRIS, M and LEVY, G, 1983. dsorption of sulphate from orally administered magnesium sulfate in man. Journal of Toxicology - Clinical Toxicology. 1983. No. 20, p. 74–114.
4. SILVA, R, CADORIN, L and RUBIO, J, 2010. Salts, sulphate ions removal form aqueous solutions: I. Co-precipitation with hydrolysed aluminium-bearing. Mineral Engineering. 2010. P. 1–7.
5. SINCHE, M, LEVAY, G and ZANIN, M, 2013. A case study on the effect of recycled process water on Cu-Mo sulphide flotation. In: 10th International Mineral Processing Seminar, Procemin 2013. 2013.
6. WEINSTEIN, Lawrence and DASH, Ranjan, 2013. Capacitive Deionization: Challenges and Opportunities. Desalination & Water Reuse. 2013. No. November-December, p. 34–37. Weinstein, L. Dash, R. (2013). Capacitive Deionization: Challenges and Opportunities, Desalination & Water Reuse, November-December, 34-37.

#### *Usuwanie siarczanów z wody procesowej za pomocą dejonizacji pojemnościowej*

*Usuwanie uwolnionych jonów siarczanowych w wodzie jest jednym z głównych wyzwań w przemyśle. Uwolnione jony siarczanowe są wszechobecne w wodach będących pod wpływem działań górniczych ze względu na ich fizyczną i chemiczną stabilność w roztworach wodnych, wliczając w to wody procesowe stosowane podczas procesów wzbogacania. Jest to główny problem dla przemysłu górniczego ponieważ ma to negatywny wpływ na proces wzbogacania oraz powodować może także problemy sprzętowe i infrastruktury rurowej. Ponadto, nie należy zapominać o wpływie takiej wody na środowisko naturalne. Dla przykładu, kiedy woda jest kierowana do procesów przeróbczych, uwolnione siarczany mogą się namnażać do poziomów wysokiej koncentracji a to ma negatywny wpływ na prowadzone procesy. Praca ta proponuje nowe podejście do problemu usuwania jonów siarczanowych z przemysłowych wód górniczych, wliczając w to wody procesowe, którym jest zastosowanie dejonizacji pojemnościowej. Technika ta daje dobrej jakości wodę o niskiej zawartości siarczanów, która jest odpowiednia dla procesów wzbogacania i jest zgodna z wymogami jakościowymi dla recyklingu a tym samym bezpieczna dla środowiska naturalnego. Sztuczna woda procesowa o zawartości siarczanów podobnej do wody przemysłowej z zakładów przeróbczych sektora górniczego została przygotowana i poddana procesowi CADI w stałych warunkach napięcia elektrycznego i czasu. Oryginalna koncentracja siarczanów w wodzie wynosiła 1000, 2000, 3000 mg/L a stopień redukcji osiągnięty wyniósł, odpowiednio, 275 mg/L, 712 mg/L oraz 1015 mg/L. Wyniki pokazały efektywność w usuwaniu jonów siarczanowych z wody procesowej.*

**Słowa kluczowe:** woda, siarczan, dejonizacja objętościowa



# Explosion Characteristics of Syngas from Gasification Process

Jan SKRÍNSKÝ<sup>1)</sup>, Ján VEREŠ<sup>2)</sup>, Jakub ČESPIVA<sup>2)</sup>, Tadeáš OCHODEK<sup>2)</sup>,  
Karel BOROVEC<sup>2)</sup>, Jan KOLONIČNÝ<sup>2)</sup>

<sup>1)</sup> VSB-Technical University of Ostrava, Energy Research Center, 17. listopadu 2172/15, 708 00 Ostrava, Czech Republic; email: jan.skrinsky@vsb.cz

<sup>2)</sup> VSB-Technical University of Ostrava, Energy Research Center, 17. listopadu 2172/15, 708 00 Ostrava, Czech Republic

<http://doi.org/10.29227/IM-2020-01-66>

Submission date: 04-01-2020 | Review date: 13-03-2020

## Abstract

*This paper describes a series of experiments performed to study the explosion parameters of syngas and its flammable component air mixtures. More than 100 pressure-time curves were recorded allowing to investigate the effects of three different gasification process conditions on the maximum explosion pressure and deflagration index. The representative syngas samples were prepared by thermochemical wood-pellets gasification. The experiments were performed in 20-L oil-heated spherical experimental arrangement for different concentrations at representative explosion initial temperature of 65°C. The experimental results were further compared with the explosion parameters of pure gases, namely hydrogen, methane, carbon monoxide and propane as the main flammable syngas components. The most important results are the maximum values of explosion pressure  $7.2 \pm 0.2$  bar and deflagration index  $170 \pm 14$  bar.m/s derived for start-up process conditions. These knowledge could be used to understand the effects of operating conditions to both the optimization design on syngas-fueled applications and the safety protection strategies.*

**Keywords:** explosion parameter, carbon monoxide, hydrogen, methane, propane, syngas, vessel

## Introduction

Due to its many significant advantages as a fuel in stationary power generation, syngas is a candidate among the alternatives being explored for energy conversion and to produce liquid biofuels from renewable resources (Saad and Williams, 2017). Apart from the alternative fuel interest, the non-standard operation regime of such process could lead to an explosion. The composition of syngas from gasification unit vary significantly with different operation conditions. Therefore, for main operating conditions the explosion parameters would have to be determined. In the literature the syngas composition is frequently referred to only stable operation condition. As a result, the explosion parameters are generally underestimated (Skrinsky, 2018). Small-scale characterization of the syngas explosion parameters over a range of fuel concentrations, temperatures and pressures has been published starting from 2014. Sarli et al. presents the  $p_{max} = 4.7\text{--}5.9$  and  $K_G = 9.4 - 35.6$  bar.m/s of wood chip-derived syngas at 283 K.

The study was performed in 5-L cylindrical vessel at two initial temperatures, 283 K and 573 K, and at atmospheric pressure (Sarli et al., 2014). Xie et al. studied the pressure history in the explosion syngas/air mixtures with  $H_2O$  addition. The maximum values have been determined  $p_{max} = 5.1\text{--}5.9$  and  $K_G = 65\text{--}225$  bar.m/s measured in 5-L cylindrical vessel at 373 K (Xie, 2016). Skrinsky et al. presents the results of an experimental evaluation of the safety characteristics for syngas stable operation conditions at temperatures of 323 K, 373 K and 423 K and at elevated pressures of 0.50 bar, 0.75 and 1.00 bar (Skrinsky, 2018). He evaluated the values of  $p_{max} = 5.4\text{--}7.0$  bar and  $KG = 45\text{--}63$  bar.m/s at 20-L oil-heated spherical experimental arrangement. Tran et al. described the influence

of hydrocarbon additions and dilutions on explosion behavior of syngas/air mixtures. In his study, explosion behaviors of hydrocarbon-added and diluted syngas/air mixtures were investigated experimentally in a 6.9-L constant volume combustion chamber (Tran, 2017). The explosion parameters have been found  $p_{max} = 8.3\text{--}9.2$  bar and  $K_G = 238\text{--}467$  bar.m/s at 298 K. The goal of this paper is to investigate the effect of initial process conditions on explosion parameters of syngas-air mixture. The practical aim of interest is to explore if the substantial variation in syngas composition due to different gasification conditions will cause a significant influence on the explosion parameters and which gasification regime is among the most dangerous.

## Materials

The average composition of syngas produced for the explosion experiments are summarized in Table 1.

Syngas consists of flammable hydrogen ( $H_2$ ), methane ( $CH_4$ ), carbon monoxide (CO), and propane ( $C_3H_8$ ). It is diluted with inert constituents of carbon dioxide ( $CO_2$ ) and nitrogen ( $N_2$ ) which results in decrease of the flammability range. The synthetic gas has been produced by gasification of a carbon containing lignocellulose biomass fuel (wood pellets). Wood pellets is one of the main organic materials used as gasification feedstock (Sarli et al, 2014). The small scale autothermal gasification technology (Temex Ltd., Czech patent no. 304091) is described schematically in Figure 1 (reproduced with permission from (Čespiva, 2018)).

The goal of this technology is the research and development of the biomass gasification process. The gasification reactor (gasifier) with a fixed bed, operates in an autothermal mode with heat output up to 100 kW, gasification ratio is be-

Tab. 1. The average composition (in vol. %) of syngas produced for the experiments (dry basis)  
 Tab. 1. Średni skład (w % obj.) gazu syntezowego wyprodukowanego dla potrzeb eksperymentu (sucha podstawa)

Chemical	H <sub>2</sub>	CH <sub>4</sub>	CO	C <sub>3</sub> H <sub>8</sub>	CO <sub>2</sub>	O <sub>2</sub>	N <sub>2</sub>
Start-up	6.0	3.5	22.0	0.6	8.0	1.0	58.9
Process	17.1	1.3	20.0	1.2	11.8	0.1	48.5
Shut-down	5.5	4.5	21.0	0.6	7.0	2.0	59.4

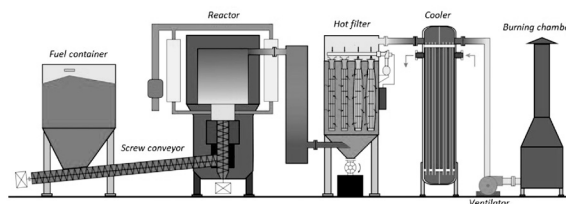


Fig. 1a. Schematic introduction of the ERC's autothermal gasification technology  
 Rys. 1a. Wstęp schematyczny do technologii autotermicznego zgazowania ERC

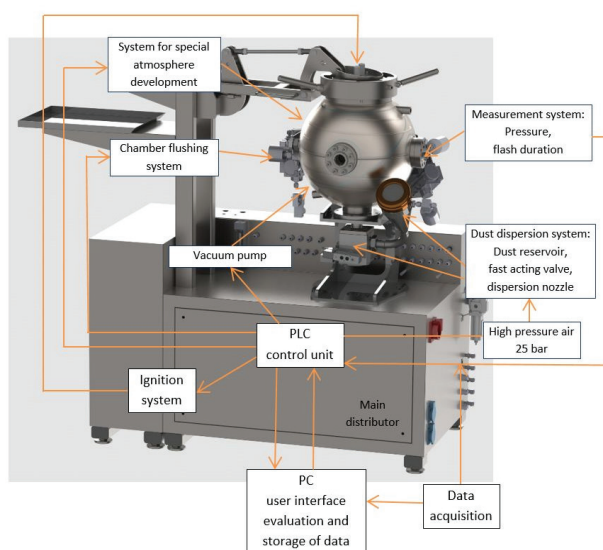


Fig. 1b. Scheme of the 0.02 m<sup>3</sup> experimental set-up  
 Rys. 1b. Schemat ustawienia eksperymentalnego 0,02 m<sup>3</sup>

tween 0.2–0.4 (fuel to gas) and gasification temperature between 850–1000°C. Syngas was measured after pre-treatment on dry basis and at ambient temperature. The composition of gaseous alkanes, carbon monoxide, hydrogen, oxygen and carbon dioxide at ambient temperature were measured by the portable Syngas analyzer (Pollutek, GAS 3000P, Pellenberg, Belgium) with resolution 0.01 vol. %. The subsequent utilization (filter, cooling with water) of the produced synthetic gas depends on its quality and content of undesirable components. All the pure gas samples have the purity higher than 99.8 mass %.

## Methods

The experiments have been performed in a constant volume stainless steel double wall vessel of spherical shape with an internal diameter of 336 mm (SN: 497-OZM-15, OZM Research, s.r.o., Hrochův Týnec, Czech Republic) adopted for the high-temperature experiments. The set-up consists of spherical vessel, cooling system, spark generator, and data acquisition system. Digitally adjustable temperature control device Presto A 30 (SN: 10291377, JULABO GmbH, Seelbach, Germany) has been used to heat the oil in the instrument to

the specified temperature close to the expected. Temperature control system has been used to heat the system of the vessel up to 65 °C. The system allows to hold the internal vessel temperature 65°C with a temperature fluctuation of less than 2°C. The initial temperature in time of ignition has been measured using the calibrated thermocouple (SN: 10291377, Jakar, Karviná, Czech Republic) with an accuracy 0.5°C located on the top of the explosion vessel (Skrinsky and Ochodek, 2019).

The data acquisition system comprises the pressure sensors, transducer sensors, signal conditioning system and signal convertor system connected to PC. The explosion pressures have been recorded by pair of piezoelectric pressure sensors (SN: 4512821 and SN: 4512822, model 701A, Kistler, Winterthur, Switzerland) and with a transducer sensor charge amplifier (Kistler, model 5041E1). Operating temperature range of the sensors is from -150°C to 200°C that is satisfactory for presented experiments. The calibrated partial range for the sensors is from 0 bar to 20 bar. The signal conditioning module (Tedia, model UDAQ-3644) has worked at a sampling frequency 50 kHz with a sampling period of 0.02 ms with a high resolution 16-bit A/D convertor connected to PC's USB. Whole acquisition is controlled by user interface PROMOT-

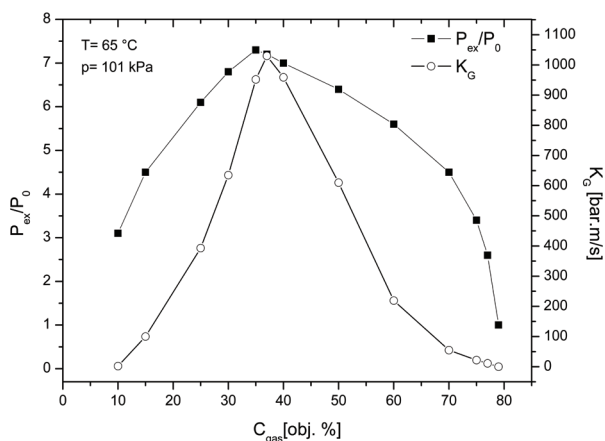


Fig. 2.  $P_{ex}/P_0$  and  $K_G$  versus concentration for  $H_2$   
Fig. 2.  $P_{ex}/P_0$  oraz  $K_G$  w układzie ze stężeniem  $H_2$

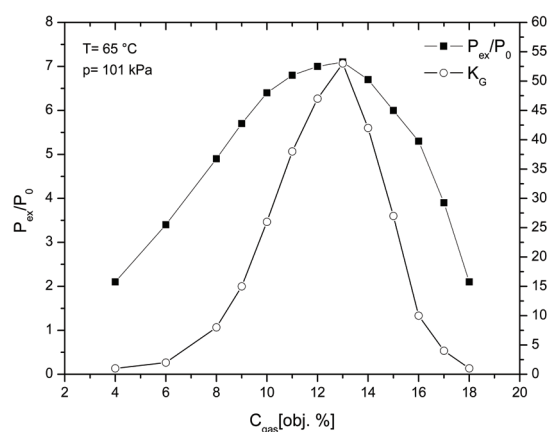


Fig. 3.  $P_{ex}/P_0$  and  $K_G$  versus concentration for  $CH_4$   
Fig. 3.  $P_{ex}/P_0$  oraz  $K_G$  w układzie ze stężeniem  $CH_4$

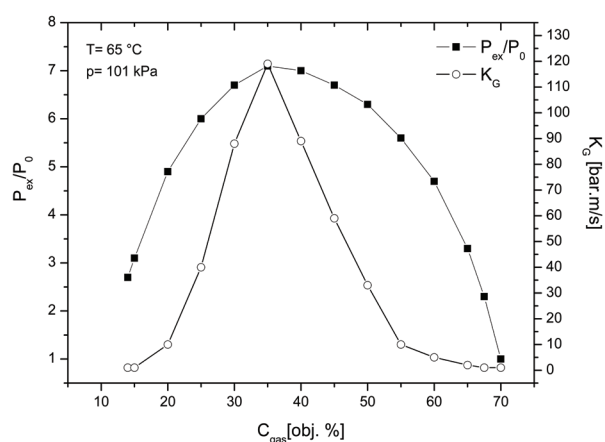


Fig. 4.  $P_{ex}/P_0$  and  $K_G$  versus concentration for  $CO$   
Fig. 4.  $P_{ex}/P_0$  oraz  $K_G$  w układzie ze stężeniem  $CO$

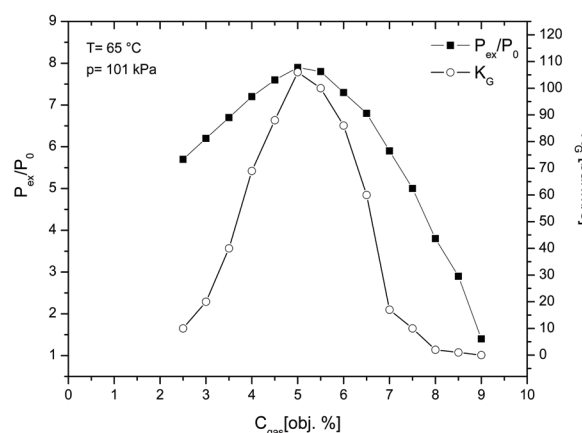


Fig. 4.  $P_{ex}/P_0$  and  $K_G$  versus concentration for  $C_3H_8$   
Fig. 4.  $P_{ex}/P_0$  oraz  $K_G$  w układzie ze stężeniem  $C_3H_8$

IC system (MICROSYS, spol. s.r.o., Ostrava, Czech Republic). Programmable logic control station (model 5073A211, Simatic, Siemens, Munich, Germany) connected to PC have been adapted to automatically control procedures for partial pressure method (gas feeding), fast acting valve timing and bottom rotating fan ensuring mixing of the fuel with air mixture. The mixture was ignited by the electric discharge from permanent spark generator (10 J) with ignition delay time 60 ms. The rods of the electrodes are positioned in the center of the testing vessel with the distance between the tips of 5 mm. The spark discharge time is adjusted to 200 ms (Skrinsky and Ochodek, 2019). The whole system is schematically introduced at Figure 1.

The methodology being applied to investigate the explosion parameters is based upon the European Standard EN 15967:2011. This method allows the measurement at atmospheric conditions and have been adapted for high temperature studies. Syngas test mixture is ignited by a defined ignition source which is positioned in the center of a test vessel. By means of a pressure measuring system, the highest pressure  $p_{ex}$  developed following the ignition of the test mixture is measured. The maximum explosion pressure  $p_{max}$  is determined during measurements of the explosion pressure  $p_{ex}$  by varying stepwise the content of flammable gas in the mixture,

until the maximum value of  $p_{ex}$  is found. The pressure-time curve developed following ignition of the test mixture is recorded and the highest rate of explosion pressure rise  $(dp/dt)_{ex}$  is calculated as the derivation. The maximum rate of explosion pressure rise  $(dp/dt)_{max}$  is normalized to vessel volume by which the deflagration index is found (EN 15967:2011).

## Results and discussion

Figures 2–5 plot the atmospheric pressure normalized explosion pressure ( $P_{ex}/P_0$ ) and the deflagration index ( $K_G$ ) versus concentration. Both parameters are measured for pure hydrogen, pure methane, pure carbon monoxide, and pure propane at initial temperature (65°C) and ambient initial pressure (101 kPa).

All the explosion pressure curves of the individual syngas flammable components possess a similar behavior. The pressure and deflagration index increases until reaching its maximum value at stoichiometric concentration and then decreases due to heat loss. The results of the  $P_{ex}/P_0$  and  $K_G$  versus concentration for the hydrogen ( $H_2$ ), methane ( $CH_4$ ), carbon monoxide ( $CO$ ), and propane ( $C_3H_8$ ) are summarized in Table 2.

The data evaluation is well described in (Skrinsky and Ochodek, 2019). The experimental uncertainty in a statistical sense is given by the used experimental method and is ac-

Tab. 2. Average values of the explosion parameters at  $t_0 = 65^\circ\text{C}$  and  $p_0 = 101\text{ kPa}$

Tab. 2. Średnie wartości parametrów eksplozji dla  $t_0 = 65^\circ\text{C}$  oraz  $p_0 = 101\text{ kPa}$

Characteristic	Unit	H <sub>2</sub>	CH <sub>4</sub>	CO	C <sub>3</sub> H <sub>8</sub>
$P_{\max}/P_0$	[-]	$7.3 \pm 0.2$	$7.1 \pm 0.2$	$7.1 \pm 0.2$	$7.9 \pm 0.2$
$K_G$	[bar·m/s]	$1030 \pm 82$	$53 \pm 4$	$119 \pm 10$	$106 \pm 9$

Tab. 3. Average values of the explosion characteristics at  $\Phi = 1,0$  and  $p_0 = 101\text{ kPa}$

Tab. 3. Średnie wartości charakterystyk eksplozji dla  $\Phi = 1,0$  oraz  $P_0 = 101\text{ kPa}$

Characteristic	Unit	Start-up	Stable	Shut-down
$P_{\max}/P_0$	[-]	$7.1 \pm 0.2$	$6.8 \pm 0.1$	$7.0 \pm 0.2$
$K_G$	[bar·m/s]	$170 \pm 14$	$147 \pm 12$	$159 \pm 13$

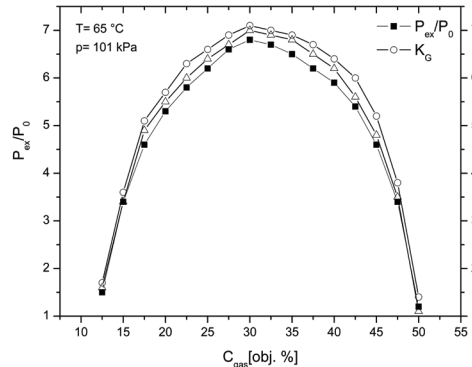


Fig. 6.  $P_{\text{ex}}/P_0$  at  $C=12.5-50.0\text{ vol. \%}$ ,  $P_0=101\text{ kPa}$  and  $T_0=65^\circ\text{C}$  for syngas-air mixtures

Rys. 6.  $P_{\text{ex}}/P_0$  dla  $C=12,5-50,0\text{ \% obj.}$ ,  $P_0=101\text{ kPa}$ ,  $T_0=65^\circ\text{C}$  dla mieszaniny powietrza i gazu syntezowego

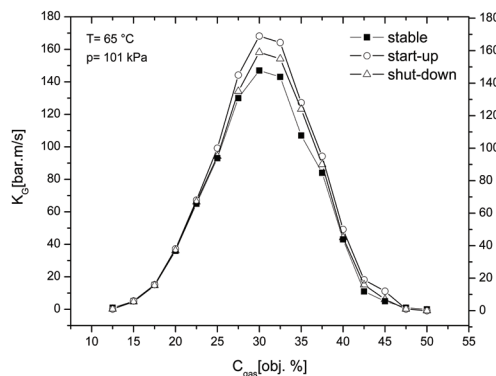


Fig. 7.  $K_G$  at  $C=12.5-50.0\text{ vol. \%}$ ,  $P_0=101\text{ kPa}$  and  $T_0=65^\circ\text{C}$  for syngas-air mixtures

Rys. 7.  $K_G$  dla  $C=12,5-50,0\text{ \% obj.}$ ,  $P_0=101\text{ kPa}$ ,  $T_0=65^\circ\text{C}$  dla mieszaniny powietrza i gazu syntezowego

according to EN 15967:2011. It has been well established that a progressive change occurs in the variety of some explosion properties of gases when mixed them together. A very interesting example of such differences is given by Figure 6–7 for three different H<sub>2</sub>-CH<sub>4</sub>-CO-C<sub>3</sub>H<sub>8</sub>-air mixtures compositions from Table 1. The search for the explosion parameters of the syngas was initiated in the concentration range from 10 vol. % up to 50 vol. % where the lowest explosion pressure has been expected according to previous studies (Skrinsky, 2018).

We consequently focused on the determination of maximum explosion parameters in the region close to  $C = 50.0\text{ vol. \%}$  according to our previous calculations (Skrinsky, 2018). After several attempts consisting in adjusting the experimental apparatus, they were found close to  $C = 30.0\text{ vol. \%}$ . The

results of the  $P_{\text{ex}}/P_0$  and  $K_G$  versus concentration for three operational regimes of gasifier are summarized in Table 3.

## Conclusion

The most important results of the presented experiments is the analysis of syngas-air mixture explosion behaviour at specific gasification process conditions. Explosion pressure and deflagration index of the syngas-air mixtures were determined in the 0.02 m<sup>3</sup> closed spherical vessel for the three different gasification process regimes start-up, stable and shut-down.

The main conclusions are summarized as follows:

1. Among syngas-air process regimes, the normalized explosion pressure and deflagration index increase in the or-

der process, shut-down and start-up at given experimental and process conditions.

2. Explosion pressure and deflagration index of the syngas mixture reach maximum values at the stoichiometric concentration  $C = 30.0$  vol. % within the studied range from 12.5 to 50.0 vol. % at initial temperature of 65°C and initial pressure of 101 kPa.

3. The maximum explosion pressure,  $p_{max}$ , was determined as the highest  $p_{ex}$  found for the mixture compositions investigated and is equal to  $7.1 \pm 0.2$  bar.

4. The deflagration index was calculated from the experimentally determined  $(dp/dt)_{max}$  value and is equal to  $170 \pm 14$  bar.m/s.

### Acknowledgements

This work would not have been possible without the financial support of Innovation for Efficiency and Environment - Growth, reg. no. LO1403 supported by National Programme for Sustainability and financed by the Ministry of Education, Youth and Sports and by "Research of conversion processes and utilization of waste heat in the framework of fuel-energy technological complexes", grant number SP 2019/89. Authors are very thankful to dr inż. Mateusz Wnukowski and mgr inż. Łukasz Niedźwiecki for their strong help during the preparation of samples from gasification technology with an autothermal generator located at the Energy Research Centre at the Technical University of Ostrava.



## Literatura – References

1. ČESPIVA, J. Adjustment of the Gasification Reactor Technology: Master thesis. Ostrava: VŠB – Technical University of Ostrava, Faculty of Mechanical Engineering, Department of Power Engineering, 2018, 54p. Thesis supervisor: Skřínský, J.
2. EN 15967 (2012). Determination of maximum explosion pressure and the maximum rate of pressure rise of gases and vapors. Berlin: Beuth Verlag, 2012. 36 s.
3. SAAD, J. M. and WILLIAMS, P. T. Manipulating the H<sub>2</sub>/CO ratio from dry reforming of simulated mixed waste plastics by the addition of steam. In Fuel Processing Technology, 156, 2017, p. 331-338. ISSN 0378-3820.
4. SARLI, V., CAMMAROTA, F., SALZANO, E. Explosion parameters of wood chip-derived syngas in air. In Journal of Loss Prevention in the Process Industries, 32, 2014, p. 399-403. ISSN 0950-4230.
5. SKRINSKY J., Influence of pressure and temperature on safety characteristics of syngas-air mixture produced by auto-thermal gasification technology. Chemical Engineering Transactions, 65, 2018, p. 133-138. ISSN 2283-9216.
6. SKRINSKY J., OCHODEK, T. Explosion Characteristics of Propanol Isomer–Air Mixtures. In Energies. 12(8), 2019, p. 1574. EISSN 1996-1073.
7. TRAN, M. V., SCRIBANO, G., CHONG C. T. et al. Influence of hydrocarbon additions and dilutions on explosion behavior of syngas/air mixtures. In International Journal of Hydrogen Energy, 42(44), 2017, p. 27416-27427. ISSN 0360-3199.
8. TRAN, M. V., SCRIBANO, G., CHONG C. T. et al. Simulation of explosion characteristics of syngas/air mixtures. In Energy Procedia, 153, 2018, p. 131-136. ISSN 1876-6102.
9. XIE, Y., WANG, J., CAI, X. et al. Pressure history in the explosion of moist syngas/air mixtures. In Fuel, 185, 2016, p. 18-25. ISSN 0016-2361

### *Charakterystyka eksplozji gazu syntezowego z procesu zgazowania*

Artykuł opisuje serię eksperymentów wykonanych w celu zbadania parametrów eksplozji gazu syntezowego oraz jego części palnych w mieszaninie z powietrzem. Więcej niż 100 krzywych w układzie ciśnienie-czas zostało zarejestrowanych pozwalając na zbadanie efektów trzech różnych warunków procesu zgazowania przy maksymalnym ciśnieniu eksplozji i wskaźniku deflagracji. Reprezentatywne próbki gazu syntezowego zostały przygotowane za pomocą zgazowania termochemicznego drewnianych granulek. Eksperymenty zostały wykonane w podgrzewanej olejowej instalacji o kształcie sferycznym, której objętość wynosiła 20 l wykorzystana została dla różnych stężeń oraz reprezentatywnej temperatury wstępnej na poziomie 65°C. Wyniki doświadczalne były następnie porównane z parametrami wybuchu czystych gazów, którymi były wodór, metan, tlenek węgla oraz propan, jako główne składniki gazu syntezowego. Najważniejszymi wynikami okazały się maksymalne wartości ciśnienia wynoszące  $7,2 \pm 0,2$  barów oraz wskaźnik deflagracji na poziomie  $170 \pm 14$  bar.m/s wyznaczony dla warunków startowych procesu. Informacje te mogą zostać wykorzystane w celu zrozumienia wpływu warunków operacyjnych dla optymalizacji zastosowań gazu syntezowego oraz strategii bezpieczeństwa związanego z jego wykorzystaniem.

**Słowa kluczowe:** parametry eksplozji, tlenek węgla, wodór, metan, propan, gaz syntezowy



# XPS (X-Ray Photoelectron Spectroscopy) Study of Removing Iron Ions from Water by Zeolite and Bentonite

Anna ŠKVARLOVÁ<sup>1)</sup>, Mária KAŇUCHOVÁ<sup>1)</sup>, Ľubica KOZÁKOVÁ<sup>1)</sup>,  
Tomáš BAKALÁR<sup>1)</sup>, Andrea ORAVCOVÁ<sup>1)</sup>, Jiří ŠKVARLA<sup>1)</sup>

<sup>1)</sup> Technical University of Košice, Faculty of Mining, Ecology, Process Control and Geotechnology, Letná 9, 042 00 Košice, Slovakia; email: anna.skvarlova@tuke.sk, maria.kanuchova@tuke.sk, lubica.kozakova@tuke.sk, tomas.bakalar@tuke.sk, andrea.oravcova@tuke.sk, jiri.skvarla@tuke.sk

<http://doi.org/10.29227/IM-2020-01-67>

Submission date: 03-12-2020 | Review date: 28-02-2020

## Abstract

Zeolites as a member of family of hydrated aluminosilicate minerals contains alkali and alkaline-earth metals. They are noted for their lability toward ion-exchange and reversible dehydration. Their framework structure encloses interconnected cavities occupied by large metal cations and water molecules. Bentonites are clays generated frequently from the alteration of volcanic ash, consisting predominantly of smectite minerals, usually montmorillonite. They present strong colloidal properties and its volume increases several times when coming into contact with water, creating a gelatinous and viscous fluid. The special properties of bentonite (hydration, swelling, water absorption, viscosity, thixotropy) make it a valuable material for a wide range of uses and applications. The purpose of this paper is to document an ability of a zeolite and bentonite to remove iron ions and various other pollutants from water. The surface analysis of zeolite and bentonite was performed by the very sensitive analytical device – XPS (X-ray photoelectron spectroscopy).

**Keywords:** XPS, bentonite, zeolite, iron, adsorption

## Introduction

With increasing rate of urbanization is hand in hand increasing a rate of the environmental pollution. Today, a world is facing a water crisis. It is necessary to reduce negative impacts of human industrialization on environment and develop such technologies, which will be more ecological and will be helpful in environmental cleaning processes. A huge quantity of wastewater has been produced from industrial processes and was discharged into soils and water systems. Contained pollutants such as cationic and anionic ions, oil and organics have poisonous and toxic effects on the whole ecosystem.

For the removal of these contaminants, a variety of techniques, such as chemical precipitation, electro-flotation, membrane separation, reverse osmosis, electro dialysis and others, have been developed. Currently, adsorption is believed to be a simple and effective technique for water and wastewater treatment and the success of the technique largely depends on the development of an efficient adsorbent. Application of natural zeolites for water and wastewater treatment is a promising technique in environmental recovery processes.

## Zeolites

Zeolites as crystalline aluminosilicates have a microporous structure with elevated thermal stability and high chemical resistance. Due to their thermal stability, high exchange capacity, easy modification and selectivity, zeolites are considered to be excellent adsorbents, which have large adsorption capacity with good cationic exchange properties [1].

In chemical industry they are usually used for purifications and separations. Their ion exchange capacity is associated with amount of Al and makes them suitable for their application in detergents, metals removal, and recovery industries, among others [2].

They consist of honeycomb structure with pores. The structure of zeolite is shown in Fig.1.

The primary building block of zeolite framework is the tetrahedron, the centre of which is occupied by a silicon or aluminium atom, with four atoms of oxygen. Substitution of Si<sup>4+</sup> by Al<sup>3+</sup> defines the negative charge of the framework, which is compensated by monovalent or divalent cations located together with water. The aluminosilicate framework is the most conserved and stable component and defines the structure type. The water molecules can be present in voids of large cavities and bonded between framework ions and exchangeable ions via aqueous bridges. The water can also serve as bridges between exchangeable cations.

The ion-exchange behaviour of natural zeolite depends on several factors, such as the framework structure, ion size and shape, charge density of the anionic framework, ionic charge and concentration of the external electrolyte solution. The adsorption characteristics of any zeolite depends on the detailed chemical/structural makeup of the adsorbent. The Si/Al ratio, cation type, number and location are particularly influential in adsorption. These properties can be changed by several chemical treatments to improve separation efficiency of raw natural zeolite. Acid/base treatment and surfactant impregnation by ion exchange are commonly employed to change the hydrophilic/hydrophobic properties for adsorption of various ions or organics [3].

The sorption of metal ion by zeolite is significantly affected by the pH. The lower metal uptake in more acidic conditions is probably attributed to competition between the metal ions and the hydrogen ions. It is documented, that the most optimal pH is 7. It was also observed, that the adsorption capacity has a correlation with the mass of sorbent [4].

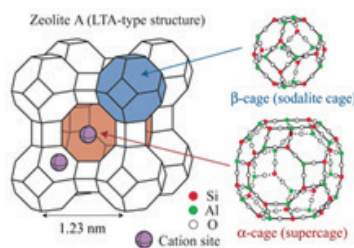


Fig. 1. The structure of zeolite [5]

Rys. 1. Struktura zeolitu [5]

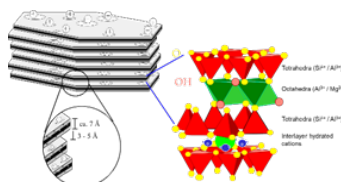


Fig. 2. The structure of bentonite [6]

Rys. 2. Struktura bentonitu [6]

## Bentonites

The main clay mineral of bentonite is montmorillonite, which is a good sorbent because it has high cation exchange capacity and a large specific surface area. Raw montmorillonite can sorb cations, but not anions, because of the negative charges on the crystal lattice. Therefore, several methods have been investigated in order to sorb anionic pollutants by montmorillonite [7].

Montmorillonite is a layered, dual-dimensional mineral. It consists of hydrated aluminium silicate [8] [9]. The crystal unit of montmorillonite is Tetrahedral-Octahedral-Tetrahedral (TOT) layer structure, which is assembled by two silicon-oxygen tetrahedral sheets fused to one edge-shared aluminium-oxygen octahedral sheet. The structure of bentonite is shown in Fig. 2. The cations in the interlayer space of montmorillonite can be exchanged which is the cation exchange property of bentonite [8] [9] [10] [11].

It is used to line the base of landfills to prevent migration of leachate, for quarantining metal pollutants of groundwater, and for the sealing of subsurface disposal systems for spent nuclear fuel. Similar uses include making slurry walls, waterproofing of below-grade walls, and forming other impermeable barriers, e.g., to seal off the annulus of a water well, to plug old wells [12].

Sodium bentonites absorb large quantities of water, swelling to many times their original volume. They have been used for building a seal dams, in portland cements and concrete, ceramics, emulsions, insecticides, soaps, pharmaceuticals, and paints, in the manufacture of paper they are using for clarifying water and as a water softener to remove calcium from hard water.

## Materials and methods

X-ray photoelectron spectroscopy is a sensitive and non-destructive method for analysing the surface of materials, based on the binding energy of chemical species, providing information about the chemical composition and the electron structure of the surface to the depth of 10 nm.

The XPS measurements were conducted using PHOIBOS 100 SCD model of XPS instrument that was equipped with a non-monochromatic X-ray source. The survey spectra were measured at the transition energy of 70 eV and the core spectra

at 30 eV at room temperature. All spectra were obtained at a basic pressure of  $2 \times 10^{-8}$  mbar with the AlK $\alpha$  excitation at 10 kV (150 W) and were corrected with the reference to aliphatic carbon at 285 eV. XPS data were processed using the CASA XPS software.

The samples were derived using distilled water, ferric sulfate non-hydrate  $\text{Fe}_2(\text{SO}_4)_3 \cdot 9\text{H}_2\text{O}$  and sorbents consisted of Bentonite Brown, Bentonite Blue (from Kramost a.s. company of Braňany), zeolite Zeocem M-20 and Zeocem M-50 ((klinoptilolite) from Zeocem a.s. company Bystré of Nižný Hrabovec). The mass of 1g of each sorbent was placed into the PET bottles with 10 ml of distilled water. Calibration mixture of ferric sulfate was prepared by using 100 and 2000 mg/l of ferric sulfate non-hydrate. The corresponding mass of the ferric sulfate non-hydrate and 100 ml of distilled water were placed into the beakers, of which 10 ml was taken out. The rest of the solution was decanted to the PET bottles with the sorbents. The filter apparatus with the filter papers isolated the adsorbents with the ferric sulfate from distilled water and un-adsorbed residues. The samples were dried, homogenized in achate mortar and subjected to XPS analyse.

## Results and discussion

As shown on Fig. 3, with the iron concentration of 100 mg/l by using bentonite brown – Ca, Al, Fe species are bonded on the adsorbent, while Si species were desorbed. With the iron concentration of 2000 mg/l, the opposite effect occurred. Fig. 4 illustrates the desorption process of the Al, Si and Ca species with the iron concentration of 100 mg/g by using bentonite blue. Only amount of Fe increased. With the iron concentration of 2000 mg/l, the amount of Si and Al species were increasing together with the Fe species, as well. The decrease of the Ca species is visible for both cases.

In case of adsorption on zeolite M-20 (Fig.5) it is visible, that with the iron concentration of 100 and 2000 mg/l, the amount of the Al and K species is decreasing. On the other hand, with the different iron concentrations we can see the differences in amount of Si and Ca species. Their quantity is decreasing with the iron concentration of 100 mg/l, while increasing with the iron concentration of 2000 mg/l.

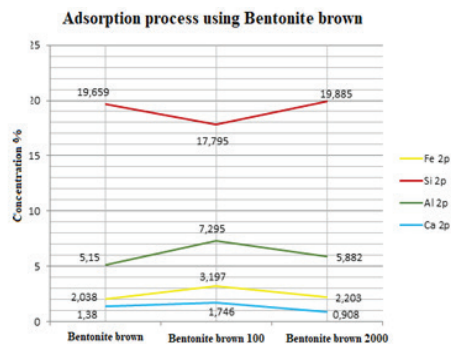


Fig. 3. Bentonite brown  
Rys. 3. Bentonit brązowy

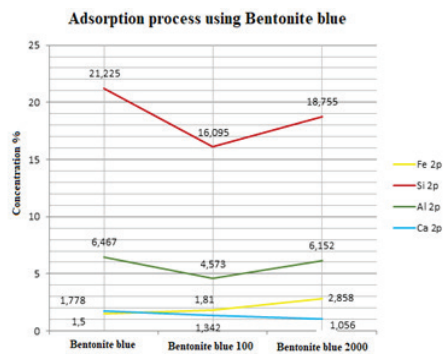


Fig. 4. Bentonite blue  
Rys. 4. Bentonit niebieski

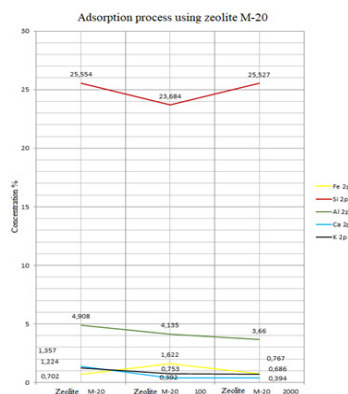


Fig. 5. Zeolite M-20  
Rys. 5. Zeolit M-20

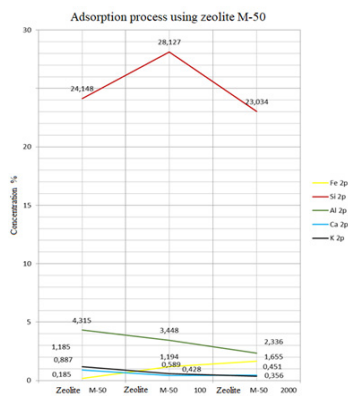


Fig. 6. Zeolite M-50  
Fig. 6. Zeolite M-50

Fe species are behaving in the opposite way. The highest adsorption is occurring with the lower concentration of iron ions.

As we can see on the Fig. 6, after the adding 100 mg/l of iron ions into the zeolite M-50, it is documented increase of the Fe and Si species, but only Fe species are still increasing even in iron concentrations of 2000 mg/l. In both cases, the quantity of Al and K species is decreasing. Calcium species are decreasing at first (100 mg/l of iron ions added), but then increasing (2000 mg/l of iron ions added).

## Conclusion

The results showed, that the best adsorption process occurred by using bentonite blue with the iron concentration of 2000 mg/l. In the primary structure of bentonite blue is

amount of Fe 1.5%. After the adsorption we measured 2,858%. In case of zeolites, the best results were shown by zeolite M-50 with the iron concentration of 2000 mg/l. In basic structure of zeolite M-50 is amount of Fe 0,185%. After the adsorption was this amount increased to value 1,655%.

## Acknowledgements

This work was supported by the Scientific Grant Agency of the Ministry of Education of Slovak Republic VEGA (Project No. 2/0055/19 and No. 1/472/18) and by the Research & Development Operational Programme (ERDF No. 26220120038, Research excellence centre on earth sources, extraction and treatment – 2nd phase).

## Literatura – References

1. Yan, J., Li, Y., Li, H., Zhou, Y., Xiao, F., Li, B., & Ma, X. (2018). Effective removal of ruthenium (III) ions from wastewater by amidoxime modified zeolite X. *Microchemical Journal*. doi:10.1016/j.microc.2018.10.047.
2. Martínez Galeano, Y., Negri, F., Moreno, M. S., Múnera, J., Cornaglia, L., & Tarditi, A. M. (2018). Pt encapsulated into NaA zeolite as catalyst for the WGS reaction. *Applied Catalysis A: General*.doi:10.1016/j.apcata.2018.12.034.
3. Shaobin Wang,, Yuelian Peng. Natural zeolites as effective adsorbents in water and wastewater treatment, *Chemical Engineering Journal* 156 (2010) 11-24. doi:10.1016/j.cej.2009.10.029
4. M.A. Shavandi, Z. Haddadian, M.H.S. Ismail, N. Abdullah, Z.Z. Abidin, Removal of Fe(III), Mn(II), and Zn(II) from palm oil mill effluent (POME) by natural zeolite, *Journal of the Taiwan Institute of Chemical Engineers* 43, (2012) 750-759
5. Abdullahi T., Harun Y., Othman M.H.D., A review on sustainable synthesis of zeolite from kaolinite resources via hydrothermal process, *Advanced Powder Technology* 28(8) (2017) 1827-1840 DOI:10.1016/j.apt.2017.04.028
6. Bentonite. [online] [cit. 25.4.2019]. Available online : <<http://www.imerys-additivesformetallurgy.com/our-resources/bentonite/>>
7. Buzetzky, D., Tóth, N. C., Nagy, N. M., & Kónya, J. (2018). Application of Modified Bentonites for Arsenite (III) Removal from Drinking Water. *Periodica Polytechnica Chemical Engineering*, 63(1), 113–121.doi:10.3311/ppch.12197
8. Bergaya F., Theng BKG., Lagaly G., Cation and anion exchange, *Handbook of clay science*, (2006) 979-1001 DOI: 10.1016/S1572-4352(05)01036-6
9. Sun J.L., Zhuang G.Z., Wu S.Q., Zhang Z.P., Structure and performance of anionic-cationic-organo-montmorillonite in different organic solvents, *RSC Advanced* (2016) 54747-54753. DOI: 10.1039/c6ra05364e
10. Zhang H.L., Yu J.Y., Kuang D.L., The Effect of Sodium and Organic Montmorillonites on the Thermal Aging Properties of Bitumen, *Petroleum Science and Technology* 31 (2013) 2074-2081 DOI: 10.1080/10916466.2012.678538
11. Petra L., Billik P., Melichova Z., Komadel P., Mechanochemically activated saponite as materials for Cu<sup>2+</sup> and Ni<sup>2+</sup> removal from aqueous solutions, *Applied Clay Science* 143 (2017) 22-28 DOI: 10.1016/j.clay.2017.03.012
12. Bentonite. [online] [cit. 9.4.2019]. Available online: <<https://en.wikipedia.org/wiki/Bentonite>>

## *Badanie z użyciem XPS (roentgenowskiej spektroskopii fotoelektronowej) usuwania jonów z wody za pomocą zeolitów i bentonitów*

*Zeolity należą do rodziny uwodnionych minerałów glinowokrzemianowych, zawierających metale alkaliczne oraz alkaliczno-ziemne. Są zauważane ze względu na ich zdolność wymiany jonowej oraz odwrotnej dehydratacji. Ich struktura zawiera wewnątrznie połączone wgłębienia zajęte przez duże kationy metali oraz cząsteczki wody. Bentonity to ily tworzone często poprzez alterację popiołu wulkanicznego, zawierające głównie minerały smektytu a zazwyczaj montmorillonitu. Wykazują silne właściwości koloidalne a ich objętość wzrasta kilkukrotnie podczas wejścia w kontakt z wodą, tworząc w ten sposób galaretowatą i lepłą ciecz. Specjalne właściwości bentonitu (hydratacja, puchnięcie, absorpcja wody, lepkość, tiksotropia) powodują, że jest to cenny materiał dla szerokiej gamy zastosowań. Celem tego artykułu jest udokumentowanie zdolności zeolitów oraz bentonitów do usuwania jonów żelaza oraz różnych innych zanieczyszczeń z wody. Analiza powierzchni zeolitu i bentonitu została wykonana za pomocą bardzo czułego urządzenia analitycznego – XPS (roentgenowska spektroskopia fotoelektronowa)*

**Słowa kluczowe:** XPS, bentonit, zeolit, żelazo, adsorpcja XPS, bentonit, zeolit, żelazo, adsorpcja



# What Antibiotic Threat Do the Heavy Metals Contaminated Sites of Mine Hide?

Ivana TIMKOVÁ<sup>1)</sup>, Miroslava LACHKÁ<sup>1)</sup>, Lea NOSÁLOVÁ<sup>1)</sup>,  
Lenka MALINIČOVÁ<sup>1)</sup>, Peter PRISTASŠ<sup>1)</sup>, Jana SEDLÁKOVÁ-KADUKOVÁ<sup>1)</sup>

<sup>1)</sup> Pavol Jozef Šafárik University in Košice, Faculty of Science, Šrobárova St. 2, 041 80 Košice, Slovak Republic; email: ivana.timkova1@student.upjs.sk, miroslava.lachka@student.upjs.sk, lea.nosalova@student.upjs.sk, lenka.malinicova@upjs.sk, peter.pristas@upjs.sk, jana.sedlakova@upjs.sk

<http://doi.org/10.29227/IM-2020-01-68>

Submission date: 02-01-2020 | Review date: 28-02-2020

## Abstract

The environment contaminated by antibiotics and heavy metals as a consequence of human activities is of great concern nowadays. Many pieces of research proved that the environment could act as a reservoir of antibiotic resistance determinants allowing them to spread among different bacterial species via the process called horizontal gene transfer. The result is antibiotic resistance even in pathogen microorganisms. Heavy metals act as important factors in this process because of their potential to select antibiotic resistant bacteria thanks to linkage among antibiotic resistance genes and heavy metals resistance genes.

Thus, this experiment was conducted to screen the antibiotic tolerance profile of bacteria obtained from heavy metal contaminated environment of mine, dump and the contaminated soil near the entry of mine.

Several samples were collected from the only active gold mine in Slovakia in Hodruša – Hámre. The presence of cultivable bacteria was proved via cultivation approaches with subsequent MALDI – TOF MS (Matrix – Assisted Laser Desorption/Ionisation Time of Flight Mass Spectrometry) identification of selected isolates. Representative bacterial isolates were screened for their antibiotic tolerance against chosen antibiotics (ampicillin (AMP), chloramphenicol (CHLOR), tetracycline (TET) and kanamycine (KAN)) with the aim to define their minimal inhibitory concentration (MIC).

The cultivable bacteria from studied environments were dominated by Gram-negative proteobacteria of *Pseudomonas* and *Rhizobium* genera. Among more than 150 isolates the resistance to ampicillin (MIC>100µg/ml – 49% isolates), kanamycine (MIC>100µg/ml – 18% isolates), and chloramphenicol (MIC>20µg/ml – 16% isolates) dominated. The resistance to tetracycline (MIC>20µg/ml) was detected in less than 1% of isolates. Overall counts of antibiotic resistance and multi-resistance were alarmingly high taking in account that industrial environments with no known antibiotic exposure were analysed.

Our data indicate that heavy metals contaminated environment could influence the occurrence and the spread of antibiotic resistance. Possibly, metal contaminated environment act as a reservoir of antibiotic resistant bacteria.

**Keywords:** mines, antibiotic resistance, heavy metals resistance, cross resistance, heavy metals contamination

## Introduction

Increased industrialization and urbanization have led to substantial quantities of toxic pollutants which are continuously released into the environment worldwide. Some of these compounds occur naturally, but many of them are present in the nature due to anthropogenic activities, especially mining activities. Although mining provides irreplaceable economic and social benefits, its long-term unfavorable impact on the environment cannot be underestimated (Fashola et al. 2016).

Manganese, copper, cobalt, zinc or nickel are essential metals inevitable for growth of microbes, but their higher concentrations in the environment have poisonous effects on not only bacteria, but also on human health (Hobman a Crossman 2015).

Microorganisms are the first line organisms affected by heavy metals contamination. It has also been reported that microbial communities are more influenced by high heavy metals concentrations compared to fungal communities (Piotrowska-Seget et al. 2005; Rajapaksha et al. 2004). In order to survive such hostile conditions of the environment, bacteria were forced to evolve various mechanisms to withstand potentially lethal circumstances (Gadd 2010). These mechanisms include the efflux of metal ions outside the cell, accumulation and complexation of the metal ions inside the cell, reduction of the heavy metal ions to a less toxic state etc. (Issazadeh et al. 2013). Resistance genes

coding for these mechanisms are often found on plasmids. But so are the antibiotic resistance genes (Foster 1983; Ghosh et al. 2000; Stepanauskas et al. 2005; Baker-Austin et al. 2006; Stokes a Gillings 2011; Sandegren et al. 2012). Thus, the close co-occurrence of these two different resistance determinants on the same mobile genetic element together with their physical linkage result in the co-selection also in the case, when only one resistance determinant is being selected by the conditions of the environment (Baker-Austin et al. 2006). And thanks to their location on the mobilizable genetic element, they may be transferred together in the process of horizontal gene transfer between different bacterial communities, even pathogenic ones (Suzuki et al. 2012; Andersson a Hughes 2014). Another potential mechanism involved in the selection and proliferation of antibiotic resistance in the conditions of heavy metals contamination, is cross-resistance. This mechanism could manifest itself through efflux of structurally dissimilar compounds using the same mechanism – efflux pumps, which are relatively non-specific and they are able to pump out of the cell antibiotics and heavy metals in order to lower their intracellular concentration (Baker-Austin et al. 2006). Observational studies showed, that antibiotic resistant bacteria are more often found at locations contaminated with metals (Stepanouskas et al. 2005; Hölzel et al. 2012; Zhu et al. 2013) in comparison with non-metal contaminated areas, what suggest, that

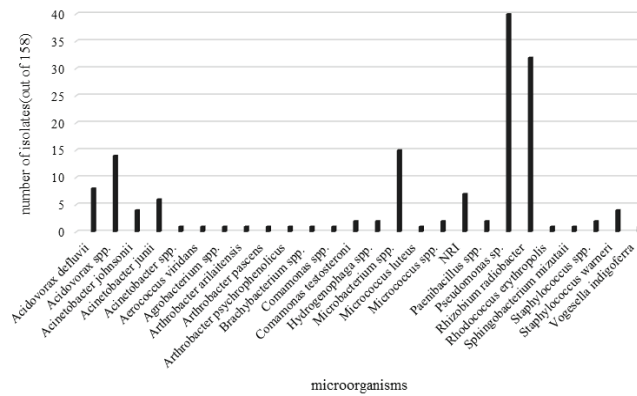


Fig. 1 MALDI-TOF MS identification of bacteria  
Rys. 1. Identyfikacja bakterii MALDI – TOF MS

heavy metals may be an additional factor indirectly selecting for antibiotic resistance (Alonso et al. 2001). Accordingly, accumulation of antibiotic resistance genes in soil environment and their assumed linkage to metal resistance genes in microbiota are of concern. Hence, the main objective of this study was to screen the antibiotic tolerance profile of bacteria obtained from heavy metals contaminated environment of mine, dump and the contaminated soil near the entry of mine.

#### Materials and methods

Two soil samples from the mine, one sample from the dump located near the mine and one sample of the contaminated soil near the entry of mine were collected from the only active gold mine in Hodruša – Hámre, Slovakia (GPS N 48°45.658' E 18°85.166').

Approx. 50 g of each sample were collected from the top layer (5–10 cm) into the sterile ziplock bag. After the collection, the samples were kept on ice and transported to the laboratory, where the material was processed until 24 hours.

1 g of thoroughly homogenized sample was suspended in 10 ml PBS-T and intensively shaken for 30 minutes. Then, 50µl of appropriate serial 10-fold dilutions of soil suspensions were plated onto the TSA (Tryptic Soy Agar), NA2 (Nutrient Agar no. 2), 100x diluted NA2 agar and R2A (Reasoner's 2A agar) agar plates, which were cultivated at 25°C for 48 hours. After the cultivation, based on the variable phenotype of bacterial colonies, 40 isolates from each type of cultivation media from one sampling site were selected (i. e. 160 isolates per one sampling site) for MALDI – TOF MS (Matrix – Assisted Laser Desorption/Ionisation Time of Flight Mass Spectrometry) identification. After the MALDI – TOF MS identification, representative isolates from each clade of phylogenetic tree were tested for their antibiotic tolerance. Antibiotic tolerance testing of bacterial isolates was performed on MH (Mueller-Hinton) agar using dilution method with the addition of antibiotics – ampicillin (AMP), chloramphenicol (CHLOR), tetracycline (TET) and kanamycine (KAN). Antibiotics were added to the medium in an appropriate amount to the achievement of final concentrations of antibiotics in the medium. Concentrations of antibiotics were as follows: AMP – 10, 20, 50, 100 µg/ml; CHLOR – 1, 2, 5, 10, 20 µg/ml; TET – 2, 5, 10, 20, 50 µg/ml and KAN – 5, 10, 20, 50, 100, 200 µg/ml. The plates were incubated in the dark at 25°C for 48 hours and then the growth of bacterial isolates was evaluated.

#### Results and discussion

In our experiments, using MALDI-TOF MS analysis of bacterial isolates, we identified cultivable microflora of studied environments. Our isolates were dominated by Gram-negative bacteria of *Pseudomonas* and *Rhizobium* genera followed by Gram-positive *Microbacterium* sp. microorganisms (Figure 1). Tomova et al. (2015) in their study of bacteria obtained from sediment and soil samples of Antarctic island also determined *Pseudomonas* genus as the most prevalent one. On the other hand, Safari Sinegani and Younessi (2017) in the research of microbial antibiotic resistance present in different soils samples observed the prevalence of *Bacillus* spp., *Micrococcus* spp. and *Staphylococcus* spp genera.

Furthermore, they detected TET resistance in the majority of the isolates cultivated from mine soil samples (44.33%), whereas in our research, this tolerance was found as the lowest one (less than 1% of overall number of isolates) (Figure 2). However, our findings are in accordance with Berg et al. (2005), who determined AMP resistance as the most abundant one; nearly 100% of their Cu-resistant microorganisms were resistant to AMP. In our experiments, AMP resistance was also observed as the predominant one, but with only 49% of tolerable microorganisms able to withstand antibiotic concentrations higher than 100 µg/ml. Berg et al. also noticed that Cu-resistant bacteria had a significantly higher occurrence of multiple antibiotic resistances, what was confirmed later in 2010 (Berg et al. 2010). This study also defined CHLOR resistance as the second most prevalent with nearly 80% of resistant microorganisms at the concentration 16 µg/ml, what is significantly more than in case of our bacteria, which resembled tolerance to this antibiotic at the concentration > 20 µg/ml in only 16%. Similarly high CHLOR tolerance pattern as in the case Berg et al. was observed in Tomova et al. (2015) – in 58% of the isolates. Inversely, only 8% resistance was observed in their KAN testing (30 µg/ml), whereas our study revealed 18% tolerance to > 100 µg/ml of this antibiotic.

#### Conclusion

Taking in account industrial habitat with no known antibiotic exposure, the results revealed alarmingly high antibiotic resistance and multi-resistance pattern in bacteria. Microorganisms exposed to elevated concentrations of heavy metals in their natural habitat are forced to develop resistance mechanisms maintaining their fitness even under the stressful conditions of

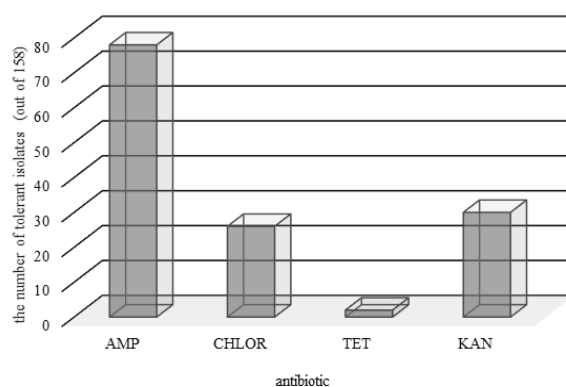


Fig. 2. Antibiotic tolerance of bacteria  
Rys. 2. Tolerancja bakterii na antybiotyki

the environment. The widespread presence of metal resistance mechanisms is of concern because of the linkage between metal resistance genes and antibiotic resistance genes, what makes this issue interesting also from the medical point of view. Linkage and subsequent interspecific co-transfer of these two groups of genes via the horizontal transport could become a serious health problem which can cause difficulties with the therapy of bacterial diseases in human. Our data indicate that heavy metals contaminated environment could influence the occurrence and the spread of

antibiotic resistance. Possibly, metal contaminated environment act as a reservoir of antibiotic resistant bacteria.

#### Acknowledgements

The work was fully supported by a grant from the Slovak National Grant Agency under the VEGA Project no. 1/0229/17 and a grant from the Slovak Research and Development Agency under the APVV Project no. 16-0171 and SK-PL-18-0012.



## Literatura – References

1. ANA ALONSO, Patricia Sánchez and José L. Martínez, Ana ALONSO a Patricia SA, 2001. Environmental selection of antibiotic resistance genes. *Environmental Microbiology*. 2001, roč. 3, s. 1–9.
2. ANDERSSON, Dan I. a Diarmaid HUGHES, 2014. Microbiological effects of sublethal levels of antibiotics. *Nature Reviews Microbiology* [online]. 2014, roč. 12, č. 7, s. 465–478. ISSN 17401534. Dostupné na: doi:10.1038/nrmicro3270
3. BAKER-AUSTIN, Craig, Meredith S. WRIGHT, Ramunas STEPANAUSKAS a J. V. MCARTHUR, 2006. Co-selection of antibiotic and metal resistance. *Trends in Microbiology* [online]. 2006, roč. 14, č. 4, s. 176–182. ISSN 0966842X. Dostupné na: doi:10.1016/j.tim.2006.02.006
4. BERG, J., A. TOM-PETERSEN a Ole NYBROE, 2005. Copper amendment of agricultural soil selects for bacterial antibiotic resistance in the field. *Letters in Applied Microbiology* [online]. 2005, roč. 40, č. 2, s. 146–151. ISSN 02668254. Dostupné na: doi:10.1111/j.1472-765X.2004.01650.x
5. BERG, Jeanette, Maja K. THORSEN, Peter E. HOLM, John JENSEN, Ole NYBROE a Kristian K. BRANDT, 2010. Cu exposure under field conditions coselects for antibiotic resistance as determined by a novel cultivation-independent bacterial community tolerance assay. *Environmental Science and Technology* [online]. 2010, roč. 44, č. 22, s. 8724–8728. ISSN 0013936X. Dostupné na: doi:10.1021/es101798r
6. FASHOLA, Muibat Omotola, Veronica Mpoke NGOLE-JEME a Olubukola Oluranti BABALOLA, 2016. Heavy metal pollution from gold mines: Environmental effects and bacterial strategies for resistance. *International Journal of Environmental Research and Public Health* [online]. 2016, roč. 13, č. 11. ISSN 16604601. Dostupné na: doi:10.3390/ijerph13111047
7. FOSTER, T.J., 1983. Plasmid-Determined Resistance to Antimicrobial Drugs and Toxic Metal Ions in Bacteria. *Microbiology and molecular biology reviews* [online]. 1983, roč. 47, č. 3, s. 361–409. ISSN 0146-0749. Dostupné na: doi:10.1016/s1473-3099(05)70243-7
8. GADD, Geoffrey Michael, 2010. Metals, minerals and microbes: Geomicrobiology and bioremediation. *Microbiology* [online]. 2010, roč. 156, č. 3, s. 609–643. ISSN 13500872. Dostupné na: doi:10.1099/mic.0.037143-0
9. GHOSH, Anjali, Amarika SINGH, P. W. RAMTEKE a V. P. SINGH, 2000. Characterization of large plasmids encoding resistance to toxic heavy metals in *Salmonella abortus equi*. *Biochemical and Biophysical Research Communications* [online]. 2000, roč. 272, č. 1, s. 6–11. ISSN 0006291X. Dostupné na: doi:10.1006/bbrc.2000.2727
10. HOBMAN, Jon L. a Lisa C. CROSSMAN, 2015. Bacterial antimicrobial metal ion resistance. *Journal of Medical Microbiology* [online]. 2015, roč. 64, č. 2014, s. 471–497. ISSN 00222615. Dostupné na: doi:10.1099/jmm.0.023036-0
11. HÖLZEL, Christina S., Christa MÜLLER, Katrin S. HARMS, Sabine MIKOLAJEWSKI, Stefanie SCHÄFER, Karin SCHWAIGER a Johann BAUER, 2012. Heavy metals in liquid pig manure in light of bacterial antimicrobial resistance. *Environmental Research* [online]. 2012, roč. 113, s. 21–27. ISSN 00139351. Dostupné na: doi:10.1016/j.envres.2012.01.002
12. ISSAZADEH, Khosro, Nadiya JAHANPOUR, Fataneh POURGHORBANALI, Golnaz RAEISI a Kamileh FAEKHONDEH, 2013. Heavy metals resistance by bacterial strains. *Annals of Biological Research*. 2013, roč. 4, č. 2, s. 60–63. ISSN 0976-1233.
13. PIOTROWSKA-SEGET, Z., M. CYCON a J. KOZDRÓJ, 2005. Metal-tolerant bacteria occurring in heavily polluted soil and mine spoil. *Applied Soil Ecology* [online]. 2005, roč. 28, č. 3, s. 237–246. ISSN 09291393. Dostupné na: doi:10.1016/j.apsoil.2004.08.001
14. RAJAPAKSHA, R. M C P, M. A. TOBOR-KAPŁON a E. BÅÅTH, 2004. Metal toxicity affects fungal and bacterial activities in soil differently. *Applied and Environmental Microbiology* [online]. 2004, roč. 70, č. 5, s. 2966–2973. ISSN 00992240. Dostupné na: doi:10.1128/AEM.70.5.2966-2973.2004
15. SAFARI SINEGANI, Ali Akbar a Nayereh YOUNESSI, 2017. Antibiotic resistance of bacteria isolated from heavy metal-polluted soils with different land uses. *Journal of Global Antimicrobial Resistance* [online]. 2017, roč. 10, s. 247–255. ISSN 22137173. Dostupné na: doi:10.1016/j.jgar.2017.05.012
16. SANDEGREN, Linus, Marius LINKEVICIUS, Birgitta LYTSY, Åsa MELHUS a Dan I. ANDERSSON, 2012. Transfer of an *Escherichia coli* ST131 multiresistance cassette has created a *Klebsiella pneumoniae*-specific plasmid associated with a major nosocomial outbreak. *Journal of Antimicrobial Chemotherapy* [online]. 2012, roč. 67, č. 1, s. 74–83. ISSN 03057453. Dostupné na: doi:10.1093/jac/dkr405
17. STEPANAUSKAS, Ramunas, Travis C. GLENN, Charles H. JAGOE, R. Cary TUCKFIELD, Angela H. LINDELL a J. V. MCARTHUR, 2005. Elevated microbial tolerance to metals and antibiotics in metal-contaminated industrial environments. *Environmental Science and Technology* [online]. 2005, roč. 39, č. 10, s. 3671–3678. ISSN 0013936X. Dostupné na: doi:10.1021/es048468f
18. STOKES, Hatch W. a Michael R. GILLINGS, 2011. Gene flow, mobile genetic elements and the recruitment of antibiotic resistance genes into Gram-negative pathogens. *FEMS Microbiology Reviews* [online]. 2011, roč. 35, č. 5, s. 790–819. ISSN 01686445. Dostupné na: doi:10.1111/j.1574-6976.2011.00273.x
19. SUZUKI, Satoru, Midori KIMURA, Tetsuro AGUSA a Habibur M. RAHMAN, 2012. Vanadium accelerates horizontal

transfer of tet(M) gene from marine Photobacterium to Escherichia coli. FEMS Microbiology Letters [online]. 2012, roč. 336, č. 1, s. 52–56. ISSN 03781097. Dostupné na: doi:10.1111/j.1574-6968.2012.02653.x

20. TOMOVA, Iva, Margarita STOILOVA-DISHEVA, Irina LAZARKEVICH a Evgenia VASILEVA-TONKOVA, 2015. Antimicrobial activity and resistance to heavy metals and antibiotics of heterotrophic bacteria isolated from sediment and soil samples collected from two Antarctic islands. *Frontiers in Life Science* [online]. 2015, roč. 8, č. 4, s. 348–357. ISSN 21553777. Dostupné na: doi:10.1080/21553769.2015.1044130
21. ZHU, Yong-Guan, Timothy A. JOHNSON, Jian-Qiang SU, Min QIAO, Guang-Xia GUO, Robert D. STEDTFELD, Syed A. HASHSHAM a James M. TIEDJE, 2013. Diverse and abundant antibiotic resistance genes in Chinese swine farms. *Proceedings of the National Academy of Sciences* [online]. 2013, roč. 110, č. 9, s. 3435–3440. ISSN 0027-8424. Dostupné na: doi:10.1073/pnas.1222743110

## *Jakie zagrożenie dla działania antybiotyków stanowią górnicze tereny zanieczyszczone metalami ciężkimi?*

Środowisko zanieczyszczone przez antybiotyki i metale ciężkie jako konsekwencja działalności ludzkiej jest obecnie przedmiotem wielu zmartwień. Wiele badań udowodniło, że środowisko może stanowić swoisty zbiornik odporności bakterii na działanie antybiotyków, pozwalając im na swobodne rozprzestrzenianie się wśród różnych bakterii poprzez proces zwany poziomym transferem genów. Wynikiem jest obecność odporności na antybiotyki nawet u mikroorganizmów patogenicznych. Metale ciężkie działają jako ważne czynniki w tym procesie ze względu na swój potencjał wyboru bakterii, która opiera się antybiotykowi ze względu na swego rodzaju połączenie pomiędzy genami opierającymi się antybiotykowi oraz genami opierającymi się metalom ciężkim. Zatem, wykonano eksperyment aby zbadać tolerancję na antybiotyk dla bakterii uzyskanych ze środowiska kopalni, składowiska oraz gleby z pobliza kopalni będących zanieczyszczonymi metalami ciężkimi. Pobrano próbki z jedynej aktywnej kopalni złota w Słowacji, zlokalizowanej w Hodruša – Hámre. Obecność bakterii kultywacyjnych został udowodniony za pomocą badań kultywacji a następnie techniki identyfikacyjnej MALDI – TOF MS (Matrix – Assisted Laser Desorption/Ionisation Time of Flight Spectrometry). Reprezentatywne izolaty bakteryjne zostały zbadane ze względu na ich tolerancję na wybrane antybiotyki (ampicylina (AMP), chloramfenikol (CHLOR), tetracyklina (TET) oraz kanamycyna (KAN) w celu zdefiniowania ich minimalnego stężenia inhibicyjnego (MIC). Bakterie kultywacyjne z badanych środowisk były zdominowane przez Gram-ujemne proteobakterie rodzaju *Pseudomonas* oraz *Rhizobium*. Spośród więcej niż 150 izolatów, odporność na ampicylinę (MIC > 100 µg/ml - 49% izolatów), kanamycynę (MIC > 100 µg/ml – 18% izolatów) oraz chloramfenikol (MIC > 20 µg/ml – 16% izolatów) dominowała. Odporność na tetracyklinę (MIC > 20 µg/ml) został stwierdzony w mniej niż 1% przypadku izolatów. Ogólna liczba odporności na antybiotyki oraz multi-odporności była alarmująco duża, biorąc pod uwagę, że środowiska przemysłowe z nieznanym stopniem wystawienia na antybiotyki była analizowana. Nasze dane wskazały, że środowisko zanieczyszczone metalami ciężkimi może wpływać na obecność i rozwój odporności na antybiotyki. Możliwym jest, że środowisko zanieczyszczone metalami zachowuje się jak zbiornik dla bakterii odpornych na działanie antybiotyków.

**Słowa kluczowe:** kopalnie, odporność na antybiotyki, odporność na metale ciężkie, odporność krzyżowa, metale ciężkie



# Quantifying Mineral Liberation – A Conventional and New Automatic Sophisticated Techniques Approach

Rudolf TOMANEC, Marina BLAGOJEV<sup>1)</sup>

<sup>1)</sup> Institute for Technology of Nuclear and Other Mineral Raw Materials, Franchet d'Esperey 86, 11000 Belgrade, Serbia;  
email: marina.blagojev@rgf.rs

<http://doi.org/10.29227/IM-2020-01-72>

Submission date: 01-02-2020 | Review date: 12-04-2020

## Abstract

*The characterization of textural properties of minerals is closely related to the process of their respective liberation. Measurements of mineral liberation, related to grinded ore, can be performed using optical ore microscope, by conventional, classical methods – point counting, linear intercepts method or planimetric measurements method (2D). Modern automatic devices and sophisticated measurement techniques (QEMSCAN/MLA) imply recording free surfaces area of mineral grains on polished sections samples in order to determine mineral degree of liberation. Value of mineral liberation obtained over free surfaces area can be of interest to flotation concentration, although not for gravity separation or, for example, magnetic separation. The prediction accuracy for behavior of one feed ore during the concentration process depends on the method of measuring/recording mineral liberation. Considering raw materials with complex textural characteristics it is crucial which method will be applied for determination of mineral liberation respecting whether for concentration process is crucial physical or chemical method.*

**Keywords:** mineral liberation, free surface area, texture characterization, prediction, ore microscopy

## Introduction

The calculation of the mineral liberation degree of the given mineral is made on representative samples of a classified grinded ore, on polished surfaces of mineral grain cross-sections (2D) applying the ore microscopy. Measurements are performed using point counting (Glagolev-Chayes method), linear intercepts method (The Rosiwal-Schand method) or planimetric measurements method (De Lesse method). After measurements have been performed, so called Gaudin correction coefficient- the stereological error correction is added. Based on the measurements of the liberation degree of the mineral of interest, it is possible to predict the behaviour of the raw material during the concentration and predict the quality of the future concentrate, i.e. the loss causes of the useful mineral in the tailings. Nowadays, due to current devices and sophisticated techniques of automatic characterization of minerals (QEMSCAN/MLA) some researchers (Al Cropp, 2013.) determine the calculation of mineral liberation on the basis of the size of free surfaces area of the mineral of interest. Namely, the total mineral surface area whereby a flotation reagent can make a direct contact is determined. This "calculation of liberation" (obtained over the size of free surface area of the mineral of interest particles) can point to possible (high) recovery, but at the same time to the very low quality of the concentrate. Figure 1 shows the concept according to which the categories of calculation of mineral liberation, measured over the size of free surface areas, can be compared with conventional understanding of the mineral liberation (modified Cropp, 2013).

According to conventional, widely accepted definitions of liberation of the given mineral in the ground ore, the raw material grains/particles cannot be liberated partially, i.e. more or less, in a very wide range (from a few percents to almost

completely free). Multiphase grain/particle is always non-liberated, middling particle, which can be classified as intermediate product and sent to regrinding – additional liberation. Therefore, the intergrown grains cannot be further classified into classes according to the liberation degree of the mineral of interest. They can be categorized into groups according to the size of the free surface areas, regarding the external contacts over which the mineral grains can interact with the reagents for concentration. For the category of intergrown grains, only the percentage (volume, mass) average-middle share of the measured mineral in the intergrowths can be expressed, for all the measured intergrown grains, or these data can be classified into certain group intervals (interval of 10%). The figure 1, showing example of simulated particles containing ore mineral grains classified by both – degree of liberation and the free surface area.

## Methods of measurement

Mineral liberation determination. The distribution of linear intercept lengths on polished sections of the feed ore samples gives a very useful characterization of the mineralogical texture such as grain and crystal aggregate sizes and shape, specific surface areas, mineral-mineral association, surface coatings, proximity index, contiguity index, degree of liberation etc.

Calculation of the contiguity index. In order to enable the successful concentration of useful minerals from the raw material, it is necessary, before crushing, to determine a number of characteristics of associated minerals related to non grinded, raw ore, such as crystal size, shape, type of intergrowth, frequency and the complexity of contact surfaces of some mineral pairs and other structural characteristics like their distribution, etc.

	Free and intergrowth simulated particles classified by free surface area (external free contacts) (u %)	Locking characteristics of particles with ore and gangue Degree mineral liberation of particles classified at 100%, 75%, 50% and 25%			
		100%	75%	50%	25%
The mineral liberation of particles classified by free surface area, %	100% Free surface area of the mineralized particles (free external surface area)				
	75% Free surface area of the mineralized particles (free external surface area)				
	50% Free surface area of the mineralized particles (free external surface area)				
	25% Free surface area of the mineralized particles (free external surface area)				
	0% Free surface area of the mineralized particles (free external surface area)				

Fig. 1. The degree of mineral liberation and mineralized particles liberation by free surface area (free external surface area) – textural classifications, are a key driver in all mineral separation processis (modified after Al Cropp, 2013). Legend: marked particles, all 11, are intergrowth, not free. Conventional degree of liberation is 14.81%. At the same time the liberation of minerals expressed as a free surface area is 85.18%

Rys. 1. Stopień uwolnienia minerałów oraz ziaren zmineralizowanych za pomocą oceny zewnętrznej powierzchni wolnej – klasyfikacje tekstur są kluczowe we wszystkich procesach przeróbki mineralnej (poprawione wg AlCropp, 2013). Legenda: zaznaczone ziarna, których jest 11, są zrostami. Tradycyjny stopień uwolnienia wynosi 14,81%. Uwolnienie minerałów wyrażone jako pole powierzchni wolnej wynosi 85,18%

Textural characterization of ore-contained minerals can be performed and represented by descriptive (Amstutz, 1960; Craig and Vaughan, 1994; Amstutz and Giger, 1972), and accurate numerical data which are commonly more convenient for operating engineers. For a mineral liberation prediction based on microscopy of the textural-structural properties of the ore, one must determine: first, the mode and degree of mineral intergrowth; secondly, the minerals which intergrow with mineral of interest in the technological process, when the ore contains deleterious components.

Associations of the selected pairs of minerals may be expressed by the "contiguity index" or, as termed by some authors (Gurland, 1958), "intergrowth, locking or proximity index" witch is approximately the same as the connectivity (Amstutz and Giger; 1972). Where ground ore is concerned, this index is closely related to the free surface area of the selected mineral and its relationship with other associated minerals. The contiguity index relates the given grain surface area of the selected mineral and its total surface. This parameter is useful for parent ore, as the input processing material, to predict the mineral liberation, and even more for the analysis of liberation from comminuted ore to characterize the intergrown grains.

The coordination number or coordination index (Jeulin, 1981), has been extensively used in textural characterizations of various rocks (Amstutz and Giger, 1972) and their classifications. Thus the coordination number between  $A_i$  and  $A_k$  phases is given by the relation:

$$K_{(A_i, A_k)} = \frac{N_{(A_i, A_k)} \cdot N}{N_{i, \dots} \cdot N_{j, \dots}}$$

where:

$N_{(A_i, A_k)}$  – number of contacts between  $A_i$  and  $A_k$ ,

$N$  – total number of investigated grains,

$N_{(A_i)}$  – number of grains  $A_i$ ,

$N_{(A_k)}$  – number of grains  $A_k$ .

Contiguity index of mineral A to mineral B can be written (Gurland, 1958; Jones and Barbery, 1975) as:

$$V_{A/B} = S_{A,B}/S_A = S_{V(A,B)}/S_{V(A)}$$

or

$$P_{A/B} = S_{A/B} \cdot 100/S_A$$

where

$V_{A/B}$  – is the proximity index,

$S_{(A,B)}$  – is the surface area of A in contact with B,

$S_A$  – is the total surface area of mineral A;

$S_{V(A,B)}$  – is the specific surface area of A in contact with B (i.e. the contact area per unit volume of A),

$S_{V(A)}$  – is the specific surface area of A, and

$P_{A/B}$  – proximity index of minerals A and B (%).

The specific surface area of mineral is calculated from the relation (Jones and Barbery, 1975):

$$S_{V(A)} = S_{(A)}/V_{(A)} = 4/\bar{L}_{(A)}$$

where

$S_{V(A)}$  – specific surface area of mineral A,

$S_{(A)}$  – total surface of mineral A,

$V_{(A)}$  – volume of A, and

$\bar{L}_{(A)}$  – mean intercept length on mineral A.

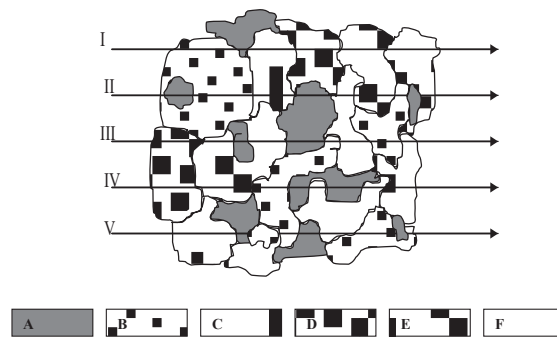


Fig. 2. Illustration of contiguity index measurement on a simulated surface area of a polished section of an raw ore (Amstutz and Giger; 1972). Legend: Polished sections of on multiphasic feed ore samples; Linear Rosiwal-Schand method of measurement; The target mineral is red phase A; The set of parallel test lines across each grain on the surface of polished section I – V; Polimineral raw ore with 5 tipe of minerals, from A to F phase; Phase A – the target, mineral of interest

Rys. 2. Ilustracja pomiaru wskaźnika przyległości wykonanego na symulowanym polu powierzchni wypolerowanego przekroju rudy (Amstutz i Giger, 1972). Legenda: wypolerowane przekroje próbek wielofazowej nadawy rudy; liniowa metoda pomiaru Rosiwala-Schanda; minerały celowe są czerwoną fazą A; zbiór równoległych linii testowych wzdłuż każdego ziarna na powierzchni wypolerowanego przekroju I – V; wielomineralna ruda z pięcioma typami minerałów, od fazy A do F; Faza A – cel, czyli mineral będący przedmiotem zainteresowania

Along a set of parallel lines across the surface of an ore polished section, volume percentages of minerals were measured and their textures characterized, and the number of contact points, both internal and external, on the set lines was registered. The number of transitions from one phase to another, or one mineral into another, was registered with the purpose of defining mineral association across the contact areas of mineral grains in the analyzed material (Fig. 2).

Sizes of contact areas of this association mineral pairs, as an important textural characteristic, are expressed by the contiguity index. A statistical processing of results (density of contact points) was used to calculate areas of direct contacts between mineral pairs in the analyzed ore. The calculated contiguity indices suggest the behaviour of the ore in crushing and grinding, the behaviour of each mineral during its liberation, and the effects of processing on the concentrate.

When the contiguity index among certain minerals is very low, due to the absence of the direct contact (genetic relationship) of the two given minerals, then the intergrown grains of these two minerals cannot be expected in the concentrate of the basic mineral as undesirable.

### Mineral liberation – prediction

The known value of the contiguity index for the given mineral can be used to deduce other ore characteristics. The empirical expression relating the degree of liberation for the given (selected) mineral phase ( $\alpha$ ) and the specific surface area (Steiner, 1975) is the following:

$$L_{\alpha}(D) = 1 - S_{V_{\alpha}}^{(i)}(D) / S_{V_{\alpha}}^{(e)}(D) \quad S_{V_{\alpha}}^{(e)}(D) > S_{V_{\alpha}}^{(i)}(D)$$

where:

$L_{\alpha}(D)$  – is the proportion of  $\alpha$  that is liberated at particle size (D),

$S_{V_{\alpha}}^{(i)}(D)$  – is the interfacial  $\alpha/\beta$  area per unit volume of  $\alpha$ , for particles of size (D),

$S_{V_{\alpha}}^{(e)}(D)$  – is the external surface area of  $\alpha$  per unit volume of  $\alpha$ , for particles of size (D).

Most of these (free) areas in the above relation can be estimated from either linear or planimetric measurements as mentioned earlier. It may be used to deduce the liberation by stereologic method following the expression (Steiner, 1975):

$$L_{\alpha}(D) = 1 - B_{\alpha}^{(i)}(D) / B_{\alpha}^{(e)}(D) = 1 - I_{\alpha}^{(i)}(D) / I_{\alpha}^{(e)}(D)$$

where:

$B_{\alpha}^{(i)}(D)$  – is the boundary length of  $\alpha/\beta$  interfaces measured on sections through particles of size (D),

$B_{\alpha}^{(e)}(D)$  – is the boundary length of  $\alpha$ /matrix interfaces measured on sections through particles of size (D),

$I_{\alpha}^{(i)}(D)$  – is the number of intersections of a test line with  $\alpha/\beta$  interfaces, for particles of size (D),

$I_{\alpha}^{(e)}(D)$  – is the number of intersections of a test line with  $\alpha$ /matrix interfaces, for particles of size (D).

Classical mineral liberation can be expressed by two different parameters: weight ratio and exposure ratio. In single particles, the former indicates the weight proportion of one mineral with regard to the total particle weight, while the latter quantifies the proportion of exposed perimeter occupied by this mineral (Perez-Barnuevo et al, 2012). The degree of mineral liberation and mineralized particles liberation by free surface area (free external surface area) – textural classifications, are a key driver in all mineral separation processes (Reyes et al, 2018).

A prediction of mineral liberation in ore grinding is possible on the basis of the identified distribution law (distribution of linear intercepts, and use of Gauss-Laplace probability function) and modeling the mineral texture (Tomanec and Milovanović, 1994).

Frequency distribution, classified intercept lengths and sample means provided, based on the identified lognormal distribution and the use of Gauss-Laplace integral probability function can be used the following:

$$F(d) = [\exp\{-(\log d - \log \bar{d})^2 / 2(\log \sigma)^2\}] / \{\log \sigma \cdot (2\pi)^{(1/2)}\}$$

for the prediction of particle size to which ore should be ground for the desired mineral liberation (Tomanec and Milovanović 1994a).

Where is:

$F(d)$  – normal distribution (probability) function,

$d$  – grain size diameter and  $\bar{d}$  – geometric mean intercept, ( $d = 1$ );

$\sigma$  – standard deviation.

## Results and discussion

In the past ten and more years, the mineral liberation has been expressed in two ways. The first, based on the volumetric/mass distribution of one mineral in free grains in relation to its total presence, in free and intergrown grains in the ore. The second way, adjusted to contemporary devices and sophisticated automatic measurement methods, based on the size of the free surface area, namely the external boundary zone of mineral particle contacts which can result in the contact of concentration reagents and the given mineral. In the 2D space, that is the grain perimeter, the size of the free peripheral line on the product surface. In real 3D conditions, all such grains are intergrowths, and they are by no means really free grains. Certainly, both methods of measurement contribute to the general characterization of mineral grains and indicate, i.e. provide a better evaluation of the mineral grains behaviour during their concentration, especially flotation.

The mass distribution of the measured free grain mineral in the sample is obtained by multiplying the results with the density of the given mineral, while the size of the measured perimeter (free edges) on the intergrown grains is obtained by putting in relation to the total free surface of the given miner-

al measured in the 2D level. Both perimeters can be calculated using Barbier's formula (Perez-Barnuevo et al, 2012).

## Conclusions

We should bear in mind that once obtained results of calculation of liberation of the given mineral must be interpreted adequately depending on the device or the recording method. The final values, as well as the integral mineral liberation, will not be comparable if the measurement is carried out by different methods.

At the same time, the prediction of the grinding fineness, the concentrate quality, the recovery, possible losses of useful minerals in the tailings will differ significantly depending on the method of liberation recording.

This paper, among other things, should serve to clarify how important the mineral textural characteristics of the preparation processes involved are, and how important it is to understand the relation of the mineral liberation and the size of the free surface areas of the mineral in the ground raw material.

The liberation and free surface areas of minerals are crucial for concentration processes and must be a high priority for engineers engaged in dressing processes.

## Literatura – References

1. AMSTUTZ, Gerhardt Christian. A geometric classification of basic intergrowth patterns of minerals. *Geotimes*, vol. 5, 1960. p. 24.
2. AMSTUTZ, Gerhardt Christian, GIGER, Hans. Stereological methods applied to mineralogy, petrology, mineral deposits and ceramics. *Journal of Microscopy*, vol. 95, 1972, p. 145-164.
3. CRAIG James; VAUGHAN David. *Ore Microscopy and Ore petrography*. 2nd edition. New York : John Wiley & Sons Inc, 1994. p. 434, ISBN 0-471-55175-9.
4. CROPP, Al. Liberation And Free Surface Area In The Float Feed. *Minassist*, [online]. Accessed 11.9.2018. Available at: <http://www.minassist.com.au/blog/liberation-and-free-surface-area-in-the-float-feed/> .
5. GURLAND, John: The measurement of grain contiguity in two-phase alloys. *Trans. Metallurgical Society of AIME*, Vol. 212, 1958, p.452-455.
6. JEULIN Dominique. *Mathematical morphology and multiphase materials*. 3rd European Symposium on Stereology, Ljubljana, 1981. p. 265–86.
7. JONES, M.P, BARBERY, Gilles. The size distribution and shapes of mineral in multiphase materials: particle determination and use in mineral process design and control. XIth International Mineral Processing Congress, Cagliari, 1975, paper 36.
8. PEREZ-BARNUEVO Laura, PIRARD Eric, CASTROVIEJO Ricardo. Textural Descriptors for Multiphase ore Particles. – *Image Anal Stereol* 31, 2012, p.175-184.
9. REYES Francisco, CILLIERS Jan., NEETHLING Steven. Quantifying mineral liberation by grade and surface exposure using X-ray micro-tomography for flotation processes, 29th International Mineral Processing Congress, 2018, Moscow – Russia, 2019, p. 3985-3994.
10. SPENCER, Stiven and SUTHERLAND, David. Stereological correction of mineral liberation grade distributions estimated by single sectioning of particles. *Image Anal Stereol*, 19, 2000, p. 175-182.
11. STEINER H J. Liberation, kinetics in grinding operations. XIth International mineral processing congress, Caligari, Ente Minerario Sardo, 1975, p. 35-58.
12. TOMANEC, Rudolf. Degree of Mineral Liberation Depending on Useful Component Concentration and Fineness of Grind, Faculty of Mining and Geology, University of Belgrade. Doctoral thesis, 1989.
13. TOMANEC Rudolf, MILOVANOVIĆ Jelica. Mineral liberation and energy saving strategies in mineral processing. *Physicochemical Problems of Mineral Processing Journal*, vol 28, and XXXI Polish Mineral Processing Symposium, Wroclaw - Poland, 1994, p. 195-205.
14. TOMANEC Rudolf, MILOVANOVIĆ Jelica. 1994a: Mineral liberation prediction based on texture characterization, 5th International Mineral Processing Symposium, Cappadocia - Turkey, 1994a, p 3-9.

### *Ocena uwolnienia minerałów – podejście konwencjonalne i nowe techniki automatyczne*

*Charakterystyka właściwości tekstury minerałów jest blisko związana z procesem ich uwolnienia. Pomiar uwolnienia minerałów powiązane są z mieleniem rudy i mogą być wykonane za pomocą mikroskopu optycznego przy zastosowaniu konwencjonalnych metod – liczenia punktów, metody linii przecięcia albo metody pomiarów planimetrycznych (2D). Nowoczesne urządzenia automatyczne, jak również wyrafinowane techniki pomiarowe (QEMSCAN/MLA) stosują pomiar pól powierzchni wolnych ziaren minerału na próbkach wypolerowanych przekrojów w celu określenia stopnia uwolnienia minerałów. Wartość tego uwolnienia otrzymana na podstawie pola powierzchni wolnej może być przedmiotem zainteresowania w kontekście prowadzenia procesu flotacji, aczkolwiek nie w przypadku wzbogacania grawitacyjnego, czy magnetycznego. Prawdliwość prognozy odnośnie zachowania rudy podczas procesu zależy od metody oceny uwolnienia minerałów. Biorąc pod uwagę surowce o skomplikowanej teksturze bardzo ważnym jest, którą metodę stosuje się w celu określenia stopnia uwolnienia minerałów pamiętając także o tym, czy dany proces jest oparty o metody fizyczne, czy też chemiczne.*

**Słowa kluczowe:** uwolnienie minerałów, pole powierzchni wolnej, charakterystyka tekstury, prognoza, mikroskopia rudy







# Determination of Risk Elements in Mine Waste Dump Soil Sample Using Sequential BCR Extraction

Barbora VALOVÁ<sup>1)</sup>, Iva KOTALOVÁ<sup>2)</sup>, Silvie HEVIÁNKOVÁ<sup>3)</sup>

<sup>1)</sup> VSB- Technical University of Ostrava, Faculty of Mining and Geology, 17. listopadu Str. 15, 708 33 Ostrava – Poruba, Czech Republic; email: barbora.val@seznam.cz

<sup>2)</sup> VSB- Technical University of Ostrava, Faculty of Mining and Geology, 17. listopadu Str. 15, 708 33 Ostrava – Poruba, Czech Republic; email: iva.kotalova@vsb.cz

<sup>3)</sup> VSB- Technical University of Ostrava, Faculty of Mining and Geology, 17. listopadu Str. 15, 708 33 Ostrava – Poruba, Czech Republic; email: silvie.heviankova@vsb.cz

<http://doi.org/10.29227/IM-2020-01-69>

Submission date: 28-12-2019 | Review date: 028-01-2020

## Abstract

The article deals with the determination of mobility of selected risk elements in soil samples of thermally active dump resulting from mining activities in the Ostrava region. The samples were taken from Hedvika dump during 2017 to 2018. Extraction of soil samples was performed using three-step sequential extraction of BCR (Bureau Community of Reference). Sequential extraction can provide information about the processes that normally take place in the environment. The solid soil component is gradually leached in the various extraction agents from the weakest to the strongest. This provides information on the total amount of risk elements potentially available under specific environmental conditions. Selected risk elements (Cr, Cu, Ni, Zn) were determined by ICP - MS method (Inductively coupled plasma mass spectrometry) and AAS (Atomic absorption spectrometry) (Zn). Nitric acid leaching was performed to supplement the total BCR extraction analysis.

**Keywords:** BCR sequence analysis, dump, ICP – MS, mobility, mining waste, risk elements, soil

## Introduction

Soil is an important component of the environment and forms the basis for human life on Earth.

The current problem of the soil environment is the strong civilization pressure behind many of the degradations. One of the forms is also chemical degradation of soil, which is caused by pollution, which also includes toxic metals. These are included in the list of global environmental issues.

The most important soil properties influencing the bio-availability and mobility of metals in soils include soil acidity (pH), oxidation and reduction processes as well as sorption properties of soils.

Potentially toxic metals are considered to be a significant source of environmental pollution, especially in urban areas where industry and mining are cumulative. Intensive deep mining of hard coal in the Ostrava-Karviná district (OKR) left behind a large amount of mining waste, mainly in heaps and dumps. The negative impact of dumps on the environment, besides land occupation and changes in landscape character, is primarily their thermal activity. This is often caused by un-professional intervention, for example due to poor sorting of waste. Spontaneous combustion can then occur primarily by aeration with carbon-rich carbon. Oxygen and water vapour are therefore critical factors for this process. The greatest amount of heat is released by the oxidation of unsaturated organic substances and is exothermic. [1] This is related to the release of toxic substances, the formation and spread of fine dust to the environment, the formation of burned-out cavities inside the dump, the risk of fire on the surface of the dump, the emergence and escape of large amounts of thermal energy,

the death of vegetation on the surface of the dump, sinks and dips, smoke, burns, etc. [2, 3]

However, the total content of metals, not just those at risk, in the ecosystem components is not entirely relevant information. In particular, in order to be harmful, the substance must be available for plants and animals. Therefore, bioavailability is being investigated. This is to what extent hazardous metals will be mobile in other environmental compartments and to what extent they are dangerous to the environment.

As part of the project, the thermally active dump of Hedvika was monitored. It is located on the eastern edge of the cadastral part of Radvanice and Michálkovice (Ostrava) in the cadastral districts of Chotěbuz and Zaryje. It lies on the border of the former districts of Ostrava and Karviná. The eastern part of Karviná is part of the Petřvald cadastre near Karviná. The exact date of foundation of the dump is unknown. The first mention dates back to 1903, from excavation and opening works. Probably the material from the digging of the pit and the opening of the Hedvika mine (the original name of the Albrecht Mine) was stored here. The surface was expanded from the original area of its own area Hedvika to the surroundings, especially in the northwest direction, directly to Michálkovice. At the turn of the 1960s and 1970s, a period of intense expansion of the dump into today's form occurred. Storage of tailings ended in 1998. [3, 4]

Hedvika dump forms a massive and flat-sprawling formation of about 32 ha. On the northern and western sides, it forms the border with the former J. Fučík Mine. It is then bordered by the Michalkovice-Petřvald road in the northeast. In the southwest it is adjacent to a mining site. At present,

the dump consists of a massive surface formation of gangue with an area of approximately 40.6 ha and an average height of disposed material in the range of 12–15 m. The mass is thus destined to produce smoke and endogenous fires. [4]

Thermal processes have been recorded in various parts of the dump since the 1950s. However, according to the preserved documentation, they were locally eliminated, mainly by firefighters, covering with an insulating layer or by extraction. However, these interventions could not completely prevent the massive development of thermal activity. The temperature at the focal point exceeds 500°C. The last experimental remediation of thermal activity in 2006 by flooding the outbreak of existing vapours with liquid clay suspension was not entirely effective. Thus, since 2010, temperature monitoring and thermal activity observation have been carried out on the dump by means of thermometric probes. [4, 5]

## Materials and Methods

### Sampling and sampling methodology

Samples were taken from the entire Hedvika area. Samples were taken from a depth of at least 10 cm. If the topsoil was present, it was removed with a spade. Subsequently, these samples were mixed to give a representative and mixed sample. Soil sampling was carried out according to ČSN ISO 10381-6 (836151) Soil Quality – Sampling – Part 6: Guidance for sampling, handling and storage of soil samples under aerobic conditions for the study of microbial processes, biomass and diversity in the laboratory. Subsequently, the samples were treated according to the ČSN ISO 11464 (836160) Soil Quality - Sample Preparation for Physico-chemical Analyses. Grain size was adjusted using Retsch stainless steel sieves with a grain size of 2 mm.

The treated samples were dried to constant weight in a MEMMERT oven at  $105 \pm 2$  °C for 2 hours. Samples were stored in a desiccator to prevent moisture sorption.

### Method to determine physical parameters of soil samples

Soil analyses were carried out as follows: dry matter and water content in the sample according to ČSN 11465 (836635) Soil quality – Determination of dry weight and soil moisture content – Gravimetric method; conductivity according to ČSN EN 13038 (836211) Soil quality were monitored in the soil analysis. Auxiliary Soil Substances and Substrates – Determination of Electrical Conductivity Using a WtW inoLab Cond.; pH value according to ČSN ISO 10390 (836221) Soil quality – Determination of pH and exchange capacity according to ČSN E ISO 14254 (836223). Soil Quality – Determination of exchange acidity in extracts with barium chloride, laboratory pH meter inoLab® pH 7110. Oxidation reduction potential (ORP) was measured using an MP-6 Hach Lange multimeter in mVH units. Hydrolytic soil reaction (Ha), exchange of basic cations (S), and maximum sorption capacity of exchangeable base cations (T) were calculated.

### BCR sequential extraction method

Sequential extraction can provide information about the processes that normally take place in the environment. Extraction of soil samples was performed by three-steps sequential BCR (Bureau Community of Reference) extraction. A modified version of the sequential extraction method was

used according to the procedure of Pueyo et al. [6] The procedure in the individual steps is given in Table 1.

### Methodology of risk metals analysis

For the analysis of the contents of hazardous metals, individual extracts of samples from the three-step sequential BCR extraction and extraction of samples from nitric acid ( $2.0 \text{ mol}^{-1}$ ) were used. Selected risk elements (Cr, Cu, Ni, Zn) were determined by mass spectrometry AAS (Zn) and inductively coupled plasma ICP - MS (Inductively coupled plasma mass spectrometers, X Series II, Thermo Scientific, Germany). The values were always measured 3 times, so the final values are the arithmetic means. The total metal content was determined by XRF method.

## Result and Discussion

### Results of physical parameters

The oxidation reduction potential ranged from +155 mV to +278 mV. The average ORP was around + 203 mV. Thus, it is the case of reduction conditions. The measured values did not have negative values, so it can be concluded that there will be no significant anaerobic processes in the soil. According to Blueberry [7], the soil environment can be evaluated as hypoxic, so it can be assumed that there will be a reduction of  $\text{FeOH}_3$  and  $\text{NO}_3^-$ . A characteristic feature will also be the slow decomposition of organic matter. If the ORP is increased, there may be significant oxygen loss and denitrification (nitrate reduction begins in the ORP range between +300 mV to +400 mV).

Conductivity values ranged from  $741 \mu\text{S cm}^{-1}$  to  $1395 \mu\text{S cm}^{-1}$ . The average value was about  $1,048 \mu\text{S cm}^{-1}$ . The values exceeded the limit value for soil with a higher salt content ( $120 \mu\text{S cm}^{-1}$ ), so we classify the soil on the Hedvika as heavily salted. As a result, there should be unfavourable conditions for plant growth and subsequent reclamation.

Soil reaction values ranged from 4.2 to 5.3. The mean value of the active soil reaction was around 5. This parameter is relatively constant in the period under review and there are no fluctuations. According to the classification of Blueberries [7] it is a strongly acidic active soil reaction. pH values from 4.2 to 5.0 may cause processes in the soil in which cation exchange capacity and basic cations from the sorption complex occur.

For the soil exchange reaction, the values varied between 4.0 and 4.8. The average soil reaction exchange rate was 4.5, a strongly acidic soil reaction. In general, the measured values of the soil exchange reaction are lower by 0.2 to 1.0 than the soil reaction. This phenomenon occurs because hydrogen protons bound in the sorption complex are also determined together with protons from the soil solution.

Potentially hydrolytic Ha soil reaction values ranged from  $35.8 \text{ mmol } 100 \text{ g}^{-1}$  to  $157.2 \text{ mmol } 100 \text{ g}^{-1}$ . The average value was about  $72 \text{ mmol } 100 \text{ g}^{-1}$ . All Ha values are very high and outweigh the Borůvka criteria [7]. It is therefore a very strong soil reaction.

The instantaneous exchangeable base cation contents ranged from  $54.7 \text{ mmol } 100 \text{ g}^{-1}$  to  $66.3 \text{ mmol } 100 \text{ g}^{-1}$ . The average value was about  $60.3 \text{ mmol } 100 \text{ g}^{-1}$ . These values also exceeded the table values, so this parameter can be classified as very strong.

Tab. 1. BCR sequence extraction in 1 g soil sample  
 Tab. 1. Ekstrakcja sekwencyjna BCR w próbce 1 g gleby

Step	Isolated fraction	Reagent used	Volume [ml]	Temperature [°C]	Extraction time
1	Exchange fraction and fractions bound to carbonates	0.11 M CH <sub>3</sub> COOH	40	22 (± 5)	Shaking for 16 h
2	Fractions bound to oxides and hydroxides of Fe / Mn - reducible fraction	0.1 M NH <sub>2</sub> OH·HCl acidified 2M HNO <sub>3</sub>	40	22 (± 5)	Shaking for 16 h
3	Fractions bound to organic matter and sulfides - oxidizable fraction	8.8 M H <sub>2</sub> O <sub>2</sub> , pH = 2	10	22 (± 5)	Extraction 1 h
				85 (± 5)	Extraction 1 h
		1 M NH <sub>4</sub> OAc, pH= 2	50	22 (± 5)	Shaking for 16 h

The saturation levels of the sorption complex were calculated from 78 to 94%. The average value was about 89%, and thus it is a fully saturated sample.

The maximum sorption capacity of the exchangeable basic cations was calculated as the sum of the degree of saturation of the sorption complex and the hydrolytic acidity. These values were between 63.7 mmol 100 g<sup>-1</sup> and 70.4 mmol 100 g<sup>-1</sup>. Due to high input values, exceeding the table values, this is a very high maximum sorption capacity.

#### Chemical parameters

The total chromium content was 104 mg kg<sup>-1</sup> of dry matter. The nitric acid leachate was 0.47 mg kg<sup>-1</sup> of dry matter. In the first BCR extraction step, the value was 2.07 mg kg<sup>-1</sup> of dry matter, in the second step the lowest measured value was 0.25 mg kg<sup>-1</sup> of dry matter. The highest value (7.27 mg kg<sup>-1</sup> of dry matter) was measured in the third step analysis step. Thus, a significant amount of chromium was released from the oxidizable fraction. Under anaerobic conditions, CrIV is reduced to CrIII. Metal mobility, toxicity, binding to organic matter, or low-solubility precipitates are also reduced.

The total copper value was 32.3 mg kg<sup>-1</sup> of dry matter. The highest measured value for the extract was 6.73 mg kg<sup>-1</sup> of dry matter. The lowest copper content was measured for the BCR analysis fraction of 0.66 mg kg<sup>-1</sup> of dry matter. In the second step, the value was 1.97 mg kg<sup>-1</sup> of dry matter. In the third step, the oxidizable fraction, the copper content was 3.53 mg kg<sup>-1</sup> of dry matter. Due to the high leachate values and low values found in the BCR analysis, it can be assumed that copper has low mobility. This metal is not released from the soil under normal conditions. From the third step, it is apparent that copper is strongly sorbed to clay materials.

Total nickel content in soil 25.5 mg kg<sup>-1</sup> of dry matter. The nitric acid extract was 2.13 mg kg<sup>-1</sup>. In the first step of the sequence analysis, the nickel content was 2.23 mg kg<sup>-1</sup> of dry matter, in the second step it increased to 3.00 mg kg<sup>-1</sup> of dry matter. In the third step, the oxidizable fraction, the highest

measured value was 3.59 mg kg<sup>-1</sup> of dry matter. In acidic soil, the mobility of nickel is more pronounced, but with increasing pH, a strong affinity for organic matter is manifested. This leads to the formation of solid complexes. This corresponds to the values of the third extraction step.

The values measured for the zinc content of the individual soil fractions ranged from 4 mg kg<sup>-1</sup> dry weight to 21 mg kg<sup>-1</sup> dry weight. The highest measured value (21 mg kg<sup>-1</sup> of dry matter) was from the leachate in nitric acid. The lowest value of 4 mg kg<sup>-1</sup> of dry matter was for the sample from the first step of the sequence analysis. In the second step, the zinc value was 12 mg kg<sup>-1</sup> of dry matter and in the third step 7 mg kg<sup>-1</sup> of dry matter was measured. The total zinc content of the soil was 94 mg kg<sup>-1</sup> of dry matter. In contrast to the other metals to be determined, zinc is likely to be reluctant in forming complexes with organic compounds.

#### Conclusion

It is true that soil reaction affects sorption and affects the availability and mobility of both nutrients and hazardous metals. It follows from the measured values that the soil at the back of Hedvika is acidic, and it can be assumed that the most accessible elements will be Fe, Mn, Cu and Zn. The activity of microorganisms and earthworms may slow down, resulting in deterioration of the soil structure. Furthermore, the content of bioavailable Cd, Zn and Pb will increase. In conclusion, however, it can be stated that none of the determined risk metals in the total concentration exceeded the values of the indicators from the methodological guideline of the Ministry of the Environment. However, it should be noted that these are areas with high loading with salts, which may have negative effects on vegetation growth.

#### Acknowledgements

This article is written as part of the projects no. CZ.11.4.120/0.0/0.0/15\_006/0000074 TERDUMP Spolupráce VŠB-TUO/GIG Katowice na průzkumu hořčících hald na obou stranách společné hranice. [8]

## Literatura – References

1. TRÁVNÍČKOVÁ, J. Transport kovů v systému půda/roślina. Porovnání metody aktivního a pasivního vzorkování (technika difúzního gradientu v tenkých filmech). Brno, 2008. Dizertační práce. Vysoké učení technické v Brně, Fakulta chemická, Ústav chemie a technologie ochrany životního prostředí. Vedoucí práce Hana Dočekalová.
2. PERTILE E., SUROVKA D. a BOŽOŇ A. The study of occurrences of selected PAHs adsorbed on PM 10 particles in coal mine waste dumps Heřmanice and Hrabůvka (Czech Republic). International Multidisciplinary Scientific GeoConference Surveying Geology and Mining Ecology Management, SGEM[online]. 2016, 3(BOOK 4), 161-168 [cit. 2019-03-25]. Dostupné z: <https://www.scopus.com/inward/record.uri?eid=s2-2.085034781162&partnerID=40&md5=bb79daf1a214eb09cf9def3a7338d4a7>
3. PERTILE E., SUROVKA D., SARČÁKOVÁ E., BOŽOŇ A. Monitoring of pollutants in an active mining Dump Ema, Czech Republic. Inżynieria Mineralna [online]. 2017, (1), 45-50 [cit. 2019-04-02]. DOI 10.29227/IM-2017-01-09. ISSN 16404920.
4. SUROVKA D., PERTILE E., DOMBEK V., VASTYL M., a LEHER V. Monitoring of Thermal and Gas Activities in Mining Dump Hedvika, Czech Republic. IOP Conference Series: Earth and Environmental Science [online]. 2017, 92 [cit. 2019-03-26]. DOI: 10.1088/1755-1315/92/1/012060. ISSN 1755-1307.
5. HÁJOVSKÝ, Radovan. Monitoring hald [online]. Ostrava: VŠB-TU Ostrava, © 2015 [cit. 2019-03-015]. Dostupné z: <http://www.monitoring-hald.com/>.
6. PUEYO, M., G. RAURET, D. LÜCK, M. YLI-HALLA, H. MUNTAU, Ph. QUEVAUVILLER a J. F. LÓPEZ-SÁNCHEZ. Certification of the extractable contents of Cd, Cr, Cu, Ni, Pb and Zn in a freshwater sediment following a collaboratively tested and optimised three-step sequential extraction procedure. Journal of Environmental Monitoring [online]. 3(2), 243-250 [cit. 2019-03-26]. DOI: 10.1039/b010235k. ISSN 14640325.
7. BORŮVKA, Luboš. Pedogeochemie. V Praze: Česká zemědělská univerzita, 2005. ISBN 80-213-1309-9.
8. TERDUMP: Spolupráce VŠB-TUO/GIG Katowice na průzkumu hořících hald na obou stranách společné hranice [online]. © 2019 [cit. 2019-03-23]. Dostupné z: <https://t4.gig.eu/node/27>.

## Określenie składowych ryzyka na podstawie próbki gleby ze składowiska górniczego przy zastosowaniu sekwencyjnej ekstrakcji BCR

Przedmiotem artykułu jest określenie mobilności pierwiastków ryzyka w próbkach gleby termicznie aktywnego składowiska, będącego efektem działalności górniczych w regionie Ostrawy. Próbki zostały pobrane ze składowiska Hedvika w okresie 2017–2018. Ekstrakcja prób gleby została wykonana za pomocą trzystopniowej ekstrakcji sekwencyjnej BCR (Bureau Community of Reference). Ekstrakcja sekwencyjna daje informacje na temat procesów, które normalnie mają miejsce w środowisku. Składnik stały gleby jest stopniowo wyplukiwany w różnych odczynnikach ekstrakcyjnych, począwszy od najsłabszego aż do najsilniejszego. To dostarcza danych na temat ogólnej ilości pierwiastków ryzyka obecnych w określonych warunkach środowiskowych. Wybrane pierwiastki ryzyka (Cr, Cu, Ni, Zn) zostały określone za pomocą metody ICP – MS (Inductively plasma mass spectrometry) oraz AAS (atomic absorption spectrometry) (Zn). Wyplukiwanie kwasu azotowego zostało zastosowane aby uzupełnić ogólną analizę ekstrakcji BCR.

**Słowa kluczowe:** analiza sekwencyjna BCR, składowisko, ICP – MS, mobilność, odpady górnicze, pierwiastki ryzyka, gleba



# Biohydrometallurgical Processing Methods for Low-Grade Sulfide Ores in the Arctic

Elena YANISHEVSKAYA<sup>1)</sup>, Andrey GORYACHEV<sup>2)</sup>, Nadezhda FOKINA<sup>3)</sup>,  
Eugenia KRASAVTSEVA<sup>4)</sup>

<sup>1)</sup> Institute of North Industrial Ecology Problems, Kola Science Centre of the Russian Academy of Sciences, 14a, Akademgorodok St., Apatity, 184209, Russia; email: drygina\_es@mail.ru

<sup>2)</sup> Institute of North Industrial Ecology Problems, Kola Science Centre of the Russian Academy of Sciences, 14a, Akademgorodok St., Apatity, 184209, Russia; email: andrej.goria4ev@yandex.ru

<sup>3)</sup> Institute of North Industrial Ecology Problems, Kola Science Centre of the Russian Academy of Sciences, 14a, Akademgorodok St., Apatity, 184209, Russia; email: nadezdavf@yandex.ru

<sup>4)</sup> Institute of North Industrial Ecology Problems, Kola Science Centre of the Russian Academy of Sciences, 14a, Akademgorodok St., Apatity, 184209, Russia; email: vandeleur2012@yandex.ru

<http://doi.org/10.29227/IM-2020-01-73>

Submission date: 05-01-2020 | Review date: 29-03-2020

## Abstract

*Microorganisms capable of oxidizing sulfide minerals were isolated for the bioleaching experiments. Ore samples from the Allarechensk mining waste dump and low-grade ore samples from the deposit Nud II were studied. The samples have a similar ore mineral composition – pyrrhotite, pentlandite, chalcopyrite, and magnetite. In the study, the solution was recycled to make the process environmentally friendly.*

**Keywords:** *bioleaching, heap leaching, sulfide ores, non-ferrous metals*

## Introduction

Multiple major deposits of the most important mineral resources are concentrated in Russia's Murmansk region. The study area is characterized by a unique combination of natural and anthropogenic factors – challenging climatic conditions and intensive industry growth. The exhaustion of the reserves of high-grade ores that can be concentrated by conventional methods raises the question concerning the prospects of the development of low-grade natural and anthropogenic mineral resources. At the same time, long-term storage of mining waste is a major environmental problem. Storage of the mining waste and concentration tailings of sulfide ores involves intense hypergene processes, in particular, the oxidation of sulfides. As a result, heavy metals pass into water-soluble salts and enter the soil, surface and groundwater, thereby polluting the environment. The total content of the valuable components accumulated in the waste has already reached a level comparable with commercial deposits, and the average grade sometimes exceeds that of many newly developed deposits. At the same time, mining waste and concentration tailings, as well as low-grade ores often remain unprocessed due to the lack of an efficient technology. Recovering non-ferrous metals contained in mining waste using microorganisms is a cost-effective alternative to conventional hydrometallurgical processes. The development of biohydrometallurgical processes for the recovery of non-ferrous metals from anthropogenic copper-nickel resources and low-grade copper-nickel ores will reduce the environmental footprint and solve the problem of mining waste storage in the Arctic.

The global experience with hydrometallurgical processes shows that heap leaching is a promising method for the further recovery of valuable components from low-grade off-balance ores (Brierley and Brierley, 2001; Watling, 2008; Khalezov, 2013). One of the developments in mineral processing is the use

of the combined processing technology, allowing to significantly improve the utilization level of the mineral resources, reduce processing costs, and ensure effective environmental protection. An example of such technology could be a combination of concentration and metallurgical processes with bacterial leaching, which is a biotechnology. The use of native bacterial strains adapted to the given environmental conditions is most appropriate.

The bioleaching technology has been commercially implemented in the recovery of copper and uranium, processing of gold ores and concentrates (Watling, 2006; Johnson, 2014; Wang et al., 2011). Henna et al. (2016) report experience with heap leaching at a polymetallic deposit in northern Finland.

Murmansk Region has a number of mineral resources, whose development requires the implementation of efficient processing methods. Such resources include the Monchepluton copper-nickel ores (Pripachkin, 2013). Anthropogenic resources that can potentially be processed include the copper-nickel concentration tailings at Kola MMC, as well as the Allarechensk waste dump composed of the mining wastes of the sulfide copper-nickel ores of the Allarechensk primary deposit.

The goal of this research was to conduct lab-scale bioleaching tests using native bacterial strains on the non-ferrous metals (copper and nickel) held in the concentration tailings from the waste dump at the Allarechensk deposit and in the low-grade ore of the Nud II deposit.

## Materials and methods

The following mineral resources were chosen for this study: a) waste dumps of the Allarechensk deposit; b) low-grade ore of the Nud II copper-nickel ore deposit.

Allarechensk waste dump holds the mining waste of the sulfide copper-nickel deposit that was developed for 10 years

Tab. 1. The chemical composition of the Allarechensk ore sample preliminarily processed by magnetic separation

Tab. 1. Skład chemiczny próbki rudy z Allarachska, wstępnie poddanej procesowi separacji magnetycznej

Component	Content, %
Na <sub>2</sub> O	0.069
MgO	8.138
Al <sub>2</sub> O <sub>3</sub>	0.798
SiO <sub>2</sub>	14.653
S	24.962
CaO	1.756
TiO <sub>2</sub>	0.337
Cr <sub>2</sub> O <sub>3</sub>	0.130
Fe <sub>2</sub> O <sub>3</sub>	38.494
CoO	0.360
NiO	7.189
CuO	3.107

starting in the 1960s. The main ore minerals are pyrrhotite, pentlandite, and less often chalcopyrite, which are in close paragenetic association with magnetite. Since the average non-ferrous grade is estimated based on the average Ni grade and is 1%, the samples were pre-processed by magnetic separation. The chemical composition of the sample is given in Table 1.

The mineralized rocks of the Nud II deposit are mainly meso- and leucocratic norites and gabbro-norites, forming a series of alternating layers with gradual transitions. The main ore minerals are pyrrhotite, pentlandite, chalcopyrite, magnetite. Pyrite, mackinawite, violarite, molybdenite are also found. Sulfides are characterized by dissemination, nodes, schlierens, and veins (Pripachkin, 2013).

The chemical composition of the sample is given in Table 2.

To study the leaching processes of the anthropogenic and natural mineral materials, water samples were taken in a swamp below the Allarechensk waste dump. The pH of the samples was 3.59, which is considered favorable for the growth of acidophilic microorganisms. A wide range of liquid and solid nutrient media was used to isolate bacteria: Towson (with agar), Liske agar medium; sulfur bacteria medium (using the recipe recommended by the American Public Health Association), Postgate, Leten, Silverman, and Lundgren 9K. In the samples, iron and sulfur-oxidizing acidophilic microorganisms promoting leaching of sulfide ores were found.

For the further research, in a biostat at a temperature of 27°C and continuous aeration, a bacterial biomass was obtained with a population density of 109 cells/ml. The bacterial population was measured by fluorescence microscopy using polycarbonate membrane filters.

The samples from the Allarechensk waste dump were used in an experiment with a circulating solution feed (bacterial solution and 2% sulfuric acid). Ore size was -5+2 mm, percolator charge 800 g, ore bed height 16 cm, column diameter 5 cm. Two columns were operated: A1 – bioleaching with a circulating bacterial solution, A2 – leaching with circulating 2% sulfuric acid. On the first day, the columns were moistened. The solutions were fed 2 times a week into each column.

Nud II ore size was -5+1 mm, percolator charge 200 g, ore bed height 12 cm, column diameter 3 cm. Two columns were

Tab. 2. The chemical composition of the Nud II ore sample

Tab. 2. Skład chemiczny próbki rudy z Nud II

Component	Content, %
Na <sub>2</sub> O	0.025
MgO	7.282
Al <sub>2</sub> O <sub>3</sub>	2.348
SiO <sub>2</sub>	32.340
S	14.930
CaO	4.576
TiO <sub>2</sub>	0.301
Cr <sub>2</sub> O <sub>3</sub>	0.147
Fe <sub>2</sub> O <sub>3</sub>	33.191
CoO	0.261
NiO	2.417
CuO	2.175

operated: H1 – bioleaching with a circulating bacterial solution, H2 – leaching with circulating 2% sulfuric acid. On the first day of the experiment, the ore was moistened. Then, the leaching solutions were fed twice weekly.

During the experiment, the parameters of the leaching and spent solutions were constantly monitored: pH, Eh, ferrous and ferric iron ion concentrations. At the outlet of the columns, the solutions were examined by atomic absorption spectrometry using the spectrophotometer SF-2000.

## Results and discussion

Pregnant solution parameters are shown in Figure 1.

As can be seen from the presented results, the pH of the bacterial medium ranged throughout the experiment from 1.8 to 2.3, the pH of the sulfuric acid solution ranged from 0.7 to 1.1. The high pH values of 5.8 indicate saturation of the ore with moisture. The Allarechensk samples were found to have a higher pH value of the solutions due to the high content of pyrrhotite in the ore, which actively consumes acid. The concentration of ferric iron in the bacterial solutions (A1, H1), which at the beginning of the experiment was 12.9 g/l, increased by the end of the experiment to 16.4 g/l, while the concentration of ferrous iron decreased. In the sulfuric acid solutions (A2, H2), the content of ferrous and ferric iron increased throughout the experiment (Table 3).

The results of the experiments on the ore sample after magnetic separation demonstrate that the grade of the filtrates after leaching with a bacterial solution significantly exceeds the grade of the filtrates when leached with a weakly acidic sulfuric solution (Fig. 2). The average nickel grade of the filtrates of the column treated with the bacterial solution was 679.1 mg/l, with a maximum value of 1.55 g/l on the 40th day of the experiment. The average copper grade was 83.9 mg/l, with a maximum value of 211 mg/l on the 49th day of the experiment. Leaching with a 2% sulfuric acid solution produced the following results: the average Ni grade was 349.1 mg/l, with a maximum value of 1.67 g/l on the 7th day; the average Cu grade was 17.3 mg/l, with a maximum value of 111.2 mg/l on the 7th day.

The results of the heap leaching experiments on the low-grade ore sample demonstrate that the grade in the filtrates af-

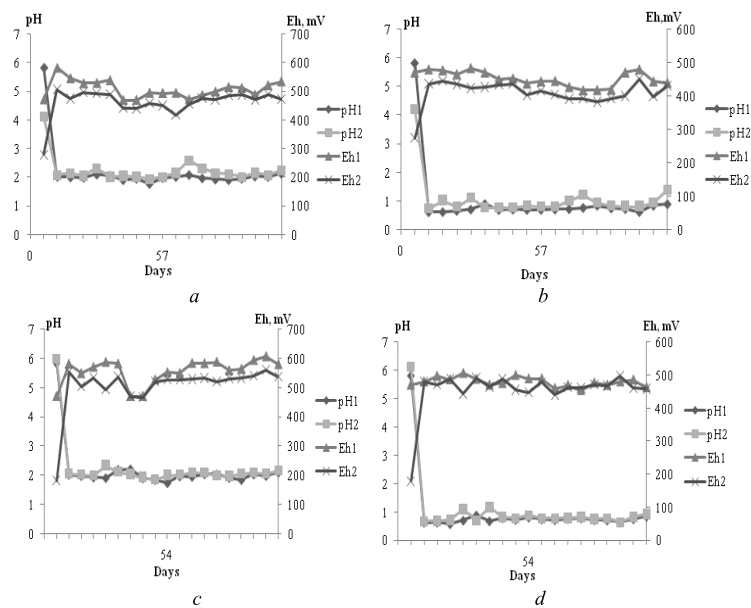


Fig. 1. Parameters of solutions: 1 – before, 2 – after: a – bioleaching of the samples from the Allarechensk waste dump, b – sulfuric acid leaching of the samples from the Allarechensk waste dump, c – bioleaching of the ore from the Nud II deposit, d – sulfuric acid leaching of the ore from the Nud II deposit  
 Rys. 1. Parametry roztworów: 1- stan przed, 2 – stan po: a – biolugowanie próbek ze składowiska odpadów Allarachenski, b – ługowanie kwasem siarkowym próbek ze składowiska odpadów Allarachenski, c – biolugowanie rudy ze złoża Nud II, d – ługowanie kwasem siarkowym rudy ze złoża Nud II

Tab. 3. Iron ion concentrations in the pregnant solutions  
 Tab. 3. Stężenia jonowe żelaza w roztworach dominujących

	Fe <sup>2+</sup> , g/l	Fe <sup>3+</sup> , g/l
A1	1,4 - 3	12,9 -16,48
A2	0 - 1,8	0 - 2,4
H1	0,9 - 1,79	12,9-16,41
H2	0,77 - 1,1	0 - 1,2

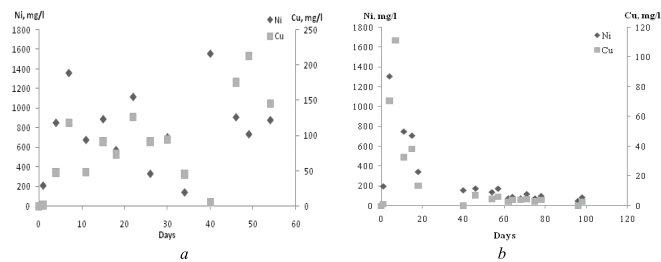


Fig. 2. Metals grade of the circulating solutions in the leaching experiment on the samples from the Allarechensk waste dump after magnetic separation. a – 2% H<sub>2</sub>SO<sub>4</sub> solution; b – bacterial solution

Rys. 2. Zawartość metali w roztworach będących w obiegu podczas eksperymentu ługowania próbek ze składowiska odpadów Allarachenski po przeprowadzeniu separacji magnetycznej. a – 2% roztwór H<sub>2</sub>SO<sub>4</sub>; b – roztwór bakteryjny

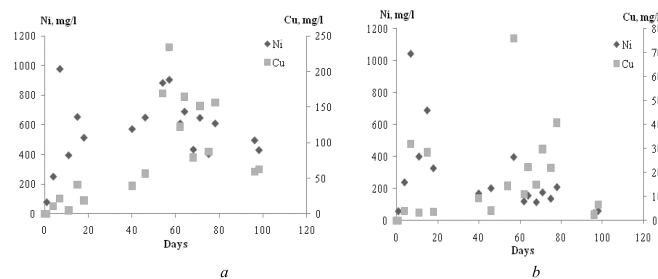


Fig. 3. Metals grade of the circulating solutions in the leaching experiment on the samples from the Nud II deposit. a – 2% H<sub>2</sub>SO<sub>4</sub> solution; b – bacterial solution

Rys. 3. Zawartość metali w roztworach będących w obiegu podczas eksperymentu ługowania próbek ze złoża Nud II. A – 2% roztwór H<sub>2</sub>SO<sub>4</sub>; b – roztwór bakteryjny



ter leaching with a bacterial solution significantly exceeds the grade of the filtrates when leached with a weakly acidic sulfuric solution, similarly to the magnetically separated ore (Fig. 3).

The average nickel grade of the filtrates of the column treated with the bacterial solution was 566.8 mg/l, with a maximum value of 904.8 mg/l on the 57th day of the experiment. The average copper grade was 81.8 mg/l, with a maximum value of 233 mg/l on the 57th day of the experiment. Leaching with a 2% sulfuric acid solution produced the following results: the average Ni grade was 364.5 mg/l, with a maximum value of 1.04 g/l on the 7th day; the average Cu grade was 18 mg/l, with a maximum value of 75.9 mg/l on the 57th day.

### Conclusion

The leaching experiments on samples of open-cut mining waste and low-grade ores demonstrated the advantages of using native iron-oxidizing microorganisms over the use of a sulfuric acid solution.

For instance, the average copper grade of the pregnant solutions after bioleaching exceeded that after leaching with a sulfuric acid solution by a factor of 4.5, the average nickel grade – by a factor of 2.

Over the 100 days of the experiment, 5.5% of nickel and 0.98% of copper was recovered into the bacterial solution, and only 2.26% and 0.18%, respectively, into the sulfuric acid solution. It should be noted that further improvements in the recovery of non-ferrous metals into the solution can potentially be achieved by tank leaching. In the leaching experiment on the Nud II low-grade ores, 31.35% of nickel and 16.31% of copper was recovered into the bacterial solution, and only 11.9% and 1.96%, respectively, into the sulfuric acid solution.

Heap leaching appears to be a promising process for the recovery of metals in the Arctic, allowing to reduce the negative impact of heavy metals on the fragile arctic ecosystems. When designing process flows for heap leaching in the arctic climate, it should be taken into account that the oxidation of sulfides contributes to the heating of the heap, which, in turn, increases the efficiency of the process by preventing the solution from freezing.

### Acknowledgments

The study has been performed with financial support of the RFFR (project No 18-05-60142 Arctic).

### Literatura – References

1. BRIERLEY, J. A., BRIERLEY, C. L. Present and future commercial applications of biohydrometallurgy // Hydrometallurgy. – 2001. – T. 59. – №. 2-3. – C. 233-239. ISSN: 0304-386X
2. JOHNSON, D. B. Biomining — biotechnologies for extracting and recovering metals from ores and waste materials // Current Opinion in Biotechnology. 2014. Vol. 30. P. 24–31. ISSN: 0958-1669
3. KHALEZOV, B. D. Heap leaching of copper and copper-zinc ores: (domestic experience): monograph. Ekaterinburg: RIO UB RAS, 2013. 346 p. ISBN: 978-5-7691-2365-8
4. OLLAKKA, H. et al. The application of principal component analysis for bioheapleaching process – Case study: Talvivaara mine // Minerals Engineering. 2016. V. 95. P. 48–58. ISSN: 0892-6875
5. PRIPACHKIN, P.V. et al. Cu-Ni-PGE and Cr deposit of the Monchegorsk area, Kola Peninsula, Russia. Guidebook of geological excursions, Apatity: Geological Institute KSC RAS, 2013, 56 p
6. WANG, X., et al. An industrial bioleaching of fluorine-bearing uranium ore // Proceedings of the 19th International Biohydrometallurgy Symposium (IBS 2011) / ed. G. Qiu, T. Jiang, W. Qin, X. Liu, Y. Yang, H. Wang. Changsha, China, 2011. P. 601–604.
7. WATLING, H. R. The bioleaching of nickel-copper sulfides // Hydrometallurgy. 2008. V. 91, Iss. 1–4. P. 70–88. ISSN: 0304-386X
8. WATLING, H. R. The bioleaching of sulphide minerals with emphasis on copper sulphides—a review // Hydrometallurgy. – 2006. – T. 84. – №. 1-2. – C. 81-108. ISSN: 0304-386X

### *Biohydrometalurgiczne metody przeróbki dla ubogich siarczkowych rud w Arktyce*

*Mikroorganizmy zdolne do utleniania minerałów siarczkowych zostały wyizolowane w celu przeprowadzenia eksperymentów biologicznego. Próbkę rudy ze składowiska odpadów pogórnictwa Allarechensk, jak również próbki rudy ze złoża Nud II zostały zbadane. Próbkę mają podobny skład mineralny – pirotyt, pentlandyt, chalkopiryt oraz magnetyt. W badaniu zastosowano recykling, aby proces był przyjazny dla środowiska.*

**Słowa kluczowe:** *biologiczne, wycinanie odpadów, rudy siarczkowe, metale ciężkie*



# Comparison of Flotation and Screening as Separation Method in Coal Recovery From Tailings by Agglomeration

Özüm YAŞAR<sup>1)</sup>, Tuncay USLU<sup>1)</sup>

<sup>1)</sup> Karadeniz Technical University, Mining Engineering Department, Trabzon, Turkey

<http://doi.org/10.29227/IM-2020-01-70>

Submission date: 08-01-2020 | Review date: 16-03-2020

## Abstract

Dependency of Turkey on foreign energy adversely affects the economy of the country and may cause energy shortage in the near future. As a primary domestic energy source, coal is used for energy production in addition to imported oil and gas. However, significant amount of fine coal is lost together with tailings in coal washeries. Recovering of fine coals from these tailings will make an economic contribution to country. In the present study, fine coals were recovered from tailings of a coal washery in Turkey by using oil agglomeration method. Flotation was used in agglomerate separation stage of oil agglomeration. Results were compared with that of previous study in which agglomerates were recovered by screening. The performance of the process increased sharply when flotation was used instead of screening in agglomerate separation stage. A clean coal with 28% ash was recovered from the washery tailings containing 55% ash by 85% combustible recovery.

**Keywords:** coal, coal processing oil agglomeration, fine coal tailings, waste vegetable oil

## Introduction

Turkey has heavy dependence on foreign countries for energy (Düzgün and Kömürgöz, 2014; Elsland et al., 2014; Öztürk and Yüksel, 2016). Since large natural gas and petroleum reserves will not be discovered in the near future, coal, as only domestic energy source, should be produced and used efficiently without being wasted (Yaşar et al., 2018). Although Turkey has considerable amount of coal reserves, their quality is low (Atılğan and Azapacı, 2017). Low quality coals are cleaned in coal washeries to increase the quality. However, considerable amounts of fine coals are disposed together with the mineral matters. Fine coals reported to tailings mean loss of an economically valuable energy source and potential environmental pollution due to accumulation in tailings areas. 1 million ton/year fine coal is estimated to be lost (Çiçek et al., 2008; Özgen et al., 2011; Özgen and Sezgin, 2011). It was stated that over 6 million tons of tailings were accumulated in Tunçbilek tailings area (Erdem et al., 2010).

Fine coal cleaning is difficult as the small size of the particles limits the efficiency of traditional gravity separation techniques. Although different improvements have been made in gravity concentrators and flotation machines, several problems including handling, transportation and dewatering of fine coal product have not been solved yet. In addition, treatment of high clay-slime coals by using existing technologies is difficult (Netten et al., 2015). The oil agglomeration process is very promising for beneficiation of fine coal (Meshram et al., 2015; Netten et al., 2015; Netten et al., 2016). It is more suitable method for oxidized and high clay-slime coals. Its dewatering stage is low cost (Şahinoğlu and Uslu, 2015). Agglomerate- tailings separation stage is simple (Şahinoğlu and Uslu, 2013). In oil agglomeration method, hydrophobic particles are agglomerated by using a bridging oil, while hydrophilic particles remain in suspension. The clean coal can be separated from the suspension by floating, skimming

and screening (Şahinoğlu and Uslu, 2013; Şahinoğlu and Uslu, 2015).

In the previous study (Yaşar et al., 2018) that is the first to use oil agglomeration method for fine coal recovery from the washeries of Turkey, recovery of approximately 50% of economically valuable clean coal from the tailings of Tunçbilek coal washery was achieved and the further detailed studies were recommended for increasing the performance of the process in term of combustible recovery to make additional improvement in the economy of the process. In the present study, fine coals from the same tailings was tried to be recovered by oil agglomeration in which agglomerates were separated from gangue and slurry by using flotation instead of screening. Because it was seen in the previous study (Yaşar et al., 2018) that small agglomerates whose size was not sufficiently large to retain on separation screen could not be recovered and considerable amount of coal was lost despite their agglomeration activity. No study on comparison of screening and flotation for agglomerate separation in oil agglomeration has been meet before.

## Materials and methods

### Material

Sample of fine washery tailings was taken from Tunçbilek Coal Washery of G.L.I of TKI before entering thickener for dewatering. Proximate-calorific value analysis, petrographic analysis and particle size analysis of the sample including also ash values are illustrated in Table 1-3, respectively. +0.5 mm fraction and slime fraction (-0.025mm) was not subjected to cleaning process. Tests were undertaken for cleaning the sample of -0.5+0.025mm whose proximate analysis is given in Table 4. As bridging material, filtrated waste sunflower oil was used. Its viscosity and density are 35.81mm<sup>2</sup>/s and 0.918 g/cm<sup>3</sup>, respectively.

Tab. 1. Proximate-calorific value analysis of the sample

Tab. 1. Analiza wartości opalowej próbki

Proximate Analysis	Air Dried	Dried
Moisture (%)	4.83	-
Ash (%)	55.60	58.42
Volatile Matter (%)	21.92	23.03
Fixed Carbon (%)	17.65	18.55
Lower Calorific Value (kcal/kg)	2353	2472
Upper Calorific Value (kcal/kg)	2501	2628

Tab. 2. Petrographic analysis of the sample

Tab. 2. Analiza petrograficzna próbki

Macerals (% Volume)			Minerals (% Volume)	
Huminite	Liptinite	Inertite	Pyrite	Other Minerals
50	5	3	2	40

Tab. 3. Particle size analysis of the sample

Tab. 3. Analiza składu ziarnowego próbki

Particle size (mm)	Amount (%)	Ash (%)
+0.5	37.14	33.45
-0.5+0.25	12.07	53.49
-0.25+0.125	5.62	51.72
-0.125+0.075	2.55	43.51
-0.075+0.038	3.98	52.76
-0.038+ 0.025	2.31	60.95
-0.025	36.33	80.35

Tab. 4. Proximate analysis of the sample (-0,5+0,025 mm)

Tab. 4. Analiza próbki (-0,5+0,025 mm)

Proximate Analysis	Air Dried	Dried
Moisture	3.62	-
Ash	52.6	54.58
Volatile Matter	25.13	26.07
Fixed Carbon	18.65	19.35

## Methods

Agglomeration experiments were undertaken in cylindrical glass vessel whose diameter was 11.7 cm. Four portable baffles were inserted to vessel. The stirring process was achieved by means of RZR 2021 type overhead stirrer. Water was distilled before the experiments. Coal samples were mixed with water (solid ratio: 10%). Coal-water mixtures were stirred at 1000 rpm for 5 min. to provide perfect wetting of coal grains. The oil (15wt. % of coal) was then put as agglomerant and mixture of coal-oil-water was stirred at 1400 rpm for 10 min. The experiments were performed at ambient pH of the mixture. After agglomeration, the suspension was transferred to a flotation cell. The suspension was conditioned at 1000 rpm for 3 min. After air addition into system, suspension was agitated at the same rate for different flotation times (0.5–2 min.) In addition, tests were undertaken for determining the effect of agitation rates (800–1400 rpm) at optimum flotation time (1min). Clean coal (float product) was skimmed from the cell.

Then, vacuum filtering and acetone washing for de-oiling were applied for agglomerates. After drying of oil-free agglomerates at  $105 \pm 5$  °C, weighing was carried out and cleaned coal products were stored for analyses. Finally, ash analyses were undertaken. The yield, combustible recovery (CR), ash reduction (AR) and ash separation efficiency (ASE) were calculated by means of following equations:

$$CR (\%) = [(MP / MF) \times ((100 - AP) / (100 - AF))] \times 100 \quad (\text{Eq.1})$$

$$AR (\%) = [1 - ((MP) \times (AP) / (MF) \times (AF))] \times 100 \quad (\text{Eq.2})$$

$$ASE (\%) = CR + AR - 100 \quad (\text{Eq.3})$$

where, MF: Mass of dry feed (g), MP: Mass of dry and oil-free product (g), AF: Ash in dry feed (wt.%), AP: Ash in dry and oil-free product (wt.%).

## Results and discussion

As seen from Figure 1, increasing flotation time from 0.5 min to 1 min improved the combustible recovery from 67.8% to 85.2%. Further increase in time had no considerable effect on amount of recovered combustible coal matter that became 86.3% at flotation time of 2 min. Increasing flotation time affected the ash contents of produced clean coals adversely. Ash rejection reduced from 78.6% to 63.2% as a result of increasing time from 0.5 min to 2 min. Clean coal with minimum ash percent was achieved to be 27.5% at 0.5 min. Increasing time reduced the selectivity of the process and led entrainments of mineral matter into voids of agglomerates. Maximum ash separation efficiency that is the indicator of optimum performance was calculated as 57.5% at 1 min flotation time at which a clean coal with 28.1% ash was produced by combustible recovery of 85.2%.

As seen from Figure 2, combustible recovery and ash separation efficiency reduced after 1000 rpm agitation rate. Further increase of rate to 1400 rpm reduced the combustible recovery from 85.2% to 82.1%. Ash separation efficiency

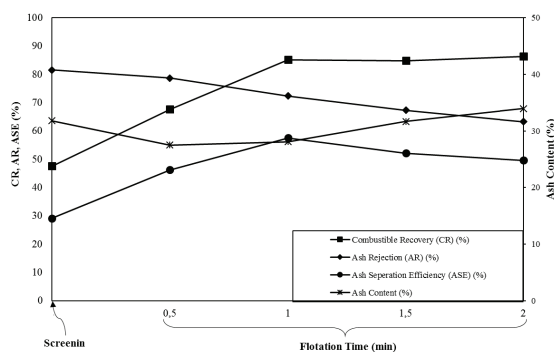


Fig. 1. Effect of flotation time on the performance of the process  
Rys. 1. Wpływ czasu flotacji na przebieg procesu

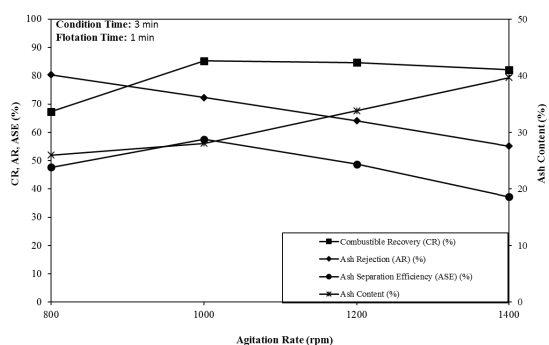


Fig. 2. Effect of the agitation rate on the performance of the process  
Rys. 2. Wpływ stopnia agitacji na przebieg procesu

reduced from 57.5% to 37.2%. It can be attributed to destroying of some agglomerates due to increasing turbulence and change of medium from mild to severe resulted from excess agitation rates. High ash coal products and lower ash rejection ratios at higher agitation rates are results of moving of fine clay particles and other mineral matters to the surfaces and voids of agglomerates.

Ash content of coal product obtained as 26.0% at 800 rpm increased sharply to 39.7% at 1400 rpm.

When the performance of the screening applied in previous study and that of flotation used in the present study as agglomerate separation methods was compared (Figure 1), it was seen that flotation caused recovery of cleaner and higher amount coal from washery tailings. Although screening produced a clean coal with 31.8% ash by combustible recovery of 47.6%, flotation ensured the production of clean coal with 28.1% ash by recovering the 85.2% of combustible matter. It was concluded that small agglomerates lost as undersize of -0.5mm separation screen could be recovered by flotation. In

addition, difficulty in removing some of mineral matter from screen during water washing was eliminated by using flotation instead of screening. Therefore, cleaner coal product was produced.

## Conclusion

By using oil agglomeration method in which flotation is applied for agglomerate separation, a clean coal with 28.1% ash was recovered from the washery tailings with 54.6% ash by combustible recovery of 85.2%. Optimum combination of flotation time-agitation rate giving the maximum ash separation efficiency was found to be 1min-1000 rpm. Performance of the flotation in agglomerate separation was proved to be greater than that of screening. It was seen that small sized agglomerates lost during screening was reported to clean coal product in case of usage of flotation instead of screening. By using flotation, combustible recovery and ash separation efficiency was improved sharply.

## Literatura – References

1. ATILGAN, Burcin et al. Energy challenges for Turkey: Identifying sustainable options for future electricity generation up to 2050, Sustainable Prod. Consumpt., 2017, <http://dx.doi.org/10.1016/j.spc.2017.02.001>.
2. CICEK, Tayfun et al. An efficient process for recovery of fine coal from tailings of coal washing plants, Energy Sources, Part A, 30, 2008 p.1716-1728.
3. DUZGUN, Bilal et al. Turkey's energy efficiency assessment: White Certificates Systems and their applicability in Turkey, Energy Policy, 65, 2014, p. 465–474.
4. Elsland, Rainer et al. Turkey's strategic energy efficiency plan – An ex ante impact assessment of the residential sector, Energy Policy 70, 2014, p. 14-29.
5. ERDEM, Ayşe et al. Beneficiation of coal fines from tailings pond of Tuncbilek washing plants, in: Proceedings of International Mineral Processing Congress (IMPC), AIMM, Brisbane, 2010, p.3737-3742.
6. NETTEN, Kim Van et al. Selective agglomeration of fine coal using a water-in-oil emulsion, Chem. Eng. Res. Des., 110, 2016, p. 54-61.
7. NETTEN, Kim Van et al. A kinetic study of a modified fine coal agglomeration process, Procedia Eng., 102, 2015, p.508 – 516.
8. OZGEN, Selcuk et al.. Studies on hydrocyclone to produce clean coal from Turkish lignite tailings (Tunçbilek/Kütahya and Soma/Manisa), El-Cezerî Journal of Science and Engineering 1, 2014, p.12-18.
9. OZGEN, Selcuk et al. Optimization of a Multi Gravity Separator to produce clean coal from Turkish lignite fine coal tailings, Fuel, 90, 2011, p. 1549-1555.
10. OZTURK, Murat et al. Energy structure of Turkey for sustainable development, Renew. and Sustain. Energy Rev., 53, 2016, p. 1259-1272.
11. SAHINOGLU, Ercan et al. Cleaning of high sulphur coal by agglomeration with waste vegetable oil, Energy Sources Part A, 37, 2015, p. 2724-2731.
12. SAHINOGLU, Ercan et al. Increasing coal quality by oil agglomeration after ultrasonic treatment, Fuel Process. Technol., 116, 2013, p. 332–338.

## Porównanie flotacji i przesiewania jako metod separacji w odzysku węgla z odpadów w procesie aglomeracji

Zależność Turcji od energii z zagranicy wpływa negatywnie na gospodarkę państwa i może powodować niedostatek ilości energii w niedalekiej przyszłości. Jako główne rodzime źródło energii traktowany jest węgiel, który stosowany jest do produkcji energii jako dodatek do importowanych ropy naftowej i gazu. Jednakże, znacząca ilość drobnego węgla jest tracona wraz z odpadami w płuczkach węgla. Odzysk drobnego węgla z tych odpadów spowoduje poprawę sytuacji ekonomicznej kraju. W prezentowanym badaniu, drobny węgiel został odzyskany z odpadów z płuczki węglowej w Turcji za pomocą metody aglomeracji olejowej. Flotacja została zastosowana na etapie rozdziału podczas tego procesu. Wyniki zostały porównane z tymi z poprzednich badań, gdzie aglomeraty były odzyskiwane poprzez przesiewanie. Wydajność procesu wzrosła znacząco kiedy zastosowano flotację w miejsce przesiewania na etapie rozdziału aglomeratów. Czysty węgiel o zawartości popiołu 28% został odzyskany z odpadów płuczki, zawierających 55% popiołu przy odzysku 85% części palnych.

**Słowa kluczowe:** węgiel, przeróbka węgla, aglomeracja olejowa, odpady drobnego węgla, odpadowy olej roślinny



# Study of Extraction of Rare Earth Elements from Hard Coal Fly Ash

Ingrid ZNAMENÁČKOVÁ<sup>1)</sup>, Silvia DOLINSKÁ<sup>1)</sup>, Slavomír HREDZÁK<sup>1)</sup>,  
Vladimír ČABLÍK<sup>2)</sup>, Michal LOVÁS<sup>1)</sup>, Dana GEŠPEROVÁ<sup>1)</sup>

<sup>1)</sup> VŠB – Technical University of Ostrava, Faculty of Mining and Geology, Institute of Clean Technologies for Extraction and Utilization of Energy Resources, 17. listopadu 15, 708 00 Ostrava-Poruba, Czech Republic; email: znamenackova@saske.sk, sdolinska@saske.sk, hredzak@saske.sk, lovasm@saske.sk

<sup>2)</sup> Institute of Geotechnics of SAS, Watsonova 45, 040 01 Košice, Slovak Republic

<http://doi.org/10.29227/IM-2020-01-71>

Submission date: 29-12-2019 | Review date: 03-03-2020

## Abstract

Rare earth elements (REEs) extraction from wastes and/or by-products is alternative possibility of their winning. The occurrence of REEs, namely 50.1 ppm of La, 100.1 ppm of Ce and 44.3 ppm of Nd was confirmed in solid fly ash samples from the coal fired heating plant (TEKO, Inc. Košice, eastern Slovakia). The submitted contribution presents laboratory results of REEs leaching from coal fly ash using 3M HCl, HNO<sub>3</sub>, H<sub>2</sub>SO<sub>4</sub> and H<sub>3</sub>PO<sub>4</sub> at 80°C during 120 min.

It was found, that recoveries 65.5% of La, 64.4% Ce and 64.3% of Nd into liquor may be attained after grain size reduction to below 5 μm.

**Keywords:** coal fly ash, REEs extraction, inorganic acids

## Introduction

Recently, REEs consumption continually increases due to their extensive application in various areas.

The content and distribution of lanthanides in rocks and coal is confirmed by the presence of REE-bearing uncommon minerals, such as monazite (Ce,La,Nd,Th)PO<sub>4</sub>, allanite (Ce,Ca,Y)<sub>2</sub>(Al,Fe<sup>3+</sup>)<sub>3</sub>(SiO<sub>4</sub>)<sub>3</sub>(OH), zircon (Zr,REE)<sub>3</sub>SiO<sub>4</sub>, xenotime YPO<sub>4</sub> (Kolker et al., 2017; Finkelman, 1981), rhabdophane (Ce,La,Y)PO<sub>4</sub>·H<sub>2</sub>O (Dai et al., 2014), florencite CeAl<sub>3</sub>(PO<sub>4</sub>)<sub>2</sub>(OH)<sub>6</sub> and Ce-Nd-bearing (fluoro)carbonates, e.g. bästnasite (Ce,La,Y)CO<sub>3</sub>F (Dai et al., 2016; Dai et al., 2017; Zhao et al., 2017). Besides electronic scrap, the wastes from mining and metallurgical industry and also coal combustion (by)products (CCPs), e.g. fly ash can consider to be a potential source of REEs. CCPs landfills often negatively influence the surroundings by their elutriation and in such way contaminate surface and ground waters. On the other hand performed scientific studies confirmed an interesting content of REEs in CCP. Moreover, within the frame of European Union REEs were recognized as critical raw materials by European Commission. All above mentioned facts caused the intensive research on REEs winning from coal fly ash.

Generally, the extraction of REEs from mineral resources is energy intensive and ecologically undesirable process. Moreover, from technological viewpoint, this process is also complicated and it includes various physical separation methods to obtain REE-bearing mineral concentrates and hydrometallurgical techniques for processing the concentrates, i.e. metals extraction from minerals by using suitable leaching agents.

Lin et al. (2017) dealt with the enrichment of REEs from coal, coal by-products and shales.

The samples of fly ash contained 312–623 ppm of REE or 378–754 REY, respectively. An enrichment of REEs was attained in non-magnetic product using magnetic separation.

As to gravity concentration, it is interesting that the highest REE content was not found in the heaviest fraction, probably due to insufficiently liberated REE-bearing minerals from others ones.

Blisset et al. (2014) evaluated the REEs content in six coal fly ashes from the United Kingdom (UK) and Poland. Apart from other things they presented REO content of four samples obtained from semi-anthracitic coal combustion at various places of processing scheme (flotation/rougher product to magnetic separation/non-magnetic product to hydrocycloning) at upgrading of fly ash. Thus, they assayed organic concentrate (REO 398 ppm) from rougher froth, magnetic concentrate (REO 270 ppm), fines from hydrocyclone overflow (REO 637 ppm) and coarse from hydrocyclone underflow (REO 560 ppm) from the feed of REO 505 ppm. After above mentioned it seems that REEs concentrate in inorganic non-magnetic matter.

Naturally, an application of hydrometallurgical techniques in REEs winning from coal fly ashes is also intensively investigated. The researchers pay attention to several technological parameters of leaching with the aim to attain maximal attainable REEs recovery. So, various leaching agents, pH value at leaching, influence of temperature, pressure, and stirring speed in consideration of coal fly ash composition are studied.

Cao et al. (2018) studied the coal fly ash containing 489 ppm REE. The leaching of fly ash in 3M HCl at 60°C, at 200 rpm during 120 min. resulted in the following values of recovery: 71.9% La, 66.0% Ce and 61.9% Nd. Kashiwakura et al. (2013) studied the extraction of REE from coal fly ashes by leaching using H<sub>2</sub>SO<sub>4</sub>. King et al. (2018) dealt with acid and alkaline leaching of REEs from fly ashes from combustion of various coals. In dependence on origin of fly ash and pH of leaching they observed leachability of REEs. It was shown that acid leaching is suitable for one group of coal fly ashes, but

Tab. 1. Chemical analysis of coal fly ash  
 Tab. 1. Analiza chemiczna popiołu węglowego

SiO <sub>2</sub> [%]	MgO [%]	CaO [%]	Fe <sub>2</sub> O <sub>3</sub> [%]	Al <sub>2</sub> O <sub>3</sub> [%]	MnO [%]	K <sub>2</sub> O [%]	La [ppm]	Ce [ppm]	Nd [ppm]	LOI [%]
44.6	1.68	4.22	6.22	21.20	0.085	1.07	55.6	100.1	49.5	15.22

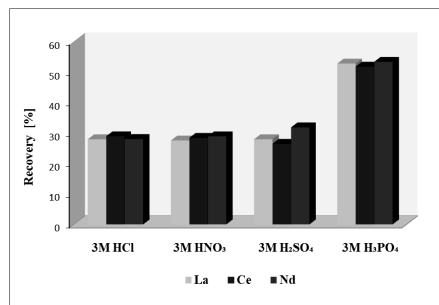


Fig. 1. Extraction La, Ce and Nd from coal fly ash (grain size –100 μm)  
 Rys. 1. Ekstrakcja La, Ce oraz Nd z popiołu węglowego (wielkość ziarna – 100 μm)

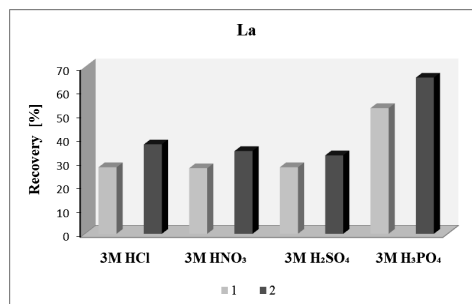


Fig. 2. Influence of grain size on extraction for La in 3M HCl, 3M HNO<sub>3</sub>, 3M H<sub>2</sub>SO<sub>4</sub> and 3M H<sub>3</sub>PO<sub>4</sub> 1 – grain size –100 μm, 2 – grain size –5 μm  
 Rys. 2. Wpływ wymiaru ziarna na ekstrakcję La w 3M HCl, 3M HNO<sub>3</sub>, 3M H<sub>2</sub>SO<sub>4</sub> i 3M H<sub>3</sub>PO<sub>4</sub> 1 – wielkość ziarna – 100 μm, 2 – wielkość ziarna – 5 μm

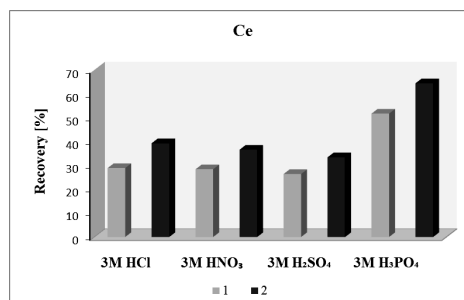


Fig. 3. Influence of grain size on extraction for Ce in 3M HCl, 3M HNO<sub>3</sub>, 3M H<sub>2</sub>SO<sub>4</sub> and 3M H<sub>3</sub>PO<sub>4</sub> 1 – grain size –100 μm, 2 – grain size – 5 μm  
 Rys. 3. Wpływ wielkości ziarna na ekstrakcję Ce w 3M HCl, 3M HNO<sub>3</sub>, 3M H<sub>2</sub>SO<sub>4</sub> i 3M H<sub>3</sub>PO<sub>4</sub> 1 – wielkość ziarna – 100 μm, 2 – wielkość ziarna – 5 μm

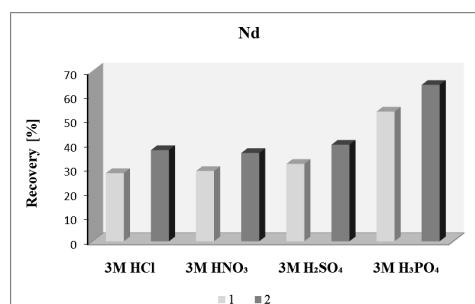


Fig. 4. Influence of grain size on extraction for Nd in 3M HCl, 3M HNO<sub>3</sub>, 3M H<sub>2</sub>SO<sub>4</sub> and 3M H<sub>3</sub>PO<sub>4</sub> 1 – grain size –100 μm, 2 - grain size –5 μm  
 Rys. 4. Wpływ wielkości ziarna na ekstrakcję Nd w 3M HCl, 3M HNO<sub>3</sub>, 3M H<sub>2</sub>SO<sub>4</sub> i 3M H<sub>3</sub>PO<sub>4</sub> 1 – wielkość ziarna – 100 μm, 2 – wielkość ziarna – 5 μm

on the other hand higher REEs recoveries into liquor were achieved using alkaline leaching in the case of the second sample group.

Wang et al. (2019) performed the study of bottom and fly ashes from the Luzhou power plant in Sichuan, (Southwest China) as a promising alternative resource for rare earth elements and yttrium (REE+Y or REY) recovery. The fly ash is characterized by an aluminosilicate composition with a low CaO content and it consists of >70% amorphous glass and <30% mineral phases such as mullite, quartz and iron oxides. Dissolution of the fly ash with 4% HF showed that ~90% of all the REY are associated with the amorphous glass. The optimal NaOH-HCl sequential leaching resulted in 41.10% removal of active silica from the fly ash and 88.15% REY extraction.

### Materials and methods

The sample of fly ash from the coal fired heating plant (TEKO, Inc. Košice, Slovakia) was subjected to leaching experiments on REEs extraction. The content of major components and lanthanides in fly ash is introduced in Table 1. The extraction was realized in glass banks in water bath at the temperature 80°C in 3M solutions of HCl, HNO<sub>3</sub>, H<sub>2</sub>SO<sub>4</sub> a H<sub>3</sub>PO<sub>4</sub>. The time of leaching was 120 min at the stirring speed 200 rpm. The ratio of leaching agent to solid phase was 100 ml of solution to 1g of solid sample. The content of lanthanides, namely La, Ce and Nd was determined by ICP-MS (Agilent 7700, USA). Silicon dioxide and Loss On Ignition (LOI) were assayed using gravimetric analysis (GA). The content of other metals was determined by AAS (Varian AA240FS, Australia).

The grain size reduction of fly ash sample to ~100 µm was performed using a vibrating mill (VM-1, KSMH – Hranice, Czech Rep.). Further diminishing to grain size below 5 µm realised by means of a planetary mill (Pulverisette 6, Fritsch, Germany) in grinding bowls at rotational speed of main disk 550 rpm. Tungsten carbide balls with diameter 10 mm were used as grinding media.

### Results and Discussion

The results of laboratory experiments of lanthanides extraction from fly ash sample of grain size below 100 µm in

3M HCl, HNO<sub>3</sub>, H<sub>2</sub>SO<sub>4</sub> and H<sub>3</sub>PO<sub>4</sub> at 80°C during 120 min are shown in Fig. 1. Thus, leachability of observed lanthanides was confirmed by using all acid solutions. The highest recoveries 52.7% of La, 51.7% of Ce and 53.3% of Nd were attained using 3M H<sub>3</sub>PO<sub>4</sub>.

Naturally, a grain size reduction of fly ash sample to ~5 µm favourably resulted in the enhancement of REEs recovery into liquor by 5–12.8%. The highest recoveries into liquor, namely 65.5% of La, 64.4% of Ce and 64.3% of Nd and the highest recovery increases by 12.8% of La, 12.7% of Ce and by 11% of Nd were again received by using 3M H<sub>3</sub>PO<sub>4</sub>. The influence of grain size reduction on individual REE recovery is graphically illustrated in Figs. 2–4.

### Conclusion

An attention to REEs recovery from hard coal fly ash was paid in submitted contribution. The samples of grain size below 100 µm and 5 µm, respectively were subjected to acid leaching by using 3M HCl, HNO<sub>3</sub>, H<sub>2</sub>SO<sub>4</sub> and H<sub>3</sub>PO<sub>4</sub>. Firstly, as to grain size below 100 µm the recoveries 27.5–52.7% of La, 26.4–51.7% of Ce and 28–53.3% of Nd into liquor were obtained. Secondly, in the case of grain size below 5 µm the recoveries 32.9–65.5% of La, 33.4–64.4% Ce and 36.3–64.3% of Nd were won. The highest REEs recoveries were attained using 3M H<sub>3</sub>PO<sub>4</sub>. Conversely, the application of HNO<sub>3</sub> and H<sub>2</sub>SO<sub>4</sub> as leaching agents seems to be inadequate. Finally, it can be stated, that grain size reduction resulted in higher REEs recovery into liquor by 5–12.8%, mostly using H<sub>3</sub>PO<sub>4</sub> (by 11–12.8%).

### Acknowledgements

This work was supported by the Slovak Grant Agency for Science VEGA grant No. 2/0055/17.

This publication is the result of the project implementation Research excellence centre on earth sources, extraction and treatment – 2nd phase supported by the Research & Development Operational Programme funded by the ERDF (ITMS: 26220120038).



## Literatura – References

1. BLISSETT, R.S.; SMALLEY, N.; ROWSON, N.A. An investigation into six coal fly ashes from the United Kingdom and Poland to evaluate rare earth element content. In *Fuel*, 119, 2014, p. 236–239.
2. CAO, S.; ZHOU, C.; PAN, J.; LIU, C.; TANG, M.; JI, W.; HU, T.; ZHANG, N. Study on influence factors of leaching of rare earth elements from coal fly ash. In *Energy Fuels* 32, 2018, 7, p. 8000-8005.
3. DAI, S.; LUO, Y.; SEREDIN, V.V.; WARD, C.R.; HOWER, J.C.; ZHAO, L.; LIU, S.; TIAN, H.; ZOU, J. Revisiting the late Permian coal from the Huayingshan, Sichuan, southwestern China: Enrichment and occurrence modes of minerals and trace elements. In *International Journal of Coal Geology* 122, 2014, p. 110-128.
4. DAI, S.; LIU, J.; WARD, C.R.; HOWER, J.C.; FRENCH, D.; JIA, S.; HOOD, M.M.; GARRISON, T.M. Mineralogical and geochemical compositions of Late Permian coals and host rocks from the Guxu Coalfield, Sichuan Province, China, with emphasis on enrichment of rare metals. In *International Journal of Coal Geology* 166, 2016, p. 71-95.
5. DAI, S.; XIE, P.; JIA, S.; WARD, C.R.; HOWER, J.C.; YAN, X.; FRENCH, D. Enrichment of U-Re-V-Cr-Se and rare earth elements in the Late Permian coals of the Moxinpo Coalfield, Chongqing, China: Genetic implications from geochemical and mineralogical data. In *Ore Geology Reviews* 80, 2017, p. 1-17.
6. FINKELMAN, R.B. Modes of occurrence of trace elements in coal U.S. Geological Survey Open File Report 81-99, 1981, 301 p.
7. KASHIWAKURA, S.; KUMAGAI, Y.; KUBO, H.; WAGATSUMA, K. Dissolution of rare earth elements from coal fly ash particles in a dilute H<sub>2</sub>SO<sub>4</sub> solvent. In *Open Journal of Physical Chemistry* 3, No. 2, 2013, Article ID: 31621, 7 p.
8. KING, J.F.; TAGGART, R.K.; SMITH, R.C.; HOWER, J.C.; HSU-KIM, H. Aqueous acid and alkaline extraction of rare earth elements from coal combustion ash. In *International Journal of Coal Geology* 195, 2018, p. 75-83.
9. KOLKER, A.; SCOTT, C.; HOWER, J.C.; VAZQUEZ, J.A.; LOPANO, C.L.; DAI, S. Distribution of rare earth elements in coal combustion fly ash, determined by SHRIMP-RG ion microprobe. In *International Journal of Coal Geology* 184, 2017, p. 1-10.
10. LIN, R.; HOWARD, B.H.; ROTH, E.A.; BANK, T.L.; GRANITE, E.J.; SOONG, Y. Enrichment of rare earth elements from coal and coal by-products by physical separations. In *Fuel* 200, 2017, p. 506-520.
11. WANG, Z.; DAI, S.; ZOU, J.; FRENCH, D.; GRAHAM, I.T. Rare earth elements and yttrium in coal ash from the Luzhou power plant in Sichuan, Southwest China: Concentration, characterization and optimized extraction. In *International Journal of Coal Geology* 203, 2019, p. 1-14.
12. ZHAO, L.; DAI, S.; GRAHAM, I.T.; LI, X.; LIU, H.; SONG, X.; HOWER, J.C.; ZHOU, Y. Cryptic sediment-hosted critical element mineralization from eastern Yunnan Province, southwestern China: Mineralogy, geochemistry, relationship to Emeishan alkaline magmatism and possible origin. In *Ore Geology Reviews* 80, 2017, p. 116-140.

### *Badanie ekstrakcji pierwiastków ziem rzadkich z popiołu węgla kamiennego*

*Ekstrakcja pierwiastków ziem rzadkich (REEs) z odpadów oraz/albo z produktów jest alternatywną możliwością ich uzyskania. Obecność REEs, konkretnie 50,1 ppm La, 100,1 ppm Ce oraz 44,2 ppm Nd została potwierdzona w próbkach popiołu z węgla z elektrociepłowni (TEKO, Inc. Košice, wschodnia Słowacja). Prezentowany artykuł pokazuje wyniki laboratoryjne ługowania REEs z popiołu węglowego za pomocą 3M HCl, HNO<sub>3</sub>, H<sub>2</sub>SO<sub>4</sub> oraz H<sub>3</sub>PO<sub>4</sub> w 80°C w czasie 120 minut. Odkryto, że odzysk 65,5% La, 64,4% Ce oraz 64,3% Nd w formie ciekłej może być osiągnięte przy redukcji wymiaru ziaren do poniżej 5 μm.*

**Słowa kluczowe:** popiół węglowy, ekstrakcja REEs, kwasy nieorganiczne



Comparison of Mineral Processing Methods for Metal Recycling from Waste Printed Circuit Board .....	7
Gordan BEDEKOVIĆ, Vitomir PREMUR, Anđela IVIĆ Environmental Pollution Monitoring by Thin Metal Electrodes Prepared by Physical Vapor Deposition .....	13
Jaroslav BRIANČIN, Iraidia KOLCUNOVÁ, Bystrík DOLNÍK, Juraj KURIMSKÝ, Jaroslav DŽMURA, Roman CIMBALA, Martin FABIÁN The Need of Elastic Material Component between Rock Pressure Load and Metallic Structure Way of Receiving it in Order to Obtain a Uniform Load .....	17
Dănuț CHIRILĂ, Tamara Cristina DUMITRAȘCU, Aronel MATEI, Sorin MANGU The Evaluation Potential as Micronized Calcite of White Marble Waste .....	21
Vedat DENİZ, Ercan POLAT Use of Solar Energy in Power Equipment .....	29
Ioan Lucian DIODIU, Daniel Alexandru DRAGOMIR, Aronel MATEI, Roxana Claudia HERBEI Sensory Network Monitoring the Air Condition, Installed in the Town of Litomerice .....	33
Josef DOUŠA EU Documents of Major Importance Relevant to Issues of Mineral Resource Utilisation .....	37
Jaroslav DVOŘÁČEK, Radmila SOUSEDÍKOVÁ, Ladislav MORAVEC Reducing Environmental Degradation Caused by the Open-Cast Coal Mining Activities .....	41
Tudor GOLDAN, Catalin Marian NISTOR, Aronel MATEI, Dimian MARU Selected Characteristics of the Atmospheric Deposition in the Area of Košice .....	45
Jozef HANČULÁK, Tomislav ŠPALDON, Oľga ŠESTINOVÁ Land Assessment Techniques .....	51
Roxana Claudia HERBEI, Aronel MATEI, Clementina MOLDOVAN, Danut CHIRILA Carbon Quantum Dots (CQDs) Prepared from Waste Biomass as a New Class of Biomaterials with Luminescent Properties .....	57
Łukasz JANUS, Marek PIĄTKOWSKI, Julia RADWAN-PRAĞŁOWSKA, Aleksandra SIERAKOWSKA Removal of Contaminants from Water by Bacterial Activity .....	63
Jana JENČAROVÁ, Alena LUPTÁKOVÁ, Daniel KUPKA Effect of Wastewater Sample Pre-Treatment on Determination of Selected Heavy Metals Using ICP-MS Method .....	67
Iva KOTALOVÁ, Katrin CALÁBKOVÁ, Martina NOVÁČKOVÁ, Silvie DRABINOVÁ, Silvie HEVIÁNKOVÁ Removal of Fluoride Ions from the Mine Water .....	71
Eugenia KRASAVTSEVA, Anton SVETLOV, Andrey GORYACHEV, Dmitry MAKAROV, Vladimir MASLOBOEV Technical Infrastructure Increasing Resistance in the Natural Environment .....	75
Šárka KROČOVÁ Steelmaking Dust: Speciation of Zinc by Sequential Leaching .....	79
Christof LANZERSTORFER, Wilfried PREITSCHOPF Combination of Chemical and Biological-Chemical Methods for Elimination of Metals from Acid Mine Drainage .....	83
Alena LUPTÁKOVÁ, Eva MACINGOVÁ, Stefano UBALDINI, Miloslav LUPTÁK Development of Filling Material with Fly Ash and Slag as Lubricant in Pipe Jacking Under Acid Sulfate Soils .....	89
Kazuki MAEHARA, Hideki SHIMADA, Takashi SASAOKA, Akihiro HAMANAKA Hidden Microcosmos in Slovak Gold Mine Rozalia – Microbial Gold Miners? .....	95
Lenka MALINIČOVÁ, Lea NOSÁLOVÁ, Ivana TIMKOVÁ, Peter PRISTAŠ, Jana SEDLÁKOVÁ-KADUKOVÁ Concepts of Necessary Costs to Be Used in the Minimum Enterprise Decisions .....	99
Sorin-Iuliu MANGU, Diana-Cornelia CSIMINGA, Mirela ILOIU, Roxana Claudia HERBEI Possibilities of Tetrahedrite Separation from Polymetallic Ore .....	105
Michal MARCIN, Martin SISOL, Peter VARGA, Ivan BREZÁNI, Michal MAŤÁŠOVSKÝ, Andrea ORAVCOVA Study of Chemical Pollutants and the Methods of Economic Reconstruction of the Rovinar Basin .....	109
Raluca MATEI, Emilia-Cornelia DUNCA, Aronel MATEI Investigation of Groundwater Flow Using $\Delta^{18}\text{O}$ and $\Delta\text{D}$ in a Sulfur Mine in Japan .....	115
Shinji MATSUMOTO, Isao MACHIDA Essement of IM-50 and TOFA Adsorbed Layer on Cassiterite in Flotation of Tin Sulfide Wastes .....	121
Tamara MATVEEVA, Nadezhda GROMOVA The Influence of Coal Tars over the Environment .....	125
Clementina MOLDOVAN, Aronel MATEI, Roxana Claudia HERBEI, Raluca MATEI Utilization Range of By-Products from Coal Combustion in Earth Structures of Transport Infrastructure .....	131
Václav MRÁZ, Jan SUDA, Vít LOJDA, Adam CULKA, Jakub TRUBAČ Biosorption of Lead and Cadmium Ions on the Green Parts of <i>Daucus Carota</i> .....	139
Martin MUCHA Online X-Ray Fluorescence Monitoring of Coarse Ore for Silver at the Process Conveyors at Kazakhmys Corporation LLC .....	145
Aydar NIGMATULIN, Zauze ABDRAKHMANOVA, Andrey KAN, Sergey EFIMENKO, Dmitry MAKAROV Oil Production by Polish Companies in Poland and Abroad .....	149
Tadeusz OLKUSKI, Janusz ZYSK, Barbara TORA, Wacław ANDRUSIKIEWICZ, Adam SZURLEJ, Kaja JEDLIŃSKA An Investigation on the Turbidity Removal from Natural Stone Processing Plant Wastewater by Flocculation .....	157
Savas OZUN, Dilan AGIRTMIS ULUS Advanced Biomaterials with Semiconductive Properties Based on Fungal Chitosan .....	163
Marek PIĄTKOWSKI, Aleksandra SIERAKOWSKA, Łukasz JANUS, Julia RADWAN-PRAĞŁOWSKA Bioactive Scaffolds for Skin Tissue Engineering Doped with Gold Nanoparticles Prepared from Waste Biomass .....	169
Julia RADWAN-PRAĞŁOWSKA, Łukasz JANUS, Marek PIĄTKOWSKI, Aleksandra SIERAKOWSKA, Dariusz BOGDAŁ Reduction of Pollution During Composite Machining .....	175
Jan RAŠKA, Libor HLAVÁČ, Adam ŠTEFEK, Martin TYČ Influence of High-Power Electromagnetic Pulses on the Structural-Chemical and Physicochemical Properties of Rare-Earth Minerals .....	179
Valentine A. CHANTURIYA, Igor Zh. BUNIN, Maria V. RYAZANTSEVA Study on Addition of Surfactants Agents to Improve the Behavior of High Water Content Sediment for Rare Earth Mining in Deep Sea .....	183
Takashi SASAOKA, Akihiro HAMANAKA, Takahiro FUNATSU, Hideki SHIMADA, Keisuke TAKAHASHI Sulphate Removal from Mining-Process Water by Capacitive Deionization .....	189
Maria SINCHÉ-GONZÁLEZ, Raul MOLLEHUARA CANALES Explosion Characteristics of Syngas from Gasification Process .....	195
Jan SKŘIŇSKÝ, Ján VEREŠ, Jakub ČESPIVA, Tadeáš OCHODEK, Karel BOROVEC, Jan KOLONIČNÝ XPS (X-Ray Photoelectron Spectroscopy) Study of Removing Iron Ions from Water by Zeolite and Bentonite .....	201
Anna ŠKVARLOVÁ, Mária KAŇUCHOVÁ, Ľubica KOZÁKOVÁ, Tomáš BAKALÁR, Andrea ORAVCOVÁ, Jiří ŠKVARLA What Antibiotic Threat Do the Heavy Metals Contaminated Sites of Mine Hide? .....	205
Ivana TIMKOVÁ, Miroslava LACHKÁ, Lea NOSÁLOVÁ, Lenka MALINIČOVÁ, Peter PRISTAŠ, Jana SEDLÁKOVÁ-KADUKOVÁ Quantifying Mineral Liberation – A Conventional and New Automatic Sophisticated Techniques Approach .....	211
Rudolf TOMANEC, Marina BLAGOJEV Determination of Risk Elements in Mine Waste Dump Soil Sample Using Sequential BCR Extraction .....	217
Barbora VALOVÁ, Iva KOTALOVÁ, Silvie HEVIÁNKOVÁ Biohydrometallurgical Processing Methods for Low-Grade Sulfide Ores in the Arctic .....	221
Elena YANISHEVSKAYA, Andrey GORYACHEV, Nadezhda FOKINA, Eugenia KRASAVTSEVA Comparison of Flotation and Screening as Separation Method in Coal Recovery From Tailings by Agglomeration .....	225
Özüm YAŞAR, Tuncay USLU Study of Extraction of Rare Earth Elements from Hard Coal Fly Ash .....	229
Ingrid ZNAMENÁČKOVÁ, Silvia DOLINSKÁ, Slavomír HREDZÁK, Vladimír ČABLÍK, Michal LOVÁS, Dana GEŠPEROVÁ	

